UNIVERSIDAD COMPLUTENSE DE MADRID
FACULTAD DE CIENCIAS BIOLÓGICAS

TESIS DOCTORAL

Further steps in systematics, biology and ecology of the phylum Kinorhyncha

Nuevas aportaciones en sistemática, biología y ecología del filo Kinorhyncha

MEMORIA PARA OPTAR AL GRADO DE DOCTOR

PRESENTADA POR

Diego Cepeda Gómez

Directores

Fernando Pardos Martínez
Nuria Sánchez Santos

Madrid

Further Steps in Systematics, Biology and Ecology of the Phylum Kinorhyncha

Nuevas Aportaciones en Sistemática, Biología y Ecología del Filo Kinorhyncha

Diego Cepeda Gómez

Tesis Doctoral 2021

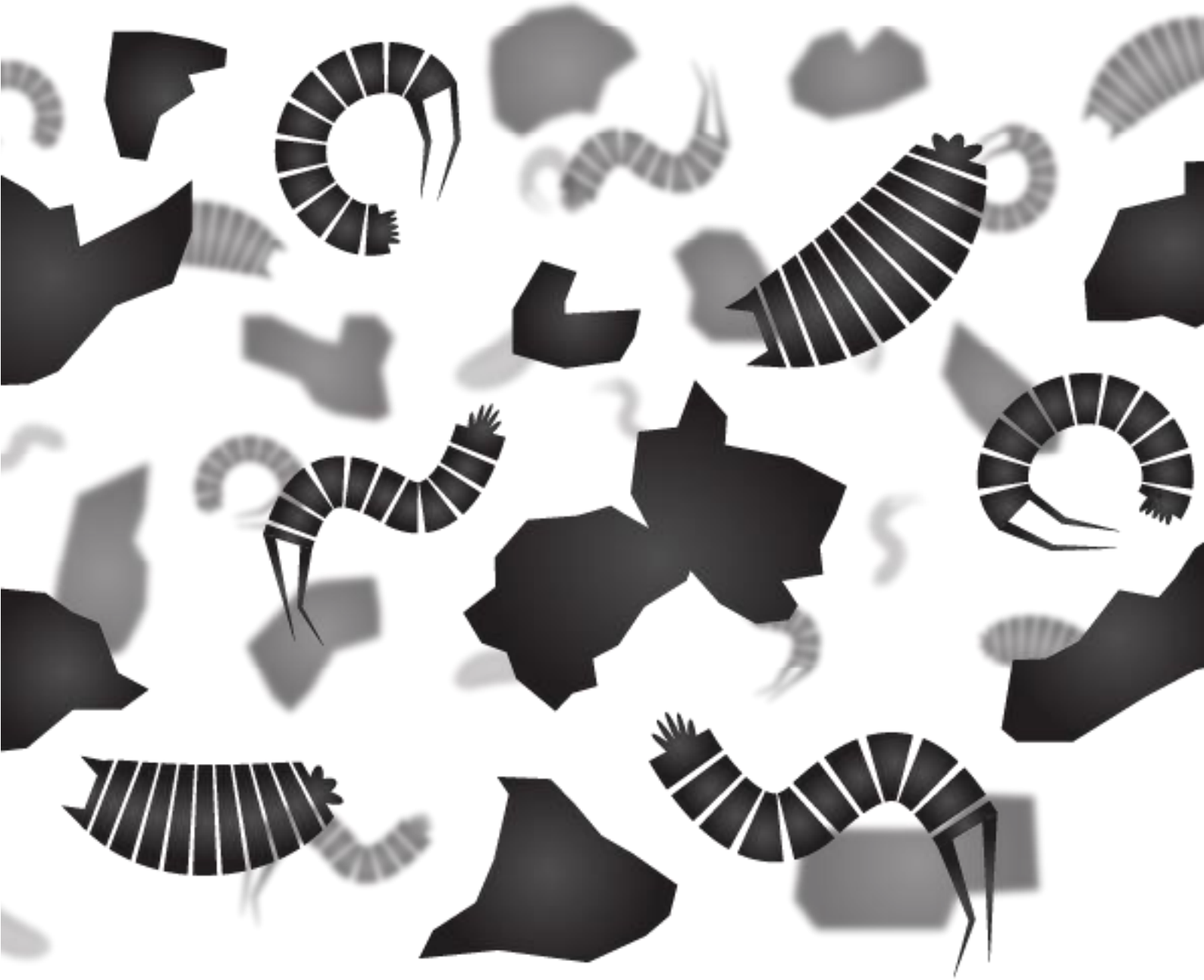

Universidad Complutense de Madrid

Facultad de Ciencias Biológicas

Departamento de Biodiversidad, Ecología y Evolución

UNIVERSIDAD COMPLUTENSE DE MADRID

FACULTAD DE CIENCIAS BIOLÓGICAS

DEPARTAMENTO DE BIODIVERSIDAD, ECOLOGÍA Y EVOLUCIÓN (BEE)

TESIS DOCTORAL

Further steps in systematics, biology and ecology of the phylum Kinorhyncha

Nuevas aportaciones en sistemática, biología y ecología del filo Kinorhyncha

MEMORIA PARA OPTAR AL TÍTULO DE DOCTOR
PRESENTADA POR

Diego Cepeda Gómez

Directores:

Fernando Pardos Martínez

Nuria Sánchez Santos

Madrid, 2021

La presente tesis doctoral ha sido financiada por:

- Ayuda para contratos predoctorales de personal investigador en formación que forma parte del Programa de Formación de Personal Investigador de la Universidad Complutense de Madrid (UCM) y del Programa de Financiación de la UCM y el Banco Santander (CT27/16-CT28/16).
- Ayuda para estancias breves en España y en el extranjero de los beneficiarios del Programa de Formación de Personal Investigador de la UCM (EB14/19).

Asimismo, los estudios realizados fueron parcialmente financiados por:

- Proyecto del Plan Nacional PGC2018-095851-B-C62 ("Fauna Ibérica XII: Escalidóforos de la península Ibérica y Baleares"), financiado por el Ministerio de Ciencia, Innovación y Universidades (MICINN) de España.
- Proyecto "PAssive Margin Exploration LAboratoires (PAMELA)", financiado por Total e Ifremer, Francia.
- Projectos IN-217306-3 y IN-202116 del Programa de Apoyo a Proyectos de Investigación e Innovación Tecnológica (PAPIIT) financiado por la Dirección General de Asuntos del Personal Académico (DGAPA) de México.
- Projecto BIO03/2017 de la Unión Iberoamericana de Universidades (UIU).

AGRADECIMIENTOS

Nunca pensé que escribir una sección de agradecimientos pudiera llegar a ser tan complicado, en algunas ocasiones, incluso más que la propia tesis. Primero, por la gran cantidad de personas que, una vez te pones a pensar, han influido y contribuido a que tu proyecto doctoral fuese posible. Segundo, por los recuerdos y memorias que me vienen a la mente conforme escribo estas palabras, y que en muchas ocasiones me hacen divagar y dejar el teclado para rememorarlos una vez más. Han sido cinco años…aparentemente cinco largos años que, sin embargo, han pasado de un plumazo. Parece que fue ayer cuando mi director de tesis, Fernando, me llamó por teléfono un 27 de octubre de 2016 para comunicarme que me habían concedido la beca predoctoral. Esto significó el inicio inminente de mi tesis. Recuerdo ese día perfectamente porque me encontraba visionando la película El crepúsculo de los dioses, de Billy Wilder, en los cines Renoir de Princesa, y tuve que salirme de la sala para contestar.

Quiero empezar agradeciéndole a él, por tanto, esta tesis, no solo por haberme dado la oportunidad de comenzarla y por haber confiado en mí desde un principio (teniendo solo mi TFM como referencia), sino también por su guía, su ayuda, su conocimiento científico, sus consejos y su inmejorable labor de director a lo largo de todo el proceso. Gracias por haber visto en mí algo de lo que yo no estaba tan seguro. Y por supuesto, esta tesis no habría llegado al punto que ha alcanzado si no hubiera sido por mi otra directora, Nuria, a la que quiero agradecer por todas sus propuestas y comentarios, su conocimiento, y su irremplazable ayuda. Sé que, sin ella, esta tesis no habría sido lo mismo, y no solo me llevo a una excelente compañera de trabajo sino también a una gran amiga.

Pero si me remonto a tiempos pretéritos, he de agradecer a mis padres que yo me halle aquí, escribiendo estos agradecimientos, y finalizando la tesis. A mi padre, Jesús, por haberme inculcado desde muy pequeño el amor y la curiosidad que hoy siento por la naturaleza y, especialmente, por los animales; por todos esos días paseando por el campo y observando mil y un bichos, mil y una plantas, mil y un hongos. Y a mi madre, Teresa, por haberme infundido la paciencia y la perseverancia tan necesarias en esto de la ciencia, por haber creído en mí desde que quise ser biólogo y dedicarme a la investigación, y por

haberme ayudado y alentado a no abandonar este camino. Tengo muy claro que, sin vosotros, esto no hubiera sido posible. Por supuesto, muchos otros familiares me han visto comenzar este proyecto y también me han apoyado a lo largo del mismo: mi hermana Ángela, mi cuñado Adrián, mis sobris Eider y Noa, mi abuela Ino…a todos ellos, que igualmente han aportado su granito de arena, gracias.

Gran parte de esta tesis la he realizado en la facultad de Biología de la Complu, de modo que he pasado mucho tiempo con mis compañeros de laboratorio y del departamento. Gracias inmensas a Irene, que empezamos casi a la par este camino, y que siempre ha estado ahí cuando la he necesitado, para tomar un café los días lluviosos y nublados que opacaban nuestras tesis; o un buen tercio en Forestales los viernes (y no solo los viernes) tras el curro en el labo; y los gintonics a ritmo del mejor petardeo ochentero y noventero los findes. Y, como Irene, muchos otros compañeros de la planta 10, que ya estaban antes que yo llegase, o que fueron viniendo después, y con los que he compartido grandes momentos (y mejores quedadas postlab): Dani, Natasha, Fer, Sergio, Tiago, Francesca, Ana… A todos vosotros, muchas gracias, porque hacer la tesis no solo es crecer como científico, sino también crecer como persona, conocer gente nueva…y todos vosotros habéis contribuido a ello. Y por supuesto, gracias también a los compañeros más veteranos, a los profesores que, como Fernando, cuando yo me encontraba en la carrera, siguieron despertando y desarrollando en mí el espíritu investigador: Jesús, Juan, Darío, Dolores, Mónica, Marta, Ana, Pablo, Tito, Carmen.

Y antes de llegar a la facultad, comencé mi carrera científica en el Museo Nacional de Ciencias Naturales. Y mucha gente de allí me apoyó en su día y continuó apoyándome en la actualidad con esta tesis. No podría olvidarme de Patri, quien me enseñó todo lo básico e hizo de mí un mejor científico, quien siempre me ayudó cuando lo necesité, y que me apoyó desde un principio. Y gracias también a Annie, a Viole, a Marian, a Jonathan, a Mar, a Teresa, a Pepa, a Iván, a Paula, a Javier y a Paco de colecciones, y por supuesto, a Dani, a Bego y a Santi de seguridad.

Algunos de vosotros habéis estado ahí desde hace mucho más tiempo, y me habéis ayudado a recorrer este camino de una manera más que esencial. Habéis sido piezas clave en mi camino científico y, sobre todo, personal. Habéis estado ahí en los momentos buenos y en los malos, en los que había algo que celebrar y en los que necesitaba desahogarme desesperadamente. Me habéis hecho mejorar, me habéis aconsejado, me habéis ayudado, y mucho. Así que este párrafo, quizás uno de los más importantes, va por

vosotros. A Lidia, que descubrió mi lado más rosa y me ayudó a que conviviera en perfecta armonía con mi lado oscuro, y que supo hacerme ver que no podía permanecer cerrado al mundo para siempre; gracias, gracias por haber estado ahí siempre, por cuando te he necesitado para pedirte consejo (científico o no), para charlar, o, simplemente, para contemplar el mar tomando vino (aún guardo aquel primer borrador de mi antiguo proyecto de tesis, con las corrientes por las rías gallegas…y siempre lo guardaré). A Fer, que siempre ha creído en mí, incluso en esos momentos más oscuros que yo no era capaz de hacerlo; juntos hemos creciendo científica y personalmente, en una ciudad como Madrid que no podría haber sido más perfecta para todo este proceso (también recordaré siempre tu celebración y tu alegría cuando, tras salir del cine, te conté que había conseguido la beca predoctoral). A Valle y Alberto, que desde Toledo siempre me han apoyado, y siempre han estado ahí cuando he vuelto a mi ciudad natal. A Vera, que siempre fue mi desconexión perfecta, y que, aunque nos hallemos a gran distancia, sabemos que podemos contar el uno con el otro para lo que sea...Madrid y yo te echamos mucho de menos. A mis compis de piso, actuales o no: Álex, Ana, Raquel, Dani, que he tenido la inmensa suerte de conocer y de tenerles no solo como compañeros sino también como amigos; habéis sido piezas clave en esto, me habéis visto en mis mejores y en mis peores momentos, me habéis apoyado siempre que lo he necesitado, y hemos compartido tantos y tantos momentos buenos…que no podría imaginarme la tesis y mi vida en Madrid sin vosotros. A Natalia, Rocío, Yoli y Carmen, que empezamos juntos en esto de la biología, y aunque ya no nos veamos tanto como antes, por una u otra circunstancia, sé que siempre mantendremos un vínculo entre nosotros; gracias por todo. A Rosa, Sergio y Jorge, por las fiestas padre que nos hemos pegado, por las risas y los momentos compartidos, y por vuestro apoyo.

Y luego llegaste tú. Y no podría haber sido en mejor momento. Te conocí tiempo después de haber empezado esta tesis, y te quedaste en mi vida. Siempre me reiré recordando que, cuando te conté que me dedicaba a la biología marina, me imaginabas limpiando playas de plásticos y desperdicios. Siempre me has hecho sonreír cuando más lo he necesitado. Siempre me has apoyado cuando más lo he necesitado. Siempre me has respetado, y siempre me has entregado incondicionalmente todo tu cariño. Y espero que continuemos riéndonos juntos, compartiendo experiencias y momentos, muchos años más. Gracias bebu. Gracias Frankie.

A todos vosotros **GRACIAS**, en mayúsculas. Me siento muy afortunado de teneros en mi vida. Porque sin vosotros esta tesis no hubiera sido posible. Porque sin vosotros no sé qué habría sido de mí. Porque sin vosotros Madrid no sería mi Madrid. Y si me he dejado a alguien en el tintero, perdón, porque escribir esto no es fácil, y ya todos sabéis que mi memoria es un poco Dory, pero que sepáis que esas gracias también van por **vosotros**.

"The sea, once it casts its spell,

*holds one in its net of wonder forever" (**Jacques Yves Cousteau**)*

"Nothing in biology makes sense except

*in the light of evolution" (**Theodosius Dobzhansky**)*

"What we know is a drop,

*what we don't know is an ocean" (**Isaac Newton**)*

"Science is simply the word we use to describe

*a method for organizing our curiosity" (**Tim Minchin**)*

"The cure for anything is salt water:

*sweat, tears, or the sea" (**Karen von Blixen-Finecke**)*

"You know how the time flies, only yesterday

*was the time of our lives" (**Someone like you, Adele**)*

"I'm big! It's the pictures

*that got small" (**Sunset Boulevard, Billy Wilder**)*

"We are like the dreamer who dreams, and then lives inside

*the dream. But…who is the dreamer?" (**Twin Peaks: The Return, David Lynch**)*

"Callar y quemarse es el castigo más grande

*que nos podemos echar encima" (**La Novia, Paula Ortiz**)*

"Hai detto che le emozioni sono sopravvalutate? Ma è una stronzata: ¡le emozioni

*sono tutto quello che abbiamo!" (**La Giovinezza, Paolo Sorrentino**)*

"There's no such thing as perfect writing,

*just like there's no such thing as perfect despair" (**Haruki Murakami**)*

"To see a world in a grain

*of sand" (**William Blake**)*

INDEX

ABSTRACT / RESUMEN

General aspects and background.

The phylum Kinorhyncha encompasses a group of exclusively marine and estuarine, holobenthic, free-living, ecdysozoan invertebrates that are part of the meiofaunal communities. Meiofauna is a widely applied term that refers to those animal taxa intermediate in body size between the macrofauna and the microbes that pass by a 1 mm sieve but are retained in a 42 μm sieve. This range of body size makes the meiofaunal component of marine benthos inhabit the small crevices and interstices of the ocean floor sediment grains. Thus, the meiofaunal communities in general and the kinorhynch populations in particular, are strongly influenced by the features of the marine sediment in which they inhabit. Kinorhynchs are worldwide distributed from the intertidal zone to hadal depths, and may be found in a great variety of marine and estuarine sediments.

Kinorhynch morphology is relatively preserved and homogeneous, as all the current representatives possess a body divided into three main regions: head, neck and trunk. The head, composed of a mouth cone and an introvert, constitutes the most anterior region of the body and is responsible for feeding, locomotion and nervous coordination. The neck may be considered as a closing apparatus that allows the complete retraction of the head inside the trunk. The trunk is segmented in a constant number of eleven segments, and this segmentation implies the serial repetition of various external and internal structures of ectodermal and mesodermal origin. Many of these external structures (*e.g.* cuticular plates, cuticular appendages, sensory spots, etc.) have been traditionally used by taxonomists to classify the observed Kinorhyncha biodiversity, yet little is known about their actual function, their evolutionary history, and/or their ecological implications or adaptations to the environment.

Kinorhyncha comprises ca. 314 species currently divided in two monophyletic classes, namely Allomalorhagida and Cyclorhagida. Although these classes are well defined and generally accepted by the phylum specialists, the internal relationships of the lower taxonomic levels suffer from a significant lack of knowledge. Kinorhyncha is included into the monophyletic superclade Scalidophora, together with the phyla

Loricifera and Priapulida, which in turn is grouped with the superclade Nematoida (phyla Nematoda and Nematomorpha) to constitute the Cycloneuralia, whose monophyly is still controversial. Cycloneuralians are included together with panarthropods (phyla Arthropoda, Onycophora and Tardigrada) in the monophyletic Ecdysozoa, characterized by the presence of a non-ciliated, external cuticle periodically moulted by hormonal control.

In recent years, the number of studies related to the phylum Kinorhyncha has skyrocketed, mainly due to an increase in the number of specialists dedicated to this animal group. Most of these studies focus on systematics and description of new species, which is essential to create a basic knowledge foundation to posteriorly develop new research lines in other fields. However, many aspects of this animal phylum still remain unexplored and are biased by specialist sampling strategies, making some ocean areas completely uncharted. Even in supposedly well known areas, new species are frequent to be found. Moreover, little is known about the main abiotic and biotic factors that sort the kinorhynch communities, despite the peculiar habitat they are part of, or basic aspects of their biology, including the reproduction strategies or what they feed on. In this way, it is necessary to expand the research dedicated to the phylum Kinorhyncha if we want to continue with the lines of knowledge established by prior pioneers.

Antecedentes y aspectos generales.

El filo Kinorhyncha está compuesto por un grupo de invertebrados ecdisozoos de aguas salobres y marinas, holobentónicos y de vida libre que forman parte de las comunidades de la meiofauna. El término meiofauna se acuñó para designar a aquellos taxones animales cuyo tamaño corporal es un intermedio entre el de los microorganismos y el de los animales de la macrofauna, de modo que son capaces de pasar por un tamiz de luz de 1 mm, pero quedan retenidos en un tamiz de luz de 42 μm. Este rango de tamaño corporal hace que los organismos meiofaunísticos del bentos marino vivan en los pequeños espacios e intersticios que quedan entre las partículas de sedimento que conforman el lecho oceánico. De este modo, los organismos de la meiofauna en general, y las poblaciones de kinorrincos en particular, están fuertemente influenciados por las características de los sedimentos marinos. Los kinorrincos se distribuyen en todos los

océanos del mundo desde la región intermareal hasta las profundidades abisales, y pueden encontrarse en una gran varidad de ambientes bentónicos marinos y salobres.

La morfología de los kinorrincos se encuentra bastante conservada, de modo que todas las especies conocidas actuales poseen el cuerpo dividido en tres regiones principales: cabeza, cuello y tronco. La cabeza, a su vez formada por el cono bucal y el introverto, constituye la región más anterior del cuerpo de estos animales, y lleva a cabo funciones tan esenciales como la toma del alimento, la locomoción y la coordinación nerviosa. El cuello conforma una especie de cierre cuando la cabeza, de carácter retráctil, queda dentro del tronco del animal. El tronco está segmentado en un número constante de once segmentos, y dicha segmentación afecta a estructuras y órganos tanto internos como externos de origen ectodérmico y mesodérmico. Muchas de estas estructuras (*e.g.* placas cuticulares, apéndices cuticulares, fosetas sensoriales, etc.) se han utilizado tradicionalmente en taxonomía para clasificar a los kinorrincos, aunque se sabe muy poco de cuál es su función, su historia evolutiva, sus implicaciones ecológicas, o sus adaptaciones morfológicas al ambiente.

El filo Kinorhyncha engloba actualmente unas 314 especies divididas en dos clases, a saber, Allomalorhagida y Cyclorhagida. Aunque estas clases están bien definidas, y son aceptadas por todos los especialistas del filo, las relaciones filogenéticas internas todavía distan de estar bien establecidas. Kinorhyncha queda incluido dentro del superclado Scalidophora, que es monofilético, junto a los filos Loricifera y Priapulida, los cuales, a su vez, se agrupan junto al superclado Nematoida (conformado por la unión de los filos Nematoda y Nematomorpha) para formar el clado Cycloneuralia, cuya monofilia está sometida a controversia. Los cicloneuralios se incluyen junto a los panartrópodos (a su vez conformados por los filos Arthropoda, Onycophora y Tardigrada) en el clado monofilético Ecdysozoa, que se caracteriza por la presencia de una cutícula exterior carente de cilios que es mudada periódicamente por control hormonal.

Recientemente, se ha disparado el número de estudios relacionados con el filo Kinorhyncha, principalmente debido al aumento en el número de especialistas dedicados a este grupo de animales. La mayoría de dichos estudios son de carácter sistemático o describen nuevas especies, lo cual resulta esencial para generar una base de conocimiento y desarrollar otras líneas de investigación posteriores. Sin embargo, muchos aspectos de los kinorrincos aún permanecen completamente inexplorados y están fuertemente sesgados por las estrategias de muestreo de los especialistas, de modo que ciertas regiones

oceánicas se encuentran tremendamente inexploradas. Incluso en áreas que se suponen bien conocidas en términos de su biodiversidad de kinorrincos, es relativamente frecuente que nuevas especies se describan. Además, se conoce muy poco de los principales factores abióticos y bióticos que definen a las comunidades de kinorrincos, a pesar de lo peculiar de sus hábitats, así como de aspectos básicos de su biología, incluyendo el modo de reproducción o sus fuentes de alimentación. De este modo, se hace necesario promover la cantidad y variedad de estudios dedicados al filo Kinorhyncha si queremos continuar con las líneas de conocimiento generadas por anteriores investigadores en este campo.

Objectives.

Given the previous context of the phylum Kinorhyncha, it seems quite obvious that the studies focused on these metazoans are still in an early stage of knowledge, specially when compared to other taxa traditionally more studied by researchers, such as the macrofaunal ones. In order to fulfil some of the numerous gaps of knowledge surrounding kinorhynchs, we carried out several new, original studies on systematics (mainly focused on taxonomy and biodiversity), morphology, ecology, morpho-ecology, macroecology and biogeography of the phylum Kinorhyncha.

The main objectives of the present thesis are summarized as follows:

- To explore new ocean areas of interest where kinorhynchs have been scarcely reported and/or described.
- To revisit supposedly well known ocean areas in terms of Kinorhyncha biodiversity to find out if there are still new species to science.
- To study whether the cuticular characters most traditionally used in taxonomy remain relevant to specific kinorhynch taxa, and whether they are subject of evolutionary processes of the phylum such as allometric growth.
- To explore the possible function and adaptation of those previously mentioned cuticular characters to particular meiofaunal environments.
- To determine ecological, macroecological and biogeographical patterns that may be useful to generate a more global vision of knowledge of the phylum Kinorhyncha.

Objetivos.

Una vez hecha esta introducción previa, resulta evidente que los estudios del filo Kinorhyncha se encuentran todavía en una etapa preliminar de desarrollo, sobre todo si los comparamos con el estado de conocimiento de otros grupos que tradicionalmente han recibido mayor atención, como aquellos de la macrofauna. Para suplir esta falta de conocimiento del filo Kinorhyncha, se han realizado una serie de estudios originales sobre sistemática (con especial hincapié en taxonomía y biodiversidad), morfología, ecología, morfoecología, macroecología y biogeografía de este grupo.

Los objetivos principales de la presente tesis pueden resumirse de la siguiente forma:

- Explorar la fauna de kinorrincos de zonas de interés donde este grupo ha sido escasamente reportado o descrito.
- Volver a estudiar áreas donde se han muestreado kinorrincos de manera más o menos intensiva para averiguar si todavía quedan especies por descubrir.
- Determinar si los caracteres cuticulares que tradicionalmente se han empleado en la taxonomía del grupo siguen siendo relevantes (con especial hincapié en grupos taxonómicos de interés), y si dichos caracteres se encuentran sometidos a procesos evolutivos concretos (por ejemplo, si exhiben patrones evolutivos de crecimiento alométrico).
- Explorar la posible función que estos caracteres cuticulares puedan tener, así como sus posibles adaptaciones morfológicas al ambiente.
- Determinar si existen patrones ecológicos, macroecológicos y biogeográficos que ayuden a generar una visión más global del grupo.

Main results.

Taxonomy and biodiversity.

In this field, we focused on identifying the unexplored kinorhynch fauna from ocean areas of biological interest, including the Caribbean Sea, which is recognized as a global hotspot of marine biodiversity, and the deep-sea, which in recent years has shown to host a unique metazoan fauna richer in species that once thought. Additionally, we wanted to

revisit some supposedly well known areas in terms of Kinorhyncha biodiversity, to better understand the taxonomic background of known species and elucidate the presence of still undescribed new species.

We described nine new species and report eleven previously known species from the Caribbean Sea, which represents an increase of ca. 38 % of the total Caribbean Kinorhyncha biodiversity. Thus, the present thesis has greatly helped to reveal the hidden kinorhynch fauna from the Caribbean Basin, making this area one of the best known nowadays for the phylum. Though we cannot confirm that the Caribbean Sea is a hotspot of Kinorhyncha biodiversity, because the obtained data just reflect a more intensive sampling effort in the area compared to others, the results are promising and encourage to continue with the Caribbean samplings in the future.

Regarding the deep-sea, we described two new species from the Gulf of California and three new species from the Mozambique Channel, and reported for the first time eight previously known and still undescribed species for the later. From these studies, new hypotheses about the distribution of deep-sea kinorhynchs came to light, as these species seem to somehow possess wider ranges of distribution than the congeners from shallow waters. Thus, new lines of research about the kinorhynch biogeography are opened, whose unknowns require more systematic studies about deep-sea kinorhynchs to be elucidated.

We furthermore explored supposedly well known areas, in terms of Kinorhyncha biodiversity, to determine if still undescribed species are present, selecting the North Sea for this objective. We described a new species of the recently established genus *Setaphyes* from the Skagerrak region, emphasizing, once again, that there are still species to be discovered even in areas that have previously been intensively sampled.

Morphology, morpho-ecology, ecology, macroecology and biogeography.

We selected some of the main external, cuticular characters frequently used for kinorhynch systematics and taxonomy to ascertain if they are subject of evolutionary trends, such as allometric growth, or conversely, whether they are more influenced by the environment and/or may have some kind of ecological relevance or morphological adaptation to particular habitats.

The segments that constitute the body of kinorhynchs, whose number remains constant throughout the phylum, follow evolutionary, allometric trends. The segments that include essential structures for the animal (most anterior and posterior ones), and that are already developed from the earlier development stages, have a generalized, negative allometric growth in all kinorhynch groups. This result is consistent with the negative allometric trend of essential body regions of other metazoans, such as the cephalic region of certain arthropods and chordates. In contrast, the intermediate body segments may exhibit different allometric trends apparently depending on the differential number of cuticular structures (and associated organs) that harbour.

In addition to these allometric trends in the growth of the body segments, the body shape seems to be morphologically adapted to the different meiofaunal habitats where kinorhynchs are found. In this way, it was determined that species inhabiting coarser sediments, or sediments with a wider range of grain sizes, tend to possess plumper, stubbier and more robust bodies. Conversely, species that inhabit finer sediments, or sediments with a greater homogeneity of particle sizes, show more vermiform, elongated bodies. For metazoans such as kinorhynchs, that move by active displacement of sediment particles using the introvert scalids, this would be a clear adaptation to take advantage of said movement, since the stubbier shapes would allow kinorhynchs to move more efficiently by exerting a greater force to displace the coarser particles, whereas the more vermiform shapes would allow species to better move trough the smaller interstices of the finer sediments. However, it should not be forgotten that phylogenetic history constitutes an important part of the morphological adaptation of extant kinorhynchs, marking important exceptions to the above mentioned statements.

Contrarily to body segments, cuticle spines, which are the most conspicuous body appendages of kinorhynchs, showed no correlation to body growth (or to corresponding segment growth), and evolutionary, allometric trends were not detected. However, lateral terminal spines shape was strongly correlated to sediment features, as it happened to body shape. Species with stouter and widened spines inhabiting coarser sediments, that in most occasions are result of areas with higher hydrodynamics, could cling more tightly to the sediment particles under episodes of strong currents, whereas species bearing slender spines (which is linked to more flexible structures) could move more efficiently through the smaller interstices of the finer sediments.

Among the main abiotic factors studied in the present thesis, granulometry was detected as relevant for kinorhynch morphological adaptations, as above mentioned. However, organic matter, pH and concentrations of particular substances in extreme habitats, such as methane and hydrogen sulphide, seem to determine relevant variations in the composition of the kinorhynch communities.

On a more global scale, the worldwide distribution of kinorhynchs appears to be influenced by latitude and certain environmental factors that vary with latitude, including the sea surface temperature and the net primary productivity. There does not seem to be a general latitudinal pattern that homogeneously explains the biogeography of kinorhynchs, but rather a complex interaction of several factors that yields a great variety of patterns throughout hemispheres, coastlines and taxonomic groups. These results agree with those obtained for other marine taxa such as copepods, bivalves and tardigrades.

Resultados principales.

Taxonomía y biodiversidad.

En esta área de conocimiento, se ha hecho hincapié en identificar y describir la fauna de kinorrincos de áreas de especial interés donde se tenía escasa información, como el mar Caribe, reconocido como una zona megadiversa a nivel global, o el océano profundo, cuyo estudio ha despuntado en los últimos años revelando la existencia de una fauna bentónica muy diferente a la de aguas someras y más rica en especies de lo que se pensaba. Además, se han estudiado también muestras procedentes de áreas donde el estado de conocimiento de la fauna de kinorrincos se encuentra más avanzado, para analizar los antecedentes taxonómicos de especies ya conocidas y determinar si todavía quedan especies por descubrir en esas áreas.

Se han descrito nueve especies nuevas y se han registrado once previamente conocidas para el mar Caribe, lo que supone un incremento del 38 % en el conocimiento de la fauna de kinorrincos caribeña. Además, esta tesis ha ayudado enormemente a desvelar la fauna de kinorrincos otrora desconocida para la cuenca caribeña, haciendo de esta área una de las más estudiadas para el filo a nivel mundial. Aunque no podemos afirmar que el mar Caribe sea una zona megadiversa de kinorrincos, ya que los datos obtenidos simplemente son un reflejo de un esfuerzo de muestreo mayor comparado con

el aplicado en otras áreas, los resultados son prometedores y animan a continuar con muestreos extra en un futuro.

Respecto al océano profundo, se han descrito dos especies nuevas para el golfo de California y tres especies nuevas para el canal de Mozambique; además, se han registrado por primera vez ocho especies ya conocidas, o bien por describir, para el canal de Mozambique. Como resultado de estos estudios, se refuerza la idea de comparar las áreas de distribución de los kinorrincos del océano profundo, que aparentemente son muy amplias, con las de sus parientes de aguas someras, mucho más restringidas. De este modo, se abren nuevas líneas de investigación sobre la biogeografía de los kinorrincos, cuyas incógnitas requieren de más muestreos sistemáticos en el mar profundo para ser desveladas.

Además, se seleccionó el mar del Norte como un área donde se conoce relativamente bien la fauna de kinorrincos existente para determinar si todavía quedan especies por descubrir. Como resultado, se describió una nueva especie del género *Setaphyes*, recientemente establecido, procedente de la zona de Skagerrak, lo que apoya la idea, una vez más, de que aún quedan muchas especies por descubrir incluso en áreas donde el esfuerzo de muestreo ha sido intensivo.

Morfología, morfoecología, ecología, macroecología y biogeografía.

Se seleccionaron una serie de caracteres cuticulares externos de relevancia en la sistemática y taxonomía del grupo para averiguar si están sometidos a procesos evolutivos determinados (*i.e.*, de crecimiento alométrico), o si por el contrario dichos caracteres se ven más influenciados por las condiciones ambientales y/o pueden tener algún tipo de implicación ecológica o adaptación morfológica a hábitats particulares.

Los segmentos que constituyen el cuerpo de los kinorrincos, cuyo número se mantiene constante en todos los taxones del filo, parecen seguir tendencias evolutivas de crecimiento alométrico. Los segmentos que albergan estructuras vitales para los kinorrincos (correspondientes a las regiones anterior y posterior del tronco), que ya se encuentran desarrollados desde los primeros estadios de la ontogenia, poseen un crecimiento alométrico negativo generalizado en todos los taxones de kinorrincos. Este resultado coincide con el obtenido en otros metazoos, como ocurre con la región cefálica

de ciertos grupos de artrópodos y de cordados. Por otro lado, los segmentos intermedios parecen tener un crecimiento alométrico más variable, dependiendo del número de estructuras cuticulares (con sus órganos asociados) que albergan.

Además de estas tendencias evolutivas de crecimiento alométrico, la forma corporal de los kinorrincos parece encontrarse adaptada a los diferentes ambientes meiofaunísticos. De este modo, se comprobó que las especies que viven en sedimentos gruesos, o sedimentos con amplio rango de tamaños de partícula, poseen una forma corporal más robusta y rechoncha. Por el contrario, aquellas especies que viven en sedimentos finos, o sedimentos homogéneos con tendencia de grano fino, poseen formas corporales más alargadas y vermiformes. Para metazoos como los kinorrincos, que se mueven por desplazamiento activo de las partículas de sedimento gracias a la actuación de las escálidas del introverto, esta variación de la forma corporal resulta adaptativa, ya que permite aumentar la eficacia de la locomoción por el medio; las formas corporales más rechonchas y robustas pueden ejercer una fuerza de empuje mayor de las partículas para desplazar esos granos de sedimento más gruesos, mientras que las formas más alargadas y vermiformes pueden moverse más fácilmente por los intersticios más estrechos de los granos finos de sedimento. Sin embargo, ha de tenerse en cuenta que la historia filogenética juega un rol fundamental a la hora de definir las adaptaciones morfológicas de las especies actuales de kinorrincos, revelando importantes excepciones a lo mencionado con anterioridad.

A diferencia de los segmentos corporales, las espinas cuticulares (los apéndices corporales más evidentes de los kinorrincos) no mostraron ningún tipo de tendencia evolutiva alométrica, ni con el tronco ni con el segmento que las porta. No obstante, la forma de las espinas laterales terminales mostró correlación con el tipo de sedimento del medio, como ocurrió con la forma corporal. Especies de kinorrincos con espinas más robustas y ensanchadas muestran tendencia a vivir en sedimentos más gruesos, que en muchos casos son el resultado de fuertes corrientes oceánicas, de modo que podrían servir para anclarse de manera más eficaz a los granos de sedimento para evitar salir despedidos, mientras que especies con espinas más alargadas y estrechas (y, probablemente, más flexibles) facilitarían el movimiento por los intersticios de menor tamaño correspondientes a sedimentos finos.

Entre los principales factores abióticos estudiados en esta tesis, la granulometría del sedimento se erigió como la variable ambiental de mayor relevancia a la hora de

determinar las adaptaciones morfológicas de los kinorrincos al ambiente. Sin embargo, la cantidad de materia orgánica, el pH y las concentraciones de determinados compuestos en ambientes extremos (como el metano y el ácido sulfhídrico) también parecen ser importantes a la hora de definir la composición de las diferentes comunidades de kinorrincos.

En una escala más global, la distribución mundial de los kinorrincos parece estar influenciada en cierto grado por la latitud y ciertas variables ambientales que muestran cambios latitudinales, como la temperatura superficial del mar o la productividad primaria neta. No parece existir un patrón latitudinal homogéneo que explique la distribución actual de los kinorrincos, sino que más bien es el resultado de una compleja interacción de diversos factores que deriva en una gran variedad de patrones latitudinales entre los diferentes hemisferios, líneas de costa y grupos taxonómicos. Estos resultados concuerdan con los obtenidos para otros taxones marinos como los copépodos, los bivalvos y los tardígrados.

List of compiled publications.

The present thesis is composed of ten publications, one appendix with still unpublished data, and four appendices with complementary samplings and material.

Published studies.

Cepeda D, Álamo D, Sánchez N, Pardos F. 2019. Allometric growth in meiofaunal invertebrates: do all kinorhynchs show homogeneous trends? *Zoological Journal of the Linnean Society* **187(4)**: 1041-1060. https://doi.org/10.1093/zoolinnean/zlz083.

Cepeda D, Álvarez-Castillo L, Hermoso-Salazar M, Sánchez N, Gómez S, Pardos F. 2019. Four new species of Kinorhyncha from the Gulf of California, eastern Pacific Ocean. *Zoologischer Anzeiger* **282**: 140-160. https://doi.org/10.1016/j.jcz.2019.05.011.

Cepeda D, González-Casarrubios A, Sánchez N, Pardos F. 2020. *Setaphyes elenae* sp. nov., a new species of mud dragon (Kinorhyncha: Allomalorhagida) from Skagerrak (north-eastern Atlantic Ocean). *European Journal of Taxonomy* **637**: e637. https://doi.org/10.5852/ejt.2020.637.

Cepeda D, Pardos F, Sánchez N. 2019. A new species and first record of *Dracoderes* (Kinorhyncha: Allomalorhagida: Dracoderidae) from American waters, with an identification key of the genus. *Zoologischer Anzeiger* **282**: 106-115. https://doi.org/10.1016/j.jcz.2019.05.019.

Cepeda D, Pardos F, Sánchez N. 2019. Kinorhyncha from the Caribbean, with the description of two new species from Puerto Rico and Barbados. *Zoologischer Anzeiger* **282**: 127-139. https://doi.org/10.1016/j.jcz.2019.05.014.

Cepeda D, Pardos F, Sánchez N. 2021. From biggest to smallest mud dragons: size-latitude trends in a group of meiobenthic animals worldwide. *Organisms Diversity & Evolution* **21**: 43-58. https://doi.org/10.1007/s13127-020-00471-y.

Cepeda D, Pardos F, Zeppilli D, Sánchez N. 2020. Dragons of the deep-sea: Kinorhyncha communities in a pockmark field at Mozambique Channel, with the description of three new species. *Frontiers in Marine Science* **7**: e665. https://doi.org/10.3389/fmars.2020.00665.

Cepeda D, Sánchez N, Pardos F. 2019. First extensive account of the phylum Kinorhyncha from Haiti and the Dominican Republic (Caribbean Sea), with the description of four new species. *Marine Biodiversity* **49(3)**: 2281-2309. https://doi.org/10.1007/s12526-019-00963-x.

Cepeda D, Sánchez N, Pardos F. 2019. First report of the family Zelinkaderidae (Kinorhyncha: Cyclorhagida) for the Caribbean Sea, with the description of a new species of *Triodontoderes* Sørensen & Rho, 2009 and an identification key for the family. *Zoologischer Anzeiger* **282**: 116-126. https://doi.org/10.1016/j.jcz.2019.05.017. Q1

Cepeda D, Trigo D, Pardos F, Sánchez N. 2020. Does sediment composition sort kinorhynch communities? An ecomorphological approach through geometric morphometrics. *Nature Scientific Reports* **10(1)**: e2603. https://doi.org/10.1038/s41598-020-59511-4.

Unpublished studies.

Appendix I. Cepeda D, González-Casarrubios A, Sánchez N, Pardos F. Submitted. Kinorhyncha diversity in the Caribbean Sea: a compilation of prior and new knowledge, description of a new species of *Echinoderes* (Cyclorhagida: Echinoderidae) and a dichotomous key to the species level. *European Journal of Taxonomy.*

Complementary samplings and material.

Appendix II. New species of *Setaphyes* from Portugal.

Appendix III. New species of kinorhynchs from the Clarion-Clipperton deep-sea zone.

Appendix IV. New species of *Leiocanthus* from the Gulf of Mexico.

Appendix V. Use of isotopes for determination of feed intake in kinorhynchs – Preliminary results.

1 - INTRODUCTION

"The most beautiful thing we can experience is the mysterious.

It is the source of all true art and science" (Albert Einstein)

1.1 Marine biodiversity and meiofauna.

Marine biodiversity includes intertidal and subtidal species, their genetic pool, the habitats and ecosystems they are part of, and the ecological processes that support them (Thorne-Miller, 1999). Most of multicellular organisms are metazoans, and at least 97 % of all animal species are invertebrates (Castro and Huber, 2007). All the major invertebrate groups possess marine representatives, and even certain phyla are exclusively marine (*e.g.* Ctenophora, Echinodermata, Kinorhyncha, Hemichordata). The oceans consequently comprise a far greater biodiversity of animal taxa than the terrestrial environment, which is not surprising taking into account that organisms firstly appeared in the seas several hundred millions years before life on land developed (Costello and Chaudhary, 2017).

According to the occupied habitat, functional diversity in marine ecosystems is classified into three main categories: plankton, nekton and benthos (Seibold and Berger, 1993). Plankton are those primary producers and consumers that drift with ocean currents, nekton includes species that actively swim through the water and benthos are living organisms on the ocean floor (Fig. 1) (Castro and Huber, 2007). Benthos plays a critical role in the functioning of marine ecosystems, being a major link in the food chains and nets, and is also important for the breakdown of organic matter in nutrient cycling processes. Benthos is also responsible for removing pollutants and sediments suspended in the water column, maintaining healthy water quality (Snelgrove, 1997).

Most studies of marine benthic communities usually focus on organisms large enough to be recognized with relative ease (*i.e.* benthic macrofauna) (Higgins and Thiel, 1988). However, benthos is also composed of smaller organisms intermediate in size between the microbes and macrofauna, which are called meiofauna (from the Ancient Greek *meiōn*, less or smaller, plus the Latin *Faunus*, in reference to the Roman god

Faunus protector of the fields, forests and herds) (Palmer and Strayer, 1996). In this context, meiofauna refers to the fauna that pass by a 1 mm sieve but is retained in a 42 μm sieve (Fig. 2) (Higgins and Thiel, 1988). These categories of body size, such as macro- and meiofauna, have little relationship with taxonomic classification and/or ecological implications.

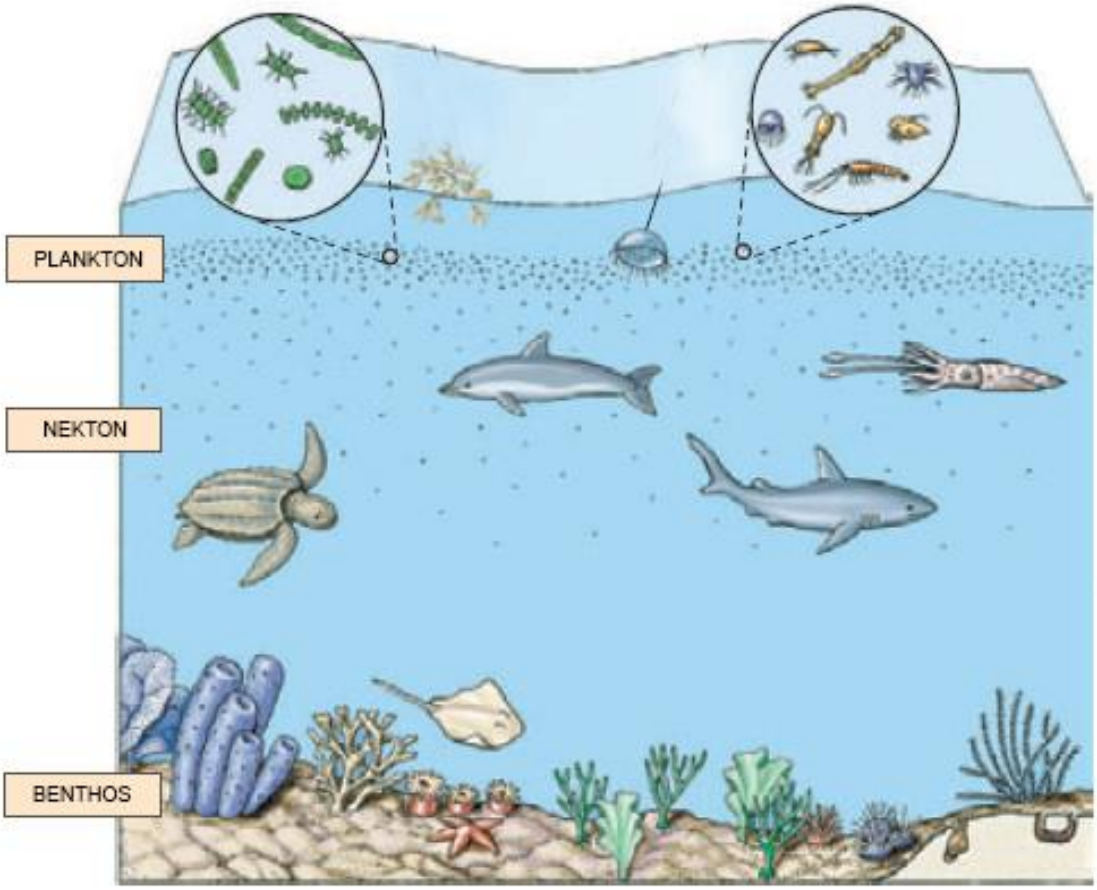

Figure 1. Classification of the functional diversity in marine ecosystems. Modified from Castro and Huber (2007).

Size definition separating macro- and meiofauna has not been always applied by marine benthologists, using other terms instead that refer to the way of movement through the sediment. Thus, interstitial fauna are animals living in the interstitial spaces and crevices of marine sediments, passively digging through the sediment particles or living sedentarily near the surface (Nicholls, 1935; Remane, 1940). On the other hand, sediment-dwellers are organisms that move by active displacement of sediment (Martens and Schockaert, 1986; Traunspurger and Majdi, 2017). Some taxa are catalogued as epibiontic, living on top of other organisms, and others are described as hyperbenthic, being able to swim through the water column from time to time (Tita *et al.*, 1999; Giere,

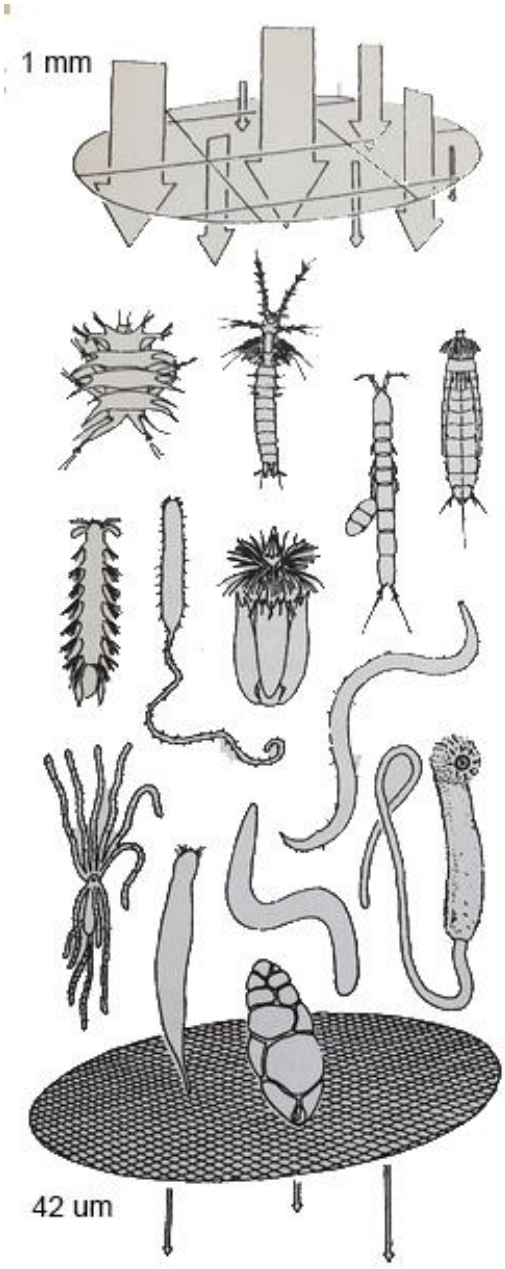

Figure 2. Representation of the concept of meiofauna based on the body size approach. Modified from Higgins and Thiel (1988).

2009). It is important to emphasize that not all organisms living in interstitial spaces or acting as sediment-dwellers are of meiofaunal body dimensions, consequently not all these species are meiofauna (Higgins and Thiel, 1988).

Meiofaunal taxa, from a body size point of view, have representatives in most of the animal phyla, and even some phyla are exclusively part of the meiofaunal communities (*e.g.* Gastrotricha, Kinorhyncha, Loricifera, Tardigrada). The study of these poorly known organisms suffers from the constraints caused by minute body size, difficult extraction from sediment, and expensive sampling and processing equipments. This leads to a reduced scientific community devoted to meiofauna in contrast to other fields of study.

1.2 Introduction to the phylum Kinorhyncha.

Kinorhyncha (from the Ancient Greek *κινέω*, movement, plus *ῥύγχος*, snout), commonly known as mud dragons, is one of the referred, exclusively marine, meiofaunal phylum of metazoan species. The representatives of this phylum freely inhabit in muddy to coarse sandy sediments, from the intertidal zone to deep-sea habitats in the oceans worldwide (Sørensen and Pardos, 2008; Neuhaus, 2013). Currently, Kinorhyncha is included in the superclade Ecdysozoa, forming the Scalidophora clade together with Priapulida and Loricifera (Dunn *et al.*, 2014).

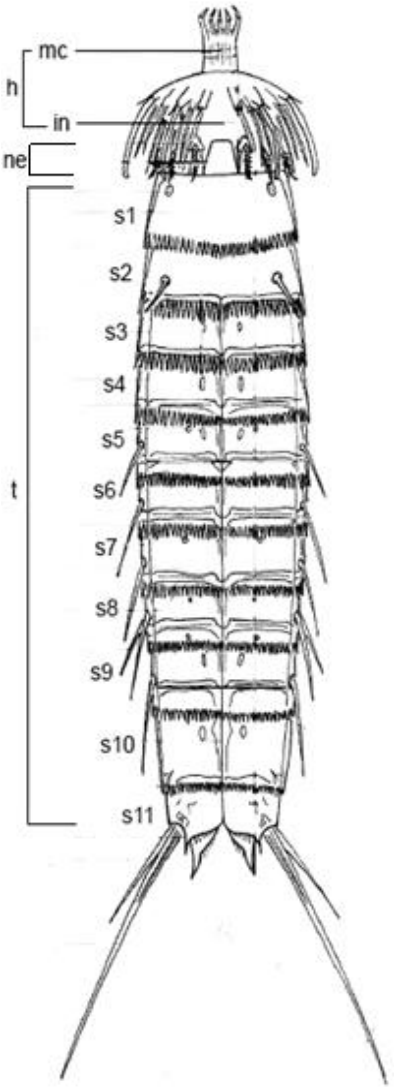

Figure 3. Generalized external kinorhynch morphology. Abbreviations: h, head; in, introvert; mc, mouth cone; ne, neck; t, trunk; s, segment (followed by number of corresponding segment). Modified from Sørensen and Pardos (2008).

Kinorhynchs are morphologically homogeneous, with a body divided into head, neck and trunk (Fig. 3) (Sørensen and Pardos, 2008; Neuhaus, 2013). The head, composed of an eversible introvert and a mouth cone, is responsible for feeding, locomotion and reception of sensory stimuli. The neck constitutes a closing system when the head is completely retracted inside the animal. The trunk is elongated and divided into eleven segments (Sørensen and Pardos, 2008; Neuhaus, 2013). This segmentation affects to cuticle, cuticular appendages, muscles, nervous system, epidermal glands and sensory structures (Brusca *et al.*, 2016).

1.3 Kinorhynch external morphology.

1.3.1 HEAD.

The head is an eversible structure located at the most anterior region of the body, and is divided in two parts: mouth cone and introvert, as previously mentioned. The mouth cone represents the beginning of the digestive tract and is composed of four rings of oral styles (Neuhaus, 2013). The most external ring (ring 00) bears nine outer oral styles, which may consist of a single, elongated, rod-like piece with hooked, pointed end (Fig. 4A) or be divided in two or three portions (Fig. 4B-F). The following three inner rings (rings -01 to -03) carry up to twenty inner oral styles, which are slender and smaller than previous ones (Zelinka, 1928; Brown, 1989; Neuhaus, 1991; 1994; 2013). The inner oral styles never come out in living animals, being only visible if the mouth cone is protruded abnormally during the fixation process (Sørensen and Pardos, 2008) (Fig. 4E).

The introvert consists of seven rings of scalids (rings 01 to 07) maximally, which are sensory and locomotor appendages divided in a basal sheath that usually bear a tuft

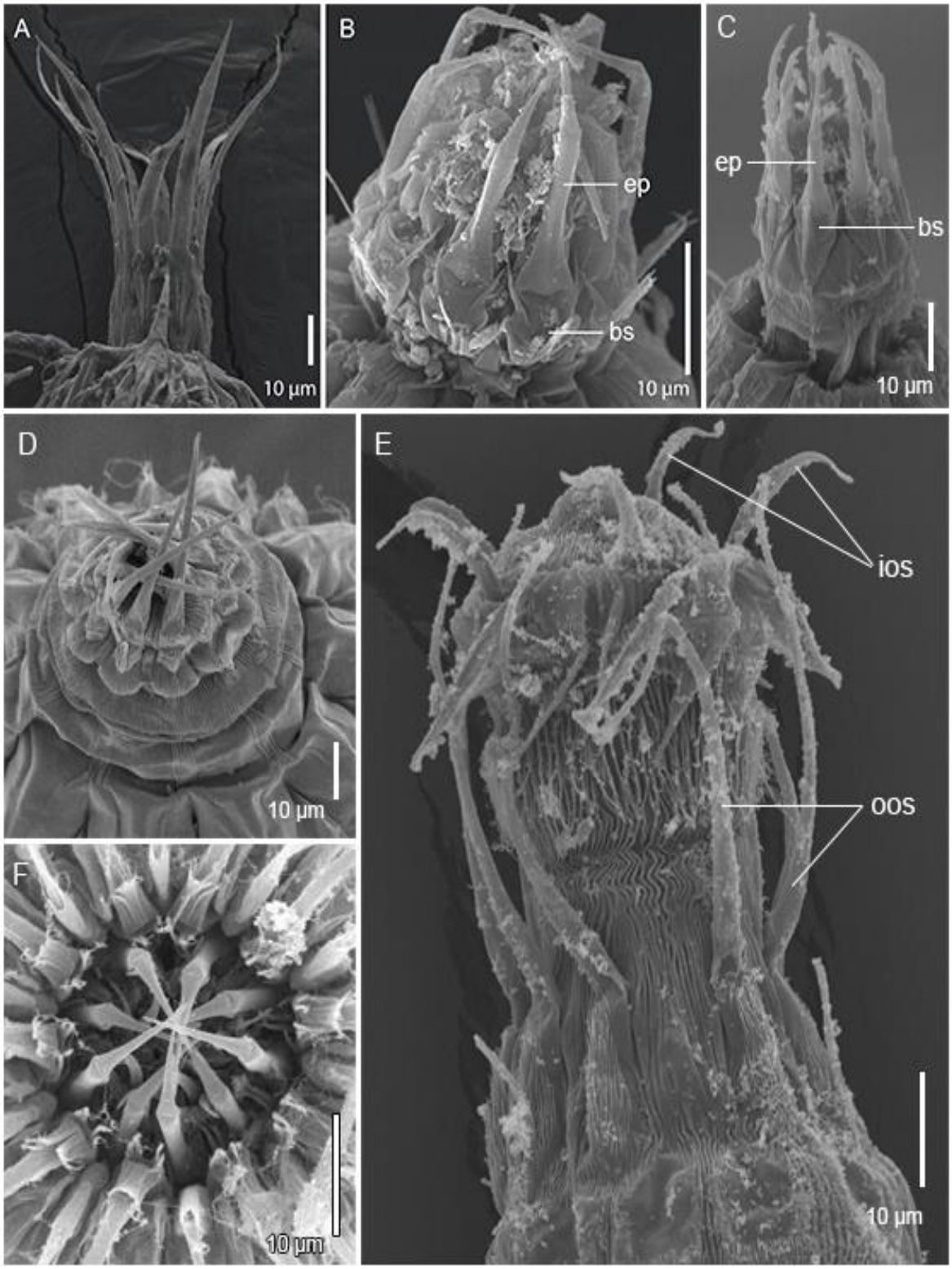

Figure 4. Mouth cone of *Triodontoderes lagahoo* Cepeda, Sánchez and Pardos, 2019 (in Cepeda *et al.*, 2019a) from Tobago (A), *Echinoderes augustae* Sørensen and Landers, 2014 from Venezuela (B), *E. hispanicus* Pardos, Higgins and Benito, 1998 from Spain (C), *Pycnophyes aulacodes* Sánchez, Pardos, Herranz and Benito, 2011 from Spain (D), *Setaphyes kielensis* (Zelinka, 1928) from Norway (E) and *E. cantabricus* Pardos, Higgins and Benito, 1998 from Spain (F). Abbreviations: bs, basal sheath; ep, end piece; ios, inner oral styles; oos, outer oral styles. Photo E kindly provided by Dr M.V. Sørensen.

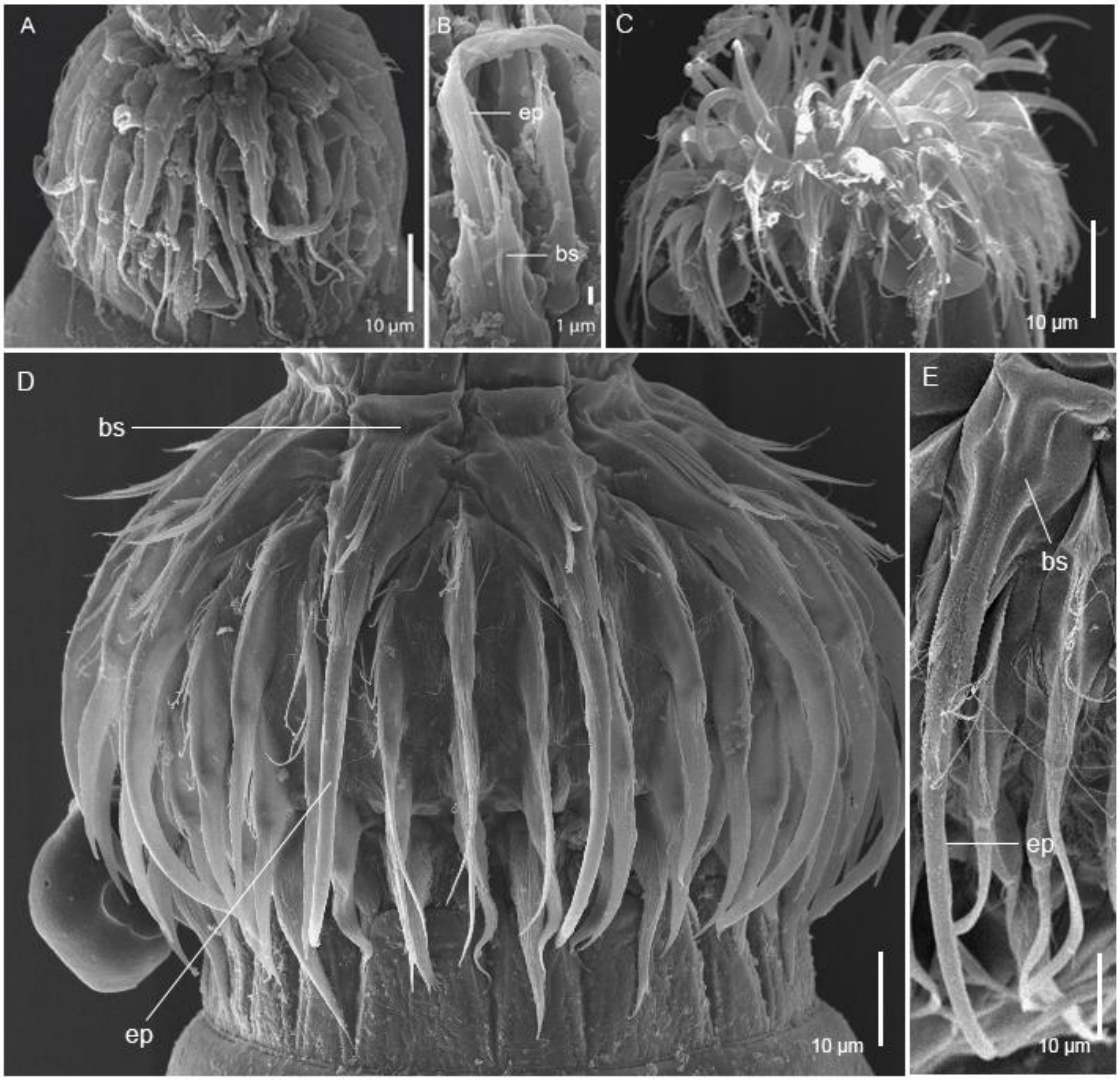

Figure 5. Introvert of *Echinoderes augustae* from Venezuela (A), *E. cantabricus* from Spain (C) and *E. hispanicus* from Spain (D), and detail of primary spinoscalids of *E. augustae* from Venezuela (B) and *P. aulacodes* from Spain (E). Abbreviations: bs, basal sheath; ep, end piece.

of spinous projections and a distal end-piece (Fig. 5A-E) (Zelinka, 1928; Brown, 1989; Sørensen and Pardos, 2008; Neuhaus, 1991; 1994; 2013). The arrangement of oral styles and scalids follows a radial symmetry pattern, hence the exact location of each appendage can be described in a polar projection (Fig. 6) (Sørensen and Pardos, 2008). In this projection, each ring represents either a mouth cone ring or an introvert ring, while the radial lines that start from the center divide the projection into the different introvert sectors; the black symbology represents the mouth cone appendages, whereas the white symbology is used to represent the introvert appendages, with a different symbol for the diverse types of scalids and oral styles (Fig. 6). The outermost and thickest concentric circle represents the neck placids (Fig. 6).

1.3.2 NECK.

The neck is usually composed of small, rectangular to trapezoidal, sclerotized plates with rounded edges called placids which are used as a closing apparatus when the head is completely retracted (Fig. 7A, C, F-H) (Sørensen and Pardos, 2008; Neuhaus, 2013). In some taxa (*e.g.* Zelinkaderidae), placids are indistinct and basally fused to the first trunk segment, being difficult to distinguish (Fig. 7B) (Higgins, 1990). Some placids may bear trichoscalids (attached to trichoscalid plates or not), which are short, cone-shaped appendages superficially covered by dense tufts of minute hairs (Fig. 7D-E) (Sørensen and Pardos, 2008).

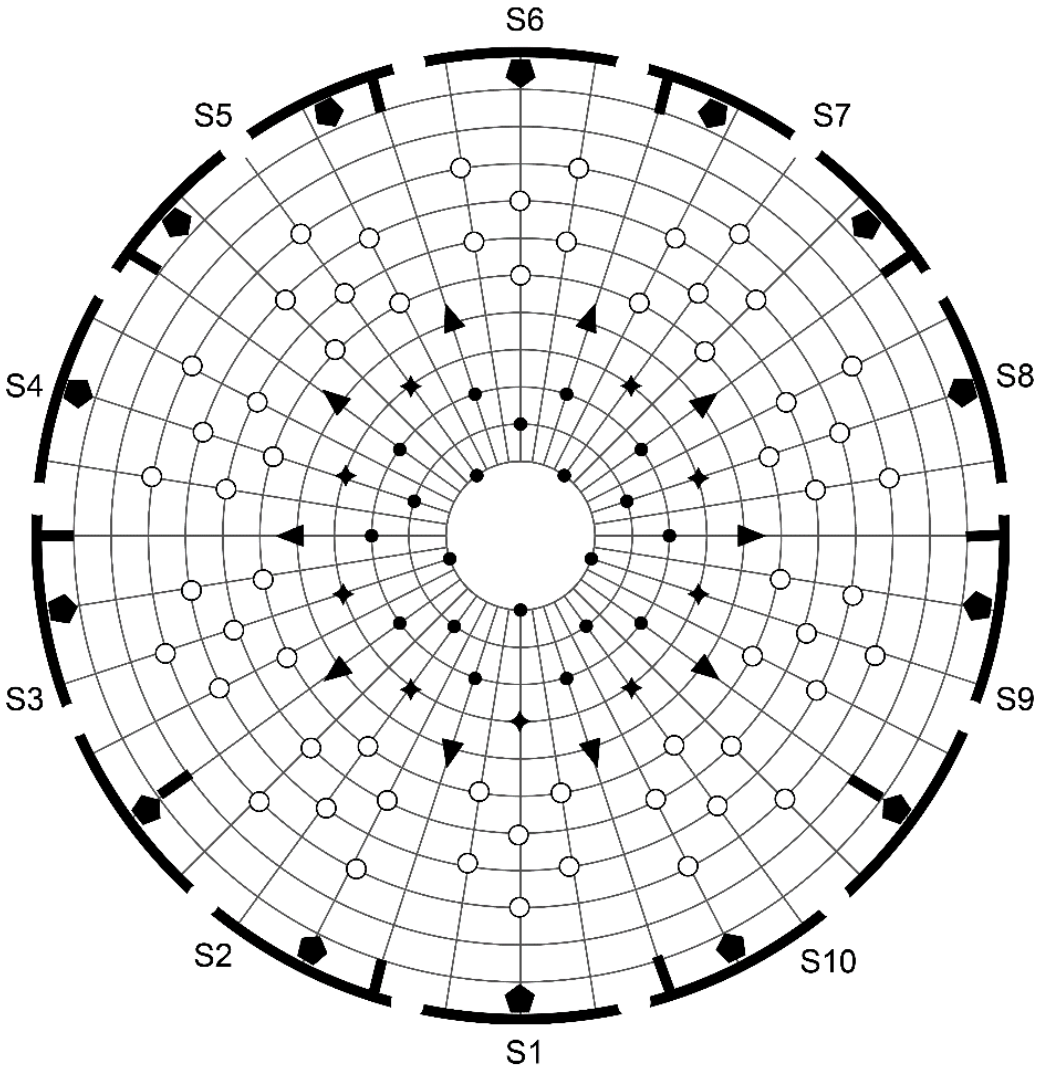

Figure 6. Example of a diagram of kinorhynch mouth cone, introvert, trichoscalids and placids. Abbreviations: S, sector (followed by number of corresponding sector); black circles represent inner oral styles, white circles represent regular-sized scalids, stars represent outer oral styles, triangles represent primary spinoscalids, pentagons represent trichoscalids.

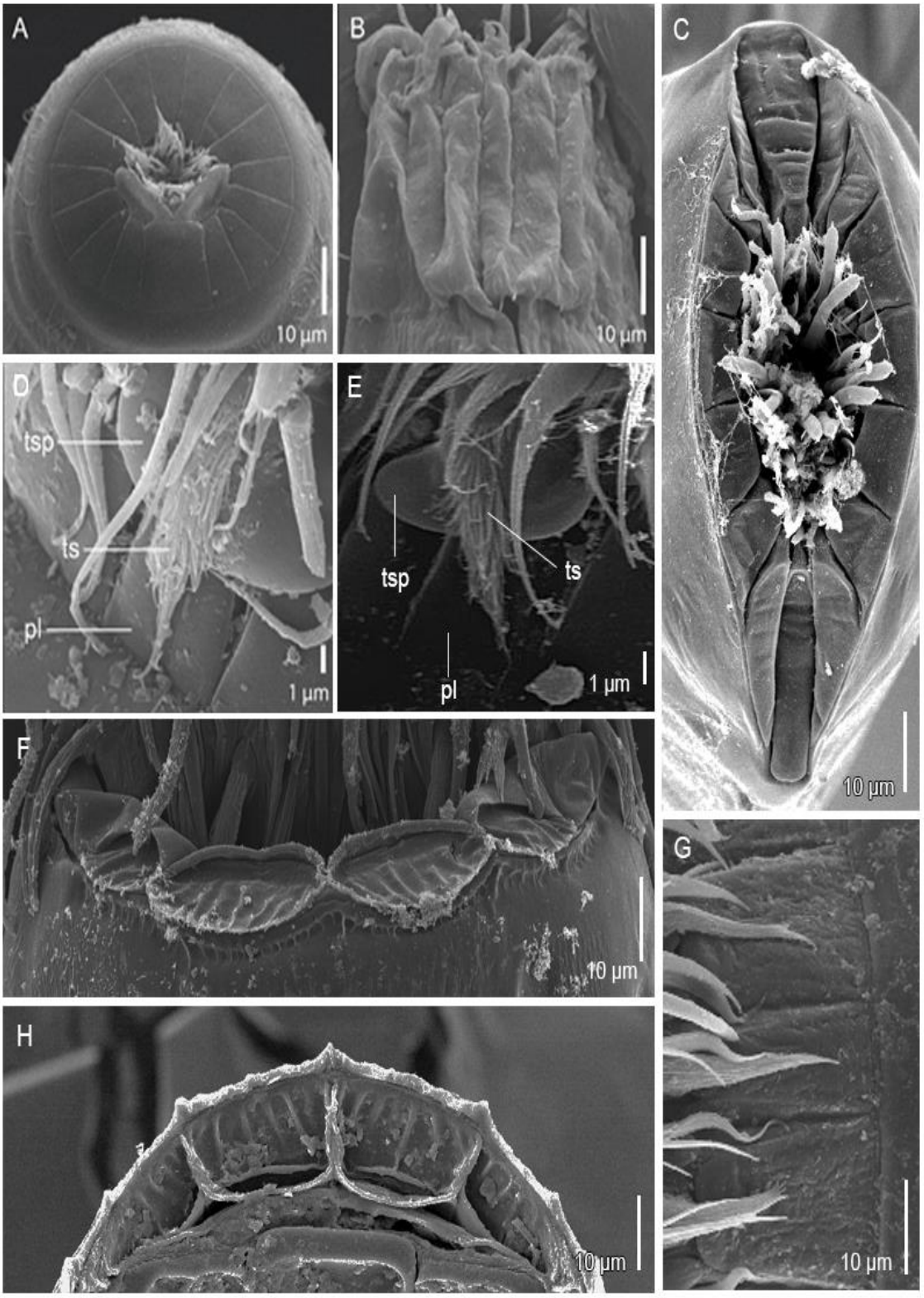

Figure 7. Neck of *Echinoderes sublicarum* Higgins, 1977 (in Higgins, 1977b) from Venezuela (A), *Triodontoderes lagahoo* from Tobago (B), *Sphenoderes aspidochelone* Sørensen and Landers, 2018 from the Gulf of Mexico (C), *Setaphyes kielensis* from Norway (F), *Pycnophyes aulacodes* from Spain (H) and *E. cantabricus* from Spain (G), and detail of a trichoscalid and its associated plate of *E. augustae* from Venezuela (D) and *E. cantabricus* from Spain (E). Abbreviations: pl, placid; ts, trichoscalid; tsp, trichoscalid plate. Photos C and F kindly provided by Dr M.V. Sørensen.

1.3.3 TRUNK.

The trunk is composed of eleven segments and may vary from spindle- or cigar-like shape (*e.g.* Echinoderidae) (Fig. 8A) to more rectangular, box-like shape (*e.g.* Pycnophyidae) (Fig. 8B, E-F) or vermiform (*e.g.* Antygomonidae, Zelinkaderidae) (Fig. 8C-D) (Neuhaus, 2013). Each segment is externally composed of a single, closed, ring-like cuticular plate or divided in two or more cuticular plates. The single dorsal plate is referred to as the tergal plate, while the ventral ones (up to three) are called sternal plates. Both tergal and sternal plates articulate laterally at the so-called tergosternal junctions, whereas when there are two sternal plates, they mesially meet in the midventral junction (Sørensen and Pardos, 2008). The cuticle of each segment (except that of segment 11) partly overlaps the following segment as a free flap, whose posterior edge may be fringed, being called primary pectinate fringe (Fig. 9A-C) (Neuhaus, 2013). On the other hand, the anterior margin of a segment (except that of segment 1) may bear one or more rows of fringes, which are known as secondary pectinate fringes (Fig. 9A-C), which are usually overlapped by the primary pectinate fringe of the precedent segment.

1.3.4 TRUNK APPENDAGES.

Several cuticular appendages, with sensory and/or glandular function, may be observed throughout the cuticular surface of a kinorhynch:

- **Acicular spines.** Elongated, spinous, rounded in cross-section appendages with basal ball-and-socket articulation, and pointed tip (Fig. 10A-B, D). The most conspicuous ones are the so-called lateral terminal spines, located in segment 11 in lateroventral position.
- **Cuspidate spines.** Syringe-shaped, oval in cross-section, spinous appendages with basal ball-and-socket articulation, superficially covered by minute hairs, and an abruptly tapered, narrowed tip (Fig. 10B, D).
- **Crenulated spines.** Moniliform, rounded in cross-section, very flexible, spinous appendages with basal ball-and-socket articulation (Fig. 10C). They are only present in the males of certain taxa (*e.g. Centroderes* Zelinka, 1907; *Echinoderes* Claparède, 1863).

- **Tubes.** Tubular, thin-walled, oval in cross-section, very flexible, elongated appendages with basal articulation and a terminal pore, usually with paired, winged extensions laterally (Fig. 10E).
- **Setae.** Tubular, thin-walled, oval in cross-section, very flexible, tiny appendages with basal articulation, a terminal pore and blunt tip (Fig. 10F). They are exclusive of the families Neocentrophyidae and Pycnophyidae.
- **Elevations.** Posterior bulges usually associated with intracuticular, butterfly-like atria of sensory spots, that never surpass the margin of a segment (Fig. 10G). They are always present in middorsal position in some species of the families Neocentrophyidae and Pycnophyidae.
- **Processes.** Distally pointed, posterior bulges that always surpass the margin of a segment (Fig. 10I). They are always present in middorsal position in some species of the families Neocentrophyidae and Pycnophyidae.
- **Glandular cell outlets.** Oval, rounded or slightly reniform glandular cell openings, connected to subcuticular glands. Two types of glandular outlets are recognized: type-1, with several pores in a circular, slight depression (Fig. 10J, N); and type-2, with a single, wide opening usually slightly elevated above the trunk cuticle's surface with pear-shaped cuticular walls inside the trunk cuticle (Fig. 10O).
- **Sensory spots.** Circular to oval areas with several rings of micropapillae surrounding one or more sensory pores from which a cilium may emerge, and that are connected to subcuticular sensory cells (Fig. 10H, K, M, P). Up to five kinds of sensory spots are recognized depending on their morphology.
- **Papillae.** Short, conical elevations superficially covered by minute micropapillae. They are present in a few kinorhynch taxa (*e.g. Echinoderes*), frequently only in females.
- **Hairs.** Elongated, bristle-like appendages with pointed tip, usually emerging from perforation sites. Hairs may be bracteate, when their cuticular junction is covered by a scale-like structure (Fig. 10L), or not.

Kinorhynch appendages can be present in different positions throughout the cuticular plates. The most frequent positions are: middorsal, paradorsal, subdorsal, laterodorsal, midlateral, sublateral, lateral accessory, lateroventral, ventrolateral, ventromedial and paraventral (Fig. 11). For instance, if a spine is present in lateroventral position, it is

referred as lateroventral spine. The function of spines, setae and tubes still remains unknown, although they are attributed a possible relationship with secretion and/or reception of sensory stimuli (Zelinka, 1928; GªOrdóñez *et al.*, 2000; Neuhaus, 2013).

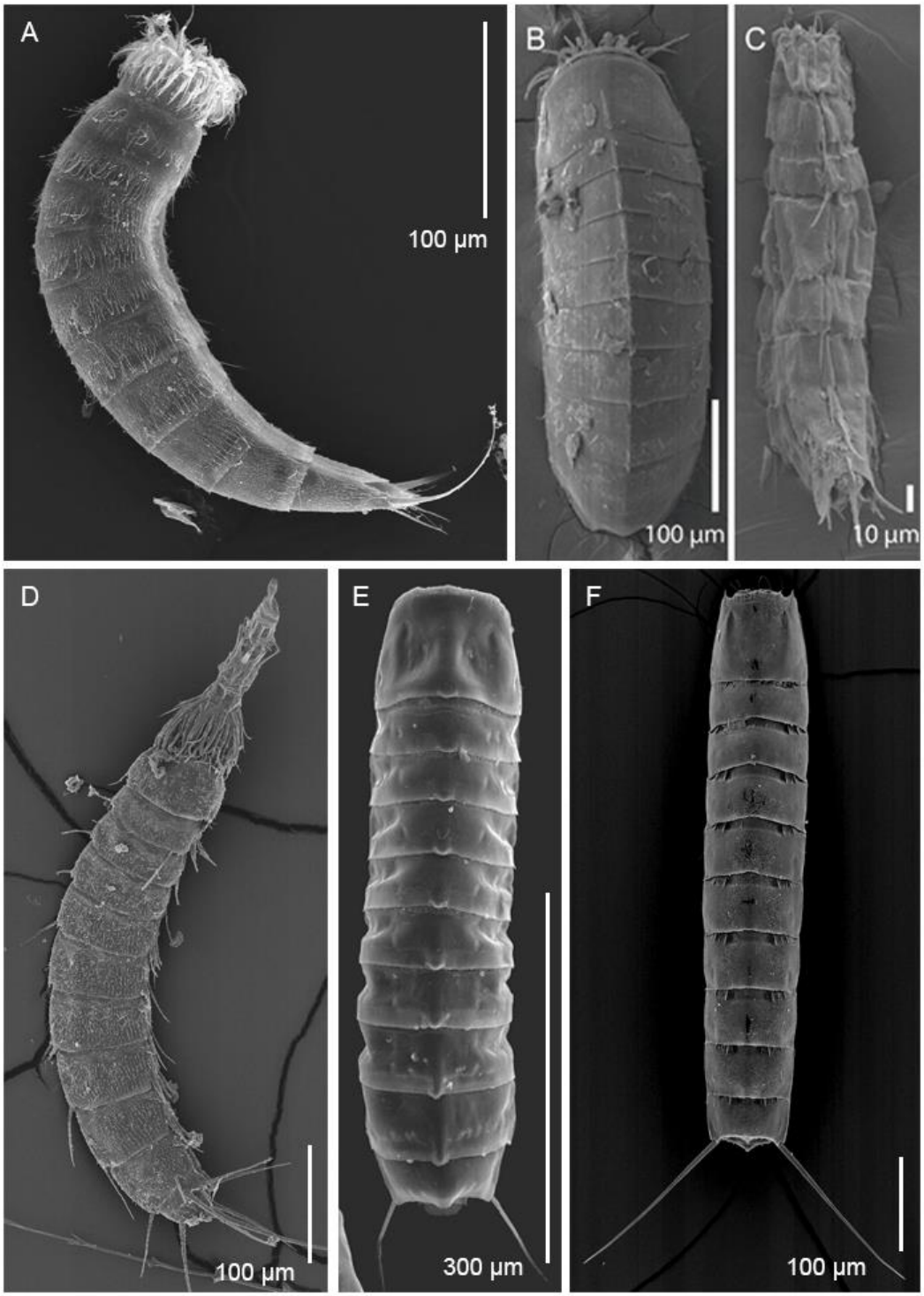

Figure 8. Trunk general overview of *Echinoderes cantabricus* from Spain (A), *Higginsium erismatum* (Higgins, 1983) from Tobago (B), *Triodontoderes lagahoo* from Tobago (C), *Antygomonas incomitata* Nebelsick, 1990 from Italy (D), *Pycnophyes communis* Zelinka, 1908 from Spain (E) and *Pycnophyes* sp. from Norway (F). Photos D and F kindly provided by Dr M.V. Sørensen.

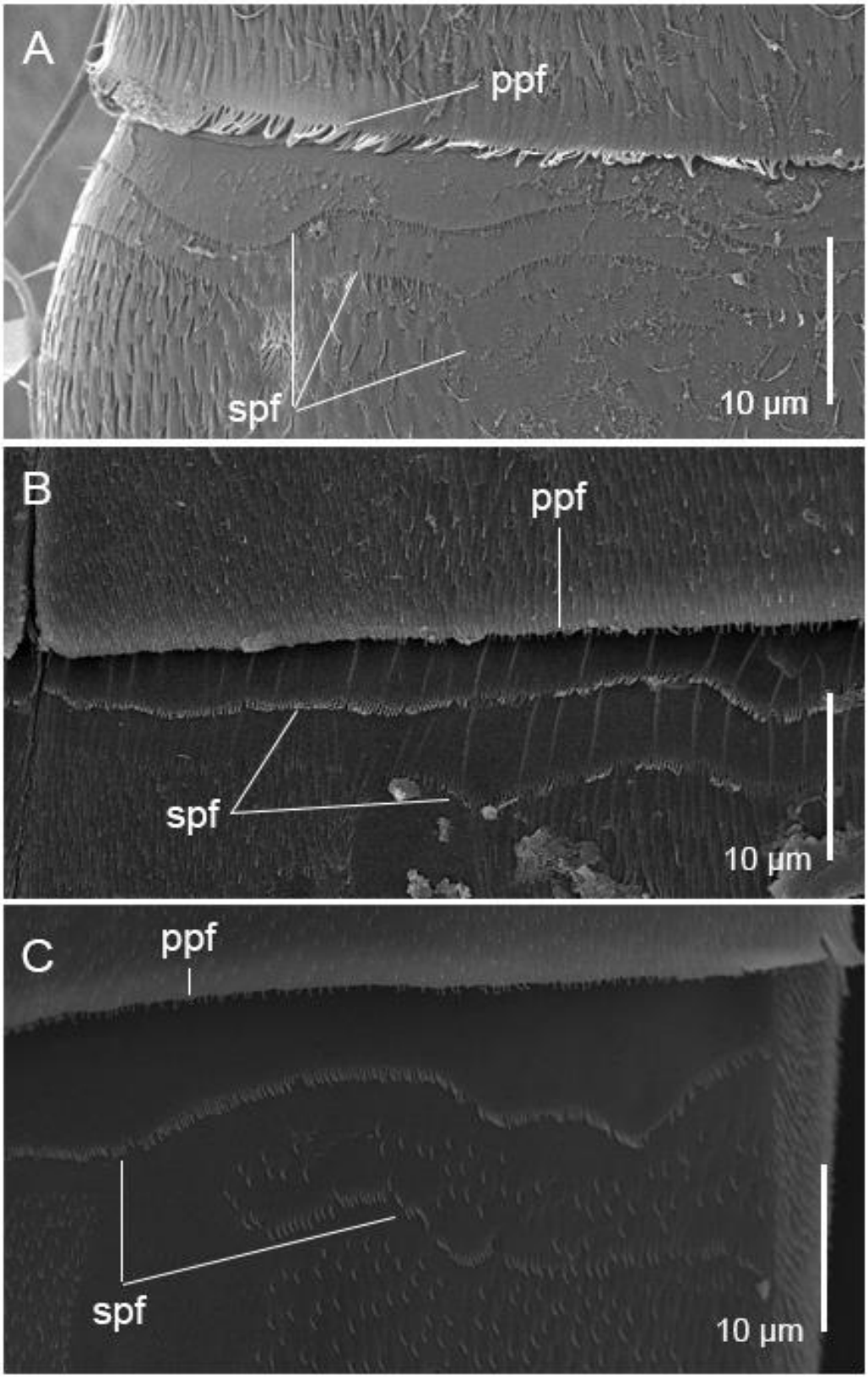

Figure 9. Primary and secondary pectinate fringes of *Campyloderes vanhoeffeni* Zelinka, 1913 from an unknown location (A), *Cristaphyes carinatus* (Zelinka, 1912) from Spain (B) and *Pycnophyes norenburgi* Herranz, Sánchez, Pardos and Higgins, 2014 from Florida (C). Abbreviations: ppf, primary pectinate fringe; spf, secondary pectinate fringe. Photo A kindly provided by Dr M.V. Sørensen.

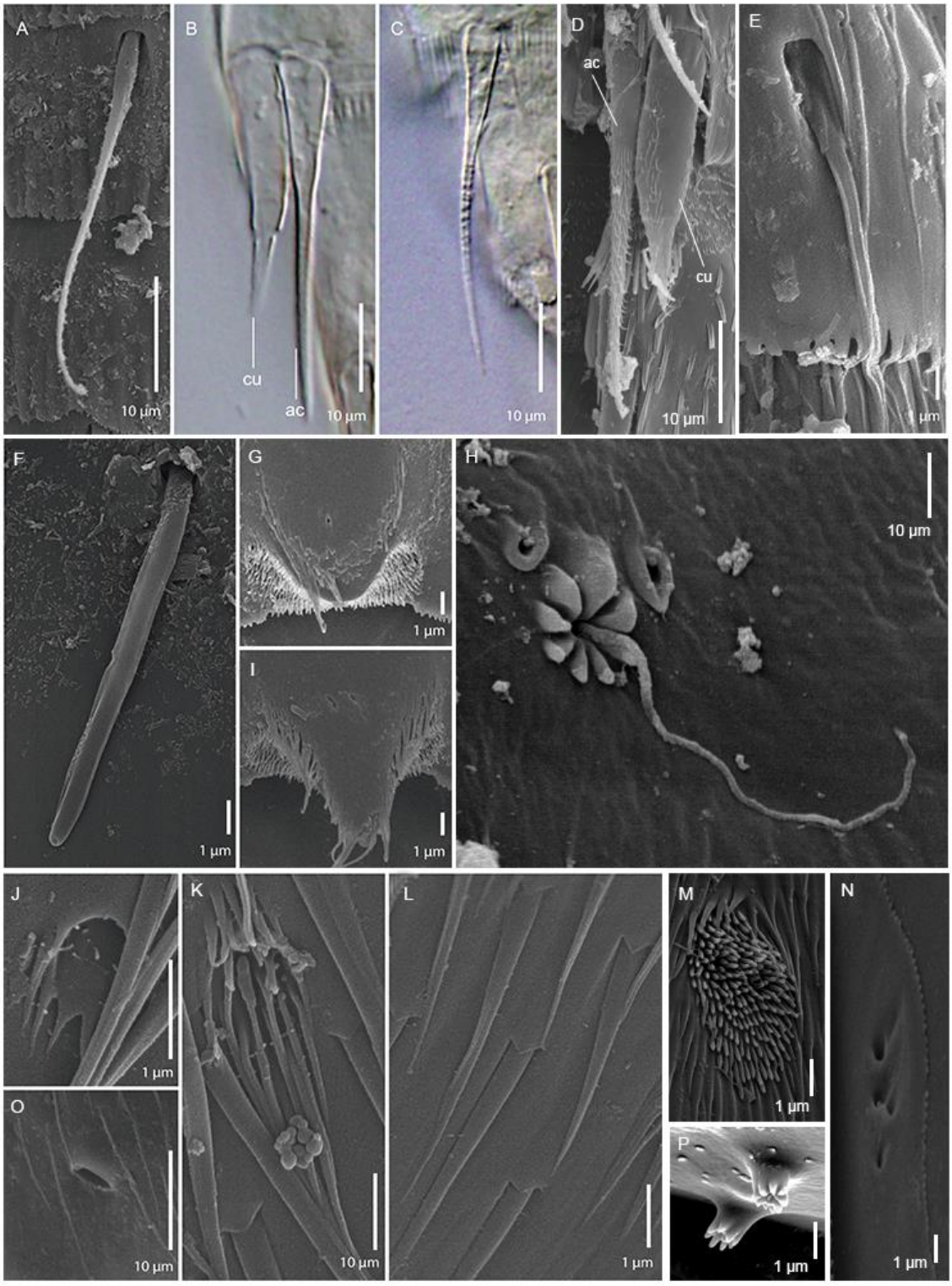

Figure 10. Cuticular appendages: acicular spine of *Dracoderes spyro* Cepeda, Pardos and Sánchez, 2019 (in Cepeda *et al.*, 2019b) from La Española (A), acicular, cuspidate (B) and crenulated (C) spines of *Triodontoderes lagahoo* from Tobago (B), acicular and cuspidate spines of *Antygomonas incomitata* from Italy (D), tube of *Echinoderes parahorni* Cepeda, Sánchez and Pardos, 2019 (in Cepeda *et al.*, 2019c) from La Española (E), seta of *Pycnophyes ancalagon* Sørensen and Grzelak, 2018 from Sweden (F), elevation (G) and process (I) of *Setaphyes elenae* from Sweden, flosculi-like sensory spot of *Leiocanthus lageria* (Sánchez, Herranz, Benito and Pardos, 2014 in Sánchez *et al.*, 2014c) from Florida (H), sensory spot of *E. sublicarum* from Venezuela (K) and *Cristaphyes carinatus* from Spain (M), type 3

sensory spot of *P. tubuliferus* Adrianov, 1989 from Norway (P), type 1 glandular cell outlet of *E. sublicarum* from Venezuela (J) and *P. tubuliferus* from Norway (N), type 2 glandular cell outlet of *Echinoderes* sp. from the Clarion-Clipperton Zone (O), and bracteate hairs of *E. sublicarum* from Venezuela (L). Abbreviations: ac, acicular spine; cu, cuspidate spine. Photos D, N and P kindly provided by Dr M.V. Sørensen.

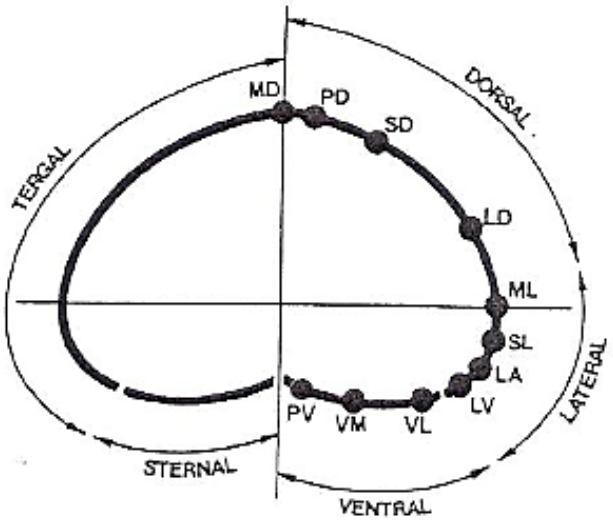

Figure 11. Generalized cross-section of the kinorhynch trunk, showing the disposition of the cuticular plates and the different position that are currently recognized to describe the cuticular appendages' arrangement. Abbreviations: LA, lateral accessory; LD, laterodorsal; LV, lateroventral; MD, middorsal; ML, midlateral; PD, paradorsal; PV, paraventral; SD, subdorsal; SL, sublateral; VL, ventrolateral; VM, ventromedial.

1.4 Kinorhynch internal morphology.

1.4.1 BODY WALL.

Kinorhynch body wall is externally surrounded by a cuticle secreted by the underlying epidermis, which is composed of a basal layer of chitin and a unilamellar, membrane-like epicuticle (Jeuniaux, 1975; Adrianov *et al.*, 1990; Neuhaus, 1993; Adrianov and Malakhov, 1994; GªOrdóñez *et al.*, 2000; Neuhaus and Higgins, 2002). The thickness of the cuticle is not homogeneous, but in certain regions it thickens into the body cavity forming what is known as pachycyclus, to which muscles attach (Zelinka, 1928). The family Pycnophyidae furthermore exhibits another kind of cuticular thickening in the tergosternal junction: the tergal plate generates a cuticular process that fits into a ring-like depression of the sternal plate, forming the so-called ball-and-socket joint (Zelinka, 1928). Cuticular thickenings of Pycnophyidae are also observed in paraventral position, where they can be extremely developed forming rounded, kidney-shaped or oval apodemes (Zelinka, 1928). Epidermal glands have been also described as unicellular,

merocrine gland cells, but a relationship with spines, setae or tubes is not confirmed (Nebelsick, 1992; GªOrdóñez *et al.*, 2000).

1.4.2 MUSCULAR SYSTEM.

Kinorhynch musculature is characterized by a certain degree of variability among genera, especially that of the head and neck (Herranz *et al.*, 2020). In general terms, the main muscles of kinorhynchs known up to now are the following (Zelinka, 1928; Nyholm and Nyholm, 1976a; 1976b; Kristensen and Higgins, 1991; Adrianov and Malakhov, 1994; Neuhaus, 1994; Müller and Schmidt-Rhaesa, 2003; Rothe and Schmidt-Rhaesa, 2004; Schmidt-Rhaesa and Rothe, 2006; Herranz *et al.*, 2014; 2020; Altenburger, 2016):

- Head with two mouth cone circular muscles, several longitudinal pairs of oral style muscles (absent in some species, *e.g. Pycnophyes ilyocryptus* (Higgins, 1961), *Setaphyes kielensis*), several sets of introvert retractors (Fig. 12B) usually associated with shorter muscles whose insertion alternates with that of the spinoscalids, at least one introvert circular muscle (Fig. 12B), and a variable number of introvert circular muscle retractors (Fig. 12B). These muscles mainly attach basally to the first two trunk segments, although some of them extend towards the more distal segments, and are responsible for the protraction and retraction of the head.
- Neck with a highly variable muscular system depending on the type of closing apparatus, but generally bearing a single circular muscle, several ring-like or longitudinal muscles associated with the placids, and both dorsal and ventral placid retractors (Fig. 12A), the latter basally attached to the first trunk segment. Transverse and dorsoventral muscles may be also present in some species, *e.g. Antygomonas* Nebelsick, 1990; *Echinoderes*.
- Trunk with paired, both dorsal and ventral longitudinal muscles (Fig. 12A); paired dorsoventral muscles (Fig. 12A); paired diagonal muscles (absent in some taxa, *e.g.* Pycnophyidae); continuous longitudinal muscles throughout segments 1-7; terminal spines muscles (Fig. 12A); and one pair of male, penile spines muscles (Fig. 12A). These muscles are responsible for the movements of the cuticular plates along the anterior-posterior axis, as well as dorsoventral and lateral trunk movements.

- Pharynx with a complex system of protractors and retractors; intestine with a grid of longitudinal and circular muscles (Fig. 12A).
- Gonads with a complex net of both longitudinal and circular muscles.

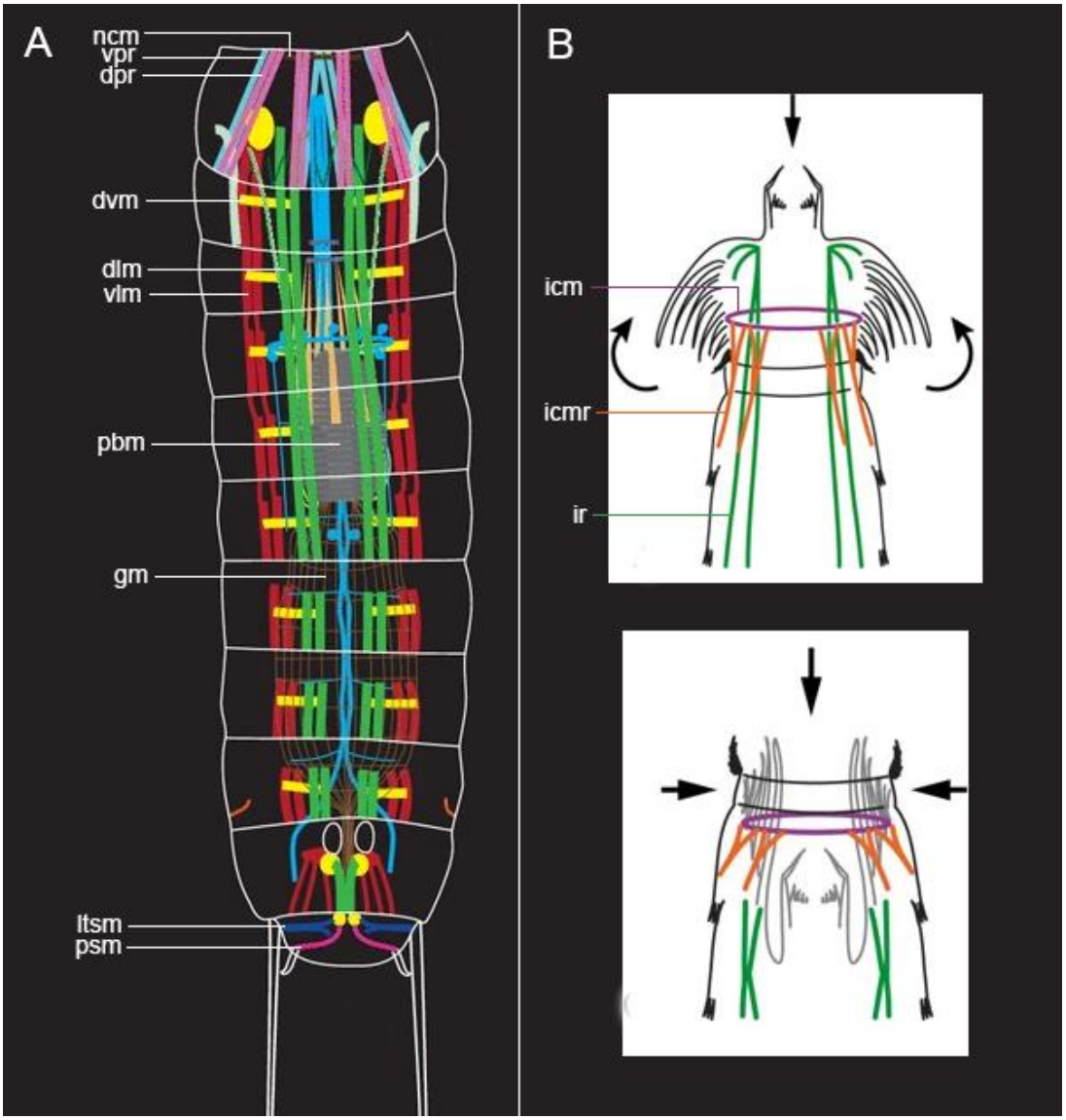

Figure 12. Schematic reconstruction of the muscular system of *Setaphyes kielensis* (A) and *Echinoderes* spp (B). Modified from Altenburger (2016) and Herranz *et al.* (2014). Abbreviations: dlm, dorsal longitudinal muscle; dpr, dorsal placid retractor; dvm, dorsoventral muscle; icm, introvert circular muscle; icmr, introvert circular muscle retractor; ir, introvert retractor; gm, gut muscles; ltsm, lateral terminal spine muscle; ncm, neck circular muscle; pbm, pharynx bulb muscles; psm, penile spine muscle; vlm, ventral longitudinal muscle; vpr, ventral placid retractor.

1.4.3 NERVOUS SYSTEM AND SENSORY ORGANS.

The kinorhynch nervous system is composed of a circumpharyngeal, ring-like, ten-lobed brain and five longitudinal nerves that extend throughout the trunk, of which the ventral one is ganglionated. These longitudinal nerves are connected by transverse neurites (Zelinka, 1928; Adrianov and Malakhov, 1990; 1994; Kristensen and Higgins, 1991; Neuhaus, 1991; 1994; Nebelsik, 1993; Neuhaus and Higgins, 2002; Herranz *et al.*, 2019b). Morphological variations between species in the nervous system have been observed.

Sensory structures have been mainly described in the head, as oral styles, spinoscalids and trichoscalids usually possess one or more ciliary sensory cells that link externally through a terminal pore, suggesting a chemoreceptive function (Moritz and Storch, 1972; Brown, 1989; Adrianov and Malakhov, 1990; Kristensen and Higgins, 1991; Nebelsick, 1993; Neuhaus, 1994). Some of these sensory structures lack a terminal pore, and a mechanoreceptive function has been suggested (Moritz and Storch, 1972; Kristensen and Higgins, 1991). Sensory spots are well-known throughout the trunk, and seem to be composed of two monociliary sensory cells and a single sheath cell, also suggesting a chemoreceptive function (Nebelsick, 1992; Neuhaus, 2013). Some spines have been reported to be coupled with sensory cells without connection to the outside, suggesting a mechanoreceptive function (Nebelsick, 1992). Finally, some species possess pigmented eyes or presumed photoreceptors (Zelinka, 1928; Brown, 1985; Kristensen and Higgins, 1991; Neuhaus, 1997; Sørensen, 2006).

1.4.4 DIGESTIVE SYSTEM.

The digestive tract begins in the mouth cone and the pharyngeal crown, continuing with the pharynx, a short oesophagus and a gut, ending in the anus (Neuhaus, 2013). The pharynx may be piriform or cylindrical, with an inner epithelium which has embedded monociliary receptor and gland cells and an outer multilamellar cuticle (Zelinka, 1928; Nebelsick, 1990; Neuhaus 1991; 1994). The gut also possesses epithelial, gland and receptor cells internally and an epicuticle externally with fine-granular basal layer and multilamellar epicuticle (Neuhaus, 2013).

1.4.5 EXCRETORY SYSTEM.

The excretory system is protonephridial, with ciliated, mace-shaped organs located laterodorsally in segment 8, which open to the outside sublaterally in segment 9 (Reinhard, 1885; Zelinka, 1928). Each protonephridium forms externally a sieve plate with a minimum of ten pores (Fig. 13A-C) (Neuhaus, 2013).

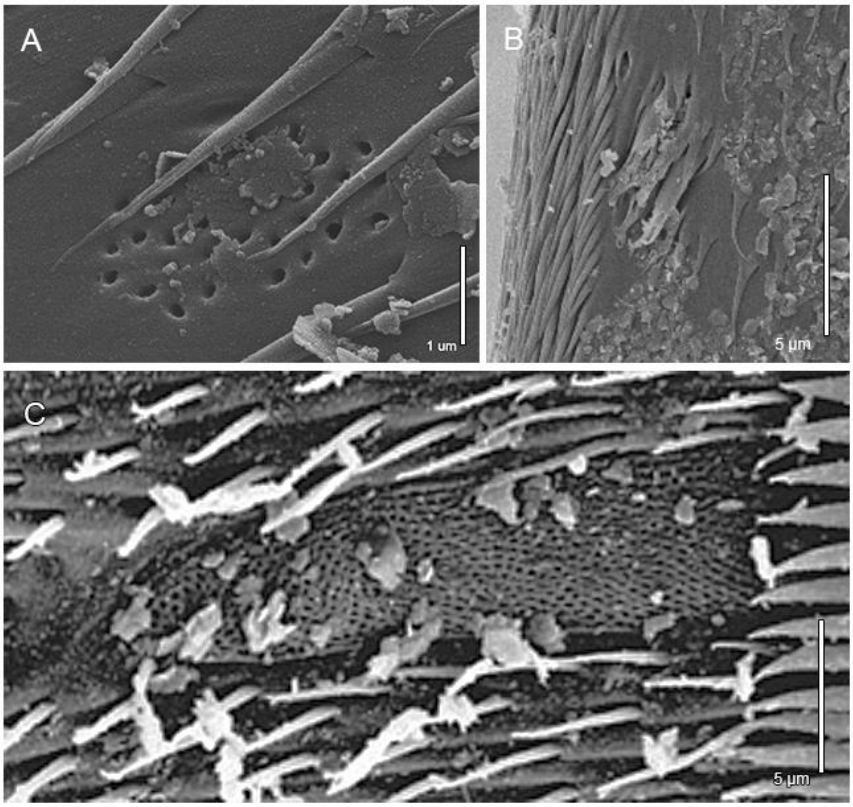

Figure 13. Protonephridial sieve plate of *Echinoderes augustae* from Venezuela (A), *Pycnophyes tubuliferus* from Norway (B) and *E. applicitus* Ostmann, Nordhaus and Sørensen, 2012 from Java (C). Photo C modified from Ostmann *et al.* (2012)

1.4.6 REPRODUCTIVE SYSTEM AND SEXUAL DIMORPHISM.

Kinorhynchs are dioecious and reproduce sexually. The gonads are sack-shaped, extending along the body cavity and, once mature, can occupy a very large volume (Zelinka, 1928; Higgins, 1974). The gonads are continued in gonoducts covered by cuticle (Zelinka, 1928; Brown, 1983; Adrianov and Malakhov, 1991; 1994; 1999a; Kristensen and Higgins, 1991). Paired, strongly sclerotized gonopores and seminal receptacles have been described in females (Neuhaus, 2013). In mature male gonads, spermatogonia, spermatocytes, spermatids, and spermatozoids develop anterior-posteriorly (Higgins, 1974; Nyholm and Nyholm, 1982; Adrianov and Malakhov, 1991; 1994; 1999a); spermatozoids possess a cilium and a central, rod-shaped nucleus enclosed

by vesicles, whereas an acrosomal structure is missing (Nyholm, 1976; Nyholm and Nyholm, 1982; Adrianov and Malakhov, 1994; 1999a). Females of certain species of the family Pycnophyidae have been observed bearing a mucous mass at their posterior trunk end containing male gametes; this structure has been sometimes interpreted as a spermatophore (Brown, 1983; Kristensen and Higgins, 1991; Adrianov and Malakhov, 1999a) (Fig. 17A). In other species, sperm has been identified inside the seminal receptacles (Zelinka, 1928; Kristensen and Higgins, 1991).

In addition to the nature of the gonads, there are other morphological characters of sexual dimorphism in Kinorhyncha. Species of several genera have males bearing two or three pairs of penile spines laterally on segment 11 (Fig. 14A, C) and females may possess a single pair of lateral terminal accessory spines also on segment 11 (Fig. 14B) or not (Fig. 14D) (Neuhaus, 2013). In the family Pycnophyidae, most species are characterized by males possessing a pair of ventromedial tubes on segment 2 (Fig. 14E), which are absent in females (Fig. 14F). Moreover, males and females of a species may differ in the number and arrangement of glandular cells, papillae, sensory spots, morphology of some spines (*e.g.* acicular in females vs. crenulated in males), length of spines and body dimensions (Neuhaus, 2013).

1.5 Systematics.

1.5.1 PHYLOGENY.

The phylum Kinorhyncha is divided in two monophyletic classes: Allomalorhagida and Cyclorhagida (Fig. 15) (Sørensen *et al.*, 2015). A summary of the orders, families and genera currently recognized, as well as number of species per genera, can be seen in Table 1 (Yamasaki, 2021).

Some important gaps in the phylogeny of Kinorhyncha still need further analyses. The species-richest allomalorhagid family, Pycnophyidae, was studied by a total-evidence analysis by Sánchez *et al.* (2016), but up to 64 species were only represented by morphological data. Additionally, the remaining allomalorhagid families (Dracoderidae, Franciscideridae and Neocentrophyidae) have their internal relationships still unresolved. Regarding cyclorhagids, the exact relationship between the three orders should be further

explored in future studies. Furthermore, the internal relationships within the two large clades Echinoderidae and Kentrorhagata are still unresolved.

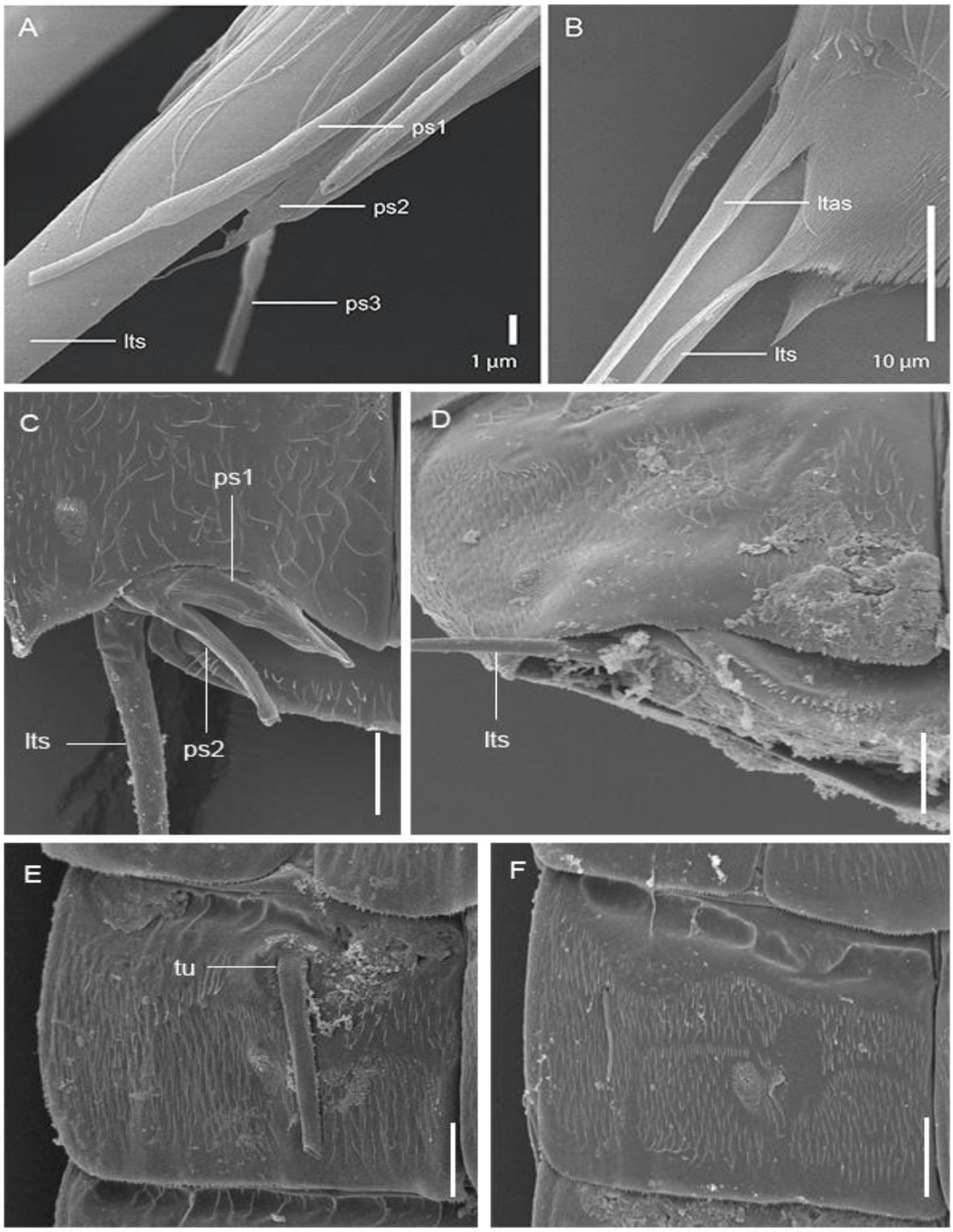

Figure 14. Sexually dimorphic characters of segment 11 spines in *Echinoderes sublicarum* from Venezuela [showing the three pairs of male penile spines (A) and the single pair of female lateral terminal accessory spines (B)] and in *Setaphyes kielensis* from Norway [showing the two pairs of male penile spines (C) and the absence of these structures in the female (D)], and sexually dimorphic characters of segment 2 tubes in *S. kielensis* from Norway [showing the male ventromedial tubes (E) and the absence of these structures in the female (F)]. Abbreviations: ltas, lateral terminal accessory spine; lts, lateral terminal spine; ps, penile spine (followed by number of corresponding pair); tu, tube. Photos C-F kindly provided by Dr M.V. Sørensen.

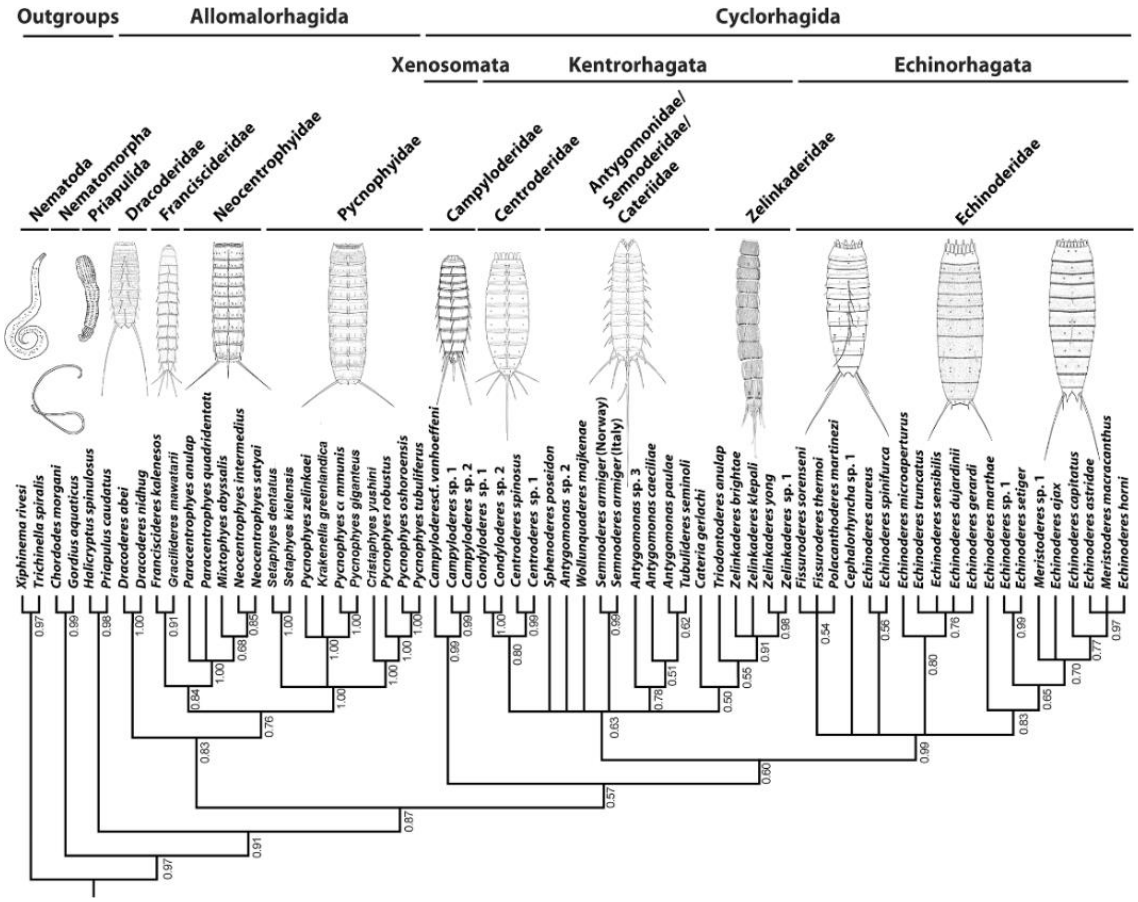

Figure 15. Phylogenetic tree showing taxonomic groups on top resulting from Bayesian Inference of combined morphological and molecular data. Modified from Sørensen *et al.*, 2015.

Table 1. Summary of current kinorhynch classes, orders, families and genera, as well as number of species per genus.

Class	Order	Family	Genus	Nº species
Allomalorhagida	/	Dracoderidae	*Dracoderes*	7
		Franciscideridae	*Franciscideres*	1
			Gracilideres	1
		Neocentrophyidae	*Mixtophyes*	1
			Neocentrophyes	2
			Paracentrophyes	4
		Pycnophyidae	*Cristaphyes*	25
			Fujuriphyes	9
			Higginsium	5
			Krakenella	11
			Leiocanthus	13

			Pycnophyes	27
			Setaphyes	7
Cyclorhagida	Echinorhagata	Echinoderidae	*Cephalorhyncha*	6
			Echinoderes	134
			Fissuroderes	7
			Meristoderes	9
			Polacanthoderes	1
	Kentrorhagata	Antygomonidae	*Antygomonas*	5
		Cateriidae	*Cateria*	2
		Centroderidae	*Centroderes*	6
			Condyloderes	10
		Semnoderidae	*Parasemnoderes*	1
			Semnoderes	4
			Sphenoderes	4
		Zelinkaderidae	*Triodontoderes*	2
			Zelinkaderes	5
		Incertae sedis	*Tubulideres*	1
			Wollunquaderes	1
	Xenosomata	Campyloderidae	*Campyloderes*	2
			Ryuguderes	1

1.5.2 TAXONOMY.

The arrangement of the cuticular plates throughout the trunk segments is a key taxonomic character in the phylum to distinguish families and genera (Sørensen and Pardos, 2008). As previously mentioned, the cuticle around a segment may be a closed, ring-like plate (*i.e.* tergal plate) or be divided into two to four cuticular plates (always a single tergal plate dorsally and up to three sternal plates ventrally). The number and arrangement of the oral styles and scalids also has a certain taxonomic value while discriminating between genera.

Placids of the neck do not usually offer taxonomic information, except for their number, which varies between genera (Sørensen and Pardos, 2008). In the genus *Condyloderes* Higgins, 1969, however, the number and disposition of a series of knob-shape projections is diagnostic of the different species.

The most informative characters in terms of taxonomy are, doubtlessly, the trunk morphology and the nature and arrangement of the cuticular appendages (Sørensen and

Pardos, 2008). This refers to the disposition of the ball-and-socket joints (in Pycnophyidae), the morphology of the primary and secondary pectinate fringes, and the distribution and kind of spines, tubes, setae, hairs, papillae, glandular cell outlets and sensory spots throughout the trunk, which are diagnostic of each species.

1.6 Geographical distribution.

Since its discovery, studies on the phylum Kinorhyncha have mainly focused on taxonomy and morphology. Thus, the current biogeographic knowledge on kinorhynchs primarily reflects the sampling strategy of the researchers rather than a real representation of the phylum distribution (Neuhaus, 2013).

Most of the known species are distributed throughout the continental shelf, disregarding deeper waters (Neuhaus, 2013). Extensive samplings have been carried out along the Atlantic coasts of Europe and the Mediterranean Sea (Claparède, 1863; Reinhard, 1881; 1885; Southern, 1914; Zelinka, 1928; Karling, 1955; Reimer, 1963; Gerlach, 1969; Sheremetevskij, 1974; Higgins, 1977a; 1978; 1985; Huys and Coomans, 1989; Nebelsick, 1990; Neuhaus, 1993; Pardos *et al.*, 1998; Gª Ordóñez *et al.*, 2008; Sánchez *et al.*, 2011; 2014; 2017; Herranz *et al.*, 2012; Sørensen *et al.*, 2012a; Dal Zotto, 2015; Neves *et al.*, 2016; Yamasaki and Durucan, 2018; Yildiz *et al.*, 2016; Sørensen and Grzelak, 2018; Dal Zotto *et al.*, 2019), the North American coasts (Higgins, 1960; 1961; 1964; 1977b; 1986; 1990; Adrianov and Higgins, 1996; Sørensen *et al.*, 2005; 2007; 2019; Sørensen, 2007; Herranz and Pardos, 2013; Herranz *et al.*, 2014; Neuhaus *et al.*, 2014; Sørensen and Landers, 2014; 2017a; 2017b; Landers and Sørensen, 2016; Herranz *et al.*, 2017; Sánchez *et al.*, 2019b; Varney *et al.*, 2019), and the northwestern Pacific coast of Russia and the waters surrounding the Korean Peninsula and Japan (Adrianov, 1989; Higgins and Shirayama, 1990; Adrianov and Malakhov, 1999b; Adrianov *et al.*, 2002; Chang and Song, 2002; Sørensen *et al.*, 2010a; 2010b; 2010c; 2012b; 2013; Lundbye *et al.*, 2011; Yamasaki *et al.*, 2012; Sánchez *et al.*, 2013; Yamasaki and Fujimoto, 2014; Altenburger *et al.*, 2015; Yamasaki, 2015; 2016; 2019; Sánchez and Yamasaki, 2016).

Some much smaller geographic areas have also been deeply sampled, as more or less isolated regions, such as the coral reef ecosystem at Carrie Bow Cay, Twin Cays, Belize (Higgins, 1983), the area surrounding Bocas del Toro, Panama (Sørensen, 2006;

Pardos *et al.*, 2016a; 2016b) or the Arctic waters (Higgins, 1966; Higgins and Kristensen, 1988; Higgins and Korczynski, 1989; Adrianov, 1995; Adrianov and Malakhov, 1999b; Grzelak and Sørensen, 2018; Sørensen and Grzelak, 2018).

Studies on deep-sea kinorhynchs are rather scarce, although they have experienced a relative boost in recent years. The first papers about this usually reported unidentified species of kinorhynchs from the Indian, Pacific and Atlantic Oceans (Zeppilli *et al.*, 2018). More recently, studies to the species level have flourished, with the description and report of new deep-sea species (Neuhaus and Blasche, 2006; Sørensen, 2008a; Neuhaus and Sørensen, 2013; Sánchez *et al.*, 2014a; 2014b; 2019; Adrianov and Maiorova, 2015; 2016; 2018a; 2018b; 2019; Grzelak and Sørensen, 2018; Sørensen and Grzelak, 2018; Sørensen *et al.*, 2018; 2019; Yamasaki *et al.* 2018a; 2018b; 2018c; 2019).

The patched distribution that is currently known of the phylum Kinorhyncha (Fig. 16) shows there are still large and completely uncharted geographic areas as far as these animals are concerned, such as the Indian Ocean, the Antarctic region, the Caribbean Sea, the deep-sea worldwide or the waters surrounding the African and the South America continents. Therefore, it is vital to promote basic research studies whose main objective is to know and describe the unexplored biodiversity of Kinorhyncha that inhabit these waters in order to fill gaps and achieve a reasonable knowledge of distribution patterns of the phylum worldwide.

1.7 Biology.

1.7.1 REPRODUCTION AND DEVELOPMENT.

It is hypothesized that kinorhynchs have internal fertilization, although this phenomenon (or what has been interpreted as such) has only been observed in a single species, *Setaphyes kielensis*. Two specimens from the aforementioned species, a male and a female, were found attached to each other through their ventral posterior ends, completely wrapped in that area by a brownish mucous mass. It is supposed that males create and transfer a spermatophore to the female (Fig. 17A). Females of *Echinoderes kozloffi* Higgins, 1977 (in Higgins, 1977b), *Pycnophyes communis* and *Setaphyes flaveolatus* (Zelinka, 1928) have been observed depositing eggs inside their exuvias after moulting, and even covering those eggs with a thick layer of detritus as protection (Nyholm, 1947;

Lang, 1963; Kozloff, 1972). Kozloff (2007) studied the eggs of kinorhynchs, which are spherical to oval (ca. 54-72 μm diameter), oligolecithal and covered by a thick shell of about 30-40 μm thickness.

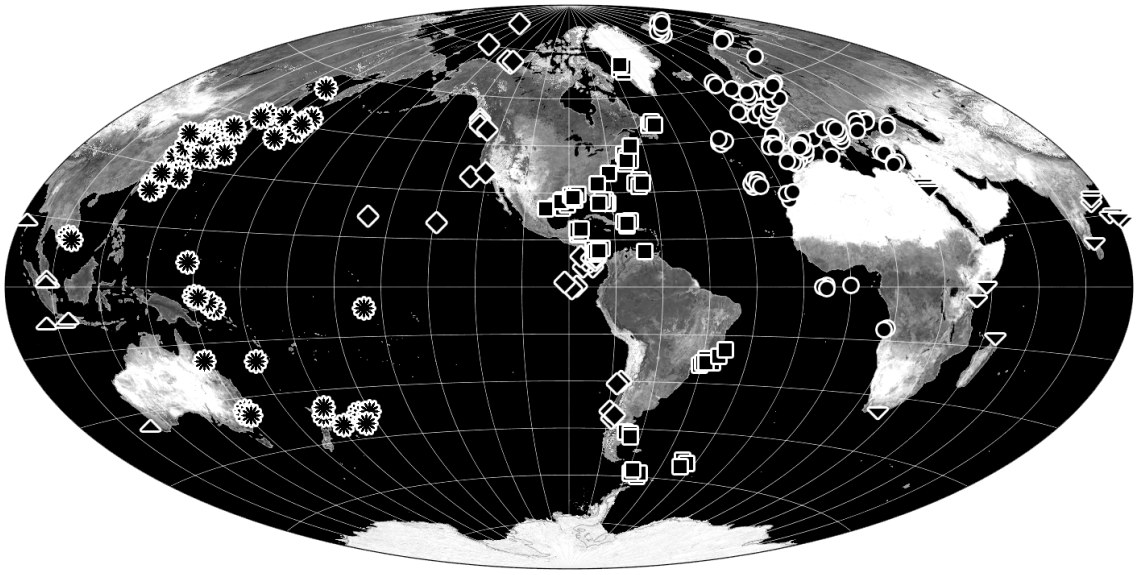

Figure 16. Current distribution of the phylum Kinorhyncha worldwide.

Postembryonic development is direct, with six juvenile stages (Fig. 17B-C) and, sometimes, a pre-adult stage before the adult (Sørensen and Pardos, 2008; Neuhaus, 2013). The first juvenile stage begins with seven to eight differentiated segments. Throughout the following stages, the number of segments increases until reaching the eleven of the adults. The segments are differentiated in a subcaudal region, but do not arise *de novo*. During the juvenile stages, the head also undergoes morphological modifications. Initially, the introvert develops prescalids and protoscalids that later become regular scalids; the number of scalid rings also increases throughout the ontogeny (Brown, 1985; Neuhaus, 1995; Sørensen *et al.*, 2010d). Juveniles' cuticle is always thinner and more flexible than that of adults, lacking pachycycli (Zelinka, 1928). The number of cuticular plates also vary during the course of the ontogeny, so that in the earliest juvenile stages there is usually no differentiation in plates (Neuhaus, 1993; Sørensen *et al.*, 2010d). The number, proportional size and type of cuticular appendages also vary from juveniles to adults (Zelinka, 1928; Brown, 1985; Higgins and Kristensen, 1988; Neuhaus, 1993; 1995; Sørensen *et al.*, 2010d).

1.7.2 FEEDING AND LOCOMOTION.

Other aspects of the kinorhynch biology, such as feeding, locomotion, behaviour or number of chromosomes, are still poorly known. It is hypothesized that kinorhynchs take food using the mouth cone, and that the sensory cells embedded in the oral styles are chemoreceptors and evaluate the quality of food (Neuhaus, 2013). It is completely unknown what these animals feed on, although it is likely detritus, bacteria and/or algae, specially diatoms (Zelinka, 1928; Higgins, 1990).

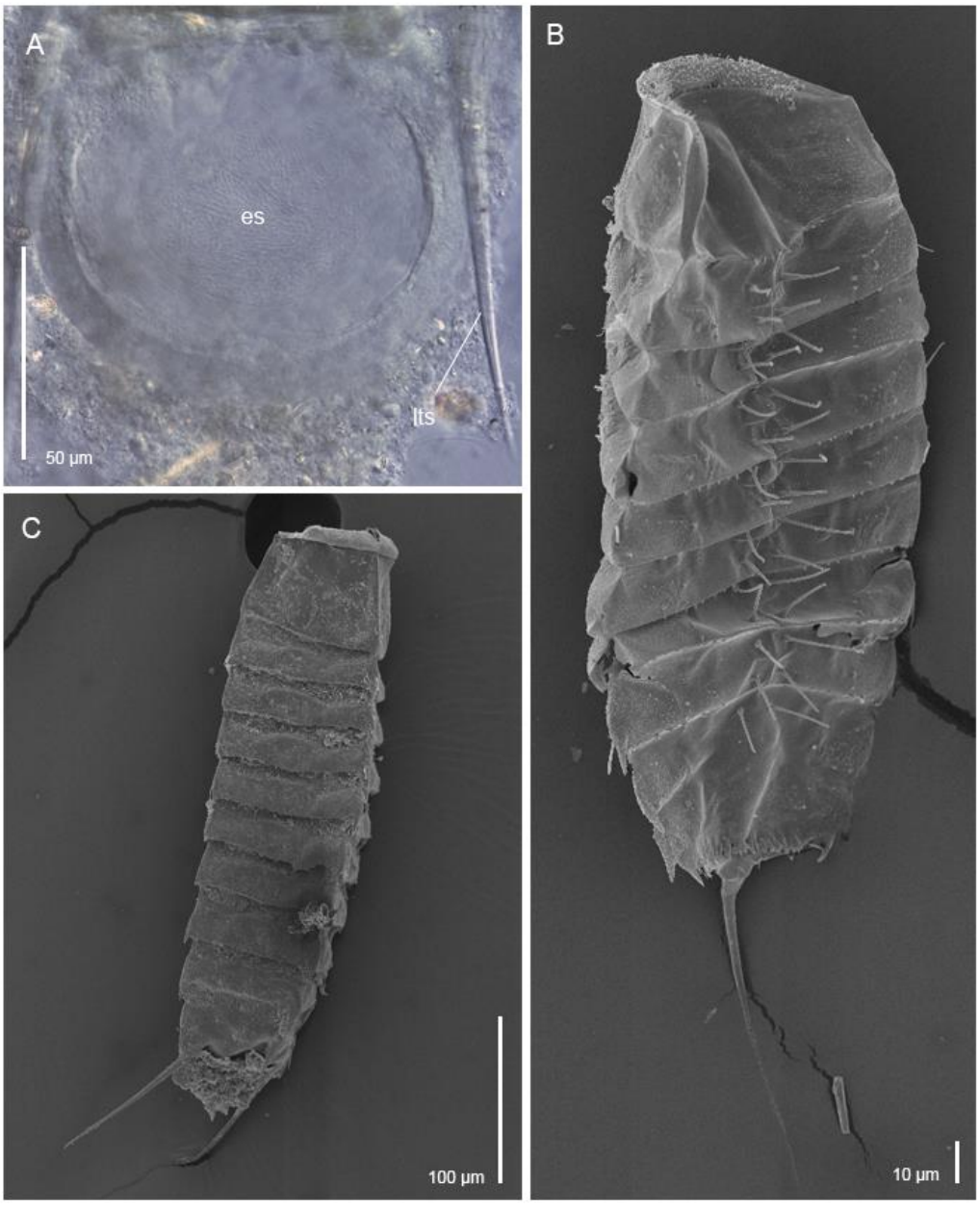

Figure 17. Reproduction and development: Posterior trunk end of a female of *Pycnophyes norenburgi* from Florida holding a spermatophore (A), and juvenile stages of Pycnophyidae from Korea (B-C). Abbreviations: es, spermatophore; lts, lateral terminal spine. Photos B-C kindly provided by Dr M.V. Sørensen.

With regard to locomotion, it is thought that kinorhynchs use the introvert scalids to anchor to the substrate; then, when retracting the introvert inside the trunk, it would pull the animal forward, and the animal would actively move through the substrate as a sediment-dweller (Neuhaus, 2013; Traunspurger and Majdi, 2017).

1.8 Ecology.

Again, little is known about the ecological aspects related to the phylum Kinorhyncha, including the abiotic and biotic factors that most influence when sorting the meiofaunal communities of which kinorhynchs are part of, or their ability to respond to changes in the environment (whether natural or human origin).

Kinorhynchs mainly inhabit the small spaces and crevices of fine-grained marine and estuarine sediments, although some species are adapted to coarse-grained substrates. Indeed, several species also crawl on algae, marine phanerogams or other larger invertebrates (Neuhaus, 2013). Although they are not usually abundant, some studies have shown they can become the third most abundant taxon in the meiofaunal communities (De Bovée and Soyer, 1974; Jensen, 1983; Herman and Dahms, 1992; Santos *et al.*, 2009; Sánchez *et al.*, 2021).

Little is known about sediment preferences despite almost all kinorhynchs live in these habitats. Grzelak and Sørensen (2019) determined that sediment particle size is the most important factor sorting kinorhynch populations in the Svalbard Archipelago. Landers and colleagues (Landers *et al.*, 2018; 2019; 2020) determined that kinorhynchs are most abundant in sediments that are rich in silt and clay, and are also positively correlated with high abundances of organic matter and some metal traces in the Gulf of Mexico. The aforementioned studies are the only ones up to now that have analysed the influence of sediment on the specific composition of Kinorhyncha communities. Nothing is known, on the other hand, of possible morphological adaptations of kinorhynchs to sediment nature.

Kinorhynchs seem to endure fluctuations in both temperature and salinity, but prolonged maintenance of extreme conditions can cause a high mortality rate in their populations (Hummon, 1975; Uozumi *et al.*, 2018). However, some species have been found living in environments with low values of salinity and temperature, *e.g.*

Echinoderes applicitus at 20.4-33.4 psu, *Echinoderes levanderi* Karling, 1955 at 3.68 ‰, *Campyloderes vanhoeffeni* Zelinka, 1913 at -1.85 ºC (Zelinka, 1913; Karling, 1955; Ostmann *et al.*, 2012). Kinorhynchs are usually found in the upper, well-oxygenated centrimetres of marine and estuarine sediments (Neuhaus, 2013), but also seem to tolerate low levels of dissolved oxygen (up to 0.2 mg/l), drastically affecting reproduction and development (Murrell and Fleeger, 1989; Modig and Ólafsson, 1998; Sergeeva *et al.*, 2012).

Human pollution based on metal traces, tributyltin, aromatic hydrocarbons, petroleum, domestic sewage, organic matter from aquaculture and fertilizers significantly reduces kinorhynch abundance (Ansari *et al.*, 1984; Frithsen *et al.*, 1985; Warwick *et al.*, 1990; Lysykh, 2005; Sutherland *et al.*, 2007; Grego *et al.*, 2009; Santos *et al.*, 2009). However, opposite trends, with kinorhynchs being able to flourish in environments with high concentrations of metal traces and other contaminants have also been reported (Ostmann *et al.*, 2012; Landers *et al.* 2018; 2020). Natural disturbances, such as strong currents, summer blossoms of toxic cyanobacteria, iceberg scouring and typhoons, do not affect to kinorhynch abundances, or initially decrease the kinorhynch populations but they quickly recolonized the substrate (up to only 50 days) (Thistle and Levin, 1998; Lee *et al.*, 2001a; 2001b; Nascimento *et al.*, 2008; Hua *et al.*, 2010).

Relationships with other organisms have been reported. Kinorhynch specimens are frequently found hosting epibionts, such as diatoms, bacteria, fungi and protozoan Ciliophora (Zelinka, 1928; Adrianov and Higgins, 1996; Dovgal *et al.*, 2008; Ostmann *et al.*, 2012; Neuhaus, 2013; Herranz *et al.*, 2017). Moreover, zooxanthellae endosymbionts have been reported by Zelinka (1928) in *Cristaphyes carinatus* (Zelinka, 1928), *Echinoderes dujardinii* Claparède, 1863, *E. capitatus* (Zelinka, 1928), *Pycnophyes communis* and *Setaphyes flaveolatus*. Internal protozoan parasites are also known (Higgins, 1990; Adrianov and Rybakov, 1991; Neuhaus, 1991; Adrianov *et al.*, 1993). In addition to this, kinorhynchs have been proved to be a food source for other benthic organisms, including crustacean decapods (Martorelli & Higgins, 2004).

1.9 Objectives of the present thesis.

Based on the aforementioned gaps of knowledge characterizing the phylum Kinorhyncha, the main objectives of the present thesis can be grouped into the following topics:

Taxonomy and biodiversity

- To increase the still unknown kinorhynch fauna from interesting areas of high biodiversity and ecological relevance (*e.g.* Caribbean Basin, deep-sea), given the large number of knowledge gaps existing in many parts of the planet.
- To revisit previous areas with certain background of known kinorhynch species to detect the potential presence of still undescribed taxa (*e.g.* Iberian Peninsula, North Sea).
- To detect relevant, systematic features of phylogenetically remarkable taxa of Kinorhyncha that could be useful for future total-evidence analyses. This type of studies will be vital to clarify the internal relationships between the different kinorhynch groups.
- To create a foundation of basic knowledge on Kinorhyncha, based on the identification and description of new species, that could promote future investigations on other fields (phylogeny, ecology, etcetera) and become the base for the construction of identification keys.

Morphology, morpho-ecology, ecology, macroecology and biogeography

- To elucidate if the main cuticular characters of the phylum Kinorhyncha (segments and certain cuticular appendages such as spines), extensively used for systematic and taxonomic purposes, are subject to evolutionary allometric growth and, if so, whether it can be used for systematic studies, or rather they depend on extrinsic factors.
- To further step into basic aspects on the biology and ecology of the phylum Kinorhyncha to better understand the functioning and way-of-life of these meiofaunal organisms, including how they relate to their environment and the main abiotic factors of it.
- To increase the previous geographic knowledge on Kinorhyncha taxa and determine which general, global trends can potentially help to explain the observed distributional patterns of the different Kinorhyncha groups.

2 – Material and methods

"Our world is built on biology and once we begin to understand it, it then becomes a technology" (Ryan Bethencourt)

This section encompasses methodology and samples generalities used in the present thesis, but further details may be seen in the corresponding papers.

2.1 Material used in the present thesis and sampling areas.

Kinorhynch specimens studied in the present thesis were obtained from different sources, including loan of both type and non-type material stored at different institutions and collected specimens from various marine samplings. A total of 1921 specimens belonging to 67 extant species were studied (Table 2).

The main advances of the present thesis are based on material collected from the Caribbean Sea (western Atlantic), the Gulf of California (eastern Pacific), the Mozambique Channel deep-sea (western Indian), the North Sea (eastern Atlantic) and the waters surrounding France and Spain (eastern Atlantic and Mediterranean) (Table 3, Figs. 18 and 19). Supplementary samplings were also carried out in the Gulf of Mexico (western Atlantic) and the Clarion-Clipperton Fracture Zone (central Pacific). Extensive samplings were exclusively carried out through the Caribbean Basin (Fig. 19), whilst in the remaining locations the samplings were rather punctual and scattered for specific purposes. A summary of the collected/studied kinorhynch species and sampling areas may be seen in Tables 2 and 3.

Samples from the Caribbean Sea (Table 3) were originally collected by Dr R. P. Higgins and his colleagues from 1967 to 1991, then stored at the facilities of the Smithsonian National Museum of Natural History (NMNH) of Washington DC, United States. Most samples from the Iberian Peninsula (Table 3) were collected by Drs F. Pardos, N. Sánchez, J. Benito and M. Herranz in 2011 and 2012, then stored at the facilities of the Meiofaunal Collection, Faculty of Biological Sciences, Universidad Complutense de Madrid (UCM), Spain. Samples from the Mozambique Channel deep-

sea (Table 3) were collected by the teams of the *PAMELA-MOZ01* and *PAMELA-MOZ04* oceanographic campaigns led by Drs K. Olu, G. Jouet and E. Deville in 2014 and 2015, then stored at the facilities of the Deep-Sea Laboratory of the Institut Fançais de Recherche pour l'Exploitation de la Mer (IFREMER) of Brest, France. Samples from the North Sea (Table 3) were collected by Drs U. Jondelius and F. Pleijel in 2017, then kindly given to the author. The remaining samples from Spain, France and the Gulf of California (Table 3 and Appendices) were collected *de novo* for the present thesis.

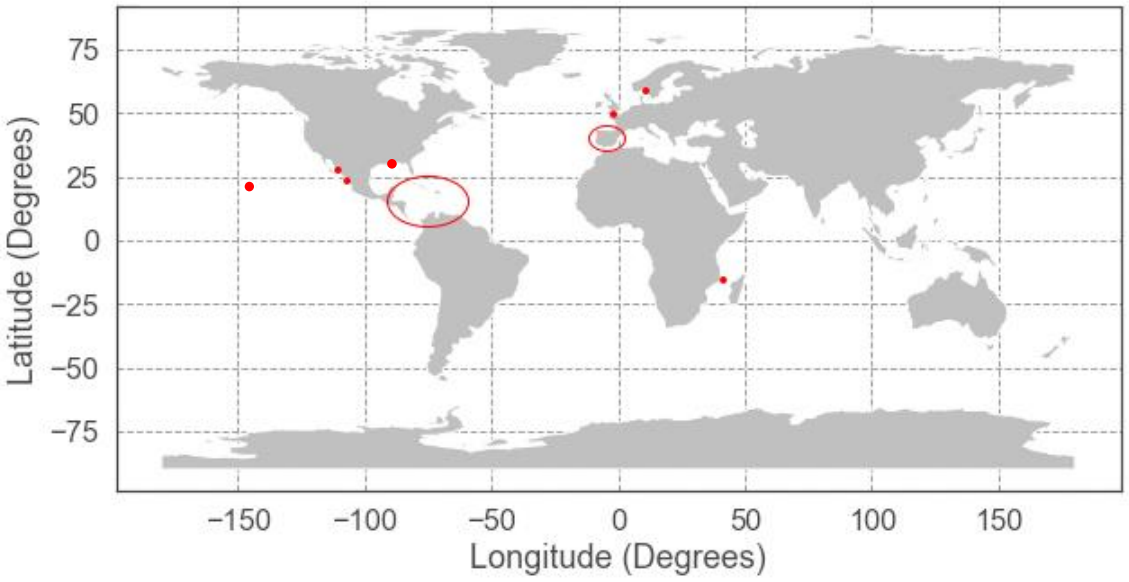

Figure 18. Worldwide map in a geographic Coordinate Reference System showing the sampling areas and localities of the present thesis.

Table 2. List of the examined material included in the present thesis.

Species	Sampling area	Studied specimens	Related section(s)
Antygomonas sp.	Iberian Peninsula	18	Appendix V
Centroderes spinosus	North Sea	5	3.7
Cephalorhyncha nybakkeni	California	1 (holotype)	3.5
Cephalorhyncha teresae	Gulf of California	13	3.5
Condyloderes sp.1	Mozambique Channel	3	3.6
Cristaphyes cornifrons	Caribbean Sea	5	3.2, Appendix I
Cristaphyes fortis	Gulf of California	4	3.5
Cristaphyes longicornis	Caribbean Sea	8	3.1, Appendix I
Cristaphyes retractilis	Caribbean Sea	17	3.1, Appendix I
Cristaphyes sp.1	Caribbean Sea	1	Appendix I
Dracoderes gallaicus	Iberian Peninsula	23	3.9
Dracoderes spyro	Caribbean Sea	196	3.3, Appendix I
Echinoderes apex	Mozambique Channel	1	3.6
Echinoderes astridae	Caribbean Sea	69	3.1, Appendix I

Echinoderes barbadensis	Caribbean Sea	28	3.2, Appendix I
Echinoderes brevipes	Caribbean Sea	5	3.1, Appendix I
Echinoderes cantabricus	Iberian Peninsula	189	3.9, Appendix V
Echinoderes cf. *capitatus*	Iberian Peninsula	10	3.9
Echinoderes cf. *dubiosus*	Mozambique Channel	4	3.6
Echinoderes dujardinii	France, Iberian Peninsula	70	3.9, Appendix V
Echinoderes cf. *eximus*	North Sea	1	3.7
Echinoderes hispanicus	Iberian Peninsula	17	3.9
Echinoderes horni	Caribbean Sea	68	3.1, Appendix I
Echinoderes hviidarum	Mozambique Channel	45	3.6
Echinoderes imperforatus	Caribbean Sea	10	3.1, Appendix I
Echinoderes intermedius	Caribbean Sea	196	Appendix I
Echinoderes orestauri	Caribbean Sea	12	Appendix I
Echinoderes parahorni	Caribbean Sea	110	3.1, Appendix I
Echinoderes spinifurca	Caribbean Sea	6	3.1, Appendix I
Echinoderes sublicarum	Caribbean Sea	26	Appendix I
Echinoderes unispinosus	Mozambique Channel	226	3.6
Echinoderes wallaceae	Caribbean Sea	7	Appendix I
Echinoderes worthingi	Iberian Peninsula	2	3.9
Echinoderes xalkutaat	Gulf of California	3	3.5
Echinoderes sp. 1	Caribbean Sea	2	Appendix I
Echinoderes sp. 2	Caribbean Sea	5	Appendix I
Echinoderes sp. 3	Mozambique Channel	2	3.6
Echinoderes sp. I	Clarion-Clipperton Zone	18	Appendix III
Echinoderes sp. II	Clarion-Clipperton Zone	8	Appendix III
Echinoderes sp. III	Clarion-Clipperton Zone	4	Appendix III
Fissuroderes cthulhu	Mozambique Channel	36	3.6
Fujuriphyes dagon	Mozambique Channel	23	3.6
Fujuriphyes dalii	Caribbean Sea	21	3.1, Appendix I
Fujuriphyes deirophorus	Caribbean Sea	33	Appendix I
Fujuriphyes distentus	Caribbean Sea	2	Appendix I
Fujuriphyes hydra	Mozambique Channel	6	3.6
Higginsium cf. *erismatum*	Caribbean Sea	69	3.2, Appendix I
Higginsium mazatlanensis	Gulf of California	4	3.5
Leiocanthus corrugatus	Caribbean Sea	4	Appendix I
Leiocanthus lageria	Iberian Peninsula	2	3.9
Leiocanthus sp. I	Gulf of Mexico	5	Appendix IV
Leiocanthus sp. II	Gulf of Mexico	5	Appendix IV
Pycnophyes almansae	Iberian Peninsula	1	3.9
Pycnophyes ancalagon	North Sea	12	3.7
Pycnophyes aulacodes	Iberian Peninsula	102	3.9, Appendix V
Pycnophyes communis	Iberian Peninsula	15	3.9
Pycnophyes sp.1	Caribbean Sea	1	Appendix I
Ryuguderes sp.1	Mozambique Channel	4	3.6
Semnoderes armiger	North Sea	3	3.7
Semnoderes lusca	Caribbean Sea	1	Appendix I

Setaphyes dentatus	Iberian Peninsula	61	3.9
Setaphyes elenae	North Sea	12	3.7
Setaphyes flaveolatus	Iberian Peninsula	15	3.7
Setaphyes sp.1	Caribbean Sea	1	Appendix I
Setaphyes sp. I	Iberian Peninsula	22	Appendix II
Sphenoderes cf. *indicus*	Mozambique Channel	1	3.6
Triodontoderes lagahoo	Caribbean Sea	22	3.4

Table 3. List of sampling locations included in the present thesis.

CARIBBEAN SAMPLES					
Locality	**Coordinates**	**Date**	**Species**	**Habitat**	**Depth (m)**
Guantánamo, Cuba	19 52 30N, 75 10 00W	17/03/76	*Echinoderes astridae, E. imperforatus, E. wallaceae*	Mangroves, mud	2
Kingston Harbour, Jamaica	17 57 00N, 76 51 18W	09/03/76	*Dracoderes spyro*	Mud	-
	17 56 24N, 76 50 00W	10/03/76	*Cristaphyes* cf. *longicornis, Echinoderes imperforatus, E. parahorni, E. sublicarum*	Gravelly and sandy mud	2
	17 56 36N, 76 49 18W	10/03/76	*Echinoderes horni*	Mangroves, muddy sand	1.5
Ocho Ríos, Jamaica	17 56 30N, 76 49 12W	10/03/76	*Echinoderes horni, E. parahorni, E. sublicarum*	Mangroves, gravelly mud	1
	17 57 18N, 76 50 24W	11/03/76	*Echinoderes astridae, E. parahorni*	Gravelly and shelly sand	4
	-	13/06/66	-	-	-
Puerto Príncipe, La Española	-	15/03/76	*Dracoderes spyro, Echinoderes astridae, E. parahorni*	Mangroves, mud	5
Cabo Haitiano, La Española	19 46 12N, 72 11 00W	10/11/80	*Dracoderes spyro, Pycnophyes* sp, *Echinoderes parahorni*	Mud	4
Cabo Rojo, La Española	-	01/04/76	*Echinoderes horni, E. imperforatus, E. spinifurca*	-	0.3

CARIBBEAN SAMPLES					
Locality	**Coordinates**	**Date**	**Species**	**Habitat**	**Depth (m)**
Puerto Plata, La Española	19 48 12N, 70 42 00W	02/11/80	*Dracoderes spyro, Cristaphyes retractilis, Fujuriphyes dalii*	Sandy mud	5
			Dracoderes spyro	Mud	5
			Cristaphyes retractilis, Fujuriphyes dalii	Mud	4
Puerto Blanco, La Española	19 54 24N, 70 56 24W	03/11/80	*Dracoderes spyro, Cristaphyes* cf. *longicornis, Echinoderes astridae, E. parahorni, E. spinifurca*	Mangroves, mud	3
			Dracoderes spyro	Mud	2
La Isabela, La Española	19 53 18N, 71 05 36W	04/11/80	*Dracoderes spyro*	Mud	4
Monte Cristi, La Española	19 53 12N, 71 40 00W	06/11/80	*Cristaphyes retractilis, Echinoderes astridae, E. horni, E. imperforatus, E. parahorni, E. spinifurca*	Muddy sand with *Thalassia testudinum*	3.5
Bahía de Icaquitos, La Española	19 53 12N, 71 38 30W	07/11/80	*Echinoderes horni, E. parahorni*	Mangroves, muddy sand with *Thalassia testudinum*	2
Santo Domingo, La Española	18 28 00N, 69 57 00W	08/05/76	*Echinoderes brevipes*	-	0.7-1
	-	09/05/76	-	-	-
La Matica, La Española	-	19/03/76	-	Mud	0.5
			-	Sand	0.5-1
Oranjestad, Aruba	12 30 00N, 70 01 00W	25/06/77	*Echinoderes sublicarum, Echinoderes* sp. 1	-	-
Saint James, Barbados	13 13 12N, 59 37 12W	-	*Echinoderes barbadensis*	-	-

CARIBBEAN SAMPLES					
Locality	**Coordinates**	**Date**	**Species**	**Habitat**	**Depth (m)**
La Parguera, Puerto Rico	-	07/06/67	*Dracoderes spyro, Cristaphyes cornifrons, C. retractilis, Echinoderes astridae, E. horni, E. spinifurca, E. orestauri*	Coral mud	15
		08/06/67	*Echinoderes sublicarum*	*Enteromorpha* sp.	-
		08/06/67	*Cristaphyes retractilis, Cristaphyes* sp, *Echinoderes horni*	Mangroves, mud	5
Klein Bonaire, Bonaire	12 10 12N, 68 18 12W	25/06/77	*Echinoderes intermedius*	Sand	100
Guadeloupe	16 21 40N, 61 39 00W	11/03/78	*Echinoderes wallaceae*	Fine sand	3.5
			Echinoderes wallaceae	Coral sand	3
			Echinoderes wallaceae	-	1.5
Tyrrel's Bay, Tobago	11 18 00N, 60 30 00W	13/05/91	*Triodontoderes lagahoo*	Fine sand	5
Bon Accord, Tobago	11 10 00N, 60 50 00W	15/05/91	*Cristaphyes* sp, *Echinoderes intermedius*	Mangroves, sand	3
Man O' War Bay, Tobago	11 19 00N, 60 33 00W	16/05/91	*Higginsium* cf. *erismatum*	Muddy sand	12
Bloody Bay, Tobago	11 18 00N, 60 37 00W	12/05/91	-	Fine sand	-
Little Harbor Cay, Berry Islands, Bahamas	-	04/03/82	*Echinoderes astridae*	-	-

CARIBBEAN SAMPLES					
Locality	**Coordinates**	**Date**	**Species**	**Habitat**	**Depth (m)**
Isla Margarita, Venezuela	-	15/02/77	*Echinoderes sublicarum*	Mangroves	-
		01/09/01	*Echinoderes intermedius*	Mud	1
Bahía de Mochima, Venezuela	10 21 12N, 64 20 36W	14/05/85	*Fujuriphyes deirophorus, Leiocanthus corrugatus, Echinoderes intermedius*	Mud	3
	10 20 42N, 64 21 18W	4/05/85	*Echinoderes augustae, Higginsium* cf. *erismatum, Fujuriphyes deirophorus, Leiocanthus corrugatus*	Mud	2
	10 21 30N, 64 20 36W	4/05/85	*Fujuriphyes deirophorus, Leiocanthus corrugatus*	Mud	3
	10 22 30N, 64 20 24W	4/05/85	*Echinoderes augustae, Higginsium* cf. *erismatum, Fujuriphyes deirophorus, Setaphyes* sp, *Echinoderes intermedius*	Mud	2
Playa Isla de Buche, Venezuela	10 32 30N, 66 05 42W	23/05/85	*Higginsium* cf. *erismatum, Fujuriphyes deirophorus, F. distentus, Echinoderes parahorni*	Sandy mud	-
		23/05/85	*Echinoderes augustae, Fujuriphyes deirophorus*	-	-
		23/05/85	*Echinoderes augustae, E. intermedius*	-	-
Los Roques, Venezuela	-	17/05/86	*Echinoderes parahorni*	Sandy mud	1
	-	17/05/86	*Echinoderes parahorni*	Sandy mud	-
	-	19/05/86	*Echinoderes intermedius, E. orestauri, E. wallaceae*	Sandy, coral mud	20
	-	19/05/86	*Echinoderes intermedius, Semnoderes lusca*	Coral sand	3

CARIBBEAN SAMPLES					
Locality	**Coordinates**	**Date**	**Species**	**Habitat**	**Depth (m)**
Morrocoy, Venezuela	10 50 00N, 68 14 00W	28/05/86	*Higginsium* cf. *erismatum*, *Echinoderes parahorni*	Coastal lagoon,	1
			Higginsium cf. *erismatum*	Sand with	0.5
Laguna Boca de Caño, El Supí, Venezuela	-	29/05/86	*Fujuriphyes deirophorus, F. distentus, Echinoderes imperforatus, Echinoderes* sp. 2	Coastal lagoon,	2
Magdalena, Colombia	10 59 00N,74 15 30W	15/02/86	-	Mangrove roots	0.5
IBERIAN PENINSULA SAMPLES					
Bahía de Algeciras, Spain	36 05.805N, 5 26.284W	11.02.07	*Echinoderes cantabricus, E.* cf. *capitatus, E. hispanicus*	Gravelly sand	30
	36 07.229N, 5 25.114W	11.02.07	*Echinoderes* cf. *capitatus*	Muddy, sandy	24
	36 09.272N, 5 26.296W	11.02.08	*Evhinoderes hispanicus, Setaphyes dentatus*	Gravelly sand	12
	36 10.348N, 5 26.464W	11.02.08	*Dracoderes gallaicus*	Gravelly, sandy mud	16
	36 10.583N, 5 24.620W	11.02.08	*Echinoderes cantabricus*	Gravelly, sandy mud	25
	36 10.741N, 5 23.243W	11.02.08	*Echinoderes dujardinii, E. hispanicus, Setaphyes dentatus*	Gravelly sand	8

IBERIAN PENINSULA SAMPLES					
Locality	**Coordinates**	**Date**	**Species**	**Habitat**	**Depth (m)**
	37 11.940N, 7 21.236W	11.04.11	*Echinoderes dujardinii, Setaphyes dentatus*	Muddy gravel	2
	37 10.963N, 7 16.549W	11.04.11	*Pycnophyes communis, Setaphyes dentatus*	Gravelly, muddy sand	11
Isla Cristina, Spain	37 11.527N, 7 14.601W	11.04.11	*Setaphyes dentatus*	Gravelly, muddy sand	12
	37 12.320N, 7 20.534W	11.04.11	*Setaphyes dentatus*	Gravelly sand	4
	37 11.887N, 7 13.019W	11.04.11	*Setaphyes dentatus*	Gravelly, muddy sand	7
	37 08.324N, 7 20.308W	11.04.12	*Pycnophyes communis*	Gravelly mud	15
	36 33.755N, 6 18.500W	11.11.10	*Leiocanthys lageria, Pycnophyes communis, Setaphyes dentatus*	Gravelly, muddy sand	13
	36 35.791N, 6 17.888W	11.11.10	*Setaphyes dentatus*	Gravelly, muddy sand	10
Cádiz, Spain	36 34.117N, 6 15.141W	11.11.10	*Echinoderes dujardinii, Pycnophyes communis, Setaphyes dentatus*	Gravelly, muddy sand	7
	36 32.761N, 6 15.141W	11.11.10	*Echinoderes hispanicus, Pycnophyes almansae, P. communis, Setaphyes dentatus*	Gravelly sand	11
	36 32.310N, 6 14.245W	11.11.10	*Echinoderes worthingi*	Gravelly sand	4
	36 31.930N, 6 12.960W	11.11.10	*Echinoderes dujardinii, E. worthingi*	Gravelly sand	4

IBERIAN PENINSULA SAMPLES					
Locality	**Coordinates**	**Date**	**Species**	**Habitat**	**Depth (m)**
Cádiz, Spain	36 31.124N, 6 15.692W	11.11.11	*Echinoderes* cf. *capitatus, E. dujardinii, E. hispanicus*	Gravelly sand	11
	36 28.304N, 6 10.936W	11.11.11	*Echinoderes hispanicus*	Gravelly, sandy mud	4
	36 29.798N, 6 12.871W	11.11.11	*Echinoderes cantabricus, E. hispanicus, Leiocanthus lageria*	Gravelly mud	1
Alvor, Portugal	37 07.714N, 08 36.329W	16.12.12	*Setaphyes* sp. I	Mud with *Zostera*	0
	DEEP-SEA SAMPLES				
Mozambique Channel	15 21.685S, 45 57.378E	--.11.15	*Condyloderes* sp., *Echinoderes* cf. *dubiosus, Ryuguderes* sp.	Outside pockmarks	754
	15 21.695S, 4557.388E	--.11.15	*Echinoderes apex, E.* cf. *dubiosus, E. unispinosus, Echinoderes* sp., *Fujuriphyes hydra, Ryuguderes* sp.	Outside pockmarks	757
	15 21.812S, 45 57.628E	--.11.15	*Echinoderes hviidarum, Sphenoderes* cf. *indicus*	Inside pockmarks	735
	15 31.148S, 45 42.931E	--.10.14	*Condyloderes* sp., *Echinoderes unispinosus, Fissuroderes cthulhu, Fujuriphyes dagon*	Inside pockmarks	789
Gulf of California	27 42 00N,111 38 00W	11.02.07	*Cristaphyes fortis*	Mud	1570
	27 09 08N,111 39 57W	11.02.07	*Cristaphyes fortis, Echinoderes xalkutaat*	Mud	1440

DEEP-SEA SAMPLES					
Locality	**Coordinates**	**Date**	**Species**	**Habitat**	**Depth (m)**
Clarion-Clipperton Zone	07 4.28S, 088 27.79W – 14 03.00N, 130 08.32W	26.04.10-11.05.16	*Echinoderes* sp. I, *Echinoderes* sp. II, *Echinoderes* sp. III	Nodule fields	4118-4890
GULF OF CALIFORNIA					
Mazatlán	23 05 30N,106 17 45W	18.05.18	*Cephalorhyncha teresae, Higginsium mazatlanensis*	Sandy mud	5
NORTH SEA					
Syd-Hällsö Island, Skagerrak	58 56.846′N, 11 4.896 E	--.--.17	*Centroderes spinosus, Echinoderes* cf. *eximus, Pycnophyes ancalagon, Semnoderes armiger, Setaphyes elenae*	Mud	55-65
GULF OF MEXICO					
-	-	-	*Leiocanthus* sp. I, *Leiocanthus* sp. II	-	-
FRANCE					
Île Callot, Carantec	48,684530, -3.923717	21.08.19	*Echinoderes dujardinii*	Mud	0

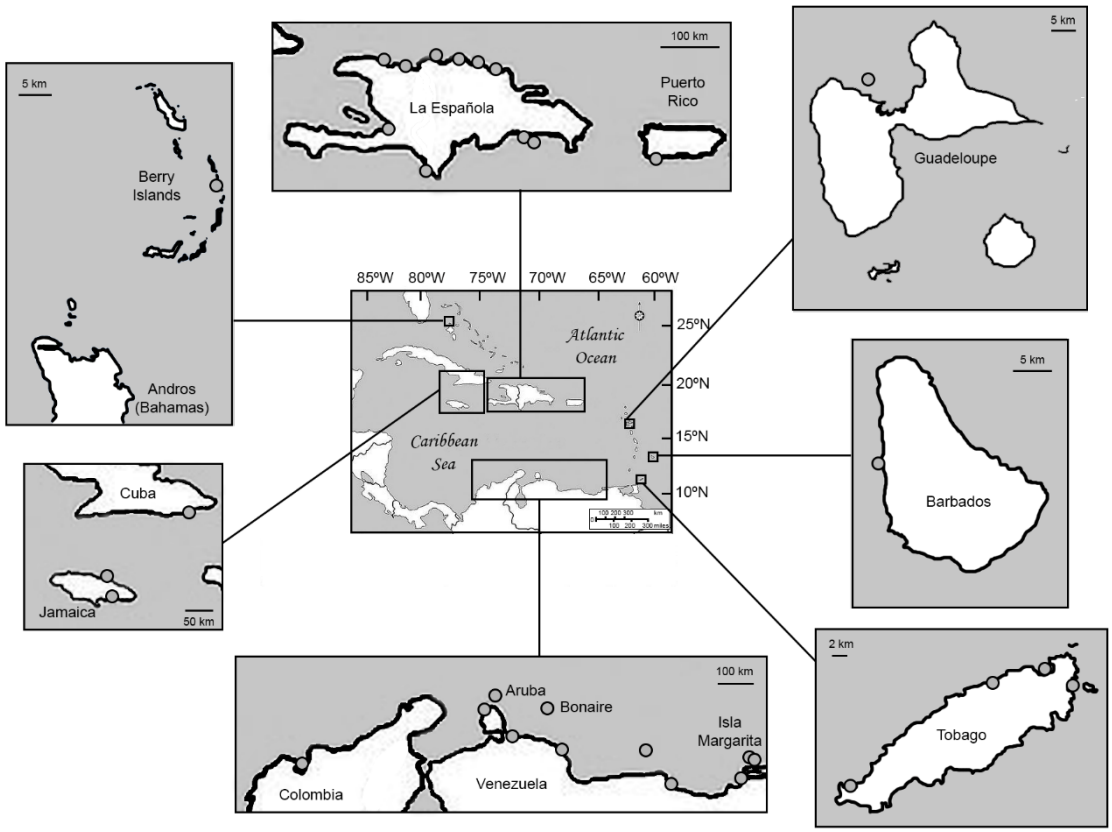

Figure 19. Geographic maps of the Caribbean Basin showing the sampling locations of the Caribbean samples studied in the present thesis.

2.2 Sampling methodology and extraction of kinorhynchs.

Figure 20. The bubble-and-blot method for extraction of meiofaunal with hard exocuticle.

Two types of samplings were performed depending on the proposed objectives: qualitative and quantitative. For qualitative samplings, sediment samples were obtained using a Higgins meiobenthic dredge (Fleeger *et al.*, 1988), which enables to collect a huge amount of the upper-most, well-oxygenated sediment layers where the greatest abundance of meiofauna is concentrated. Meiofaunal organisms were subsequently separated from the

sediment particles using the bubble-and-blot method (Higgins, 1964; Sørensen and Pardos, 2008), which creates turbulences and bubbles in the sediment to drag the animals until the water surface, where they can be easily collected and filtered using a 42 or 63 μm sieve (Fig. 20). Although the bubble-and-blot method is not quantitative either, it is able to collect about the 90-95 % of the meiofauna with hard exocuticle of a sediment sample (Higgins and Thiel, 1988). Meiofaunal organisms were fixed in 4 % neutral buffered formalin and preserved in 70 %, 100 % ethanol or propoylene glycol. Sorting of kinorhynchs was carried out using an Irwin Loop under a Motic® SMZ-168 stereo zoom microscope.

For quantitative samplings from the Mozambique Channel deep-sea, sediment samples were collected using a Barnett-type multi-corer (MTB) with three cores by deployment. Sediment samples were fixed in 4 % neutral buffered formalin and meiofaunal organisms were subsequently separated from sediment by Ludox centrifugation (Heip *et al.*, 1985).

2.3 Microscopy.

For light microscopy (LM), kinorhynchs were firstly washed with distilled water to remove remnants of ethanol or formalin, then dehydrated through a graded series of 25 %, 50 %, 75 % and 100 % glycerine to be mounted on a glass slide with Fluoromount G® sealed with Depex®. The specimens must spend a whole night in 100 % glycerine to ensure that all ethanol traces evaporate. Only a single kinorhynch specimen is mounted per glass slide to facilitate taxonomic identification and make it easier to later locate a specific specimen. The mounted specimens were studied using an Olympus© BX51-P microscope with differential interference contrast (DIC) optics, equipped with an Olympus© DP-70 camera, in the Meiofaunal Laboratory of the UCM. The DIC enhances the contrast in transparent structures and allows seeing otherwise invisible features of the kinorhynchs.

For scanning electron microscopy (SEM), kinorhynchs were washed with distilled water to remove remains of the preservative liquid and sonically cleaned during 10-15 s to eliminate the attached sediment particles. Then, specimens were dehydrated through a graded series of 70 %, 80 %, 90 % and 100 % ethanol. Hexamethyldisilazane (HMDS) was used for chemical drying through a HMDS-ethanol series. Finally, specimens were

coated with gold and mounted on aluminium stubs to be examined with a JSM® 6335-F JEOL SEM at the Centro Nacional de Microscopía Electrónica (ICTS), UCM.

Identification of kinorhynchs to genus level was done using the keys provided by Sørensen and Pardos (2008; 2020) and the genera diagnoses of Sánchez *et al.* (2016).

2.4 Statistics.

To test most of the proposed hypotheses about evolution, ecology, morpho-ecology and biogeography of kinorhynchs, statistical modelling (*i.e.* the process of applying statistical analysis of a dataset) was applied. A statistical model is a mathematical representation of observed data. Rather than scrutinizing the raw data, this practice allows identifying relationships between variables, making predictions and visualizing those data.

Due to the nature of the analyses that were necessary to test the hypotheses of the present thesis, mixed models (also known as mixed-effects or mixed-error component models) were frequently used. Biological data are usually complex and hierarchized by grouping factors (*e.g.* populations, species, collecting localities…), making them not truly independent (McCullagh and Nelder, 1989). In this context, mixed models were designed to deal with structured data saving degrees of freedom compared to standard linear models (Hajduk, 2019).

Mixed models have two components: fixed and random effects. Fixed effects are variables whose influence on the response variable we are trying to elucidate (in standard linear models, they are called explanatory variables), whilst random effects are grouping factors consequence of having hierarchical data whose effect we are trying to control (Hajduk, 2019). In our cases of study, kinorhynchs data, obtained from species and/or populations, are hierachized by Linnean taxonomy (as a result, in turn, of the group phylogeny), making the observations not independent. Although the best approach to eliminate the phylogenetic correlation of a biological dataset is phylogenetic generalized least squares, this tool requires a solid phylogenetic tree (Freckleton *et al.*, 2002; Tidière *et al.*, 2017), and many relationships of the current Kinorhyncha phylogeny still remain unresolved, making its application unsuitable. Consequently, the application of mixed models allows using the nested structure, originated by phylogeny, in the random-effect component of the model. All the statistical analyses were conducted in R (R Core Team, 2021).

3 – Results

"How inappropriate to call this planet Earth,

when it is quite clearly Ocean" (Arthur C. Clarke)

This section includes the set of papers that are part of this article-based thesis, as well as five appendices with complementary samplings and material, which can be grouped into the following categories:

TAXONOMY AND BIODIVERSITY

Taxonomy and biodiversity of Kinorhyncha in the Caribbean Sea

3.1 Cepeda D, Sánchez N, Pardos F. 2019. First extensive account of the phylum Kinorhyncha from Haiti and the Dominican Republic (Caribbean Sea), with the description of four new species. *Marine Biodiversity* **49(3)**: 2281-2309. https://doi.org/10.1007/s12526-019-00963-x. Q2

3.2 Cepeda D, Pardos F, Sánchez N. 2019. Kinorhyncha from the Caribbean, with the description of two new species from Puerto Rico and Barbados. *Zoologischer Anzeiger* **282**: 127-139. https://doi.org/10.1016/j.jcz.2019.05.014. Q1

3.3 Cepeda D, Pardos F, Sánchez N. 2019. A new species and first record of *Dracoderes* (Kinorhyncha: Allomalorhagida: Dracoderidae) from American waters, with an identification key of the genus. *Zoologischer Anzeiger* **282**: 106-115. https://doi.org/10.1016/j.jcz.2019.05.019. Q1

3.4 Cepeda D, Sánchez N, Pardos F. 2019. First report of the family Zelinkaderidae (Kinorhyncha: Cyclorhagida) for the Caribbean Sea, with the description of a new species of *Triodontoderes* Sørensen & Rho, 2009 and an identification key for the family. *Zoologischer Anzeiger* **282**: 116-126. https://doi.org/10.1016/j.jcz.2019.05.017. Q1

Appendix I Kinorhyncha diversity in the Caribbean Sea: a compilation of prior and new knowledge, description of a new species of *Echinoderes* (Cyclorhagida: Echinoderidae) and a dichotomous key to the species level.

Taxonomy and ecology of Kinorhyncha in the deep-sea

3.5 Cepeda D, Álvarez-Castillo L, Hermoso-Salazar M, Sánchez N, Gómez S, Pardos F. 2019. Four new species of Kinorhyncha from the Gulf of California, eastern Pacific Ocean. *Zoologischer Anzeiger* **282**: 140-160. https://doi.org/10.1016/j.jcz.2019.05.011. Q1

3.6 Cepeda D, Pardos F, Zeppilli D, Sánchez N. 2020. Dragons of the deep-sea: Kinorhyncha communities in a pockmark field at Mozambique Channel, with the description of three new species. *Frontiers in Marine Science* **7**: e665. https://doi.org/10.3389/fmars.2020.00665. Q1

Taxonomy of Kinorhyncha in the North Sea

3.7 Cepeda D, González-Casarrubios A, Sánchez N, Pardos F. 2020. *Setaphyes elenae* sp. nov., a new species of mud dragon (Kinorhyncha: Allomalorhagida) from Skagerrak (north-eastern Atlantic Ocean). *European Journal of Taxonomy* **637**: e637. https://doi.org/10.5852/ejt.2020.637. Q2

MORPHOLOGY, ECOLOGY AND BIOGEOGRAPHY

Morphology and morpho-ecology

3.8 Cepeda D, Álamo D, Sánchez N, Pardos F. 2019. Allometric growth in meiofaunal invertebrates: do all kinorhynchs show homogeneous trends? *Zoological Journal of the Linnean Society* **187(4)**: 1041-1060. https://doi.org/10.1093/zoolinnean/zlz083. Q1

3.9 Cepeda D, Trigo D, Pardos F, Sánchez N. 2020. Does sediment composition sort kinorhynch communities? An ecomorphological approach through geometric morphometrics. *Nature Scientific Reports* **10(1)**: e2603. https://doi.org/10.1038/s41598-020-59511-4. Q1

Macroecology and biogeography

3.10 Cepeda D, Pardos F, Sánchez N. 2021. From biggest to smallest mud dragons: size-latitude trends in a group of meiobenthic animals worldwide. *Organisms Diversity & Evolution* **21**: 43-58. https://doi.org/10.1007/s13127-020-00471-y. Q1

COMPLEMENTARY SAMPLINGS AND MATERIAL

Appendix II New species of *Setaphyes* from Portugal.

Appendix III New species of kinorhynchs from the Clarion-Clipperton deep-sea zone.

Appendix IV New species of *Leiocanthus* from the Gulf of Mexico.

Appendix V Use of isotopes for determination of feed intake in kinorhynchs.

Marine Biodiversity
https://doi.org/10.1007/s12526-019-00963-x

SENCKENBERG

ORIGINAL PAPER

First extensive account of the phylum Kinorhyncha from Haiti and the Dominican Republic (Caribbean Sea), with the description of four new species

Diego Cepeda[1] **& Nuria Sánchez**[1] **& Fernando Pardos**[1]

Received: 19 November 2018 / Revised: 15 March 2019 / Accepted: 25 April 2019

Abstract
Several meiofaunal samplings along the continental slope of Central America and the Antilles through the Caribbean Sea have revealed a rich kinorhynch fauna of undescribed species. The present contribution includes the description of two new species of the allomalorhagid genera *Cristaphyes* Sánchez et al., 2016 and *Fujuriphyes* Sánchez et al., 2016 and two new species of the cyclorhagid genus *Echinoderes* Claparède, 1863, as well as the first record of the previously known *Cristaphyes longicornis* (Higgins, 1983), *Echinoderes astridae* Sørensen, 2014, *Echinoderes horni* Higgins, 1983, *Echinoderes imperforatus* Higgins, 1983 and *Echinoderes spinifurca* Sørensen et al., 2005 for Haiti and the Dominican Republic (Hispaniola Island, Greater Antilles) together with new morphological information of the former. All the new species are formally described. Furthermore, we discuss the possibility of an expansion in the intraspecific morphological variation of *C. longicornis*, geographical remarks on the Caribbean Kinorhyncha and compare the morphological differences between the newly described species and their most similar congeners.

Keywords Kinorhynchs · Taxonomy · Morphology · *Echinoderes* · *Cristaphyes* · *Fujuriphyes*

Introduction

The phylum Kinorhyncha encompasses a group of marine, holobenthic, free-living, meiofaunal species that inhabit the upper centimetres of oceanic or estuarine sediment from intertidal to abyssal depths (Higgins 1988; Sørensen and Pardos 2008). Currently, the phylum is composed of two classes, Cyclorhagida and Allomalorhagida, based on both morphological and molecular evidence (Sørensen et al. 2015). Kinorhynchs are worldwide distributed, but the available biogeographical data is strongly biased by sampling strategies of the specialists in the phylum that have intensively sampled certain areas to the detriment of others poorly studied, being the North Sea, the Mediterranean Sea, the north-western Atlantic American shoreline and the Sea of Japan and adjacent waters as the most sampled areas of the world so far (Neuhaus 2013).

In this context, it has to be emphasised how little is known about the kinorhynch fauna of the Caribbean region, even though the region generally hosts the greatest marine biodiversity of the western Atlantic Ocean and is a global-scale hotspot of marine species (Roberts et al. 2002; Miloslavich et al. 2010). The first approach to describe the Caribbean kinorhynchs was done by Kirsteuer (1964) with the description of *Echinoderes caribiensis* Kirsteuer, 1964 from the Mochima National Park, Venezuela. A more extensive sampling campaign was accomplished by Higgins (1983), although this study was limited to the coral reef ecosystem at Carrie Bow Cay, Belize. This contribution increased the number of known Caribbean kinorhynch species to

This article is registered in ZooBank under urn:lsid:zoobank.org:pub:D10BC214-CD04-4543-B6C0-9A3A2700CD97.
Cristaphyes retractilis sp. nov. is registered in Zoobank under urn:lsid:zoobank.org:act:3D46B431-40FA-4415-B00C-63811B07252B.
Fujuriphyes dalii sp. nov. is registered in Zoobank under urn:lsid:zoobank.org:act:0C1C372B-1EA0-4B0B-854A-53D5AA947B33.
Echinoderes brevipes sp. nov. is registered in Zoobank under urn:lsid:zoobank.org:act:4E5899A5-85C8-44C1-B3C5-21A71C6C00A7.
Echinoderes parahorni sp. nov. is registered in Zoobank under urn:lsid:zoobank.org:act:F8FA16F5-75FC-47BB-A56D-7A3FF59EF0CE

Communicated by S. Gollner

* Diego Cepeda
diegocepedagomez@gmail.com

[1] Department of Biodiversity, Ecology and Evolution, Faculty of Biological Sciences, Complutense University of Madrid, José Antonio Novais St. 12, Madrid 28040, Spain

Published online: 03 July 2019

19, with the description of 5 new species of Cyclorhagida and 13 species of Allomalorhagida (Higgins 1983). More recently, the area of Bocas del Toro, Colón Island and Bastimento Island (Panama) has been extensively studied by Sørensen (2006), Neuhaus et al. (2014) and Pardos et al. (2016a, b), resulting in 5 new species of Cyclorhagida, 2 new species of Allomalorhagida and 7 new reports, bringing the total number of valid kinorhynch species for the Caribbean Sea up to 31.

All the available information on Caribbean Kinorhyncha is limited to the continental shelf, disregarding the Antilles shelves. The main aim of the present project is to describe the still unknown kinorhynch fauna of the aforementioned archipelago through the study of the Caribbean samples obtained by Dr. R. P. Higgins and his colleagues from 1966 to 1991 and deposited at the Smithsonian Institution National Museum of Natural History (NMNH). The present contribution focuses on Hispaniola Island, one of the Greater Antilles, and includes the descriptions of four new species of kinorhynchs and the first report of *Cristaphyes longicornis* (Higgins, 1983), *Echinoderes astridae* Sørensen, 2014 and *Echinoderes spinifurca* Sørensen et al., 2005 for the area, with additional details on morphology of *C. longicornis*. Further papers will deal with the remaining Caribbean samples.

Materials and methods

Hispaniola Island is a part of the Greater Antilles of the Caribbean Sea (western Atlantic Ocean) and located between Cuba and Puerto Rico, separated by the Windward Passage and the Mona Passage respectively (Fig. 1a). Samples were taken at several intertidal and subtidal localities, of which seven yielded the analysed specimens in the present study (Table 1). Stations L1 to L6 are situated off the northern coast of the island, while Station L7 is located in the southern part (Fig. 1b). Detailed data on samples and localities is summarised in Table 1. Sampling was performed using a meiobenthic dredge (Fleeger et al. 1988), and meiofauna was separated using the bubble and blot method (Higgins 1964; Sørensen and Pardos 2008). Meiofaunal specimens were fixed in 4% formalin and preserved in propylene glycol.

Unmounted kinorhynchs were observed under a Motic® SMZ-168 stereo zoom microscope and picked up with an Irwin loop. For light microscopy (LM), animals were dehydrated through a graded series of 25%, 50%, 75% and 100% glycerine to be mounted on a glass slide or a Cobb's aluminium slide holder with Fluoromount G® and sealed with Depex®. The mounted specimens were studied and photographed using an Olympus© BX51-P microscope with differential interference contrast (DIC) optics equipped with an Olympus© DP-70 camera. For scanning electron microscopy (SEM), specimens were transferred to 70% ethanol and then progressively dehydrated through a series of 80%, 90%, 95% and 100% ethanol. Hexamethyldisilazane (HMDS) was used for chemical drying through a HMDS-ethanol series. Specimens were coated with gold and mounted on aluminium stubs to be examined with a JSM® 6335-F JEOL SEM at the ICTS Centro Nacional de Microscopía Electrónica (Complutense University of Madrid, Spain). Identification to genus level of the cyclorhagid kinorhynchs was done according to the dichotomous key provided by Sørensen and Pardos (2008), whereas the allomalorhagid kinorhynchs were identified following the genus diagnoses provided by Sánchez et al. (2016). Line drawings and images plates composition was done using Adobe® Photoshop 6.0 and Illustrator CC-2014 software.

Results

A total of ten species belonging to four genera and three families were recorded along the Hispaniola Island coastline

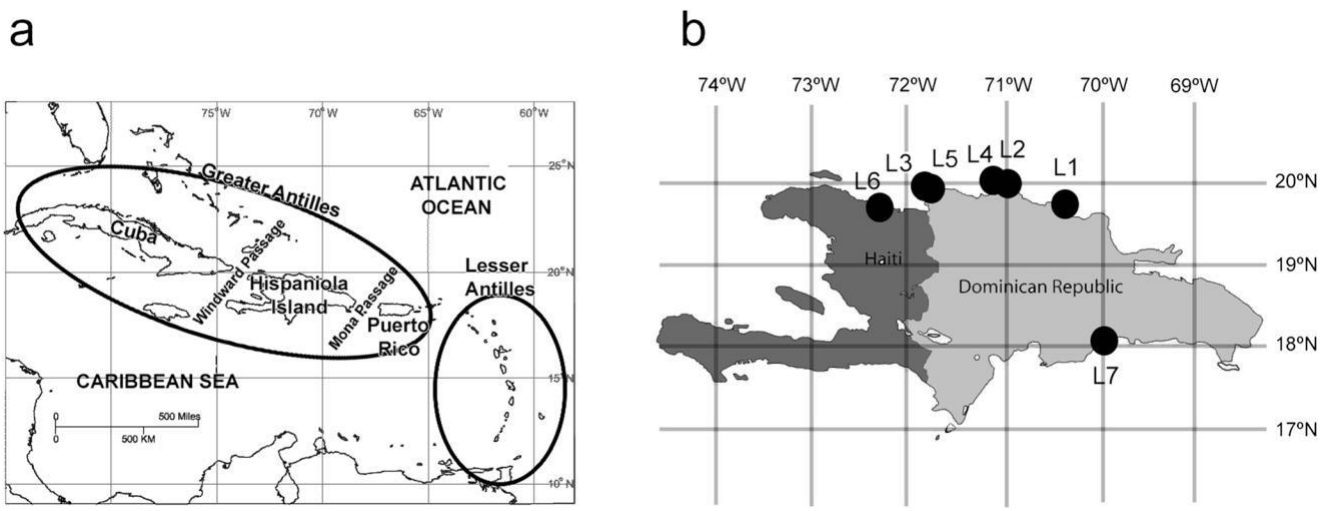

Fig. 1 Map showing the location of the Hispaniola Island as part of the Greater Antilles of the Caribbean Sea, western Atlantic Ocean (**a**) and the sampling locations of the studied kinorhynch specimens (**b**)

Table 1 Data on sampling localities, habitat of the collected specimens and collected species per sample

Station code	Location	Geographical coordinates	Sampling date	Sediment	Depth (m)	Collected species
L1	Puerto Plata, Dominican Republic	19° 48′ 12″ N 70° 42′ 00″ W	02/11/1980	Sandy mud	4–5	*Fujuriphyes dalii* sp. nov., *Dracoderes* sp.
L2	Puerto Blanco, Dominican Republic	19° 54′ 24″ N 70° 56′ 24″ W	03/11/1980	Silty mud	3	*Cristaphyes retractilis* sp. nov., *C.* cf. *longicornis*, *Dracoderes* sp., *Echinoderes astridae*, *E. spinifurca*, *E. parahorni* sp.nov.
L3	Monte Cristi Bay, Dominican Republic	19° 53′ 12″ N 71° 40′ 00″ W	06/11/1980	Muddy sand	3–4	*Cristaphyes retractilis* sp. nov., *Echinoderes astridae*, *E. horni*, *E. imperforatus*, *E. spinifurca*, *Fujuriphyes dalii* sp. nov.
L4	La Isabela, Dominican Republic	19° 53′ 18″ N 71° 05′ 36″ W	04/11/1980	Silty mud	4	*Cristaphyes retractilis* sp.nov., *Dracoderes* sp.
L5	Icaquitos Bay, Dominican Republic	19° 53′ 12″ N 71° 38′ 30″ W	07/11/1980	Muddy sand	2	*Echinoderes horni*, *E. parahorni* sp. nov.
L6	Cabo Haitiano, Haiti	19° 46′ 12″ N 72° 11′ 00″ W	10/11/1980	Mud	3–5	*Dracoderes* sp., *Echinoderes parahorni* sp.nov.
L7	Santo Domingo, Dominican Republic	18° 28′ 00″ N 69° 57′ 00″ W	08/05/1976	Unknown	0.7–1.0	*Echinoderes brevipes* sp. nov.

(Table 1). Of these, four species are herein newly described and five are newly reported for the Greater Antilles.

Class **Allomalorhagida** Sørensen et al., 2015
Family **Pycnophyidae** Zelinka, 1896
Genus ***Cristaphyes*** Sánchez et al., 2016
Cristaphyes retractilis sp. nov. (Figs. 2, 3 and 4 and Tables 2 and 3)

Material examined

Type material. Holotype, adult male, collected on 06 November 1980 at Monte Cristi Bay, Dominican Republic, Hispaniola Island, western Atlantic Ocean: 19° 53′ 12″ N, 071° 40′ 00″ W (L3) (Table 1; Fig. 1b) at 3–4 m depth in muddy sand; mounted in Fluoromount G®, deposited at NMNH under accession number: USNM 1490909. Paratypes, four adult males and five adult females; six of them with same collecting data as holotype, mounted in Fluoromount G® and deposited at NMNH under accession numbers: USNM 1490910– 1490915; two of them collected on 03 November 1980 at Puerto Blanco Harbour, Dominical Republic, Hispaniola Island, western Atlantic Ocean: 19° 54′ 24″ N, 70° 56′ 24″ W (L2) (Table 1; Fig. 1b) at 3 m depth in silty mud; mounted in Fluoromount G®, deposited at NMNH under accession num-bers: USNM 1490916–1490917; one of them collected on 04 November 1980 at La Isabela, Dominican Republic, Hispaniola Island, western Atlantic Ocean: 19°53′ 18″ N, 71° 05′ 36″ W (Table 1; Fig. 1b) at 4 m depth in silty mud; mounted in Fluoromount G®, deposited at NMNH under accession number: USNM 1490918.

Non-type material. Twenty-two additional specimens from the same localities as the holotype and paratypes (17 mounted for LM, 5 mounted for SEM), also deposited at NMNH under accession numbers: USNM 1490919–1490936.

Diagnosis

Cristaphyes with middorsal processes on segments 1–9. Pairs of paradorsal setae on segments 2, 4, 6 and 8, laterodorsal setae on segments 2–9, paralateral setae on segment 1, lateroventral setae on segments 2, 4, 6, 8 and 10, ventrolateral setae on segments 1, 3–8 and 10, one pair of ventromedial setae on segments 2–8 and two pairs of ventromedial setae on segment 9. Setae in each paradorsal pair differ in length and shape: one short and thick, the other one longer and progressively tapering towards end. Laterodorsal setae mesially shifted on uneven segments compared to those of even segments. Segments 10 and 11 retractable into segment 9. Lateral terminal spines absent.

Etymology

From the Latin 'retractilis', meaning retracting, which refers to the segments 10 and 11 that often appear retracted into the precedent segments.

Description

See Table 2 for measurements and dimensions, and Table 3 for summary of cuticular process, seta, tube, glandular cell outlet and sensory spot locations.

Head and neck. Head with retractable mouth cone and introvert. The collected specimens were not suitable for head examinations, hence data on number and arrangement of scalids and oral styles is not available.

Neck with four dorsal and two ventral sclerotized placids (Fig. 2a–c). Dorsal placids rectangular; mesial ones broader than lateral ones (Fig. 2b). Ventral placids much more elongate and trapezoidal, getting thinner towards the lateral sides (Fig. 2a, c).

Trunk. Trunk with 11 segments (Figs. 2a, b, 3a, b and 4a, b). Segment 1 with one tergal, two episternal and one trapezoidal midsternal plate (Figs. 2a–c, 3a, b and 4a, b); remaining ones

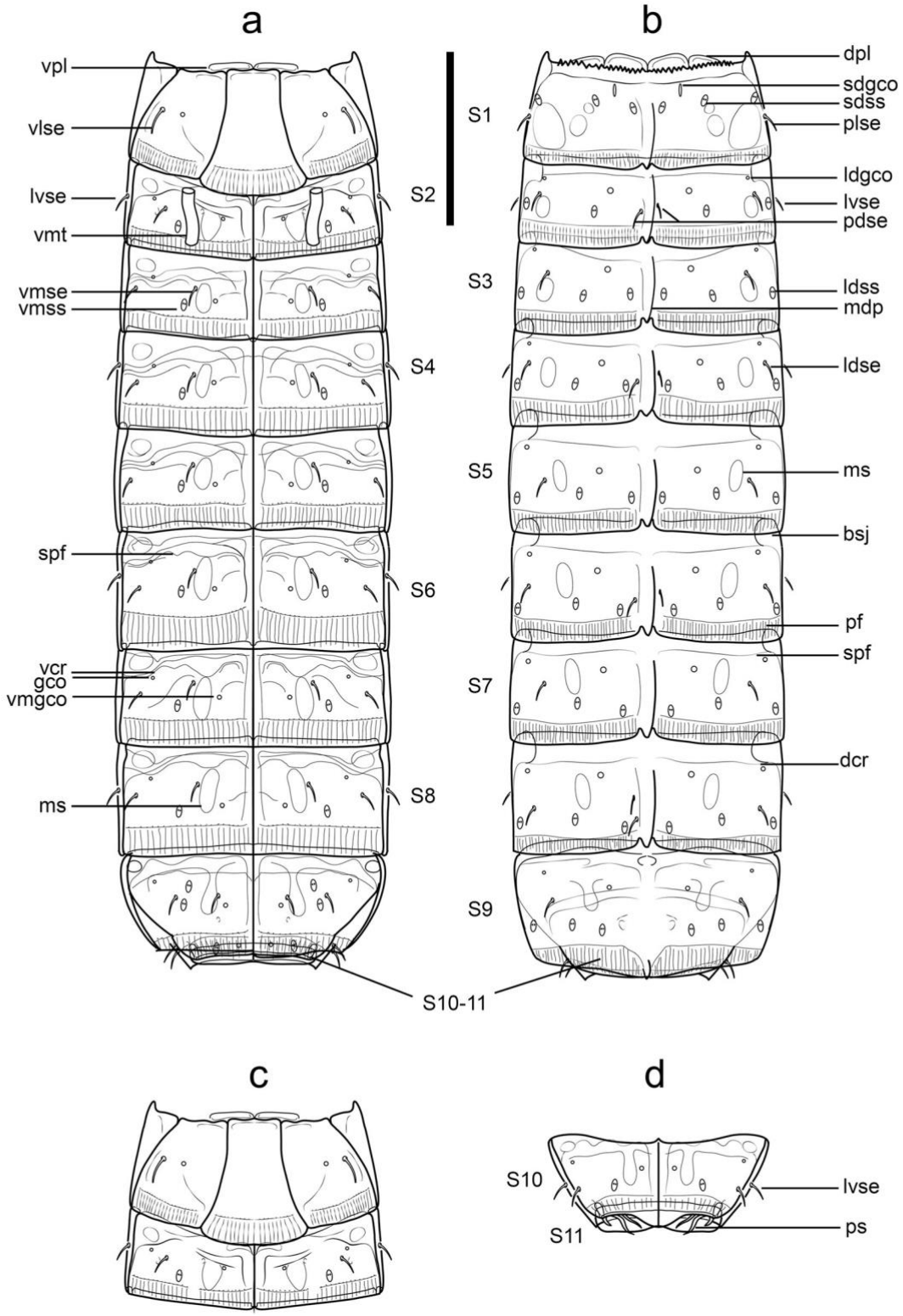

Fig. 2 Line art illustrations of *Cristaphyes retractilis* sp. nov. **a** Male, ventral view; **b** Male, dorsal view; **c** Female, segments 1–2, ventral view; **d** Male, segments 10–11, ventral view. Scale: 100 μm. *bsj* ball-and-socket joint, *dcr* dorsal cuticular ridge, *dpl* dorsal placid, *gco* glandular cell outlet, *ldgco* laterodorsal glandular cell outlet, *ldse* laterodorsal seta, *ldss* laterodorsal sensory spot, *lvse*, lateroventral seta, *mdp* middorsal process, *ms* muscular scar, *pdse* paradorsal seta, *pf* pectinate fringe, *plse* paralateral seta, *ps* penile spine, *S* segment followed by number of corresponding segment, *sdgco* subdorsal glandular cell outlet, *sdss* subdorsal sensory spot, *spf* secondary pectinate fringe, *vcr* ventral cuticular ridge, *vlse* ventrolateral seta, *vmgco* ventromedial glandular cell outlet, *vmse* ventromedial seta, *vmss* ventromedial sensory spot, *vmt* ventromedial tube, *vpl* ventral placid

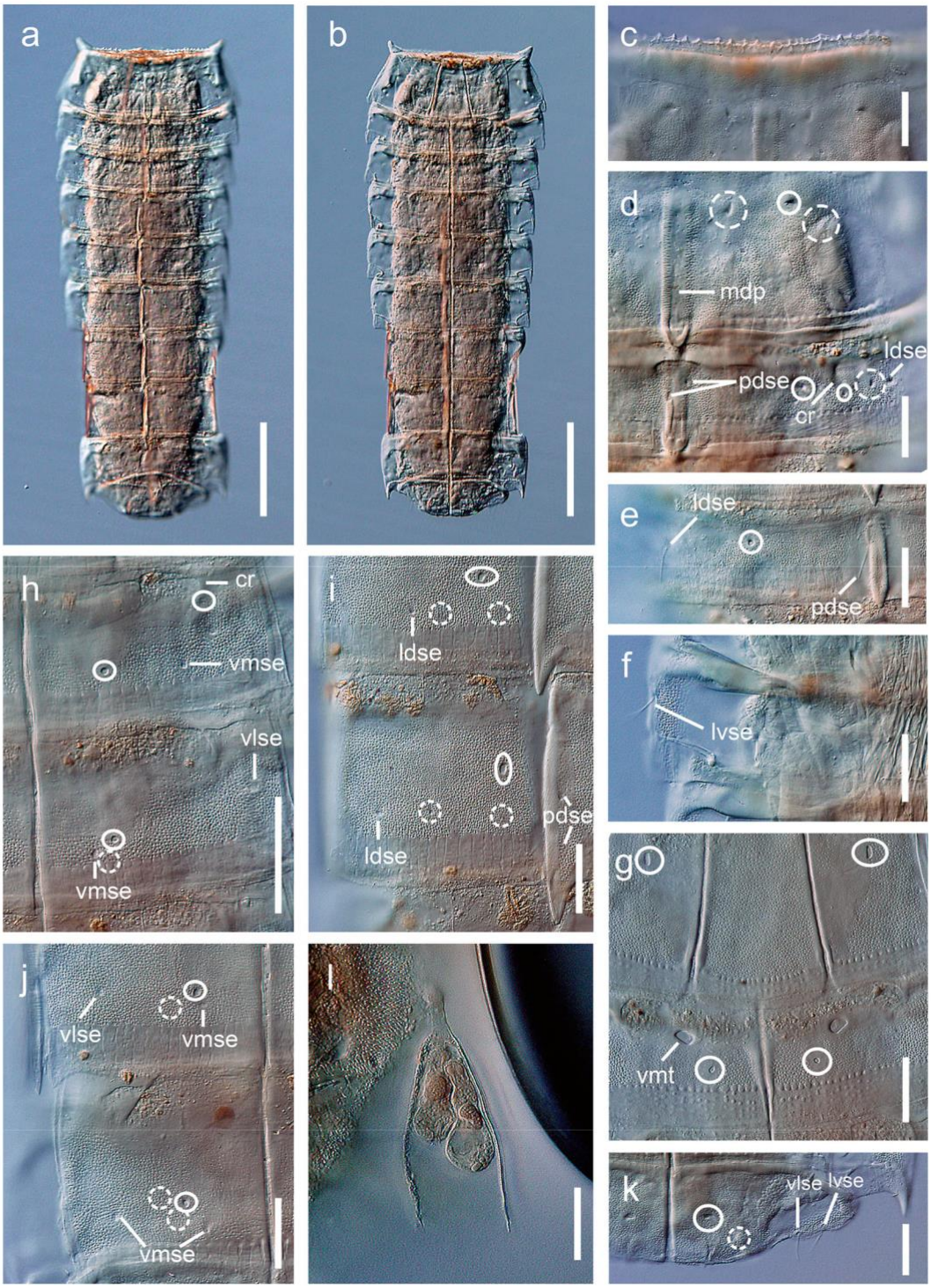

Fig. 3 Light micrographs showing trunk overview and details in the segments and the sexual dimorphism of *Cristaphyes retractilis* sp. nov. **a** Female, dorsal overview of trunk; **b** Female, ventral overview of trunk; **c** Female, dorsal overview of segment 1, showing the strongly denticulated anterior margin of the tergal plate; **d** Female, middorsal, paradorsal, subdorsal and laterodorsal regions on right half of tergal plates of segments 1–2; **e** Female, detail of the middorsal, paradorsal, subdorsal and laterodorsal regions on left half of tergal plate of segment 2; **f** Female, lateroventral region on left half of sternal plates of segment 2. **g** Male, ventromedial region of sternal plates of segments 1–2; **h** Female, ventrolateral and ventromedial regions on right half of sternal plates of segments 2–3; **i** Female, middorsal, paradorsal, subdorsal and laterodorsal reigons on left half of tergal plates of segments 7–8; **j** Female, ventrolateral and ventromedial regions of left half of sternal plates of segments 8–9; **k** Female, ventrolateral and ventromedial regions of right half of sternal plates of segment 10. **l** Epibiontic Ciliophora on the cuticle surface on the laterodorsal section of segment 9. Scales: **a**, **b**: 100 μm; **c**–**l**: 20 μm. *cr* cuticular ridge, *ldse* laterodorsal seta, *lvse* lateroventral seta, *mdp* middorsal process, *pdse* paradorsal seta, *vlse* ventrolateral seta, *vmse* ventromedial seta, *vmt* ventromedial tube; sensory spots are marked as dashed circles, and glandular cell outlets as continuous circles

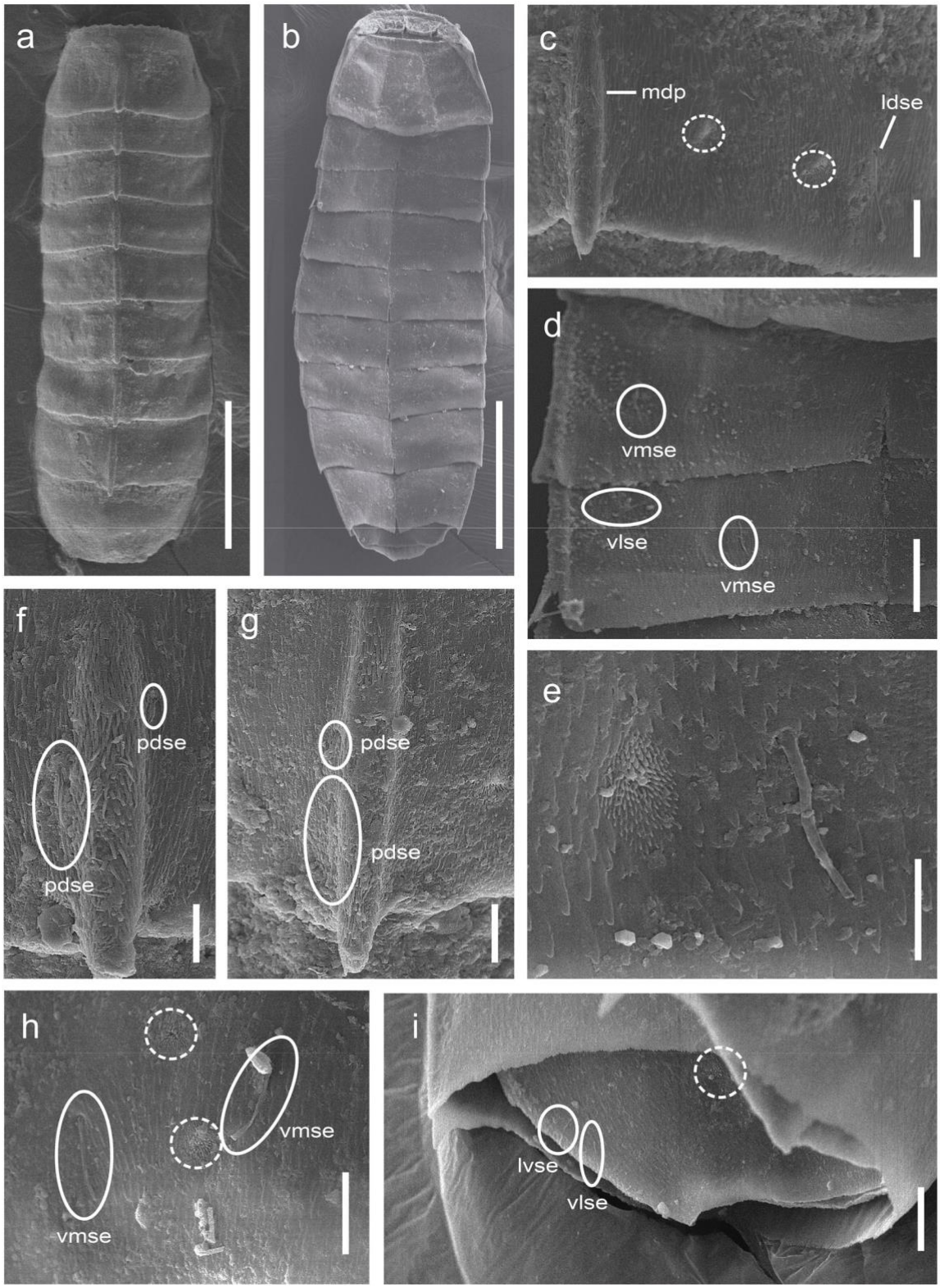

Fig. 4 Scanning electron micrographs showing overviews and details in the cuticular trunk morphology of *Cristaphyes retractilis* sp. nov. **a** Dorsal overview of trunk; **b** Ventral overview of trunk; **c** Middorsal, paradorsal, subdorsal and laterodorsal regions of right half of tergal plate of segment 3; **d** Ventrolateral and ventromedial regions on left half of sternal plates of segments 2–3; **e** Detail of ventromedial seta and sensory spot of segment 3; **f** Detail of middorsal process and paradorsal setae of segment 4; **g** Detail of middorsal process and paradorsal setae of segment 8; **h** Ventromedial region on left half of sternal plates of segment 9; **i** Lateroventral and ventrolateral regions on left half of tergal and sernal plates of segment 10. Scales: **a**, **b**: 100 μm; **c**, **d**, **h**–**i**: 10 μm; **e**–**g**: 5 μm. *ldse* laterodorsal seta, *lvse* lateroventral seta, *mdp* middorsal process, *pdse* paradorsal seta, *vlse* ventrolateral seta, *vmse* ventromedial seta; sensory spots are marked as dashed circles.

Table 2 Measurements of adult *Cristaphyes retractilis* sp. nov. from Hispaniola Island, including number of measured specimens (*n*), mean of data and standard deviation (SD). There were no remarkable differences in sizes or dimensions between the two sexes or among the sampling locations

Character	Range	Mean (SD; *n*)
TL (μm)	466.8–601.9	520.3 (64.4; 20)
MSW-5 (μm)	125.6–230.0	166.1 (23.2; 20)
MSW-5/TL (%)	20.9–32.5	32.1 (3.6; 20)
SW-10 (μm)	92.8–161.8	110.6 (17.4; 20)
SW-10/TL (%)	19.8–22.8	21.2 (1.6; 20)
S1 (μm)	71.5–115.8	83.2 (12.1; 20)
S2 (μm)	33.1–57.5	42.4 (7.7; 20)
S3 (μm)	39.6–63.2	49.5 (7.8; 20)
S4 (μm)	41.1–77.9	56.8 (9.3; 20)
S5 (μm)	45.3–87.2	58.3 (9.3; 20)
S6 (μm)	48.6–91.4	61.7 (10.4; 20)
S7 (μm)	51.1–92.3	63.0 (11.2; 20)
S8 (μm)	50.2–96.6	67.6 (10.1; 20)
S9 (μm)	53.4–86.4	66.9 (9.8; 20)
S10 (μm)	28.3–66.3	40.4 (8.7; 20)
S11 (μm)	12.6–43.6	23.3 (7.3; 20)

MSW-5 maximum sternal width (on segment 5), *S* segment lengths, *SW-10* standard width (on segment 10), *TL* total length of trunk

with one tergal and two sternal cuticular plates (Figs. 2a–d, 3a, b and 4a, b). Midsternal and tergosternal junctions, as well as junctions between midsternal and episternal plates, as conspicuous lines externally on the cuticle (Figs. 2a, d, 3b and 4b). Tergal cuticular plates slightly bulging middorsally. Sternal plates reach their maximum width at segment 5, but almost constant in width throughout the trunk, slightly tapering at the last two trunk segments (Figs. 2a, b, 3a, b and 4a, b). Sternal cuticular plates are relatively wide in the ratio maximum width to total trunk length (MSW-5:TL average ratio = 32.1%), giving the animal a plump appearance (Figs. 2a, b, 3a, b and 4a, b). Middorsal processes on segments 1–9, keel-shaped, with pointed tips that surpass the posterior segment margins, turning progressively longer towards the posterior end (Figs. 2b, 3a, d, i and 4a, c, f–g). Middorsal process of segment 9 shorter and thinner than previous ones, but also pointed and extending beyond the terminal trunk segment (Fig. 2b). Segments 1–10 with paired, rounded glandular cell outlets in subdorsal positions (Figs. 2b and 3d–e, i). Segments 2–10 with paired cuticular ridges in laterodorsal position followed by small, intracuticular wrinkled glandular cell outlets on their posterior margin (Fig. 2b). Segments 1–10 furthermore with paired, rounded glandular cell outlets in ventromedial position, those on segment 1 being laterally displaced (Figs. 2a, c–d and 3g–h, j–k). Segments 2–10 furthermore with paired ventral cuticular ridges marking the ventrolateral-ventromedial border followed by small, intracuticular wrinkled glandular cell outlets on their posterior margin (Figs. 2a, c, 3h). Cuticular hairs distributed all over the trunk cuticle; tergal plates bear elongate, very thin hairs that become thicker on middorsal processes and shorter towards posterior segment margin (Fig. 4c, f–g); sternal plates bear very short, scale-like, thick hairs that become thinner towards posterior segment margin (Fig. 4d–e, h). Pachycycli and ball-and-socket joints on segments 2–10 (Fig. 2a–d). Apodemes not observed. Primary pectinate fringe finely serrated (Fig. 2a–d), appearing smooth under LM (Fig. 3d–e, g–j); secondary pectinate fringe also finely serrated, wavy (Fig. 2a–c), dorsally protruded to the beginning of middorsal processes; free flaps covering anterior part of subsequent segment. Muscular scars as rounded to oval hairless areas (Fig. 2a–d), quite inconspicuous.

Segment 1 with middorsal process flanked by more densely covered hairy areas that slightly surpasses the posterior segment margin (Figs. 2b and 3d). Midsternal plate forming a midventral convex extension on its posterior edge (Figs. 2a, c, 3b and 4b). Anterolateral margins of the tergal cuticular plate as

Table 3 Summary of nature and arrangement of sensory spots, glandular cell outlets, cuticular processes, setae and spines in *Cristaphyes retractilis* sp. nov.

Segment	MD	PD	SD	LD	PL	LV	VL	VM
1	cp		ssx2, gco	ss	se		se, gco	
2	cp	se	ss, gco	se, gco, ss		se	gco	ss, se, tu(m), gco
3	cp		ssx2, gco	se, gco, ss			se, gco	ss, se, gco
4	cp	se	ssx2, gco	se, gco, ss		se	se, gco	ss, se, gco
5	cp		ssx2, gco	se, gco, ss			se, gco	ss, se, gco
6	cp	se	ssx2, gco	se, gco, ss		se	se, gco	ss, se, gco
7	cp		ssx2, gco	se, gco, ss			se, gco	ss, se, gco
8	cp	se	ssx2, gco	se, gco, ss		se	se, gco	ss, se, gco
9	cp		ss, gco	ssx2, se, gco			gco	se, ssx2, se, gco
10			gco	gco		se	se, gco	ss, gco
11						psx2(m)		

cp cuticular process, *gco* glandular cell outlet, *LD* laterodorsal, *LV* lateroventral, *m* male condition of sexually dimorphic character, *MD* middorsal, *PD* paradorsal, *PL* paralateral, *ps* penile spine, *se* seta, *SD* subdorsal, *ss* sensory spot, *tu* tube, *VL* ventrolateral, *VM* ventromedial

horn-shaped extensions (Figs. 2a–c, 3a, b and 4a, b). Anterior margin of tergal plate strongly denticulated, followed by a smooth area (Figs. 2b, 3a, c and 4a). Two pairs of sensory spots in subdorsal position; one pair of sensory spots in laterodorsal position, all of them located at the anterior half of the cuticular plate (Figs. 2b and 3d); sensory spots on this and remaining segments rounded to oval, with several rings of cuticular papillae surrounding a central pore (Fig. 4c, e, h, i). Paired setae in paralateral and ventrolateral position (Fig. 2a–c).

Segment 2 with middorsal process as on preceding segment (Figs. 2b and 3d–e). Paired paradorsal setae differing in size: one seta very short (ca. 2 µm long) and relatively thick, the other one longer (ca. 8 µm long) and progressively thinner towards end (Figs. 2b and 3d–e). Paired setae also in laterodorsal, lateroventral and ventromedial positions (Figs. 2a–c, 3d–f, h and 4d); laterodorsal setae located laterally to the muscular scars; ventromedial setae located near the border between the ventrolateral and ventromedial sections (Figs. 2a–c and 4d). Paired sensory spots in subdorsal, laterodorsal and ventromedial positions (Figs. 2a–c and 3d– e, h). Sexually dimorphic male tubes in ventromedial position (Figs. 2a and 3g). Tubes long, flexible, thin-walled, with blunt tip bearing a minute pore.

Segment 3 with middorsal process as on preceding segments (Figs. 2b and 4c). Paired setae in laterodorsal, ventrolateral and ventromedial positions (Figs. 2a, b, 3h and 4c–e); laterodorsal setae mesially displaced compared to those of the precedent segment; ventromedial setae located more lateral than the ventromedial muscular scars (Fig. 2a, b). Two pairs of sensory spots in subdorsal position plus one pair of sensory spots in laterodorsal and ventromedial positions (Figs. 2a, b, 3h and 4c–e).

Segment 4 with middorsal process as on preceding segments (Figs. 2b and 4f). Paired paradorsal setae differing in size: one seta very short (ca. 2 µm long) and relatively thick, the other one longer (ca. 8 µm long) and progressively narrower towards end (Figs. 2b and 4f). Paired setae also in laterodorsal, lateroventral, ventrolateral and ventromedial positions (Fig. 2a, b); laterodorsal setae located laterally to the muscular scars; ventrolateral setae located near the junction between the ventrolateral and ventromedial sections (Fig. 2a, b). Two pairs of sensory spots in subdorsal position plus one pair of sensory spots in laterodorsal and ventromedial positions (Fig. 2a, b).

Segment 5 similar to segment 3 (Fig. 2a, b).

Segment 6 similar to segment 4 (Fig. 2a, b).

Segment 7 similar to segments 3 and 5 (Figs. 2a, b and 3i).

Segment 8 with tergal plate resembling that of segments 4 and 6, but with both paradorsal setae located at the same side of the middorsal process (Figs. 2b, 3i and 4g). Sternal plates identical with those of segments 4 and 6 (Figs. 2a and 3j).

Segment 9 with poorly developed middorsal process that barely surpasses the posterior margin (Fig. 2b). A pair of setae in laterodorsal position, and two pairs in ventromedial position (Figs. 2a, b, 3j and 4 h), one of them close to the border between the ventrolateral and ventromedial sections (Fig. 2a). One pair of sensory spots in subdorsal position; two pairs of sensory spots in laterodorsal and ventromedial positions, the last one located between the ventromedial setae (Figs. 2a, b, 3j and 4h). Nephridiopores not observed. Some specimens with epibiontic Ciliophora protozoans on the dorsal cuticular surface (Fig. 3l).

Segments 10 and 11 often retracted into precedent segment (Figs. 2a, b, 3a, b and 4a, b, i). Segment 10 with paired setae in lateroventral and ventrolateral positions and paired sensory spots in ventromedial position (Figs. 2d, 3k and 4i), all of them near the posterior segment margin. Segment 11 without cuticular appendages (Fig. 2d). Males with two pairs of penile spines and genital pores surrounded by tuft of long hairs in between segments 10 and 11 (Fig. 2d). Lateral terminal spines absent.

Notes on diagnostic and taxonomic features

Cristaphyes retractilis sp. nov. may be easily distinguished from most of its congeners by the lack of lateral terminal spines. Only *C. anomalus* (Lang, 1953) from Reloncaví Estuary (Chile, eastern Pacific Ocean), *C. belizensis* (Higgins, 1983) from Carrie Bow Cay (Belize, Caribbean Sea), *C. harrisoni* (Pardos et al., 2016) from Taboga Island (Panama, eastern Pacific Ocean), *C. panamensis* (Pardos et al., 2016) from Bastimento Island (Panama, Caribbean Sea), *C. phyllotropis* (Brown and Higgins, 1983) from Hunter Bay (Australia, western Pacific Ocean), *C. rabaulensis* (Adrianov, 1999 in Adrianov and Malakhov 1999) from Rabaul (Papua New Guinea, western Pacific Ocean), *C. spinosus* (Lang, 1949) from Falkland Islands (western Atlantic Ocean) and *C. yushini* (Adrianov, 1989) from the Seto Inland Sea (Japan, western Pacific Ocean) also lack lateral terminal spines (Lang 1949, 1953; Brown and Higgins 1983; Higgins 1983; Adrianov 1989; Adrianov and Malakhov 1999; Pardos et al. 2016a, b; Sánchez et al. 2016). *Cristaphyes retractilis* sp. nov. possesses paired paradorsal setae on segments 2, 4, 6 and 8, which is only shared with *C. harrisoni* (Pardos et al. 2016b; Sánchez et al. 2016), as the remaining species having a different paradorsal setae arrangement (paired on segments 3–6 and 8–9 in *C. anomalus*; unpaired on segments 2, 6, 8 and 9–10 and paired on segment 4 in *C. belizensis*; unpaired on segments 3, 5, 7 and 9–10 and paired on segments 2, 4, 6 and 8 in *C. panamensis*; at least unpaired on segments 2, 5–6 and 8 in *C. phyllotropis*; and unpaired on segments 2, 4, 6 and 8–9 in *C. yushini*) (Lang 1953; Brown and Higgins 1983; Higgins 1983; Adrianov 1989; Adrianov and Malakhov 1999; Pardos et al. 2016a; Sánchez et al. 2016). Nevertheless, *C. retractilis* sp. nov. and *C. harrisoni* are easily distinguished by the pattern of the ventral setae: the former has paired ventrolateral setae on segments 1, 3–8 and 10, one pair of ventromedial setae on segments 2–8 and two pairs of ventromedial setae on segment 9, whereas the latter is characterised by having paired ventrolateral setae on segments

1, 5 and 10 and paired ventromedial setae on segments 3–8 (Pardos et al. 2016b; Sánchez et al. 2016). The available information on setae arrangement of *C. rabaulensis and C. spinosus* is scarce (Lang 1949; Adrianov and Malakhov 1999; Sánchez et al. 2016), but the differences with *C. retractilis* sp. nov. are in the position of lateroventral setae: *C. rabaulensis* only has lateroventral setae on segment 6 (and possibly on segment 5) and *C. spinosus* on segments 2, 4 and 9–10 (and possibly on segment 5), while *C. retractilis* sp. nov. possesses lateroventral setae on all even segments (Lang 1949; Adrianov and Malakhov 1999; Sánchez et al. 2016).

Regarding the general setae arrangement, *C. retractilis* sp. nov. is most similar to *C. carinatus* (Zelinka, 1928) from Naples (Italy, Mediterranean Sea) by the presence of several pairs of setae in ventrolateral position (segments 1, 3–8 and 10 in *C. retractilis* sp. nov. and segments 3–9 in *C. carinatus*) (Zelinka 1928; Sánchez et al. 2016), as the remaining congeners possess ventrolateral setae only on one, two or three segments (Sánchez et al. 2016). Nevertheless, *C. retractilis* sp. nov. is characterised by possessing pairs of paradorsal setae on segments 2, 4, 6 and 8, one pair of lateroventral setae on segments 2, 4, 6, 8 and 10 and two pairs of ventromedial setae on segment 9 and by lacking lateral terminal spines, while *C. carinatus* has pairs of paradorsal setae on segments 1–9, one pair of lateroventral setae on segments 2–10, two pairs of ventromedial setae on segments 3–9 and a pair of lateral terminal spines (Zelinka 1928; Sánchez et al. 2016).

The ability to retract segments 10 and 11 into the preceding segments has not previously been observed in any *Cristaphyes*, although it has been described for other kinorhynchs, including *Echinoderes applicitus* Ostmann et al., 2012 from Java (western Pacific Ocean), *E. maxwelli* (Omer-Cooper, 1957) from South Africa, *E. strii* Pardos et al., 2016 from Pedro González Island (Panama, eastern Pacific Ocean) and *Pycnophyes alexandroi* Pardos et al., 2016 from Taboga Island (Panama, eastern Pacific Ocean) (Omer-Cooper 1957; Ostmann et al. 2012; Pardos et al. 2016a, b). This character is hardly explained as an artefact of the fixation or the preservation process because it has been frequently found in many specimens of samples from different localities, as also observed by Pardos et al. (2016b). Finally, the presence of two pairs of ventromedial setae on the same segment is only present in the newly described species (segment 9), *C. belizensis* (Higgins, 1983) from Carrie Bow Cay, Caribbean Sea (segments 4–9) and *C. carinatus* (segments 3–9) (Zelinka 1928; Higgins 1983; Sánchez et al. 2016).

Cristaphyes cf. *longicornis*

Material examined.

Non-type material. Seven adult females, four prepared for LM with Fluoromount G® and three prepared for SEM, collected on 03 November 1980 at Puerto Blanco Harbour, Dominican Republic, Hispaniola Island, western Atlantic Ocean: 19° 54′ 24″ N, 70° 56′ 24″ W (L2) (Table 1; Fig. 1b) at 3 m depth in silty mud, deposited at NMHN under acces-sion numbers: USNM 1490937–1490941.

Description

The morphology of the examined specimens generally followed the original description of *Cristaphyes longicornis* (Higgins, 1983). Hence, only deviations from the original description are mentioned in the following.

Segment 1 with paired ventrolateral sensory spots located near the posterior margin of segment (Fig. 5a). Segments 6 and 8 with paired lateroventral setae (Fig. 5b), as reported in the original description but not observed in the type material by Sánchez et al. (2016). Segment 10 lacking lateroventral setae, bearing a pair of widened ventrolateral sensory spots located near the posterior margin of segment (Fig. 5c). Secondary pectinate fringe on segments 1–11 developed as three transverse finely serrated fringes, two of them near the anterior segments margins, the other one almost reaching the posterior margin (Fig. 5d). Conspicuous paraventral apodemes present on segments 9–10. Cuticular hairs on seg-ments 1–11 very small, scale-like, basally widened, abruptly tapering, randomly distributed through tergal and sternal cu-ticular plates (Fig. 5e), densely covering a middorsal bulging on segment 10 (Fig. 5f).

Notes on diagnostic and taxonomic features

Several *Cristaphyes* specimens were studied and herein reported as *C.* cf. *longicornis*, as they agree with the main diagnostic characters of the species: trunk tapering slightly beginning with segment 7, lateral terminal spines long and recurved at tip, middorsal processes on segments 2–10, unpaired paradorsal setae on segments 4, 6 and 8, laterodorsal setae on segments 2–9, paralateral setae on segment 1, lateroventral setae on segments 2, 4 and 10, ventrolateral setae on segments 5 and 10, ventromedial setae on segments 1 and 3–9 and males with sexually dimorphic tubes in ventromedial position on segment 2 (Higgins 1983; Sánchez et al. 2016).

Some morphological differences from the original description were observed, including the presence of paired ventrolateral sensory spots located near the posterior margin of segment 1 and the absence of lateroventral setae on segment 10. Additionally, Higgins (1983) determined the presence of lateroventral setae on segments 2, 4, 6 and 8, but according to the revision of the type material by Sánchez et al. (2016), *C. longicornis* possesses these structures only on segments 2 and 4. The specimens herein reported as *C.* cf. *longicornis* also possess lateroventral setae on segments 6 and 8, as originally described.

The observed morphological discrepancies may have passed unnoticed to Higgins (1983) and Sánchez et al. (2016) likely because they are barely seen under LM and the badly preserved type material, preventing proper observation of the cuticular characters. However, intraspecific variation in the arrangement

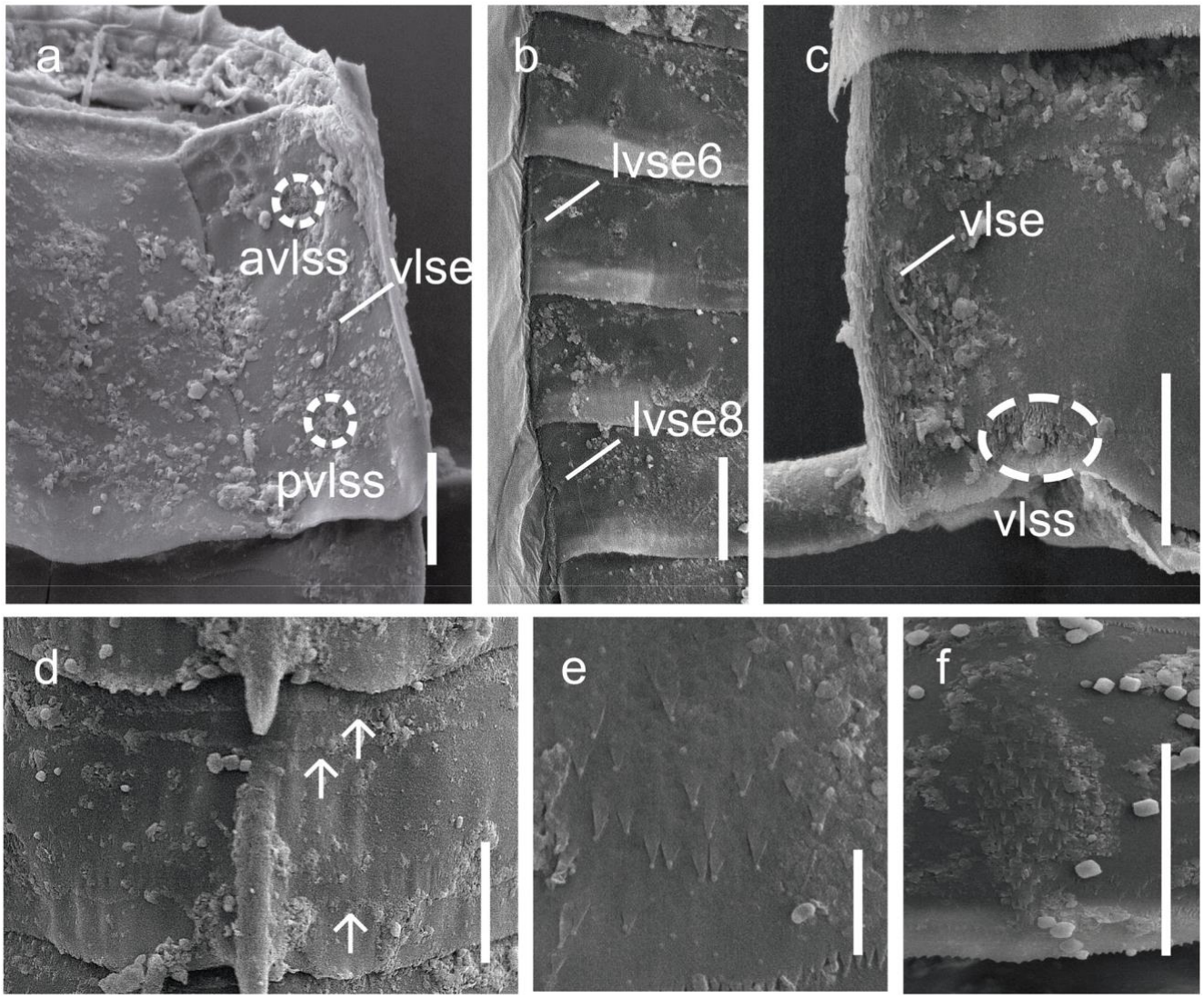

Fig. 5 Scanning electron micrographs showing details in the cuticular trunk morphology of *Cristaphyes* cf. *longicornis*. **a** Ventrolateral region on right half of sternal plates of segment 1; **b** Lateroventral region on left half of sternal plates of segments 5–8; **c** Ventrolateral region on left half of sternal plates of segment 10; **d** Middorsal, paradorsal and subdorsal regions of tergal plate of segment 3, arrows mark the secondary pectinate fringes; **e** Detail of cuticular hairs of segment 9 sternal plate; **f** Detail of cuticular, hairy bulging of segment 10. Scales: **a**, **c**, **d**, **f**: 10 μm; **b**: 20 μm; **e**: 2 μm. *avlss* anterior ventrolateral sensory spot, *lvse* lateroventral seta, *pvlss* posterior ventrolateral sensory spot, *vlse* ventrolateral seta, *vlss* ventrolateral sensory spot; sensory spots are marked as dashed circles

of sensory spots of segment 1 and lateroventral setae may exist, defining morphologically different populations through the Caribbean Basin. Moreover, the presence of paired posterior ventrolateral sensory spots on segment 1, paired lateroventral setae on segments 6 and 8 and the absence of paired lateroventral setae on segment 10 in the specimens collected from Hispaniola Island could indicate the existence of a new species. However, we do not consider this morphological variation as sufficient to erect a new species, especially when taking the bad preservation stage of the type specimens into account.

Genus ***Fujuriphyes*** Sánchez et al., 2016
Fujuriphyes dalii sp. nov.
(Figs. 6, 7 and 8 and Tables 4 and 5)

Material examined

Type material. Holotype, adult male, collected on 02 November 1980 at 200 m east of Puerto Plata Harbour, Dominican Republic, Hispaniola Island, western Atlantic Ocean: 19°48′ 12″ N, 70° 42′ 00″ W (L1) (Table 1; Fig. 1b) at 4–5 m depth in brown sandy mud; mounted in Fluoromount G®, deposited at NMHN under accession number: USNM 1490942. Paratypes, 8 adult males and 8 adult females; 14 of them with same collecting data as holotype, mounted in

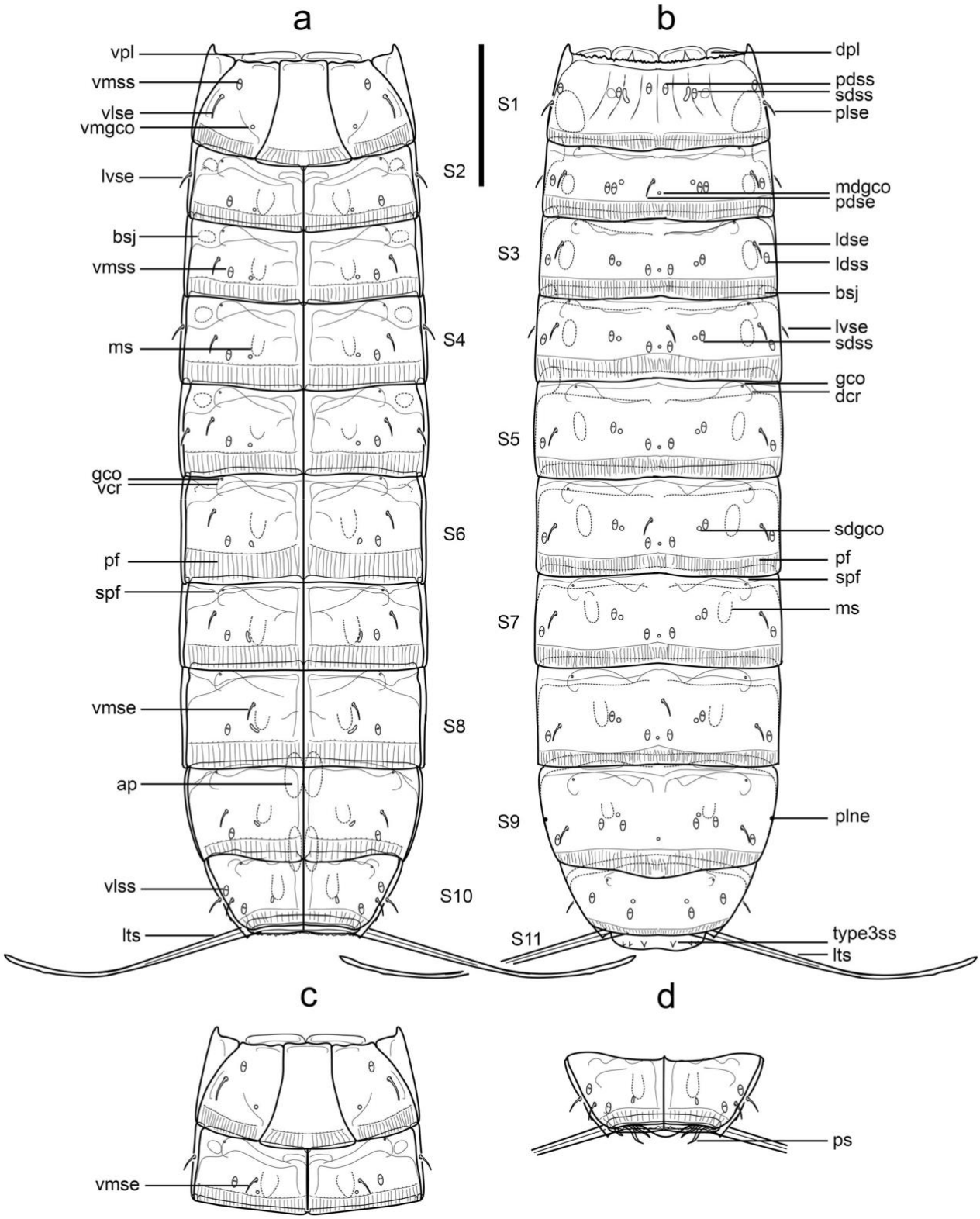

Fig. 6 Line art illustrations of *Fujuriphyes dalii* sp. nov. **a** Male, ventral view; **b** Male, dorsal view; **c** Female, segments 1–2, ventral view; **d** Male, segments 10–11, ventral view. Scale: 50 µm. *ap* apodeme, *bsj* ball-and-socket joint, *dcr* dorsal cuticular ridge, *dpl* dorsal placid, *gco* glandular cell outlet, *ldse* laterodorsal seta, *ldss* laterodorsal sensory spot, *lts* lateral terminal spine, *lvse* lateroventral seta, *mdgco* middorsal glandular cell outlet, *ms* muscular scar, *pdse* paradorsal seta, *pdss* paradorsal sensory spot, *pf* pectinate fringe, *plne* paralateral nephridiopore, *plse* paralateral seta, *ps* penile spine, *S* segment followed by number of corresponding segment, *sdgco* subdorsal glandular cell outlet, *sdss* subdorsal sensory spot, *spf* secondary pectinate fringe, *type3ss* type 3 sensory spot, *vcr* ventral cuticular ridge, *vlse* ventrolateral seta, *vlss* ventrolateral sensory spot, *vmgco* ventromedial glandular cell outlet, *vmse* ventromedial seta, *vmss* ventromedial sensory spot, *vpl* ventral placid

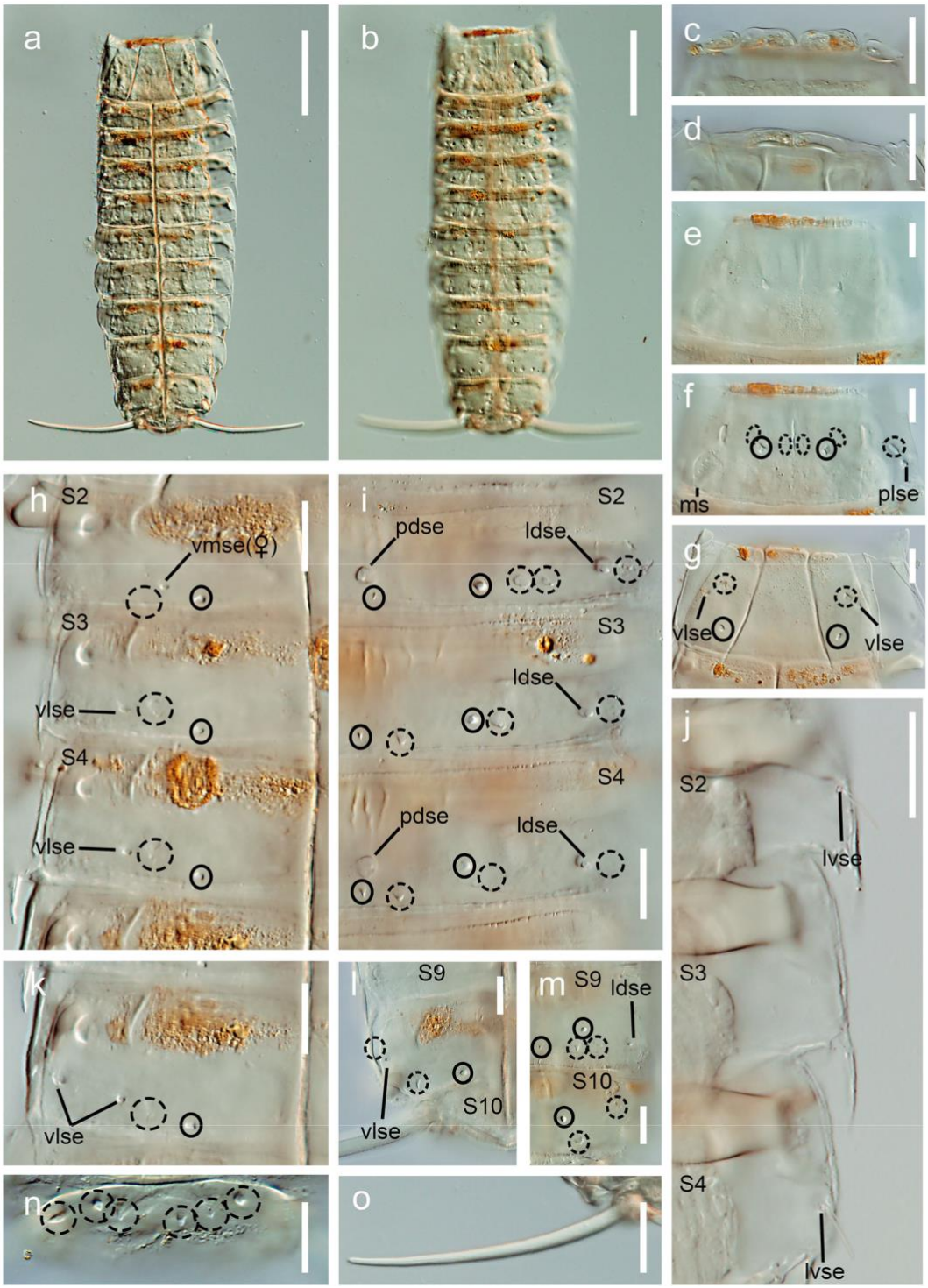

Fig. 7 Light micrographs showing trunk overview and cuticular details in the segments of *Fujuriphyes dalii* sp. nov. **a** Ventral overview of trunk; **b** Dorsal overview of trunk; **c** Dorsal placids; **d** Ventral placids; **e** Dorsal overview of segment 1, showing the strongly denticulated anterior margin of tergal plate followed by a crenulated area with high longitudinal ridges and regions of the tergal plate superficially spotted; **f** Dorsal view of segment 1; **g** Ventral view of segment 1; **h** Ventrolateral and ventromedial regions on left half of sternal plates of segments 2–4; **i** Middorsal, paradorsal, subdorsal and laterodorsal regions on right half of tergal plates of segments 2–4; **j** Lateroventral region on right half of tergal plates of segments 2–4; **k** Ventrolateral and ventromedial regions on left half of sternal plates of segment 5; **l** Ventrolateral and ventromedial regions on left half of sternal plates of segment 10; **m** Middorsal, paradorsal, subdorsal and laterodorsal regions on right half of tergal plates of segments 9–10; **n** Dorsal view of segment 11; **o** Detail of the left lateral terminal spine. Scales: **a**, **b**, 100 μm; **c**–**n**, 20 μm; **o**, 50 μm. *ldse* laterodorsal seta, *lvse* lateroventral seta, *ms* muscular scar, *pdse* paradorsal seta, *plse* paralateral seta, *S* segment followed by number of corresponding segment, *vlse* ventrolateral seta, *vmse* ventromedial seta; sensory spots are marked as dashed circles, and glandular cell outlets as continuous circles

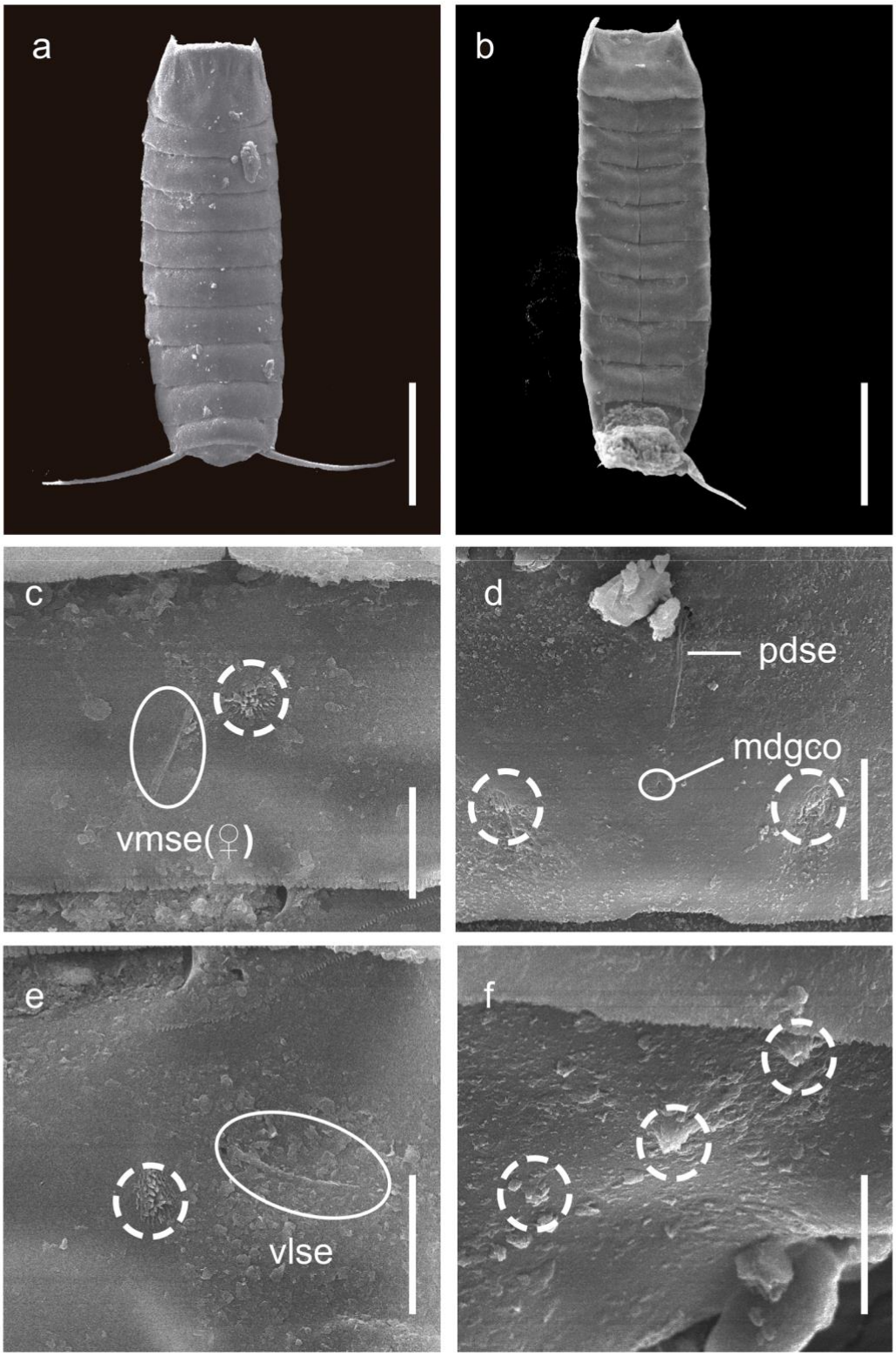

Fig. 8 Scanning electron micrographs showing overviews and details in the cuticular trunk morphology of *Fujuriphyes dalii* sp. nov. **a** Dorsal overview of trunk; **b** Ventral overview of trunk; **c** Ventromedial region on left half of sternal plates of segment 2, showing the sensory spot and the female sexually dimorphic seta; **d** Middorsal and paradorsal regions of tergal plate of segment 4, showing the middorsal glandular cell outlet, the paradorsal seta and the paradorsal sensory spots; **e** Ventrolateral region on left half of sternal plates of segment 4, showing the ventromedial sensory spot and the ventrolateral seta; **f** Subdorsal and laterodorsal regions on right half of tergal plate of segment 11, showing the type 3 sensory spots. Scales: **a**, **b**: 100 μm; **c**–**e**: 10 μm; **f**: 5 μm. *mdgco* middorsal glandular cell outlet, *pdse* paradorsal seta, *vlse* ventrolateral seta, *vmse* ventromedial seta; sensory spots are marked as dashed circles, and setae and glandular cell outlets as continuous circles

Table 4 Measurements of adult *Fujuriphyes dalii* sp. nov. from Hispaniola Island, including number of measured specimens (*n*), mean of data and standard deviation (SD). There were no remarkable differences in sizes or dimensions between the two sexes or sampling locations.

Character	Range	Mean (SD; **n**)
TL (μm)	424.1–627.6	495.0 (44.4; 17)
MSW-5 (μm)	140.9–177.6	155.5 (10.3; 17)
MSW-5/TL (%)	28.3–33.5	31.5 (1.2; 17)
SW-10 (μm)	103.2–134.9	120.4 (8.8; 17)
SW-10/TL (%)	21.5–24.9	24.4 (0.8; 17)
S1 (μm)	76.6–104.8	90.0 (8.5; 17)
S2 (μm)	34.8–65.2	47.3 (7.3; 17)
S3 (μm)	37.9–78.9	54.4 (7.6; 17)
S4 (μm)	47.8–83.6	59.2 (7.7; 17)
S5 (μm)	50.7–83.2	59.5 (7.4; 17)
S6 (μm)	50.6–83.6	61.2 (7.4; 17)
S7 (μm)	55.8–84.9	62.9 (6.6; 17)
S8 (μm)	55.5–89.9	64.0 (8.5; 17)
S9 (μm)	51.1–81.3	63.3 (8.0; 17)
S10 (μm)	45.1–91.7	53.4 (10.3; 17)
S11 (μm)	18.9–39.5	29.7 (6.3; 17)
LTS (μm)	106.7–186.4	149.6 (19.7; 17)
LTS/TL (%)	25.1–31.9	30.2 (2.1; 17)

LTS lateral terminal spine, *MSW-5* maximum sternal width (on segment 5), *S* segment lengths, *SW-10* standard width (on segment 10), *TL* total length of trunk

Fluoromount G® and deposited at NMHN under accession numbers: USNM 1490943-1490956; 2 of them collected on 06 November 1980 at Monte Cristi Bay, south-western of Capra Island, Dominican Republic, Hispaniola Island, western Atlantic Ocean: 19° 53′ 12″ N, 71° 40′ 00″ W (L3) (Table 1; Fig. 1b), at 3–4 m depth in muddy sand associated with assemblages of *Thalassia* sp., mounted in Fluoromount G®, deposited at NMHN under accession numbers: USNM 1490957-1490958.

Non-type material. Two additional specimens from the same locality of the holotype, mounted for SEM, also deposited at NMHN under accession number USNM 1490959.

Diagnosis

Fujuriphyes without middorsal processes or elevations; anterior margin of first segment strongly denticulated, followed by a crenulated area with elevated longitudinal ridges; ball-and-socket joints present on segments 2–5; unpaired paradorsal setae on segments 2, 4, 6 and 8, paired laterodorsal setae on segments 2–9, paired paralateral setae on segment 1, paired lateroventral setae on segments 2, 4 and 10, paired ventrolateral setae on segments 1, 3–7 and 10 (two pairs on segment 5), and a pair of ventromedial setae on segment 8–9.

Etymology

The name is dedicated to the prominent Spanish surrealist Salvador Dalí (1904–1989), whose peculiar moustache resembles the shape of the lateral terminal spines of the species.

Description

See Table 4 for measurements and dimensions, and Table 5 for summary of seta, spine, nephridiopore, glandular cell outlet and sensory spot locations.

Head and neck. Head with retractable mouth cone and introvert. The collected specimens were not suitable for head examinations, hence data on number and arrangement of scalids and oral styles is not available.

Neck with four dorsal and two ventral sclerotized placids (Figs. 6a–c and 7c, d). Dorsal placids rectangular, wide (Figs. 6b and 7c); mesial ones broader, with a small indentation in the middle of the posterior margin (Figs. 6b and 7c); lateral ones narrower (Figs. 6b and 7c). Ventral placids also

Table 5 Summary of nature and arrangement of sensory spots, glandular cell outlets, nephridiopores, setae and spines in *Fujuriphyes dalii* sp. nov.

Segment	MD	PD	SD	LD	PL	LV	VL	VM
1		ss	gco, ss	ss	se		se	ss, gco
2	gco	se*	gco, ssx2	gco, se, ss		se	gco	ss, se(f), gco
3	gco	ss	gco, ss	gco, se, ss			se, gco	ss, gco
4	gco	se*, ss	gco, ss	gco, se, ss		se	se, gco	ss, gco
5	gco	ss	gco, ss	gco, se, ss			sex2, gco	ss, gco
6	gco	se*, ss	gco, ss	gco, se, ss			se, gco	ss, gco
7	gco	ss	gco, ss	gco, se, ss			se, gco	ss, gco
8	gco	se*, ss	gco, ss	gco, se, ss			gco	ss, se, gco
9	gco		gco, ssx2	gco, se, ss	ne		gco	se, ss, gco
10			gco, ss	gco, ss		se	ss, se, ss, gco	gco
11			ss3	ss3x2		lts, psx2 (m)		

f female condition of sexually dimorphic character, *gco* glandular cell outlet, *LD* laterodorsal, *lts* lateral terminal spine, *LV* lateroventral, *m* male condition of sexually dimorphic character, *MD* middorsal, *ne* nephridiopore, *PD* paradorsal, *PL* paralateral, *ps* penile spine, *SD* subdorsal, *se* seta, *ss* sensory spot, *VL* ventrolateral, *VM* ventromedial; * indicates that the structure is unpaired.

rectangular but much more elongate, getting narrower towards the lateral sides (Figs. 6a, c and 7d).

Trunk. Trunk with 11 segments (Figs. 6a, b, 7a, b and 8a, b). Segment 1 with one tergal, two episternal and one trapezoidal midsternal plate; remaining segments with one tergal and two sternal cuticular plates (Figs. 6a–d, 7a, b and 8a, b). Midsternal and tergosternal junctions as conspicuous lines externally on the cuticle (Figs. 6a, c–d, 7a and 8b). Sternal plates reach their maximum width at segment 5, but almost constant in width throughout the trunk, slightly tapering at the last trunk segments (Figs. 6a, b, 7a, b and 8a, b). Sternal cuticular plates wide in ratio of maximum sternal width to trunk lenght (MSW-5:TL average ratio = 33.2%), giving the animal a plump appearance (Figs. 6a, b, 7a, b and 8a, b). Middorsal processes and elevations absent. Segments 2–9 with minute glandular cell outlets in middorsal position (Figs. 6b, 7i, m and 8d). Segments 2–10 furthermore with paired, oval, elongated glandular cell outlets in subdorsal position (Figs. 6b, and 7f, i, m). Segments 2–10 also with paired cuticular ridges in laterodorsal position followed by small, intracuticular wrinkled glandular cell outlets located on their inner posterior margin (Fig. 6b). Segments 1–10 furthermore with paired, rounded to oval glandular cell outlets in ventromedial position (first pair laterally displaced to ventrolateral position) (Figs. 6a, c and 7g–h, k, l). Segments 2–10 furthermore with paired ventral cuticular ridges marking the ventrolateral-ventromedial limit followed by small, intracuticular wrinkled glandular cell outlets located on their inner posterior margin (Fig. 6a, c). Cuticular hairs only on the tergosternal junction. Pachycycli and ball-and-socket joints on segments 2–5 (Fig. 6a, b). Paraventral apodemes on segments 9–10 (Fig. 6a). Pectinate fringe finely serrated (Figs. 6a–d), appears smooth under LM (Fig. 7f–i, k–m); secondary pectinate fringe also finely serrated (Fig. 6a, b); free flaps extend around the posterior segment margins. Muscular scars oval (Fig. 6a–d), scarcely detectable on most segments.

Segment 1 without middorsal cuticular processes and elevations. Anterolateral margins of the tergal cuticular plate as horn-shaped extensions (Figs. 6a–c, 7a, b, g and 8a, b). Anterior margin of tergal plate strongly denticulated, followed by a crenulated area with high longitudinal ridges (Figs. 6b, 7e and 8a). Paired setae in paralateral and ventrolateral positions (Figs. 6a–c and 7f–g). Paired sensory spots in paradorsal, subdorsal, laterodorsal and ventromedial positions, all of them located at the anterior half of the cuticular plates (Figs. 6a–c and 7f, g); sensory spots on this and remaining segments rounded to oval, with several rings of cuticular papillae surrounding a central pore (Fig. 8c–e).

Segment 2 without middorsal cuticular processes and elevations. Unpaired seta in paradorsal position (Figs. 6b and 7i). Paired setae in laterodorsal and lateroventral positions (Figs. 6a–c and 7i, j); laterodorsal pair located a bit more lateral than the muscular scar (Fig. 6b). Two pairs of sensory spots in subdorsal position; one pair of sensory spots in laterodorsal and ventromedial positions (Figs. 6a–c, 7h, i and 8c). Both males and females without ventromedial tubes, females with paired ventromedial setae (Figs. 6c, 7h and 8c).

Segment 3 without middorsal cuticular processes and elevations. Paired setae in laterodorsal and ventrolateral positions (Figs. 6a, b and 7h, i). Paired sensory spots in paradorsal, subdorsal, laterodorsal and ventromedial positions (Figs. 6a, b and 7h, i).

Segment 4 without middorsal cuticular processes and elevations. Unpaired seta in paradorsal position (Figs. 6b, 7i and 8d). Paired setae in laterodorsal, lateroventral and ventrolateral positions (Figs. 6a, b, 7h–j and 8e). Paired sensory spots in paradorsal, subdorsal, laterodorsal and ventromedial positions (Figs. 6a, b, 7h, i and 8d, e).

Segment 5 without middorsal cuticular processes and elevations. A pair of setae in laterodorsal position; two pairs of setae in ventrolateral position (Figs. 6a, b and 7k). A pair of sensory spots in paradorsal, subdorsal, laterodorsal and ventromedial positions (Figs. 6a, b and7k).

Segment 6 without middorsal cuticular processes and elevations. Unpaired seta in paradorsal position (Fig. 6b). Paired setae in laterodorsal and ventrolateral positions (Fig. 6a, b). Paired sensory spots in paradorsal, subdorsal, laterodorsal and ventromedial positions (Fig. 6a, b).

Segment 7 similar to segment 3 (Fig. 6a, b).

Segment 8 without middorsal cuticular processes and elevations. Unpaired seta in paradorsal position (Fig. 6b). Paired setae in laterodorsal and ventromedial positions (Fig. 6a, b). Paired sensory spots in paradorsal, subdorsal, laterodorsal and ventromedial positions (Fig. 6a, b).

Segment 9 without middorsal cuticular processes and elevations. Protonephridial opnenings in paralateral position (Fig. 6b). Paired setae in laterodorsal and ventromedial positions; ventromedial setae laterally shifted, not aligned with segment 8 ventromedial setae (Fig. 6a, b). Two pairs of sensory spots in subdorsal position plus one pair of sensory spots in laterodorsal and ventromedial positions (Figs. 6a, b and 7m).

Segment 10 without middorsal cuticular processes and elevations. Paired setae in lateroventral and ventrolateral positions (the latter flanked by the sensory spots) (Figs. 6a, b and 7l, m). A pair of sensory spots in subdorsal and laterodorsal positions (the latter near the posterior margin of the tergal plate); two pairs of sensory spots in ventrolateral position (Figs. 6a, b and 7l,m).

Segment 11 with three pairs of type 3 sensory spots, one pair in subdorsal and two pairs in laterodorsal positions (Figs. 6b, 7n and 8f). Posterior ventral margin conspicuously serrated. Males with two pairs of penile spines and genital pores surrounded by tuft of long hairs in between segments 10 and 11 (Fig. 6d). Lateral terminal spines long (LTS:TL average ratio = 30.2%), stout, wide, apparently flexible (Figs. 6a, b, 7a, b, o and 8a, b).

Notes on diagnostic and taxonomic features

Currently, the genus accomodates six species: two from the Caribbean Sea, *Fujuriphyes deirophorus* (Higgins, 1983) and *Fujuriphyes distentus* (Higgins, 1983), one from the Gulf of Mexico, *Fujuriphyes viserioni* Sánchez, et al. 2019, one from the East China Sea, *Fujuriphyes longispinosus* Sánchez and Yamasaki, 2016, one from the Black and Mediterranean Seas, *Fujuriphyes ponticus* (Reinhard, 1881) and one from the Mediterranean Sea, *Fujuriphyes rugosus* (Zelinka, 1928) (Reinhard 1881; Zelinka 1928; Higgins 1983; Sánchez et al. 2012, 2016, 2019; Sánchez and Yamasaki 2016). *Fujuriphyes dalii* sp. nov. is easily distinguished from its congeners by the presence of paralateral setae on segment 1, lateroventral setae on segments 2, 4 and 10, a single pair of ventrolateral setae on segments 1, 3–7 and 10, with an extra pair on segment 5, ventromedial setae only on segments 8–9 and by the absence of male ventromedial tubes on segment 2 (see Reinhard 1881; Zelinka 1928; Higgins 1983; Sánchez and Yamasaki 2016; Sánchez et al. 2019 for original description of all known species of the genus and appendix of Sánchez et al. 2016 for updated morphological characters).

Fujuriphyes dalii sp. nov. lacks middorsal cuticular processes and elevations, whereas the remaining congeners posseess middorsal elevations on segments 1–9 (*F. deirophorus* and *F. distentus*), on segments 2–9 (*F. ponticus* and *F. rugosus*), on segment 3 (*F. viserioni*) or, at least, on segments 1–6 (*F. longispinosus*) (Reinhard 1881; Zelinka 1928; Higgins 1983; Sánchez and Yamasaki 2016; Sánchez et al. 2016, 2019). Regarding the setae arrangement, the recently described *F. longispinosus* from Nagannu Island, Japan (East China Sea) shows most resemblance to *F. dalii* sp. nov., as both species have two pairs of ventrolateral setae on segment 5 and a relatively low number of ventromedial setae (*F. dalii* sp. nov. possesses a pair of ventromedial setae on segments 8–9 and *F. longispinosus* is characterised by having paired, ventromedial setae on segments 2 and 9) (Sánchez and Yamasaki 2016; Sánchez et al. 2016). However, the arrangement of ventrolateral setae of *F. dalii* sp. nov. (one pair on segments 1, 3, 4, 6, 7 and 10, and two pairs on segment 5) is unique among its congeners. Furthermore, *F. dalii* sp. nov. lacks male-specific ventromedial tubes on segment 2 as *F. longispinosus*, *F. ponticus* and *F. rugosus* (Reinhard 1881; Zelinka 1928; Sánchez and Yamasaki 2016; Sánchez et al. 2016), whereas *F. deirophorus* and *F. distentus* possess these structures (Higgins 1983; Sánchez et al. 2016). Moreover, *F. dalii* sp. nov. has lateral terminal spines as *F. longispinosus*, *F. ponticus* and *F. rugosus* (Reinhard 1881; Zelinka 1928; Sánchez and Yamasaki 2016; Sánchez et al. 2016), while *F. deirophorus* and *F. distentus* lack lateral terminal spines (Higgins 1983; Sánchez et al. 2016).

Class **Cyclorhagida** (Zelinka, 1896) Sørensen et al. 2015
Family **Echinoderidae** Zelinka, 1894
Genus ***Echinoderes*** Claparède, 1863.
Echinoderes brevipes sp. nov.
(Figs. 9 and 10 and Tables 6 and 7)

Material examined.

Type material. Holotype, adult male, collected on 08 May 1976 off Santo Domingo, Dominican Republic, Hispaniola Island, Caribbean Sea: 18° 28′ 00″ N, 69° 57′ 00″ W (L7) (Table 1; Fig. 1b) at 0.7–1.0 m depth in an unknown sediment; mounted in Fluoromount G®, deposited at NMNH under accession number: USNM 1490960. Paratypes, two adult females and two adult males; all of them same collecting data as holotype, mounted in Fluoromount G® and deposited at NMNH under accession numbers: USNM 1490961–1490964.

Diagnosis

Echinoderes with middorsal spines on segments 4, 6, 8, increasing in length posteriorly; subdorsal and ventrolateral tubes plus sublateral glandular cell outlets type 2 on segment 2; lateroventral tubes on segment 5 and lateroventral spines on segments 6–9; lateral accessory tubes on segments 6–8; laterodorsal tubes on segments 8 and 10. Lateral terminal spines very short.

Etymology

From the Latin ‘brevis’, meaning short, and ‘pes’, meaning foot, which refers to the possession of conspicuously very short lateral terminal spines compared to the total trunk length of the species.

Description

See Table 6 for measurements and dimensions, and Table 7 for summary of spine, tube, nephridiopore, glandular cell out-let and sensory spot locations.

Head and neck. Head with retractable mouth cone and introvert (Fig. 10a–d). Internal part of mouth cone with several rings of inner oral styles; exact number, arrangement and morphology of inner oral styles not determined. External part of mouth cone with nine outer oral styles (Fig. 10c, d). Outer oral styles alternate in size between slightly longer and slightly shorter ones (Fig. 10c, d). Five long styles appear anterior to the odd numbered introvert sections, whereas four slightly shorter ones appear anterior to the even numbered ones, except in the middorsal section 6 where a style is missing (Fig. 10c, d). Outer oral styles with two jointed subunits, with a rectangular basis bearing a short fringe at its base, and a triangular, hook-like distal structure (Fig. 10c, d).

Introvert with seven rings of cuticular spinoscalids (Fig. 10c, d). Ring 01 with ten primary spinoscalids consisting of a short basal sheath and a distal end piece (Fig. 10c, d). Basal sheath with a proximal long fringe situated very close to the insertion point, bearing several flexible, elongated fringe tips, followed by a smooth part bearing another fringe with several long, flexible tips (Fig. 10c, d). Distal piece of the primary spinoscalids wide, rounded in cross-section, smooth, hook-like, with blunt tip (Fig. 10c, d). Remaining rings bear spinoscalids laterally compressed, with a long, smooth basis and elongate, thin, hook-like distal piece (Fig. 10c, d). Exact number, arrangement and detailed morphology of these spinoscalids not determined as they tended to be collapsed when mounted.

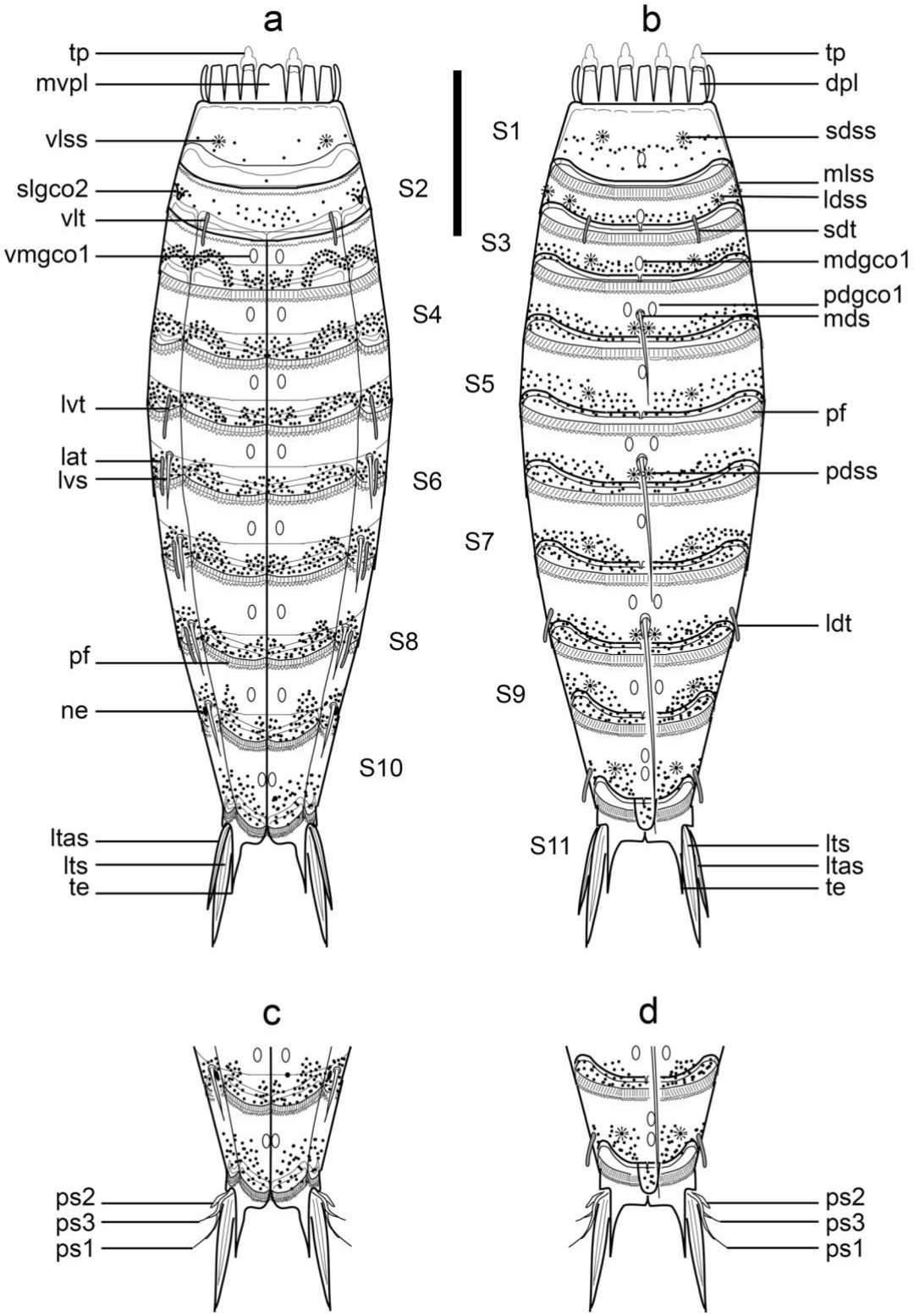

Fig. 9 Line art illustrations of *Echinoderes brevipes* sp. nov. **a** Female, ventral view; **b** Female, dorsal view; **c** Male, segments 10–11, ventral view; **d** Male, segments 10–11, dorsal view. Scale: 50 μm. *dpl* dorsal placid, *lat* lateral accessory tube, *ldss* laterodorsal sensory spot, *ldt* laterodorsal tube, *ltas* lateral terminal accessory spine, *lts* lateral terminal spine, *lvs* lateroventral spine, *lvt* lateroventral tube, *mdgco1* middorsal type 1 glandular cell outlet, *mds* middorsal spine, *mlss* midlateral sensory spot, *mvpl* midventral placid, *ne* nephridiopore, *pdgco1* paradorsal type 1 glandular cell outlet, *pdss* paradorsal sensory spot, *pf* pectinate fringe, *ps* penile spine, *sdss* subdorsal sensory spot, *sdt* subdorsal tube, *slgco2* sublateral type 2 glandular cell outlet, *te* tergal extension, *tp* trichoscalid plate, *vlss* ventrolateral sensory spot, *vlt* ventrolateral tube, *vmgco1* ventromedial type 1 glandular cell outlet

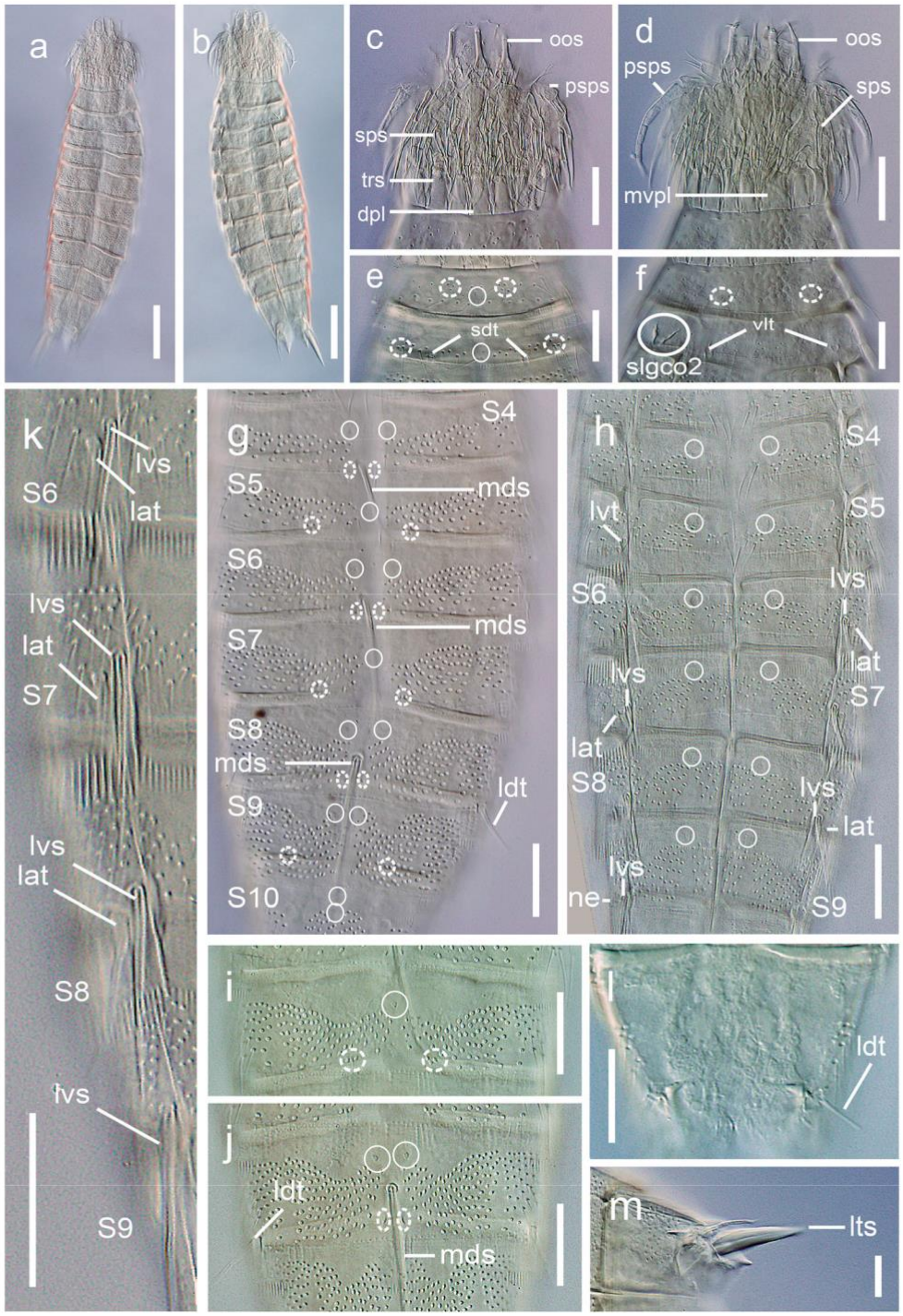

Fig. 10 Light micrographs showing trunk overview and cuticular details in the segments of *Echinoderes brevipes* sp. nov. **a** Dorsal overview of trunk; **b** Ventral overview of trunk; **c** Dorsal view of introvert and neck, showing the dorsal placids and some trichoscalids, spinoscalids and outer oral styles; **d** Ventral view of introvert and neck, showing the ventral placids and some spinoscalids and outer oral styles; **e** Dorsal view of segments 1–2; **f** Ventral view of segments 1–2; **g** Dorsal overview of segments 4–10; **h** Ventral overview of segments 4–9; **i** Middorsal, paradorsal, subdorsal and laterodorsal regions of tergal plate of segment 7; **j** Middorsal, paradorsal, subdorsal and laterodorsal regions of tergal plate of segment 8; **k** Lateroventral region on left half of tergal plate of segments 6–9; **l** Middorsal, paradorsal, subdorsal and laterodorsal regions of tergal plate of segment 10; **m** Detail of a lateral terminal spine. Scales: **a**, **b**: 50 µm; **c**–**m**: 20 µm. *dpl* dorsal placid, *lat* lateral accessory tube, *ldt* laterodorsal tube, *lts* lateral terminal spine, *lvs* lateroventral spine, *lvt* lateroventral tube, *mds* middorsal spine, *mvpl* midventral placid, *oos* outer oral style, *psps* primary spinoscalid, *S* segment followed by number of corresponding segment, *sdt* subdorsal tube, *slgco2* sublateral type 2 glandular cell outlet, *sps* spinoscalid, *trs* trichoscalid, *vlt* ventrolateral tube; type 1 glandular cell outlets are marked as continuous circles and sensory spots as dashed circles

Table 6 Measurements of adult *Echinoderes brevipes* sp. nov. from Hispaniola Island, including number of measured specimens (*n*), mean of data and standard deviation (SD). There were no remarkable differences in sizes or dimensions between the two sexes

Character	Range	Mean (SD; *n*)
TL (µm)	235.7–265.6	252.3 (12.9; 5)
MSW-5 (µm)	58.4–65.6	61.9 (2.9; 5)
MSW-5/TL (%)	22.0–26.2	24.6 (2.0; 5)
SW-10 (µm)	47.5–53.8	50.5 (2.6; 5)
SW-10/TL (%)	17.9–22.1	20.0 (1.7; 5)
S1 (µm)	26.3–29.4	28.2 (1.3; 5)
S2 (µm)	19.4–30.7	25.2 (4.2; 5)
S3 (µm)	18.1–27.2	25.1 (4.9; 5)
S4 (µm)	21.8–33.3	27.7 (4.5; 5)
S5 (µm)	28.8–40.5	32.7 (4.6; 5)
S6 (µm)	36.5–49.1	39.5 (5.4; 5)
S7 (µm)	36.6–42.9	39.1 (2.5; 5)
S8 (µm)	35.8–44.6	41.1 (3.2; 5)
S9 (µm)	35.2–43.0	39.4 (3.0; 5)
S10 (µm)	38.4–42.4	40.5 (1.7; 5)
S11 (µm)	28.5–30.1	28.6 (1.3; 5)
SD2 (tu) (µm)	9.21–15.9	14.8 (3.4; 5)
VL2 (tu) (µm)	8.7–16.3	13.0 (3.1; 5)
MD4 (ac) (µm)	29.9–31.5	30.6 (0.8; 3)
LV5 (tu) (µm)	10.3–17.4	14.6 (3.8; 5)
MD6 (ac) (µm)	38.4–54.7	44.0 (7.4; 4)
LV6 (ac) (µm)	17.5–24.6	20.9 (2.6; 5)
LA6 (tu) (µm)	10.4–14.0	12.1 (1.3; 5)
LV7 (ac) (µm)	22.7–28.1	24.7 (2.7; 5)
LA7 (tu) (µm)	11.0–14.4	12.2 (1.6; 5)
MD8 (ac) (µm)	69.0–85.5	76.6 (8.4; 4)
LD8 (tu) (µm)	15.1–17.0	15.9 (0.7; 5)
LV8 (ac) (µm)	24.1–29.9	26.7 (2.3; 5)
LA8 (tu) (µm)	9.8–17.9	13.4 (3.4; 5)
LV9 (ac) (µm)	21.2–29.0	24.9 (3.1; 5)
LD10 (tu) (µm)	10.8–13.0	11.8 (0.9; 5)
LTS (µm)	26.9–36.6	31.8 (5.2; 4)
LTAS (µm)	18.0–19.3	18.7 (0.6; 2)
LTS/TL (%)	10.1–14.7	12.5 (2.5; 4)

ac acicular spine, *LA* lateral accessory, *LTAS* lateral terminal accessory spine, *LTS* lateral terminal spine, *LV* lateroventral, *MD* middorsal, *MSW-5* maximum sternal width (on segment 5), *S* segment lengths, *SD* subdorsal, *SW-10* standard width (on segment 10), *TL* total length of trunk, *tu* tube, *VL* ventrolateral

Neck with 16 trapezoidal placids, wider at base, with a distinct joint between the neck and segment 1 (Figs. 9a, b and 10c, d); midventral one widest (ca. 12 µm wide at base) (Figs. 9a and 10d), remaining ones alternate between wider and narrower (6–9 µm at base) (Figs. 9b and 10c). Placids closely situated together at base, distally separated by cuticular folds (Figs. 9a, b and 10c, d). A ring of six long, hairy trichoscalids associated with the placids of the neck is present, attached to small trichoscalid plates (Fig. 10c, d).

Trunk. Trunk with 11 segments (Figs. 9a, b and 10a, b). Segments 1–2 as closed cuticular rings; remaining ones with one tergal and two sternal cuticular plates (Figs. 9a, b and 10a, b). Midsternal junction as conspicuous line on the cuticle; tergosternal junctions mostly subcuticular (Figs. 9a, c and 10a, b). Tergal plates of anterior segments slightly bulging middorsally; posterior ones more flattened, giving the animal a tapering outline in lateral view. Sternal plates reach their maximum width at segment 5, progressively tapering towards the last trunk segments (Figs. 9a,b and 10a, b). Sternal plates relatively narrow compared to the total trunk length (MSW-5:TL average ratio = 24.6%), giving the animal a slender appearance (Figs. 9a, b and 10a, b).

Segment 1 without spines and tubes. Cuticular hairs distributed in two irregular, transvers rows mainly in the posterior half of the plate, that merge together in a single transverse row from ventrolateral to ventromedial area (Fig. 9a, b). Cuticular hairs on this and remaining segments long, filiform. Unpaired type 1 glandular cell outlet in middorsal position (Figs. 9b and 10e). Paired sensory spots in subdorsal and ventrolateral positions (Figs. 9a, b and 10e, f). Posterior segment margin straight, showing a pectinate fringe with a very weak serration (Fig. 9a, b).

Segment 2 with paired, thick tubes in subdorsal and ventrolateral positions (Figs. 9a,b and 10e, f). Cuticular hairs distributed in two irregular, transvers rows only on the posterior half of the plate, that merge together in an irregular ventral patch showing no definite pattern (Fig. 9a, b). Unpaired type 1 glandular cell outlet in middorsal position; paired type 2 glandular cell outlets in sublateral position (Figs. 9a, b and 10e, f). Paired sensory spots in laterodorsal and midlateral positions (Figs. 9b and 10e). Posterior segment margin and pectinate fringe as on the precedent segment (Fig. 9a, b).

Segment 3 with cuticular plates lacking spines and tubes. Cuticular hairs dorsally arranged in four wavy, transvers rows that increase in length posteriorly, plus a pair of paraventral patches (Fig. 9a, b). Unpaired type 1 glandular cell outlet in middorsal position; paired type 1 glandular cell outlets in ventromedial position (Fig. 9a, b). Paired sensory spots in subdorsal position (Fig. 9b). Primary pectinate fringe well-developed, with regular tips (Fig. 9a, b).

Segment 4 with a middorsal spine exceeding the posterior edge of the segment but not reaching the posterior margin of the following segment (Figs. 9b and 10g). Cuticular hairs arranged in five wavy, transvers rows that increase in length posteriorly, plus a pair of paraventral patches (Fig. 9a, b). Paired type 1 glandular cell outlets in paradorsal and ventromedial positions (Figs. 9a, b and 10g, h). Paired sensory spots in paradorsal position, located posteriorly to middorsal spine near the posterior margin of the segment (Figs. 9b and 10g). Pectinate fringe as on the precedent segment (Fig. 9a, b).

Table 7 Summary of nature and arrangement of sensory spots, glandular cell outlets, nephridiopores, tubes and spines in *Echinoderes brevipes* sp. nov.

Segment	MD	PD	SD	LD	ML	SL	LA	LV	VL	VM
1	gco1		ss						ss	
2	gco1		tu	ss	ss	gco2			tu	
3	gco1		ss							gco1
4	ac	gco1, ss								gco1
5	gco1		ss					tu		gco1
6	ac	gco1, ss					tu	ac		gco1
7	gco1		ss				tu	ac		gco1
8	ac	gco1, ss		tu			tu	ac		gco1
9		gco1	ss				ne	ac		gco1
10	gco1x2		ss	tu						gco1
11					psx3 (m)		ltas(f)	lts		

ac acicular spine, *f* female condition of sexually dimorphic character, *LA* lateral accessory, *gco* glandular cell outlet, *LD* laterodorsal, *ltas* lateral terminal accessory spine, *lts* lateral terminal spine, *LV* lateroventral, *m* male condition of sexually dimorphic character, *MD* middorsal, *ML* midlateral, *ne* nephridiopore, *PD* paradorsal, *ps* penile spine, *SD* subdorsal, *SL* sublateral, *ss* sensory spot, *tu* tube, *VL* ventrolateral

Segment 5 with paired, long, narrow tubes in lateroventral position (Figs. 9a and 10h). Cuticular hairs arranged in 5–6 wavy, transvers rows that increase in length posteriorly, plus a pair of paraventral patches (Fig. 9a, b). Unpaired type 1 glandular cell outlet in middorsal position; paired type 1 glandular cell outlets in ventromedial position (Figs. 9a, b and 10g, h). Paired sensory spots in subdorsal position (Figs. 9b and 10g). Pectinate fringe as on the precedent segment (Fig. 9a, b).

Segment 6 with a middorsal spine longer than that of segment 4, exceeding the posterior margin of the following segment, and paired, robust, lateroventral spines (Figs. 9a, b and 10g, h, k). Paired, long, narrow tubes in lateral accessory position (Figs. 9a and 10h, k). Cuticular hairs as on the preceding segment (Fig. 9a, b). Paired type 1 glandular cell outlets in paradorsal and ventromedial positions (Figs. 9a, b and 10g, h). Paired sensory spots in paradorsal position, located posteriorly to middorsal spine near the posterior margin of the segment (Figs. 9b and 10g). Pectinate fringe as on the precedent segment (Fig. 9a, b).

Segment 7 with paired, robust, lateroventral spines (Figs. 9a and 10h, k) and long, narrow tubes in lateral accessory position (Figs. 9a and 10h, k). Cuticular hairs as on the preceding segment (Fig. 9a, b). Unpaired type 1 glandular cell outlet in middorsal position; paired type 1 glandular cell outlets in ventromedial position (Figs. 9a, b and 10g, i). Paired sensory spots in subdorsal position (Figs. 9b and 10g, i). Pectinate fringe as on the preceding segment (Fig. 9a, b).

Segment 8 with a middorsal spine much longer than that of segment 6, almost reaching the posterior margin of the last trunk segment, and paired, robust, lateroventral spines (Figs. 9a, b and 10g, h, j, k). Paired, long, narrow tubes in laterodorsal and lateral accessory positions (Figs. 9a, b and 10g, h, j, k). Cuticular hairs arranged in 7–8 wavy, transverse rows that increase in length posteriorly, plus a pair of paraventral patches (Fig. 9a, b). Paired type 1 glandular cell outlets in paradorsal and ventromedial positions (Figs. 9a, b and 10g, h, j). Paired sensory spots in paradorsal position, located posteriorly to middorsal spine near the posterior margin of the segment (Fig. 9b and 10g, j). Pectinate fringe as on the preceding segment (Fig. 9a, b).

Segment 9 with paired, robust, lateroventral spines (Figs. 9a and 10h, k). Cuticular hairs arranged in 9–10 wavy, transversal rows that increase in length posteriorly, plus a pair of paraventral patches (Fig. 9a, b). Paired type 1 glandular cell outlets in paradorsal and ventromedial positions (Figs. 9a, b and 10g, h). Paired sensory spots in subdorsal position (Figs. 9b and 10g). Nephridiopore as a very small sieve plate, in lateral accessory position (Figs. 9a and 10h). Pectinate fringe as on the preceding segment (Fig. 9a, b).

Segment 10 with paired, long, narrow tubes in laterodorsal position in both sexes (Figs. 9b, d and 10l). Cuticular hairs arranged in 7–9 wavy, transvers rows that increase in length posteriorly, forming two separated dorsal patches on the tergal plate (Fig. 9a, b). Two unpaired type 1 glandular cell outlets in middorsal position; paired type 1 glandular cell outlets in ventromedial position, mesially displaced, not aligned with the previous ventromedial type 1 glandular cell outlets (Figs. 9a–d and 10g). Paired sensory spots in subdorsal position (Figs. 9b). Posterior segment margin deeply curved, extending in the ventromedial area, with a pectinate fringe as on the preceding segment (Fig. 9a–d).

Segment 11 with lateral terminal spines very thick and short (LTS:TL average ratio = 12.5%), robust and distally pointed, showing a hollow central cavity (Figs. 9a–d and 10m). Females with a pair of lateral terminal accessory spines, even shorter, about two thirds of length of lateral terminal spines (Fig. 9a, b). Males with three pairs of penile spines arising laterally under the pectinate fringe of the precedent segment; ventral and dorsal penile spines

(ps1 and ps3) filiform, midlateral penile spine (ps2) shorter and coarser (Fig. 9c, d). Tergal plate with a middorsal, hairy protuberance, and two relatively long, distally pointed tergal extensions (Fig. 9b, d).

Notes on diagnostic and taxonomic features

Echinoderes brevipes sp. nov. has middorsal spines on segments 4, 6 and 8 as well as short, robust lateral terminal spines (LTS). There are only three species with the same pattern of features: *Echinoderes abbreviatus* Higgins, 1983 from Carrie Bow Cay (Belize, Caribbean Sea), *Echinoderes belenae* Pardos et al., 2016 from Taboga Island (Panama, eastern Pacific Ocean) and *Echinoderes rociae* Pardos et al., 2016 from Bocas del Toro, Bastimento Island (Panama, Caribbean Sea) (Higgins 1983; Pardos et al. 2016a, b). Nevertheless, *Echinoderes brevipes* sp. nov. can be unequivocally distinguished from the aforementioned congeners by the arrangement of the remaining spines and tubes. The four species share the presence of lateroventral spine/tubes on segments 5–9 (Higgins 1983; Pardos et al. 2016a, b), but *E. abbreviatus* and *E. belenae* have lateral accessory tubes only on segment 8 (Higgins 1983; Pardos et al. 2016b), and *E. rociae* on segments 7–8 (Pardos et al. 2016a), whereas the newly described species possesses lateral accessory tubes on segments 6–8.

Furthermore, the middorsal spines (MDS) of *E. brevipes* sp. nov. are remarkably longer than those of the aforementioned congeners (MDS4 average: 16.2 µm in *E. abbreviatus*, 17.0 µm in *E. belenae*, 13.0 µm in *E. rociae* and 30.6 µm in *E. brevipes* sp. nov.; MDS6 average: 23.2 µm in *E. abbreviatus*, 21.0 µm in *E. belenae*, 16.0 µm in *E. rociae* and 44.0 µm in *E. brevipes* sp. nov.; MDS8 average: 34.8 µm in *E. abbreviatus*, 25.0 µm in *E. belenae*, 20.0 µm in *E. rociae* and 76.6 µm in *E. brevipes* sp. nov.) (Higgins 1983; Pardos et al. 2016a, 2016b).

Echinoderes parahorni sp. nov.

(Figs. 11, 12 and 13 and Tables 8 and 9)

Synonymy

Echinoderes horni Sørensen et al. 2005: p. 507.

Echinoderes horni Herranz et al. 2014a: p. 3, 10, 23–24; Table 1, 2 and 3; Figs. 1b, 8, 9 and 10a, c.

Echinoderes horni Herranz et al. 2014b: p. 71, 78, 86.

Echinoderes horni Sørensen et al. 2015: p. 4; Table 1, including the 18S RNA sequence EU669453 submitted to GenBank.

Material examined.

Type material. Holotype, adult male, collected on 06 Nov 1980 off Monti Cristi Bay, Dominican Republic, Hispaniola Island, western Atlantic Ocean: 19° 53′ 12″ N, 71° 40′ 00″ W (L3) (Table 1; Fig. 1b) at 3–4 m depth in muddy sand associated with assemblages of *Thalassia* sp., mounted in Fluoromount G®, deposited at NMNH under accession number: USNM 1490965. Paratypes, 18 adult males and 25 adult females, all of them same collecting data as holotype, mounted in Fluoromount G® and deposited at NMNH under accession numbers: USNM 1490966-1491008; one adult male and one adult female collected on 03 Nov 1980 off Puerto Blanco, Dominican Republic, Hispaniola Island, western Atlantic Ocean: 19° 54′ 24″ N, 70° 56′ 24″ W (L2) (Table 1; Fig. 1b) at 3 m depth in silty mud, mounted in Fluoromount G®, deposited at NMNH under accession numbers: USNM 1491009-1491010; four adult females collected on 07 Nov 1980 off Icaquitos Bay, Dominican Republic, Hispaniola Island, western Atlantic Ocean: 19° 53′ 12″ N, 71° 38′ 30″ W (L5) (Table 1; Fig. 1b) at 2 m depth in muddy sand associated with assemblages of *Thalassia* sp., mounted in Fluoromount G®, deposited at NMNH under accession numbers: USNM 1491011-1491018; one adult male collected on 10 Nov 1980 off Cabo Haitiano, Haiti, Hispaniola Island, western Atlantic Ocean: 19° 46′ 12″ N, 72° 11′ 00″ W (L6) (Table 1; Fig. 1b) at 3–5 m depth in mud, mounted in Fluoromount G®, deposited at NMNH under accession number: USNM 1491019.

Non-type material. Four specimens from the same locality of the holotype (mounted for SEM), also deposited at NMNH under accession number: USNM 1491020.

Additional material. Nine additional specimens from Fort Pierce, Florida, western Atlantic Ocean (27° 29.96′ N, 80° 12.67′ W) at 15 m depth, collected in May 2006 by Dr. M. V. Sørensen and Dr. T. M. Jespersen, mounted in Fluoromount G®, deposited at the Natural History Museum of Denmark under accession numbers: NHMD 288580-188585. Two additional specimens from Fort Pierce, Florida, western Atlantic Ocean (27° 29.56′ N, 80° 12.23′ W) at 15 m depth, collected in June 22, 2003 by Dr. M. V. Sørensen and Dr. R. M. Kristensen, mounted in Fluoromount G®, also deposited at the Natural History Museum of Denmark under accession numbers: NHMD 288578-288579.

Diagnosis

Echinoderes lacking middorsal spines; ventrolateral tubes and subdorsal type 2 glandular cell outlets on segment 2; lateroventral tubes on segment 5, laterodorsal tubes on segment 10 (very reduced in females) and lateroventral spines on segments 6–9; lateral accessory tubes on segment 8.

Etymology

From the Ancient Greek ‘παρά’ (pará), meaning next to or similar to, which refers to the similar morphological features that the newly described species shares with its congener *E. horni*.

Description

See Table 8 for measurements and dimensions, and Table 9 for summary of spine, tube, nephridiopore, glandular cell outlet and sensory spot locations.

Head and neck. Head with retractable mouth cone and introvert (Fig. 13a, b). Internal part of mouth cone with several rings of inner oral styles; exact number, arrangement and morphology of inner oral styles not determined. External part of mouth cone with nine outer oral styles (Fig. 13a, b). Outer oral

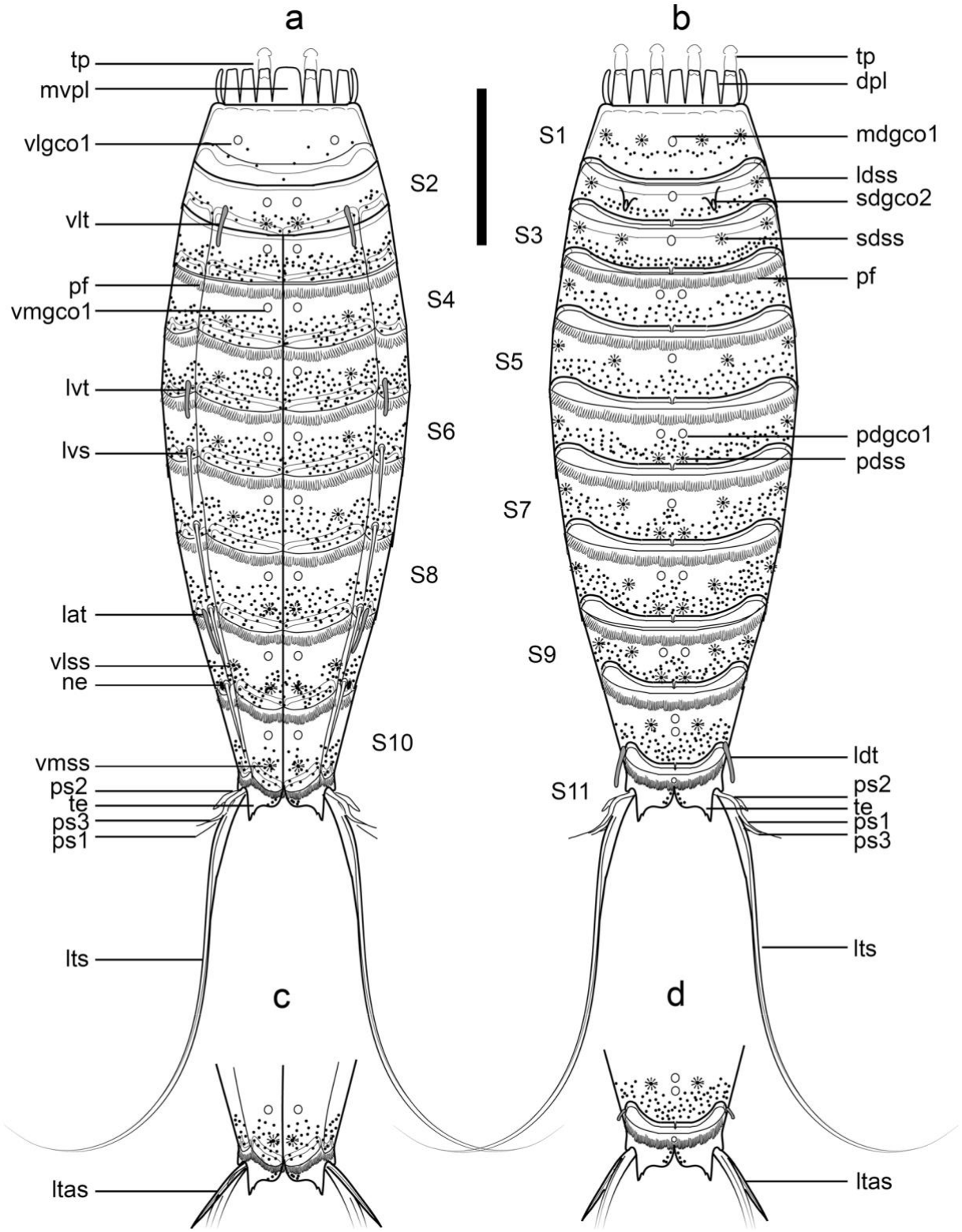

Fig. 11 Line art illustrations of *Echinoderes parahorni* sp. nov. **a** Male, ventral view; **b** Male, dorsal view; **c** Female, segments 10–11, ventral view; **d** Female, segments 10–11, dorsal view. Scale: 50 μm. *dpl* dorsal placid, *lat* lateral accessory tube, *ldss* laterodorsal sensory spot, *ldt* laterodorsal tube, *ltas* lateral terminal accessory spine, *lts* lateral terminal spine, *lvs* lateroventral spine, *lvt* lateroventral tube, *mdgco1* middorsal type 1 glandular cell outlet, *mvpl* midventral placid, *ne* nephridiopore, *pdgco1* paradorsal type 1 glandular cell outlet, *pdss* paradorsal sensory spot, *pf* pectinate fringe, *ps* penile spine, *sdgco2* subdorsal type 2 glandular cell outlet, *sdss* subdorsal sensory spot, *te* tergal extension, *tp* trichoscalid plate, *vlss* ventrolateral sensory spot, *vlt* ventrolateral tube, *vmgco1* ventromedial type 1 glandular cell outlet, *vmss* ventromedial sensory spot

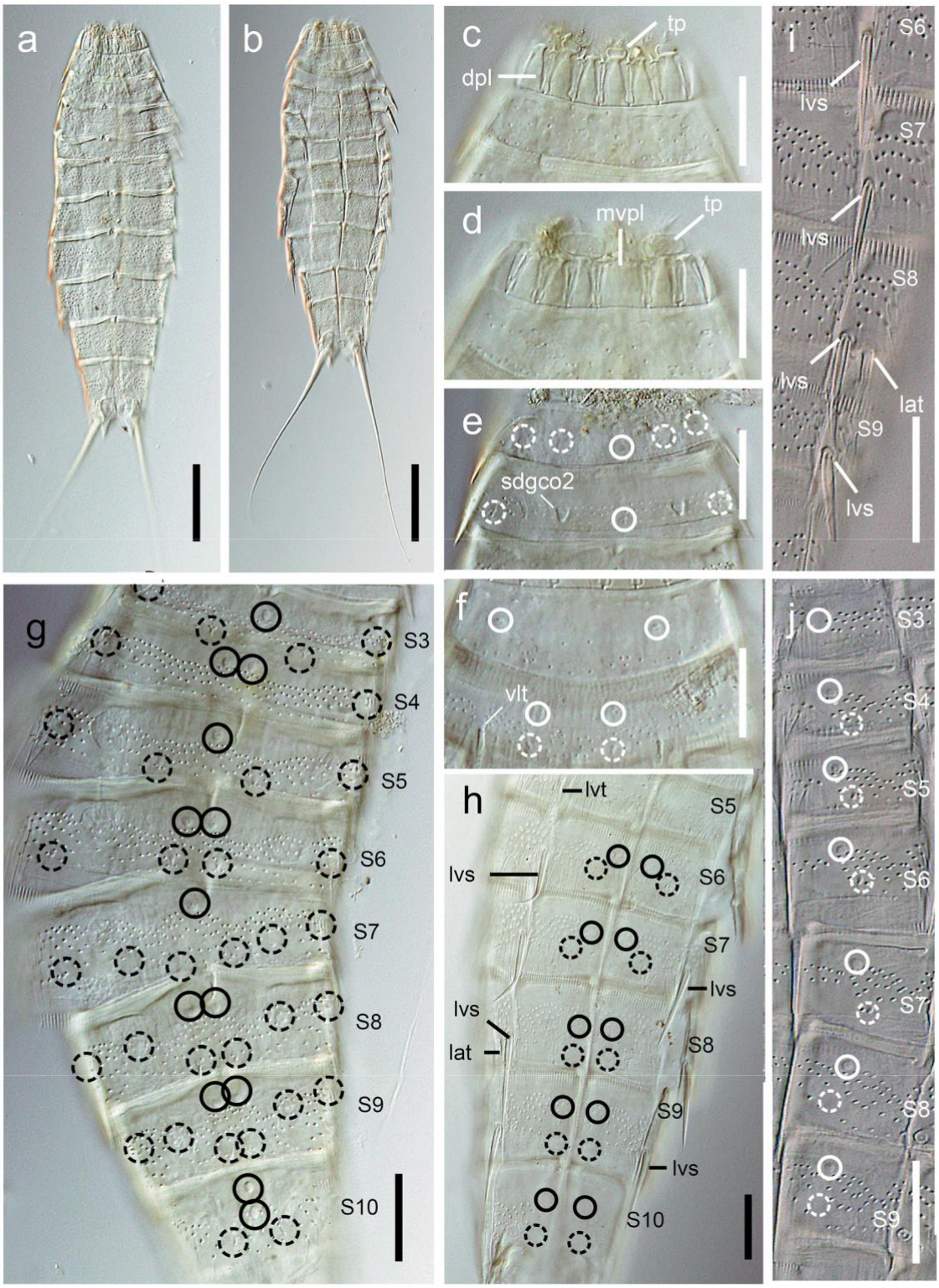

Fig. 12 Light micrographs showing trunk overview and cuticular details in the segments of *Echinoderes parahorni* sp. nov. **a** Dorsal overview of trunk; **b** Ventral overview of trunk; **c** Dorsal view of neck, showing the dorsal placids and the trichoscalid plates; **d** Ventral view of neck, showing the ventral placids and the trichoscalid plates; **e** Dorsal overview of segments 1–2; **f** Ventral overview of segments 1–2; **g** Dorsal overview of segments 3–10; **h** Ventral overview of segments 5–10; **i** Lateroventral region on right half of tergal plates of segments 6–9; **j** Ventrolateral and ventromedial regions on right half of sternal plates of segments 3–9. Scales: **a**–**b**: 50 μm; **c**–**j**: 20 μm. *dpl* dorsal placid, *lat* lateral accessory tube, *lvs* lateroventral spine, *lvt* lateroventral tube, *mvpl* midventral placid, *S* segment followed by number of corresponding segment, *sdgco2* subdorsal glandular cell outlet type 2, *tp* trichoscalid plate, *vlt* ventrolateral tube; sensory spots are marked as dashed circles, and type 1 glandular cell outlets as continuous circles

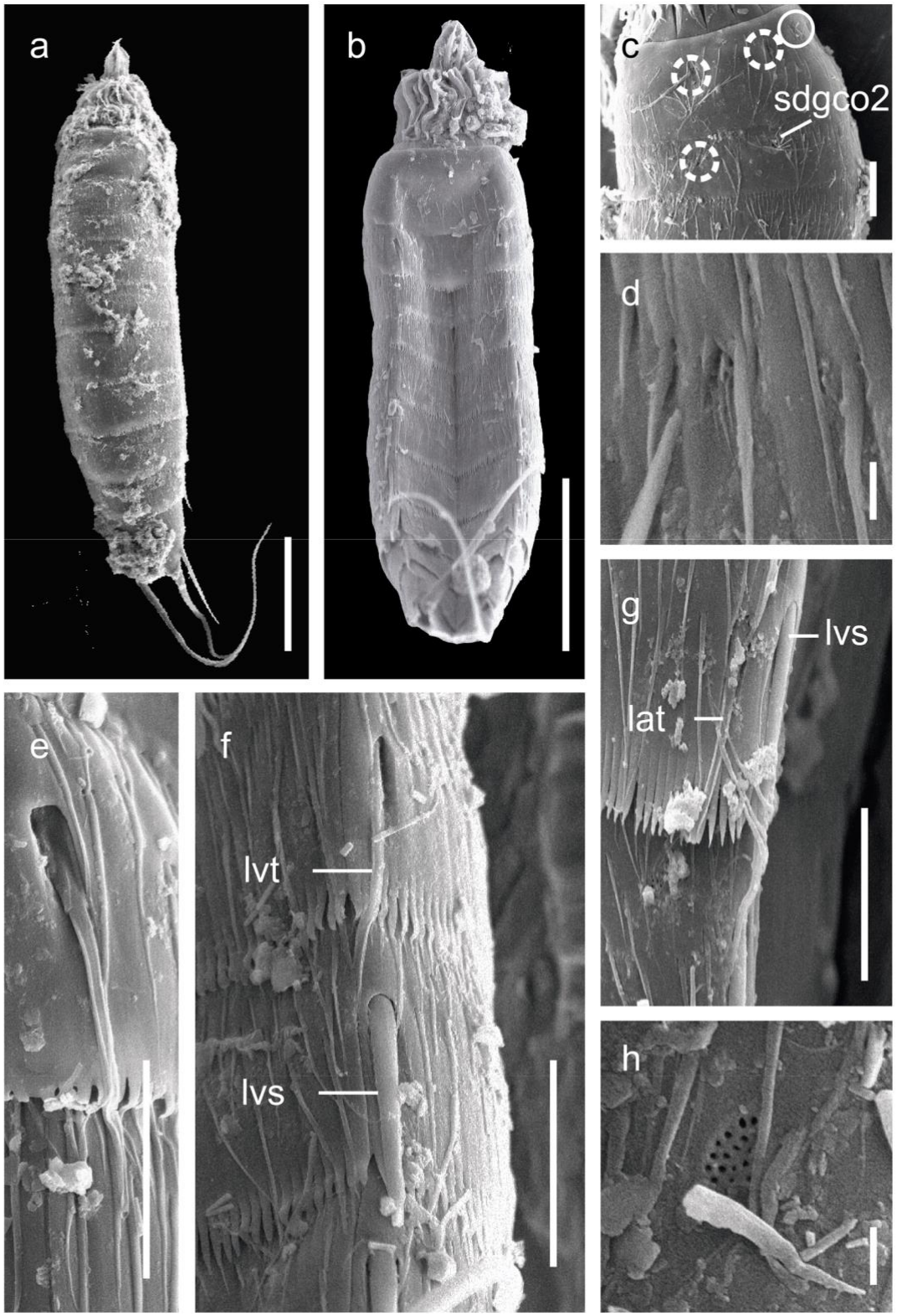

Fig. 13 Scanning electron micrographs showing overviews and details in the cuticular trunk morphology of *Echinoderes parahorni* sp. nov. **a** Dorsal overview of trunk; **b** Ventral overview of trunk; **c** Middorsal, subdorsal and laterodorsal regions on left half of cuticular plate of segments 1–2; **d** Detail of a ventromedial sensory spot of segment 5; **e** Ventrolateral region on right half of cuticular plate of segment 2, showing a ventrolateral tube; **f** Lateroventral region on right half of sternal plates of segments 5–6, showing the lateroventral spines; **g** lateroventral and lateral accessory regions on right half of sternal plates of segment 8, showing a lateroventral spine and a lateral accessory tube; **h** detail of the segment 9 nephridiopore. Scales: **a**, **b**: 40 μm; **c**, **f**, **g**: 10 μm; **d, h**: 1 μm; **e**: 4 μm. *lat* lateral accessory tube, *lvs* lateroventral spine, *lvt* lateroventral tube, *sdgco2* subdorsal glandular cell outlet type 2; sensory spots are marked as dashed circles, and type 1 glandular cell outlets as continuous circles

Table 8 Measurements of adult *Echinoderes parahorni* sp. nov. from Hispaniola Island, including number of measured specimens (*n*), mean of data and standard deviation (SD). There were no remarkable differences in sizes or dimensions between the two sexes or sampling locations

Character	Range	Mean (SD; *n*)
TL (μm)	191.0–263.3	216.9 (18.3; 20)
MSW-5 (μm)	31.8–52.3	45.0 (4.5; 20)
MSW-5/TL (%)	16.6–19.9	20.7 (1.2; 20)
SW-10 (μm)	29.2–42.5	37.1 (3.5; 20)
SW-10/TL (%)	15.3–16.2	17.1 (0.8; 20)
S1 (μm)	15.9–24.7	21.6 (2.2; 20)
S2 (μm)	18.9–26.9	23.3 (2.4; 20)
S3 (μm)	24.2–30.1	27.5 (1.6; 20)
S4 (μm)	29.5–34.7	30.9 (1.2; 20)
S5 (μm)	21.7–34.9	32.5 (2.7; 20)
S6 (μm)	32.7–42.7	36.8 (2.3; 20)
S7 (μm)	27.6–39.0	36.4 (2.8; 20)
S8 (μm)	31.2–39.0	36.6 (2.3; 20)
S9 (μm)	28.1–36.7	33.8 (1.8; 20)
S10 (μm)	25.8–35.2	31.2 (2.5; 20)
S11 (μm)	23.9–31.1	26.6 (1.7; 20)
LV2 (tu) (μm)	5.5–12.2	8.4 (1.7; 20)
LV5 (tu) (μm)	7.4–12.6	9.8 (1.4; 20)
LV6 (ac) (μm)	15.5–22.2	18.2 (1.9; 20)
LV7 (ac) (μm)	14.9–26.3	20.4 (2.8; 20)
LV8 (ac) (μm)	16.7–35.0	21.7 (3.8; 20)
LA8 (tu) (μm)	7.4–16.1	10.9 (2.3; 20)
LV9 (ac) (μm)	15.4–29.0	22.0 (2.9; 20)
LTS (μm)	109.6–183.8	138.0 (17.9; 18)
LTAS (μm)	32.87–40.51	36.4 (2.6; 20)
LTS/TL (%)	47.6–86.0	63.6 (9.8; 18)

ac acicular spine, *LA* lateral accessory, *LTAS* lateral terminal accessory spine, *LTS* lateral terminal spine, *LV* lateroventral, *MSW-5* maximum sternal width (on segment 5), *S* segment lengths, *SW-10* standard width (on segment 10), *TL* total length of trunk, *tu* tube

styles alternate in size between slightly longer and slightly shorter ones (Fig. 13a, b). Five long styles appear anterior to the odd numbered introvert sections, whereas four slightly shorter ones appear anterior to the even numbered ones, except in the middorsal section 6 where a style is missing (Fig. 13a, b). Outer oral styles with two jointed subunits, with a rectangular basis bearing a short fringe at its base, and a triangular, hook-like distal portion (Fig. 13a, b).

Introvert with seven rings of cuticular spinoscalids (Fig. 13a, b). Ring 01 with ten primary spinoscalids, each one with long, rectangular basal sheath and distal end piece (Fig. 13a, b). Basal sheath with very long fringe situated near its basis that exceeds the joint between the two subunits, bearing several flexible and elongated fringe tips. Distal piece narrow, oval in cross-section, smooth, hook-like, with blunt tip. Remaining rings bear spinoscalids laterally compressed, all with basal sheath and elongate, thin, hook-like distal piece (Fig. 13a, b). Exact number, arrangement and detailed morphology of these spinoscalids not determined as they tended to be collapsed when mounted for LM; furthermore, specimens mounted for SEM did not have the introvert completely extended, so full examination of this structure was not possible.

Neck with 16 trapezoidal placids, wider at base, with distinct joint between the neck and segment 1 (Figs. 11a, b and 12c, d); midventral placid widest (ca. 9–10 μm wide at base) (Figs. 11a and 12d), remaining ones alternating between slightly wider and slightly narrower, varying between 5 and 7 μm at base (Figs. 11b and 12c). Placids closely situated together at base, distally separated by flexible cuticular folds (Figs. 11a, b and 12c, d). A ring of six, long, hairy trichoscalids associated with the neck is present, attached to small trichoscalid plates (Figs. 11a, b and 12c, d).

Trunk. Trunk with 11 segments (Figs. 11a, b, 12a, b and 13a-b). Segments 1–2 as closed cuticular rings; remaining ones with one tergal and two sternal cuticular plates (Figs. 11a, b, 12a, b and 13a, b). Midsternal and tergosternal junctions as conspicuous lines on the cuticle (Figs. 11a, c, 12b and 13b). Tergal plates of anterior segments slightly bulging middorsally; posterior ones more flattened, giving the animal a tapering outline in lateral view. Sternal plates reach their maximum width at segment 5, progressively tapering towards the last trunk segments (Figs. 11a, b, 12a, b and 13a, b). Sternal plates relatively narrow in ratio to the total trunk length (MSW-5:TL average ratio = 20.9%), giving the animal a slender general aspect (Figs. 11a, b, 12a, b and 13a, b).

Segment 1 without spines and tubes. Cuticular hairs irregularly distributed through the cuticular surface, without any recognisable pattern (Fig. 11a, b). Cuticular hairs on this and following segments long, bracteate, filiform (Fig. 13c–h). Unpaired type 1 glandular cell outlet in middorsal position (Figs. 11b, 12e and 13c); paired type 1 glandular cell outlets in ventrolateral position (Figs. 11a and 12f). Paired sensory spots in subdorsal and laterodorsal positions (Figs. 11b, 12e and 13c). Sensory spots on this and remaining segments with a single pore surrounded by few, short micropapillae and flanked by one or two non-bracteate cuticular hairs (Fig. 13d). Posterior segment margin straight, showing a pectinate fringe with a very weak serration (Fig. 11a, b).

Segment 2 with paired, narrow tubes located in ventrolateral position (Figs. 11a, 12f and 13e). Cuticular hairs distributed in three continuous, transvers rows only in the posterior half of the plate (Fig. 11a, b). Unpaired type 1 glandular cell outlet in middorsal position (Figs. 11b and 12e); paired type 1 glandular cell outlets in ventromedial position (Figs. 11a and 12f). Paired type 2 glandular cell outlet in subdorsal position (Figs. 11b, 12e and 13c). Paired sensory spots in laterodorsal and ventromedial positions (Figs. 11b, 12e and 13c). Posterior segment margin and pectinate fringe as on the precedent segment (Fig. 11a, b).

Table 9 Summary of nature and arrangement of sensory spots, glandular cell outlets, nephridiopores, tubes and spines in *Echinoderes parahorni* sp. nov.

Segment	MD	PD	SD	LD	ML	LA	LV	VL	VM
1	gco1		ss	ss				gco1	
2	gco1		gco2	ss				tu	gco1, ss
3	gco1		ss	ss					gco1
4		gco1		ss					gco1, ss
5	gco1		ss	ss			tu		gco1, ss
6		gco1, ss		ss			ac		gco1, ss
7	gco1	ss	ss	ss			ac		gco1, ss
8		gco1, ss	ss	ss		tu	ac		gco1, ss
9		gco1, ss	ss	ss		ne	ac	ss	gco1, ss
10	gco1x2		ss	tu					gco1, ss
11	gco1				psx3 (m)	ltas (f)	lts		

ac acicular spine, *f* female condition of sexually dimorphic character, *LA* lateral accessory, *gco* glandular cell outlet, *LD* laterodorsal, *ltas* lateral terminal accessory spine, *lts* lateral terminal spine, *LV* lateroventral, *m* male condition of sexually dimorphic character, *MD* middorsal, *ML* midlateral, *ne* nephridiopore, *PD* paradorsal, *ps* penile spine, *SD* subdorsal, *ss* sensory spot, *tu* tube, *VL* ventrolateral, *VM* ventromedial

Segment 3 without spines and tubes. Cuticular hairs arranged in 4–5 wavy, transvers rows that increase in length posteriorly, plus a pair of paraventral patches (Fig. 11a, b). Unpaired type 1 glandular cell outlet in middorsal position; paired type 1 glandular cell outlets in ventromedial positions (Figs. 11a, b and 12g, j). Paired sensory spots in subdorsal and laterodorsal positions (Figs. 11b and 12g). Posterior segment margin and pectinate fringe as on the precedent segment (Fig. 11a, b).

Segment 4 without spines and tubes. Cuticular hairs arranged in 4–5 wavy, transvers rows that increase in length posteriorly, plus a pair of paraventral patches (Fig. 11a, b). Paired type 1 glandular cell outlets in paradorsal and ventromedial positions (Figs. 11a, b and 12g, j). Paired sensory spots in laterodorsal and ventromedial positions (Figs. 11a, b and 12g, j). Posterior segment margin and pectinate fringe as on the precedent segment (Fig. 11a, b).

Segment 5 with paired tubes in lateroventral position (Figs. 11a, 12h and 13f). Cuticular hairs arranged in 5–6 wavy, transverse rows that increase in length posteriorly, plus a pair of paraventral patches (Fig. 11a, b). Unpaired type 1 glandular cell outlet in middorsal position; paired type 1 glandular cell outlets in ventromedial position (Figs. 11a, b and 12g, j). Paired sensory spot in subdorsal, laterodorsal and ventromedial positions (Figs. 11a, b and 12g, h, j). Pectinate fringe as on precedent segment (Fig. 11a, b).

Segment 6 with paired spines on lateroventral position (Figs. 11a, 12h, i and 13f). Cuticular hairs arranged as on precedent segment (Fig. 11a, b). Paired type 1 glandular cell outlets in paradorsal and ventromedial positions (Figs. 11a, b and 12g, h, j). Paired sensory spots in paradorsal, laterodorsal and ventromedial positions, the former located posteriorly to middorsal spine (Figs. 11a, b and 12g, h, j). Pectinate fringe as on precedent segment (Fig. 11a, b).

Segment 7 with paired spines in lateroventral position (Figs. 11a and 12h, i). Cuticular hairs arranged in 5–6 wavy, transverse rows that increase in length posteriorly, plus a pair of paraventral patches (Fig. 11a, b). Unpaired type 1 glandular cell outlet in middorsal position; paired type 1 glandular cell outlets in ventromedial position (Figs. 11a, b and 12g, h, j). Paired sensory spots in paradorsal, subdorsal, laterodorsal and ventromedial positions (Figs. 11a, b and 12g, h, j). Pectinate fringe as on precedent segment (Fig. 11a, b).

Segment 8 with paired spines on lateroventral position plus paired tubes in lateral accessory position (Figs. 11a, 12h, i and 13g). Cuticular hairs arranged in 6–7 wavy, transverse rows that increase in length posteriorly, plus a pair of paraventral patches (Fig. 11a, b). Paired type 1 glandular cell outlets in paradorsal and ventromedial positions (Figs. 11a, b and 12g, h, j). Paired sensory spots in paradorsal, subdorsal, laterodorsal and ventromedial positions (Figs. 11a, b and 12g, h, j). Pectinate fringe as on precedent segment (Fig. 11a, b).

Segment 9 with paired spines on lateroventral position (Figs. 11a and 12h, i). Cuticular hairs arranged in 8–9 wavy, transverse rows of cuticular hairs that increase in length posteriorly, plus a pair of paraventral patches (Fig. 11a, b). Paired type 1 glandular cell outlets in paradorsal and ventromedial positions (Figs. 11a, b and 12g, h, j). Paired sensory spots in paradorsal, subdorsal, laterodorsal, ventrolateral and ventromedial positions (Figs. 11a, b and 12g, h, j). Nephridiopore as a sieve plate, in lateral accessory position (Figs. 11a and 13h).

Segment 10 with paired tubes in laterodorsal position, almost completely reduced in females but still with a cuticular marking that indicates the presence of the structure. Cuticular hairs arranged into 5–6 wavy, transverse rows of cuticular hairs that increase in length posteriorly, not reaching the midventral

section (Fig. 11a, b). Two unpaired type 1 glandular cell outlets in middorsal position; paired type 1 glandular cell outlets in ventromedial position (Figs. 11a, b and 12g, h). Paired sensory spots in subdorsal and ventromedial positions, the former mesially shifted, not aligned with precedent subdorsal sensory spots (Figs. 11a, b and 12g, h). Posterior segment margin deeply curved, extending in the ventromedial area, with a pectinate fringe as on the precedent segment (Fig. 11a–d).

Segment 11 with long, narrow lateral terminal spines (LTS:TL average ratio = 63.6%), being swollen in its proximal quarter, distally slender and pointed, showing a hollow central cavity in LM (Figs. 11a, b, 12a, b and 13a, b). Unpaired type 1 glandular cell outlet in middorsal position (Fig. 11b, d). Females with a pair of lateral accessory terminal spines relatively short, about one-fifth of the length of lateral terminal spines (Fig. 11c, d). Males with three pairs of penile spines arising laterally under the pectinate fringe of the precedent segment; ventral and dorsal penile spines (ps1 and ps3) filiform, midlateral penile spine (ps2) shorter and thicker (Fig. 11a, b). Tergal plate carrying two relatively short, distally pointed, laterally hairy tergal extensions (Fig. 11b, d).

Notes on diagnostic and taxonomic features

Echinoderes parahorni sp. nov. shares the absence of middorsal spines together with 14 congeners: *E. andamanensis* Higgins and Rao, 1979; *E. applicitus*, *E. aspinosus* Sørensen et al., 2012; *E. bengalensis* (Timm, 1958); *E. caribiensis*, *E. coulli* Higgins, 1977; *E. filispinosus* Adrianov, 1989; *E. horni* Higgins, 1983; *E. hwiizaa* Yamasaki and Fujimoto, 2014; *E. komatsui* Yamasaki and Fujimoto, 2014; *E. malakhovi* Adrianov, 1999 in Adrianov and Malakhov, 1999; *E. marthae* Sørensen, 2014; *E. multisetosus* Adrianov, 1989 and *E. strii* (Omer-Cooper 1957; Timm 1958; Kirsteuer 1964; Higgins 1977, 1983; Higgins and Rao 1979; Adrianov 1989; Adrianov and Malakhov 1999; Ostmann et al. 2012; Sørensen et al. 2012; Yamasaki and Fujimoto 2014; Pardos et al. 2016a). Of these, only *E. horni* from Carrie Bow Cay, Belize (Caribbean Sea) possesses a similar arrangement of spines and tubes with *E. parahorni* sp. nov., as both have lateroventral tubes on segment 5, lateroventral spines on segments 6–9 and lateral accessory tubes on segment 8 (Higgins 1983). However, *E. horni* has lateroventral tubes on segment 2 (Higgins 1983), while *E. parahorni* sp. nov. carries these structures in ventrolateral position. Moreover, *E. parahorni* sp. nov. is characterised by having type 2 glandular cell outlets in subdorsal position on segment 2 and tubes in laterodorsal position on segment 10, two morphological features that are absent in *E. horni* (Higgins 1983). Although the morphological description of *E. horni* is relatively old, Sørensen et al. (2016) revised the type material deposited at NMNH and did not determined discrepancies with the original description of the species. Thus, the morphological differences reported herein clearly support the erection of the new species.

The re-examination of several kinorhynchs previously reported as *E. horni* from Fort Pierce, Florida (western Atlantic Ocean) determined they are conspecific with *E. parahorni* sp. nov. adding relevant biogeographical information of this newly described species. Thus, all the ecological, morphological, phylogenetical and biogeographical information previously published for these specimens must be considered for *E. parahorni* (Sørensen et al. 2005; Herranz et al. 2014a, b; Sørensen et al. 2015).

Discussion

Current knowledge of the kinorhynch Caribbean fauna and new reports for Hispaniola Island

Until now, the kinorhynch fauna of the Caribbean Sea was composed of 12 genera and 31 species, including 2 species without confirmation (*Antygomonas* cf. *paulae* and *Semnoderes* cf. *pacificus*) plus three determined only to genus level (*Campyloderes* sp., *Cephalorhyncha* sp. and *Echinoderes* sp.) (Sørensen 2006; Pardos et al. 2016a). With the present study, the knowledge of the Caribbean kinorhynchs has been increased with the description of four new species (*Cristaphyes retractilis* sp. nov., *Fujuriphyes dalii* sp. nov., *Echinoderes brevipes* sp. nov. and *E. parahorni* sp. nov.), and the first report of *Echinoderes astridae* and *E. spinifurca* for the area. *Echinoderes horni* and *E. imperforatus* Higgins, 1983 are also firstly reported for Hispaniola Island, although previously known in the Caribbean Sea.

Echinoderes astridae was originally described from Araçá Bay, São Sebastião (Brazil), western Atlantic Ocean, in grey mud mixed with sand at 10 m depth (Sørensen 2014). The presence of the species in Monte Cristi Bay and Puerto Blanco (Dominican Republic) represents the first record of the species in Caribbean waters and its first report since the original description. Moreover, the Caribbean sediment samples consisted of mud and silty mud collected at 3–4 m depth. *Echinoderes horni* and *E. imperforatus* were described from Twin Cays (Belize), Caribbean Sea, in calcareous sediment with detritus and sand at 1–2 m depth (Higgins 1983). In the present study, both species were collected in Monte Cristi Bay and Icaquitos Bay in muddy sand at 2–4 m depth, being their first record for the Great Antilles. *Echinoderes spinifurca* was first described off Fort Pierce (Florida), in *Dentalium* sand at 15 m depth (Sørensen et al. 2005); here, we report this species in Monte Cristi Bay and Puerto Blanco (Dominican Republic)

in mud and silty mud at 3–4 m depth. These new records extend the biogeographical and ecological ranges for each species.

Geographic distribution of Caribbean kinorhynchs

Overall, the 35 known Caribbean species of Kinorhyncha are distributed as follows:

1. Ten species only known from Carrie Bow Cay, Belize: *Cristaphyes belizensis*, *Echinoderes abbreviatus*, *Fujuriphyes deirophorus*, *Higginsium erismatum* (Higgins, 1983), *H. trisetosum* (Higgins, 1983), *Leiocanthus corrugatus* (Higgins, 1983), *L. ecphantor* (Higgins, 1983), *Pycnophyes apotomus* (Higgins, 1983), *P. stenopygus* (Higgins, 1983) and *Setaphyes iniorhaptus* (Higgins, 1983).
2. Four species only known from the Caribbean Panama: *Cristaphyes panamensis* Pardos et al., 2016, *Echinoderes collinae* Sørensen, 2006, *E. orestauri* Pardos et al., 2016 and *E. rociae*.
3. One species only known from Mochima, Venezuela: *Echinoderes caribiensis*.
4. Three species only known from Hispaniola Island, Greater Antilles: *Cristaphyes retractilis* sp. nov., *Echinoderes brevipes* sp. nov. and *Fujuriphyes dalii* sp. nov.
5. Six species only found in the Caribbean Sea (more than a single locality): *Cristaphyes longicornis*, *Echinoderes imperforatus*, *E. wallaceae* Higgins, 1983, *Fujuriphyes distentus*, *Leiocanthus emarginatus* (Higgins, 1983) and *Paracentrophyes praedictus* Higgins, 1983.
6. Eleven species found both inside and outside the Caribbean Sea: *Antygomonas paulae* Sørensen, 2007, *Centroderes barbanigra* Neuhaus et al., 2014, *Echinoderes astridae*, *E. horni*, *E. intermedius* Sørensen, 2006, *E. parahorni* sp. nov. *E. spinifurca*, *E. truncatus* Higgins, 1983, *Pycnophyes alexandroi* Pardos et al., 2016, *P. beaufortensis* Higgins, 1964 and *Semnoderes pacificus* Higgins, 1967.

The geographic distribution of most of the Caribbean Kinorhyncha is limited to the Caribbean Sea. The Caribbean constitutes one distinctive biogeographical subregion of the Tropical North Western Atlantic Province, but is biogeographically heterogeneous and scarcely isolated (Briggs 1995; Miloslavich et al. 2010). Moreover, nearby regions, including the Atlantic coast of Mexico and South America, have been scarcely studied regarding the kinorhynch fauna. In addition, the new records of *Cristaphyes longicornis*, *Echinoderes astridae*, *E. horni*, *E. imperforatus* and *E. spinifurca* for Haiti and the Dominican Republic suggest that the biogeographical range of the previously known Caribbean kinorhynchs could be wider.

Echinoderes horni, *E. intermedius*, *Pycnophyes alexandroi* and *Semnoderes pacificus* have been reported in both the Caribbean and the Pacific Ocean (Higgins 1967; Sørensen 2006; Pardos et al. 2016a, b). The only existing connection between these two bodies of water is the Panama Canal. Although the canal could act as a passageway for ma-rine fauna exchange between the two oceans (Menzies 1968; Schloder et al. 2013; Ros et al. 2014), meiofaunal species encounter great physical, chemical and biological limitations to achieve the migration (Pardos et al. 2016b). Thus, deeper studies would be necessary to clarify the biogeographical status of the aforementioned species.

Acknowledgements We thank Kathryn Ahlfeld and Dr. Jon L. Norenburg from the Smithsonian Institution of Washington for their efficiency in sending the examined material and Dr. Robert P. Higgins for collecting the material and making it available for all researchers. We also thank Dr. M. V. Sørensen and Dr. H. Yamasaki for their useful revision, suggestions and comments that strongly improved the present paper. Cepeda was supported by a predoctoral fellowship of the Complutense University of Madrid (CT27/16-CT28/16).

Compliance with ethical standards

Conflict of interest The authors declare that they have no conflict of interest.

Ethical approval This article does not contain any studies with animals performed by any of the authors.

Sampling and field studies All necessary permits for sampling and observational field studies have been obtained by the authors from the competent authorities and are mentioned in the acknowledgements, if applicable.

Data availability statement Data sharing not applicable to this article as no datasets were generated or analysed during the current study.

References

Adrianov AV (1989) The first report on Kinorhyncha of the Sea of Japan. Zool Zh 68:17–27

Adrianov AV, Malakhov VV (1999) Cephalorhyncha of the world ocean. KMK Scientific Press, Moscow

Briggs J (1995) Global biogeography. Elsevier Science, Amsterdam

Brown R, Higgins RP (1983) A new species of *Kinorhynchus* (Homalorhagida, Pycnophyidae) from Australia with a redescription and range extension of other Kinorhyncha from the South Pacific. Zool Scr 12(3):161–169

Claparède ARE (1863) Zur Kenntnis der Gattung *Echinoderes* Duj. Beobachtungen über Anatomie und Entwicklungsgeschichte wirbelloser Thiere an der Küste von Normandie angestellt. Verlag von Wilhelm Engelmann, Leipzig

Fleeger JW, Thistle D, Thiel H (1988) Sampling Equipment. In: Higgins RP, Thiel H (eds) Introduction to the study of meiofauna, 1st edn. Smithsonian Institution Press, Washington D.C., pp 115–133

Herranz M, Boyle MJ, Pardos F, Neves RC (2014a) Comparative myoanatomy of *Echinoderes* (Kinorhyncha): a comprehensive investigation by CLSM and 3D reconstruction. Front Zool 11:31

Herranz M, Sánchez N, Pardos F, Higgins RP (2014b) New Kinorhyncha from Florida coastal waters. Helgol Mar Res 68:59–87

Higgins RP (1964) Three new kinorhynchs from the North Carolina coast. Bull Mar Sci 14:479–493

Higgins RP (1967) The Kinorhyncha of New Caledonia. In: Expédition Française Sur les Recifs Coralliens de la nouvelle-Calédonie 2, 1st edn. Fondation Singer-Polignac, Paris, pp 75–90

Higgins RP (1977) Two new species of *Echinoderes* (Kinorhyncha) from South Carolina. Trans Am Microsc Soc 96:340–354

Higgins RP (1983) The Atlantic Barrier Reef ecosystem at Carrie Bow Cay, Belize, II: Kinorhyncha. Smithson Contrib Mar Sci (18):1–13

Higgins RP (1988) Kinorhyncha. In: Higgins RP, Thiel H (eds) Introduction to the study of meiofauna, 1st edn. Smithsonian Institution Press, Washington D.C., pp 328–331

Higgins RP, Rao GC (1979) Kinorhynchs from the Andaman Islands. Zool J Linnean Soc 67:75–85

Kirsteuer E (1964) Zur Kenntnis der Kinorhynchen Venezuelas. Zool Anz 173:388–393

Lang K (1949) Echinoderida. Further zoological results of the Swedish Antarctic expedition 1901–1903 4:1–22

Lang K (1953) Reports of the Lund University Chile expedition 1948-1949. 9. Echinoderida. Acta Univ Lund 49(4):3–8

Menzies RJ (1968) Transport of marine life between oceans through the Panama Canal. Nature 220:802–803

Miloslavich P, Díaz JM, Klein E, Alvarado JJ, Díaz C, Gobin J, Escobar-Briones E, Cruz-Motta JJ, Weil E, Cortés J, Bastidas AC, Robertson R, Zapata F, Martín A, Castillo J, Kazandjian A, Ortiz M (2010) Marine biodiversity in the Caribbean: regional estimates and distribution patterns. PLoS ONE 5(8): e11916.

Neuhaus B (2013) 5. Kinorhyncha (=Echinodera). In: Schmidt-Rhaesa A (ed) Handbook of zoology. Gastrotricha, Cycloneuralia and Gnathifera. Volume 1: Nematomorpha, Priapulida, Kinorhyncha, Loricifera, 1st edn. De Gruyter, Göttingen, pp 181–348

Neuhaus B, Pardos F, Sørensen MV, Higgins RP (2014) New species of *Centroderes* (Kinorhyncha: Cyclorhagida) from the Northwest Atlantic Ocean, life cycle and ground pattern of the genus. Zootaxa 3901:1–69

Omer-Cooper J (1957) Deux nouvelles especes de Kinorhyncha en Provenance de l'Afrique du Sud. Bull Mens Soc Linn Lyon 26: 213–216

Ostmann A, Nordhaus I, Sørensen MV (2012) First recording of kinorhynchs from Java, with the description of a new brackish water species from a mangrove-fringed lagoon. Mar Biodivers 42:79–91

Pardos F, Sánchez N, Herranz M (2016a) Two sides of a coin: the phylum Kinorhyncha in Panama. I Caribbean Panama. Zool Anz 265:3–25

Pardos F, Herranz M, Sánchez N (2016b) Two sides of a coin: the phylum Kinorhyncha in Panama. II Pacific Panama. Zool Anz 265:26–47

Reinhard W (1881) Uber *Echinoderes* und *Desmoscolex* der Umgebung von Odessa. Zool Anz 4:588–592

Roberts CM, McClean CJ, Veron JE, Hawkins JP, Allen GR, McAllister DE, Mittermeier CG, Schueler FW, Spalding M, Wells F, Vynne C, Werner TB (2002) Marine biodiversity hotspots and conservation priorities for tropical reefs. Science 295:1280–1284

Ros M, Ashton GV, Lacerda MB, Carlton JT, Vázquez-Luis M, Guerra-García JM, Ruiz GM (2014) The Panama Canal and the transoceanic dispersal of marine invertebrates: evaluation of the introduced amphipod *Paracaprella pusilla* Mayer, 1890 in the Pacific Ocean. Mar Environ Res 99:204–211

Sánchez N, Yamasaki H (2016) Two new Pycnophyidae species (Kinorhyncha: Allomalorhagida) from Japan lacking ventral tubes in males. Zool Anz 265:80–89

Sánchez N, Herranz M, Benito J, Pardos F (2012) Kinorhyncha from the Iberian Peninsula: new data from the first intensive sampling campaigns. Zootaxa 3402:24–44

Sánchez N, Yamasaki H, Pardos F, Sørensen MV, Martínez A (2016) Morphology disentangles the systematics of a ubiquitous but elusive meiofaunal group (Kinorhyncha: Pycnophyidae). Cladistics 32: 479–505

Sánchez N, Sørensen MV, Landers SC (2019) Pycnophyidae (Kinorhyncha: Allomalorhagida) from the Gulf of Mexico: *Fujuriphyes viserioni* sp. nov. and a redescription of *Leiocanthus langi* (Higgins, 1964), with notes on its intraspecific variation. Mar Biodivers. https://doi.org/10.1007/s12526-019-00947-x.

Schloder C, Canning-Clode J, Saltonstall K, Strong EE, Ruiz GM, Torchin ME (2013) The Pacific bivalve *Anomia peruviana* in the Atlantic: a recent invasion across the Panama Canal? Aquat Invasions 8:443–448

Sørensen MV (2006) New kinorhynchs from Panama, with a discussion of some phylogenetically significant cuticular structures. Meiofauna Mar 15:51–77

Sørensen MV (2007) A new species of *Antygomonas* (Kinorhyncha: Cyclorhagida) from the Atlantic coast of Florida, USA. Cah Biol Mar 48:155–168

Sørensen MV (2014) First account of echinoderid kinorhynchs from Brazil, with the description of three new species. Mar Biodivers 44:251–274

Sørensen MV, Pardos F (2008) Kinorhynch systematics and biology—an introduction to the study of kinorhynchs, inclusive identification keys to the genera. Meiofauna Mar 16:21–73

Sørensen MV, Heiner I, Ziemer O (2005) A new species of *Echinoderes* from Florida (Kinorhyncha: Cyclorhagida). Proc Biol Soc Wash 118:499–508

Sørensen MV, Rho HS, Min WG, Kim D, Chang CY (2012) An exploration of *Echinoderes* (Kinorhyncha: Cyclorhagida) in Korean and neighboring waters, with the description of four new species and a redescription of *E. tchefouensis* Lou, 1934. Zootaxa 3368:161–196

Sørensen MV, Dal Zotto M, Rho HS, Herranz M, Sánchez N, Pardos F, Yamasaki H (2015) Phylogeny of Kinorhyncha based on morphology and two molecular loci. PLoS ONE 10(7): e0133440

Sørensen MV, Herranz M, Landers SC (2016) A new species of *Echinoderes* (Kinorhyncha: Cyclorhagida) from the Gulf of Mexico, with a redescription of *Echinoderes bookhouti* Higgins, 1964. Zool Anz 265:48–68

Timm RW (1958) Two new species of *Echinoderella* (phylum Kinorhyncha) from the Bay of Bengal. J Bombay Nat Hist Soc 55: 107–109

Yamasaki H, Fujimoto S (2014) Two new species in the *Echinoderes coulli* group (Echinoderidae, Cyclorhagida, Kinorhyncha) from the Ryukyu Islands, Japan. ZooKeys 382:27–52

Zelinka C (1894) über die Organisation von *Echinoderes*. Verh Dtsch Zool Ges 4:46–49

Zelinka C (1896) Demonstration von Tafeln der *Echinoderes* Monographie. Verh Dtsch Zool Ges 6:197–199

Zelinka C (1928) Monographie der Echinodera. Engelmann, Leipzig

.

Zoologischer Anzeiger 282 (2019) 127-139

Contents lists available at ScienceDirect

Zoologischer Anzeiger

journal homepage: www.elsevier.com/locate/jcz

Research paper

Kinorhyncha from the Caribbean, with the description of two new species from Puerto Rico and Barbados*

Diego Cepeda [a, *], **Fernando Pardos** [a], **Nuria Sánchez** [a, b]

[a] Departamento de Biodiversidad, Ecología y Evolucion, Facultad de Ciencias Biologicas, Universidad Complutense de Madrid (UCM), Jose Antonio Novais St. 12, 28040, Madrid, Spain

[b] Laboratoire Environment Profond, Institut Français de Recherche pour l'Exploitation de la Mer (IFREMER), Centre Bretagne e ZI de la Pointe du Diable, CS 10070, 29280, Plouzane, France

ARTICLE INFO

Article history:
Received 26 February 2019
Received in revised form 20 March 2019 Accepted 23 May 2019 Available online 5 June 2019

Keywords:
Kinorhynchs
Biodiversity
Meiofauna
Morphology
Taxonomy

ABSTRACT

Two new kinorhynch species from Puerto Rico (Greater Antilles) and Barbados (Lesser Antilles) are described herein from Dr R. P. Higgins' unexamined Caribbean meiofaunal samples, which have been stored in the Smithsonian Institution collections. The species from Puerto Rico, *Cristaphyes cornifrons* sp. nov., belongs to the class Allomalorhagida, whereas the species from Barbados, *Echinoderes barbadensis* sp. nov., belongs to the class Cyclorhagida. *C. cornifrons* sp. nov. is easily distinguished from most of its congeners by the presence of lateral terminal spines and the absence of male, sexually dimorphic, ventromedial tubes on segment 2, as only other two species of the genus lack these features. Of these, *C. cornifrons* sp. nov. may be easily differentiated by its pattern of paradorsal, ventrolateral and ventromedial setae. *E. barbadensis* sp. nov. is unique among its congeners by the combined presence of middorsal spines on segments 4-8, lateroventral spines on segments 6-9, lateral accessory tubes on segment 8, lateroventral tubes on segment 5, ventrolateral tubes on segment 2 and type 2 glandular cell outlets in subdorsal position on segment 2 and in midlateral position on segment 4.

1. Introduction

Kinorhynchs, commonly known as mud dragons, are small, holobenthic, meiofaunal organisms that inhabit the spaces and crevices between the sediment particles of worldwide oceans (Sørensen & Pardos 2008; Neuhaus 2013). Much of the currently known biodiversity of the phylum includes intertidal to circalittoral species, biased by samplings being done in the most accessible marine areas (Neuhaus 2013; Sørensen & Grzelak 2018). However, many shoreline regions still remain poorly studied, as it is the case of the Caribbean Basin. The Caribbean is a tropical sea bounded by Mexico and Central America to the west and south west, by the Greater Antilles to the north, by the Lesser Antilles to the east and by the northern coast of South America to the south (Miloslavich et al. 2010). To date, a total of 30 species have been reported for the whole Basin (Kirsteuer 1964; Higgins 1983; Sørensen 2006; Pardos et al. 2016b), but the study of several samples from different Caribbean localities stored at the Smithsonian National Museum of Natural History (NMNH) has revealed a still unknown, rich diversity of Caribbean kinorhynchs (Cepeda et al. 2019b, 2019c).

The present contribution is part of an extensive survey of Caribbean Kinorhyncha that take advantage of the series of samples deposited by Dr R. P. Higgins during several decades, samples that still remain unsorted and unexamined in the NMNH. Specifically, this paper focuses on Puerto Rico, part of the Greater Antilles, and Barbados, which is part of the Lesser Antilles, locations where the kinorhynch fauna is completely unknown. The present study describes two species new to science.

2. Material and methods

Studied kinorhynchs were collected by Dr R. P. Higgins at two different localities throughout the Caribbean Antilles (Fig. 1A): La Parguera (Puerto Rico) in 1967 (Fig. 1B) and St. James (Barbados) in 1968 (Fig. 1C). All the samplings were done using a meiobenthic dredge (Higgins 1988).

After sampling, meiofauna was extracted from sediment using the bubble and blot method defined by Higgins (1964). Meiofaunal specimens were fixed

urn:lsid:zoobank.org:pub:2966A891-8F2A-453C-930A-5326DDE12AE3.

* This article is a part of the Fifth International Scalidophora Workshop special issue published in Zoologischer Anzeiger 282C, 2019.

* Corresponding author.
E-mail address: diegocepeda@ucm.es (D. Cepeda).

https://doi.org/10.1016/j.jcz.2019.05.014
0044-5231/

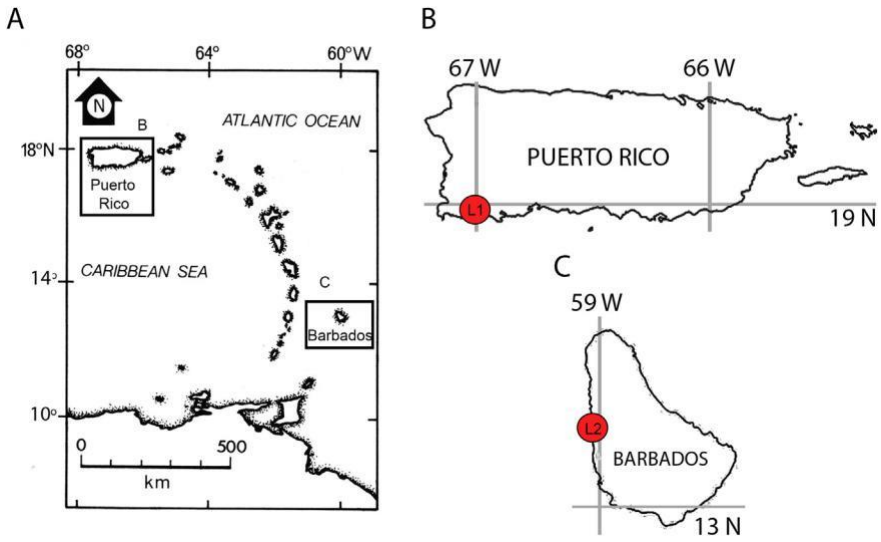

Fig. 1. General map (A) showing the sampling localities (B-C) through the Caribbean Sea (western Atlantic Ocean).

in 4% formalin and finally preserved in Carosafe®. Fixed kinorhynchs were picked up with an Irwin loop using a Motic® SMZ-168 stereo zoom microscope and washed with distilled water to remove remnants of formalin. For light microscopy (LM), specimens were dehydrated though a series of 25%, 50%, 75% and 100% glycerine and mounted on glass slides using Fluoromount G® sealed with Depex®. Mounted specimens were studied and photographed using an Olympus® BX51-P microscope equipped with differential interference contrast (DIC) optics and an Olympus® DP-70 camera. Morphometrics were obtained with Olympus cellSens® software. For scanning electron microscopy (SEM), specimens were transferred to 70% ethanol and progressively dehydrated through a graded series of 80%, 90%, 95% and 100% ethanol. Hexamethyldisilazane (HMDS) was used for chemical drying through a HMDS-ethanol series. Specimens were finally coated with gold and mounted on aluminium stubs to be examined with a JSM® 6335-F JEOL SEM at the ICTS Centro Nacional de Microscopía Electronica (Complutense University of Madrid, Spain). Type material is deposited at the NMNH, Smithsonian Institution, Washington, while non-type material is deposited at the Invertebrates Collection of the Meiofaunal Laboratory at the Universidad Complutense de Madrid (UCM), Spain. Line drawings and image plates composition were done using Adobe® Photoshop CC-2014 and Illustrator CC-2014 software.

3. Results and discussion

Class **Allomalorhagida** Sørensen et al. 2015.
Family **Pycnophyidae** Zelinka 1896.
Genus ***Cristaphyes*** Sánchez et al., 2016.

3.1. ***Cristaphyes cornifrons*** sp. nov.
urn:lsid:zoobank.org:act:5F5572D9-EB13-4205-8706-6D3BC6413DC3.
(Figs. 2-5 and Tables 2 and 3).

3.1.1. Type material

Holotype, adult female, collected by Dr R. P. Higgins on 7 June 1967 at La Parguera, Puerto Rico, western Atlantic Ocean (L1): 17º57'00"N, 67°03'00"W (Table 1; Fig. 1A, B), 15 m depth, mud; mounted in Fluoromount G®, NMNH accession number: USNM 1550583.

Two paratypes, one adult male and one adult female, with same collecting data as holotype, mounted in Fluoromount G®, NMNH accession numbers: USNM 1550584 and 1550585.

3.1.2. Non-type material

Two additional specimens with same collecting data as holotype and paratypes, prepared for SEM, deposited at the Invertebrates Collection of the Meiofaunal Laboratory of the Universidad Complutense de Madrid (UCM), Spain.

3.1.3. Diagnosis

Cristaphyes with middorsal processes on segments 2-9, with small pointed projection of the tergal plate of segment 10. Anterior margin of first segment strongly denticulated, with "teeth" of different sizes. Unpaired paradorsal setae on segments 2, 4 and 6. Paired paralateral setae on segment 1; paired laterodorsal setae on segments 2-9; paired lateroventral setae on segments 2, 4, 6, 8 and 10; paired ventrolateral setae on segments 2, 3 (in some specimens mesially shifted to ventromedial position on segment 3) and 5 (females furthermore with sexually dimorphic, ventrolateral setae on segment 10); paired ventromedial setae on segments 4-9. Lateral terminal spines long, about 34% of total trunk length.

3.1.4. Etymology

From the latin "cornifrons", which refers to the lateral anterior horn-shaped extensions of segment 1 that are markedly elongated, curved and pointed.

3.1.5. Description

See Table 2 for measurements and dimensions, and Table 3 for summary of cuticular process, seta, glandular cell outlet, nephridiopore, spine and sensory spot locations.

Head with retractable mouth cone and introvert (Fig. 3C, D). Although two of the examined specimens had the introvert completely everted, oral styles and scalids tended to be collapsed when mounted for LM (Fig. 3C, D), so only some details can be provided. External ring of mouth cone (ring 00) with nine equally-sized outer oral styles (Fig. 3C), arranged as one anterior to each introvert sector except for the middorsal sector 6 where a style is missing. Each outer oral style composed of a single, very flexible, superficially smooth piece with a basal, short, fringed sheath (Fig. 3C). Ring

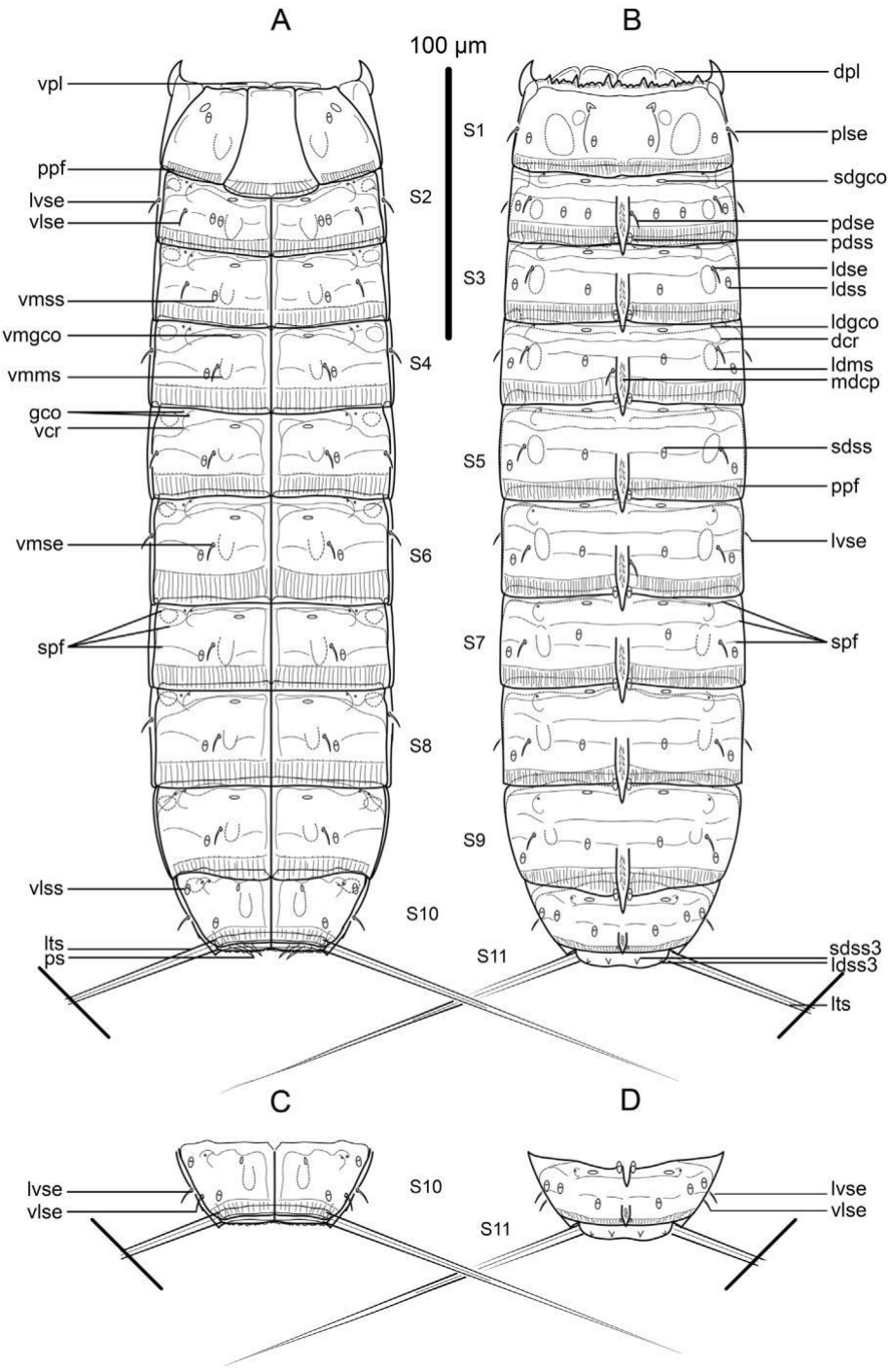

Fig. 2. Line art illustrations of *Cristaphyes cornifrons* sp. nov. (A) Male, ventral overview; (B) Male, dorsal overview; (C) Female, segments 10-11, ventral view; (D) Female, segments 10-11, dorsal view. Abbreviations: dcr, dorsal cuticular ridge; dpl, dorsal placid; gco, glandular cell outlet; ldgco, laterodorsal glandular cell outlet; ldms, laterodorsal muscular scar; ldse, laterodorsal seta; ldss, laterodorsal sensory spot; ldss3, laterodorsal type 3 sensory spot; lts, lateral terminal spine; lvse, lateroventral seta; mdcp, middorsal cuticular process; pdse, paradorsal seta; pdss, paradorsal sensory spot; plse, paralateral seta; ppf, primary pectinate fringe; ps, penile spine; S, segment followed by number of corresponding segment; sdgco, subdorsal glandular cell outlet; sdss, subdorsal sensory spot; sdss3, subdorsal type 3 sensory spot; spf, secondary pectinate fringes; vcr, ventral cuticular ridge; vlse, ventrolateral seta; vlss, ventrolateral sensory spot; vmgco, ventromedial glandular cell outlet; vmms, ventromedial muscular scar; vmse, ventromedial seta; vmss, ventromedial sensory spot; vpl, ventral placid.

01 with ten primary spinoscalids, each one composed of a basal sheath and a distal, elongated piece; basal sheath equipped with a median, dense fringe (Fig. 3D). Remaining rings of introvert (rings 02-06) with regular scalids morphologically similar to the primary spinoscalids but shorter (Fig. 3D).

Neck with four dorsal and two ventral, sclerotized placids (Figs. 2A, B and 3E, F). Dorsal placids rectangular; mesial ones broader than lateral ones (Figs. 2B and 3E). Ventral placids much more elongated and trapezoidal, getting thinner towards the lateral sides (Figs. 2A and 3F). Fourteen elongated, hairy trichoscalids are present, without trichoscalid plates (Fig. 3D).

Trunk markedly rectangular, stout, triangular in cross-section, composed of eleven segments (Figs. 2A, B, 3A, B and 5A, B).

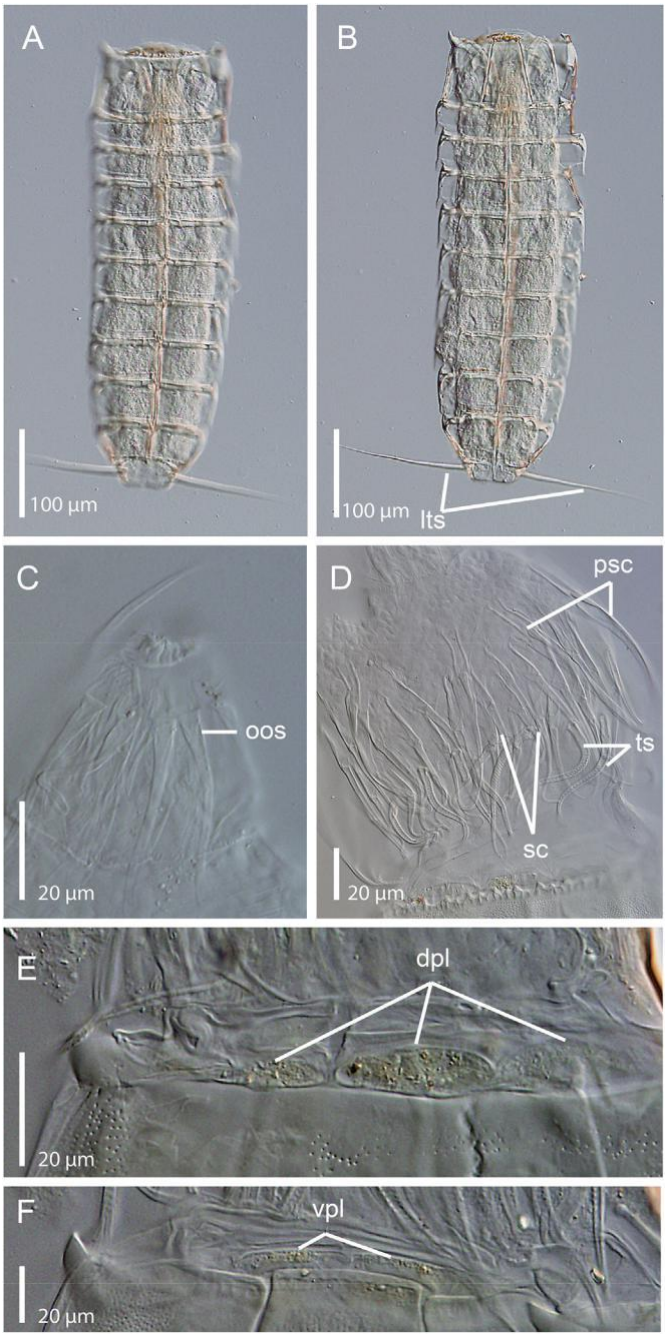

Fig. 3. Light micrographs showing trunk overviews and details in the head and neck of female holotype USNM 1550583 (A-B) and male paratype USNM 1550585 (C-F) of *Cristaphyes cornifrons* sp. nov. (A) Dorsal overview of trunk; (B) ventral overview of trunk; (C) mouth cone, showing the outer oral styles (ring 00); (D) introvert, showing primary spinoscalids (ring 01), regular scalids and neck's trichoscalids (ring 07); (E) dorsal view of neck, showing the dorsal placids; (F) ventral view of neck, showing the ventral placids. Abbreviations: dpl, dorsal placid; lts, lateral terminal spines; oos, outer oral style; psc, primary spinoscalid; sc, scalid; ts, trichoscalid; vpl, ventral placid.

Segment 1 with one tergal, two episternal and one trapezoidal, midsternal plate; remaining segments with one tergal and two sternal plates (Figs. 2A, B, 3A, B and 5A, B). Midsternal and tergosternal junctions as conspicuous lines externally on the cuticle (Fig. 2A, C). Sternal plates reach their maximum width at segment 5, but almost constant in width throughout the trunk, slightly tapering at the posterior trunk end (Figs. 2A, B, 3A, B and 5A, B). Sternal plates are relatively narrow (MSW-5:TL average ratio = 23.6%), giving the animal a slender appearance. Middorsal processes on segments 2-9, keel-shaped, with pointed tips that surpass the posterior segment margins, turning progressively longer towards the posterior end (Figs. 2B, D, 3A, 4C, D, F, I and 5A, C, D); segment 10 with a small pointed projection towards the posterior segment margin (Figs. 2B, D and 4C). Segments 1-10 with oval-shaped glandular cell outlets in subdorsal and ventromedial position (Figs. 2A-D, and 4A-J). Segments 2-10 with paired cuticular ridges in laterodorsal position, not always detectable, followed by one small glandular cell outlet; segments 2-10 furthermore with paired cuticular ridges at the ventrolateral-ventromedial limit, followed by small glandular cell outlets with two cuticular openings (Figs. 2A-D and 5G). Cuticular hairs acicular, distributed all over the trunk cuticle, except the mesial halves of the episternal plates. Muscular scars very conspicuous as superficially smooth, hairless, rounded to oval-shaped areas on the cuticle, in laterodorsal and ventromedial positions (Figs. 2A-D and 4A-J). Pachycycli and ball-and-socket joints on segments 2-10 (Fig. 2A, B). Apodemes not observed. Posterior margin of segments straight, showing poorly-developed primary pectinate fringes with a very weak serration (Fig. 2A-D). Secondary pectinate fringes developed as three transverse, wavy rows with a very weak dentation, two of them located near the anterior margin of segments, one of them located near the posterior margin of segments (Fig. 2A-D). Some specimens were found carrying epibiontic Ciliophora on both tergal and sternal plates throughout the trunk.

Segment 1 without middorsal process (Figs. 2B and 4A). Anterolateral margins of the tergal plate large, elongated as horn-shaped extensions, curved inwards, distally pointed (Figs. 2A, B, 3A, B, F, 4B and 5A, B). Anterior margin of the tergal plate strongly denticulated, with projections of different sizes, followed by a smooth area (Figs. 2B, 3A and 5A). Paired setae in paralateral position (Figs. 2B and 4A). Paired sensory spots in subdorsal position, posterior to the dorsal cuticular scars; in laterodorsal position, lateral to the dorsal cuticular scars; and in ventrolateral position, lateral to the ventral muscular scars (Figs. 2A, B and 4A, B). Sensory spots on this and remaining segments rounded to oval, with several rings of cuticular papillae surrounding a central pore (similar to Fig. 5F, I).

Segment 2 with keel-like middorsal process that surpasses the posterior segment margin, with a median, densely-covered fringe of cuticular hairs (Figs. 2B, 4D and 5D). Unpaired seta in paradorsal position, and paired setae in laterodorsal, lateroventral and ventrolateral positions, the former immediately lateral to the dorsal muscular scars (Figs. 2A, B, 4D, E and 5D, E). Two pairs of sensory spots in subdorsal and ventromedial positions, the latter lateral to the ventral muscular scars; plus one pair of sensory spots in paradorsal and laterodorsal positions, the latter lateral to the laterodorsal setae (Figs. 2A, B, 4D, E and 5D, E). Sexually dimorphic male tubes absent.

Segment 3 with middorsal process as on preceding segment (Figs. 2B, 4F and 5D). Paired setae in laterodorsal and ventrolateral positions (Figs. 2A, B, 4F, G and 5D, F), the latter showing intraspecific variation as one of the examined specimens had this pair of setae mesially shifted to ventromedial position (Fig. 5E). Paired sensory spots in paradorsal, subdorsal, laterodorsal and ventromedial positions (Figs. 2A, B, 4F, G and 5D-F).

Segment 4 with middorsal process as on the preceding segment (Figs. 2B and 4I). Unpaired seta in paradorsal position, plus paired setae in laterodorsal, lateroventral and ventromedial positions (Figs. 2A, B and 4I, J). Paired sensory spots in paradorsal, subdorsal, laterodorsal and ventromedial positions (Figs. 2A, B and 4I, J).

Segment 5 with tergal plate similar to that of segment 3 and sternal plates similar to those of segment 4 but also with paired ventrolateral setae (Figs. 2A, B and 4I, J).

Fig. 4. Light micrographs showing trunk cuticular details of male paratype USNM 1550585 of *Cristaphyes cornifrons* sp. nov. (A) Left half of tergal plate of segment 1; (B) ventrolateral and ventromedial views on left half of segment 1; (C) left halves of tergal plates of segments 8-11; (D) left half of tergal plate of segment 2; (E) left sternal plate of segment 2; (F) left half of tergal plate of segment 3; (G) left sternal plate of segment 3; (H) lateroventral to ventromedial view on left sternal plates of segments 8-11; (I) left halves of tergal plates of segments 4-7; (J) left sternal plates of segments 4-7. Abbreviations: ldse, laterodorsal seta; lvne, lateroventral nephridiopore; lvse, lateroventral seta; mdcp, middorsal cuticular process; mdcpr, middorsal cuticular projection; pdse, paradorsal seta; plse, paralateral seta; vlse, ventrolateral seta; vmse, ventromedial seta; sensory spots are marked as closed circles, and glandular cell outlets as dashed circles; numbers after abbreviations indicate the corresponding segment.

Segment 6 similar to segment 4 (Figs. 2A, B and 4I, J). Segment 7 with tergal plate similar to that of segment 3 and sternal plates similar to those of segment 4 (Figs. 2A, B, 4I, J and 5I). Segment 8 similar to segment 4, but lacking paradorsal seta (Figs. 2A, B, 4C, H and 5C).

Segment 9 with tergal plate similar to that of segment 3, but with lateroventral nephridiopores present, and sternal plates similar to those of segment 4 (Figs. 2A, B and 4C, H).

Segment 10 with small pointed projection towards the posterior margin of the tergal plate (Figs. 2B, D and 4C). Paired setae in lateroventral position; females furthermore with sexually dimorphic, paired setae in ventrolateral position (Figs. 2A-D and 4C, H). Two pairs of sensory spots in laterodorsal position, plus one pair of sensory spots in paradorsal, subdorsal, ventrolateral and ventromedial positions (Figs. 2A-D, 4C, H and 5H).

Segment 11 with two pairs of type 3 sensory spots, one in subdorsal and one in laterodorsal position (Figs. 2B, D and 4C). Males with two pairs of stout, penile spines and genital pores surrounded by tuft of long hairs (Figs. 2A and 5H). Lateral terminal spines long (LTS:TL average ratio = 34.0%),

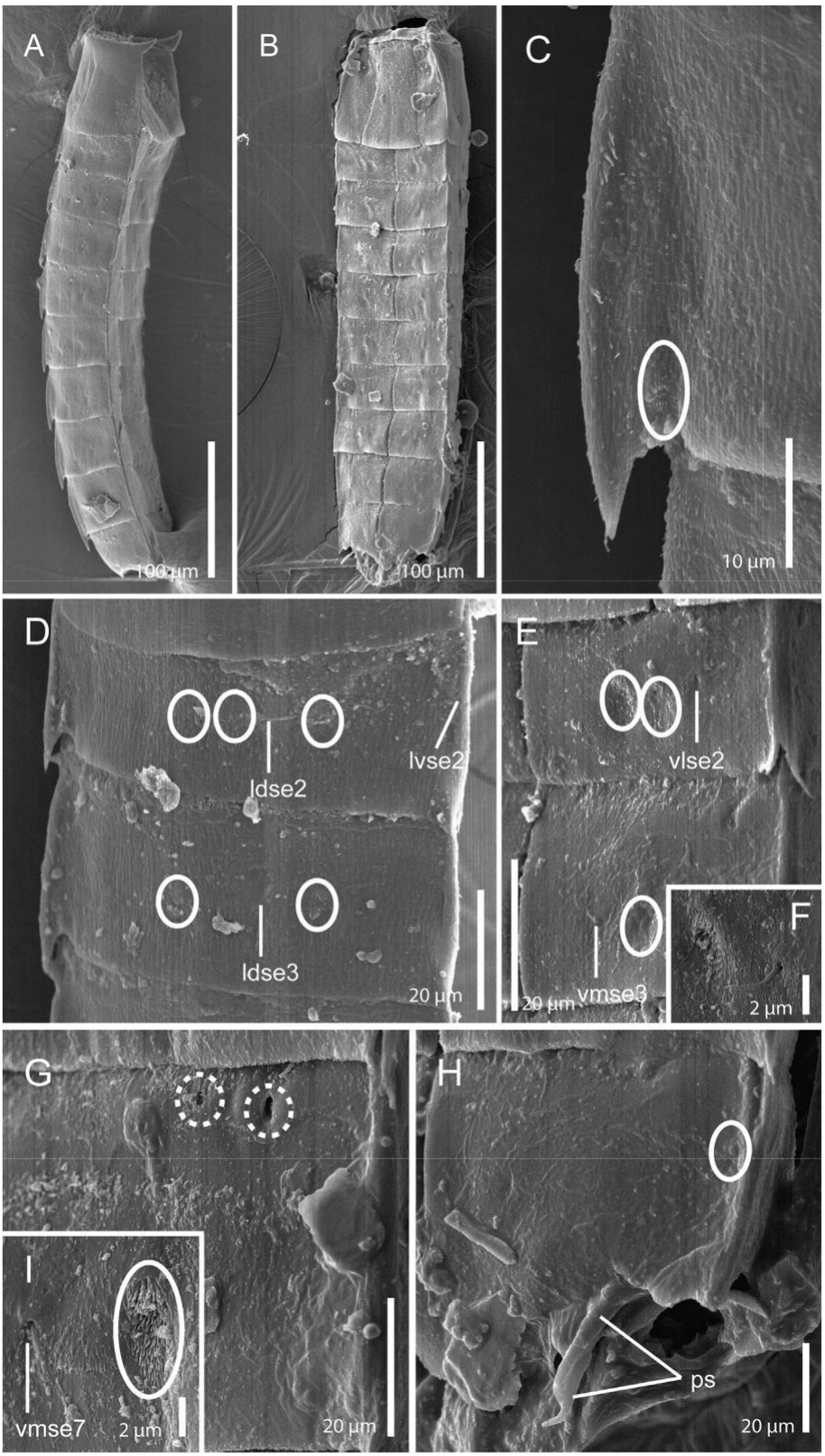

Fig. 5. Scanning electron micrographs showing general overviews and details of the cuticular trunk morphology of non-type male of *Cristaphyes cornifrons* sp. nov. (A) Lateral overview of trunk; (B) ventral overview of trunk; (C) paradorsal view on right half of segment 8, with detail of the middorsal process and the paradorsal sensory spot; (D) subdorsal to lateroventral view on right half of segments 2-3; (E) left sternal plates of segments 2-3; (F) detail of ventrolateral seta and ventromedial sensory spot of segment 3; (G) left sternal plates of segment 7, with detail of the ventral cuticular ridge and the associated glandular cell outlets; (H) left sternal plates of segments 10-11, showing the male penile spines; (I) ventromedial view on left half of segment 7, with detail of the ventromedial seta and the ventromedial sensory spot. Abbreviations: ldse, laterodorsal seta; lvse, lateroventral seta; ps, penile spine; vlse, ventrolateral seta; vmse, ventromedial seta; sensory spots are marked as closed circles, and glandular cell outlets as dashed circles; numbers after abbreviations indicate the corresponding segment.

Table 1
Data on sampling localities and habitat of the collected specimens.

Station code	Location	Geographical coordinates	Sampling date	Sediment	Depth (m)
L1	La Parguera (Puerto Rico)	17°57′00″N 67°03′00″W	07/06/1967	Mud	15
L2	St. James (Barbados)	13°13′12″N 59°37′12″W	23/08/1968	Unknown	Unknown

Table 2
Measurements of adult *Cristaphyes cornifrons* sp. nov. from Puerto Rico, including number of measured specimens (*n*), mean of data and standard deviation (SD).

Character	Range	Mean (SD; *n*)
TL (µm)	422.6-481.8	447.9 (30.5; 3)
MSW-5 (µm)	101.0-111.7	105.3 (5.6; 3)
MSW-5/TL (%)	21.5-24.0	23.6 (2.0; 3)
SW-10 (µm)	76.9-104.2	88.1 (14.3; 3)
SW-10/TL (%)	16.0-23.7	19.8 (3.9; 3)
S1 (µm)	68.5-82.0	76.2 (7.0; 3)
S2 (µm)	35.1-40.6	38.5 (3.0; 3)
S3 (µm)	43.3-50.0	46.0 (3.3; 3)
S4 (µm)	44.7-49.8	47.0 (2.6; 3)
S5 (µm)	45.8-51.6	48.9 (2.9; 3)
S6 (µm)	48.3-53.5	50.6 (2.6; 3)
S7 (µm)	47.1-52.5	48.9 (3.1; 3)
S8 (µm)	47.8-54.5	50.6 (3.5; 3)
S9 (µm)	46.9-58.7	53.4 (6.0; 3)
S10 (µm)	35.5-49.0	43.4 (7.1; 3)
S11 (µm)	24.6-38.7	29.6 (7.8; 3)
LTS (µm)	111.7-181.8	151.6 (36.0; 3)
LTS/TL (%)	25.4-43.0	34.0 (8.8; 3)

Abbreviations: LTS, lateral terminal spine; MSW-5, maximum sternal width (on segment 5); S, segment lengths (numbers after S indicate the corresponding segment); SW-10, standard sternal width (on segment 10); TL, total length of trunk.

stout, wide, apparently flexible (Figs. 2A-D, 3A, B and 5B).

3.1.6. Remarks on diagnostic characters

Of the 23 species currently belonging to *Cristaphyes*, the newly described species may be distinguished from eight of them by the possession of lateral terminal spines, as *Cristaphyes anomalus* (Lang, 1953), *Cristaphyes belizensis* (Higgins, 1983), *Cristaphyes harrisoni* Pardos et al., 2016a,b, *Cristaphyes panamensis* Pardos et al., 2016a,b (in Pardos et al., 2016a), *Cristaphyes phyllotropis* (Brown & Higgins, 1983), *Cristaphyes rabaulensis* (Adrianov, 1999 in Adrianov & Malakhov, 1999), *Cristaphyes spinosus* (Lang 1949) and *Cristaphyes yushini* (Adrianov, 1989) lack these structures. Additionally, males of *C. cornifrons* sp. nov. do not have ventral tubes on segment 2, whereas males of eleven of the remaining congeners do, namely *Cristaphyes abyssorum* (Adrianov & Maiorova, 2015), *Cristaphyes arctous* (Adrianov, 1999 in Adrianov & Malakhov, 1999), *Cristaphyes carinatus* (Zelinka, 1928), *Cristaphyes chukchiensis* (Higgins, 1991), *Cristaphyes cristatus* (Sánchez et al., 2013), *Cristaphyes cryopygus* (Higgins & Kristensen 1988), *Cristaphyes dordaidelosensis* Sørensen & Grzelak, 2018, *Cristaphyes furugelmi* (Adrianov, 1999 in Adrianov & Malakhov, 1999), *Cristaphyes glaurung* Sørensen & Grzelak, 2018, *Cristaphyes odhneri* (Lang, 1949) and *Cristaphyes scatha* Sørensen & Grzelak, 2018. Male specimens of *Cristaphyes nubilis* (Sánchez et al., 2014) are unknown, so this species cannot be assumed to lack these tubes. Of the four remaining congeners, *Cristaphyes chilensis* (Lang, 1953) and *C. nubilis* possess middorsal processes from segment 1, unlike *C. cornifrons* sp. nov. that has these structures from segment 2. Moreover, both species differ from the new species by keel-shaped middorsal process at segment 10 clearly surpassing beyond the posterior margin of the segment (Lang 1953; Sánchez et al. 2014).

C. cornifrons sp. nov. is most similar to *Cristaphyes fortis* Cepeda et al., (in Cepeda et al. 2019a) and *Cristaphyes longicornis* (Higgins, 1983) as all three of them share the presence of lateral terminal spines and the lack of ventral tubes on segment 2 in males. However, there are some remarkable differences in the setae arrangement, which justifies the erection of the new species: *C. cornifrons* sp. nov. possesses unpaired setae in paradorsal position on segments 2, 4 and 6, whereas *C. longicornis* carries these structures on segments 2, 4, 6 and 8. Additionally, *C. cornifrons* sp. nov. has paired setae in ventrolateral position on segments 2-3, 5 and 10 (only in females) and in ventromedial position on segments 4-9, while *C. longicornis* bears ventrolateral setae on segments 2, 5 and 10 and in ventromedial position on segments 1 and 3-9. Main morphological differences in the setae location between *C. cornifrons* sp. nov. and *C. fortis* are found in the sternal plates. Thus, *C. cornifrons* sp. nov. is characterized by a single pair of ventrolateral setae on segments 2-3, 5 and 10 (only in females), while *C. fortis* has two pairs of ventrolateral setae on segment 5 and a single pair on segments 2-4, 6-7 and 10. Moreover, *C. cornifrons* sp. nov. has ventromedial setae on segments 4-9 whereas *C. fortis* bears these structures only on segments 8-9.

Additionally, *C. longicornis* and *C. fortis* are larger species than *C. cornifrons* sp. nov. (TL average of *C. cornifrons*: 447.9 µm; *C. fortis*: 644.5 µm; *C. longicornis*: 636.7 µm), and although the three species are characterized by having the anterolateral margins of segment 1 forming horn-shaped extensions, these are much more elongated and curved inwards in *C. cornifrons* sp. nov. than those of *C. fortis* and *C. longicornis*. *C. fortis* also

Table 3
Summary of nature and arrangement of sensory spots, glandular cell outlets, cuticular processes, setae, nephridiopores and spines in adults of *Cristaphyes cornifrons* sp. nov.

Segment	MD	PD	SD	LD	PL	LV	VL	VM
1			gco, ss	ss	se		ss, gco	
2	cp	se*, ss	gco, ss, ss	gco, se, ss		se	se, gco	ss, ss, gco
3	cp	ss	gco, ss	gco, se, ss			se⋮, gco	ss, gco
4	cp	se*, ss	gco, ss	gco, se, ss		se	gco	ss, se, gco
5	cp	ss	gco, ss	gco, se, ss			se, gco	ss, se, gco
6	cp	se*, ss	gco, ss	gco, se, ss		se	gco	ss, se, gco
7	cp	ss	gco, ss	gco, se, ss			gco	ss, se, gco
8	cp	ss	gco, ss	gco, se, ss		se	gco	ss, se, gco
9	cp	ss	gco, ss	gco, se, ss		ne	gco	ss, se, gco
10	cp	ss	gco, ss	gco, ssx, ss		se	se (f), ss, gco	ss, gco
11			ss3	ss3		lts, psx2 (m)		

Abbreviations: cp, cuticular process; f, female condition of sexually dimorphic character; gco, glandular cell outlet; LD, laterodorsal; lts, lateral terminal spine; LV, lateroventral; m, male condition of sexually dimorphic character; MD, middorsal; ne, nephridiopore; PD, paradorsal; PL, paralateral; ps, penile spine; se, seta; ss, sensory spot; ss3, type 3 sensory spot; SD, subdorsal; VL, ventrolateral; VM, ventromedial; ⋮, indicates intraspecific variation between ventrolateral or ventromedial position; *, indicates unpaired structures.

has the pachycycly and ball-and-socket joints much more developed than *C. cornifrons* sp. nov, being thicker and stouter in the former, but this could be related to the age of the type specimens of *C. fortis*. Finally, *C. longicornis* possesses conspicuous apodemes in segments 8-10, which are absent in *C. cornifrons* sp. nov.

3.1.7. Associated kinorhynch fauna

C. cornifrons sp. nov. co-occurred with the cyclorhagids *Echinoderes astridae* Sørensen, 2014, *Echinoderes horni* Higgins, 1983, *Echinoderes orestauri* Pardos et al., 2016 (in Pardos et al. 2016b) and *Echinoderes spinifurca* Sørensen et al., 2005, and the allomalorhagids *Cristaphyes* sp. and *Dracoderes spyro* Cepeda et al., (in Cepeda et al. 2019b).

Class **Cyclorhagida** (Zelinka 1896) Sørensen et al. 2015.
Family **Echinoderidae** Zelinka 1894.
Genus ***Echinoderes*** Claparède, 1863.

3.2. ***Echinoderes barbadensis*** sp. nov.
urn:lsid:zoobank.org:act:BCF2D1F5-A0AF-480E-B1E1-3E5AB93E1083.
(Figs. 6-8 and Tables 4 and 5).

3.2.1. Type material

Holotype, adult male, unknown collector, sampling done on 23 Aug 1968 at St. James (Barbados), Caribbean Sea, eastern Atlantic Ocean (L2): 13º13′12″N, 59º37′12″W (Table 1; Fig. 1A, C), depth and sediment unknown; mounted in Fluoromount G®, NMNH accession number: USNM 1550576. Paratypes, three adult males and three adult females, with same collecting data as holotype; mounted in Fluoromount G®, NMNH accession numbers: USNM 1550577-1550582.

3.2.2. Non-type material

Six additional specimens with same collecting data as holotype and paratypes, mounted for SEM, deposited at the Invertebrates Collection of the Meiofaunal Laboratory at the Universidad Complutense de Madrid (UCM), Spain.

3.2.3. Diagnosis

Echinoderes with short middorsal spines on segments 4-8, lateroventral spines on segments 6-9, lateral accessory tubes on segment 8, lateroventral tubes on segment 5 and ventrolateral tubes on segment 2. Type 2 glandular cell outlets present in subdorsal position on segment 2 and in midlateral position on segment 4. Cuticular hairs densely distributed through all cuticular surface (except on segment 11), very long, bracteate. Segment 11 with a middorsal, triangular, protuberance-like structure emerging between segments 10 and 11, located near the anterior segment margin. Sternal extensions of segment 11 bearing paired, very long, thick cuticular hairs.

3.2.4. Etymology

The species name refers to Barbados, the type locality where the species was found.

3.2.5. Description

See Table 4 for measurements and dimensions, and Table 5 for summary of spine, tube, nephridiopore, glandular cell outlet and sensory spot locations.

Head with retractable mouth cone and introvert. Although some of the paratypes have the introvert partially everted, oral styles and scalids tended to collapse when mounted for LM; furthermore, specimens for SEM were not suitable for head examination, so details on the exact number, arrangement and morphology of oral styles and scalids cannot be provided.

Neck with sixteen trapezoidal placids, wider at base, with a deep indentation on its anterior margin, and distinguished joint between the neck and segment 1 (Figs. 6A, B and 7B, C). Midventral placid widest (ca. 12-13 µm wide at base) (Figs. 6A and 7C), remaining ones alternate between wider and narrower (ca. 8-10 µm at base) (Figs. 6A, B and 7B, C). Placids situated closely together at base, distally separated by cuticular folds (Figs. 6A, B and 7B, C). Six long, hairy trichoscalids attached to trichoscalid plates present (Figs. 6A, B and 7B, C).

Trunk outline orbicular, stubby, strongly sclerotized, hairy, heart-shaped in cross-section, composed of eleven trunk segments (Figs. 6A, B, 7A and 8A). Segments 1-2 as closed cuticular rings; remaining ones with one tergal and two sternal plates (Figs. 6A-D and 7A). Midsternal and tergosternal junctions as conspicuous lines on the cuticle (Figs. 6A-D and 7A). Tergal anterior plates noticeably bulging middorsally; posterior ones more flattened, giving the animal a tapering outline in lateral view (Fig. 8A). Sternal plates reach their maximum width at segment 5, slightly tapering towards the last trunk segments (Figs. 6A and 7A). Sternal plates conspicuously wide compared to the total trunk length (MSW-5:TL average ratio = 25.9%), giving the animal a globose, stout appearance (Figs. 6A, B and 7A). Cuticular hairs densely distributed all over the trunk cuticle, except on segment 11, in wavy, continuous, transversely arranged rows along the surface of the cuticle (Figs. 6A-D, 7A-Q and 8A-C, E). Cuticular hairs on all segments bracteate, long, slender, apparently flexible (Fig. 8A-E). Posterior margin of segments straight, with well-developed primary pectinate fringes with an elongated, strongly serrated free flap (Figs. 6A-D, 7A-Q and 8A, C); secondary pectinate fringes absent.

Segment 1 without spines and tubes. Unpaired type 1 glandular cell outlet in middorsal position, near the anterior segment margin; in LM, the glandular cells appear like a row of vertically arranged light refracting granules (Figs. 6B and 7D). Paired sensory spots in subdorsal, laterodorsal and ventrolateral positions, all of them located near the anterior segment margin (Figs. 6A-B and 7D-E). Sensory spots on this and remaining segments are small, circular to oval-shaped areas composed of a ring with few (ca. 8-10) micropapillae varying in size that surround a central pore with an emerging, quite long cilium, not flanked by cuticular hairs (similar to Fig. 8D, F). Cuticular hairs distributed in 7-9 rows (Figs. 6A-B and 7D, E).

Segment 2 with paired tubes in ventrolateral position (Figs. 6A and 7G). Type 1 glandular cell outlet unpaired in middorsal and paired in ventromedial positions, both located near the anterior segment margin, as rows of horizontally arranged light refracting granules (Figs. 6A, B and 7F, G). Paired type 2 glandular cell outlets in subdorsal position, (Figs. 6B, 7F and 8B). Paired sensory spots in laterodorsal position (Figs. 6B and 7F). Cuticular hairs distributed in 5-6 rows (Figs. 6A, B and 7F, G).

Segment 3 without spines and tubes. Type 1 glandular cell outlet unpaired in middorsal and paired in ventromedial positions, similar to those of preceding segments (Figs. 6A, B and 7H, I). Paired sensory spots in ventrolateral position (Figs. 6A and 7I). Cuticular hairs distributed as on the preceding segment.

Segment 4 with a short, acicular middorsal spine not exceeding the posterior edge of the segment (Figs. 6B and 7H). Paired type 1 glandular cell outlets in paradorsal and ventromedial positions, similar to those of preceding segments (Figs. 6A, B and 7H, I). Paired type 2 glandular cell outlets in midlateral position, near the posterior segment margin, smaller than those of the second trunk segment (Figs. 6A and 7I). Paired sensory spots in paradorsal and ventrolateral positions, the former anterior to the base of the middorsal spine, the latter near the posterior margin of segment (Figs. 6A, B and 7H, I). Cuticular hairs distributed in 8-10 rows (Figs. 6A, B and 7H, I).

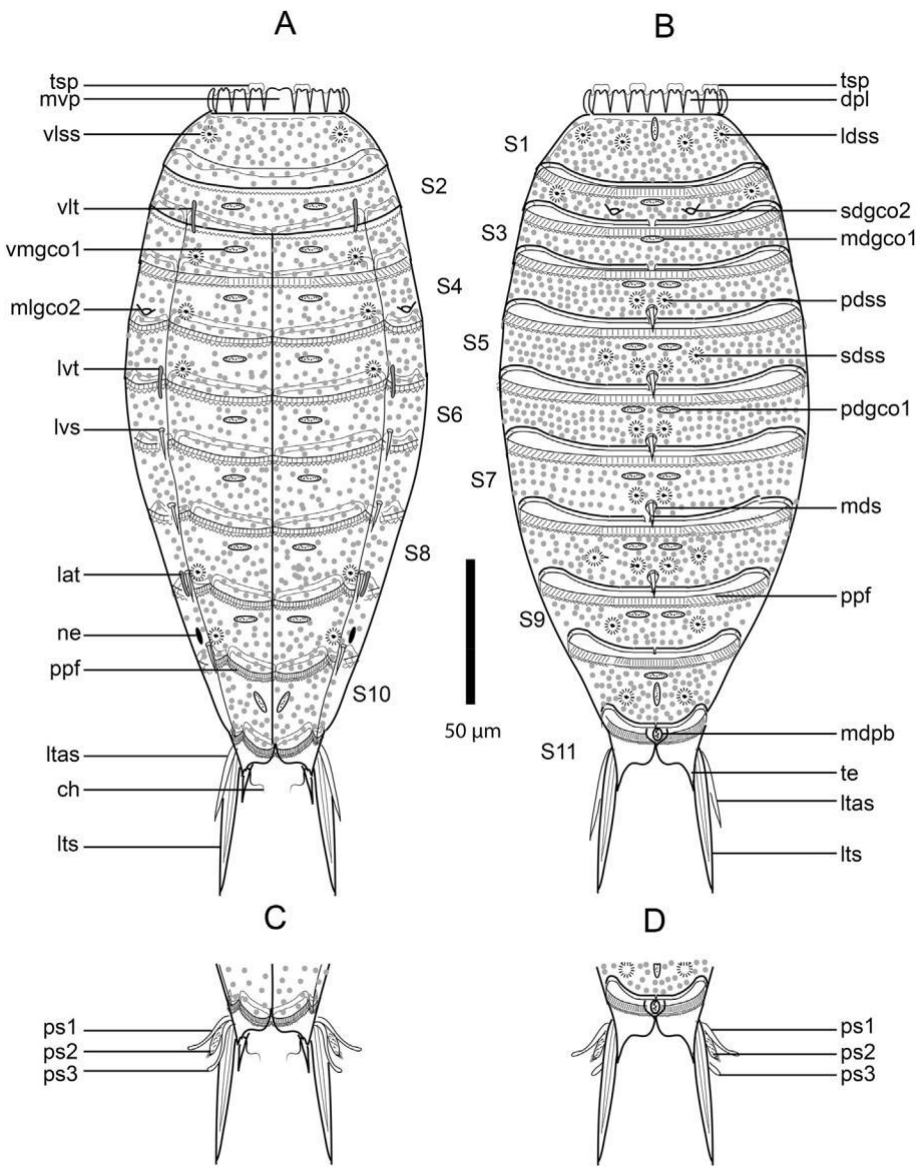

Fig. 6. Line art illustrations of *Echinoderes barbadensis* sp. nov. (A) Female, ventral overview; (B) Female, dorsal overview; (C) Male, segments 10-11, ventral view; (D) Male, segments 10-11, dorsal view. Abbreviations: ch, cuticular tuft of hairs; dpl, dorsal placid; lat, lateral accessory tube; ldss, laterodorsal sensory spot; ltas, lateral terminal accessory spine; lts, lateral terminal spine; lvs, lateroventral spine; lvt, lateroventral tube; mdgco1, middorsal type 1 glandular cell outlet; mdpb, middorsal protuberance; mds, middorsal spine; mlgco2, midlateral type 2 glandular cell outlet; mvp, midventral placid; ne, nephridiopore; pdgco1, paradorsal type 1 glandular cell outlet; pdss, paradorsal sensory spot; ppf, primary pectinate fringe; ps, penile spine; S, segment followed by number of corresponding segment; sdgco2, subdorsal type 2 glandular cell outlet; sdss, subdorsal sensory spot; te, tergal extension; tsp, trichoscalid plate; vlss, ventrolateral sensory spot; vmgco1, ventromedial type 1 glandular cell outlet; vlt, ventrolateral tube; cuticular hairs are drawn as grey dotes to make the interpretation of the remaining cuticular characters easier.

Segment 5 with a short, acicular middorsal spine not exceeding the posterior edge of the segment and paired tubes in lateroventral position (Figs. 6A, B, 7L, M and 8C). Paired type 1 glandular cell outlets in paradorsal and ventromedial positions, similar to those of preceding segments (Figs. 6A, B and 7L, M). Paired sensory spots in paradorsal, subdorsal and ventrolateral positions, the former anterior to the base of the middorsal spine, the latter near the posterior margin of segment (Figs. 6A, B and 7L, M). Cuticular hairs distributed in 7-10 rows (Figs. 6A, B and 7L, M).

Segment 6 with a short, middorsal spine not exceeding the posterior edge of the segment and paired spines in lateroventral position (Figs. 6A, B, 7L, M and 8C). Paired type 1 glandular cell outlets in paradorsal and ventromedial positions, similar to those of preceding segments (Figs. 6A, B and 7L, M). Paired sensory spots in paradorsal position, located anteriorly to the base of the middorsal spine (Figs. 6B and 7L). Cuticular hairs distributed in 7-9 rows (Figs. 6A, B and 7L, M).

Segment 7 similar to segment 6 but with the cuticular hairs distributed in 9-11 rows (Figs. 6A, B, 7J, K and 8C).

Segment 8 with a middorsal spine not exceeding the posterior margin of the segment and paired spines in lateroventral position (Figs. 6A, B, 7J, K and 8C, E). Paired tubes in lateral accessory position (Figs. 6A, 7K and 8C, E). Paired type 1 glandular cell outlets in paradorsal and ventromedial positions, similar to those of preceding segments (Figs. 6A, B and 7J, K). Paired sensory spots in paradorsal, subdorsal and ventrolateral positions, the former anterior to the base of the middorsal spine, the latter close to the lateroventral spines near the anterior margin of segment (Figs. 6A, B, 7J, K and 8D). Cuticular hairs distributed in 9-12 rows (Figs. 6A, B and 7J, K).

Segment 9 with paired spines in lateroventral position (Figs. 6A, 7O and 8C). Cuticular hairs distributed in 10-13 wavy, continuous, transversely arranged rows along the surface of the cuticle (Figs. 6A, B and 7N, O). Paired

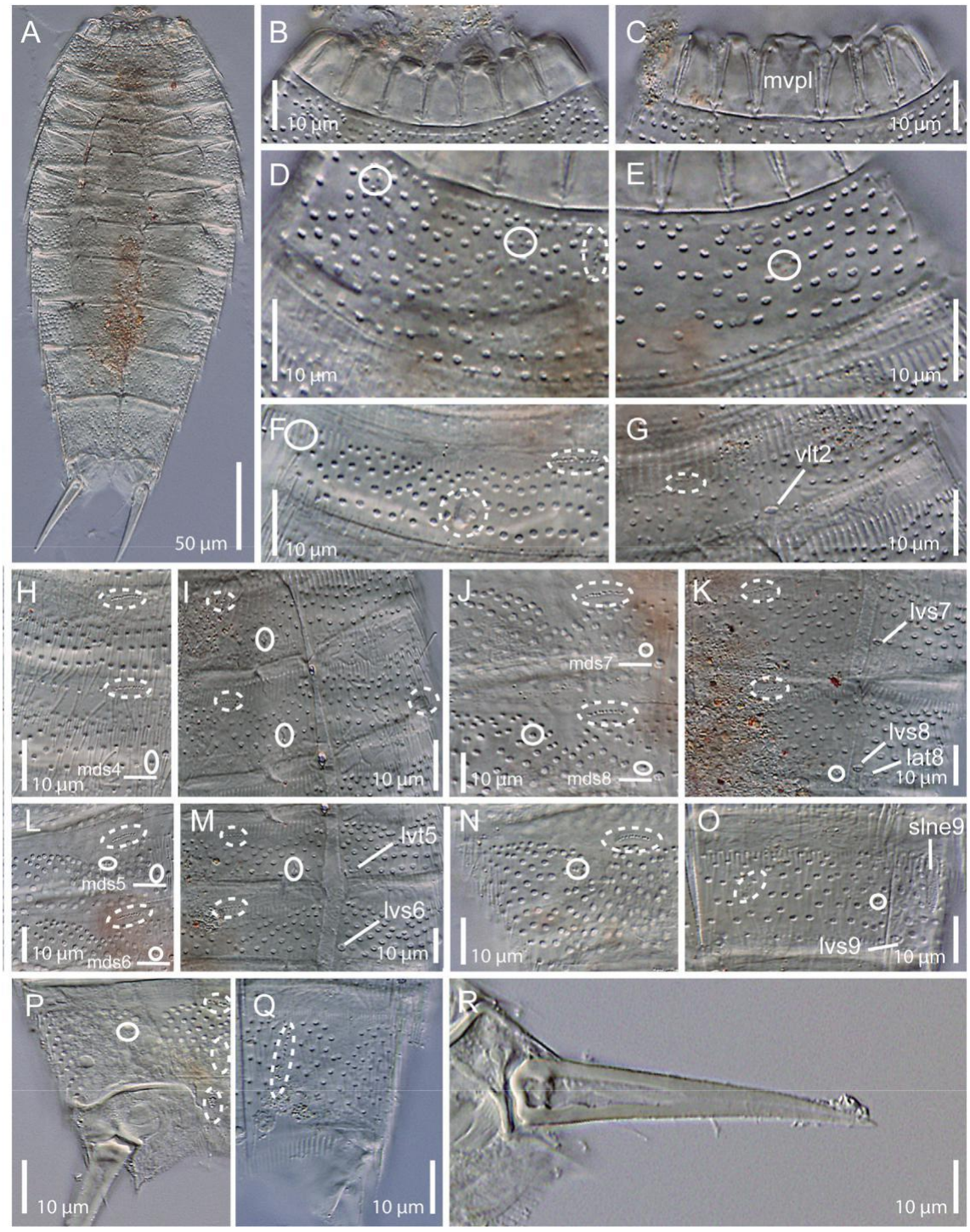

Fig. 7. Light micrographs showing overviews, neck and trunk cuticular details and structures of male holotype USNM 1550576 of *Echinoderes barbadensis* sp. nov. (A) Ventral overview of trunk; (B) dorsal view of neck, showing the dorsal placids; (C) ventral view of neck, showing the ventral placids; (D) middorsal to laterodorsal view on left half of segment 1; (E) lateroventral to ventromedial view on left half of segment 1; (F) middorsal to laterodorsal view on left half of segment 2; (G) lateroventral to ventromedial view on left half of segment 2; (H) left halves of tergal plates of segments 3-4; (I) sublateral to ventromedial view on left half of segments 3-4, (J) middorsal to subdorsal view on left half of segments 7-8; (K) lateroventral to ventromedial view on left half of segments 7-8; (L) middorsal to subdorsal view on left half of segments 5-6; (M) lateroventral to ventromedial views on left half of segments 5-6; (N) middorsal to subdorsal view on left half of segment 9; (O) lateroventral to ventromedial view on left half of segment 9; (P) left halves of tergal plates of segments 10-11; (Q) left sternal plates of segments 10-11; (R) lateral terminal spine. Abbreviations: lat, lateral accessory tube; lvs, lateroventral spine; lvt, lateroventral tube; mds, middorsal spine; mvpl, midventral placid; slne, sublateral nephridiopore; vlt, ventrolateral tube; sensory spots are marked as closed circles, and glandular cell outlets as dashed circles; numbers after abbreviations indicate the corresponding segment.

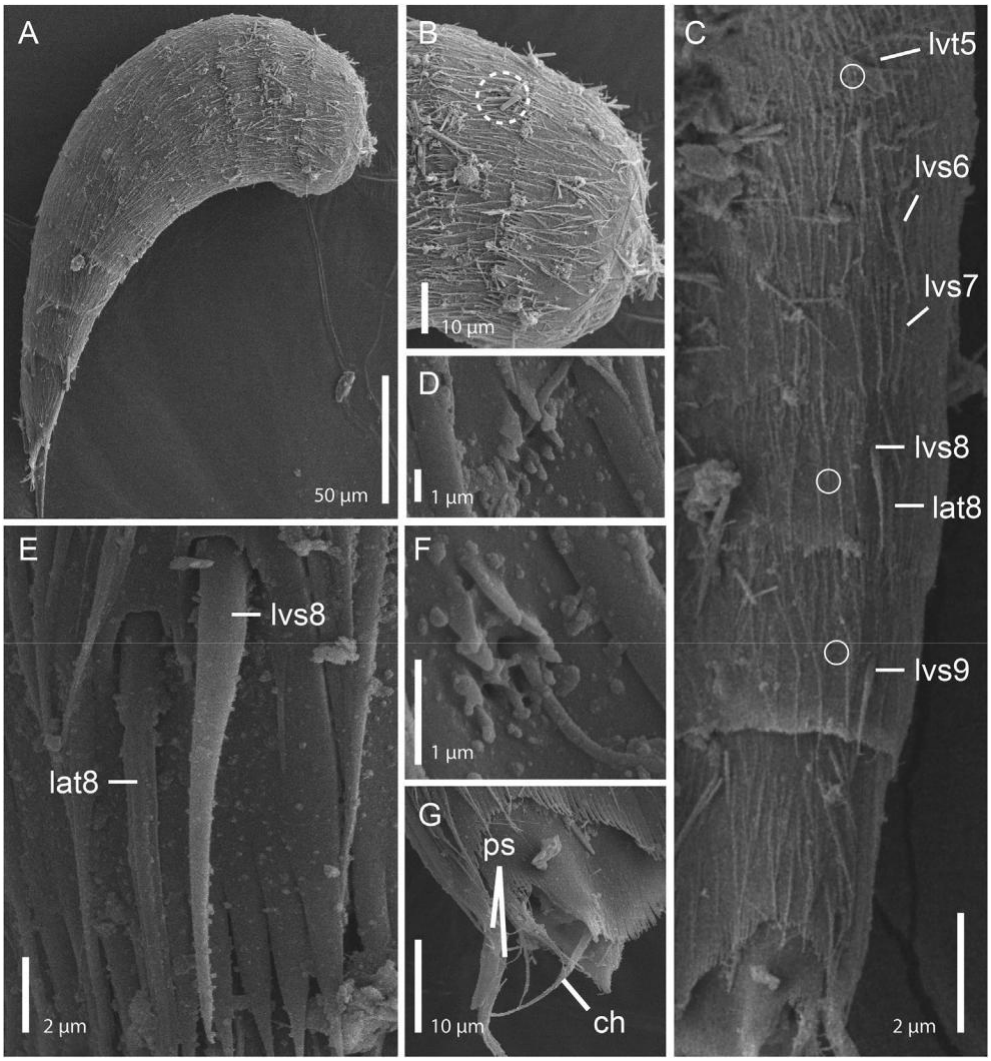

Fig. 8. Scanning electron micrographs showing general overview and details of the cuticular trunk morphology of non-type female (A-B) and male (C-G) of *Echinoderes barbadensis* sp. nov. (A) Lateral overview of trunk; (B) subdorsal to lateroventral view on left half of segments 1-2; (C) lateroventral overview of segments 5-10; (D) detail of ventrolateral sensory spot of segment 8; (E) detail of the lateral accessory tube and the lateroventral spine of right side of tergal plate of segment 8; (F) detail of the ventrolateral sensory spot of sternal plates of segment 8; (G) ventral overview of right sternal plate of segments 10-11, with detail of the penile spines and the elongated, basal, thick cuticular hair of the tergal extensions. Abbreviations: ch, cuticular tuft of hairs; lat, lateral accessory tube; lvs, lateroventral spine; lvt, lateroventral tube; ps, penile spines; sensory spots are marked as closed circles, and glandular cell outlets as dashed circles; numbers after abbreviations indicate the corresponding segment.

type 1 glandular cell outlets in paradorsal and ventromedial positions, similar to those of preceding segments (Figs. 6A, B and 7N, O). Paired sensory spots in subdorsal and ventrolateral positions, the latter close to the lateroventral spines, near the posterior margin of segment (Figs. 6A-B and 7N, O). Paired nephridiopores in sublateral position, as a longitudinally elongated, oval-shaped sieve plate (Fig. 7O).

Segment 10 without spines and tubes. Two unpaired type 1 glandular cell outlets in middorsal position, one horizontally arranged and near the anterior margin of segment, the other one vertically arranged and posterior to the other outlet (Figs. 6B and 7P). Paired type 1 glandular cell outlets in ventromedial position, near the anterior margin of segment, obliquely arranged (Figs. 6A and 7Q). Paired sensory spots in subdorsal position, not aligned with those of the previous segments, mesially shifted, near the posterior margin of segment (Figs. 6B and 7P). Cuticular hairs distributed in 10-12 rows (Figs. 6A, B and 7P, Q).

Segment 11 with quite short lateral terminal spines (LTS:TL average ratio = 20.1%), stout, rigid, distally pointed, showing a central cavity (Fig. 6A-D and 7A, R). Females with paired lateral terminal accessory spines (LTAS:LTS average ratio = 34.7%), slender, flexible, distally pointed (Fig. 6A, B). Males with three pairs of penile spines, first and third pairs longer and slender, superficially smooth and distally rounded, second pair shorter and stouter, superficially hairy with a distal tuft of hairs (Figs. 6C, D and 8G). Dorsal plate with an anterior, middorsal, triangular, protuberance-like structure that emerges between segments 10 and 11 (Fig. 6B, D). Unpaired type 1 glandular cell outlet in middorsal position, vertically arranged near the posterior margin of segment (Figs. 6B, D and 7P). Tergal extensions quite long, distally elongated and pointed (Figs. 6B, D and 7P). Sternal extensions wide, distally rounded, bearing a basal tuft of thick, long hairs (Figs. 6A, C, 7Q and 8G).

Table 4
Measurements of adult *Echinoderes barbadensis* sp. nov. from Barbados, including number of measured specimens (*n*), mean of data and standard deviation (SD).

Character	Range	Mean (SD; *n*)
TL (µm)	223.7-307.0	275.0 (18.6; 20)
MSW-5 (µm)	62.5-86.6	71.0 (4.8; 20)
MSW-5/TL (%)	23.2-32.1	25.9 (2.0; 20)
SW-10 (µm)	53.6-67.0	59.2 (4.1; 20)
SW-10/TL (%)	20.0-24.5	21.6 (1.8; 20)
S1 (µm)	29.0-33.9	31.1 (1.3; 20
S2 (µm)	27.2-33.5	30.1 (1.7; 20)
S3 (µm)	29.7-35.9	32.9 (1.7; 20)
S4 (µm)	26.5-40.4	36.8 (2.9; 20)
S5 (µm)	31.8-42.1	37.1 (2.3; 20)
S6 (µm)	32.6-42.7	38.8 (2.4; 20)
S7 (µm)	37.1-42.6	40.5 (1.4; 20)
S8 (µm)	40.3-44.3	42.4 (1.4; 20)
S9 (µm)	39.4-46.9	44.2 (1.8; 20)
S10 (µm)	41.1-48.7	45.8 (1.8; 20)
S11 (µm)	22.3-39.2	31.7 (3.9; 20)
MD4 (ac) (µm)	6.5-12.6	9.6 (1.6; 18)
MD5 (ac) (µm)	6.8-12.2	9.7 (1.4; 19)
MD6 (ac) (µm)	7.7-13.6	10.5 (1.7; 19)
MD7 (ac) (µm)	6.7-14.8	11.0 (2.1; 19)
MD8 (ac) (µm)	7.3-12.8	10.5 (1.2; 20)
VL2 (tu) (µm)	6.3-11.5	8.6 (1.4; 15)
LV5 (tu) (µm)	6.3-11.1	8.4 (1.2; 19)
LV6 (ac) (µm)	8.0-13.6	11.0 (1.4; 20)
LV7 (ac) (µm)	8.0-13.7	10.4 (1.3; 20)
LV8 (ac) (µm)	9.1-15.0	10.6 (1.4; 20)
LA8 (tu) (µm)	6.3-10.9	7.7 (1.0; 20)
LV9 (ac) (µm)	9.5-13.4	11.3 (1.3; 19)
LTS (µm)	48.4-58.3	55.1 (2.5; 19)
LTS/TL (%)	17.4-24.9	20.1 (1.9; 19)
LTAS (µm)	17.2-21.6	19.0 (1.2; 10)
LTAS/LTS (%)	31.8-44.6	34.7 (3.5; 10)

Abbreviations: ac, acicular spine; LA, lateral accessory; LTAS, lateral terminal accessory spine; LTS, lateral terminal spine; LV, lateroventral; MD, middorsal; MSW-5, maximum sternal width (on segment 5); S, segment lengths (numbers after S indicate the corresponding segment); SW-10, standard sternal width (on segment 10); TL, total length of trunk; tu, tube; VL, ventrolateral.

3.2.6. Remarks on diagnostic characters

E. barbadensis sp. nov. possesses middorsal spines on segments 4-8 and short, robust lateral terminal spines. There are only seven species with this pattern of characters: *Echinoderes aquilonius* Higgins & Kristensen, 1988, *Echinoderes augustae* Sørensen & Landers, 2014, *Echinoderes brevicaudatus* Higgins, 1966, *Echinoderes cavernus* Sørensen et al., 2000, *Echinoderes lusitanicus* Neves et al., 2016 (only females), *Echinoderes obtuspinosus* Sørensen et al., 2012 and *Echinoderes ulsanensis* Adrianov, 1999 in Adrianov & Malakhov, 1999. Nonetheless, *E. barbadensis* sp. nov. can be unambiguously distinguished from the aforementioned congeners by the arrangement of the remaining spines and tubes, and the pattern of type 2 glandular cell outlets.

E. lusitanicus and *E. ulsanensis* are the species that most differ from *E. barbadensis* sp. nov., as only possess lateroventral spines on segments 8-9 and 6-8 respectively, whereas *E. barbadensis* has lateroventral spines on segments 6-9.

The pattern of tubes allows distinguishing *E. aquilonius* and *E. obtuspinosus* from *E. barbadensis* sp. nov.: the first two bear these structures only in lateroventral position on segment 5, whereas the latter has tubes in lateral accessory position on segment 8, lateroventral position on segment 5 and ventrolateral position on segment 2. The pattern of the type 2 glandular cell outlets is also different: *E. aquilonius* bears these structures in subdorsal position on segments 2 and 4, laterodorsal position on segment 10, sublateral position on segment 8, midlateral position on segments 2 and 5, and ventrolateral position on segment 2; *E. obtuspinosus* has the glands in subdorsal position on segments 2 and 4, laterodorsal position on segment 2, sublateral position on segments 2 and 8, and ventrolateral position on segment 2; *E. barbadensis* sp. nov. only has type 2 glandular cell outlets in subdorsal position on segment 2 and midlateral position on segment 4.

E. augustae, *E. brevicaudatus* and *E. cavernus* are similar to *E. barbadensis* sp. nov. in the possession of lateroventral spines on segments 6-9, lateroventral tubes on segment 5 and lateroventral/ventrolateral tubes on segment 2. However, *E. augustae* also possesses tubes in midlateral position on segment 4, laterodorsal position on segment 10 (only males), and sublateral position on segment 8, whereas *E. barbadensis* sp. nov. carries these structures only in lateral accessory position on segment 8. Additionally, *E. brevicaudatus* and *E. cavernus* lack tubes in lateral accessory position on segment 8 and type 2 glandular cell outlets, structures present in *E. barbadensis* sp. nov. as mentioned above.

3.2.7. Associated kinorhynch fauna

No other kinorhynch species co-occurred with *E. barbadensis* sp. nov. in the studied location.

Table 5
Summary of nature and arrangement of sensory spots, glandular cell outlets, spines, tubes and nephridiopores in adults of *Echinoderes barbadensis* sp. nov.

Segment	MD	PD	SD	LD	ML	SL	LA	LV	VL	VM
1	gco1		ss	ss					ss	
2	gco1		gco2	ss					t	gco1
3	gco1								ss	gco1
4	ac	gco1, ss			gco2				ss	gco1
5	ac	gco1, ss	ss					t	ss	gco1
6	ac	gco1, ss						ac		gco1
7	ac	gco1, ss						ac		gco1
8	ac	gco1, ss	ss				t	ac	ss	gco1
9		gco1	ss			ne		ac	ss	gco1
10	gco1, gco1		ss							gco1
11	pr, gco1						psx3 (m), ltas (f)	lts		

Abbreviations: ac, acicular spine; f, female condition of sexually dimorphic character; gco1/2, glandular cell outlet type 1/2; LA, lateral accessory; LD, laterodorsal; ltas, lateral terminal accessory spine; lts, lateral terminal spine; LV, lateroventral; m, male condition of sexually dimorphic character; MD, middorsal; ML, midlateral; ne, nephridiopore; PD, paradorsal; pr, protuberance; ps, penile spine; SD, subdorsal; SL, sublateral; ss, sensory spot; t, tube; VL, ventrolateral; VM, ventromedial.

Funding sources

Cepeda was supported by a predoctoral fellowship of the Complutense University of Madrid (CT27/16-CT28/16).

Conflicts of interest

The authors declare no conflicts of interest.

Acknowledgements

We thank Dr Jon Norenburg and Katie Ahlfeld from the NMNH for loaning the studied kinorhynch specimens.

References

Adrianov, A.V., 1989. The first report on Kinorhyncha of the Sea of Japan. Zool. Zh. 68, 17-27.

Adrianov, A.V., Maiorova, A.S., 2015. *Pycnophyes abyssorum* sp. n. (Kinorhyncha: Homalorhagida), the deepest kinorhynch species described so far. Deep Sea Res. Part 2 Top. Stud. Oceanogr. 111, 49-59. https://doi.org/10.1016/j.dsr2.2014.08. 009.

Adrianov, A.V., Malakhov, V.V., 1999. Cephalorhyncha of the World Ocean, first ed. KMK Scientific Press, Moscow.

Brown, R., Higgins, R.P., 1983. A new species of *Kinorhynchus* (Homalorhagida, Pycnophyidae) from Australia with a re-description and range extension of other Kinorhyncha from the South Pacific. Zool. Scr. 12 (3), 161-169. https://doi.org/10.1111/j.1463-6409.1983.tb00561.x.

Cepeda, D., Álvarez-Castillo, L., Hermoso-Salazar, M., Sánchez, N., Gómez, S., Pardos, F., 2019a. Four new species of Kinorhyncha from the Gulf of California. Zool. Anz. 282, 140-160. https://doi.org/10.1016/j.jcz.2019.05.011.

Cepeda, D., Pardos, F., Sánchez, N., 2019b. A new species and first record of *Dracoderes* (Kinorhyncha: Allomalorhagida: Dracoderidae) from American waters, with an identification key of the genus. Zool. Anz. 282, 106-115. https://doi.org/10.1016/j.jcz.2019.05.019.

Cepeda, D., Sánchez, N., Pardos, F., 2019c. First report of the family Zelinkaderidae (Kinorhyncha: Cyclorhagida) for the Caribbean Sea, with the description of a new species of *Triodontoderes* Sørensen and Rho, 2009 and an identification key for the family. Zool. Anz. 282, 116-126. https://doi.org/10.1016/j.jcz.2019.05.017.

Claparède, A.R.E., 1863. Zur Kenntnis der Gattung *Echinoderes* Duj. Beobachtungen über Anatomie und Entwicklungsgeschichte wirbelloser Thiere an der Küste von Normandie angestellt, first ed. Verlag von Wilhelm Engelmann, Leipzig.

Higgins, R.P., 1964. Three new kinorhynchs from the North Carolina Coast. Bull. Mar. Sci. 14, 479-493.

Higgins, R.P., 1966. Faunistic studies in the Red Sea (in winter, 1961-1962). Part II. Kinorhynchs from the area of Al-Ghardaqa. Zool. Jahrb. Abt. Anat. Ontog. Tiere 93, 118e126.

Higgins, R.P., 1983. The Atlantic Barrier Reef ecosystem at Carrie Bow Cay, Belize, II: Kinorhyncha. Smithson. Contrib. Mar. Sci. 18, 1-131. https://doi.org/10.5479/si. 01960768.18.1.

Higgins, R.P., 1988. Kinorhyncha. In: Higgins, R.P., Thiel, H. (Eds.), Introduction to the Study of Meiofauna. Smithsonian Institution Press, Washington D.C., pp. 328-331

Higgins, R.P., 1991. *Pycnophyes chukchiensis*, a new homalorhagid kinorhynch from the Arctic Sea. Proc. Biol. Soc. Wash. 104 (1), 184-188.

Higgins, R.P., Kristensen, R.M., 1988. Kinorhyncha from Disko Island, west Greenland. Smithson. Contrib. Zool. 458, 1-56. https://doi.org/10.5479/si. 00810282.458.

Kirsteuer, E., 1964. Zur Kenntnis der Kinorhynchen Venezuelas. Zool. Anz. 173, 388-393.

Lang, K., 1949. Echinoderida. Furth. Zool. Results Swed. Antarct. Expedition 1901e1903 (4), 1-22.

Lang, K., 1953. Reports of the Lund University Chile expedition 1948-1949. 9. Echinoderida. Lunds universitets Årsskrift N. F. Avd. 2 49 (4), 3-8.

Miloslavich, P., Díaz, J.M., Klein, E., Alvarado, J.J., Díaz, C., et al., 2010. Marine biodiversity in the Caribbean: regional estimates and distribution patterns. PLoS One 5 (8), e11916. http://doi.org/10.1371/journal.pone.0011916.

Neuhaus, B., 2013. Kinorhyncha (=Echinodera). In: Schmidt-Rhaesa, A. (Ed.), Handbook of Zoology, Gastrotricha, Cycloneuralia and Gnathifera, Volume 1: Nematomorpha, Priapulida, Kinorhyncha, Loricifera. De Gruyter, Hamburg, pp. 181-350.

Neves, R., Sørensen, M.V., Herranz, M., 2016. First account on kinorhynchs from Portugal, with the description of two new species: *Echinoderes lusitanicus* sp. nov. and *E. reicherti* sp. nov. Mar. Biol. Res. 12 (5), 1-16. https://doi.org/10.1080/ 17451000.2016.1154973.

Pardos, F., Herranz, M., Sánchez, N., 2016a. Two sides of a coin: the phylum Kinorhyncha in Panama. II) Pacific Panama. Zool. Anz. 265, 26-47. https://doi.org/10. 1016/j.jcz.2016.06.006.

Pardos, F., Sánchez, N., Herranz, M., 2016b. Two sides of a coin: the phylum Kinorhyncha in Panama. I) Caribbean Panama. Zool. Anz. 265, 3-25. https://doi.org/ 10.1016/j.jcz.2016.06-005.

Sánchez, N., Pardos, F., Sørensen, M.V., 2014. Deep-sea Kinorhyncha: two new species from the Guinea Basin, with evaluation of an unusual male feature. Org. Divers. Evol. 14 (4), 349-361. https://doi.org/10.1007/s13127-014-0182-6.

Sánchez, N., Rho, M.S., Min, W.G., Kim, D., Sørensen, M.V., 2013. Four new species of *Pycnophyes* (Kinorhyncha: Homalorhagida) from Korea and the East China Sea. Sci. Mar. 77 (2), 353-380. https://doi.org/10.1007/s13127-014-0182-6.

Sánchez, N., Yamasaki, H., Pardos, F., Sørensen, M.V., Martínez, A., 2016. Morphology disentangles the systematics of a ubiquitous but elusive meiofaunal group (Kinorhyncha: Pycnophyidae). Cladistics 32 (5), 479-505. https://doi.org/10. 1111/cla.12143.

Sørensen, M.V., 2006. New kinorhynchs from Panama, with a discussion of some phylogenetically significant cuticular structures. Meiofauna Mar. 15, 51-77.

Sørensen, M.V., 2014. First account of echinoderid kinorhynchs from Brazil, with the description of three new species. Mar. Biodivers. 44, 251-274. https://doi.org/ 10.1007/s12526-013-0181-4.

Sørensen, M.V., Dal Zotto, M., Rho, H.S., Herranz, M., Sánchez, N., Pardos, F., Yamasaki, H., 2015. Phylogeny of Kinorhyncha based on morphology and two molecular loci. PLoS One 10 (7), e0133440. https://doi.org/10.1371/journal.pone. 0133440.

Sørensen, M.V., Grzelak, K., 2018. New mud dragons from Svalbard: three new species of *Cristaphyes* and the first arctic species of *Pycnophyes* (Kinorhyncha: Allomalorhagida: Pycnophyidae). PeerJ 6, e5653. https://doi.org/10.7717/peerj. 5653.

Sørensen, M.V., Heiner, I., Ziemer, O., 2005. A new species of *Echinoderes* from Florida (Kinorhyncha: Cyclorhagida). Biol. Soc. Wash. 118 (3), 499-508. https://doi.org/10.2988/0006-324X.

Sørensen, M.V., Jørgensen, A., Boesgaard, T.M., 2000. A new *Echinoderes* (Kino-rhyncha: Cyclorhagida) from a submarine cave in New South Wales, Australia. Cah. Biol. Mar. 41, 167-179.

Sørensen, M.V., Landers, S.C., 2014. Two new species of *Echinoderes* (Kinorhyncha: Cyclorhagida) from the Gulf of Mexico. Front. Mar. Sci. 1, e8. https://doi.org/10. 3389/fmars.2014.00008.

Sørensen, M.V., Pardos, F., 2008. Kinorhynch systematics and biology – an introduction to the study of kinorhynchs, inclusive identification keys to the genera. Meiofauna Mar. 16, 21-73.

Sørensen, M.V., Rho, H.S., Min, W.G., Kim, D., Chang, C.Y., 2012. An exploration of *Echinoderes* (Kinorhyncha: Cyclorhagida) in Korean and neighboring waters, with the description of four new species and a redescription of *E. tchefouensis* Lou, 1934. Zootaxa 3368, 161-196.

Zelinka, C., 1894. Über die Organisation von *Echinoderes*. Verh. Dtsch. Zool. Ges. 4, 46-49.

Zelinka, C., 1896. Demonstration der Tafeln der *Echinoderes* e Monographie. Verh. Dtsch. Zool. Ges. 6, 197-199.

Zelinka, C., 1928. Monographie der Echinodera, first ed. Engelmann Press, Leipzig.

Zoologischer Anzeiger 282 (2019) 106-115

Contents lists available at ScienceDirect

Zoologischer Anzeiger

journal homepage: www.elsevier.com/locate/jcz

Research paper

A new species and first record of *Dracoderes* (Kinorhyncha: Allomalorhagida: Dracoderidae) from American waters, with an identification key of the genus*

Diego Cepeda [a, *], **Fernando Pardos** [a], **Nuria Sanchez** [a, b]

[a] *Departamento de Biodiversidad, Ecología y Evolucion, Facultad de Ciencias Biologicas, Universidad Complutense de Madrid, Jose Antonio Novais St. 12, 28040, Madrid, Spain*

[b] *Laboratoire Environnement Profond, Institut Français de Recherche pour l'Exploitation de la Mer (IFREMER), Centre Bretagne - ZI de la Pointe du Diable, CS 10070, 29280, Plouzane, France*

ARTICLE INFO

Article history:
Received 25 February 2019
Received in revised form 20 May 2019
Accepted 23 May 2019
Available online 6 June 2019

Corresponding Editor: Sørensen

Keywords:
Kinorhynchs
Taxonomy
Morphology
Caribbean Sea
Dominican Republic
Haiti

ABSTRACT

A new species of *Dracoderes*, *Daracoderes spyro* sp. nov., is described from Hispaniola Island (Caribbean Sea), and represents the first record of this genus in American waters. The new species is distinguished from its congeners by the presence of lateroventral spines on segments 3-4 and 6-9, lateral accessory spines on segment 5, lateroventral tubes on segments 2, 5 and 10, and laterodorsal tubes on segment 8. Additionally, a dichotomous key to the species level for the genus *Dracoderes* is included.

1. Introduction

The phylum Kinorhyncha comprises a group of meiofaunal, holobenthic, free-living organisms that inhabit the upper centimetres of sandy and muddy marine soft bottoms (Sørensen & Pardos 2008; Neuhaus 2013). Until recently, the phylum was composed of two orders, Cyclorhagida and Homalorhagida (Zelinka 1896; Higgins 1964), comprising 23 genera (Dal Zotto et al. 2013; Sørensen 2013; Sanchez et al. 2014). However, more recent analyses, based on either ribosomal genes, or ribosomal genes combined with morphology, indicated the paraphyly of Cyclorhagida, as the former cyclorhagid genus *Dracoderes* Higgins & Shirayama, 1990 turned out to be more closely related with homalorhagid taxa (Dal Zotto et al. 2013; Yamasaki et al. 2013; Sørensen et al. 2015). As a result, the systematics of the phylum were modified, accommodating the family Dracoderidae within the new class Allomalorhagida, together with the former homalorhagid taxa and the recently established genus *Franciscideres* Dal Zotto et al., 2013 (Sørensen et al. 2015).

Kinorhynchs spend their whole life cycle in the sediment, have a limited locomotion and are gonochoristic. Thus, kinorhynch species have been considered to usually show regional distribution patterns limited to a few hundreds of kilometres (Kozloff 1972; Artois et al. 2011; Yamasaki et al. 2014). Nevertheless, unequal species richness and biogeographical distribution patterns may be found among kinorhynch species by focussing on upper taxonomic categories such as genera or families (Sørensen et al. 2012; Neuhaus 2013). Thus, there are some highly diverse taxa, *e.g.*, the genus *Echinoderes* Claparede, 1863 and the family Pycnophyidae, that are distributed worldwide and together represents more than two thirds of the total number of known kinorhynch species. On the contrary, other taxa display much more restricted biogeographical distributions and are composed of a single or a few species, *e.g.*, the monotypic *Polacanthoderes* Sørensen, 2008 only known from the South Shetland Archipelago in the Antarctic

urn:lsid:zoobank.org:pub:10560CCC-9BF0-4603-A4D6-69A6ABCEF5F0.

* This article is a part of the Fifth International Scalidophora Workshop special issue published in Zoologischer Anzeiger 282C, 2019.

* Corresponding author.
E-mail address: diegocepeda@ucm.es (D. Cepeda).

https://doi.org/10.1016/j.jcz.2019.05.019
0044-5231/

Ocean (Sørensen 2008) or *Neocentrophyes* Higgins, 1969 composed of two species restricted to the Indian Ocean (Higgins 1969). This was also the case of the genus *Dracoderes* that appeared to have a distribution limited to the Seto Inland Sea and the Sea of Japan until the description of a new species from the Atlantic coast of Spain (Sørensen et al. 2012).

Dracoderes currently accommodates six species, five from the northwestern Pacific Ocean, namely *Dracoderes abei* Higgins & Shirayama, 1990 (Seto Inland Sea, Sea of Japan and northwest Pacific); *Dracoderes nidhug* Thomsen et al., 2013 (Korea, Sea of Japan); *Dracoderes orientalis* Adrianov, 1999 in Adrianov & Malakhov, 1999 (Korea, Sea of Japan); *Dracoderes snufkini* Yamasaki, 2015 (Okinawa, East China Sea); and *Dracoderes toyoshioae* Yamasaki, 2015 (Okinawa, East China Sea); and one from Galicia at the Atlantic coast of Spain: *Dracoderes gallaicus* Sørensen et al., 2012. The genus is morphologically characterized by a combination of mouth cone with nine outer oral styles alternating in size, neck with nine placids dorsal and midlaterally interrupted by cuticular foldings, cuticle of first segment as a closed ring, cuticle of remaining segments divided into one tergal and two sternal plates, dorsal spines on at least segments 3-9 with the anteriormorst spine middorsally located, following ones in paradorsal position alternatingly displaced left or right regarding to the middorsal line and posterior-most spine middorsal or paradorsally located, and lateroventral spines on at least segments 6-9 (Higgins & Shirayama 1990; Sørensen et al. 2012; Yamasaki 2015). The most significant morphological differences among species of *Dracoderes* are the position of tubes and dorsal spines, the shape and size of trunk segments, the shape of pectinate fringe and the shape of tergal extensions (Sørensen et al. 2012; Thomsen et al. 2013; Yamasaki 2015). There is also sexual dimorphism in *Dracoderes*, as males possess three pairs of penile spines on segment 11 (Sørensen et al. 2012).

Samples of meiofauna from the Caribbean Sea and adjacent waters collected by Dr R. P. Higgins in 1976 and 1980 and deposited in the Smithsonian National Museum of Natural History of Washington (NMNH) gave the authors the opportunity to study several specimens of *Dracoderes* from Hispaniola Island, the second largest land mass of the Greater Antilles after Cuba, where kinorhynchs have been scarcely studied. There are few papers dealing with the biodiversity of this phylum in the Caribbean Sea (Kirsteuer 1964; Higgins 1983; Sørensen 2006; Neuhaus et al. 2014; Pardos et al. 2016). The present study contributes to the understanding of the taxonomy and biogeographical distribution of the allomalorhagid *Dracoderes* as well as to the knowledge of kinorhynch biodiversity of the Caribbean Sea and adjacent waters.

2. Material and methods

The studied specimens of *Dracoderes* were collected at four different localities in Hispaniola Island, Caribbean Sea (western Atlantic Ocean). Detailed information on the localities and sampling data are summarized in Fig. 1A-C and Table 1. Samplings were performed using a meiobenthic dredge (Higgins 1988). After sampling, meiofauna was extracted from sediment using the bubble and blot method defined by Higgins (1964). Meiofaunal specimens were fixed in 4% formalin and then preserved in Carosafe® or 70% ethanol.

The fixed kinorhynchs were picked up under a Motic® SMZ-168 stereo zoom microscope with the help of an Irwin loop. Initially, specimens were washed with distilled water in order to remove formalin. For light microscopy (LM), specimens were dehydrated through a graded series of 25%, 50%, 75% and 100% glycerin and finally mounted on a glass slide or a Cobb's aluminium slide holder in Fluoromount G® and sealed with Depex®. The mounted specimens were studied and photographed using an Olympus® BX51-P microscope with differential interference contrast (DIC) optics equipped with an Olympus® DP-70 camera. Measurements were obtained with Olympus cellSens® software. The identification at genus level of the specimens was done according to the dichotomous key provided by Sørensen & Pardos (2008). For scanning electron microscopy (SEM), specimens were dehydrated through a graded series of 80%, 90%, 95% and 100% ethanol. Then, specimens were cleaned by an ultrasonic cleaner for 10-15 s, transferred to acetone and critical point dried. Finally, the kinorhynchs were mounted on aluminium stubs, coated with gold and examined with a JSM® 6335-F JEOL SEM in the ICTS Centro Nacional de Microscopía Electronica (Universidad Complutense de Madrid, Spain). Images and line drawing were mounted using Adobe® Photoshop 6.0 and Illustrator CC-2014 software.

3. Results

Taxonomic account

Class **Allomalorhagida** Sørensen et al. 2015

Family **Dracoderidae** Higgins & Shirayama 1990

Genus ***Dracoderes*** Higgins & Shirayama, 1990

Dracoderes spyro sp. nov.

urn:lsid:zoobank.org:act:1C598D96-958E-4A3D-82A7-3E07270089F9

(Figs. 2-4 and Tables 2 and 3)

3.1. Type material

Holotype, adult female, collected on 10 November 1980 at Cabo Haitiano, Haiti, Hispaniola Island, western Atlantic Ocean: 19 46 12N, 072 11 00W (L4) (Fig. 1C) at 3-5 m depth in mud; mounted in Fluoromount G®, deposited at NMNH under accession number: USNM1480327. Paratypes, six adult females and five males; three of them with same collecting data as holotype, mounted in Fluoromount G®, deposited at NMNH under accession numbers: USNM1480328, USNM1480329, USNM1480333; two of them collected on 02 November 1980 at Puerto Plata, Dominican Republic, Hispaniola Island, western Atlantic Ocean: 19 48 12N, 070 42 00W (L1) (Fig. 1C) at 5 m depth in sandy mud, mounted in Fluoromount G®, deposited at NMNH under accession numbers: USNM1480330, USNM1480334; two of them collected on 04 November 1980 at Isabela Bay, Dominican Republic, Hispaniola Island, western Atlantic Ocean: 19 53 18N, 071 05 36W (L3) (Fig. 1C) at 4 m depth in silty mud, mounted in Fluoromount G®, deposited at NMNH under accession numbers: USNM1480331, USNM1480335; two of them collected on 03 November 1980 at Puerto Blanco, Dominican Republic, Hispaniola Island, western Atlantic Ocean: 19 54 24N, 070 56 24W (L2) (Fig. 1C) at 3 m depth in silty mud, mounted in Fluoromount G®, deposited at NMNH under accession numbers: USNM1480332, USNM1480336; two of them collected on 15 March 1976 at Puerto Príncipe, Haiti, Hispa-niola Island, western Atlantic Ocean: 18 32 21N, 072 20 05W (L5) (Fig. 1C) at 5 m depth in mud, mounted in Fluoromount G®, deposited at NMNH under accession numbers: USNM1480337, USNM1480338.

3.2. Non-type material

159 additional specimens from all the previous localities, mounted for LM, deposited at NMNH under accession numbers USNM1480339-USNM1480496; and 3 additional specimens mounted for SEM and stored at the Invertebrates Collection of the Meiofaunal Laboratory of the Universidad Complutense de Madrid (UCM), Spain.

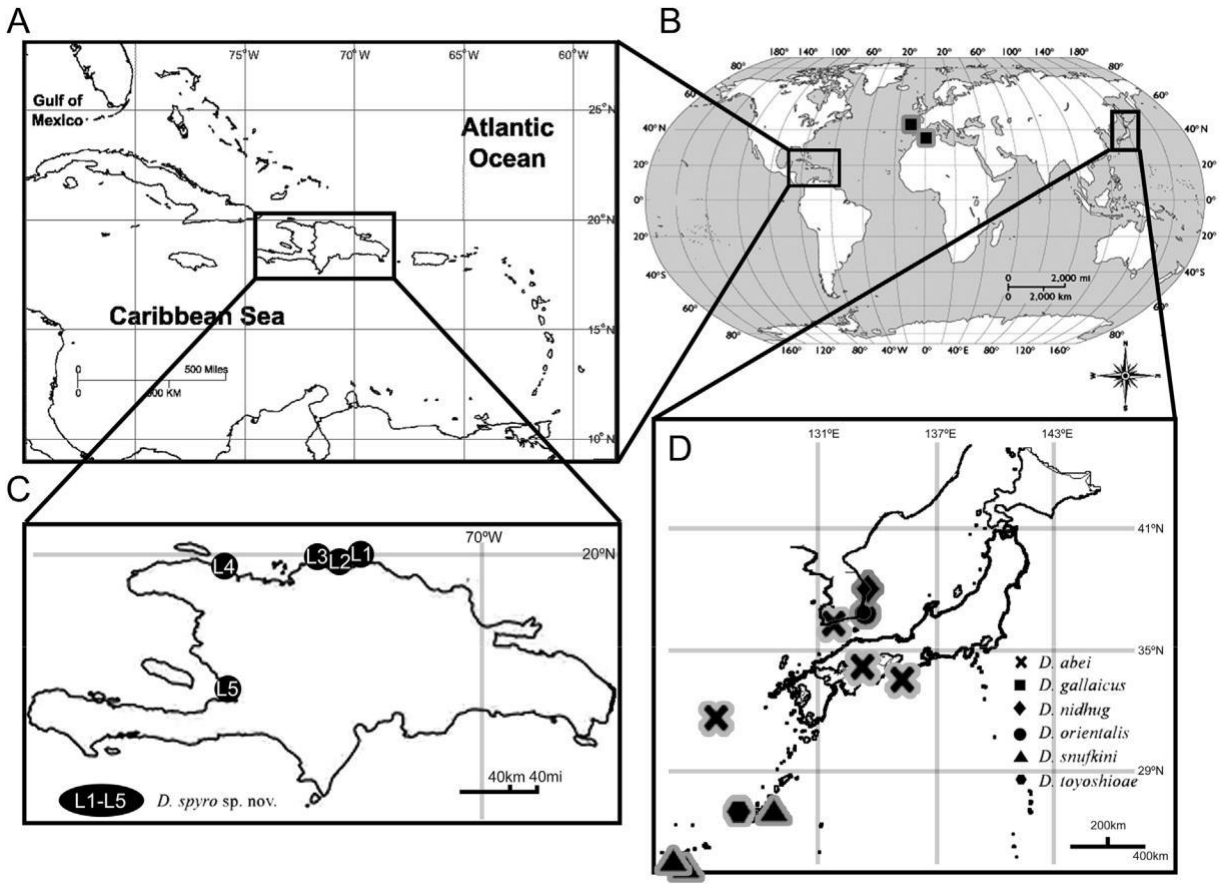

Fig. 1. Map showing the sampling locations of *Dracoderes spyro* sp. nov. in Hispaniola Island, Caribbean Sea, western Atlantic Ocean (A, C) and the distribution of the remaining species of the genus (B, D).

Table 1
Data on sampling localities and habitat of the collected specimens.

Station code	Location	Geographical coordinates	Sampling date	Sediment	Depth (m)
L1	Puerto Plata, Dominican Republic	19 48 12 N 70 42 00 W	02/11/1980	Sandy mud	5
L2	Puerto Blanco, Dominican Republic	19 54 24 N 70 56 24 W	03/11/1980	Silty mud	3
L3	Isabela Bay, Dominican Republic	19 53 18 N 71 05 36 W	04/11/1980	Silty mud	4
L4	Cabo Haitiano, Haiti	19 46 12 N 72 11 00 W	10/11/1980	Mud	3-5
L5	Puerto Príncipe, Haiti	18 32 21 N 72 20 05 W	15/03/1976	Mud	5

3.3. Diagnosis

Dracoderes with middorsal spines on segments 2 and 9, paradorsal spines on segments 3-8, lateroventral spines on segments 3-4 and 6-9, lateral accessory spines on segment 5, lateroventral tubes on segments 2, 5 and 10 and laterodorsal tubes on segment 8.

3.4. Etymology

The species is named after the dragon “Spyro”, the main character of the platform video games series Spyro the Dragon™, originally released by the defunct Universal Interactive Studios.

3.5. Description

See Table 2 for measurements and dimensions, and Table 3 for summary of spine, tube, nephridiopore and sensory spot locations.

Head consists of retractable mouth cone and introvert (Fig. 2A-B, D and 4A-C). Internal part of mouth cone with three rings of inner oral styles. Exact number, arrangement and morphology of inner oral styles not determined. External part of mouth cone with 9 outer oral styles (Fig. 2B). Outer oral styles alternate in size between longer and shorter ones. Five long styles appear anterior to the odd numbered introvert sections, whereas four shorter ones appear anterior to the even numbered ones, except in the middorsal section 6 where a style is missing. Both longer and shorter styles with two jointed subunits, terminating into a hook-like structure, and a basis with lateral, pectinate fringes

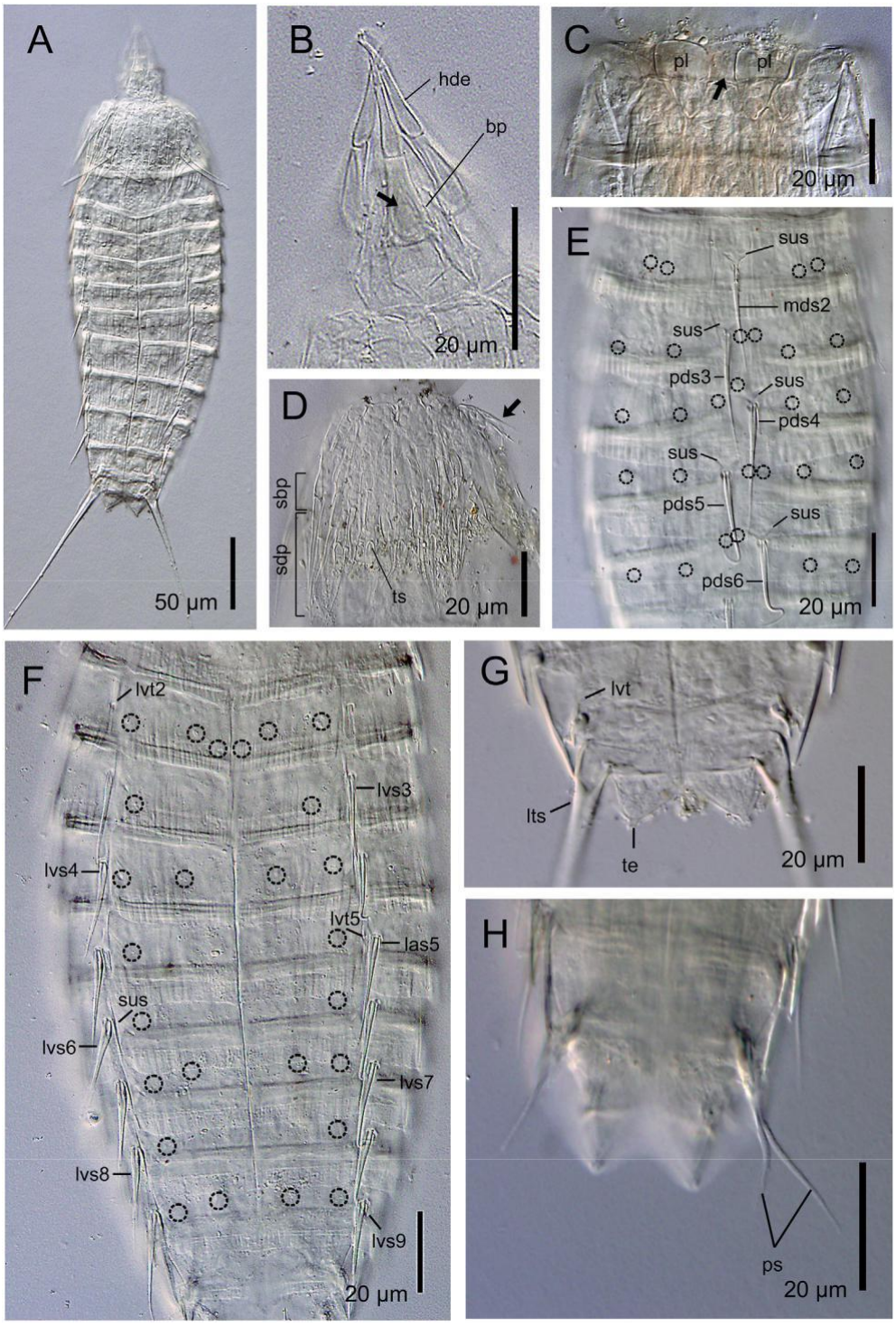

Fig. 2. Light micrographs showing trunk overview and details in the head and the sexual dimorphism of female holotype USNM1480327 (A-G) and male paratype USNM140333 (H) of *Dracoderes spyro* sp. nov. (A) Ventral overview of head and trunk; (B) Mouth cone, showing the outer oral styles; arrow indicates the median area bushy fringe tips; (C) Neck, showing the placids; arrowhead indicates cuticular folds; (D) Introvert, showing the scalids; arrow indicates the filiform fringes of the basal region; (E) middorsal, paradorsal, subdorsal and laterodorsal regions of tergal plates of segments 2-7 (F) lateroventral, ventrolateral and ventromedial regions of tergal and sternal plates of segments 2-10 (G) lateroventral, ventrolateral and ventromedial regions of tergal and sternal plates of segments 10-11; (H) posterior end of the trunk, showing the sexually dimorphic male penile spines. Abbreviations: bp, basal part of outer oral style; hde, hook-like distal end of outer oral style; las, lateral accessory spine; lts, lateral terminal spine; lvs, lateroventral spine; lvt, lateroventral tube; mds, middorsal spine; pds, paradorsal spine; pl, placid; ps, penile spines; sbp, scalid basal part; sdp, scalid distal part; sus, subcuticular line; te, tergal extension; ts, trichoscalid; sensory spots are marked as dotted-line circles; numbers after abbreviation indicate the corresponding segment.

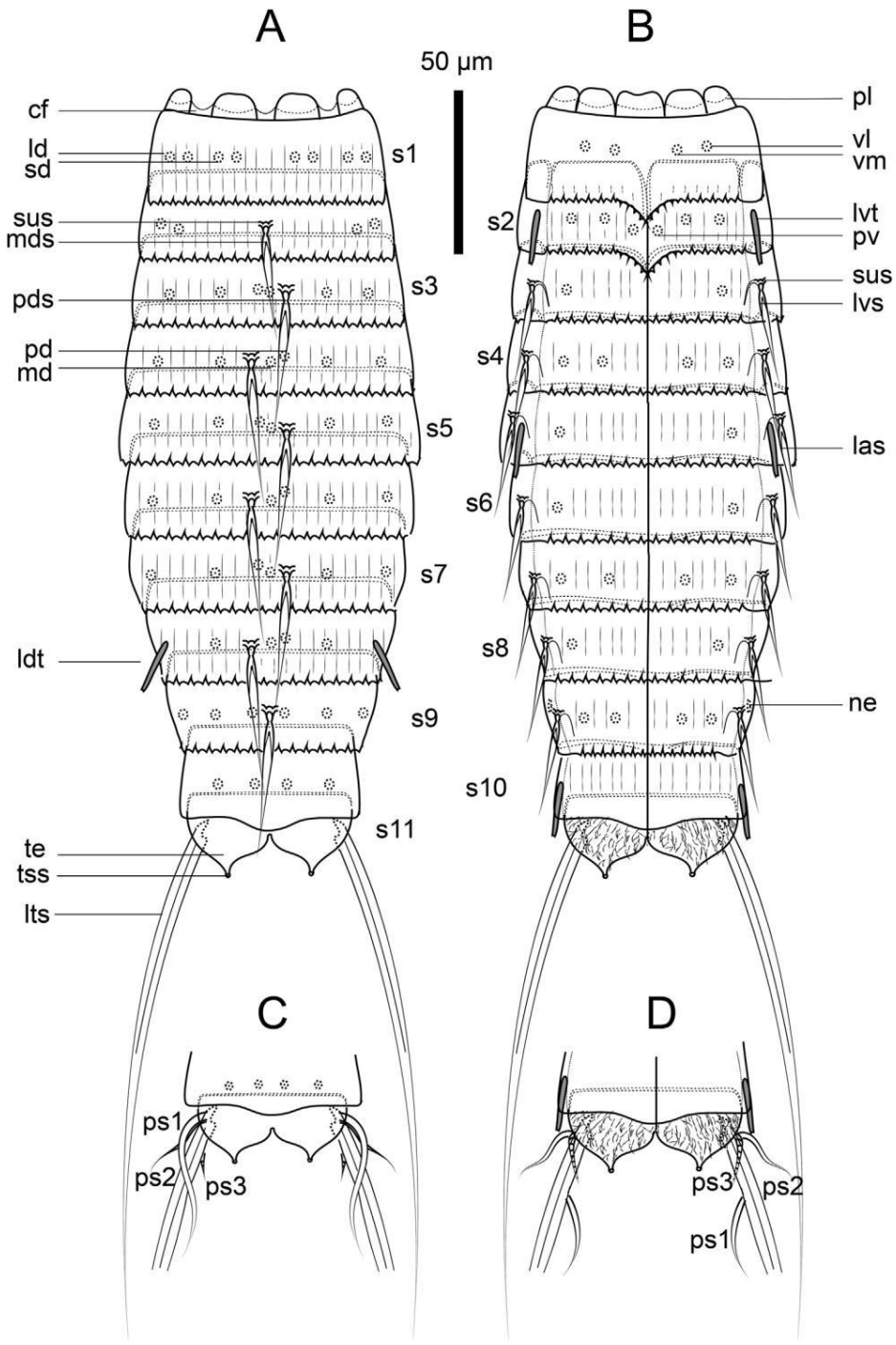

Fig. 3. Line-art illustrations of *Dracoderes spyro* sp. nov. (A) Female, dorsal view; (B) Female, ventral view; (C) Male, segments 10-11, dorsal view; (D) Male, segments 10-11, ventral view. Abbreviations: cf, cuticular folding; las, lateral accessory spine; ld, laterodorsal sensory spot; ldt, laterodorsal tube; lts, lateral terminal spine; lvs, lateroventral spine; lvt, lateroventral tube; md, middorsal sensory spot; mds, middorsal spine; ne, nephridial pore; pd, paradorsal sensory spot; pds, paradorsal spine; pl, placid; ps, penile spines followed by penile spine number; pv, paraventral sensory spot; s, segment followed by segment number; sd, subdorsal sensory spot; sus, subcuticular line; te, tergal extension; tss, terminal sensory spot; vm, ventromedial sensory spot; vl, ventrolateral sensory spot.

and a widened median area with bushy fringe tips (Fig. 2B). Introvert with seven rings of scalids. Scalids with a long distal part and a shorter basal sheath. Basal sheath laterally extending into long, filiform fringes (Figs. 2D and 4C). Nine trichoscalids (Figs. 2D and 4C) distributed as single ones in sections 2, 4, 6, 8 and 10, and as paired ones in sections 5 and 7. Exact number, arrangement and detailed morphology of scalids not determined as they tended to be collapsed when mounted, so further examination was not possible.

Neck with nine placids and a distinct joint between the neck and segment 1 (Figs. 2C and 3A, B); midventral and midlateral placids

wider (17 µm wide at base) than others (10-14 µm wide at base). Ventral placids close each other; subdorsal, laterodorsal and midlateral placids separated by cuticular folds (Figs. 2C and 3A, B).

Trunk with eleven segments (Figs. 2A and 3A, B and 4A, B); segment 1 consists of closed cuticular ring; segments 2-11 consist of one tergal and two sternal plates (Figs. 2A and 3A, B and 4A, B). Tergosternal junctions intracuticular (only visible with LM) (Fig. 2F). Midsternal junctions externally visible as conspicuous lines in both LM and SEM (Figs. 2F, 3B and 4B, F, G). Cuticle of segments 1-8 with longitudinal ridges in dorsal, lateral and ventral areas (Fig. 2A, E, 3A, B and 4A, B, D, F, G, I). Tergal anterior plates middorsally bulging; posterior ones flattened, with tapering outline in lateral view (Fig. 4B). Sternal plates widest at segment 5, but almost constant in width throughout the trunk, tapering at the last trunk segments (Fig. 2A, F, 3A, B and 4B). Sternal plates relatively (MSW-5:TL average ratio = 30.5%), giving the animal a plump general appearance (Figs. 2A and 3A, B and 4A, B). Cuticular hairs absent (except on sternal plates of segment 11). Posterior margin of segments 1-2 serrated, with a convex midventral V-shaped extension and rounded indentations without serrated edges in the lateroventral position (Fig. 2E and F, 3A, B and 4F); posterior margin of remaining segments strongly serrated without V-shaped extension, with rounded indentations without serrated edges in the lateroventral position (Fig. 2E and F, 3A, B and 4A, B, F, G). Well-developed pectinate fringes absent.

Segment 1 without spines or tubes. Pair of sensory spots in ventrolateral and ventromedial positions, two pairs of sensory spots in subdorsal and laterodorsal positions (Fig. 3A and B); sensory spots on this and remaining segments small, rounded, with a ring of cuticular papillae surrounding a central pore (Fig. 4I).

Segment 2 with middorsal spine (Figs. 2E, 3A and 4A, D); dorsal spines on this and remaining segments thin and acicular, composed of a basal sheath with two deep incisions accompanied by a central pore, and an acicular end portion with smooth margins (Fig. 4E). Trunk cuticles around the insertion points of the spines on this and following segments with conspicuous subcuticular structures (Fig. 2E and F and 3A, B); most basal part of the spine inside the segments' cuticle shows spherical, condyle-like articulation, similar to a ball-and-socket articulation. Paired tubes present in lateroventral position (Figs. 2F, 3B and 4F); tubes on this and remaining segments short, flattened, stouter basally, distally with a median, longitudinal cleft surrounded by two flat, membranous wings (Fig. 4H). Two pairs of sensory spots in subdorsal position (Figs. 2E and 3A); paired sensory spots in ventrolateral, ventromedial and paraventral positions (Figs. 2F and 3B).

Segment 3 with paradorsal spine located to the left or to the right (Figs. 2E, 3A and 4A, D). Left or right displacement of paradorsal spines along the whole trunk varies among specimens (Figs. 2E, 3A and 4A) within the same population, and there are no apparent left/right preference correlated with sex or sampling location. Additional spines in lateroventral position (Figs. 2F, 3B and 4F); trunk cuticle around the insertion point of lateroventral acicular spines on this and following segments enforced, forming conspicuous subcuticular lines longitudinally directed (Figs. 2F and 3B). Unpaired sensory spots in middorsal and paradorsal positions, the latter located in a paradorsal position opposite to the side of the dorsal spine on the same segment (Figs. 2E and 3A); paired sensory spots in subdorsal, laterodorsal and ventrolateral positions (Fig. 2E and F and 3A, B).

Segment 4 with paradorsal spine located on the opposite side of that on the preceding segment (Figs. 2E, 3A and 4A, D). Additional spines in lateroventral position (Figs. 2F, 3B and 4F). Unpaired sensory spots in middorsal and paradorsal positions, the latter located in a paradorsal position opposite to the side of the dorsal spine on the same segment (Figs. 2E and 3A); paired sensory spots in subdorsal, laterodorsal, ventrolateral and ventromedial positions (Fig. 2E and F, 3A).

Segment 5 with paradorsal spine located on the opposite side of that on the preceding segment (Figs. 2E and 3A). Additional spines in lateral accessory position (Figs. 2F, 3B and 4G, H). Paired tubes present in lateroventral position (Figs. 2F, 3B and 4G, H). Arrangement of sensory spots identical with segment 3 (Fig. 2E and F and 3A, B).

Segment 6 with paradorsal spine located on the opposite side of that on the preceding segment (Figs. 2E and 3A). In a single specimen, the paradorsal spines of this and the subsequent segment occurred on the same side (*i.e.*, did not alternatingly shift sides), which is a deviation of the general morphological pattern of the species (Fig. 4A). Additional spines in lateroventral position (Figs. 2F, 3B and 4G, J). Arrangement of sensory spots identical with segment 3 (Fig. 2E and F and 3A, B).

Segment 7 similar to segment 4, except for the paradorsal spine and paradorsal sensory spot located on the opposite side of those on the segment 4 (Fig. 3A).

Segment 8 with paradorsal spine located on the opposite side of that on the preceding segment (Fig. 3A). Additional spines in lateroventral position (Figs. 2F, 3B and 4G, J). Paired tubes in laterodorsal position (Figs. 3A and 4J). Unpaired sensory spots in middorsal and paradorsal positions, the latter located in a paradorsal position opposite to the side of the dorsal spine on the same segment (Fig. 3A); paired sensory spots in subdorsal and ventrolateral positions (Figs. 2F and 3A, B).

Segment 9 with unpaired middorsal and paired lateroventral spines (Figs. 2F, 3A, B and 4A, G). Longitudinal cuticular ridges lacking dorsal, lateral and ventrally (Fig. 3A and B and 4A, B). Pair of sensory spots in paradorsal, subdorsal, laterodorsal, ventrolateral and ventromedial positions (Figs. 2F and 3A, B). Nephridiopores in lateral accessory positions (Fig. 3B); pore not sieve-like, formed by a minute, posteriorly directed opening with a few papillae.

Segment 10 lacking spines, with paired lateroventral tubes (Figs. 2G and 3B, D and 4K, L). Pair of sensory spots in paradorsal and subdorsal positions (Fig. 3A, C).

Segment 11 with lateral terminal spines (Fig. 2A, G, 3A, B and 4A, B, K, L). Gonopores of females not observed. Males with three pairs of penile spines; dorsal one longest, with very thick basis, smooth; medial one slightly shorter, attaching on the basis of the longest penile spine; ventral one shortest, crenulated, attaching on the outer lateral margin of the lateral terminal spine (Figs. 2H and 3C, D and 4L). Pair of sensory spots on the tips of the tergal extensions, giving these extensions a nipple-like appearance (Figs. 2G and 3A-D and 4K, L). Tergal extensions bulged, triangular, extending well beyond sternal plates (Figs. 2G, 3A-D and 4A, B, K, L); dorsal side of tergal extensions smooth (Fig. 3A, C), with ventral surface densely covered with short, papillary hairs (Fig. 3B, D and 4K, L). Posterior margins of sternal plates slightly rounded, without any projecting parts (Figs. 2G and 3B, D and 4K, L).

3.6. *Remarks on morphological features*

One of the examined specimens showed a modified alternate pattern of paradorsal spines, possessing three consecutive spines in the same side of the paradorsal position (Fig. 4A).

Two of the examined specimens carried ciliophoran epibionts attached to the laterodorsal surface of the segment 9 (Fig. 5A and B).

3.7. *Associated kinorhynch fauna*

D. spyro sp. nov. appeared together with *Cristaphyes* sp (Cepeda et al. in press), *Cristaphyes* cf. *longicornis* (Higgins 1983), *Echinoderes*

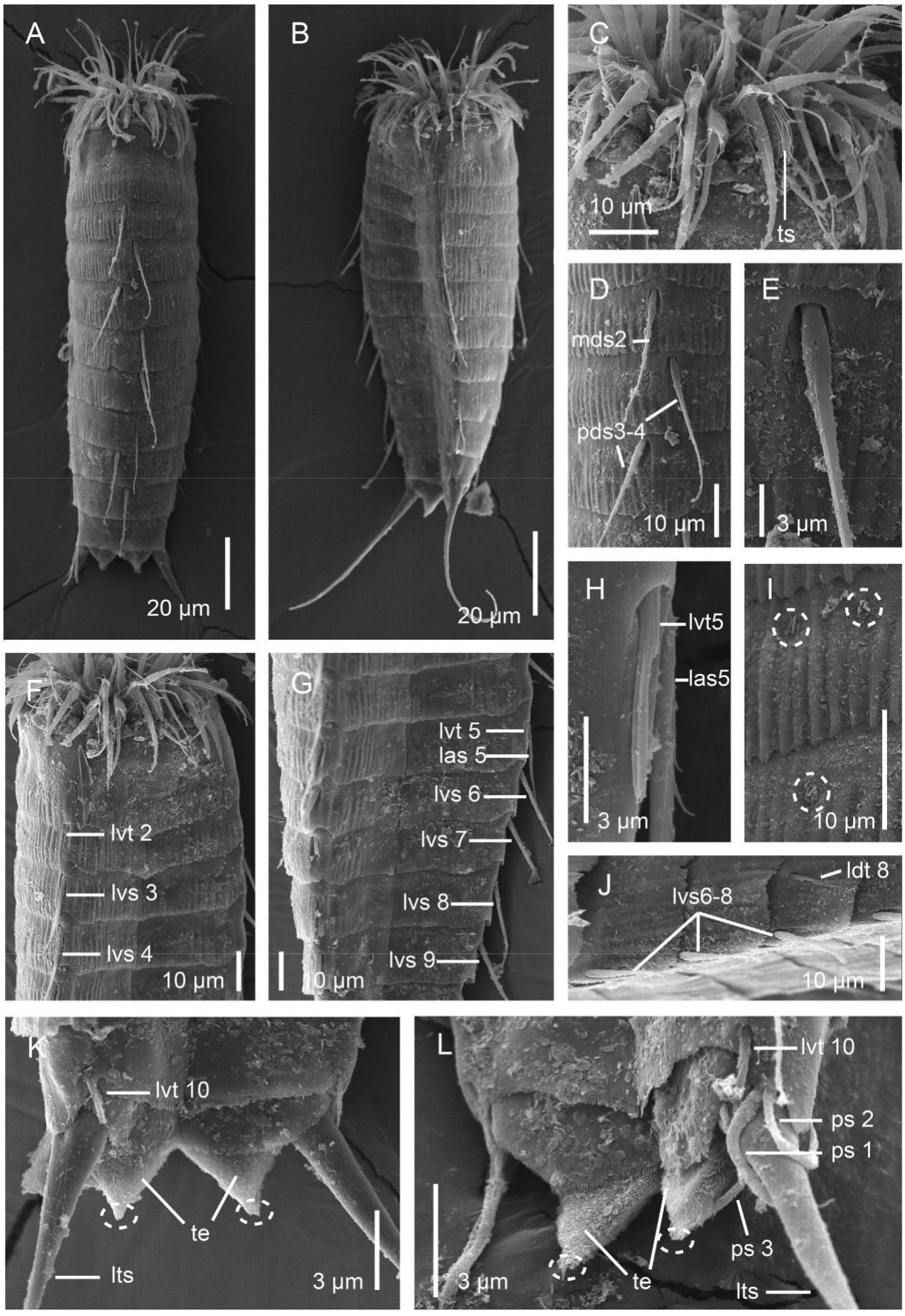
A
20 µm
B
20 µm
C
10 µm
ts
D
mds2
pds3-4
10 µm
E
3 µm
H
lvt5
las5
3 µm
I
10 µm
J
ldt 8
lvs6-8
10 µm
F
lvt 2
lvs 3
lvs 4
10 µm
G
lvt 5
las 5
lvs 6
lvs 7
lvs 8
lvs 9
0 µm
K
lvt 10
te
lts
3 µm
L
lvt 10
ps 2
ps 1
ps 3
te
lts
3 µm

Table 2

Measurements of adult *Dracoderes spyro* sp. nov. from Hispaniola Island, including number of measured specimens (*n*), mean and standard deviation (SD). Because there were no remarkable differences in sizes or dimensions between the two sexes or sampling locations, measurements are not shown by sexes or populations.

Character	Range	Mean (SD; *n*)
TL (µm)	158.8-275.3	196.8 (25.8; 34)
MSW-5 (µm)	47.8-63.9	59.3 (3.0; 34)
MSW-5/TL (%)	22.6-33.6	30.5 (3.0; 34)
SW-10 (µm)	32.4-49.6	43.4 (5.0; 34)
SW-10/TL (%)	14.0-26.6	22.4 (3.6; 34)
S1 (µm)	28.7-37.6	33.9 (2.1; 34)
S2 (µm)	18.8-30.2	27.0 (2.9; 34)
S3 (µm)	18.8-33.4	25.5 (3.9; 34)
S4 (µm)	21.1-35.8	31.8 (4.0; 34)
S5 (µm)	24.5-37.9	33.0 (3.6; 34)
S6 (µm)	24.1-39.8	33.2 (3.9; 34)
S7 (µm)	22.2-38.8	31.1 (4.0; 34)
S8 (µm)	23.7-35.6	28.9 (3.0; 34)
S9 (µm)	20.0-37.2	27.7 (3.3; 34)
S10 (µm)	17.1-30.6	25.7 (3.0; 34)
S11 (µm)	18.8-30.5	25.0 (2.8; 34)
MD 2 (ac) (µm)	15.9-36.4	29.3 (4.0; 34)
PD 3 (ac) (µm)	21.7-37.9	32.0 (4.1; 34)
PD 4 (ac) (µm)	19.7-41.9	34.5 (5.2; 34)
PD 5 (ac) (µm)	26.4-45.2	36.0 (4.7; 34)
PD 6 (ac) (µm)	14.9-38.7	33.9 (4.8; 33)
PD 7 (ac) (µm)	23.7-41.6	31.4 (4.2; 33)
PD 8 (ac) (µm)	17.6-34.4	28.3 (3.9; 32)
MD 9 (ac) (µm)	20.9-34.1	29.0 (3.1; 30)
LV 2 (tu) (µm)	5.5-13.2	10.1 (1.6; 34)
LV 3 (ac) (µm)	14.7-26.6	19.8 (2.5; 34)
LV 4 (ac) (µm)	14.0-26.0	21.6 (2.7; 34)
LV 5 (tu) (µm)	6.3-15.7	9.6 (2.0; 34)
LA 5 (ac) (µm)	18.9-29.0	23.4 (2.5; 34)
LV 6 (ac) (µm)	17.4-28.6	23.1 (2.6; 34)
LV 7 (ac) (µm)	16.4-29.9	23.8 (3.1; 34)
LD 8 (tu) (µm)	5.1-9.9	7.5 (1.1; 20)
LV 8 (ac) (µm)	18.5-31.5	23.7 (3.5; 34)
LV 9 (ac) (µm)	16.2-30.5	24.3 (3.5; 34)
LV 10 (tu) (µm)	6.0-11.3	8.4 (1.6; 20)
LTS (µm)	108.2-152.5	130.8 (9.7; 34)

Abbreviations: ac, acicular spine; LA, lateral accessory, LD, laterodorsal; LTS, lateral terminal spine; LV, lateroventral spine/tube; MD, middorsal spine; MSW-5, maximum sternal width (on segment 5); PD, paradorsal spine; S, segment lengths; SWe10, standard width (on segment 10); TL, total length of trunk; tu, tube.

Table 3

Summary of nature and arrangement of sensory spots, spines and tubes in *Dracoderes spyro* sp. nov.

Segment	MD	PD	SD	LD	LA	LV	VL	VM	PV
1			ss ss	ss ss			ss	ss	
2	ac		ss ss			tu	ss	ss	ss
3	ss	ac* ss*	ss	ss		ac	ss		
4	ss	ss* ac*	ss	ss		ac	ss	ss	
5	ss	ac* ss*	ss	ss	ac	tu	ss		
6	ss	ss* ac*	ss	ss		ac	ss		
7	ss	ac* ss*	ss	ss		ac	ss	ss	
8	ss	ss* ac*	ss	tu		ac	ss		
9	ac	ss	ss	ss	n-	ac	ss	ss	
10		ss	ss			tu			
11			ss			lts, psx3 (m)			

Abbreviations: LA, lateral accessory; LD, laterodorsal; LV, lateroventral; MD, middorsal; PD, paradorsal; PV, paraventral; SD, subdorsal; VL, ventrolateral; VM, ventromedial; ac, acicular spine; lts, lateral terminal spine; m, male condition of sexually dimorphic character; ne, nephridiopore; ps, penile spine; ss, sensory spot; tu, tube; * indicates unpaired structures.

astridae Sørensen, 2014, *Echinoderes* sp (Cepeda et al., in press), *Echinoderes spinifurca* Sørensen et al., 2005 and *Fujuriphyes* sp (Cepeda et al., in press) in Puerto Blanco (L2); with *Cristaphyes* sp in Isabela Bay (L3); with *Fujuriphyes* sp in Puerto Plata (L1); and with *Echinoderes* sp in Cabo Haitiano (L4).

4. Discussion

4.1. Taxonomy

D. spyro sp. nov., clearly belongs to the genus *Dracoderes* by the combination of the following morphological features: mouth cone with 9 outer oral styles alternating in size between longer and shorter ones, neck consisting of nine placids with the dorsal and midlateral ones separated by cuticular folds, segment 1 of trunk composed of a ring cuticular plate and remaining segments composed of one tergal and two sternal cuticular plates, dorsal spines on segments 2-9 of which the first and the last ones appear in middorsal position and the remaining ones in paradorsal position alternatingly laterally displaced and males possessing three pairs of penile spines (Sørensen et al. 2012; Yamasaki 2015). *D. spyro* sp. nov. can be easily distinguished from its congeners by the arrangement of the spines, tubes and the sensory spots locations, namely, having two pairs of subdorsal sensory spots on segment 1 and a single middorsal (perispinal) and paradorsal sensory spots on segments carrying paradorsal spines, whereas the remaining *Dracoderes* species possess one pair of subdorsal (if present in this position) sensory spots and a pair of perispinal sensory spots on segments carrying paradorsal spines (Sørensen et al. 2012; Thomsen et al. 2013; Yamasaki 2015).

Regarding the nature and arrangement of spines/tubes, the recently described *D. toyoshioae* from Okinawa, Japan (northwest Pacific Ocean) shows most resemblance with *D. spyro* sp. nov. Nevertheless, the description of *D. toyoshioae* was based on a single adult female exoskeleton lacking most spines and tubes, only inferred by the presence of the respective subcuticular structures. Thus, the author assumed the nature of these spines/tubes, stating the need of additional specimens in order to better determine the morphological characters of this species (Yamasaki 2015). *D. toyoshioae* is characterized by having lateroventral spines/tubes on segments 2-10, lateral accessory spines/tubes on segments 2-8, ventrolateral acicular spines on segment 1 and dorsal cuticular structures (possibly spines) on segments 1-9 (Yamasaki 2015), while *D. spyro* sp. nov. also has lateroventral spines/tubes on segements 2-10 (tubes on segments 2, 5 and 10, and acicular spines on segments 3-4 and 6-9) but possesses lateral accessory spines only on segment 5, lacks ventrolateral acicular spines on segment 1 and has dorsal spines on segments 2-9. Furthermore, *D. spyro* sp. nov. possesses laterodorsal tubes on segment 8 which are absent in *D. toyoshioae*. The remaining congeners of the genus are characeterized by having lateroventral spines/tubes on segments 5-9 or 5-10 (Adrianov & Malakhov 1999; Sørensen et al. 2012; Thomsen et al. 2013; Yamasaki 2015), while *D. spyro* sp. nov. also has latereoventral spines on segments 3 and 4. Another morphological feature that makes *D. spyro* sp. nov. easily recognizable, as previously mentioned, is the presence of

←**Fig. 4.** Scanning electron micrographs showing overviews and details in the cuticular trunk morphology of a non-type male (A, C-J and L) and a non-type female (B and K) of *Dracoderes spyro* sp. nov. (A) Dorsal overview of trunk; (B) lateral and ventral overviews of trunk; (C) introvert partially everted, showing some scalids; (D) middorsal and paradorsal regions of tergal plates of segments 2-4; (e) detail of a paradorsal spine of segment 3; (F) lateroventral, ventrolateral and ventromedial regions of tergal and sternal plates of segments 1-4; (G) lateroventral, ventrolateral and ventromedial regions of tergal and sternal plates of segments 5-9; (H) detail of a lateroventral tube and a lateral accessory spine of segment 5; (I) detail of subddorsal and laterodorsal sensory spots of segments 2-3; (J) laterodorsal and lateroventral regions of tergal plates of segments 6-8; (K) lateroventral, ventrolateral and ventromedial regions of tergal and sternal plates of segments 10-11 of a female; (L) lateroventral, ventrolateral and ventromedial regions of tergal and sternal plates of segments 10-11 of a male. Abbreviations: las, lateral accessory spine; ldt, laterodorsal tube; lts, lateral terminal spine; lvt, lateroventral tube; lvs, lateroventral spine; mds, middorsal spine; pds, paradorsal spine; ps, penile spine; te, tergal extension; ts, trichoscalid; sensory spots are marked as dotted-line circles; numbers after abbreviations indicate the corresponding segment.

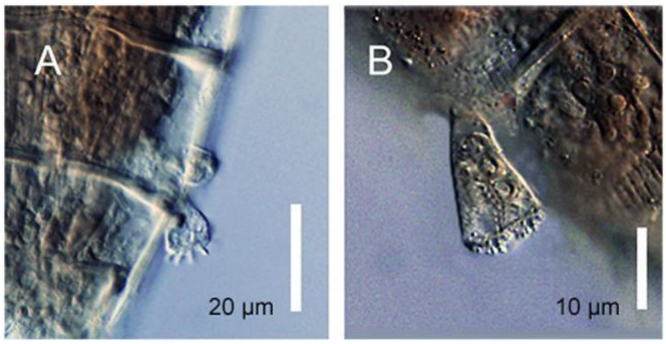

Fig. 5. Light micrographs showing details of epibiontic Ciliophora on the cuticle surface of *Dracoderes spyro* sp. nov. on the laterodorsal position of segment 9. (A) Cuticle of segment 9 showing the attached epibionts; (B) Detail of a epibiont.

laterodorsal tubes on segment 8, which are absent in the remaining known congeners.

Based on the morphology of the posterior margin of segment 1, *D. spyro* sp. nov. is similar to *D. abei*, *D. gallaicus* and *D. nidhug*, having this margin strongly serrated and extending midventrally to form a triangular expansion. However, *D. abei* and *D. gallaicus* are characterized by having the posterior margin of segment 1 with rounded indentations (not serrated) from lateroventral to ventrolateral positions, whereas *D. spyro* sp. nov. and *D. nidhug* only have these rounded indentations in the lateroventral position. Furtheremore, *D. spyro* sp. nov. also possesses the posterior margin of segment 2 extending midventrally to form a triangular extension, which is absent in *D. abei*, *D. gallaicus* and *D. nidhug* (Sørensen et al., 2012; Thomsen et al., 2013). On the other hand, *D. orientalis* and *D. toyoshioae* are characterized by having the posterior margin of segment 1 finely serrated, not extending midventrally (Adrianov & Malakhov 1999; Yamasaki 2015), whereas *D. snufkini* has long, extremely marked serrations on the ventral side (Yamasaki 2015).

4.2. Key to species of Dracoderes

1 Middorsal subcuticular structure (possibly basal structure of spine) present on segment 1; ventrolateral spines on segment 1 present … ***D. toyoshioae***
- Middorsal subcuticular structure absent on segment 1; ventrolateral spines on segment 1 absent … **2**

2 Middorsal spine on segment 2 absent; subdorsal tubes present on segment 2 … ***D. nidhug***
- Middorsal spine on segment 2 present; subdorsal tubes absent on segment 2 … **3**

3 Lateroventral spines/tubes present on segments 2-10; laterodorsal tubes on segment 8 present … ***D. spyro* sp. nov**
- Lateroventral spines/tubes present on some segments from 2 to 10 but never on segments 3-4; laterodorsal tubes on segment 8 absent … **4**
-

4 Lateroventral tubes on segment 2 absent … ***D. orientalis***
- Lateroventral tubes on segment 2 present … **5**

5 Lateral accessory spines present on segment 5 … ***D. gallaicus***
- Spines absent in lateral series on segment 5 ... **6**

6 Lateroventral tubes on segment 10 absent; primary pectinate fringe of segment 1 strongly developed, with long, wide serrations on the ventral side not forming a V-shaped extension … ***D. snufkini***
- Lateroventral tubes on segment 10 present; primary pectinate fringe of segment 1 scarcely developed, with short, rounded serrations on the ventral side forming a V-shaped extension … ***D. abei***

4.3. Distribution of the genus

Until the discovery of *D. gallaicus*, which was described from Galicia, northeastern Spain, eastern Atlantic Ocean (Sørensen et al. 2012), the genus *Dracoderes* was thought to be a kinorhynch taxon geographically limited to east Asia, as the only known species were *D. abei*, from Mukaishima yacht harbour, Japan (Higgins & Shirayama 1990) and *D. orientalis* from Ulsan Bay, South Korea (Adrianov & Malakhov 1999) (Fig. 1B, D). Later, additional three species of the genus were also described from the same area (Thomsen et al. 2013; Yamasaki 2015), leaving *D. gallaicus* as the only *Dracoderes* species outside this area (Fig. 1B, D). With the description of *D. spyro* sp. nov. from Hispaniola Island, we extend the geographical distribution of the genus to American waters (Fig. 1A-C). Furthermore, this record marks the southernmost limit of the genus' distribution, which is still unknown from the Southern Hemisphere (Fig. 1A-D).

Funding sources

Cepeda was supported by a predoctoral fellowship of the Complutense University of Madrid (CT27/16-CT28/16).

Conflicts of interest

The authors declare no conflicts of interest.

Acknowledgements

We would like to thank Dr Jon Norenburg and Katie Ahlfeld for loaning the material that made the present study possible.

References

Adrianov, A.V., Malakhov, V.V., 1999. Cephalorhyncha of the World Ocean, first ed. KMK Scientific Press, Moscow.

Artois, T., Fontaneto, D., McInnes, S., Todaro, M.A., Sørensen, M.V., Zullini, A., 2011. Ubiquity of microscopic animals? Evidence from the morphological approach in species identification. In: Fontaneto D. (ed.), Biogeography of Microscopic Organisms: Is everything Small everywhere? Cambridge University Press, Cambridge, pp. 244-283.

Cepeda, D., Sanchez, N., Pardos, F., (in press). First extensive account of the phylum Kinorhyncha from Haiti and the Dominican Republic (Caribbean Sea), with the description of four new species. Mar. Biodivers., in press.

Claparede, A.R.E., 1863. Zur Kenntnis der Gattung *Echinoderes* Duj. Beobachtungen über Anatomie und entwicklungsgeschichte wirbelloser Thiere an der Küste von Normandie angestellt. Verlag von Wilhelm engelmann, Leipzig.

Dal Zotto, M., Di Domenico, M., Garraffoni, A., Sørensen, M.V., 2013. *Franciscideres* gen. nov. - a new, highly aberrant kinorhynch genus from Brazil, with an analysis of its phylogenetic position. Syst. Biodivers. 11, 303-321. https://doi.org/10.1080/14772000.2013.819045.

Higgins, R.P., 1964. Three new kinorhynchs from the North Carolina Coast. Bull. Mar. Sci. 14, 479-493. https://doi.org/10.2307/3225864.

Higgins, R.P., 1969. Indian Ocean Kinorhyncha, 2: Neocentrophyidae, a new homalorhagid family. Proc. Biol. Soc. Wash. 82, 113-128.

Higgins, R.P., 1983. The Atlantic Barrier Reef ecosystem at Carrie Bow Cay, Belize, II: Kinorhyncha. Smithsonian Contrib. Mar. Sci. 18, 1-131. https://doi.org/10.5479/si.01960768.18.1.

Higgins, R.P., 1988. Kinorhyncha. In: Higgins, R.P., Thiel, H. (eds.), Introduction to the Study of Meiofauna. Smithsonian Institution Press, Washington D.C., pp. 328-331

Higgins, R.P., Shirayama, Y., 1990. Dracoderidae, a new family of the cyclorhagid Kinorhyncha from the Inland Sea of Japan. Zool. Sci. 7, 939-946.

Kirsteuer, E., 1964. Zur Kenntnis der Kinorhynchen Venezuelas. Zool. Anz. 173, 388-393.

Kozloff, E.N., 1972. Some aspects of development in *Echinoderes* (Kinorhyncha). Trans. Am. Microsc. Soc. 91, 119-130. https://doi.org/10.2307/3225404.

Neuhaus, B., 2013. Kinorhyncha (=Echinodera). In: Schmidt-Rhaesa, A. (ed.), Handbook of Zoology, Gastrotricha, Cycloneuralia and Gnathifera, Volume 1 Nematomorpha, Priapulida, Kinorhyncha, Loricifera. De Gruyter, Hamburg, pp. 181-350.

Neuhaus, B., Pardos, F., Sørensen, M.V., Higgins, R.P., 2014. New species of *Centroderes* (Kinorhyncha: Cyclorhagida) from the northwest Atlantic Ocean, life cycle and ground pattern of the genus. Zootaxa 3901, 1-69. https://doi.org/10. 11646/zootaxa.3901.1.1.

Pardos, F., Sanchez, N., Herranz, M., 2016. Two sides of a coin: the phylum Kinorhyncha in Panama. I) Caribbean Panama. Zool. Anz. 265, 3-25. https://doi.org/10.1016/j.jcz.2016.06.005.

Sanchez, N., Pardos, F., Sørensen, M.V., 2014. A new kinorhynch genus, *Mixtophyes* (Kinorhyncha: Homalorhagida), from the Guinea Basin deep-sea, with new data on the family Neocentrophyidae. Helgol. Mar. Res. 68, 221-239. https://doi.org/10.1007/s10152e014e0383e6.

Sørensen, M.V., 2006. New kinorhynchs from Panama, with a discussion of some phylogenetically significant cuticular structures. Meiofauna Marina 15, 51-77.

Sørensen, M.V., 2008. A new kinorhynch genus from the Antarctic deep sea and a new species of *Cephalorhyncha* from Hawaii (Kinorhyncha: Cyclorhagida: echinoderidae). Org. Divers. evol. 8, 230.1-230.18. https://doi.org/10.1016/j. ode.2007.11.003.

Sørensen, M.V., 2013. Phylum Kinorhyncha. Zootaxa 3703, 63e66. https://doi.org/10.11646/zootaxa.3703.1.13.

Sørensen, M.V., 2014. First account of echinoderid kinorhynchs from Brazil, with the description of three new species. Mar. Biodivers. 44, 251-274. https://doi.org/10.1007/s12526e013e0181e4.

Sørensen, M.V., Dal Zotto, M., Rho, H.S., Herranz, M., Sanchez, N., Pardos, F., Yamasaki, H., 2015. Phylogeny of Kinorhyncha based on morphology and two molecular loci. PLoS ONE 10, e0133440. https://doi.org/10.1371/journal.pone.0133440.

Sørensen, M.V., Heiner, I., Ziemer, O., 2005. A new species of *Echinoderes* from Florida (Kinorhyncha: Cyclorhagida). Proc. Biol. Soc. Wash. 118, 499-508. https:/doi.org/10.2988/0006e324X(2005)118[499:ANSOeF]2.0.CO;2.

Sørensen, M.V., Herranz, M., Rho, H.S., Min, W.G., Yamasaki, H., Sanchez, N., Pardos, F., 2012. On the genus *Dracoderes* Higgins & Shirayama, 1990 (Kinorhyncha: Cyclorhagida) with a redescription of its type species, *D. abei*, and a description of a new species from Spain. Mar. Biol. Res. 8, 210-231. https://doi. org/10.1080/17451000.2011.615328.

Sørensen, M.V., Pardos, F., 2008. Kinorhynch systematics and biology – an introduction to the study of kinorhynchs, inclusive identification keys to the genera. Meiofauna Marina 16, 21-73.

Thomsen, V.G., Rho, H.S., Kim, D., Sørensen, M.V., 2013. A new species of *Dracoderes* (Kinorhyncha: Dracoderidae) from Korea provides further support for a dracoderid-homalorhagid relationship. Zootaxa 3682, 133-142. https://doi.org/10.11646/zootaxa.3682.1.6.

Yamasaki, H., 2015. Two new species of *Dracoderes* (Kinorhyncha: Dracoderidae) from the Ryukyu Islands, Japan, with a molecular phylogeny of the genus. Zootaxa 3980, 359-378. https://doi.org/10.11646/zootaxa.3980.3.2.

Yamasaki, H., Hiruta, S.D., Kajihara, H., 2013. Molecular phylogeny of kinorhynchs. Mol. Phylogenet. Evol. 67, 303-310. https://doi.org/10.1016/j.ympev.2013.02.016.

Yamasaki, H., Hiruta, S.D., Kajihara, H., Dick, M.H., 2014. Two kinorhynch species (Cyclorhagida, Echinoderidae, *Echinoderes*) show different distribution patterns across Tsugaru Strait, northern Japan. Zool. Sci. 31, 421-429. https://doi.org/10. 2108/zs140011.

Zelinka, K., 1896. Demonstration von Tafeln der *Echinoderes* - Monographie. Verh. Dtsch. Zool. Ges. 6, 197-199.

Zoologischer Anzeiger 282 (2019) 116-126

Contents lists available at ScienceDirect

Zoologischer Anzeiger

journal homepage: www.elsevier.com/locate/jcz

Research paper

First report of the family Zelinkaderidae (Kinorhyncha: Cyclorhagida) for the Caribbean Sea, with the description of a new species of *Triodontoderes* Sørensen & Rho, 2009 and an identification key for the family*

Diego Cepeda [a, *], **Nuria Sánchez** [a, b], **Fernando Pardos** [a]

[a] *Departamento de Biodiversidad, Ecología y Evolucion, Facultad de Ciencias Biologicas, Universidad Complutense de Madrid, Jose Antonio Novais St. 12, 28040 Madrid, Spain*

[b] *Laboratoire Environnement Profond, Institut Français de Recherche pour l'Exploitation de la Mer (IFREMER), Centre Bretagne - ZI de la Pointe du Diable, CS 10070 - 29280 Plouzane, France*

ARTICLE INFO

Article history:
Received 23 February 2019
Received in revised form 12 March 2019 Accepted 23 May 2019 Available online 6 June 2019

Keywords:
Kinorhynchs
Biodiversity
Meiofauna
Morphology
Taxonomy
Triodontoderes lagahoo sp. nov.

ABSTRACT

A new species of Kinorhyncha, *Triodontoderes lagahoo* sp. nov., is described from Tobago Island, Caribbean Sea (western Atlantic Ocean) from a coastal, sandy habitat using both light and scanning electron microscopy. The species is characterized by the presence of middorsal acicular spines on segments 1e11 (that on segment 10 crenulated in males), laterodorsal crenulated spines on segment 10 only in males, lateroventral acicular spines on segments 3-4 and 6-8 (lateroventral spines also on segment 10 in females), lateroventral cuspidate spines on segments 5 and 9, lateral accessory acicular spines on segments 5 and 9, lateral accessory cuspidate spines on segment 8, ventrolateral acicular spines on segment 2 and ventrolateral cuspidate spines on segment 2. Females furthermore possess short papillae in ventrolateral position on segment 8 and ventromedial position on segment 9. The absence of cuspidate spines in lateral accessory position on segment 6 easily distinguishes *T. lagahoo* sp. nov. from the single known congener, *Triodontoderes anulap*. Moreover, also the arrangement of female papillae and sensory spots differ between the species. The finding of a new species of *Triodontoderes* in the Caribbean Sea is the first report of the genus for American waters and the Atlantic Ocean since its original description. Additionally, a dichotomous key for identification of the family Zelinkaderidae to species level, as well as systematic remarks on some morphological characters of the new species are included herein.

1. Introduction

Kinorhynchs are small-sized, holobenthic, free-living, marine invertebrates that inhabit sandy and muddy sediments (Higgins & Thiel 1988; Neuhaus 2013; Sørensen & Pardos 2008). Currently, the phylum comprises near 300 species distributed worldwide and arranged in two classes, Allomalorhagida and Cyclorhagida (Sørensen et al. 2015). The cyclorhagid family Zelinkaderidae was originally erected by Higgins (1990) to accommodate the newly described species *Zelinkaderes floridensis* Higgins, 1990 from Fort Pierce, Florida (western Atlantic Ocean) and the reassigned *Cateria submersa* (Gerlach, 1969), originally described from the North Sea. Not much later, *Zelinkaderes klepali* Bauer-Nebelsick, 1995 was described from the Red Sea and, more recently, *Zelinkaderes brightae* Sørensen et al., 2007 also from Fort Pierce. Two years later, the second genus of the family was erected with the description of *Triodontoderes anulap* Sørensen & Rho, 2009 from the Chuuk Islands, Micronesia (western Pacific Ocean). Finally, *Zelinkaderes yong* Altenburger et al., 2015 was described from the Korean Peninsula (western Pacific Ocean).

Zelinkaderid kinorhynchs are morphologically characterized by having an introvert with one ring of spinoscalids followed by three or four regular scalids rings, fourteen or sixteen distally tripartite placids, trunk vermiform and conspicuously circular in cross-section, at least segments 5 to 11 composed of a single tergal plate with midventral joint, acicular spines present in dorsal and lateral positions, cuspidate spines present in lateral

urn:lsid:zoobank.org:pub:7699F0E0-3F1B-451C-8E43-EB548773D1C0

* This article is a part of the Fifth International Scalidophora Workshop special issue published in Zoologischer Anzeiger 282C, 2019.

* Corresponding author.
E-mail address: diegocepeda@ucm.es (C. Diego).

https://doi.org/10.1016/j.jcz.2019.05.017
0044-5231/

position on some segments, segment 11 with lateral terminal, lateral terminal accessory and midterminal spines, at least some large and oval sensory spots with two pores in the anterior body region, scale-like cuticular hairs medially depressed and males with crenulated spines on segment 10 (Sørensen & Rho 2009). In the present contribution, a new *Triodontoderes* species, *Triodontoderes lagahoo* sp. nov., is described from Tobago Island (Caribbean Sea) using light and scanning electron microscopes. This finding is the first report of the genus for American waters and the western Atlantic Ocean since its original description from the Chuuk Archipelago, Pacific Ocean (Sørensen & Rho 2009). Additionally, a key to species level identification for Zelinkaderidae is included.

2. Material and methods

Specimens of *T. lagahoo* sp. nov. were collected at Tyrrel's Bay, Tobago Island, Caribbean Sea (western Atlantic Ocean): 11 18 00 N, 60 30 00 W (Fig. 1). The Archipelago of Trinidad and Tobago is situated at the verge of the Lesser Antilles (Fig. 1) and is part of the so-called Southern Caribbean marine ecoregion. Sampling was originally done on 13 May 1991 by Dr R. P. Higgins using a meio-benthic dredge (Higgins & Thiel 1988) at 5 m depth in very fine sand. After sampling, meiofauna was extracted from sediment using the bubble and blot method defined by Higgins (1964). Meiofaunal specimens were fixed in 4% formalin, preserved in Carosafe® and deposited in unsorted vials at the Smithsonian National Museum of Natural History (NMNH), Washington.

The aforementioned vials were loaned to the authors for the present study. Fixed kinorhynchs were picked up under a Motic® SMZ-168 stereo zoom microscope with the help of an Irwin loop and washed with distilled water in order to remove formalin. For light microscopy (LM), specimens were dehydrated through a graded series of 25%, 50%, 75% and 100% glycerin and finally mounted on a glass slide in Fluoromount G® sealed with Depex®. Mounted specimens were studied and photographed using an Olympus® BX51-P microscope equipped with differential interference contrast (DIC) optics and an Olympus® DP-70 camera. Morphological measurements were obtained with Olympus cell-Sens® software. For scanning electron microscopy (SEM), specimens were transferred to 70% ethanol and then progressively dehydrated through a series of 80%, 90%, 95% and 100% ethanol. Specimens were sonically cleaned during 5-7 s. Hexamethyldisilazane (HMDS) was used for chemical drying through a HMDS-ethanol series. Specimens were coated with gold and mounted on aluminium stubs to be examined with a JSM 6335-F JEOL SEM at the ICTS Centro Nacional de Microscopía Electronica (Complutense University of Madrid, Spain).

Line drawings, images and plates composition were done using Adobe® Photoshop CC-2014 and Illustrator CC-2014 software.

3. Results

Taxonomic account

Class **Cyclorhagida** (Zelinka 1896) Sørensen et al. 2015
Order **Kentrorhagata** Sørensen et al. 2015
Family **Zelinkaderidae** Higgins 1990
Genus ***Triodontoderes*** Sørensen & Rho, 2009.
T. lagahoo sp. nov.
(Figs. 2-6 and Tables 1-3)

The species was registered in Zoobank under: zoobank.org:pub:7699F0E0-3F1B-451C-8E43-EB548773D1C0.

3.1. Type material

Holotype, adult female, collected on 13 May 1991 at Tyrrel's Bay, Tobago Island, western Atlantic Ocean: 11 18 00 N, 60 30 00 W at 5 m depth in very fine sand; mounted in Fluoromount G®, deposited at NMHN under accession number: USNM 1550564. Paratypes, seven adult males and four adult females, all of them with same collecting data as holotype, mounted in Fluoromount G®, deposited at NMHN under accession numbers: USNM 1550565-1550575.

3.2. Non-type material

Five additional specimens with same collecting data as holotype and paratypes, mounted for SEM, deposited at the Invertebrates Collection of the Meiofaunal Laboratory at the Universidad Complutense de Madrid (UCM), Spain.

3.3. Diagnosis

Triodontoderes with middorsal acicular spines on segments 1-11 (that on segment 10 crenulated in males), laterodorsal crenulated spines on segment 10 only in males, lateroventral acicular spines on segments 3-4 and 6-8 (lateroventral spines also on segment 10 in females), lateroventral cuspidate spines on segments 5 and 9, lateral accessory acicular spines on segments 5 and 9, lateral accessory cuspidate spines on segment 8, ventrolateral acicular spines on segment 2 and ventrolateral cuspidate spines on segment 2. Females with short papillae in ventrolateral position on segment 8 and ventromedial position on segment 9. Neck and trunk segments superficially covered by small, scale-like, medially depressed cuticular hairs arranged in slightly irregular longitudinal bands.

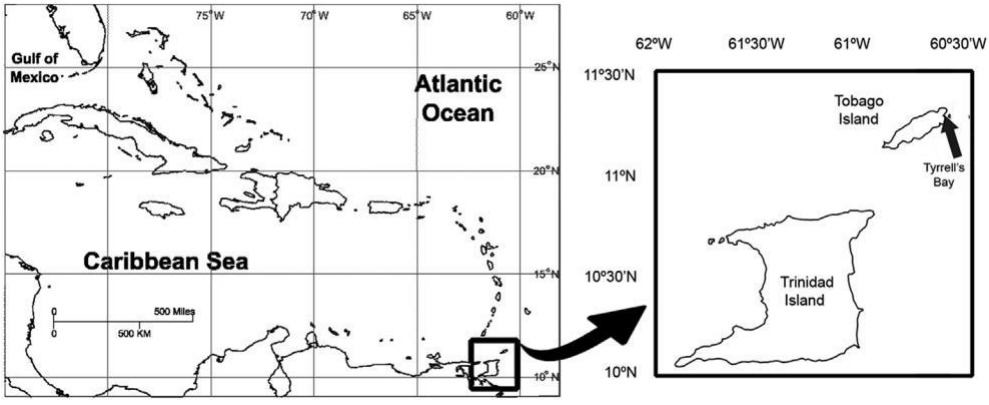

Fig. 1. Map showing the sampling locality on Tobago Island (Trinidad and Tobago), Lesser Antilles, Caribbean Sea (western Atlantic Ocean).

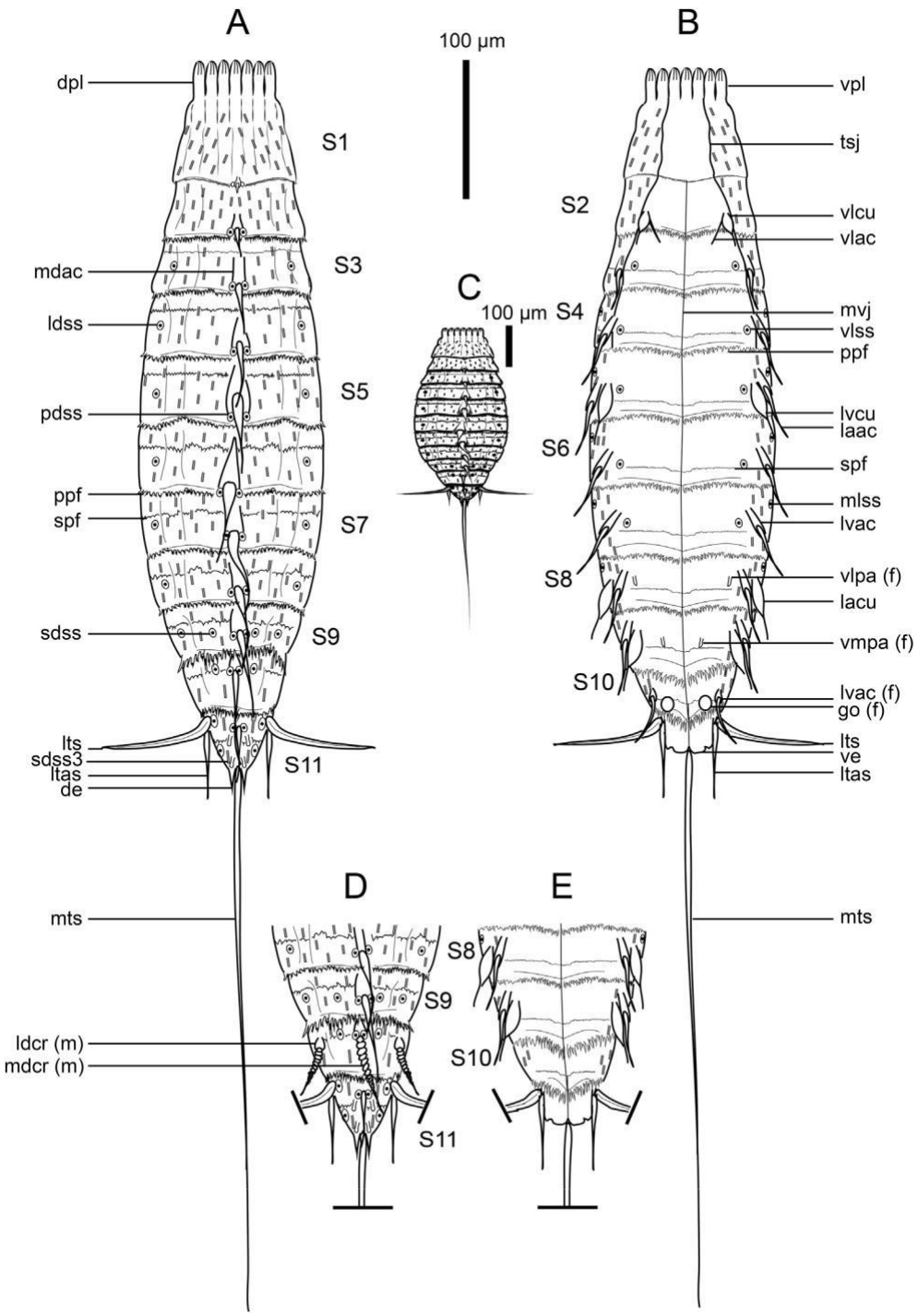

Fig. 2. Line art illustrations of *Triodontoderes lagahoo* sp. nov. (A) Female, dorsal overview; (B) Female, ventral overview; (C) Female, dorsal overview showing the fat shape of the species; (D) Male, segments 8-11, dorsal overview; (E) Male, segments 8-11, ventral overview. Abbreviations: de, dorsal extension (of segment 11); dpl, dorsal placid; f, female condition of sexually dimorphic feature; go, gonopore; laac, lateral accessory acicular spine; lacu, lateral accessory cuspidate spine; ldcr, laterodorsal crenulated spine; ldss, lat-erodorsal sensory spot; ltas, lateral terminal accessory spine; lts, lateral terminal spine; lvac, lateroventral acicular spine; lvcu, lateroventral cuspidate spine; m, male condition of sexually dimorphic feature; mdac, middorsal acicular spine; mdcr, middorsal crenulated spine; mlss, midlateral sensory spot; mts, midterminal spine; mvj, midventral junction; pdss, paradorsal sensory spot; ppf, primary pectinate fringe; S, segment followed by number of corresponding segment; sdss, subdorsal sensory spot; sdss3, subdorsal type 3 sensory spot; spf, secondary pectinate fringe; tsj, tergo-sternal junction; ve, ventral extension (of segment 11); vlac, ventrolateral acicular spine; vlcu, ventrolateral cuspidate spine; vlpa, ventrolateral papilla; vlss, ventrolateral sensory spot; vmpa, ventromedial papilla; vpl, ventral placid.

Primary pectinate fringe short on segment 1, strongly serrated with bifid tips on the remaining trunk segments. Dorsal extensions of segment 11 elongated, distally pointed, horn-like; ventral extensions of segment 11 short, wide, distally rounded.

3.4. Etymology

The species is named after the mythical shapeshifting monster “Lagahoo” (also known as “Ligahoo” or “Lugarhou”) from the folklore of Trinidad and

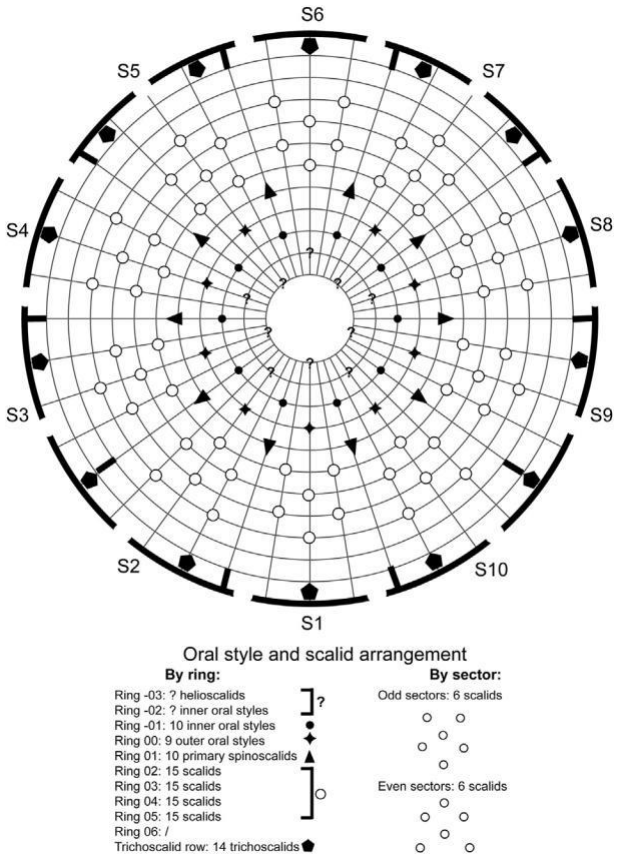

Fig. 3. Diagram of mouth cone, introvert and trichoscalids in *Triodontoderes lagahoo* sp. nov., with indication of oral style, scalid and trichoscalid arrangement. The outermost bold lines refers to the placids.

Tobago, the location where the species was found. According to the legend, Lagahoo can shapeshift into various creatures, which resembles the different trunk shapes reported herein for the species.

3.5. Description

See Tables 1 and 2 for measurements and dimensions, and Table 3 for summary of acicular, crenulated and cuspidate spine, papilla and sensory spot locations.

Head with narrow, retractable mouth cone and introvert with five rings plus an extra ring of trichoscalids attached to the neck (Figs. 3 and 4A-H). Mouth cone presumably with four rings of oral styles, incompletely observed (Fig. 3). Ring of helioscalids and the first ring of inner oral styles (rings -03 and -02) barely visible in the examined specimens. Second ring of inner oral styles (ring -01) with ten styles (Fig. 3). Observed inner oral styles of ring -01 composed of a single unit, with a trapezoidal, enlarged base bearing a short fringe and a triangular, hook-like, inwards-pointed, distal tip (Fig. 4C). Ring 00 with nine equally-sized outer oral styles that morphologically resemble the inner oral styles but much longer and flexible at their distal tips, with a fringe and paired spines arising from their bases (Figs. 3, 4C-D and 6B). Outer oral styles composed of a single unit, located anterior to each introvert sector, except in the middorsal section 6 where a style is missing (Fig. 3). Triangular, cuticular thickenings flanking the outer oral styles' bases (Fig. 4D). Posterior part of mouth cone elongated, forming a long tube (Fig. 4A, B).

Heads were only everted in the holotype (mounted for LM) and one paratype, (mounted for SEM), which disabled precise examination of the arrangement and morphology of scalids in the remaining specimens. Ring 01 with ten primary spinoscalids (Fig. 3) composed of a basal sheath and a distal elongated end-piece; basal sheath equipped with a median dense fringe with long tips (Fig. 4E, F). Tips of the fringe slightly protrude outwards when the introvert is retracted inside the trunk, and lay on top of the primary spinoscalids when the introvert is completely everted (Fig. 4F). Ring 02 with fifteen regular-sized scalids, arranged as two in the odd-numbered sectors and one in the even-numbered sectors (Figs. 3 and 4G, H). Scalids on this and remaining rings are composed of a basal sheath and a distal, elongated, hook-like end-piece (Fig. 4G, H). Ring 03 with fifteen regular-sized scalids, arranged as one in the odd-numbered sectors and two in the even-numbered sectors (Figs. 3 and 4G, H). Ring 04 similar to ring 02 (Figs. 3 and 4G, H). Ring 05 similar to ring 03 (Figs. 3 and 4G, H). The location of scalids in rings 01-05 follows a strict pattern around the introvert, and each sector carries six scalids, five following a quincunx arrangement plus a single scalid that appears anterior (in even-numbered sectors) or posterior (in odd-numbered sectors) (Figs. 3 and 4G, H).

Neck with fourteen inconspicuous, elongated, distally tripartite, soft placids of uniform size; placids are fused with the segment 1 and a transverse articulation between placids and segment 1 is missing (Figs. 2A, B, 4A, B and 6A, C). Fourteen small, triangular trichoscalids attached to the neck, whose occurrence is directly associated with the placids position (Figs. 3 and 4E). Trichoscalid plates absent.

Trunk vermiform, circular in cross-section, spindle-shaped, composed of eleven segments (Figs. 2A, B, 4A, B and 6A). Body outline variable from longer and slender to shorter and chubby (Figs. 2A-C and 4A, B, J-L). Cuticle along the whole trunk thin, soft and flexible, making the intersegmental junctions barely visible. First trunk segment with one tergal and one sternal plate (Fig. 2A, B); segments 2-4 with one tergal and two sternal plates with lateroventral and midventral joints (Fig. 2A, B); remaining segments with a single tergal plate with midventral joint (Fig. 2A, B, D, E). Segment 1 fused with the neck, without distinct articulation (Figs. 2A, B, 5A and 6A, C). Neck and all trunk segments superficially covered by small, scale-like, medially depressed cuticular hairs arranged in slightly irregular longitudinal bands (Figs. 2A, B, D, E and 6D, G, I); cuticular hairs absent at ventrolateral and ventromedial regions of trunk (Fig. 2B, E). Trunk segments with longitudinal folds on the dorsal and lateral sides that are most certainly a fixation artefact (Figs. 2A, C, D, 4A, B, 5A, B, D, E, G, H and 6A). Posterior margin of segments straight, with long primary pectinate fringes (except that of segment 1 that is conspicuously shorter); primary pectinate fringes with very weak serration on first segment, with strong serration and bifid tips on remaining segments (Figs. 2A, B, D, E and 4I). Secondary pectinate fringes on segments 2-11 less conspicuous than primary ones but also long, ventrally extending near the posterior margin of segment, also serrated and with bifid tips (Figs. 2A, B, D, E and 4I).

Segment 1 with a small, very short, extremely flexible acicular spine in middorsal position (Figs. 2A and 5A). Acicular spines on this and following segments are composed of a single flexible, elongated piece with pointed tip that basally articulates in a swollen cuticular thickening (Figs. 2A, B, D, E, 4I, 5A, K and 6A, D-F, H, J); basal swollen articulation of acicular spines with paired cuticular protuberances that flank the spine (Figs. 2A and 5A). Paired sensory spots in paradorsal position, on top of the protuberances beside the spine's basal articulation (Fig. 2A and similar to 6D). Sensory spots on this and most following segments are composed of an oval patch of numerous micropapillae surrounding a central pore (similar to 6G).

Segment 2 with acicular spine in middorsal position (Figs. 2A and 5A); paired small, very short, extremely flexible acicular spines in ventrolateral position (Figs. 2B and 5B). Paired cuspidate spines also in ventrolateral position, but located between tergosternal junction and acicular spine (Figs. 2B and 5B). Cuspidate spines on this and following segments are composed of a single syringe-like piece with broadened base, of which the latter constitutes more than 50% of the spine dimension, basally articulated (Figs. 2B, E, 5B, E, H and 6E). Paired sensory spots in paradorsal position, similar to those of the precedent segment (Figs. 2A and 5A).

Segment 3 with acicular spine in middorsal position and paired acicular spines in lateroventral position (Figs. 2A, B and 5A, B). Paired sensory spots in paradorsal, laterodorsal and ventrolateral positions (Figs. 2A, B and 5A, B).

Segment 4 with acicular spine in middorsal position and paired acicular spines in lateroventral position (Figs. 2A, B and 5D, E). Paired sensory spots in paradorsal, laterodorsal, midlateral and ventrolateral positions (Figs. 2A, B, 5D and 6G). Midlateral sensory spots on this and following segments are composed of an oval patch of numerous micropapillae surrounding two pores (similar to Fig. 6I).

Segment 5 with acicular spine in middorsal position and paired acicular spines in lateral accessory position (Figs. 2A, B, 5D, E and 6E); paired cuspidate spines in lateroventral position (Figs. 2B, 5E and 6E). Paired sensory spots in paradorsal, laterodorsal, midlateral and ventrolateral positions (Figs. 2A, B, 5D, E and 6G).

Segment 6 with arrangement of spines and sensory spots similar to segment 4 (Figs. 2A, B, 5D, E and 6F, I).

Segment 7 with arrangement of spines and sensory spots similar to segments 4 and 6 (Figs. 2A, B, 5D, H and 6F).

Segment 8 with acicular spine in middorsal position and paired acicular spines in lateroventral position (Figs. 2A, B, D, E, 5G, H and 6D, F); paired cuspidate spines in lateral accessory position (Figs. 2B, E and 5H). Paired sensory spots in paradorsal, laterodorsal and midlateral positions (Figs. 2A, B, D, E, 5G and 6D). Females with paired, small papillae in ventrolateral position (Figs. 2B and 5H); papillae on this and following segment are rounded areas with a minute tubular structure carrying a basal collar of short, flexible hairs.

Segment 9 with acicular spine in middorsal position and paired acicular spines in lateral accessory position (Figs. 2A, B, D, E and 5G, H); paired cuspidate spines in lateroventral position (Figs. 2B, E and 5H). Paired sensory spots in paradorsal, subdorsal and laterodorsal positions (Figs. 2A, D and 5G). Females with paired, small papillae in ventromedial position (Figs. 2B and 5H).

Segment 10 differing between males and females. Males with an unpaired, crenulated spine in middorsal position and paired, crenulated spines in laterodorsal position (Figs. 2D, 5J and 6H). Females with an unpaired, acicular spine in middorsal position and paired acicular spines in lateroventral position (Figs. 2A, B and 5G, H). Females with paired, large, strongly cuticularized, rounded gonopores at the intersegmental junction between segments 10 and 11 (Fig. 5I). Both males and females with paired sensory spots in paradorsal and subdorsal positions (Figs. 2A, D and 5G).

Segment 11 tapering to the base of the midterminal spine, with acicular spine in middorsal position and paired lateral terminal and lateral terminal accessory spines (Figs. 2A, B, D, E, 5C, F, G, I-K and 6A, J). Tergal plate of segment 11 carrying two elongated, distally pointed, horn-like dorsal extensions (Figs. 2A, D, 5F and 6J) as well as two short, wide, distally rounded ventral extensions (Figs. 2B, E and 5I). Paired sensory spots arranged on top of the paired cuticular protuberances beside the middorsal spine's basal articulation, in paradorsal position (Figs. 2A, D, 5G-J and 6J). Two pairs of type 3 sensory spots in subdorsal position, one posterior to the paradorsal sensory spots, another near the posterior margin of segment (Figs. 2A, D, 5C, J and 6J). Two pairs of sensory spots in laterodorsal position, one near the base of the dorsal cuticular extensions, another near the basal insertion of the lateral terminal spines (Figs. 2A, D and 6J), barely visible under LM.

4. Discussion

4.1. Remarks on morphological features

T. lagahoo sp. nov. fits well into the genus *Triodontoderes* by the combination of the following characters: oral styles of mouth cone composed of a single piece; neck composed of fourteen soft, elongated, inconspicuous, equally-sized, distally tripartite placids fused with segment 1; neck and trunk with small, scale-like, medially depressed cuticular hairs irregularly arranged in longitudinal bands; segment 1 with one tergal and one sternal plate, segments 2-4 with one tergal and two sternal plates and remaining segments with a single tergal plate with midventral joint; unpaired middorsal spines on all trunk segments; segment 2 with paired, small, very flexible acicular spines in ventrolateral position plus paired cuspidate spines also in ventrolateral position; segments 3-9 with lateral acicular and/or cuspidate spines; males with middorsal and paired laterodorsal crenulated spines on segment 10; females with paired, lateroventral acicular spines on segment 10 and paired ventral papillae on some segment from 7 to 9; segment 11 with midterminal, lateral terminal and lateral terminal accessory spines (Sørensen & Rho 2009).

Until now, the genus *Triodontoderes* was composed of a single species, *T. anulap*, from the Chuuk Archipelago, Micronesia, western Pacific Ocean (Sørensen & Rho 2009). The main morphological discrepancies between the two congeners are summarized in Table 4. Both species may be easily distinguished by their patterns of spines, female papillae and sensory spots. *T. anulap* is characterized by having paired cuspidate spines in lateral accessory position on segment 6 (Sørensen & Rho 2009), absent in *T. lagahoo* sp. nov. Moreover, females of *T. anulap* have paired papillae in ventrolateral position on segments 7-8 and in ventromedial position on segment 9 (Sørensen & Rho 2009), while females of *T. lagahoo* sp. nov. possess papillae in ventrolateral position only on segment 8 and in ventromedial position on segment 9. Additionally, the main differences between both species in sensory spot are the presence of paired sensory spots in laterodorsal position on segments 3-9 and 11 in *T. lagahoo* sp. nov. (only on segment 10 in *T. anulap*), in midlateral position on segments 4-8 (only on segment 2 in *T. anulap*) and in ventrolateral positions on segments 3-7 (displaced to ventromedial position and on segments 4, 6-8 and 10-11 in *T. anulap*) (see Sørensen & Rho 2009, for complete sensory spots arrangement of *T. anulap*).

Another morphological discrepancy between both species refer to the trunk pectinate fringes and cuticular hairs. *T. anulap* only possesses serrated posterior margin of segments with long pectinate fringes on segments 7-11 (Sørensen & Rho 2009), whereas *T. lagahoo* sp. nov. has serrated posterior margin of segments and long pectinate fringes on segments 2-11. Moreover, *T. anulap* is characterized by having several wavy secondary pectinate fringes composed of tiny scales mixed with slightly longer aciculae from segment 2 (Sørensen & Rho 2009), while *T. lagahoo* sp. nov. has a single straight secondary pectinate fringe strongly serrated and with bifid tips, also from segment 2. Finally, *T. anulap* has cuticular hairs arranged all over the integument (Sørensen & Rho 2009), whereas those of *T. lagahoo* sp. nov. are absent at ventrolateral and ventromedial regions of trunk.

A striking morphological feature of *T. lagahoo* sp. nov. is the presence of two different body outlines. Of the seventeen examined specimens, twelve

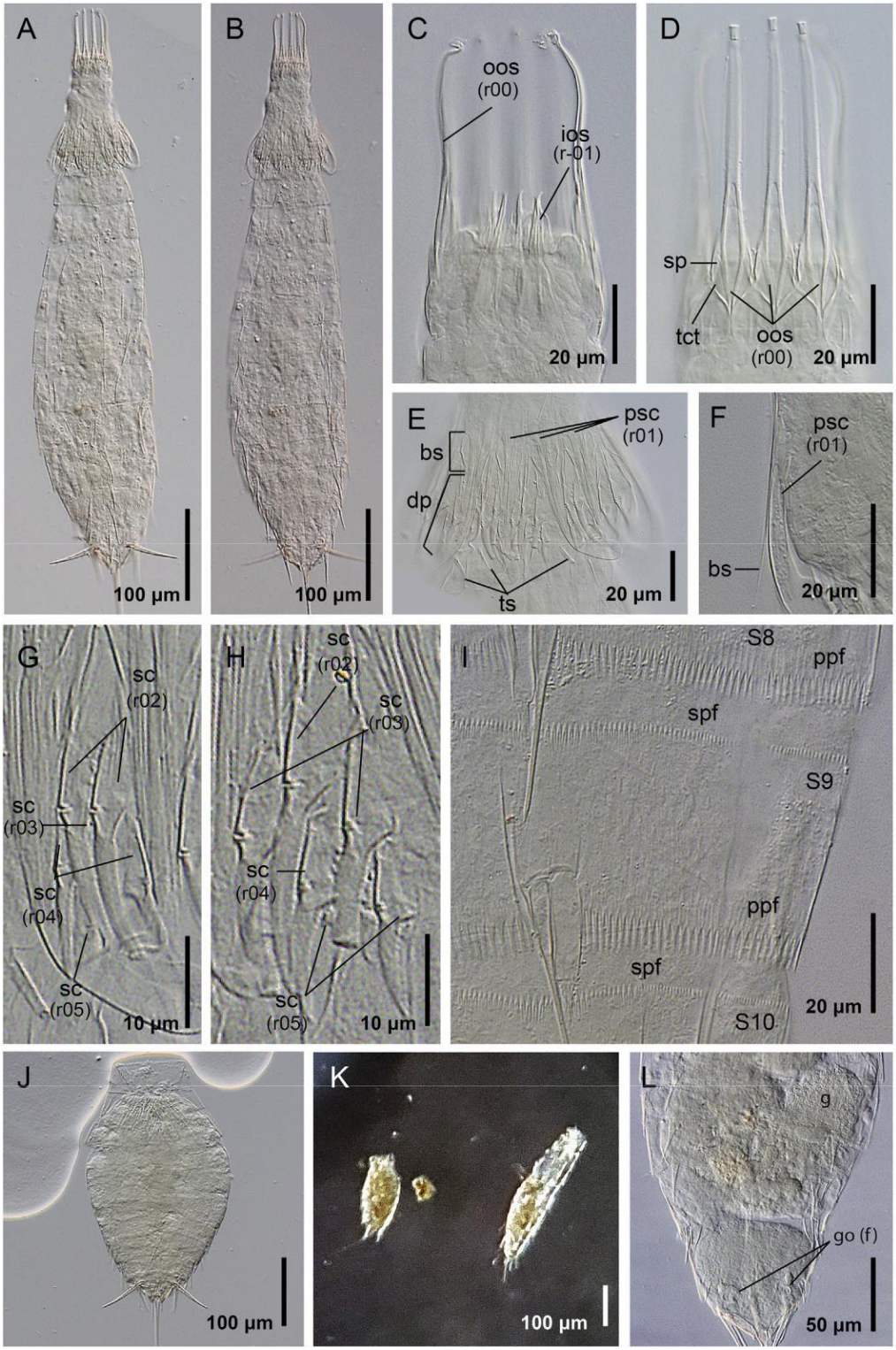

Fig. 4. Light micrographs (A-J, L) and stereomicroscope photo (K) showing trunk overviews and details in the mouth cone, introvert and general cuticular trunk characters of the female holotype NMNH USNM 1550564 (A-I), a male paratype NMNH USNM 1550565 (J), a female paratype NMNH USNM 1550572 (L) and non-mounted additional specimens (K) of *Triodontoderes lagahoo* sp. nov. (A) Dorsal overview of trunk; (B) ventral overview of trunk; (C) mouth cone, with detail of the last ring of inner oral styles (ring -01); (D) mouth cone, with detail of the ring of outer oral styles (ring 00); (E) introvert, showing the first ring of primary spinoscalids (ring 01) and trichoscalids; (F) detail of a primary spinoscalid, showing the rigid spine that extends from its basal plate; (G) sector 5 of introvert, with detail of scalids of rings 02-05; (H) sector 6 of introvert, with detail of scalids of rings 02-05; (I) midlateral and lateroventral regions on right half of tergal plate of segments 8-10, with detail of primary and secondary pectinate fringes; (J) ventral overview of a chubby body outline male; (K) slender body outline (right) and chubby body outline (left) non-mounted specimens; (L) ventral view of segments 7-11 of a chubby body outline female, showing the gonads and the gonopores. Abbreviations: bs, basal sheath; dp, distal piece; f, female condition of sexually dimorphic character; g, gonad; go, gonopore; ios, inner oral style; oos, outer oral style; ppf, primary pectinate fringe; psc, primary spinoscalid; r, ring; S; segment followed by number of corresponding segment; sp, spine; sc, scalid; spf, secondary pectinate fringe; tct, triangular cuticular thickening; ts, trichoscalid.

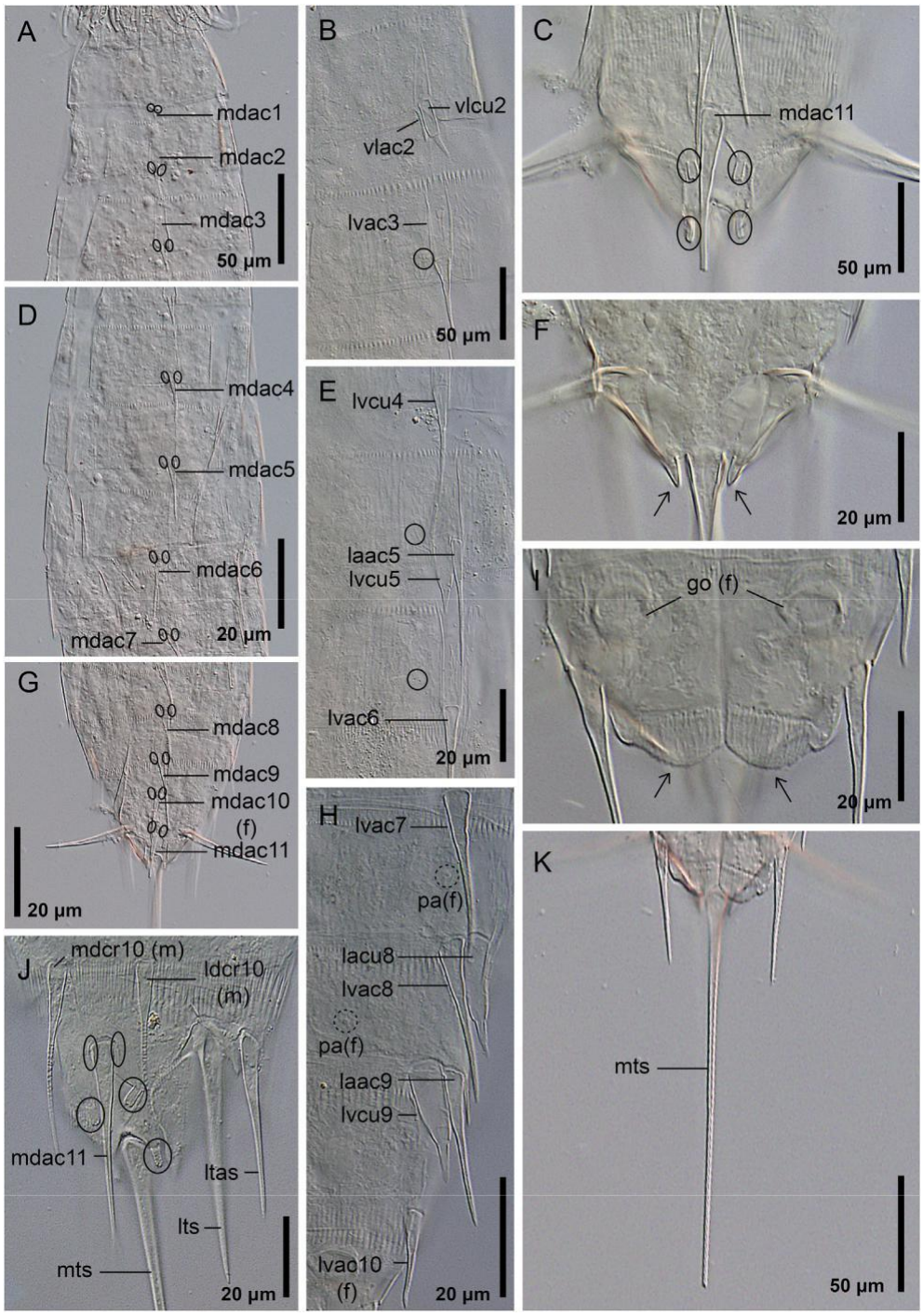

Fig. 5. Light micrographs showing details of cuticular trunk characters of female holotype NMNH USNM 1550564 (A-I, K) and male paratype NMNH USNM 1550565 (J) of *Triodontoderes lagahoo* sp. nov., with main focus on spines, sensory spots, sexually dimorphic features and segment 11 cuticular extensions. (A) Dorsal view of segments 1-3; (B) lateral view of right half of segments 2-3; (C) dorsal view of segment 11, showing the two pairs of type 3 sensory spots; (D) dorsal view of segments 4-7; (E) lateral accessory to ventromedial regions on right half of tergal and sternal plates of segments 4-6; (F) dorsal view of segment 11, showing the tergal extensions (in arrows); (G) dorsal view of segments 8-11; (H) lateral accessory to ventromedial regions on right half of tergal plates of segments 7-10; (I) ventral view of segment 11, showing the sternal extensions (in arrows) and the female gonopores; (J) lateral view of right half of a male segment 11; (K) ventral view of segment 11, showing the midterminal spine. Abbreviations: f, female condition of sexually dimorphic character; go, gonopore; laac, lateral accessory aciculate spine; lacu, lateral accessory cuspidate spine; ldcr, laterodorsal crenulated spine; ltas, lateral terminal accessory spine; lts, lateral terminal spine; lvac, lateroventral acicular spine; lvcu, lateroventral cuspidate spine; m, male condition of sexually dimorphic character; mdac, middorsal acicular spine; mdcr, middorsal crenulated spine; mts, midterminal spine; pa, papilla; vlac, ventrolateral acicular spine; vlcu, ventrolateral cuspidate spine; sensory spots are marked as continuous circles and papillae as dotted circles; numbers after spines indicate the corresponding segment.

belong to the slender body outline and five to the chubby one. Both females and males were found in the two different body outlines. Specimens with short and chubby body outline possess the same number of trunk segments and arrangement of cuticular structures than those with long and slender body outline (Fig. 4J). Moreover, these specimens also possess developed gonads

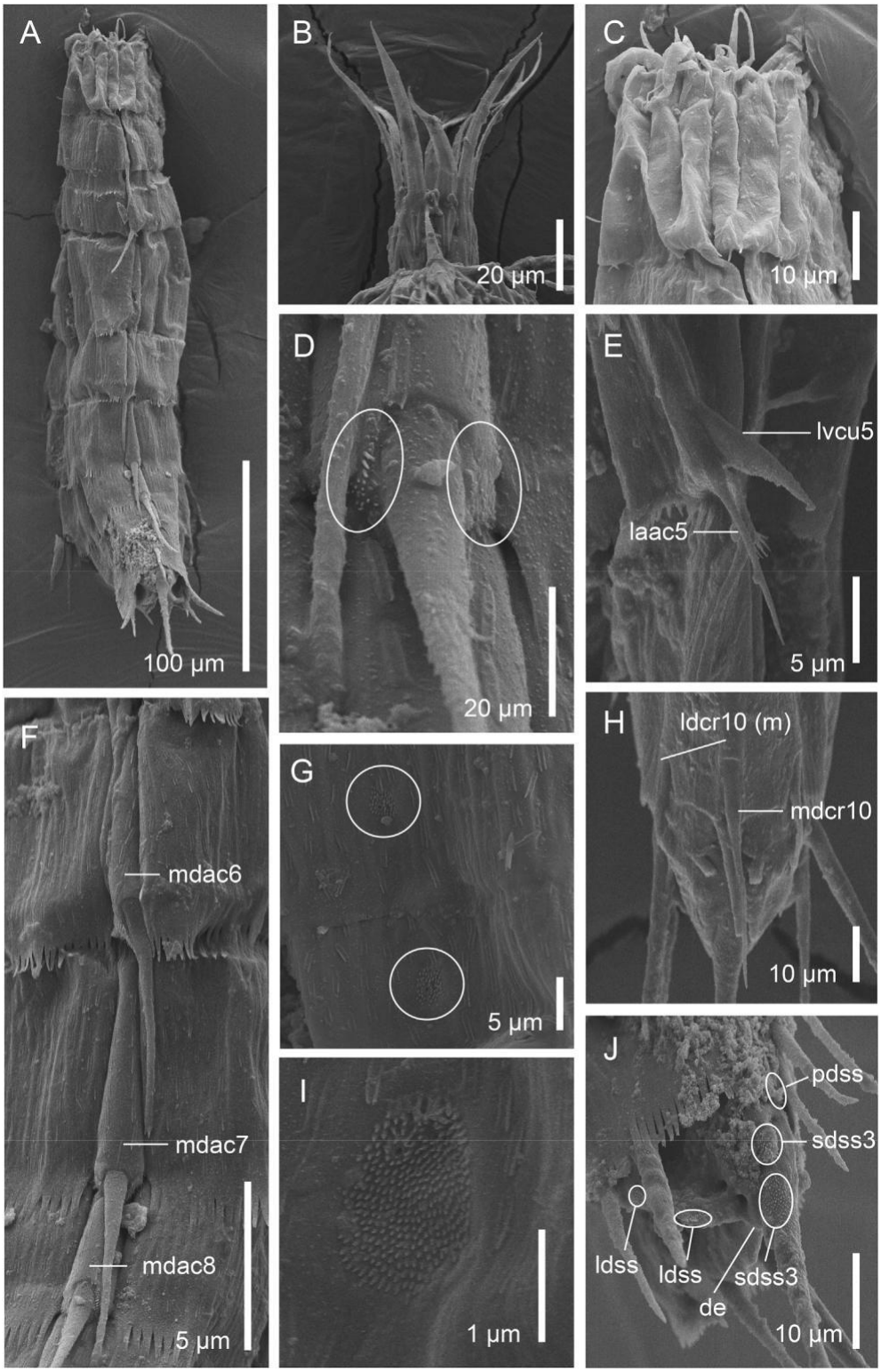

Fig. 6. Scanning electron micrographs showing general overview and details of the cuticular trunk morphology of non-type specimens of *Triodontoderes lagahoo* sp. nov. (A) Dorsal overview of trunk; (B) mouth cone, showing the outer oral styles; (C) dorsal view of neck, showing the distally tripartite placids; (D) detail of middorsal spine of segment 8, showing the swollen cuticular thickenings of its basal articulation with the paired paradorsal sensory spots; (E) lateroventral and lateral accessory regions on right half of tergal plates of segment 5; (F) middorsal and paradorsal regions of tergal plates of segments 6-8; (G) laterodorsal region on left half of tergal plates of segments 4-5; (H) dorsal view of a male segment 10, showing the crenulated middorsal and laterodorsal spines; (I) detail of midlateral sensory spot of segment 6; (J) lateral view of left half of segment 11 tergal plate, showing all sensory spots on left side. Abbreviations: de, dorsal extension (of segment 11); laac, lateral accessory acicular spine; ldcr, laterodorsal crenulated spine; ldss, laterodorsal sensory spot; lvcu, lateroventral cuspidate spine; m, male condition of sexually dimorphic character; mdac, middorsal acicular spine; mdcr, middorsal crenulated spine; pdss, paradorsal sensory spot; sdss3, subdorsal type 3 sensory spot; sensory spots are marked as continuous circles; numbers after spines indicate the corresponding segment.

Table 1
Measurements of body size, lateral terminal, lateral terminal accessory and midterminal spines of adult *Triodontoderes lagahoo* sp. nov., including number of measured specimens (*n*), mean of data and standard deviation (SD). There were no remarkable differences in sizes or dimensions between the two sexes. Abbreviations: LTAS, lateral terminal accessory spine; LTS, lateral terminal spine; MTS, midterminal spine; S, segments lengths (number after S indicates the corresponding segment); TL, total length of trunk.

Character	Range	Mean (SD; *n*)
TL (µm)	319.0-540.2	428.0 (62.0; 12)
S1 (µm)	35.5-72.8	51.1 (13.1; 12)
S2 (µm)	21.2-57.4	43.1 (12.0; 12)
S3 (µm)	25.4-62.9	47.4 (11.3; 12)
S4 (µm)	29.8-63.8	52.3 (11.9; 12)
S5 (µm)	29.4-67.2	55.4 (12.8; 12)
S6 (µm)	39.5-63.7	52.1 (7.8; 12)
S7 (µm)	37.5-65.9	53.4 (8.8; 12)
S8 (µm)	47.8-76.0	56.6 (12.0; 12)
S9 (µm)	31.5-76.2	58.4 (12.4; 12)
S10 (µm)	34.3-71.2	56.7 (11.9; 12)
S11 (µm)	26.0-51.1	43.8 (11.6; 12)
LTS (µm)	52.8-78.8	60.8 (6.9; 12)
LTS/TL (%)	10.6-21.5	14.5 (3.1; 12)
LTAS (µm)	33.7-42.4	39.7 (3.8; 12)
LTAS/TL (%)	8.2-13.3	9.5 (1.9; 12)
LTAS/LTS (%)	55.4-74.4	65.6 (4.5; 12)
MTS (µm)	117.6-288.2	214.8 (51.7; 9)
MTS/TL (µm)	27.8-72.3	39.5 (27.5; 9)

Table 2
Measurements of middorsal, laterodorsal, lateral accessory and lateroventral spines of adult *Triodontoderes lagahoo* sp. nov., including number of measured specimens (*n*), mean of data and standard deviation (SD). Abbreviations: ac, acicular (spine); cr, crenulated (spine); cu, cuspidate (spine); f, female condition of sexually dimorphic character; LAS, lateral accessory spine; LDS, laterodorsal spine; LVS, lateroventral spine; m, male condition of sexually dimorphic character; MDS, middorsal spine.

Character	Range	Mean (SD; *n*)
MDS 1 (ac) (µm)	5.0-10.5	7.5 (1.8; 11)
MDS 2 (ac) (µm)	14.3-34.2	24.9 (7.6; 12)
MDS 3 (ac) (µm)	24.5-53.2	38.9 (7.4; 11)
MDS 4 (ac) (µm)	32.5-57.7	46.1 (8.6; 11)
MDS 5 (ac) (µm)	37.6-60.5	48.9 (7.9; 12)
MDS 6 (ac) (µm)	42.5-64.5	53.3 (8.4; 12)
MDS 7 (ac) (µm)	41.3-71.9	58.6 (9.0; 12)
MDS 8 (ac) (µm)	47.9-71.1	60.8 (7.9; 12)
MDS 9 (ac) (µm)	39.3-73.4	59.9 (10.5; 11)
MDS 10 (cr, m; ac, f) (µm)	22.3-65.9	42.8 (13.2; 12)
MDS 11 (ac) (µm)	25.4-51.7	46.0 (7.6; 12)
LDS 10 (cr, m) (µm)	26.1-34.8	31.6 (3.3; 7)
VLS 2 (ac) (µm)	11.4-22.0	16.1 (4.9; 12)
VLS 2 (cu) (µm)	13.6-24.2	18.3 (5.2; 12)
LVS 3 (ac) (µm)	19.9-50.0	34.0 (8.8; 12)
LVS 4 (ac) (µm)	31.0-55.6	41.9 (7.6; 11)
LVS 5 (cu) (µm)	18.8-27.4	23.4 (3.1; 12)
LAS 5 (ac) (µm)	32.3-55.6	43.2 (8.4; 12)
LVS 6 (ac) (µm)	36.1-56.1	48.9 (6.4; 12)
LVS 7 (ac) (µm)	40.0-65.7	54.8 (8.6; 12)
LVS 8 (ac) (µm)	38.2-47.5	42.7 (2.9; 12)
LAS 8 (cu) (µm)	20.5-30.5	26.0 (3.5; 12)
LVS 9 (cu) (µm)	22.5-31.7	28.2 (2.5; 12)
LAS 9 (ac) (µm)	34.9-50.4	43.1 (6.0; 12)
LVS 10 (ac, f) (µm)	21.7-28.1	24.0 (2.8; 5)

and, in case of females, conspicuous gonopores (Fig. 4L). Though the abundance of the slender specimens were higher than that of the chubby ones, the latter body outline could be an artefact of the fixation process. As both types of body outlines were found in the vial containing non-mounted animals (Fig. 4K), the chubby shape is not result of the mounting process for LM. Nevertheless, two possibilities must be considered. On the one hand, the species may have the ability of kindly modifying its body outline due to the soft cuticle that characterizes this genus. This could be related to the proposed

Table 3
Summary of nature and arrangement of sensory spots, papillae and spines in *Triodontoderes lagahoo* sp. nov. Abbreviations: ac, acicular spine; cr, crenulated spine; cu, cuspidate spine; f, female condition of sexually dimorphic character; LA, lateral accessory; LD, laterodorsal; ltas, lateral terminal accessory spine; lts, lateral terminal spine; LV, lateroventral; m, male condition of sexually dimorphic character; MD, middorsal; mt, midterminal spine; ML, midlateral; pa, papilla; PD, paradorsal; SD, subdorsal; ss, sensory spot; ss3, type 3 sensory spot; VL, ventrolateral; VM, ventromedial.

Segment	MD	PD	SD	LD	ML	LA	LV	VL	VM
1	ac	ss							
2	ac	ss						cu, ac	
3	ac	ss		ss			ac	ss	
4	ac	ss		ss	ss		ac	ss	
5	ac	ss		ss	ss	ac	cu	ss	
6	ac	ss		ss	ss		ac	ss	
7	ac	ss		ss	ss		ac	ss	
8	ac	ss		ss	ss	cu	ac	pa(f)	
9	ac	ss	ss	ss		ac	cu		pa (f)
10	cr (m)/ac (f)	ss	ss	cr (m)			ac (f)		
11	ac, mt	ss	ss3, ss3	ss, ss		ltas	lts		

hypothesis by Yamasaki (2019) of thin-cuticle body kinorhynchs, as this kind of cuticle would allow the animal being more flexible to seep through sediment interstices more easily and absorbing physical damage when sand grains are disturbed. On the other hand, the chubby specimens may correspond to the latest juvenile stages of the species. Though both chubby females and males were found with completely developed gonads, and gonopores in case of females (Fig. 4L), the latest juvenile stages of kinorhynchs often begin to develop gonads (Neuhaus 2013).

4.2. Remarks on systematic features

Triodontoderes, together with the genus *Zelinkaderes*, belongs to the family Zelinkaderidae, whose monophyly was supported by a total-evidence analysis (Sørensen et al. 2015). This family is morphologically characterized by possessing an introvert with one ring of primary spinoscalids followed by three or four rings of regular scalids, a trunk conspicuously circular in cross-section, at least segments 5 to 10 composed of a single tergal plate with midventral joint, acicular spines present in dorsal and lateral positions, cuspidate spines present on some segments, a segment 11 with lateral terminal, lateral terminal accessory and midterminal spines, at least some large, oval sensory spots with two pores in the anterior trunk region, scale-like cuticular hairs with a medial depression and male sexually dimorphic crenulated spines on segment 10 (Sørensen & Rho 2009).

The introvert of Zelinkaderidae is characterized by the reduction of, at least, one ring of scalids. Regular scalids are completely absent on rings 02-03 in *Z. brightae* and *Z. klepali* (Bauer-Nebelsick, 1995; Sørensen et al., 2007); on ring 06 in *T. anulap* and *T. lagahoo* sp. nov. (Sørensen & Rho, 2009; this paper); on rings 05-06, odd sectors of ring 03 and even sectors of ring 02 in *Z. floridensis* (Higgins, 1990); and on ring 02, even sectors of ring 06 and odd sectors of ring 03 in *Z. yong* (Altenburger et al., 2015). In suµmary, species of *Zelinkaderes* generally shows a strong reduction of the introvert scalids, as this reduction involves more than a single ring, whereas *Triodontodere*s only shows scalid reduction in the last ring. Additionally, *Zelinkaderes* seems to show more variability in the scalid arrangement (Sørensen et al. 2007) than the genus *Triodontoderes*, with identical disposition of scalids in the two known species (Sørensen & Rho 2009; this paper). The only other cyclorhagid genus with a considerably lower number of scalids is *Cateria* Gerlach, 1956, that, besides the ten primary spinoscalids, possesses 35 regular scalids (Herranz et al. 2019; Neuhaus & Kegel 2015).

Table 4
Summary of main morphological differences between *Triodontoderes anulap* and *T. lagahoo* sp. nov.

Character	*T. anulap*	*T. lagahoo* sp. nov.
Cuspidate spines in lateral accessory position on segment 6	Present	Absent
Female papillae arrangement	Ventrolateral on segments 7-8 and ventromedial on segment 9	Ventrolateral on segment 8 and ventromedial on segment 9
Laterodorsal sensory spots	Segment 10	Segments 3-9 and 11
Midlateral sensory spots	Segment 2	Segments 4-8
Ventral sensory spots	Ventromedial on segments 4, 6-8 and 10-11	Ventrolateral on segments 3-7
Long and conspicuous trunk pectinate fringes	Segments 7-11	Segments 2-11

Furthermore, a newly described genus of Franciscideridae also possesses a reduction in the number of scalids, lacking these structures in ring 06 and the even-numbered sectors of ring 05 (Yamasaki 2019). It seems that *Cateria*, *Triodontoderes* and the new genus of Franciscideridae lost its more posterior scalid rings (Herranz et al. 2019; Sørensen & Rho 2009; Yamasaki 2019), whereas *Zelinkaderes* reduced the scalids in its more anterior rings (Altenburger et al. 2015; Sørensen et al. 2007). The reduction of scalids could have occurred independently in the four genera, as also proposed by Herranz et al. (2019). However, this hypothesis cannot be tested until a more complete systematic analysis of Kentrorhagata is performed.

The presence of distally tripartite placids seems also to be a synapomorphic feature of the family Zelinkaderidae (Sørensen & Rho 2009), with the exception of *Z. yong* that has very reduced placids (Altenburger et al. 2015). Both species of *Triodontoderes* also share the former feature (Sørensen & Rho 2009; this paper). According to the most recent phylogenetic analysis (Sørensen et al. 2015), it is likely that the plesiomorphic condition for placid morphology in Zelinkaderidae is the possession of distally tripartite placids. Then, *Z. yong* would have suffered a reversion of the character state through the placid reduction as an autapomorphy of the species. Again, this hypothesis cannot be tested until more morphological, and especially molecular phylogenetic data is available for the whole family.

One of the important morphological differences between species of *Triodontoderes* and *Zelinkaderes* is the number and arrangement of both acicular and cuspidate spines. The former genus is characterized by having middorsal acicular spines along all trunk segments (Sørensen & Rho 2009; this paper), whereas the latter has middorsal spines on segments 4, 6 and 8-11 (Sørensen et al. 2007). Additionally, lateral acicular and/or cuspidate spines are present on segment 2 and 4-9 in *Zelinkaderes* (Altenburger et al., 2015; Bauer-Nebelsick, 1995; Higgins, 1990; Sørensen et al., 2007), while they are present in at least one sex on segments 2-10 in *Triodontoderes* (Sørensen & Rho, 2009; this paper). Thus, a greater number of dorsal and lateral spines characterizes the genus *Triodontoderes* within the family Zelinkaderidae. However, it is still too early to infer an evolutionary trend towards increasing or decreasing the number of spines in Zelinkaderidae.

4.3. Key to species of Zelinkaderidae

1. Segment 1 composed of one tergal and one sternal plate; segments 2 to 4 composed of one tergal and two sternal plates; segments 5 to 11 composed of a single plate with midventral joint; neck consisting of 14 distally tripartite placids; middorsal spines present on all trunk segments; cuticular hairs irregularly arranged in scattered bands … **2** (**genus *Triodontoderes***)
- Segments 1 to 2 composed of one closed cuticular ring; segments 3 to 11 composed of a single plate with midventral joint; neck consisting of 16 entire or distally tripartite placids; middorsal spines present on segments 4, 6 and 8 to 11; cuticular hairs regularly arranged in longitudinal bands … **3 (genus *Zelinkaderes*)**

2. Lateral accessory cuspidate spines present on segment 6; female, sexually dimorphic papillae present in ventrolateral position on segments 7 to 8 and in ventromedial position on segment 9; long, conspicuous pectinate fringes on segments 7 to 11 … ***T. anulap***
- Lateral accessory cuspidate spines absent on segment 6; female, sexually dimorphic papillae present in ventrolateral position on segment 8 and in ventromedial position on segment 9; long, conspicuous pectinate fringes on segments 2 to 11 … ***T. lagahoo* sp. nov**.

3. Spines present in various lateral positions on segment 2 … **4**
- Spines absent on segment 2 … ***Z. floridensis***

4. Lateroventral or lateral accessory acicular spines present on segment 9 … **5**
- Lateroventral or lateral accessory acicular spines absent on segment 9 … ***Z. yong***

5. Cuspidate spines present in lateral series on segments 4 and 6 … **6**
- Cuspidate spines absent in lateral series on segments 4 and 6 … ***Z. klepali***

6. Cuspidate spines present in lateroventral position on segment 7 … ***Z. submersus***
- Cuspidate spines absent in lateroventral position on segment 7 … ***Z. brightae***

Funding sources

Cepeda was supported by a predoctoral fellowship of the Complutense University of Madrid (CT27/16-CT28/16).

Conflict of interest

The authors declare no conflicts of interest.

Acknowledgements

We would like to thank Dr Jon Norenburg and Kathryn Ahlfeld for loaning the material that made the present study possible.

References

Altenburger, A., Rho, H.S., Chang, C.Y., Sørensen, M.V., 2015. *Zelinkaderes yong* sp. nov. from Korea - the first recording of *Zelinkaderes* (Kinorhyncha: Cyclorhagida) in Asia. Zool. Stud. 54, 25. https://doi.org/10.1186/s4055-014-0103-6.

Bauer-Nebelsick, M., 1995. *Zelinkaderes klepali* sp. n., from shallow water sands of the Red Sea. Ann. Naturhist. Mus. Wien 97 (B), 57-74.

Gerlach, S.A., 1969. *Cateria submersa* sp. n., ein cryptorhager Kinorhynch aus dem sublitoralen Mesopsaµmal der Nordsee. Veröff. Inst. Meeresforsch. Bre-merhaven 12, 161-168.

Herranz, M., Di Domenico, M., Sørensen, M.V., Leander, B.S., 2019. The enigmatic kinorhynch *Cateria styx* gerlach, 1956 - a sticky son of a beach. Zool. Anz. 282, 10-30. https://doi.org/10.1016/j.jcz.2019.05.016.

Higgins, R.P., 1964. Three new kinorhynchs from the North Carolina Coast. Bull. Mar. Sci. 14, 479-493.

Higgins, R.P., 1990. Zelinkaderidae, a new family of cyclorhagid Kinorhyncha. Smithsonian Contrib. Zool. 500, 1-26. https://doi.org/10.5479/si.00810282.500.

Higgins, R.P., Thiel, H., 1988. Introduction to the Study of Meiofauna, first ed. Smithsonian Institution Press, Washington D.C.

Neuhaus, B., 2013. Kinorhyncha (=Echinodera). In: Schmidt-Rhaesa, A. (Ed.), Handbook of Zoology, Gastrotricha, Cycloneuralia and Gnathifera, Volume 1 Nematomorpha, Priapulida, Kinorhyncha, Loricifera. De Gruyter, Hamburg, pp. 181-350.

Neuhaus, B., Kegel, A., 2015. Redescription of *Cateria gerlachi* (Kinorhyncha, Cyclorhagida) from Sri Lanka and of *C. styx* from Brazil, with notes on *C. gerlachi* from India and *C. styx* from Chile, and the ground pattern of the genus. Zootaxa 3965, 1-77.

Sørensen, M.V., Dal Zotto, M., Rho, H.S., Herranz, M., Sanchez, N., Pardos, F., Yamasaki, H., 2015. Phylogeny of Kinorhyncha based on morphology and two molecular loci. PLoS One 10 (7), e0133440. https://doi.org/10.1371/journal.pone.0133440.

Sørensen, M.V., Heiner, I., Ziemer, O., Neuhaus, B., 2007. *Tubulideres seminoli* gen. et sp. nov. and *Zelinkaderes brightae* sp. nov. (Kinorhyncha, Cyclorhagida) from Florida. Helgol. Mar. Res. 61, 247-265. https://doi.org/10.1007/s10152-007-0073-8.

Sørensen, M.V., Pardos, F., 2008. Kinorhynch systematics and biology - an introduction to the study of kinorhynchs, inclusive identification keys to the genera. Meiofauna Mar. 16, 21-73.

Sørensen, M.V., Rho, H.S., 2009. *Triodontoderes anulap* gen. et sp. nov. - a new cyclorhagid kinorhynch genus and species from Micronesia. J. Mar. Biol. Assoc. U. K. 89 (6), 1269-1279. https://doi.org/10.1017/S0025315409000526.

Yamasaki, H., 2019. *Gracilideres mawatarii*, a new genus and species of Francisci-deridae (Allomalorhagida: Kinorhyncha) from Japan with morphological comparison of head characters, and special attention to thin-cuticle body of Kinorhyncha in relation to adaptation to interstitial environment. Zool. Anz. 282, 176-188. https://doi.org/10.1016/j.jcz.2019.05.010.

Zelinka, C., 1896. Demonstration der Tafeln der *Echinoderes* - monographie. Ver-handlungen Dtsch. Zool. Ges. 6, 197-199.

APPENDIX I. Kinorhyncha diversity in the Caribbean Sea: a compilation of prior and new knowledge, description of a new species of *Echinoderes* (Cyclorhagida: Echinoderidae) and a dichotomous key to the species level

Diego CEPEDA[1,*], Alberto GONZÁLEZ-CASARRUBIOS[2], Fernando PARDOS[3] & Nuria SÁNCHEZ[4]

[1,2,3,4] Universidad Complutense de Madrid (UCM), Faculty of Biological Sciences, Department of Biodiversity, Ecology and Evolution. C/ José Antonio Novais 12. 28040 Madrid, Spain.

* Corresponding author: diegocepeda@ucm.es

Abstract.

Studies on Caribbean Kinorhyncha diversity have focused on specific areas and scattered through time, being necessary to increase the knowledge of the region. Thanks to several meiofaunal samples originally taken by Dr Robert P. Higgins during the 60-90s and stored at the Smithsonian Institution of Washington, the authors of the present paper were able to begin with a project whose main aim was to describe the hidden Kinorhyncha diversity of the Caribbean Sea. This study represents the culmination of that project, combining all the prior and new knowledge to determine the kinorhynch diversity that inhabits the Caribbean Basin, and includes the description of a new species, *Echinoderes* sp. 1. It can be unequivocally distinguished from its congeners by the combination of middorsal spines on segments 4, 6 and 8 increasing in length posteriorly and lateroventral spines on segments 6-9, ventrolateral tubes on segment 2, lateroventral tubes on segment 5, sublateral tubes on segment 8 and laterodorsal tubes (in both sexes) on segment 10, and tergal extensions long and pointed, with a small cusp at their inner margin near the tip. Finally, a dichotomous, local key for identification to the species level of all known Caribbean kinorhynch species is included.

Keywords

Kinorhynchs, Mud dragons, Meiofauna, Caribbean Basin, Species diversity.

1. INTRODUCTION.

The phylum Kinorhyncha (commonly referred as mud dragons) covers a group of entirely marine and estuarine, holobenthic, free-living, meiofaunal organisms that inhabit different kinds of bottom sediments from the intertidal zone to the deep sea (Higgins 1988; Neuhaus 2013; Sørensen & Pardos 2020). Kinorhynchs are usually more abundant in silt and mud, but sand and gravel may also host these animals (Sørensen & Pardos 2020). In addition, although kinorhynchs are more abundant in the upper centimetres of marine sediments, where the pore water has enough available oxygen, lower abundances may be found below the redox layer (Cepeda *et al.* 2020a; Sánchez *et al.* 2020; Sørensen & Pardos 2020).

Currently, the phylum encompasses two classes, Allomalorhagida and Cyclorhagida, based on total-evidence analyses (Sørensen *et al.* 2015; Sánchez *et al.* 2016). Most kinorhynch genera are worldwide distributed, whilst species tend to show more regional distributions, frequently restricted to a few points in the same geographic area (Neuhaus 2013; Sørensen & Pardos 2020). However, kinorhynch distributions may hide artefacts due to sampling strategies of individual researchers in many cases (Neuhaus 2013; Sørensen & Pardos 2020; Cepeda *et al.* 2021), as occurs for other meiofaunal phyla (*e.g.* Fontaneto *et al.* 2012). Because of that, certain regions holding a rich diversity of marine meiofauna have been overlooked, including the Caribbean Sea, object of the present study.

The first reported species from the Caribbean Sea was *Echinoderes caribiensis* Kirsteuer, 1964 at the Bahía de Mochima, Venezuela (Kirsteuer 1964). However, it was not until 1983 that Dr R. P. Higgins published a detailed study of the coral reef kinorhynch fauna of Carrie Bow Cay and Twin Cays, Belize (Higgins 1983), including the description of eighteen new species: *Cristaphyes belizensis* (Higgins, 1983), *C. longicornis* (Higgins, 1983), *Echinoderes abbreviatus* Higgins, 1983, *E. horni* Higgins, 1983, *E. imperforatus* Higgins, 1983, *E. truncatus* Higgins, 1983, *E. wallaceae* Higgins, 1983, *Fujuriphyes deirophorus* (Higgins, 1983), *F. distentus* (Higgins, 1983), *Higginsium erismatum* (Higgins, 1983), *H. trisetosum* (Higgins, 1983), *Leiocanthus corrugatus* (Higgins, 1983), *L. ecphantor* (Higgins, 1983), *L. emarginatus* (Higgins, 1983), *Paracentrophyes praedictus* Higgins, 1983, *Pycnophyes apotomus* (Higgins, 1983), *P. stenopygus*

(Higgins, 1983) and *Setaphyes iniorhaptus* (Higgins, 1983). Posteriorly, Dr M. V. Sørensen began the study of the kinorhynchs of the Caribbean Panama (Sørensen 2006), whose samples yielded the description of two new species, *Echinoderes collinae* Sørensen, 2006 and *E. intermedius* Sørensen, 2006, and the first report for the Caribbean area of *E. spinifurca* Sørensen *et al.*, 2005, *Pycnophyes beaufortensis* Higgins, 1964, *Semnoderes* cf. *pacificus* Higgins, 1967 and two still undescribed species (*Cephalorhyncha* sp. and *Echinoderes* sp.). This work was latter supplemented by Neuhaus *et al.* (2014) with the description of *Centroderes barbanigra* Neuhaus *et al.*, 2014 from La Española and Panama, and Pardos *et al.* (2016b) with the description of *Cristaphyes panamensis* Pardos *et al.*, 2016, *Echinoderes rociae* Pardos *et al.*, 2016, *E. orestauri* Pardos *et al.*, 2016 and *Pycnophyes alexandroi* Pardos *et al.*, 2016, and reporting *Antygomonas* cf. *paulae* and *Campyloderes* sp. from the region for the first time.

More recently, we started a large project in 2017 with the main aim of increasing the scattered, rather scarce knowledge of the kinorhynch species inhabiting the Caribbean Basin. In order to achieve it, several still unprocessed meiofaunal samples from the Smithsonian Institution of Washington (SIW) Invertebrate Zoology collection were studied. These samples were originally collected by Dr R. P. Higgins and his colleagues throughout many different Caribbean localities in the 60-90s. Such research gave rise to the publication of up to four articles dedicated to the kinorhynch fauna of the Caribbean, yielding the description of eight new species, namely *Cristaphyes cornifrons* Cepeda *et al.*, 2019, *C. retractilis* Cepeda *et al.*, 2019, *Dracoderes spyro* Cepeda *et al.*, 2019, *Echinoderes barbadensis* Cepeda *et al.*, 2019, *E. brevipes* Cepeda *et al.*, 2019, *E. parahorni* Cepeda *et al.*, 2019, *Fujuriphyes dalii* Cepeda *et al.*, 2019 and *Triodontoderes lagahoo* Cepeda *et al.*, 2019, as well as the first report of *Echinoderes astridae* Sørensen, 2014 (Cepeda *et al.* 2019a; 2019b; 2019c; 2019d). In parallel to this project, Sánchez & Martínez (2019) explored the kinorhynch fauna from a Caribbean anchialine cave in Mexico, which yielded the description on a new species, *Pycnophyes kukulkan* Sánchez & Martínez, 2019, and the report of an undescribed species of *Paracentrophyes* sp.

The present contribution represents the culmination of this series of articles that belong to the aforementioned project, acting as a summary that gives a general overview of the current knowledge on Caribbean Kinorhyncha and also expands the previously known fauna with the description of a new species of *Echinoderes* and several new

records. Moreover, a dichotomous key for identification to the species level is included in order to help future research on kinorhynch diversity at the Caribbean Basin.

2. MATERIAL AND METHODS

As previously introduced, kinorhynch specimens of the present study were obtained from several meiofaunal samples collected during the 60-90s by Dr R. P. Higgins and his colleagues at the Caribbean Basin. The Caribbean localities have been classified in four main regions: Greater Antilles, Lesser Antilles, Lucayas Archipelago and continental Caribbean. This division follows that of Spalding *et al.* (2007), which classifies the Great Caribbean in nine marine ecoregions, but with some modifications based on the samples' distribution (as only those from Venezuela yielded kinorhynchs, we grouped them as continental Caribbean). There were other continental Caribbean samples available at the SIW Invertebrate Collection from Mexico, Belize, Honduras and Panama, but the COVID-19 pandemic prevented us from their study. A detailed list of all the studied Caribbean samples through the whole project, included those treated in the previous works, may be found in Table 1.

Samplings were originally done by Dr R. P. Higgins with a meiobenthic dredge (Fleeger *et al.* 1988), and meiofaunal organisms were extracted from the sediment following the bubble and blot method (Higgins 1964; Sørensen & Pardos 2020). Meiofauna was fixed in 4% neutralized formalin and preserved in Carosafe®, remaining unsorted until the present study. Kinorhynch specimens were separated from the other meiofaunal organisms using an Irwin loop and washed with distillate water (to eliminate remnants of formalin and/or Carosafe®) for the present project. The specimens of the new species described in the present study were prepared for light microscopy (LM) through a graded series of glycerine and mounted on glass slides with Fluoromount G® sealed with Depex®. The mounted specimens were studied and photographed using an Olympus© BX51-P microscope with differential interference contrast (DIC) optics equipped with an Olympus© DP-70 camera. Line art illustrations and LM plate composition were done using Adobe® Photoshop and Illustrator CC-2014 software.

To evaluate the representativeness of the sampling effort and recorded kinorhynch inventory, sample-based rarefaction curves were constructed based on the observed richness (S) for each sampling site (we included both the Caribbean sites studied for the present project and those previously sampled by other authors), while the expected richness was calculated with non-parametric estimators Chao 2, Jackknife 1, Jackknife 2 and Bootstrap using the package 'vegan' (Oksanen *et al.* 2020) in R (R Core Team 2021).

3. RESULTS

3.1 Summary of collected species at the Caribbean Sea.

A total of 28 species belonging to 10 genera and five families were recorded along the Caribbean Sea from the studied samples (Table 1), as follows:

- Greater Antilles. 16 species belonging to five genera and three families.
    - Cuba: *Echinoderes astridae, E. imperforatus* and *E. wallaceae*.
    - Jamaica: *Cristaphyes* cf. *longicornis, Dracoderes spyro, Echinoderes astridae, E. horni, E. imperforatus, E. parahorni* and *E. sublicarum* Higgins, 1977.
    - La Española (Haiti and Dominican Republic): *Cristaphyes* cf. *longicornis, C. retractilis, Dracoderes spyro, Echinoderes astridae, E. brevipes, E. horni, E. imperforatus, E. parahorni, E. spinifurca, Fujuriphyes dalii* and *Pycnophyes* sp.
    - Puerto Rico: *Cristaphyes cornifrons, C. retractilis, Dracoderes spyro, Echinoderes astridae, E. horni, E. spinifurca* and *E. orestauri.*
- Lesser Antilles. Eight species belonging to five genera and three families.
    - Aruba (The Netherlands): *Echinoderes sublicarum* and *Echinoderes* sp. 1.
    - Barbados: *Echinoderes barbadensis*.
    - Bonaire (The Netherlands): *Echinoderes intermedius.*
    - Guadeloupe: *Echinoderes wallaceae.*
    - Tobago (Trinidad and Tobago): *Cristaphyes* sp., *Echinoderes intermedius, Higginsium* cf. *erismatum* and *Triodontoderes lagahoo.*

- Lucayas Archipelago, Berry Islands (Bahamas). A single species: *Echinoderes astridae.*
- Continental Caribbean. 13 species belonging to six genera and three families.
    - Colombia: no kinorhynchs were found in this area.
    - Venezuela: *Echinoderes augustae* Sørensen & Landers, 2014, *E. imperforatus, E. intermedius, E. parahorni, E. sublicarum, E. orestauri, E. wallaceae, Echinoderes* sp., *F. deirophorus, F. distentus, Higginsium* cf. *erismatum, Leiocanthus corrugatus, Semnoderes lusca* and *Setaphyes* sp.

Data are summarized in Table 1 for easier consultation. An overall, graphic overview of this kinorhynch diversity is represented in Figure 1. A map showing all the collecting areas and localities of the present project is shown in Figure 4, and a distribution map of the different species in Figure 5.

3.2 Taxonomic account of new species.

Class **Cyclorhagida** (Zelinka, 1896) Sørensen *et al.*, 2015

Family **Echinoderidae** Zelinka, 1894

Genus ***Echinoderes*** Claparède, 1863

***Echinoderes* sp. 1**

(Figs. 2-3 and Tables 3-4)

Material examined

Holotype, adult male, collected in June 25, 1977 off Renaissance Island, Oranjestad, Aruba (The Netherlands), Caribbean Sea: 12º 30’ N, 70º 01’ W, unknown depth and sediment; mounted in Fluoromount G®. Paratype, adult female without the anterior part of the body, same collecting data as holotype; mounted in Fluoromount G®.

Diagnosis

Echinoderes with spines in middorsal position on segments 4, 6 and 8, increasing in length posteriorly; and in lateroventral position on segments 6-9. Tubes in ventrolateral

position on segment 2, in lateroventral position on segment 5, in sublateral position on segment 8 and in laterodorsal position on segment 10. Tergal extensions relatively long, distally pointed, with a small cusp at their inner margin near the tip. No sexual dimorphic characters other than the usual for the genus: males with three pairs of penile spines on segment 11, females with paired lateral terminal accessory spines instead.

Description

See Table 3 for measurements and dimensions, and Table 4 for summary of spine, tube, nephridiopore, glandular cell outlet and sensory spot locations.

Head and neck. Head with retractable mouth cone and introvert. None of the examined specimens had the head available for analysis, hence no details on the morphology and arrangement of oral styles and scalids are provided.

Neck with sixteenth elongated (approximately three to four times longer than wide), trapezoidal placids, wider at base, with a distinct joint between the neck and the first trunk segment (Figs. 2A-B, 3B); midventral one widest (ca. 17-18 μm wide at base), remaining ones alternate between slightly wider and narrower (8-10 μm wide at base) (Figs. 2A-B, 3 B). Placids closely situated each other at base, distally separated by cuticular folds (Figs. 2A-B, 3 B). A ring of six short, hairy trichoscalids associated with the placids of the neck is present, attached to small, oval trichoscalid plates (Figs. 2A-B, 3 B).

Trunk. Body trunk composed of eleven segments (Figs. 2A-D, 3A). Segments 1-2 as closed cuticular rings, remaining ones with one tergal and two sternal cuticular plates (Figs. 2A-D, 3A-E). Sternal plates reach their maximum width at segment 6, progressively tapering towards the last trunk segments; sternal plates relatively narrow compared to the total trunk length (MSW-6:TL ratio = 21.7%) (Table 3), giving the species a slender appearance. Cuticular hairs acicular, very elongated, emerging from rounded to oval perforation sites. Cuticular hairs distributed in 8-9 (dorsal) and 6-8 (ventral) straight, transverse rows on segment 1; in 3-4 (both dorsal and ventral) straight, transverse rows on segment 2; in 6-8 (both dorsal and ventral) transverse rows from paradorsal to ventrolateral region on segments 3-10 becoming wavier at the ventrolateral position; segment 11 without hairs (Fig. 2A-D). Primary pectinate fringe straight,

conspicuously serrated, showing a free flap with alternating longer and shorter tips (Fig. 2A-B). Secondary pectinate fringe not detected.

Segment 1 without spines and tubes. Unpaired type 1 glandular cell outlet in middorsal position, and paired ones in sublateral position (Figs. 2A-B, 3B). Paired sensory spots in subdorsal and laterodorsal positions, located at the anterior half of the segment (Figs. 2A-B, 3G).

Segment 2 with tubes in ventrolateral position (Figs. 2A, 3B). Unpaired type 1 glandular cell outlet in middorsal position, and paired ones in lateroventral position (Fig. 2A-B). Paired sensory spots in laterodorsal, midlateral and ventromedial positions (Figs. 2A-B, 3B, G).

Segment 3 without spines and tubes. Unpaired type 1 glandular cell outlet in middorsal position, and paired ones in ventromedial position (Fig. 2A-B). Paired sensory spots in subdorsal, laterodorsal, sublateral and ventromedial positions (Fig. 2A-B).

Segment 4 with middorsal spine exceeding the total length of the following segment (Figs. 2B, 3D). Paired type 1 glandular cell outlets in paradorsal and ventromedial positions (Fig. 2A-B). Paired sensory spots in paradorsal, subdorsal, midlateral and ventromedial positions (Fig. A-B).

Segment 5 with tubes in lateroventral position (Figs. 2A, 3C). Unpaired type 1 glandular cell outlet in middorsal position, and paired ones in ventromedial position (Fig. 2A-B). Paired sensory spots in paradorsal, subdorsal, laterodorsal, sublateral and ventromedial positions (Figs. 2A-B, 3C-D).

Segment 6 with middorsal spine exceeding the total length of the following two segments, plus lateroventral spines (Figs. 2A-B, 3C-D). Paired type 1 glandular cell outlets in paradorsal and ventromedial positions (Fig. 2A-B). Paired sensory spots in paradorsal, subdorsal, laterodorsal and ventromedial positions (Figs. 2A-B, 3C-D).

Segment 7 with lateroventral spines (Figs. 2A, 3C). Unpaired type 1 glandular cell outlet in middorsal position, and paired ones in ventromedial position (Fig. 2A-B). Paired sensory spots in paradorsal, subdorsal, laterodorsal and ventromedial positions (Figs. 2A-B, 3C-D).

Segment 8 with middorsal spine almost reaching the end of segment 11, plus lateroventral spines and sublateral tubes, the bases of the latter located more posterior to the bases of the former (Figs. 2A-B, 3C-D). Paired type 1 glandular cell outlets in paradorsal and ventromedial positions (Fig. 2A-B). Paired sensory spots in paradorsal, subdorsal, laterodorsal and ventrolateral positions, the latter located near the lateroventral spines (Figs. 2A-B, 3C-D).

Segment 9 with lateroventral spines (Figs. 2A, 3C). Unpaired type 1 glandular cell outlet in middorsal position, and paired ones in ventromedial position (Fig. 2A-B). Paired sensory spots in paradorsal and ventrolateral positions, the latter located near the lateroventral spines (Figs. 2A-B, 3C-D). Nephridiopores as oval sieve plates in lateral accessory position (Figs. 2A, 3C).

Segment 10 with long laterodorsal tubes almost reaching the end of segment 11 tergal extensions (Figs. 2B, D, 3E-F). Two unpaired type 1 glandular cell outlets longitudinally arranged in middorsal position, and paired ones in ventromedial position (Fig. 2A-D). Paired sensory spots in paradorsal position (Figs. 2B, D, 3E).

Segment 11 with lateral terminal spines long and slender (LTS:TL ratio = 59.6%) (Table 3), distally pointed, showing a hollow, central cavity (Figs. 2A-B, 3A, C). Males with three pairs of penile spines arising laterally under the segment 10 primary pectinate fringe; dorsal and ventral pairs of penile spines (ps1 and ps3) longer and filiform, median pair (ps2) shorter and coarse (Figs. 2A-B, 3F). Females with paired lateral terminal accessory spines relatively short (LTAS:LTS ratio = 30.3%) (Table 3, Figs. 2C-D, 3E). Unpaired type 1glandular cell outlet in middorsal position (Fig. 2B, D). Tergal extensions relatively long, distally pointed, with a small cusp at their inner margin near the tip (Figs. 2B, D, 3F). Sternal extensions short, wide, distally rounded (Figs. 2A, C, 3G).

Associated kinorhynch fauna

Echinoderes sp. 1 was found together with *E. sublicarum* in the analysed samples.

3.3 Dichotomous key for the identification of Caribbean Kinorhyncha.

1. Overall body rectangular; trunk triangular in cross-section; neck with 6, 7 or 9 placids … **2** (Class Allomalorhagida**)**
- Overall body spindle-shaped; trunk circular or heart-shaped in cross-section; neck with 14 or 16 placids … **22** (Class Cyclorhagida**)**

2. Neck with 5 ventral placids; first trunk segment composed of a single, ring-like cuticular plate; acicular spines present in middorsal, paradorsal and lateral positions … Family Dracoderidae; Genus *Dracoderes*: ***Dracoderes spyro***
- Neck with 2 or 3 ventral placids; first trunk segment divided in cuticular plates; acicular spines absent in middorsal, paradorsal and lateral positions … 3

3. First trunk segment composed of one tergal and one sternal plate; midterminal spine present; two pairs of ventrolateral setae on segment 1 … Family Neocentrophyidae; Genus *Paracentrophyes:* ***Paracentrophyes praedictus***
- First trunk segment composed of one tergal, two episternal and one midsternal plates; midterminal spine absent; one pair of ventrolateral setae on segment 1 (if present) … 4 (Family Pycnophyidae)

4. Middorsal cuticular specializations (elevations and/or processes) on segments 7-10 absent; ventrolateral setae only on segments 1, 5 and/or 10 … 5 (Genus *Leiocanthus*)
- Middorsal cuticular specializations (elevations and/or processes) on segments 7-10 usually present; ventrolateral setae can be in other segments different from 1, 5 and 10 … 7

5. Setae on episternal plates of segment 1 (ventrolateral) absent; laterodorsal setae on segment 9 absent; lateral terminal spines short (LTS:TL ratio < 30%) … ***Leiocanthus emarginatus***
- Setae on episternal plates of segment 1 (ventrolateral); laterodorsal setae on segment 9; lateral terminal spines long (LTS:TL ratio > 30%) … 6

6. Anterior region of the tergal surface of segment 1 with conspicuous cuticular ornamentation as parallel semicircles; sternal plates of segments 8-10 with conspicuous vertical secondary pectinate fringes near the lateral margins; ventrolateral setae on segment 10 absent; males with sexually dimorphic tubes in ventromedial position on segment 2 … ***Leiocanthus corrugatus***
- Anterior region of the tergal surface of segment 1 without such cuticular ornamentation; sternal plates of segments 8-10 without such secondary pectinate fringes; ventrolateral setae on segment 10; males without sexually dirmophic tubes in ventromedial position on segment 2 … ***Leiocanthus ecphantor***

7. Middorsal processes at least on segments 2-9, often on segments 1 and 10 as well … 8 (Genus *Cristaphyes*)
- Middorsal processes absent, or only present on any posterior segment (6-10) … 12

8. Lateral terminal spines absent … 9
- Lateral terminal spines present … 11

9. Sternal plates of segments 3-4 and 6-9 with two pairs of setae (ventrolateral and/or ventromedial); segments 10-11 retractable into segment 9 … ***Cristaphyes retractilis***
- Sternal plates of segments 3-4 and 6-9 with one pair of setae (ventrolateral or ventromedial); segments 10-11 not retractable into segment 9 … 10

10. Paradorsal setae (paired or unpaired) throughout segments 1-10; sternal plates with sensory spots more lateral than setae… ***Cristaphyes panamensis***
- Paradorsal setae (paired or unpaired) only in some segments throughout the trunk; sternal plates with sensory spots more mesial than setae … ***Cristaphyes belizensis***

11. Episternal plates of segment 1 without setae; ventromedial setae of segment 8 longitudinally aligned with those of previous and posterior segments … ***Cristaphyes cornifrons***

- Episternal plates of segment 1 with setae (ventrolateral); ventromedial setae of segment 8 more lateral than those of previous and posterior segments (not longitudinally aligned) … ***Cristaphyes longicornis***

12. Both middorsal elevations and processes throughout the trunk … 13 (Genus *Higginsium*)
- Only middorsal elevations throughout the trunk (if middorsal cuticular specializations are present) … 14

13. Secondary pectinate fringes as three transverse, wavy rows not extending beyond the anterior half of sternal plates; sternal plates of most segments with three pairs of setae… ***Higginsium trisetosum***
- Secondary pectinate fringes as three transverse, wavy rows extending beyond the anterior half of sternal plates; sternal plates of most segments with two pairs of setae … ***Higginsium erismatum***

14. Ventrolateral setae on segment 5 absent … Genus *Setaphyes:* ***Setaphyes iniorhaptus***
- Ventrolateral setae on segment 5 … 15

15. Ventrolateral setae on segments 1, 5 and on additional segments from segment 3 to 9 … 16 (Genus *Fujuriphyes*)
- Ventrolateral setae only on segment 5, often on segments 1-2 as well … 18 (Genus *Pycnophyes*)

16. Lateral terminal spines absent; males with ventromedial tubes on segment 2 … 17
- Lateral terminal spines present; males without ventromedial tubes on segment 2 … ***Fujuriphyes dalii***

17. Ventromedial setae absent; anterodorsal margin of segment 1 with a row of punctate sculpturing followed by an undulating ridge of cuticle … ***Fujuriphyes deirophorus***
- Ventromedial setae on segments 6-8 (not longitudinally aligned); anterodorsal margin of segment 1 with slightly roughened sculpture followed by a series of five looped ridges on either side of midline … ***Fujuriphyes distentus***

18. Lateral terminal spines absent … 19
- Lateral terminal spines present … 21

19. Subdorsal setae on segment 1; segments 10-11 retractable into segment 9 … ***Pycnophyes alexandroi***
- Subdorsal setae on segment 1 absent; segments 10-11 not retractable into segment 9 … 20

20. Odd-numbered trunk segments without paradorsal setae; lateroventral setae on segments 7 and 9 absent… ***Pycnophyes stenopygus***
- Odd-numbered trunk segments with paradorsal setae; lateroventral setae on segments 7 and 9… ***Pycnophyes apotomus***

21. Anterior margin of tergal surface of segment 1 with a pool of depressed annuli bearing several pores as cuticular ornamentation; setae of segments 3-8 in ventrolateral position … ***Pycnophyes kukulkan***
- Anterior margin of tergal surface of segment 1 without such cuticular ornamentation; setae of segments 3-8 in ventromedial position … ***Pycnophyes beaufortensis***

22. Midterminal spine present; cuspidate spines present on some segments … 23
- Midterminal spine absent; cuspidate spines absent … 27 (Family Echinoderidae; Genus *Echinoderes*)

23. Neck with 14 inconspicuous, elongated, distally tripartite, soft placids of uniform size; placids fused with segment 1; first trunk segment composed of one tergal and one sternal plates … Family Zelinkaderidae; Genus *Triodontoderes*: ***Triodontoderes lagahoo.***
- Neck with 16 distinct, shortened, distally entire, sclerotized placids not uniform in size; conspicuous articulation between neck and first trunk segment; first trunk segment with a single, ring-like cuticular plate … 24

24. Ventrolateral acicular spines on segment 1, conspicuously long and flexible; posterior margin of first trunk segment extended midventrally, forming a spinous process … Family Centroderidae; Genus *Centroderes:* ***Centroderes barbanigra.***
- Ventrolateral acicular spines on segment 1 absent; posterior margin of first trunk segment straight midventrally … 25

25. First trunk segment with deep middorsal and midventral incisions, forming a clamshell-like closing apparatus; midventral placid rod-shaped … 26 (Family Semnoderidae; Genus *Semnoderes*)
- First trunk segment middorsal and midventrally concave, without the aforementioned incisions; midventral placid trapezoidal … Family Antygomonidae; Genus *Antygomonas:* ***Antygomonas paulae***.

26. Primary spinoscalids with eight distal, internal septa; tergal plates with minute, scale-like cuticular hairs arranged in conspicuous lines throughout the trunk; males with middorsal acicular spine on segment 10 … ***Semnoderes pacificus***
- Primary spinoscalids with a single distal, internal septum; tergal plates with minute, leaf-like cuticular hairs forming a homogeneous sculpture pattern; males with middorsal crenulated spine on segment 10 … ***Semnoderes lusca***

27. Middorsal spines absent … 28
- Middorsal spines present … 30

28. Lateroventral spines on segments 6 and 7; lateroventral tubes on segment 2; lateral accessory tubes on segment 8 … 29
- Lateroventral spines on segments 6 and 7 absent; lateroventral tubes on segment 2 absent; lateral accessory tubes absent … ***Echinoderes caribiensis***

29. Laterodorsal tubes on segment 10; subdorsal type 2 glandular cell outlets on segment 2 … ***Echinoderes parahorni***
- Laterodorsal tubes on segment 10 absent; subdorsal type 2 glandular cell outlets absent … ***Echinoderes horni***

30. Middorsal spines only on segments 4 and 6; subdorsal and lateroventral type 2 glandular cell outlets only on segment 2 … ***Echinoderes astridae***
- Middorsal spines on segments 4, 6 and more segments; type 2 glandular cell outlets, if present, with a different arrangement … 31

31. Middorsal spine on segment 8 … 32
- Middorsal spine absent on segment 8 … ***Echinoderes collinae***

32. Middorsal spines on segments 4, 6 and 8 … 33
- Middorsal spines on segments 4-8 … 38

33. Lateral terminal spines conspicuously short and robust (LTS/TL<20%) … 34
- Lateral terminal spines conspicuously long and slender (LTS/TL>20%) … 36

34. Lateral accessory tubes only on segment 8 … ***Echinoderes abbreviatus***
- Lateral accessory tubes on more than one segment … 35

35. Lateral accessory tubes on segments 7-8 … ***Echinoderes rociae***
- Lateral accessory tubes on segments 6-8 … ***Echinoderes brevipes***

36. Lateral accessory tubes on segments 6-8; triangular tergal extensions with conspicuous papillar tips, blade-like tergal extensions … ***Echinoderes intermedius***
- Lateral accessory or sublateral tubes only on segment 8; tergal extensions with other morphology … 37

37. Lateral accessory tubes on segment 8, with the bases near the lateroventral spines; laterodorsal and lateroventral type 2 glandular cell outlets on segment 2; blade-like tergal extensions … ***Echinoderes wallaceae***
- Sublateral tubes on segment 8, with the bases posterior to the lateroventral spines; type 2 glandular cell outlets absent; triangular tergal extensions with a small cusp at their inner margin near the tip … ***Echinoderes* sp. 1**

38. Lateral terminal spines conspicuously short and robust (LTS/TL<20%) … ***Echinoderes barbadensis***
- Lateral terminal spines conspicuously long and slender (LTS/TL>20%) … 39

39. Up to 30 pairs of short, fringed tubes distributed mainly on tergal plates … ***Echinoderes orestauri***
- Such tubes absent … 40

40. Tergal extensions forming very long, triangular, spinous projections; tubes of segment 5 in lateral accessory position; tubes of segment 10 in sublateral position … ***Echinoderes spinifurca***
- Tergal extensions not forming such projections; tubes of segment 5 in lateroventral position; tubes of segment 10, if present, in laterodorsal or lateroventral positions … 41

41. Tergal extensions truncate; tubes on segment 2 absent; tubes of segment 10 in lateroventral position … ***Echinoderes truncatus***

- Tergal extensions triangular, distally pointed; tubes in lateroventral or ventrolateral position on segment 2; tubes of segment 10, if present, in laterodorsal position … 42

42. Tubes on segment 4 in midlateral position; tubes on segment 8 in sublateral position; subdorsal type 2 glandular cell outlets on segment 2 … ***Echinoderes augustae***
- Tubes on segments 4 and 8 absent … 43

43. Minute laterodorsal type 2 glandular cell outlets on segments 8-9; middorsal spines conspicuously short (longest middorsal spine<20 μm), not surpassing the posterior margin of their segments; females with ventromedial papillae on segments 6-8 … ***Echinoderes imperforatus***
- Minute laterodorsal type 2 glandular cell outlets on segment 8; middorsal spines conspicuously long (longest middorsal spine>20 μm), surpassing the posterior margin of their segments; females with ventromedial papillae on segment 8 … ***Echinoderes sublicarum***

3.4 Sample-based rarefaction curves.

The sample-based rarefaction curves showed that the observed S (27 species in our samples, 52 species in the total samples) did not tend to reach an asymptote, with a representativeness of ca. 74% (for the samples of the present project) and 63% (for the total number of Caribbean samples) with respect to the average value of the non-parametric estimators (Fig. 6A-B).

For the Caribbean samples studied in the present project, the highest estimates of expected S were obtained by Jackknife 1 (37 species) and Jackknife 2 (41 species), whilst the lowest were obtained by Chao 2 (36 species) and Bootstrap (32 species). For the total Caribbean samples, the highest estimates of expected S were yielded by Jackknife 2 (93 species) and Chao 2 (92 species), whereas the lowest were yielded by Jackknife 1 (76 species) and Bootstrap (62 species).

4. DISCUSSION

4.1 Remarks on diagnostic and taxonomic features of *Echinoderes* sp. 1

Within the family Echinoderidae, the presence of segments 1-2 consisting of a single closed, ring-like cuticular plate, and remaining body segments consisting of one tergal plus two sternal cuticular plates unequivocally allocates the new species into the genus *Echinoderes* (Claparède 1863; Sørensen *et al.* 2015; Sørensen & Pardos 2020; Yamasaki *et al.* 2020).

Echinoderes sp. 1 shows a relatively common spine and tube pattern, consisting of middorsal spines on segments 4, 6 and 8, lateroventral or ventrolateral tubes on segments 2 and 5, lateroventral spines on segments 6-9, lateral accessory or sublateral tubes on segment 8, and laterodorsal tubes on segment 10 in both sexes. Several species of the genus with a similar pattern, differing only in the lack of laterodorsal tubes on segment 10, were described with males possessing a small, seta-like cuticular appendage in laterodorsal position on segment 10 (Higgins 1966a; 1966b; 1983; 1985; Huys & Coomans 1989); at least for one of this species, *E. wallaceae* Higgins, 1983, we can confirm that this seta-like appendage is a small-sized tube based on the examination of several Caribbean specimens. Because of that, we will consider those species as also having laterodorsal tubes on segment 10 for this comparison.

Thus, *Echinoderes* sp. 1 shares a similar spine and tube arrangement with the following congeners: *E. abbreviatus* Higgins, 1983 from Belize (Caribbean Sea), *E. arlis* Higgins, 1966 from the Chukchi Sea (Arctic Ocean), *E. higginsi* Huys & Coomans, 1989 from the North Sea (eastern Atlantic Ocean), *E. kristenseni* Higgins, 1985 from France (eastern Atlantic Ocean), *E. riedli* Higgins, 1966 from Egypt (Red Sea), and *E. wallaceae* from Belize (Caribbean Sea). Of these, only *E. arlis* possesses laterodorsal tubes on segment 10 in both males and females as *Echinoderes* sp. 1 (Higgins 1966; Grzelak & Sørensen 2019) whilst the remaining ones only have males with this structure (Higgins 1966b; 1983; 1985; Huys & Coomans 1989). However, *E. arlis* is easily distinguishable in the intraspecific variation of the segment 8 sublateral tubes, that may or not be present (always present in *Echinoderes* sp. 1), and the presence of subdorsal and sublateral type 2 glandular cell outlets on segment 2, which are absent in *Echinoderes* sp. 1.

In addition to only males possessing laterodorsal tubes on segment 10, other morphological differences of the aforementioned congeners can be remarked. *Echinoderes abbreviatus* also differs in the presence of conspicuously shorter lateral terminal spines (LTS:TL ratio = 17.2% in *E. abbreviatus* vs. 59.6 % in *Echinoderes* sp. 1) (Higgins 1983). *Echinoderes kristenseni* and *E. wallaceae* possess two pairs of type 2 glandular cell outlets on segment 2 (Higgins 1983; 1985; illustrated but described as muscular scars, confirmed by the present authors in the latter species based on several Caribbean specimens) which are absent in *Echinoderes* sp. 1. *Echinoderes riedli* has conspicuously shorter middorsal spines (mean of 15, 16 and 18 μm in *E. riedli* vs. mean of 30.5, 41.7 and 51.1 μm in *Echinoderes* sp. 1) (Higgins 1983; 1985). *Echinoderes higginsi* possesses similar tergal extensions to those of *Echinoderes* sp. 1 (remarkably long and pointed, with a small cusp at the inner margin) (Huys & Coomans 1989), but the small cusp of the inner margin is situated close to the base of the tergal extension in *E. higginsi* (Huys & Coomans 1989), whereas in *Echinoderes* sp. 1 is located nearer the tip.

4.2 Status of the knowledge on the kinorhynch Caribbean diversity.

Before the beginning of the present project, the Caribbean Sea hosted 32 species of Kinorhyncha belonging to 12 genera and seven families (Kirsteuer 1964; Higgins 1983; Sørensen 2006; Pardos *et al.* 2016b; Cepeda *et al.* 2019c; Sánchez & Martínez 2019). The papers published to date related to the project, including the present one, increased this number to 52 species belonging to 15 genera and nine families (Cepeda *et al.* 2019a; 2019b; 2019c; 2019d; this paper), which represents an increase of ca. 37% of the total Caribbean Kinorhyncha diversity.

A total of nine species have been described as new to science in the area during the last five years, namely *Cristaphyes cornifrons, C. retractilis, Dracoderes spyro, Echinoderes barbadensis, E. brevipes, Echinoderes* sp. 1, *E. parahorni, Fujuriphyes dalii* and *Triodontoderes lagahoo* (Cepeda *et al.* 2019a; 2019b; 2019c; 2019d; this manuscript). This high number of new species had not been repeated for the Caribbean since the exhaustive sampling of the coral reef habitat of Carrie Bow Cay and Twin Cays (Belize) by Higgins (1983), who described 18 new species. Furthermore, several kinorhynch species previously known from other geographic areas were newly reported

for the Caribbean Sea, including *E. astridae* (originally described from Araçá Bay, São Sebastião, Brazil), *E. augustae* and *Semnoderes lusca* (originally described from the nearby Gulf of Mexico), and *E. sublicarum* (originally described from South Carolina) (Higgins 1977; Sørensen 2014; Sørensen & Landers 2014; Cepeda *et al.* 2019c; this manuscript) (Fig. 5). Finally, the distribution range of several Caribbean species have been expanded, as they were found in new Caribbean locations. This is the case of *C. longicornis*, *E. horni*, *E. imperforatus*, *E. wallaceae*, *F. deirophorus*, *F. distentus*, *Higginsium erismatum* and *Leiocanthus corrugatus* (previously known only from Carrie Bow Cay, Belize), and *E. intermedius* and *E. orestauri* (previously known only from Bocas del Toro, Panama) (Higgins 1983; Sørensen 2006; Pardos *et al.* 2016b; Cepeda *et al.* 2019a; 2019b; 2019c; this manuscript).

In summary, the Caribbean Sea seems to host a rich fauna of Kinorhyncha, as ca. 16% of the worldwide species are present in this area (and ca. 48% of the worldwide genera). This project has greatly helped to know the true hidden diversity of Kinorhyncha at the Caribbean Sea, making this area one of the best known nowadays for the phylum, together with the North Sea, the Mediterranean Sea, the north-western Atlantic American shoreline (including the Gulf of Mexico) and the Sea of Japan and adjacent waters (Neuhaus 2013; Cepeda *et al.* 2019c).

Despite the above mentioned, the results of the sample-based rarefaction curves reinforce the idea that further sampling efforts are needed in order to reach the real Caribbean kinorhynch richness. The sampling effort seems not to be completely exhaustive as indicated by the non-parametric estimators and the lack of an asymptote in the corresponding curves (Fig. 6A-B). Regarding the studied samples for the present project, La Española, Venezuela and all the Lesser Antilles (taken as a group) seem to be better sampled than the remaining Greater Antilles (Fig. 6A). When considering the Caribbean ecoregions and the total number of Caribbean samples, the continental Caribbean, which includes the ecoregions defined as western, south-western and south Caribbean by Spalding *et al.* (2007), is the best sampled area (Fig. 6B). This makes sense considering that the greatest sampling effort has been done in this area, especially by previous studies (Kirsteuer 1964; Higgins 1983; Sørensen 2006; Pardos *et al.* 2016). However, both the Greater and the Lesser Antilles suffer more from a lack of sampling effort to reflect the true Kinorhyncha diversity of their waters (Fig. 6B).

4.3 Geographic distribution of Caribbean kinorhynchs.

Most of Caribbean Kinorhyncha (24 out of 52 species, ca. 46%) are restricted to a single, specific locality or a few nearby points belonging to the same geographic zone. Thus, *Campyloderes* sp., *Cephalorhyncha* sp., *Cristaphyes panamensis*, *Echinoderes collinae*, *E. rociae* and *Echinoderes* sp.2 are only known from the continental Caribbean, specifically from Bocas del Toro, Panama (Sørensen 2006; Pardos *et al.* 2016b) (Fig. 5). On the other hand, *Cristaphyes belizensis, E. abbreviatus, Higginsium trisetosum, Leiocanthus ecphantor, Pycnophyes apotomus, P. stenopygus* and *Setaphyes iniorhaptus* have been solely recorded in Carrie Bow Cay and Twin Cays, Belize (Higgins 1983). Other Caribbean species only recorded in a single locality includes *Echinoderes* sp. 1 from Aruba, *E. barbadensis* from Barbados, *E. brevipes*, *Fujuriphyes dalii* and *Pycnophyes* sp. from La Española, *P. kukulkan* and *Paracentrophyes* sp. from Mexico, *C. cornifrons* from Puerto Rico, *Triodontoderes lagahoo* from Tobago and *E. caribiensis, Echinoderes* sp.3 and *Setaphyes* sp. from Venezuela (Kirsteuer 1964; Cepeda *et al.* 2019a; 2019b; 2019c; Sánchez & Martínez 2019; this manuscript). This pattern of distribution is commonly found within the phylum Kinorhyncha, especially in shallow water species that seem to possess rather restricted distribution ranges, which correlates with their lifecycle (without pelagic larva) and a somewhat limited dispersal ability (Neuhaus 2013; Sørensen & Pardos 2020; Cepeda *et al.* 2021). This statement has some exceptions (*e.g.* some *Echinoderes* species widely distributed through the Arctic Ocean, or the species *Campyloderes vanhoeffeni* Zelinka, 1913 which shows a cosmopolitan distribution) (Neuhaus & Sørensen 2013; Grzelak & Sørensen 2019), but seems to apply for the majority of the Caribbean Kinorhyncha. It is noteworthy to highlight that the presence on a species in a single point is the result of a sampling effort bias mixed with the patchy distribution of kinorhynch populations at local level.

Among the species that have been recorded in several localities throughout the Caribbean Sea (12 out of 52 species, ca. 23%), *Cristaphyes retractilis*, *Cristaphyes* sp. and *Dracoderes spyro* are only found off the Antilles, in La Española and Puerto Rico, Puerto Rico and Tobago, and La Española, Jamaica and Puerto Rico, respectively. Others are distributed in several localities of the continental Caribbean, including *Echinoderes orestauri* (Panama and Venezuela), *Fujuriphyes deirophorus* (Belize and Venezuela), *F. distentus* (Belize, Panama and Venezuela) and *Leiocanthus emarginatus* and

Paracentrophyes praedictus (Belize and Panama). On the other hand, several species have been reported in both the Antilles and the continental Caribbean: *C. longicornis* (Belize, La Española and Jamaica), *Echinoderes imperforatus* (Belize, Cuba, La Española, Jamaica, Puerto Rico and Venezuela), *E. wallaceae* (Belize, Cuba, Guadeloupe and Venezuela) and *Higginsium erismatum* (Belize, Tobago and Venezuela) (Higgins 1983; Sørensen 2006; Pardos *et al.* 2016b; Cepeda *et al.* 2019a; 2019b; 2019c; 2019d; this manuscript).

Moreover, 15 species (ca. 29%) are known from locations both inside and outside the Caribbean Sea. Most of these species are present, apart from the Caribbean, in the Gulf of Mexico and adjacent waters (Atlantic coast of Florida and/or Bermuda, North and South Carolina): *Antygomonas paulae* Sørensen, 2007, *Centroderes barbanigra*, *Echinoderes augustae, E. parahorni, E. spinifurca, E. sublicarum, E. truncatus, Leiocanthus corrugatus, Pycnophyes beaufortensis, P. alexandroi* and *Semnoderes pacificus* Higgins, 1967 (Higgins 1967; Sørensen *et al.* 2005; 2016; Sørensen 2007; Neuhaus *et al.* 2014; Sørensen & Landers 2014; 2018; Landers & Sørensen 2016; Pardos *et al.* 2016a; Landers *et al.* 2018; 2020; Cepeda *et al.* 2019c; Landers & Ingels 2019; Sánchez *et al.* 2019). This is not striking taking into account that the Caribbean Basin and the Gulf of Mexico are connected through the Yucatan Canal and are dynamically interdependent (Oey *et al.* 2005; Escobar-Briones 2008). Indeed, several benthic and planktonic species are shared between the two water entities (Miloslavich *et al.* 2010). Another two water entities, the Caribbean and the Pacific coasts of Panama, harbour two species in common, namely *Echinoderes intermedius and Pycnophyes alexandroi* (Pardos *et al.* 2016a; 2016b) (besides, *P. alexandroi* is also present in the Gulf of Mexico, see Sánchez *et al.*, 2019). If the Panama Canal has favoured the dispersal of these species, or whether they were present at both sides of Panama before the rising of the Panama Isthmus remains unclear, as well as the idea whether these two species are truly present at both Panamanian coasts or they are actually part of cryptic species complexes (Pardos *et al.* 2016a). Finally, three species seem to possess wider geographic distributions: *Echinoderes astridae,* present throughout the Atlantic coast of Brazil (Sørensen 2014), *E. horni* present in Florida and Hawaii (Sørensen *et al.* 2005; Dunn *et al.* 2008), and *Semnoderes pacificus* distributed through New Caledonia and California (Higgins 1967; 2007). However, with the rather limited knowledge about biogeography and dispersal

mechanisms of the phylum Kinorhyncha, we can only hypothesize about the degree of connectivity of these areas in terms of meiofaunal species.

Of all the Caribbean Kinorhyncha, four species highlight in terms of wider patterns of distribution through the Caribbean Basin: *Echinoderes astridae* (collected at Bahamas, Cuba, Jamaica, La Española and Puerto Rico; also known outside the Caribbean), *E. imperforatus* (collected at Belize, Cuba, Jamaica, La Española, Puerto Rico and Venezuela), *E. intermedius* (collected at Bonaire, Panama, Puerto Rico and Venezuela; also known outside the Caribbean) and *E. wallaceae* (collected at Belize, Cuba, Guadeloupe and Venezuela) (Table 1, Fig. 5). However, in terms of abundance, the species that we must mention are *Dracoderes spyro, E. intermedius* and *E. parahorni*, as more than 100 specimens were found throughout the Caribbean Basin (personal observation). We do not provide data on abundances in the present study since all the samples were taken by qualitative samplings, making their comparison inaccurate.

4.4 Habitat variability of Caribbean kinorhynchs.

The Caribbean Basin has an average depth of 2200 m, and its deepest point, the Cayman Trench, reaches up to 7686 m (Lemenkova 2020). Despite this, all the samples of the present project were collected in shallow coastal waters less than 100 m depth, and usually within the first 20 m (Tables 1 and 2). In fact, only the sample from Klein Bonaire, which yielded several specimens of *Echinoderes intermedius*, was taken at 100 m depth (Tables 1 and 2). Similarly, the previous records of Caribbean kinorhynchs are also from less than 20 m (Kirsteuer 1964; Higgins 1983; Sørensen 2006; Neuhaus *et al.* 2014; Pardos *et al.* 2016b; Sánchez & Martínez 2019) (Table 2). Thus, the current knowledge we have about the bathymetric distribution of Caribbean Kinorhyncha is very scarce, since it is almost exclusively limited to the first 20 m depth; it remains to study the kinorhynch Caribbean fauna from deeper waters. This fact does not take us by surprise either, since the challenges associated with sampling at greater depths makes to obtain samples from the deep sea unmanageable in many cases (Llodra & Billett 2006; Brandt *et al.* 2014). In the specific field of Kinorhyncha, again most of existing records of species are from shallow, coastal waters up to 200 m depth (Cepeda *et al.* 2021). Thus, a greater attempt should be

made to increase sampling in the deep sea in order to better understand the bathymetric distribution patterns of kinorhynchs.

The Caribbean Sea hosts a complex mosaic of marine and coastal habitats, including coral reefs, seagrass beds, mangrove forests, coastal lagoons, marine caves, high-energy sandy beaches and different kinds of soft sediment seafloors (Whalley 2011; Cortés 2016). The analysed Caribbean samples were taken from a wide variety of marine habitats (Table 2). Sediments of mangrove areas were collected at Kingston Harbour (Jamaica, consisted of sandy mud and sandy, shelly mud), Puerto Príncipe (La Española, unknown kind of sediment), Puerto Blanco (La Española, consisted of silty mud), Bahía de Icaquitos (La Española, consisted of muddy sand in *Thalassia testudinum* K.D. Koenig, 1805), Bahía de Guantánamo (Cuba, consisted of mud and sandy mud) and Isla Margarita (Venezuela, unknown kind of sediment) (Tables 1 and 2). Mangroves show specific marine conditions that usually increase the meiofauna abundance and diversity (Netto & Gallucci 2003; Pinto *et al.* 2013; Zeppilli *et al.* 2018). However, kinorhynchs are not particularly abundant in mangrove areas, and normally represent less than 1% of the total meiofaunal abundance (Hodda & Nicholas 1986; Schrijvers *et al.* 1997; Della Patrona *et al.* 2016; Zeppilli *et al.* 2018); there are some exceptions, as certain kinorhynch species have been found as the second or third most abundant taxa in mangrove samples (Ostmann *et al.* 2012; Zeppilli *et al.* 2018). The kinorhynch abundances of the Caribbean mangrove samples were quite low, with no more than 20 specimens; again, this abundance data must be taken with caution since the Caribbean samplings were mainly qualitative. Most of the kinorhynchs that have been collected in mangrove areas belong to the so-called *Echinoderes coulli* group, which is thought to be adapted to the fluctuating salinity of mangroves by possessing an enlarged nephridiopore (Ostmann *et al.* 2012; Zeppilli *et al.* 2018; Randsø *et al.* 2019). Only *E. orestauri*, that belongs to the *E. coulli* group, was found in these mangrove areas (Table 2), but either none of the remaining found species were characterized by having remarkably enlarged nephridiopores (Cepeda *et al.* 2019a; 2019b; 2019c; 2019d; this manuscript).

Samples taken near coral reefs included those of La Parguera (Puerto Rico, consisted of coral mud), Guadeloupe (consisted of coral sand), Los Roques (Venezuela, consisted of coarse coral sand and sandy coral mud) and Morrocoy (Venezuela, consisted of coral sand, silty coral sand and coral mud) (Tables 1 and 2). Coral reef sediments host

a rich community of both macro and meiobenthos (Ruiz-Abierno & Armenteros 2016), and many kinorhynch species have been found living in these habitats (*e.g.* Higgins 1966a; 1969; 1983; Coull 1970; Sørensen & Thormar 2010). Our results support this statement, as the samples consisting of coral sediment were between those with the highest diversity, special mention to La Parguera, Puerto Rico (9 species) and Los Roques and Morrocoy, Venezuela (6 species) (Table 1, Fig. 5). Indeed, the Caribbean site with the highest number of kinorhynch species is Belize (18 species), whose samples studied by Higgins (1983) were taken throughout the coral reef ecosystem at Carrie Bow Cay and Twin Cays.

Seagrass beds and their associated sediment were collected at La Parguera (Puerto Rico, consisted of *Enteromorpha* sp.), Bahía de Monte Cristi (La Española, consisted of muddy sand with *Thalassia testudinum*) and Morrocoy (Venezuela, consisted of sand with *Halimeda* sp.) (Tables 1 and 2). It is not very usual to find kinorhynchs directly on algae or seagrass, still some taxa are present in this kind of environment (Dujardin 1851; Moore 1973; Higgins 1977; Neuhaus 2013). The only sample that exclusively consisted of algae was that of La Parguera, and yielded several specimens of *Echinoderes sublicarum* (Tables 1 and 2), which was originally described in South Carolina from colonies of the hydroid *Eudendrium* sp. (Higgins 1977). Higgins (1977) hypothesized that the long spines of *E. sublicarum* could serve to retain the animal in the hydroid colony under strong current conditions, which also could apply to the *Enteromorpha* sp. assemblages. It is not striking to find *E. sublicarum* in such a peculiar habitat, taking into account that this species seems to be epibiont of other organisms (Higgins 1977). Nevertheless, the species was also found in soft sediments (Tables 1 and 2).

Marine caves were not explored in the present project, but Sánchez & Martínez (2019) reported *Pycnophyes kukulkan* from the anchialine cave Casa Cenote (Mexico), together with *Centroderes barbanigra* and *Paracentrophyes* sp. (Table 2). It was hypothesized that the annuli ornamentation of the first trunk segment of *P. kukulkan* could play a sensorial function (Sánchez & Martínez 2019), and the development of non-photoreceptor sensorial organs is considered as an adaptation of fauna to cave life (Culver & Pipan 2009; Romero 2009).

The remaining samples consisted of different kinds of soft sediments, from coarse sand with gravel to silty mud (Tables 1 and 2). Physicochemical data for sediment are not homogeneous and sometimes unavailable because samples were taken over a long time period under different circumstances and by several different collectors; the only samples that have been quantitatively studied in terms of sediment were those from Kingston Harbour (Jamaica) by Cepeda *et al.* (2020b); the variety of these sediments was considerable, from gravelly and shelly sand to gravelly mud (Cepeda *et al.* 2020b) (Table 1). The most common soft sediment for kinorhynchs is mud (Neuhaus 2013), which coincides with most of the analysed Caribbean samples, although they may be also present in sandy sediment (Tables 1 and 2).

4.5 Final perspective.

The Caribbean Sea seems to host a rich fauna of kinorhynch species, and the present study, together with the others that are part of the same project, have relevantly increased the known diversity of the phylum in the area. In this point, it is necessary to highlight the commendable scientific labour of Dr R. P. Higgins, thanks to whom we can have, nowadays, a picture of the Caribbean Kinorhyncha diversity.

However, it is necessary to emphasize the need to promote new studies of this nature to continue unravelling the hidden Kinorhyncha diversity in still uncharted regions, including Cuba and the Lesser Antilles (in the former, only a single sample from Bahía de Guantánamo was taken due to political issues), the continental Caribbean (it must be highlighted the availability of unsorted meiofaunal samples from Mexico, Honduras, Belize and Panama still stored at the SIW Invertebrate Collection), and the deeper waters of the Caribbean Basin. Revisiting the same points (or as close as possible) in the future that Dr R. P. Higgins once sampled would also be interesting, to determine if the Caribbean Kinorhyncha community has change during the last decades. Something similar was done by Pardos *et al.* (2016) that revisited some Panamanian points originally studied by Sørensen (2006), and finding only two species in common with the passage of a decade.

Taxonomic works are still needed nowadays to generate basic knowledge that can potentially contribute to develop new studies on other topics, to protect the marine diversity and earn relevant scientific information.

Acknowledgements

The authors of the present paper would like to thank and greatly emphasize the effort of the curators of the Smithsonian Institution of Washington Invertebrate Zoology collection: Jon Norenburg, Anna J. Phillips, William Moser, and specially Katie Ahlfeld. Undoubtedly, this project could not have been possible without their labour. In addition, we would like to highlight the colossal research work that Dr Robert P. Higgins did during his active working life, allowing us to use the multiple samples that he once collected to continue understanding the incredible world of the mud dragons. The present paper has been partially funded by the project "Fauna Ibérica XII: Escalidóforos de la península Ibérica y Baleares (PGC2018-095851-B-C62) of the Ministerio de Ciencia, Innovación y Universidades (MICINN) of Spain. Cepeda was supported by a predoctoral fellowship of the Universidad Complutense de Madrid (UCM, code: CT27/16-CT28/16), and Sánchez by the Research Talent Attraction Programme for incorporation into research groups of the Universidad Complutense de Madrid (UCM) and the Comunidad de Madrid (code: 2019-T2/AMB-13328).

5. References

Brandt A., Griffiths H.J., Gutt J., Linse K., Schiaparelli S., Ballerini T., Danis B. & Pfannucke O. 2014. Challenges of deep-sea biodiversity assessments in the Southern Ocean. *Advances in Polar Science* 25(3): 204-212. https://doi.org/10.13679/j.advps.2014.3.00204.

Cepeda D., Pardos F. & Sánchez N. 2019a. Kinorhyncha from the Caribbean, with the description of two new species from Puerto Rico and Barbados. *Zoologischer Anzeiger* 282: 127-139. https://doi.org/10.1016/j.jcz.2019.05.014.

Cepeda D., Pardos F. & Sánchez N. 2019b. A new species and first record of *Dracoderes* (Kinorhyncha: Allomalorhagida: Dracoderidae) from American waters, with an identification key of the genus. *Zoologischer Anzeiger* 282: 106-115. https://doi.org/10.1016/j.jcz.2019.05.019.

Cepeda D., Pardos F. & Sánchez N. 2021. From biggest to smallest mud dragons: size-latitude trends in a group of meiobenthic animals worldwide. *Organisms Diversity & Evolution* 2021. https://doi.org/10.1007/s13127-020-00471-y.

Cepeda D., Pardos F., Zeppilli D. & Sánchez N. 2020a. Dragons of the deep sea: Kinorhyncha communities in a pockmark field at Mozambique Channel, with the description of three new species. *Frontiers in Marine Science* 7: e665. https://doi.org/10.3389/fmars.2020.00665.

Cepeda D., Sánchez N. & Pardos F. 2019c. First extensive account of the phylum Kinorhyncha from Haiti and the Dominican Republic (Caribbean Sea), with the description of four new species. *Marine Biodiversity* 49: 2281-2309. https://doi.org/10.1007/s12526-019-00963-x.

Cepeda D., Sánchez N. & Pardos F. 2019d. First report of the family Zelinkaderidae (Kinorhyncha: Cyclorhagida) for the Caribbean Sea, with the description of a new species of *Triodontoderes* Sørensen & Rho, 2009 and an identification key for the family. *Zoologischer Anzeiger* 282: 116-126. https://doi.org/10.1016/j.jcz.2019.05.017.

Claparède A.R.E. 1863. Beobachtungen über Anatomie und Entwicklungsgeschichte wirbelloser Thiere an der Küste von Normandie angestellt. Verlag von Wilhelm Engelmann, Leipzig.

Cortés J. 2016. Chapter 17. The Caribbean coastal and marine ecosystems. *In*: Kappelle M. (ed.) *Costa Rican Ecosystems*: 591-617. University of Chicago Press, Chicago and London.

Coull B.C. 1970. Shallow water meiobenthos of the Bermuda Platform. *Oecologia* 4: 325-357.

Culver D.C. & Pipan T. 2009. The biology of caves and other subterranean hábitats. Oxford University Press, Oxford.

Della Patrona L., Marchand C., Hubas C., Molnar N., Deborde J. & Mezianc T. 2016. Meiofauna distribution in a mangrove forest exposed to shrimp farm effluents (New Caledonia). *Marine Environmental Research* 119: 100-113. https://doi.org/10.1016/j.marenvres.2016.05.028.

Dujardin F. 1851. Sur un petit animal marin, l'echinodère, formant un type intermédiaire entres les crustacés et les vers. *Annales des Sciences Naturelles (Série 3)* 15: 158-160.

Dunn C.W., Hejnol A., Matus D.Q., Pang K., Browne W.E., Smith S.A., Seaver E., Rouse G.W., Obst M., Edgecombe G.D., Sørensen M.V., Haddock S.H.D., Schmidt-Rhaesa A., Okuso A., Kristensen R.M., Wheeler W.C., Martindale M.Q. & Giribet G. 2008. Broad phylogenomic sampling improves resolution of the animal tree of life. *Nature* 452: 745–749. https://doi.org/10.1038/nature06614.

Escobar-Briones E. 2008. Current knowledge on benthic communities in the Gulf of Mexico. *In:* Withers K. & Nippers M. (eds.) *Environmental Analysis of the Gulf of Mexico*: 108-136. Texas A&M University Press, Corpus Christi.

Fleeger J.W., Thistle D. & Thiel H. 1988. Sampling Equipment. *In*: Higgins R.P. & Thiel H. (eds.) *Introduction to the Study of Meiofauna*: 115-133. Smithsonian Institution Press, Washington D.C.

Fontaneto D., Barbosa A.M., Segers H. & Pautasso M. 2012. The "rotiferologist" effect and other global correlates of species richness in monogonont rotifers. *Ecography* 35(2): 174-182. https://doi.org/10.1111/j.1600-0587.2011.06850.x.

Grzelak K. & Sørensen M.V. 2019. Diversity and distribution of Arctic *Echinoderes* species (Kinorhyncha: Cyclorhagida), with the description of one new species and a redescription of *E. arlis* Higgins, 1966. *Marine Biodiversity* 49: 1131-1150. https://doi.org/10.1007/s12526-018-0889-2.

Higgins R.P. 1964. Three new kinorhynchs from the North Carolina coast. *Bulletin of Marine Sciene of the Gulf and Caribbean* 14(3): 479-493.

Higgins R.P. 1966a. Faunistic studies in the Red Sea (in winter, 1961-1962), Part II: Kinorhynchs from the area of Al-Ghardaqa. *Zoologische Jahrbücher Abteilung für Systematik, Ökologie und Geographie der Tiere* 93: 118-126.

Higgins R.P. 1966b. *Echinoderes arlis*, a new kinorhynch from the Arctic Ocean. *Pacific Science* 20(4): 518-520.

Higgins R.P. 1967. The Kinorhyncha of New-Caledonia. *Expédition Française sur les Recifs coralliens de la Nouvelle-Calédonie 2. Éditions de la Fondation Singer-Polignac, Paris* 1: 75-90.

Higgins R.P. 1969. Indian Ocean Kinorhyncha, 2: Neocentrophyidae, a new homalorhagid family. *Proceedings of the Biological Society of Washington* 82(7): 113-128.

Higgins R.P. 1977. Two new species of *Echinoderes* (Kinorhyncha) from South Carolina. *Transactions of the American Microscopical Society* 96(3): 340-354.

Higgins R.P. 1983. The Atlantic barrier reef ecosystem at Carrie Bow Cay, Belize, II. Kinorhyncha. *Smithsonian Contributions to the Marine Sciences* 18: 1-131. https://doi.org/10.5479/si.01960768.18.1.

Higgins R.P. 1985. The genus *Echinoderes* (Kinorhyncha: Cyclorhagida) from the English Channel. *Journal of the Marine Biological Association of the United Kingdom* 65(3): 785-800. https://doi.org/10.1017/s0025315400052590.

Higgins R.P. 1988. Kinorhyncha. *In:* Higgins R.P. & Thiel H. (eds.) *Introduction to the Study of Meiofauna*: 328-331. Smithsonian Institution Press, Washington D.C.

Higgins R.P. 2007. Kinorhyncha, Loricifera, and Priapulida. *In:* Carlton J.T. (ed.) *The Light and Smith Manual: Intertidal Invertebrates from Central California to Oregon:* 269-273. University of California Press, Berkeley, L.A. & London.

Hodda M. & Nicholas W.L. 1986. Temporal changes in littoral meiofauna from the Hunter River estuary. *Australian Journal of Marine and Freshwater Research* 37(6): 729-741. https://doi.org/10.1071/MF9860729.

Huys R. & Coomans A. 1989. *Echinoderes higginsi* sp.n. (Kinorhyncha, Cyclorhagida) from the southern North Sea with a key to the genus *Echinoderes* Claparède. *Zoologica Scripta* 18(2): 211-221.

Kirsteuer E. 1964. Zur Kenntnis der Kinorhynchen Venezuelas. *Zoologischer Anzeiger* 173: 388-393.

Landers S.C. & Ingels J. 2019. Kinorhynch communities on the Louisiana continental shelf. *Proceedings of the Biological Society of Washington* 132(1): 1-14. https://doi.org/10.2988/18-00008.

Landers S.C. & Sørensen M.V. 2016. Two new species of *Echinoderes* (Kinorhyncha, Cyclorhagida), *E. romanoi* sp.n. and *E. joyceae* sp.n., from the Gulf of Mexico. *ZooKeys* 594: 51–71. https://doi.org/10.15468/39omei.

Landers S.C., Bassham R., Miller J.M., Ingels J., Sánchez N. & Sørensen M.V. 2020. Kinorhynch communities from Alabama coastal waters. *Marine Biology Research* 16: 1-11. https://doi.org/10.1080/17451000.2020.1789660.

Landers S.C., Sørensen M.V., Beaton K.R., Jones C.M., Miller J.M. & Stewart P.M. 2018. Kinorhynch assemblages in the Gulf of Mexico continental shelf collected during a two-year survey. *Journal of Experimental Marine Biology and Ecology* 502: 81-90. https://doi.org/10.1016/j.jembe.2017.05.013.

Lemenkova P. 2020. Geomorphology of the Puerto Rico Trench and Cayman Trough in the context of the geological evolution of the Caribbean Sea. *Annales Universitatis Mariae Curie-Sklodowska sectio B – Geographia Geologia Mineralogia et Petrographia* 75: 115-141. https://doi.org/10.17951/b.2020.75.115-141.

Llodra E.R. & Billett D.S.M. 2006. 3. Deep-sea ecosystems: pristine biodiversity reservoir and technological challenges. *In*: Duarte C.M. (ed.) *The Exploration of Marine Biodiversity. Scientific and Technological Challenges*: 65-94. Fundación BBVA, Bilbao.

Miloslavich P., Díaz J.M., Klein E., Alvarado J.J., Díaz C., Gobin J., Escobar-Briones E., Cruz-Mota J.J., Weil E., Cortés J., Bastidas A.C., Robertson R., Zapata F., Martín A., Castillo J., Kazandjian A. & Ortiz M. 2010. Marine biodiversity in the Caribbean: regional estimates and distribution patterns. *PLoS ONE* 5(8): e11916. https://doi.org/10.1371/journal.pone.0011916.

Moore P.G. 1973. *Campyloderes macquariae* Johnston, 1938 (Kinorhyncha: Cyclorhagida) from the Northern Hemisphere. *Journal of Natural History* 7: 341-354.

Netto S.C. & Gallucci F. 2003. Meiofauna and macrofauna communities in a mangrove from the island of Santa Catarina, South Brazil. *Hydrobiologia* 505: 159-170. https://doi.org/10.1023/B:HYDR.0000007304.22992.b2.

Neuhaus B. 2013. Kinorhyncha (=Echinodera). *In*: Schmidt-Rhaesa A. (ed.) *Handbook of Zoology. Gastrotricha, Cycloneuralia and Gnathifera. Volume 1: Nematomorpha, Priapulida, Kinorhyncha, Loricifera:* 1-69. De Gruyter, Göttingen. https://doi.org/10.1515/9783110272536.

Neuhaus B. & Sørensen M.V. 2013. Populations of *Campyloderes* sp. (Kinorhyncha, Cyclorhagida): One global species with significant morphological variation? *Zoologischer Anzeiger* 252(1): 48-75. https://doi.org/10.1016/j.jcz.2012.03.002.

Neuhaus B., Pardos F., Sørensen M.V. & Higgins R.P. 2014. New species of *Centroderes* (Kinorhyncha: Cyclorhagida) from the Northwest Atlantic Ocean, life cycle, and ground pattern of the genus. *Zootaxa* 3901(1): 1-69. https://doi.org/10.11646/zootaxa.3901.1.1.

Oey L.Y., Ezer T. & Lee H.C. 2005. Loop Current, Rings and Related Circulation in the Gulf of Mexico: A Review of Numerical Models and Future Challenges. *Geophysical Monograph Series* 161: 31-56. https://doi.org/10.1029/161GM04.

Oksanen J., Blanchet F.G., Friendly M., Kindt R., Legendre P., McGlinn D., Minchin P.R., O'Hara R.B., Simpson G.L., Solymos P., Stevens M.H.H., Szoecs E. & Wagner H. 2020. Package 'vegan'. https://github.com/vegandevs/vegan.

Ostmann A., Nordhaus I. & Sørensen M.V. 2012. First recording of kinorhynchs from Java, with the description of a new brackish water species from a mangrove-fringed lagoon. *Marine Biodiversity* 42: 79-91. https://doi.org/10.1007/s12526-011-0094-z.

Pardos F., Herranz M. & Sánchez N. 2016a. Two sides of a coin: the phylum Kinorhyncha in Panama. II) Pacific Panama. *Zoologischer Anzeiger* 265: 26-47. http://dx.doi.org/10.1016/j.jcz.2016.06.006.

Pardos F., Sánchez N. & Herranz M. 2016b. Two sides of a coin: the phylum Kinorhyncha in Panama. I) Caribbean Panama. *Zoologischer Anzeiger* 265: 3-25. http://dx.doi.org/10.1016/j.jcz.2016.06.005.

Pinto T.K., Austen M.C.V., Warwick R.M., Somerfield P.J., Esteves A.M., Castro F.J.V., Fonseca-Genevois V.G. & Santos P.J.P. 2013. Nematode diversity in different microhabitats in a mangrove region. *Marine Ecology* 34: 257-268. https://doi.org/10.1111/maec.12011.

R Core Team. 2021. *R: A language and environment for statistical computing*. R Foundation for Statistical Computing, Vienna. https://www.R-project.org.

Randsø P.V., Yamasaki H., Bownes S.J., Herranz M., Di Domenico M., Qii G.B. & Sørensen M.V. 2019. Phylogeny of the *Echinoderes coulli*-group (Kinorhyncha: Cyclorhagida: Echinoderidae) – a cosmopolitan species group trapped in the intertidal. *Invertebrate Systematics* 33: 501-517. https://doi.org/10.1071/IS18069.

Romero A. 2009. Cave biology: life in darkness. Cambridge University Press, Cambridge.

Ruiz-Abierno A. & Armenteros M. 2016. Coral reef hábitats strongly influence the diversity of macro- and meiobenthos in the Caribbean. *Marine Biodiversity* 47: 101-111. https://doi.org/10.1007/s12526-016-0553-7.

Sánchez N. & Martínez A. 2019. Dungeons and dragons: Two new species and records of Kinorhyncha from anchialine cenotes and marine lava tubes. *Zoologischer Anzeiger* 282: 161-175. https://doi.org/10.1016/j.jcz.2019.05.012.

Sánchez N., Sørensen M.V. & Landers S.C. 2019. Pycnophyidae (Kinorhyncha: Allomalorhagida) from the Gulf of Mexico: *Fujuriphyes viserioni* and a redescription of *Leiocanthus langi* (Higgins, 1964), with notes on its intraspecific variation. *Marine Biodiversity* 49: 1857-1875. https://doi.org/10.1007/s12526-019-00947-x.

Sánchez N., Yamasaki H., Pardos F., Sørensen M.V. & Martínez A. 2016. Morphology disentangles the systematics of a ubiquitous but elusive meiofaunal group (Kinorhyncha: Pycnophyidae). *Cladistics* 32: 479-505. https://doi.org/10.1111/cla.12143.

Sánchez N., Zeppilli, D., Baldrighi E., Vanreusel A., Gasimandova-Lahitsiresy M., Brandily C., Pastor L., Macheriotou L., García-Gómez G., Dupré S. & Olu K. 2020. A threefold perspective on the role of a pockmark in benthic faunal communities and

biodiversity patterns. *Deep Sea Research Part I: Oceanographic Research Papers* 167: e103425. https://doi.org/10.1016/j.dsr.2020.103425.

Schrijvers J., Schallier R., Silence J., Okondo J.P. & Vincx M. 1997. Interactions between epibenthos and meiobenthos in a high intertidal *Aviccnnia marina* mangrove forest. *Mangroves and Salt Marshes* 1: 137-154. https://doi.org/10.1023/A:1009936318721.

Sørensen M.V. 2006. New kinorhynchs from Panama, with a discussion of some phylogentically significant cuticular structures. *Meiofauna Marina* 15: 51-77.

Sørensen M.V. 2007. A new species of *Antygomonas* (Kinorhyncha: Cyclorhagida) from the Atlantic coast of Florida, USA. *Cahiers de Biologie Marine* 48: 155-168.

Sørensen M.V. 2014. First account of echinoderid kinorhynchs from Brazil, with the description of three new species. *Marine Biodiversity* 44(3): 251-274. https://doi.org/10.1007/s12526-013-0181-4.

Sørensen M.V. & Landers S.C. 2014. Two new species of *Echinoderes* (Kinorhyncha: Cyclorhagida) from the Gulf of Mexico. *Frontiers in Marine Science* 1(8): 1-18. https://doi.org/10.3389/fmars.2014.00008.

Sørensen M.V. & Landers S.C. 2018. New species of Semnoderidae (Kinorhyncha: Cyclorhagida: Kentrorhagata) from the Gulf of Mexico. *Marine Biodiversity* 48(7): 1-29. https://doi.org/10.1007/s12526-017-0728-x.

Sørensen M.V. & Pardos F. 2020. Kinorhyncha. *In*: Schmidt-Rhaesa A. (ed.) *Guide to the Identification of Marine Meiofauna*: 391-414. Verlag Dr. Friedrich Pfeil, München.

Sørensen M.V. & Thormar J. 2010. *Wollunquaderes majkenae* gen. et – a new cyclorhagid kinorhynch genus and species from the Coral Sea, Australia. *Marine Biodiversity* 40: 261-275. https://doi.org/10.1007/s12526-010-0048-x.

Sørensen M.V., Dal Zotto M., Rho H.S., Herranz M., Sánchez N., Pardos F. & Yamasaki H. 2015. Phylogeny of Kinorhyncha based on morphology and two molecular loci. *PLoS ONE* 10(7): e0133440. https://doi.org/10.1371/journal.pone.0133440.

Sørensen M.V., Heiner I. & Ziemer O. 2005. A new species of *Echinoderes* from Florida (Kinorhyncha: Cyclorhagida). *Proceedings of the Biological Society of Washington* 118(3): 499-508. https://doi.org/10.2988/0006-324x(2005)118[499:ansoef]2.0.co;2.

Spalding M., Fox H., Allen G., Davidson N., Ferdaña Z., Finlayson M., Halpern B.S., Jorge M.A., Lombana A., Lourie S.A., Martin K.D., McManus E., Molnar J., Recchia C.A. & Robertson J. 2007. Marine ecoregions in the world: a bioregionalization of coastal and shelf areas. *BioScience* 57(7): 573-583. https://doi.org/10.1641/B570707.

Whalley P. 2011. Sustainable management of the shared living marine resources of the Caribbean large marine ecosystem & adjacent regions. CLME regional transboundary diagnostic analysis. Caribbean LME Project.

Yamasaki H., Herranz M. & Sørensen M.V. 2020. An interactive identification key to species of Echinoderidae (Kinorhyncha). *Zoologischer Anzeiger* 287: 14-16. https://doi.org/10.1016/j.jcz.2020.05.002.

Zelinka C. 1894. Über die Organisation von *Echinoderes. Verhandlungen der Deutschen Zoologischen Gesellschaft* 4: 46-49.

Zelinka C. 1896. Demonstration von Tafeln der *Echinoderes* Monographie. *Verhandlungen der Deutschen Zoologischen Gesellschaft* 6: 197-199.

Zeppilli D., Leduc D., Fontanier C., Fontaneto D., Fuchs S., Gooday G.J., Goineau A., Ingels J., Ivenenko V.N., Kristensen R.M., Neves R.C., Sánchez N., Sandulli R., Sarrazin J., Sørensen M.V., Tasiemski A., Vanreusel A., Autret M., Bourdonnay L., Claireaux M., Coquillé V., De Wever L., Rachel D., Marchant J., Toomey L. & Fernandes D. 2018. Characteristics of meiofauna in extreme ecosystems: a review. *Marine Biodiversity* 48: 35-71. https://doi.org/10.1007/s12526-017-0815

Tables.

Table 1. Data on sampling localities, geographic coordinates, date of collecting, habitat, depth and kinorhynch species found in the Caribbean samples from the Smithsonian Institution collection.

Region	Locality	Coordinates	Date	Species	Habitat	Depth (m)
Greater Antilles	Bahía de Guantánamo, Cuba	19 52 30N, 75 10 00W	17/03/76	*Echinoderes astridae, E. imperforatus, E. wallaceae*	Mangroves, mud	2
	Kingston Harbour, Jamaica	17 57 00N, 76 51 18W	09/03/76	*Dracoderes spyro*	Mud	-
		17 56 24N, 76 50 00W	10/03/76	*Cristaphyes* cf. *longicornis, Echinoderes imperforatus, E. parahorni, E. sublicarum*	Gravelly and sandy mud	2
		17 56 36N, 76 49 18W	10/03/76	*Echinoderes horni*	Mangroves, muddy sand	1.5
		17 56 30N, 76 49 12W	10/03/76	*Echinoderes horni, E. parahorni, E. sublicarum*	Mangroves, gravelly mud	1
		17 57 18N, 76 50 24W	11/03/76	*Echinoderes astridae, E. parahorni*	Gravelly and shelly sand	4
	Ocho Ríos, Jamaica	-	13/06/66	-	-	-
	Puerto Príncipe, La Española	-	15/03/76	*Dracoderes spyro, Echinoderes astridae, E. parahorni*	Mangroves, mud	5
	Cabo Haitiano, La Española	19 46 12N, 72 11 00W	10/11/80	*Dracoderes spyro, Pycnophyes* sp, *Echinoderes parahorni*	Mud	4
	Cabo Rojo, La Española	-	01/04/76	*Echinoderes horni, E. imperforatus, E. spinifurca*	-	0.3
	Puerto Plata, La Española	19 48 12N, 70 42 00W	02/11/80	*Dracoderes spyro, Cristaphyes retractilis, Fujuriphyes dalii*	Sandy mud	5
				Dracoderes spyro	Mud	5
				Cristaphyes retractilis, Fujuriphyes dalii	Mud	4
	Puerto Blanco, La Española	19 54 24N, 70 56 24W	03/11/80	*Dracoderes spyro, Cristaphyes* cf. *longicornis, Echinoderes astridae, E. parahorni, E. spinifurca*	Mangroves, mud	3
				Dracoderes spyro	Mud	2
	La Isabela, La Española	19 53 18N, 71 05 36W	04/11/80	*Dracoderes spyro*	Mud	4

	Monte Cristi, La Española	19 53 12N, 71 40 00W	06/11/80	*Cristaphyes retractilis, Echinoderes astridae, E. horni, E. imperforatus, E. parahorni, E. spinifurca*	Muddy sand with *Thalassia testudinum*	3.5
	Bahía de Icaquitos, La Española	19 53 12N, 71 38 30W	07/11/80	*Echinoderes horni, E. parahorni*	Mangroves, muddy sand with *Thalassia testudinum*	2
	Santo Domingo, La Española	18 28 00N, 69 57 00W	08/05/76	*Echinoderes brevipes*	-	0.7-1
		-	09/05/76	-	-	-
	La Matica, La Española	-	19/03/76	-	Mud	0.5
				-	Sand	0.5-1
	La Parguera, Puerto Rico	-	07/06/67	*Dracoderes spyro, Cristaphyes cornifrons, C. retractilis, Echinoderes astridae, E. horni, E. spinifurca, E. orestauri*	Coral mud	15
			08/06/67	*Echinoderes sublicarum*	*Enteromorpha* sp.	-
			08/06/67	*Cristaphyes retractilis, Cristaphyes* sp, *Echinoderes horni*	Mangroves, mud	5
Lesser Antilles	Oranjestad, Aruba	12 30 00N, 70 01 00W	25/06/77	*Echinoderes sublicarum, Echinoderes* sp. 1	-	-
	Saint James, Barbados	13 13 12N, 59 37 12W	-	*Echinoderes barbadensis*	-	-
	Klein Bonaire, Bonaire	12 10 12N, 68 18 12W	25/06/77	*Echinoderes intermedius*	Sand	100
	Guadeloupe	16 21 40N, 61 39 00W	11/03/78	*Echinoderes wallaceae*	Fine sand	3.5
				Echinoderes wallaceae	Coral sand	3
				Echinoderes wallaceae	-	1.5
	Tyrrel's Bay, Tobago	11 18 00N, 60 30 00W	13/05/91	*Triodontoderes lagahoo*	Fine sand	5
	Bon Accord, Tobago	11 10 00N, 60 50 00W	15/05/91	*Cristaphyes* sp, *Echinoderes intermedius*	Mangroves, sand	3
	Man O' War Bay, Tobago	11 19 00N, 60 33 00W	16/05/91	*Higginsium* cf. *erismatum*	Muddy sand	12
	Bloody Bay, Tobago	11 18 00N, 60 37 00W	12/05/91	-	Fine sand	-

Lucayas Archipelago	Little Harbor Cay, Berry Islands, Bahamas	-	04/03/82	*Echinoderes astridae*	-	-
Continental America	Isla Margarita, Venezuela	-	15/02/77	*Echinoderes sublicarum*	Mangroves	-
			01/09/01	*Echinoderes intermedius*	Mud	1
	Bahía de Mochima, Venezuela	10 21 12N, 64 20 36W	14/05/85	*Fujuriphyes deirophorus, Leiocanthus corrugatus, Echinoderes intermedius*	Mud	3
		10 20 42N, 64 21 18W	14/05/85	*Echinoderes augustae, Higginsium* cf. *erismatum, Fujuriphyes deirophorus, Leiocanthus corrugatus*	Mud	2
		10 21 30N, 64 20 36W	14/05/85	*Fujuriphyes deirophorus, Leiocanthus corrugatus*	Mud	3
		10 22 30N, 64 20 24W	14/05/85	*Echinoderes augustae, Higginsium* cf. *erismatum, Fujuriphyes deirophorus, Setaphyes* sp, *Echinoderes intermedius*	Mud	2
	Playa Isla de Buche, Venezuela	10 32 30N, 66 05 42W	23/05/85	*Higginsium* cf. *erismatum, Fujuriphyes deirophorus, F. distentus, Echinoderes parahorni*	Sandy mud	-
		11 32 30N, 66 05 42W	23/05/85	*Echinoderes augustae, Fujuriphyes deirophorus*	-	-
		12 32 30N, 66 05 42W	23/05/85	*Echinoderes augustae, E. intermedius*	-	-
	Los Roques, Venezuela	-	17/05/86	*Echinoderes parahorni*	Sandy mud	1
		-	17/05/86	*Echinoderes parahorni*	Sandy mud	-
		-	19/05/86	*Echinoderes intermedius, E. orestauri, E. wallaceae*	Sandy, coral mud	20
		-	19/05/86	*Echinoderes intermedius, Semnoderes lusca*	Coral sand	3
	Morrocoy, Venezuela	10 50 00N, 68 14 00W	28/05/86	*Higginsium* cf. *erismatum, Echinoderes parahorni*	Coastal lagoon, coral sand	1
				Higginsium cf. *erismatum*	Sand with *Halimeda* sp.	0.5

	Laguna Boca de Caño, El Supí, Venezuela	-	29/05/86	*Fujuriphyes deirophorus*, *F. distentus*, *Echinoderes imperforatus*, *Echinoderes* sp	Coastal lagoon, muddy sand	2
	Magdalena, Colombia	10 59 00N, 74 15 30W	15/02/86	-	Mangrove roots	0.5

Table 2. Data on known Caribbean habitats for Kinorhyncha, listed by species (including those of previous and present works). Habitats are classified following the criteria adopted in the discussion (mangrove sediment, coral reef sediment, marine cave sediment, seagrass bed sediment, and simply sediment). As no quantitative methods were applied for granulometry, the terms calcareous, mud and sand, used to described the Caribbean sediments, are merely indicative; depth is indicated in metres.

Species	Habitat	Depth
Antygomonas paulae	Sediment (sand)	1-14
Campyloderes sp.	Mangrove sediment (sand)	10
Centroderes barbanigra	Coral reef sediment (mud), Mangrove sediment (sand), Marine cave (calcareous), Sediment (mud, sand)	10-20
Cephalorhyncha sp.	Coral reef sediment (sand)	1
Cristaphyes belizensis	Coral reef sediment (calcareous, mud, sand), Mangrove sediment (calcareous, mud, sand)	1-3
Cristaphyes cornifrons	Coral reef sediment (mud)	15
Cristaphyes longicornis	Mangrove sediment (calcareous, mud, sand), Sediment (mud)	1-15
Cristaphyes panamensis	Mangrove sediment (sand)	10
Cristaphyes retractilis	Coral reef sediment (mud), Mangrove sediment (mud), Seagrass bed sediment (sand), Sediment (mud)	3-15
Cristaphyes sp.	Mangrove sediment (sand, mud)	3
Dracoderes spyro	Coral reef sediment (mud), Mangrove sediment (mud), Sediment (mud)	2-15
Echinoderes abbreviatus	Coral reef sediment (calcareous), Mangrove sediment (calcareous)	1-2
Echinoderes astridae	Coral reef sediment (mud), Mangrove sediment (mud), Seagrass bed sediment (sand), Sediment (sand)	2-15
Echinoderes augustae	Sediment (mud)	2
Echinoderes barbadensis	-	-
Echinoderes brevipes	-	1
Echinoderes caribiensis	Mangrove sediment (mud)	-
Echinoderes collinae	Coral reef sediment (mud)	20
Echinoderes horni	Coral reef sediment (mud), Mangrove sediment (calcareous, sand, mud), Seagrass bed sediment (sand), Sediment (calcareous, mud, sand)	0-15

Echinoderes imperforatus	Coral reef sediment (calcareous, mud), Mangrove sediment (calcareous, mud), Seagrass bed sediment (sand), Sediment (calcareous, mud, sand)	0-5
Echinoderes intermedius	Coral reef sediment (mud, sand), Mangrove sediment (sand), Sediment (mud, sand)	1-100
Echinoderes orestauri	Coral reef sediment (mud), Mangrove sediment (sand)	10-20
Echinoderes parahorni	Coral reef sediment (sand), Mangrove sediment (sand, mud), Seagrass bed sediment (sand), Sediment (mud, sand)	1-5
Echinoderes rociae	Sediment (sand)	10
Echinoderes spinifurca	Coral reef sediment (mud), Mangrove sediment (mud), Seagrass bed sediment (sand)	20
Echinoderes sublicarum	Mangrove sediment (mud), Sediment (mud), Algae (*Enteromorpha* sp.)	1-2
Echinoderes truncatus	Coral reef sediment (mud), Mangrove sediment (mud)	3-20
Echinoderes wallaceae	Coral reef sediment (calcareous, mud, sand), Mangrove sediment (calcareous, mud), Sediment (calcareous, mud, sand)	1-3
Echinoderes sp. 1	-	-
Echinoderes sp. 2	Coral reef sediment (mud)	20
Echinoderes sp. 3	Sediment (sand)	2
Fujuriphyes dalii	Sediment (mud)	4-5
Fujuriphyes deirophorus	Coral reef sediment (calcareous), Mangrove sediment (calcareous), Sediment (mud, sand)	1-3
Fujuriphyes distentus	Coral reef sediment (mud, sand), Mangrove sediment (mud, sand), Sediment (mud, sand)	2-10
Higginsium erismatum	Coral reef sediment (sand), Mangrove sediment (calcareous, mud, sand), Seagrass bed sediment (sand), Sediment (mud, sand)	1-12
Higginsium trisetosum	Coral reef sediment (calcareous, sand), Mangrove sediment (calcareous, sand)	1-2
Leiocanthus corrugatus	Coral reef sediment (sand, mud), Mangrove sediment (sand, mud), Sediment (mud)	1-12
Leiocanthus ecphantor	Coral reef sediment (calcareous), Mangrove sediment (calcareous)	1-2
Leiocanthus emarginatus	Coral reef sediment (calcareous, mud, sand), Mangrove sediment (calcareous, mud, sand), Sediment (mud, sand)	1-12
Paracentrophyes praedictus	Coral reef sediment (mud, sand), Mangrove sediment (mud, sand), Sediment (mud, sand)	3-12

Paracentrophyes sp.	Marine cave (calcareous sediment)	-
Pycnophyes alexandroi	Mangrove sediment (mud), Sediment (mud)	1-2
Pycnophyes apotomus	Coral reef sediment (mud), Mangrove sediment (mud)	3
Pycnophyes beaufortensis	Coral reef sediment (mud)	20
Pycnophyes kukulkan	Marine cave (calcareous)	-
Pycnophyes stenopygus	Coral reef sediment (calcareous, mud), Mangrove sediment (calcareous, mud)	1-3
Pycnophyes sp.	Sediment (mud)	4
Semnoderes cf. *pacificus*	Coral reef sediment (sand)	1
Semnoderes lusca	Coral reef sediment (sand)	3
Setaphyes iniorhaptus	Coral reef sediment (calcareous), Mangrove sediment (calcareous)	1-2
Setaphyes sp.	Sediment (mud)	2
Triodontoderes lagahoo	Sediment (sand)	5

Table 3. Measurements of adult *Echinoderes* sp. 1. Abbreviations: ac, acicular spine; LD, laterodorsal; LTAS, lateral terminal accessory spine; LTS, lateral terminal spine; LV, lateroventral; MD, middorsal; MSW, maximum sternal width (measured at segment 6); S, segment length (followed by number of corresponding segment); SL, sublateral; SW, standard sternal width; tu, tube; TL, total trunk length; VL, ventrolateral.

Character	Specimen 1	Specimen 2
TL (µm)	197.6	-
MSW-6 (µm)	42.9	47.2
MSW-6/TL (%)	21.7	-
SW (µm)	37.6	42.2
SW/TL (%)	19	-
S1 (µm)	19.7	-
S2 (µm)	21.3	-
S3 (µm)	19.2	19.6
S4 (µm)	22.9	23.1
S5 (µm)	26.8	27.5
S6 (µm)	32.2	31.6
S7 (µm)	32.4	29.3
S8 (µm)	32.7	34.1
S9 (µm)	30.6	33.6
S10 (µm)	38.4	38.7
S11 (µm)	31.2	32.1
VL2 (tu) (µm)	6.3	-
MD4 (ac) (µm)	30.5	30.6
LV5 (tu) (µm)	9.0	16.4
MD6 (ac) (µm)	40.1	43.4
LV6 (ac) (µm)	24.0	29.0
LV7 (ac) (µm)	26.0	-
MD8 (ac) (µm)	48.1	54.2
SL8 (tu) (µm)	16.5	17.8
LV8 (ac) (µm)	28.1	29.4
LV9 (ac) (µm)	30.9	34.5
LD10 (tu) (µm)	24.4	10.1
LTS (µm)	117.8	121.1
LTS/TL (%)	59.6	-
LTAS (µm)	-	36.7
LTAS/LTS (%)	-	30.3

Table 4. Summary of nature and arrangement of spines, tubes, sensory spots, type 1 glandular cell outlets and nephridiopore of *Echinoderes* sp. 1. Abbreviations: ac, acicular spine; gcoI, type 1 glandular cell outlet; LA, lateral accessory; LD, laterodorsal; ltas, lateral terminal accessory spine; lts, lateral terminal spine; LV, lateroventral; MD, middorsal; ML, midlateral; ne, nephridiopore; PD, paradorsal; ps, penile spine; SD, subdorsal; ss, sensory spot; tu, tube; VL, ventrolateral; VM, ventromedial; * indicates unpaired structures.

Segment	MD	PD	SD	LD	ML	SL	LA	LV	VL	VM
1	gcoI*		ss	ss		gcoI				
2	gcoI*			ss	ss			gcoI	tu	ss
3	gcoI*		ss	ss		ss				gcoI, ss
4	ac*	gcoI, ss	ss		ss					gcoI, ss
5	gcoI*	ss	ss	ss		ss		tu		gcoI, ss
6	ac*	gcoI, ss	ss	ss				ac		gcoI, ss
7	gcoI*	ss	ss	ss				ac		gcoI, ss
8	ac*	gcoI, ss	ss	ss		tu		ac	ss	gcoI
9	gcoI*	ss					ne	ac	ss	gcoI
10	gcoI*x2	ss		tu						gcoI
11	gcoI*						ltas (♀), psx3 (♂)	lts		

Figures.

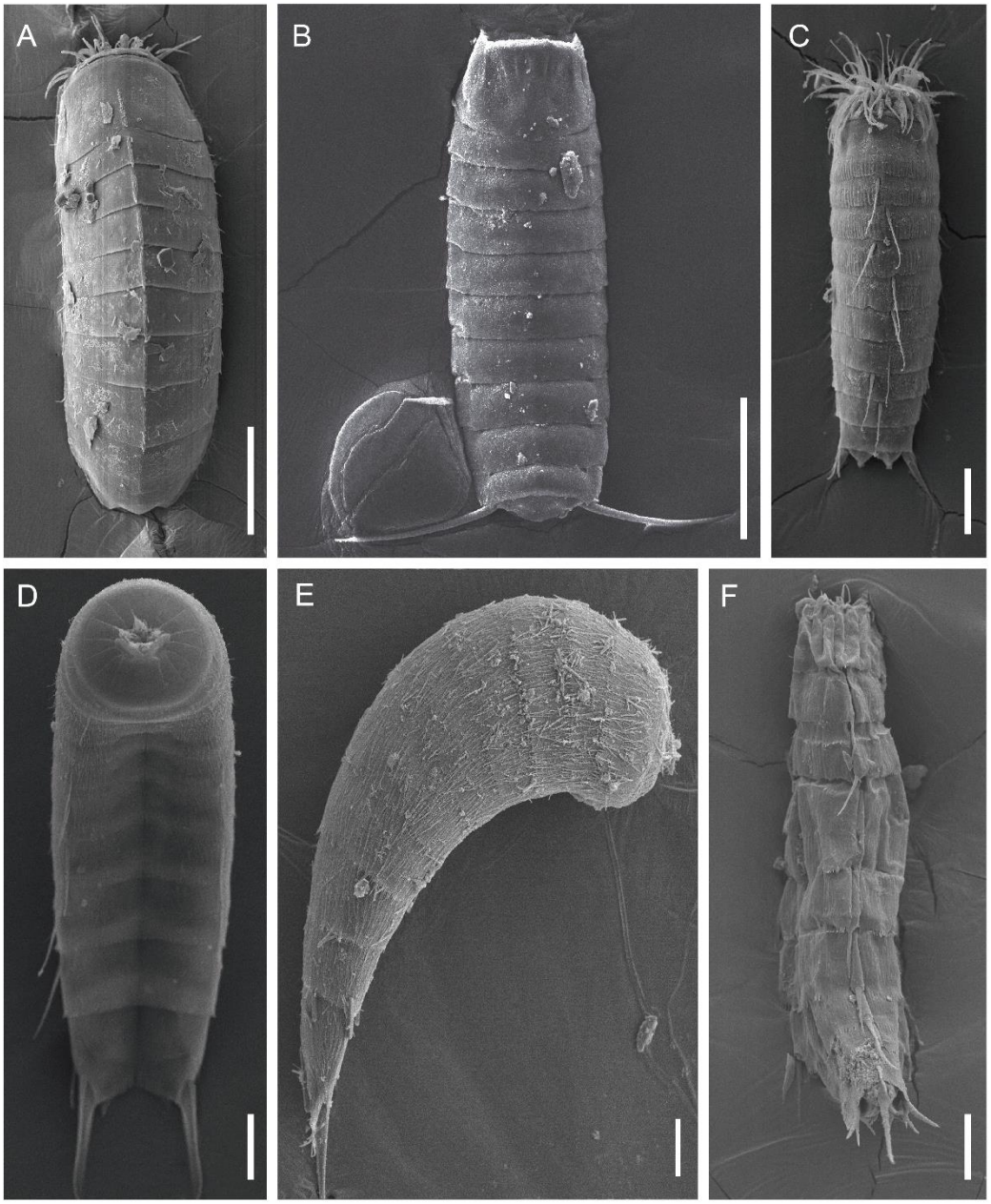

Figure 1. Selected scanning electron micrographs of kinorhynch species from the studied samples of the Caribbean Sea, showing an overall view of Kinorhyncha biodiversity in this area. (A) Dorsal view of a specimen of *Higginsium* cf. *erismatum* from Tobago; (B) dorsal view of a specimen of *Fujuriphyes dalii* from La Española; (C) dorsal view of a male of *Dracoderes spyro* from La Española; (D) ventral view of a male of *Echinoderes sublicarum* from Venezuela; (E) lateroventral view of a male of *Echinoderes barbadensis* from Barbados; (F) dorsal view of a male of *Triodontoderes lagahoo* from Tobago. Scales: A-B, 100 μm; C-F, 30 μm.

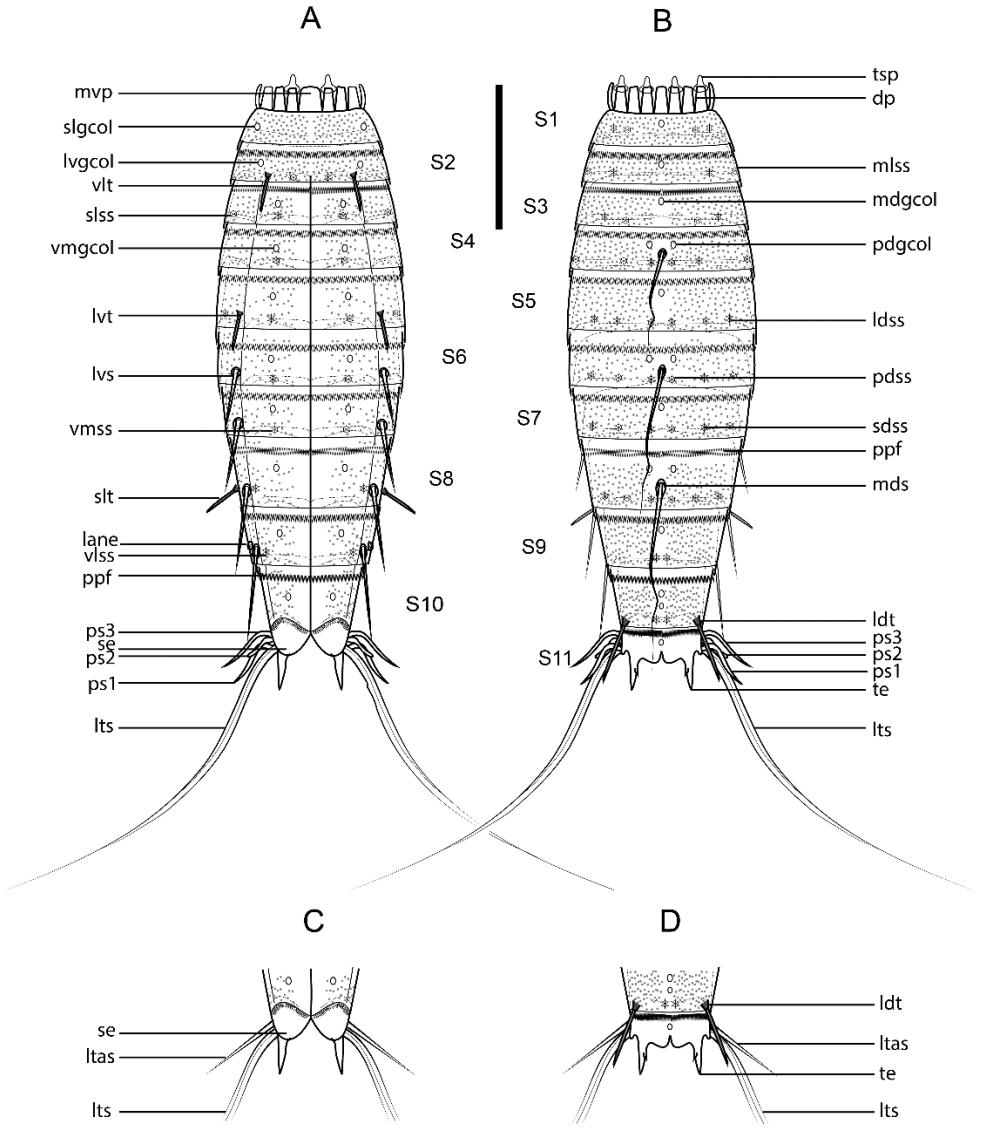

Figure 2. Line art illustrations of *Echinoderes* sp. 1 (A) Male, ventral view; (B) male, dorsal view; (C) female, segments 10-11, ventral view; (D) female, segments 10-11, dorsal view. Scale bar: 50 μm. Abbreviations: dp, dorsal placid; lane, lateral accessory nephridiopore; ldss, laterodorsal sensory spot; ldt, laterodorsal tube; ltas, lateral terminal accessory spine; lts, lateral terminal spine; lvgcoI, lateroventral type 1 glandular cell outlet; lvs, lateroventral spine; lvt, lateroventral tube; mdgcoI, middorsal type 1 glandular cell outlet; mds, middorsal spine; mlss, midlateral sensory spot; mvp, midventral placid; pdgcoI, paradorsal type 1 glandular cell outlet; pdss, paradorsal sensory spot; ppf, primary pectinate fringe; ps, penile spine (followed by number of corresponding pair); sdss, subdorsal sensory spot; se, sternal extension; slgcoI, sublateral type 1 glandular cell outlet; slss, sublateral sensory spot; slt, sublateral tube; te, tergal extension; tsp, trichoscalid plate; vlss, ventrolateral sensory spot; vlt, ventrolateral tube; vmgocI, ventromedial type 1 glandular cell outlet; vmss, ventromedial sensory spot.

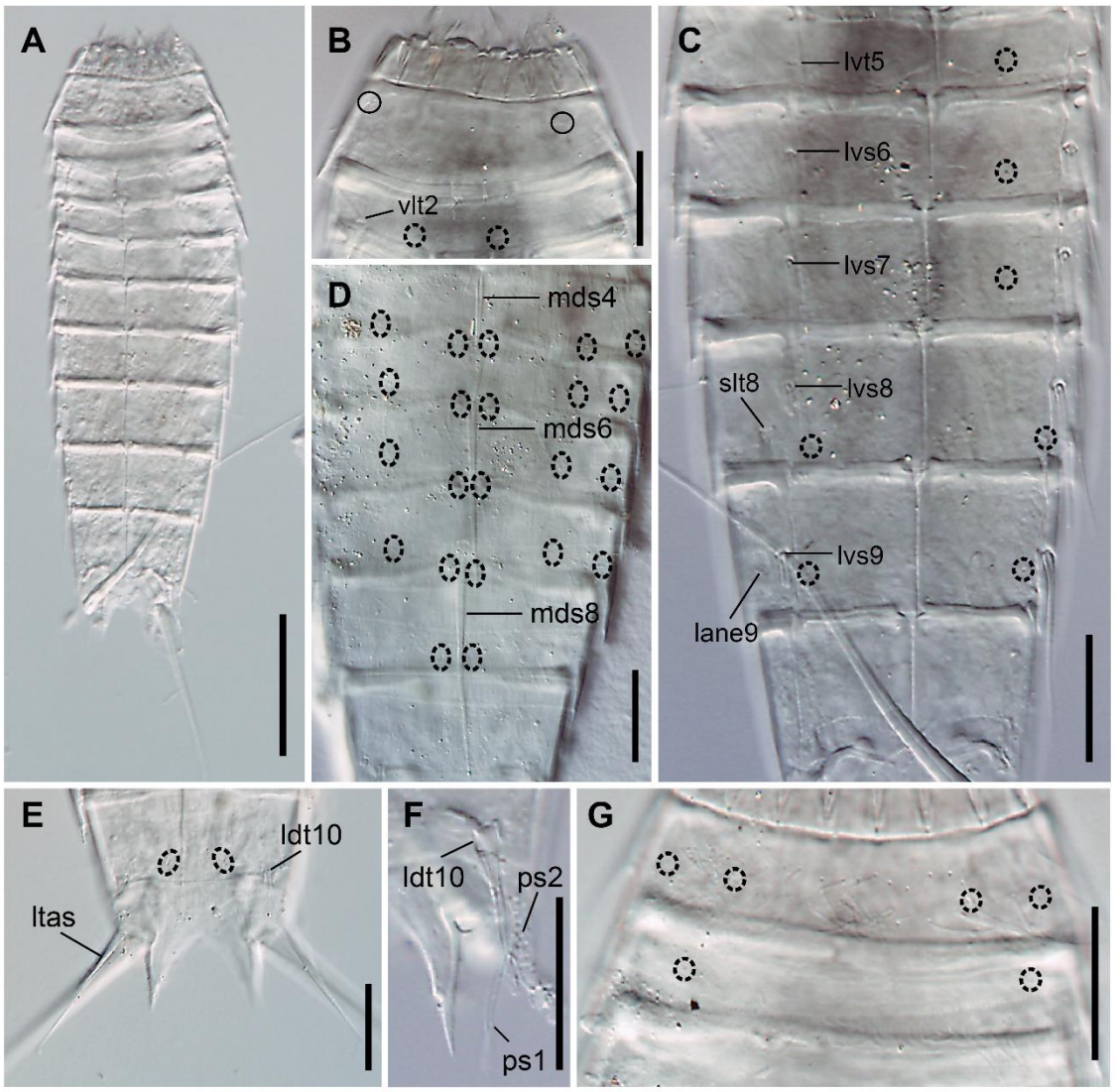

Figure 3. Light micrographs showing trunk overview and details in the main cuticular characters of male (A-C, F-G) and female (D-E) of *Echinoderes* sp. 1 (A) Ventral overview of trunk; (B) ventral overview of neck and segments 1-2; (C) lateral and ventral overviews of segments 5-10; (D) dorsal overview of segments 5-9; (E) dorsal overview of segments 10-11; (F) tergal extension; (G) dorsal overview of segments 1-2. Scale bars: A, 50 μm; B-F, 20 μm; G, 10 μm. Abbreviations: lane, lateral accessory nephridiopore; ldt, laterodorsal tube; ltas, lateral terminal accessory spine; lvs, lateroventral spine; lvt, lateroventral tube; mds, middorsal spine; ps, penile spine (followed by number of corresponding pair); slt, sublateral tube; vlt, ventrolateral tube; type 1 glandular cell outlets are marked as continuous circles, and sensory spots as dashed circles; numbers after abbreviations indicate the corresponding segment.

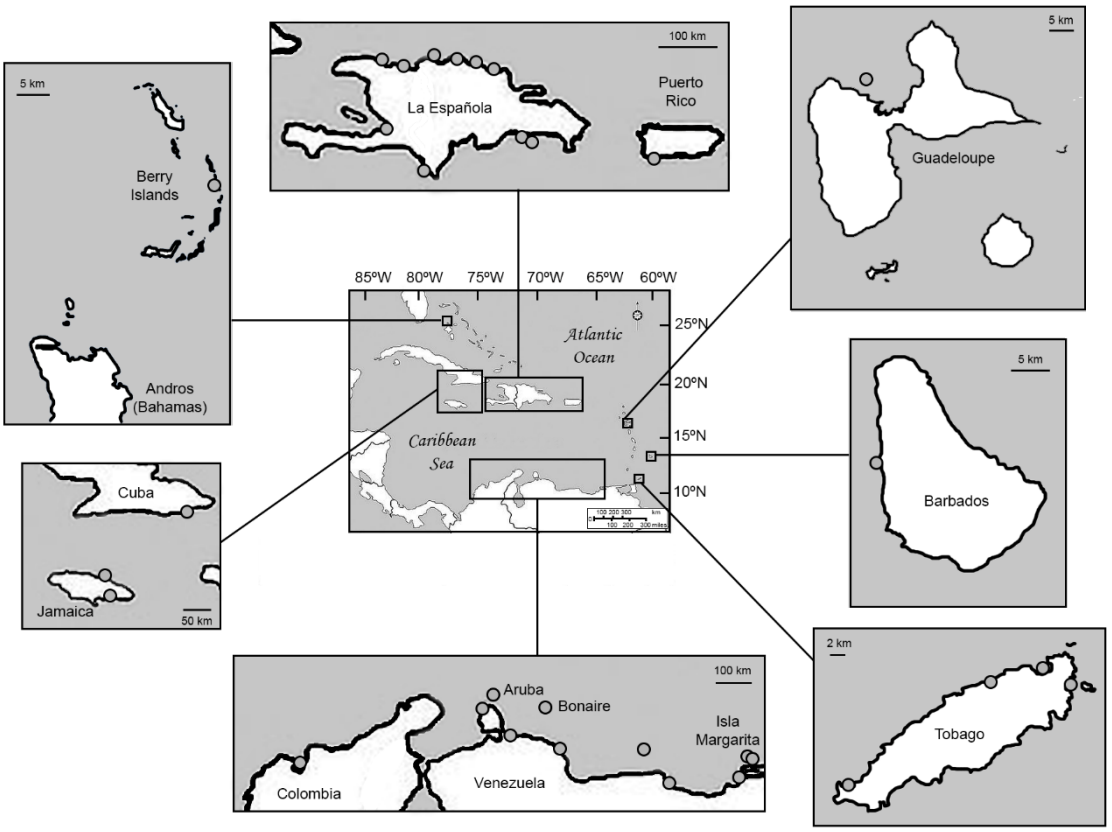

Figure 4. Map of the Caribbean Sea and nearby waters showing the collecting areas and localities (close-up in the insets for further geographic details) that are part of the present project.

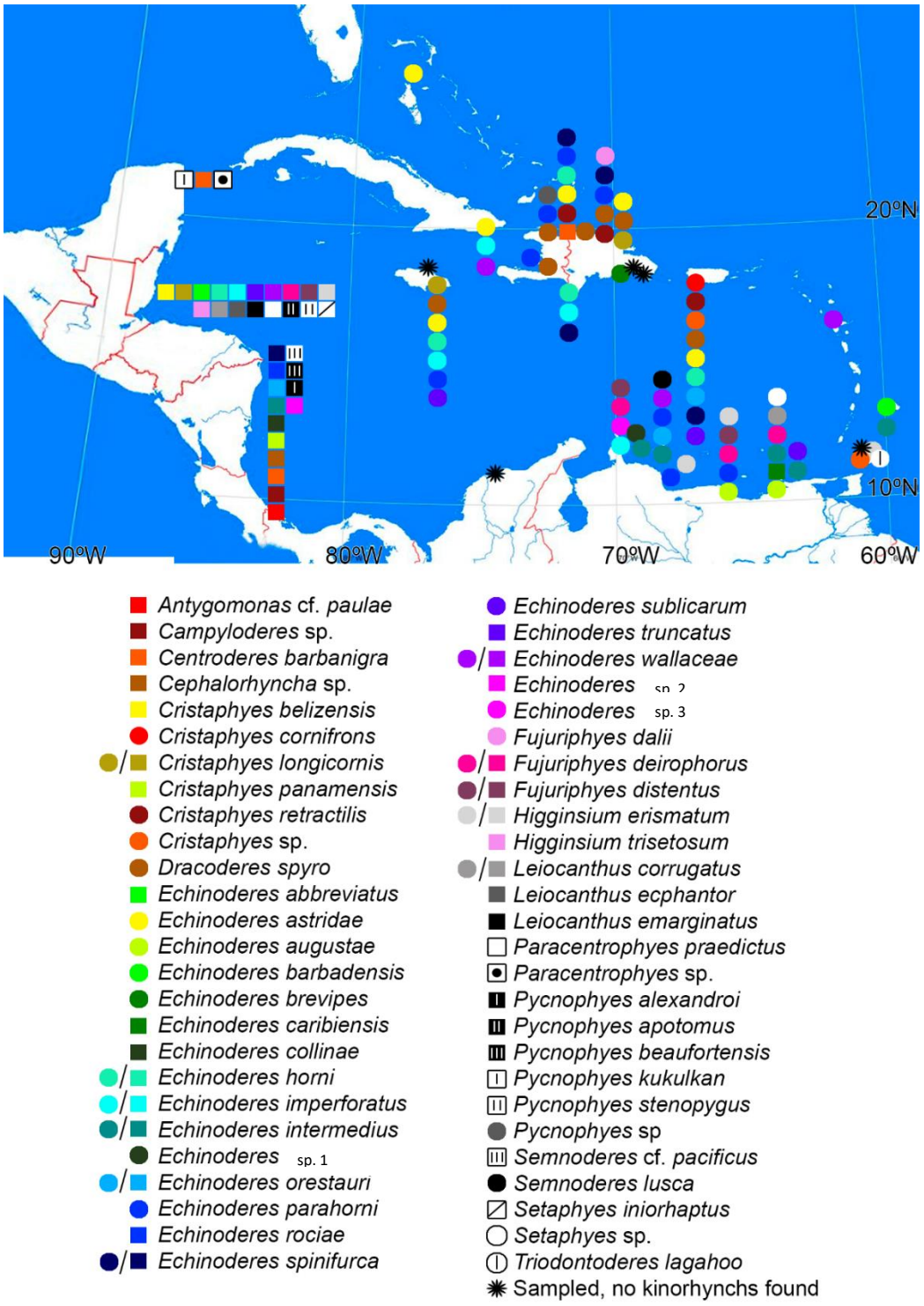

Figure 5. Map of the Caribbean Sea and nearby waters showing the distribution of all known kinorhynch species of the area, including those of previous studies (squares), those collected in the samples of the present project (circles) and sampled locations that yielded no kinorhynchs (asterisks).

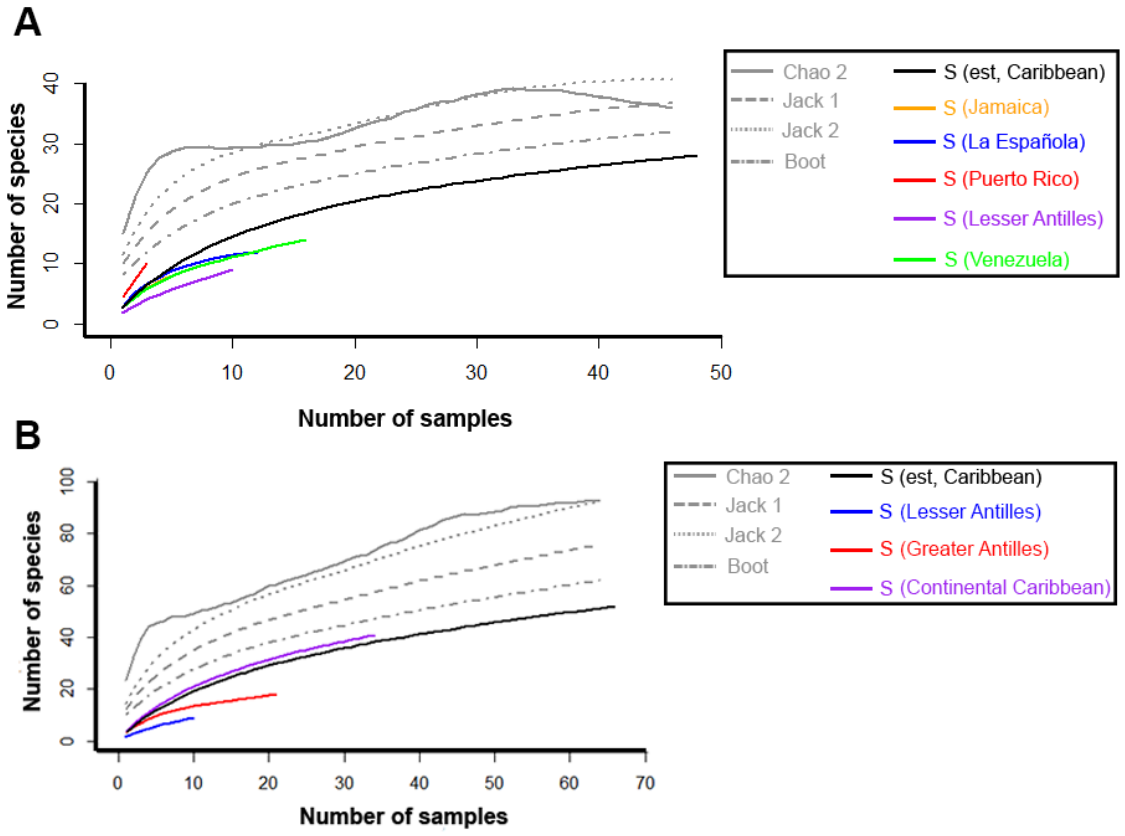

Figure 6. Sample-based rarefaction curves of the Caribbean samples studied for the present project (A) and the total number of Caribbean samples, including both those for the present project and those or previous studies done in the area, classified in the marine ecoregions proposed by Spalding *et al.* (2007) (B). Black curves represent the total area of the Caribbean Sea, coloured curves represent specific Caribbean areas, and grey curves represent the non-parametric estimators of richness. Abbreviations: est, estimated; S, richness.

Zoologischer Anzeiger 282 (2019) 140-160

Contents lists available at ScienceDirect

Zoologischer Anzeiger

journal homepage: www.elsevier.com/locate/jcz

Research paper

Four new species of Kinorhyncha from the Gulf of California, eastern Pacific Ocean*

Diego Cepeda [a, *], Lucía Álvarez-Castillo [b], Margarita Hermoso-Salazar [b], Nuria Sánchez [a, c], Samuel Gómez [d], Fernando Pardos [a]

[a] Departamento de Biodiversidad, Ecología y Evolucion, Facultad de Ciencias, Biologicas, Universidad Complutense de Madrid, Jose Antonio Novais St. 12, 28040, Madrid, Spain
[b] Facultad de Ciencias, Universidad Nacional Autonoma de Mexico, Circuito Exterior S/N, 04510, Mexico, D.F., Mexico
[c] Laboratoire Environnement Profond, Institut Français de Recherche pour, l'Exploitation de la Mer (IFREMER), Centre Bretagne - ZI de la Pointe du Diable, CS 10070, 29280, Plouzane, France
[d] Universidad Nacional Autónoma de México, Instituto de Ciencias del Mar y Limnología, Unidad Academica de Mazatlán, Cap. Joel Montes Camarena, Cerro del Vigía, 82040, Mazatlán, Sin., México

ARTICLE INFO

Article history:
Received 28 February 2019
Received in revised form 10 May 2019
Accepted 23 May 2019
Available online 6 June 2019

Corresponding Editor: Sørensen

Keywords:
Kinorhynchs
Meiofauna
Biodiversity
Taxonomy
Pycnophyidae
Echinoderidae

ABSTRACT

Several meiofaunal samples from the central and lower Gulf of California were studied. Four new species of kinorhynchs, *Cristaphyes fortis* sp. nov., *Higginsium mazatlanensis* sp. nov., *Cephalorhyncha teresae* sp. nov. and *Echinoderes xalkutaat* sp. nov., are described herein. *C. fortis* sp. nov. may be distinguished from its most similar congeners by its more strongly developed pachycycli and ball-and-socket joints and the presence of unpaired paradorsal setae on segments 2, 4 and 6, two pairs of ventrolateral setae on segment 5, one pair of ventrolateral setae on segments 2-4, 6-7 and 10, and one pair of ventromedial setae on segments 8-9. *H. mazatlanensis* sp. nov. is easily distinguished from its congeners by the combined presence of subdorsal setae only on segment 1 and lateroventral setae only on even segments. *C. teresae* sp. nov. is unique within the genus by the presence of acicular spines in middorsal position on segments 4, 6 and 8, in sublateral position on segment 7 and in lateroventral position on segments 8 and 9, as well as tubes in subdorsal position on segment 2, and in lateroventral position on segment 5. Moreover, this species has primary pectinate fringes of segments 2-7 bearing a tuft of elongated spinous projections in middorsal position, which is unique among its congeners. *E. xalkutaat* sp. nov. belongs to a group of *Echinoderes* characterized by possessing type 2 glandular cell outlets in subdorsal, laterodorsal, sublateral and ventrolateral positions on segment 2, together with middorsal spines on segments 4-8, lateroventral spines on segments 6-9 and lateroventral tubes on segment 5, but the arrangement of the remaining type 2 glandular cell outlets (in midlateral position on segment 5, in sublateral position on segment 8 and in laterodorsal position on segment 10) and the cuticular composition of segment 11 (one tergal and two sternal plates) allow its morphological differentiation.

1. Introduction

Kinorhynchs, commonly known as mud dragons, are marine, holobenthic, meiofaunal invertebrates that inhabit the upper centimetres of the bottom sea sediments (Sørensen & Pardos 2008; Neuhaus 2013). Species of kinorhynchs are distributed worldwide, and can be found from shallow waters to the deep sea (Neuhaus 2013). Despite the apparent ubiquity of the phylum, only a few regions have been extensively sampled, and little is known about the true diversity and biogeography of these invertebrates (Neuhaus 2013; Grzelak & Sørensen 2018). Meiofaunal organisms are essential for the functioning of marine food webs and ecosystem (Gerlach 1971; Hakenkamp & Morin 2001; Schmid-Araya et al. 2002; Schratzberger & Ingels 2017). The current lack of knowledge that hampers biodiversity estimations of meiofaunal taxa (Mokievsky & Azovsky 2002; Appeltans et al. 2012) leads to the need of further taxonomic studies in order to improve our understanding of meiofaunal marine communities.

urn:lsid:zoobank.org:pub:BE20AC11-DC52-4D89-80AD-3A1298838F5.

* This article is a part of the Fifth International Scalidophora Workshop special issue published in Zoologischer Anzeiger 282C, 2019.

* Corresponding author.
E-mail address: diegocepeda@ucm.es (D. Cepeda).

https://doi.org/10.1016/j.jcz.2019.05.011
0044-5231/

The Gulf of California represents an important gap in our knowledge on the distribution of Kinorhyncha from the eastern Pacific. The upper Gulf has been recently studied by Alvarez-Castillo et al. (2015, 2018). They reported the kinorhynch *Fissuroderes thermoi* Neuhaus & Blasche, 2006 and the presence of ten additional unidentified kinorhynch species of the genus *Echinoderes* and the family Pycnophyidae. However, the central and lower Gulf has received little attention, and the kinorhynch species composition of this part of the Gulf remains unexplored. The present contribution increases our knowledge on the diversity of Kinorhyncha in the central and lower Gulf of California with the description of two new Pycnophyidae and two new Echinoderidae species.

2. Material and methods

Sediment samples were collected at two localities in the central Gulf of California and one locality off Mazatlán, Sinaloa State, northwestern Mexico, lower Gulf (Fig. 1; Table 1).

Samples from the central Gulf were collected on February 11, 2007 during the course of oceanographic cruise Talud X on board of R/V El Puma (Universidad Nacional Autónoma de México). A sediment sample was collected at each station using a box corer, from which three replicas were taken using an acrylic corer of 9.2 cm of internal diameter and 19.5 cm long. The upper 3 cm layer of the sediment was recovered and preserved in 96% ethanol. Specimens of Kinorhyncha were firstly separated from the sediment particles and remaining meiofaunal organisms. Sample "St15" is located at 1570 m depth and the sediment was mainly composed of mud (sand: 4.49%, silt: 84.00%, clay: 11.96%) with a low content of organic matter (8.37%). Sample "St18" is located at 1440 m depth and the sediment was also composed of mud (sand: 17.20%, silt: 71.62%, clay: 11.19%) with a low content of organic matter too (7.13%).

The sediment sample from Mazatlán was taken at a sampling station located about 8.7 km south of Mazatlán on May 18, 2018 (sample "L3"). The sample was taken with a meiobenthic dredge during the Workshop "Tecnicas de muestreo, morfología, taxonomía y análisis genético en meiofauna: Copepodos harpacticoides (Crustacea, Copepoda) y Kinorrincos (Cephalorhyncha, Kinorhyncha) como modelos", that took place at the Instituto de Ciencias del Mar y Limnología at Mazatlán. Sample "L3" is located at 5 m depth and the sediment was mainly composed of sandy mud. Meiofaunal organisms were separated from the sediment using the bubble-and-blot method (Higgins 1964), and kinorhynchs were preserved in 100% ethanol.

All the studied kinorhynch specimens were picked up under a Motic® SMZ-168 stereo zoom microscope with an Irwin loop and treated with a series of 25%, 50%, 75% and 100% glycerin for light microscopy (LM). The specimens were mounted on glass slides with Fluoromount G® sealed with Depex®. The specimens were studied and photographed using an Olympus® BX51-P microscope equipped with differential interference contrast (DIC) and an Olympus® DP-70 camera. Measurements were obtained with Olympus cellSens® software. Line drawings and image plates were prepared with Adobe® Photoshop CC-2014 and Illustrator CC-2014 software.

The type material was deposited in the collection of the Smithsonian National Museum of Natural History (NMNH), Washington.

Fig. 1. Map showing the sampling locations of the studied kinorhynch specimens in the Gulf of California (Northeast Pacific Ocean).

Table 1
Data on sampling, localities and collected species.

Location	Geographical coordinates	Sampling date	Habitat	Depth (m)	Sampling method	Collected species
Central Gulf of California (St15)	27º42'00"N, 111º38'00"W	11/02/2007	Mud	1570	Box corer	*Cristaphyes fortis* sp.nov.
Central Gulf of California (St18)	27º09'08"N, 111º39'57"W	11/02/2007	Mud	1440	Box corer	*Cristaphyes fortis* sp.nov.; *Echinoderes xalkutaat* sp. nov.
South of Mazatlán (L3)	23º05'30"N, 106º17'45"W	18/05/2018	Sandy mud	5	Meiobenthic dredge	*Cephalorhyncha teresae* sp. nov.; *Higginsium mazatlanensis* sp. nov.

3. Results and discussion

Taxonomic account
Class **Allomalorhagida** Sørensen et al. 2015
Family **Pycnophyidae** Zelinka 1896
Genus ***Cristaphyes*** Sánchez et al., 2016

3.1. ***Cristaphyes fortis*** sp. nov

(Figs. 2-5 and Tables 2 and 3)
urn:lsid:zoobank.org:act:1909D377-717B-4708-AA5F-176EA50569F8

3.1.1. Type material

Adult male holotype (USNM 1558492) collected on February 11, 2007 in the central Gulf of California, eastern Pacific (St15): 27 42 00 N, 111 38 00 W; 1570 m depth; mounted in Fluoromount G®. One adult male paratype (USNM 1558494) with same collecting data as holotype, and two adult females paratypes (USNM 1558495-1558496) collected on February 12, 2007 in the central Gulf of California, eastern Pacific (St18): 27 09 08 N, 111 39 57 W; 1440 m depth; mounted in Fluoromount G®.

3.1.2. Diagnosis

Cristaphyes with middorsal processes on segments 2-10; process of segment 10 shorter and thinner than previous ones. Unpaired paradorsal setae on segments 2, 4 and 6. Paralateral seta on segment 1; laterodorsal setae on segments 2-9, although those of segments 5-7 and 9 may be absent or only present on one side; lateroventral setae on segments 2, 4, 6, 8 and 10; two pairs of ventrolateral setae on segment 5 and one pair on segments 2-4, 6-7 and 10; paired ventromedial setae on segments 8-9. Pachycycli and ball-and-socket joints strongly developed, thick and stout, distinctly visible on segments 2-10.

3.1.3. Etymology

The specific epithet from the Latin "fortis", strong or stout, refers to the markedly thick, robust pachycycli and ball-and-socket joints of the new species.

3.1.4. Description

See Table 2 for measurements and dimensions, and Table 3 for summary of location of cuticular processes, setae, glandular cell outlets, spines, nephridiopores and sensory spots.

Head with retractable mouth cone and introvert (Fig. 3A-E). Although all the examined specimens had the introvert completely everted, oral styles and scalids tended to collapse when mounted for LM. There were no specimens for SEM examination, and only some details of the head structures are given. Observed inner oral styles composed of a single unit with a trapezoidal, enlarged base and a triangular, straight, rigid distal tip (Fig. 3C). Following ring (ring 00) with nine outer oral styles (Fig. 3D). Outer oral styles composed of a single, very flexible piece with a basal, short, fringed sheath (Fig. 3D and E). Exact arrangement and detailed morphology of these oral styles not determined. Ring 01 of introvert with ten primary spinoscalids, each one composed of a basal sheath and a distal, elongated piece; basal sheath equipped with a median, dense fringe (Fig. 3E). Remaining rings of introvert (rings 02-06) with scalids morphologically similar to the primary spinoscalids but shorter (Fig. 3E). Fourteen elongated, hairy trichoscalids without trichoscalid plates (Fig. 3E). Exact number, arrangement and detailed morphology of scalids not determined.

Neck with four dorsal and two ventral sclerotized placids (Fig. 2A and B). Dorsal placids rectangular; mesial ones broader than lateral ones (Fig. 2B). Ventral placids much more elongated and trapezoidal, progressively thinner laterally (Fig. 2A).

Trunk markedly rectangular, stout, strongly sclerotized, triangular in cross-section, composed of eleven segments (Figs. 2A, B and 3A, B). Segment 1 with one tergal, two episternal and one trapezoidal, midsternal plate conspicuously broader at its base (Figs. 2A, B and 3A, B); remaining segments with one tergal and two sternal, cuticular plates (Figs. 2A, B and 3A, B). Sternal plates reach their maximum width at segment 5, but are almost constant in width throughout the trunk, slightly tapering at the posterior trunk end (Figs. 2A, B and 3A, B). Middorsal processes on segments 2-10, keel-shaped, with enlarged, pointed tips that reach one quarter of the total length of the following plate on most segments; middorsal processes increase in width and length segment by segment towards the posterior trunk end (Figs. 2B and 3A); middorsal process of segment 10 shorter and thinner than previous ones (Figs. 2B and 5I). Segments 1-10 with paired glandular cell outlets in subdorsal and ventromedial positions (ventromedial ones of segment 1 laterally shifted to ventrolateral position), near the anterior margin of segments, circular to oval-shaped (Figs. 2A, B, 4A-J and 5A-J). Segments 2-10 with paired, poorly-marked cuticular ridges in laterodorsal position and also at the ventrolateral-ventromedial limit, next to small glandular cell outlets (Fig. 2A, B, 4D, F, H, J and 5H, J). Muscular scars conspicuous, smooth, hairless, rounded to oval-shaped, in laterodorsal and ventromedial positions on segments 1-10 (except for the ventral muscular scars of segment 1 that are ventrolateral) (Figs. 2A, B, 4A-J and 5A-J). Pachycycli and ball-and-socket joints well-developed, thick, on segments 2-10 (Figs. 2A, B and 3A, B). Apodemes not observed. Posterior margin of segments straight, showing well-developed primary pectinate fringes weakly serrated; secondary pectinate fringes not detectable under LM (Fig. 2A, B).

Segment 1 without middorsal process (Figs. 2B and 3A). Anterolateral margins of the tergal plate as horn-shaped, straight, distally rounded extensions (Figs. 2A, B and 3A). Anterior margin of tergal plate strongly denticulated, followed by paired longitudinal grooves in subdorsal position (Figs. 2B and 4A). Paired setae in paralateral position (Figs. 2B and 4A). Paired sensory spots in laterodorsal and ventrolateral positions, distributed on the anterior half of segment, the former near the paralateral setae, the latter near the ventrolateral glandular cell outlets (Figs. 2A, B and 4A, B). Detailed morphology of sensory spots not determined.

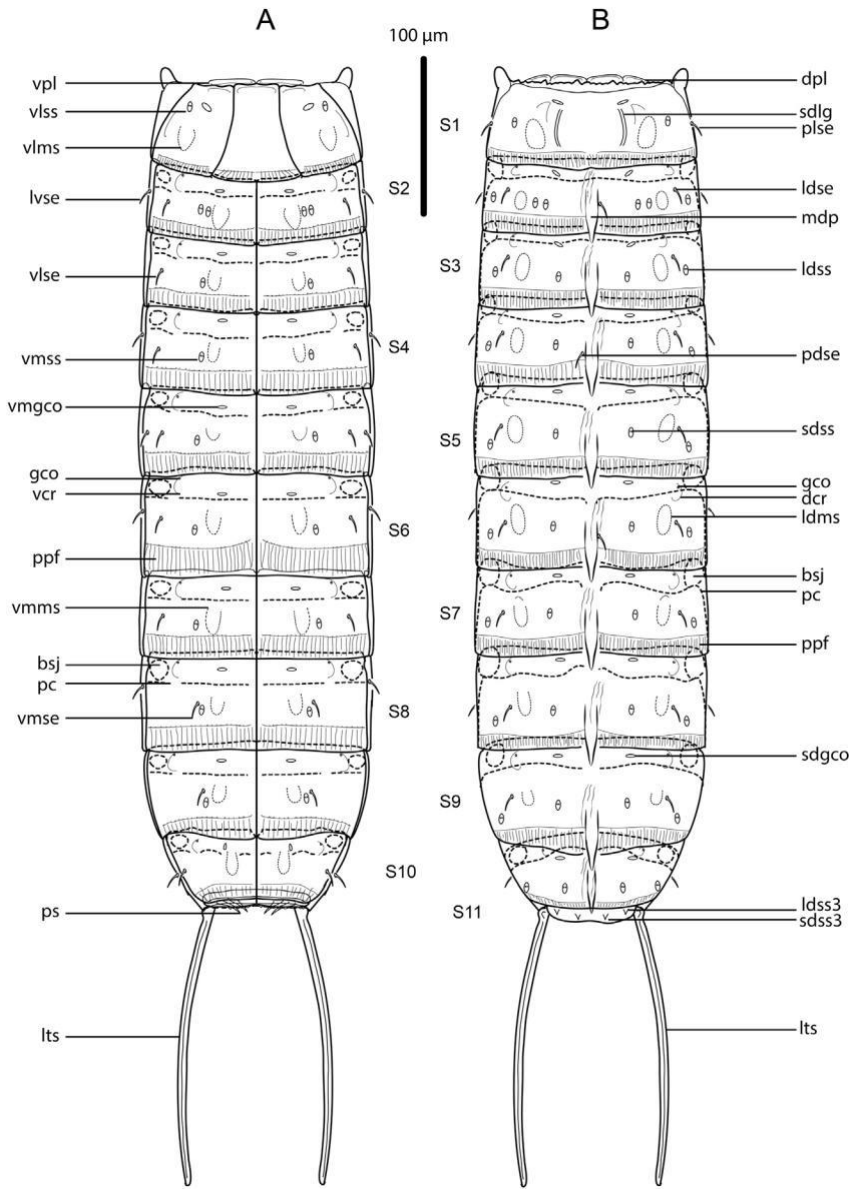

Fig. 2. Line art illustrations of male *Cristaphyes fortis* sp. nov. (A) Ventral overview of trunk; (B) dorsal overview of trunk. Abbreviations: bsj, ball-and-socket joint; dcr, dorsal cuticular ridge; dpl, dorsal placid; gco, glandular cell outlet; ldms, laterodorsal muscular scar; ldse, laterodorsal seta; ldss, laterodorsal sensory spot; ldss3, laterodorsal type 3 sensory spot; lts, lateral terminal spine; lvse, lateroventral seta; mdp, middorsal process; pc, pachycycli; pdse, paradorsal seta; plse, paralateral seta; ppf, primary pectinate fringe; ps, penile spine; S, segment (number after S indicates the corresponding segment); sdgco, subdorsal glandular cell outlet; sdlg, subdorsal longitudinal groove; sdss, subdorsal sensory spot; sdss3, subdorsal type 3 sensory spot; vcr, ventral cuticular ridge; vlms, ventrolateral muscular scar; vlse, ventrolateral seta; vlss, ventrolateral sensory spot; vmgco, ventromedial glandular cell outlet; vmms, ventromedial muscular scar; vmse, ventromedial seta; vmss, ventromedial sensory spot; vpl, ventral placid.

Segment 2 with middorsal process projecting beyond the posterior margin of segment (Figs. 2B and 4C). Unpaired seta in paradorsal position (Figs. 2B and 4C); and paired setae in laterodorsal, lateroventral and ventrolateral positions (Figs. 2A, B and 4C, D). Two pairs of sensory spots in subdorsal position, one posterior to the subdorsal glandular cell outlets, the other mesial to muscular scars (Figs. 2B and 4C); and one pair of sensory spots in laterodorsal position (Figs. 2B and 4C). Sternal plates with two pairs of sensory spots in ventromedial position, lateral to the ventral muscular scars (Figs. 2A and 4D). Sexually dimorphic male tubes absent (Fig. 2A).

Segment 3 with middorsal process as on the preceding segment (Figs. 2B and 4E). Paired setae in laterodorsal and ventrolateral positions (Figs. 2A, B and 4E, F). Paired sensory spots in subdorsal, laterodorsal and ventromedial positions, with the laterodorsal pair lateral to the setae (Figs. 2A, B and 4E, F).

Segment 4 with middorsal process as on the preceding segment (Figs. 2B and 4G). Unpaired seta in paradorsal position (Figs. 2B and 4G); paired setae in laterodorsal, lateroventral and ventrolateral positions (Figs. 2A, B and 4G, H). Paired sensory spots in subdorsal, laterodorsal and ventromedial positions, with the laterodorsal pair lateral to the setae (Figs. 2A, B and 4G, H).

Segment 5 with middorsal process as on the preceding segment (Figs. 2B and 4I). One pair of setae in laterodorsal position (Figs. 2B and 4I), and two pairs of setae in ventrolateral position (Figs. 2A and 4J). Laterodorsal setae with intraspecific variation, absent in some specimens or present only on one

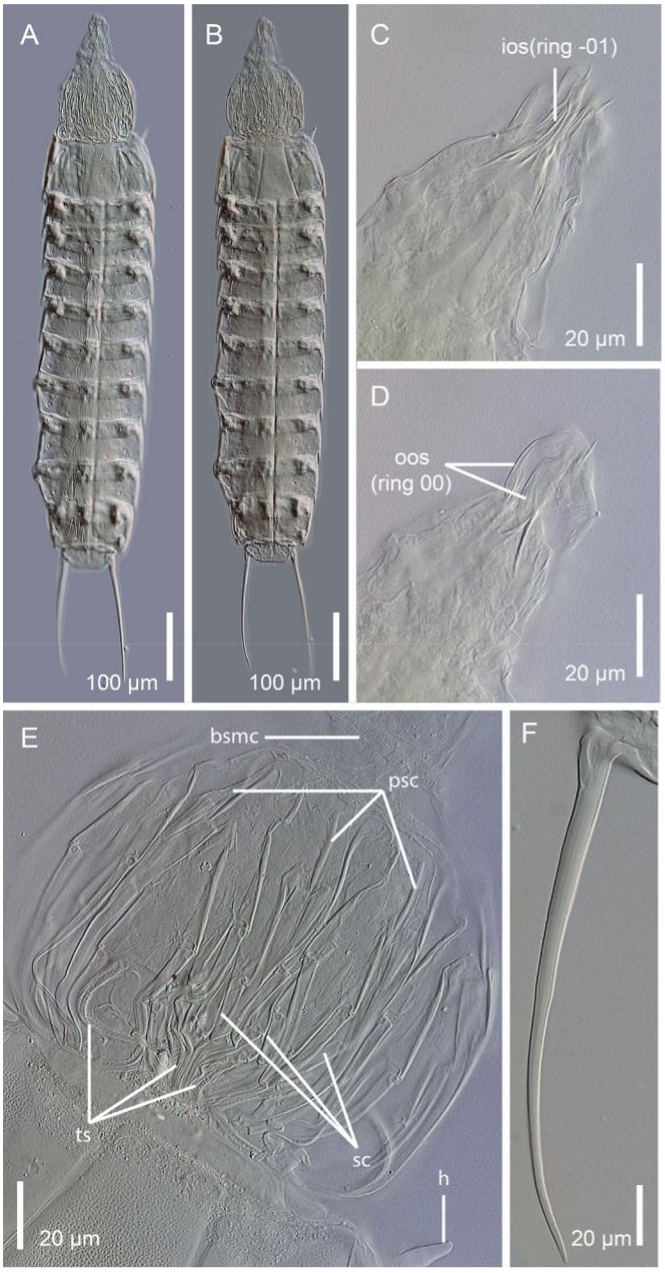

Fig. 3. Light micrographs showing trunk overviews and details in the mouth cone, introvert and lateral terminal spines characters of male holotype USNM 1558492 of *Cristaphyes fortis* sp. nov. (A) Dorsal overview of trunk; (B) ventral overview of trunk; (C) mouth cone, detail showing ring 01 of inner oral styles; (D) mouth cone, detail showing outer oral styles; (E) introvert, with detail of the first ring of primary spinoscalids (ring 01), remaining rings of regular scalids, trichoscalids; and horn-like extensions of segment 1; (F) detail of a lateral terminal spine. Abbreviations: bsmc, basal sheath of mouth cone; h, horn-like extension; ios, inner oral style; oos, outer oral style; psc, primary spinoscalid; sc, scalid; ts, trichoscalid.

side of the tergal plate. Paired sensory spots in subdorsal, laterodorsal and ventromedial positions, with the laterodorsal pair lateral to the setae (Figs. 2A, B and 4I, J).

Segment 6 similar to segment 4 in the arrangement of cuticular process, setae and sensory spots (Figs. 2A, B and 5A, B). Laterodorsal setae on this segment showing intraspecific variation as those of segment 5.

Segment 7 similar to segment 5 in the arrangement of cuticular process, setae and sensory spots, except for the presence of a single pair of ventrolateral setae (Figs. 2A, B and 5C, D).

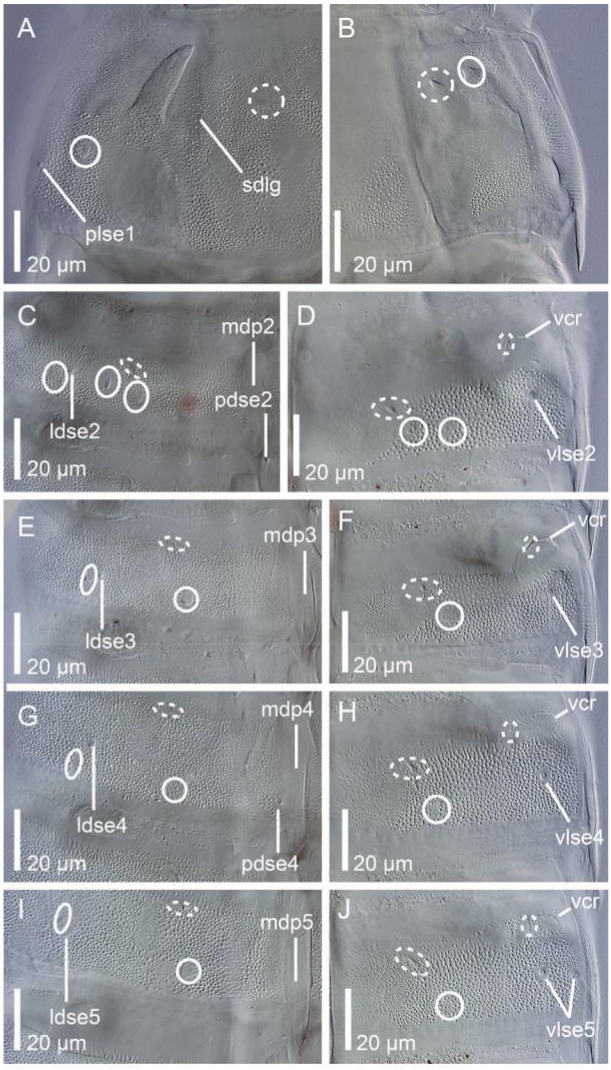

Fig. 4. Light micrographs showing details of cuticular trunk characters of segments 1-5 of male holotype USNM 1558492 of *Cristaphyes fortis* sp. nov., with main focus on glandular cell outlets, setae, sensory spots and cuticular processes. (A) Left half of tergal plate of segment 1; (B) right half of sternal plates of segment 1; (C) left half of tergal plate of segment 2; (D) right half of sternal plate of segment 2; (E) left half of tergal plate of segment 3; (F) right half of sternal plate of segment 3; (G) left half of tergal plate of segment 4; (H) right half of sternal plate of segment 4; (I) left half of tergal plate of segment 5; (J) right half of sternal plate of segment 5. Abbreviations: ldse, laterodorsal seta; mdp, middorsal process; pdse, paradorsal seta; plse, paralateral seta; sdlg, subdorsal longitudinal groove; vcr, ventral cuticular ridge; vlse, ventrolateral seta; sensory spots are marked as closed circles, and glandular cell outlets as dashed circles; numbers after abbreviation indicate the corresponding segment.

Segment 8 with middorsal process as on the preceding segment (Figs. 2B and 5E). Paired setae in laterodorsal, lateroventral and ventromedial positions (Figs. 2A, B and 5E, F). Paired sensory spots in subdorsal, laterodorsal and ventromedial positions, the latter mesial to ventromedial setae (Figs. 2A, B and 5E, F).

Segment 9 with middorsal process as on the preceding segment (Figs. 2B and 5G). Paired setae in laterodorsal and ventromedial positions (Figs. 2A, B and 5G, H). Laterodorsal setae with intraspecific variability, as those of segment 5. Paired sensory spots in subdorsal, laterodorsal and ventromedial positions (Figs. 2A, B and 5G, H), the latter lateral or mesial to the ventromedial setae. Paired nephridiopores in paralateral position; detailed morphology of nephridiopores not determined.

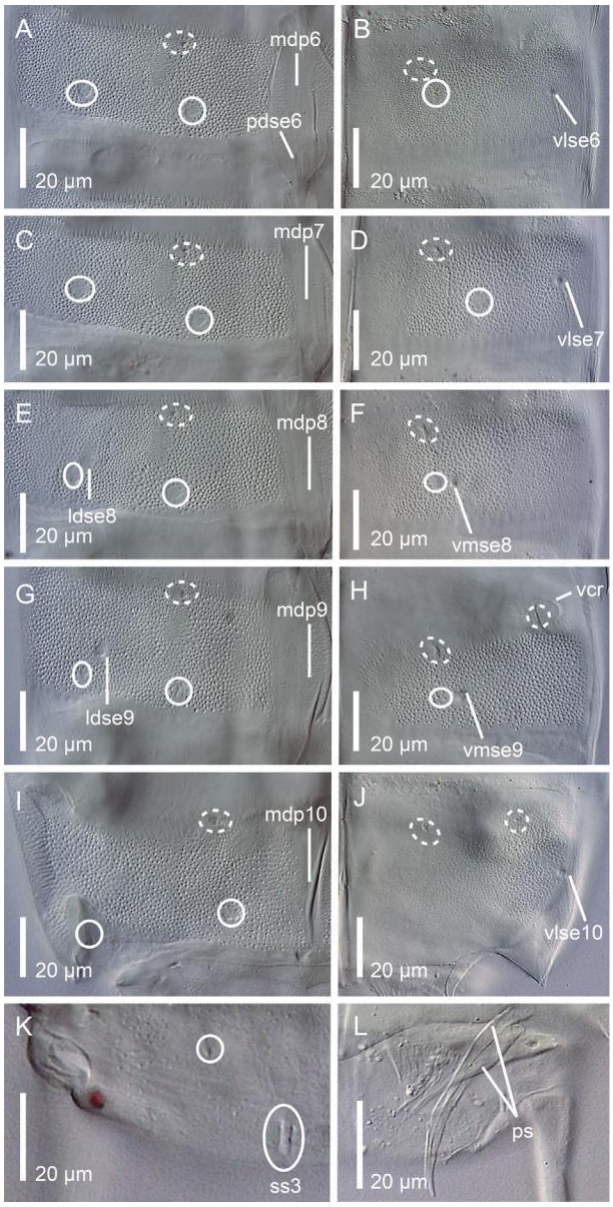

Fig. 5. Light micrographs showing details of cuticular trunk characters of segments 6-11 of male holotype USNM 1558492 of *Cristaphyes fortis* sp. nov., with main focus on glandular cell outlets, setae, sensory spots and cuticular processes. (A) Left half of tergal plate of segment 6; (B) right half of sternal plate of segment 6; (C) left half of tergal plate of segment 7; (D) right half of sternal plate of segment 7; (E) left half of tergal plate of segment 8; (F) right half of sternal plate of segment 8; (G) left half of tergal plate of segment 9; (H) right half of sternal plate of segment 9; (I) left half of tergal plate of segment 10; (J) right half of sternal plate of segment 10; (K) left half of tergal plate of segment 11; (L) right half of sternal plate of segment 11. Abbreviations: ldse, laterodorsal seta; mdp, middorsal process; pdse, paradorsal seta; ps, penile spine; ss3, type 3 sensory spot; vcr, ventral cuticular ridge; vlse, ventrolateral seta; vmse, ventromedial seta; sensory spots are marked as closed circles, and glandular cell outlets as dashed circles; numbers after abbreviation indicate the corresponding segment.

Segment 10 with short middorsal process, less developed than in previous segments (Figs. 2B and 5I). Paired setae in lateroventral and ventrolateral positions (Figs. 2A, B and 5J). Paired sensory spots in subdorsal and laterodorsal positions, near the posterior margin of segment (Figs. 2B and 5I).

Segment 11 with paired type 3 sensory spots in subdorsal and laterodorsal positions (Figs. 2B and 5K). Males with two pairs of stout, thick, penile spines and genital pores surrounded by a tuft of long hairs (Figs. 2A, B and 5L). Lateral terminal spines long (LTS:TL average ratio = 29.0%), slender, narrow, apparently rigid, with rounded tips (Figs. 2A, B and 3A, B, F).

Table 2

Measurements of adult *Cristaphyes fortis* sp. nov. from the lower Gulf of California, including number of measured specimens (*n*), mean of data and standard deviation (SD). There were no remarkable differences in size and/or dimension between the two sexes or sampling locations.

Character	Range	Mean (SD; *n*)
TL (µm)	618.8-664.6	644.5 (19.6; 4)
MSW-5 (µm)	151.6-171.2	159.9 (8.4; 4)
MSW-5/TL (%)	23.9-26.7	24.8 (1.3; 4)
SW-10 (µm)	120.6-134.4	128.8 (5.9; 4)
SW-10/TL (%)	19.5-21.0	20.0 (0.7; 4)
S1 (µm)	94.4-113.3	101.7 (8.5; 4)
S2 (µm)	54.3-67.3	60.8 (7.2; 4)
S3 (µm)	56.3-78.5	65.9 (9.4; 4)
S4 (µm)	62.6-68.0	65.2 (2.4; 4)
S5 (µm)	57.1-75.0	67.5 (7.7; 4)
S6 (µm)	65.3-86.6	72.7 (9.5; 4)
S7 (µm)	61.0-77.6	71.2 (7.1; 4)
S8 (µm)	56.7-83.6	69.6 (11.0; 4)
S9 (µm)	69.5-81.5	73.9 (5.5; 4)
S10 (µm)	76.2-86.9	81.3 (5.1; 4)
S11 (µm)	35.0-40.1	37.1 (2.3; 4)
LTS (µm)	173.6-197.4	186.5 (9.9; 4)
LTS/TL (%)	26.6-30.0	29.0 (1.6; 4)

Abbreviations: LTS, lateral terminal spine; MSW-5, maximum sternal width (on segment 5); S, segment lengths; SW-10, standard sternal width (on segment 10); TL, total length of trunk.

3.1.5. Remarks on differential characters

This species clearly belongs to the genus *Cristaphyes* by the following diagnostic features: middorsal processes on segments 2-10, surpassing the posterior margin of segments, progressively longer towards segment 9, and well-developed pachycycli and ball-and-socket joints of similar size on segments 2-10 (Sánchez et al. 2016). However, it may be distinguished from the remaining congeners by its unique arrangement of cuticular processes, setae and spines.

C. fortis sp. nov. is characterized by having lateral terminal spines on segment 11, and by lacking ventromedial, sexually dimorphic tubes in males, structures that are usually present in the family Pycnophyidae (Sánchez et al. 2016). Only *C. chilensis* (Lang, 1953), *C. cornifrons* Cepeda et al., 2019, *C. longicornis* (Higgins, 1983) and *C. nubilis* (Sánchez et al., 2014), share the combination of missing tubes and possessing lateral terminal spines with the new species. Moreover, *C. fortis* sp. nov., *C. cornifrons* and *C. longicornis* share the arrangement of middorsal processes throughout segments 2-10, whereas the middorsal processes of *C. chilensis* and *C. nubilis* are present from segment 1.

C. fortis sp. nov. can be distinguished from *C. cornifrons* and *C. longicornis* by its pattern of setae and spines. *C. longicornis* is characterized by having unpaired setae in paradorsal position on segments 2, 4, 6 and 8, whereas *C. fortis* sp. nov. possesses these unpaired paradorsal setae only on segments 2, 4 and 6. Moreover, *C. longicornis* has one pair of ventrolateral setae on segments 2, 5 and 10 and one pair of ventromedial setae on segments 1 and 3-9, while the new species has two pairs of ventrolateral setae on segment 5, one pair of ventrolateral setae on segments 2-4, 6-7 and 10, and one pair of ventromedial setae on segments 8-9. *C. cornifrons* is even more similar to *C. fortis* sp. nov. in the arrangement of the tergal setae, but differs remarkably on the sternal ones. Thus, *C. cornifrons* is characterized by having one pair of ventrolateral setae on segments 2-3, 5 and 10 (the last one only in

Table 3
Summary of nature and arrangement of sensory spots, glandular cell outlets, cuticular processes, setae, nephridiopores and spines in adults of *Cristaphyes fortis* sp. nov.

Segment	MD	PD	SD	LD	PL	LV	VL	VM
1			gco	ss	se		ss, gco	
2	cp	se:	gco, ssx2	gco, se, ss		se	se, gco	ssx2, gco
3	cp		gco, ss	gco, se, ss			se, gco	ss, gco
4	cp	se:	gco, ss	gco, se, ss		se	se, gco	ss, gco
5	cp		gco, ss	gco, se*, ss			sex2, gco	ss, gco
6	cp	se:	gco, ss	gco, se*, ss		se	se, gco	ss, gco
7	cp		gco, ss	gco, se*, ss			se, gco	ss, gco
8	cp		gco, ss	gco, se, ss		se	gco	ss, se, gco
9	cp		gco, ss	gco, se*, ss	ne		gco	ss, se, gco
10	cp		gco, ss	gco, ss		se	se, gco	gco
11			ss3	ss		lts, psx2 (m)		

Abbreviations: cp, cuticular process; gco, glandular cell outlet; LD, laterodorsal; lts, lateral terminal spine; LV, lateroventral; m, male condition of sexually dimorphic character; MD, middorsal; ne, nephridiopore; PD, paradorsal; PL, paralateral; ps, penile spine; SD, subdorsal; se, seta; ss, sensory spot; ss3, type 3 sensory spot; VL, ventrolateral; VM, ventromedial; * indicates intraspecific variation, and that structure may be paired, unpaired or absent; : indicates the presence of unpaired structures.

females) and one pair of ventromedial setae on segments 4-9, whereas *C. fortis* sp. nov. has two pairs of ventrolateral setae on segment 5, one pair of ventrolateral setae on segments 2-4, 6-7 and 10, and one pair of ventromedial setae on segments 8-9.

Genus ***Higginsium*** Sánchez et al., 2016.

3.2. ***Higginsium mazatlanensis*** sp. nov
(Figs. 6-9 and Tables 4 and 5)
urn:lsid:zoobank.org:act:0D79B812-D3CB-4CD9-8EE7-21361DF105A0

3.2.1. Type material

Adult male holotype (USNM 1558497) collected on May 18, 2018 near the mouth of Presidio River, south of Mazatlan, Sinaloa State, Mexico (southern Gulf of California), eastern Pacific (L3): 23 05 30 N, 106 17 45 W; 5 m depth; mounted in Fluoromount G®. Two adult males (USNM 1558499-1558500) and one adult female (USNM 1558498) paratypes with same collecting data as holotype; mounted in Fluoromount G®.

3.2.2. Diagnosis

Higginsium with middorsal elevations on segments 1-6, middorsal processes on segments 7-9 and middorsal small pointed projection on segment 10. Anterior margin of first segment with several minute, rounded glandular cell outlets. Unpaired seta in paradorsal position on segments 3, 5, 7 and 9-10; paired setae in paradorsal position on segments 2, 4, 6 and 8. Subdorsal setae on segment 1. Two pairs of laterodorsal setae on segments 2-9, those of even segments more mesial than those of odd segments. Paralateral setae on segment 1. Lateroventral setae on segments 2, 4, 6, 8 and 10 (two pairs on segment 10). Ventromedial setae on segments 2-9. Male with paired, sexually dimorphic ventromedial tubes on segment 2. Lateral terminal spines absent.

3.2.3. Etymology

The name makes refers to the municipality Mazatlán (Sinaloa State, Mexico), where the species was found.

3.2.4. Description

See Table 4 for measurements and dimensions, and Table 5 for summary of location of cuticular elevations, cuticular processes, setae, glandular cell outlets, nephridiopores and sensory spots.

Head with retractable mouth cone and introvert. The collected specimens were not suitable for head examination, hence data on number, morphology and arrangement of scalids and oral styles are not available.

Neck with four dorsal and two ventral sclerotized placids (Figs. 6A-C and 7C, D). Dorsal placids trapezoidal, flattened, with a lateral indentation near the posterior margin; mesial ones broader, not getting narrower towards the lateral sides; lateral ones getting narrower towards the lateral sides, with a concave anterior margin (Figs. 6B and 7C). Ventral placids similar to dorsal mesial ones (Figs. 6A, C and 7D).

Trunk markedly rectangular, stout, sclerotized, triangular in cross-section, composed of eleven segments (Figs. 6A, B and 7A, B). Segment 1 with one tergal, two episternal and one midsternal plate; midsternal plate of segment 1 trapezoidal, laterally extended at its base, with a lateral constriction near its anterior margin, with a straight posterior margin (Figs. 6A, B and 7A, B, D). Remaining trunk segments with one tergal and two sternal plates (Figs. 6A-D and 7A, B). Sternal plates reach their maximum width at segment 6, almost constant in width up to segment 9, progressively tapering towards the posterior end of trunk (Figs. 6A, B and 7A, B). Middorsal elevations on segments 1-6, short, pentagonally-shaped, distally rounded, not projecting beyond the posterior margin of segments, with intracuticular, butterfly-like atria of paradorsal sensory spots (Figs. 6A, B, 7A, 8A, C, E, G, I and 9A). Middorsal processes on segments 7-9, keel-shaped, with enlarged pointed tips, projecting beyond the posterior margin of segments, progressively longer in the last segments (Figs. 6B, 7A and 9C, E, G). Segment 10 also with a small, slightly pointed, very narrow middorsal elevation (Figs. 6B and 9I). Tergal plates of segments 1-10 with paired glandular cell outlets in subdorsal and ventromedial positions (ventral ones of segment 1 in ventrolateral position), near the anterior margin of segments, triangular to crescentic-shaped (Figs. 6A-C, 8A-J and 9A-J). Tergal plates of segments 2-7 with minute, rounded glandular cell outlets in laterodorsal position near the anterior margin of segments (Figs. 6B, 8C, E, G, I and 9A, C). Sternal plates of segments 2-10 with paired cuticular ridges marking the ventrolateral-ventromedial limit, quite inconspicuous on some segments, next to small glandular cell outlets (Figs. 6A, C, 8F, H, J and 9B, D, F, H). Segment 1 with several, minute, rounded glandular cell outlets, arranged dorsally along an anterior line running parallel to the anterior margin of segment, and ventrally in irregular patches (Figs. 6A-C and 8A, B). Muscular scars smooth, hairless, rounded to oval-shaped, in laterodorsal and ventromedial position on segments 1-10 (Figs. 6A-D, 8A-J and 9A-J). Pachycycli and ball-and-socket joints well-developed in segments 2-10 (Figs. 6A-D and 7A, B). Apodemes only slightly visible between segments 8-9, in paraventral position (Figs. 6A and 7B). Posterior margin of segments straight, with well-developed primary pectinate fringes strongly striated; secondary pectinate fringes developed as three wavy, transverse bands (Figs. 6A-D).

Segment 1 with middorsal elevation not projecting beyond the posterior margin of segment (Figs. 6B and 8A). Anterolateral margins of the tergal plate as horn-shaped, short, narrow, straight, distally pointed extensions (Figs. 6A-C, 7A, B and 8B). Paired setae in subdorsal, paralateral and ventrolateral

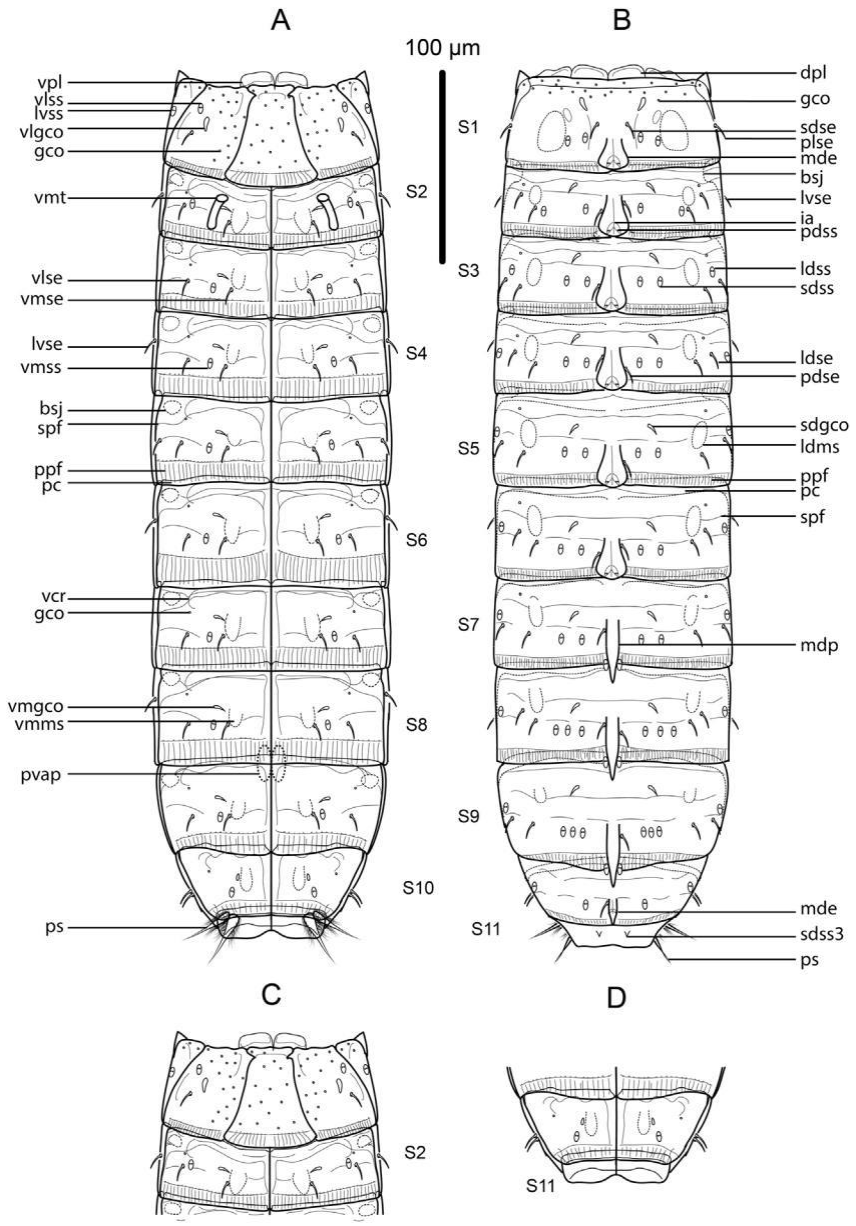

Fig. 6. Line art illustrations of *Higginsium mazatlanensis* sp. nov. (A) Male, ventral overview of trunk; (B) male, dorsal overview of trunk; (C) female, ventral overview of segments 1-2; (D) female, ventral overview of segments 10-11. Abbreviations: bsj, ball-and-socket joint; dpl, dorsal placid; gco, glandular cell outlet; ia, intracuticular atria; ldms, laterodorsal muscular scar; ldse, laterodorsal seta; ldss, laterodorsal sensory spot; lvse, lateroventral seta; lvss, lateroventral sensory spot; mde, middorsal elevation; mdp, middorsal process; pc, pachycycli; pdse, paradorsal seta; pdss, paradorsal sensory spot; plse, paralateral seta; ppf, primary pectinate fringe; ps, penile spine; pvap, paraventral apodeme; sdgco, subdorsal glandular cell outlet; sdse, subdorsal seta; sdss, subdorsal sensory spot; sdss3, subdorsal type 3 sensory spot; spf, secondary pectinate fringe; vcr, ventral cuticular ridge; vlgco, ventrolateral glandular cell outlet; vlse, ventrolateral seta; vlss, ventrolateral sensory spot; vmgco, ventromedial glandular cell outlet; vmms, ventromedial muscular scar; vmse, ventromedial seta; vmss, ventromedial sensory spot; vmt, ventromedial tube; vpl, ventral placid.

positions (Figs. 6A-C and 8A, B). Two pairs of sensory spots in subdorsal position; one pair immediately below the subdorsal glandular cell outlets, another pair lateral to the muscular scars (Figs. 6B and 8A). One pair of sensory spots in paradorsal, lateroventral and ventrolateral positions (Figs. 6A-C and 8A, B). Detailed morphology of sensory spots not determined.

Segment 2 with middorsal elevation as on the preceding segment (Figs. 6B and 8C). Two pairs of setae in laterodorsal position, more mesial than those of the following segment, aligned with the remaining laterodorsal pairs of setae of the even segments (Figs. 6B and 8C); one pair of setae in paradorsal, lateroventral, ventrolateral and ventromedial positions (Figs. 6A-C and 8C, D). Paradorsal pair of setae not transversally aligned, so one of the seta appears more anterior than the other (Figs. 6B and 8C). Paired sensory spots in paradorsal, subdorsal, laterodorsal and ventrolateral position (Figs. 6A-C and 8C, D). Sexually dimorphic male tubes in ventromedial position, lateral to the ventromedial glandular cell outlets, short and thick (Figs. 6A and 8D).

Segment 3 with middorsal elevation as on the preceding segment (Figs. 6B and 8E). Unpaired seta in paradorsal position (Figs. 6B and 8E). Two pairs of setae in laterodorsal position, more lateral than those of the preceding

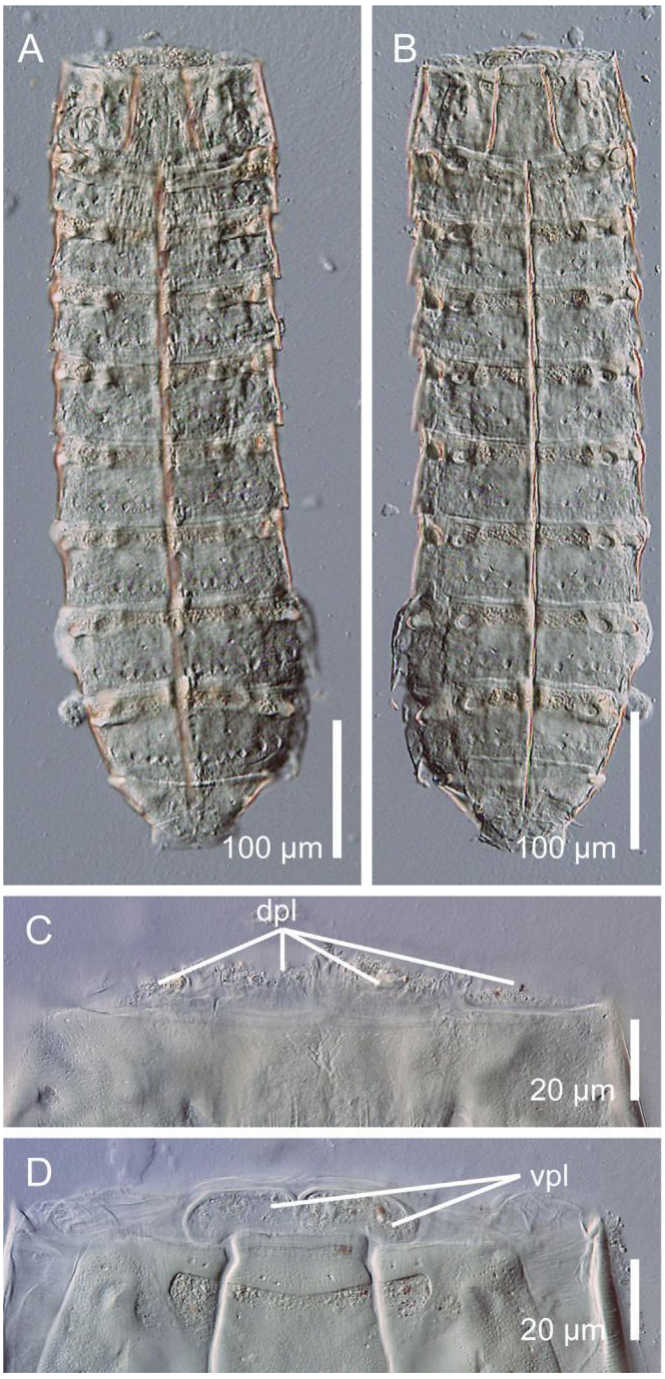

Fig. 7. Light micrographs showing trunk overviews and details in the neck of male holotype USNM 1558497 of *Higginsium mazatlanensis* sp. nov. (A) Dorsal overview of trunk; (B) ventral overview of trunk; (C) dorsal view of neck, with detail in the dorsal placids; (D) ventral view of the neck, with detail in the ventral placids. Abbreviations: dpl, dorsal placid; vpl, ventral placid.

segment, aligned with the remaining laterodorsal pairs of setae of the odd segments (Figs. 6B and 8E). One pair of setae in ventrolateral and ventromedial positions (Figs. 6A and 8F). Two pairs of sensory spots in subdorsal position (Figs. 6B and 8E); one pair of sensory spots in paradorsal, laterodorsal and ventromedial position (Figs. 6A, B and 8E, F).

Segment 4 with middorsal elevation as on the preceding segment (Figs. 6B and 8G). Two pairs of setae in laterodorsal position, aligned with the remaining laterodorsal pairs of setae of the even segments (Figs. 6B and 8G); one pair of setae in paradorsal, lateroventral, ventrolateral and ventromedial positions (Figs. 6A, B and 8G, H). Paradorsal pair of setae not transversally aligned, so one of the seta appears more anterior than the other (Figs. 6B and 8G). Two pairs of sensory spots in subdorsal position (Figs. 6B and 8G); one pair of sensory spots in paradorsal, laterodorsal and ventromedial position (Figs. 6A, B and 8G, H).

Segment 5 with middorsal elevation as on the preceding segment (Figs. 6B and 8I). Unpaired seta in paradorsal position, located on the opposite side of that of segment 3 (Figs. 6B and 8I). Two pairs of setae in laterodorsal position, aligned with the remaining laterodorsal pairs of setae of the odd segments, and in ventrolateral position (Figs. 6A, B and 8I, J); one pair of setae in ventromedial position (Figs. 6A and 8J). Two pairs of sensory spots in subdorsal position (Figs. 6B and 8I); one pair of sensory spots in paradorsal, laterodorsal and ventromedial position (Figs. 6A, B and 8I, J).

Segment 6 similar to segment 4 regarding the arrangement of cuticular elevation, setae and sensory spots (Figs. 6A, B and 9A, B).

Segment 7 with middorsal process projecting beyond the posterior margin of segment (Figs. 6B and 9C). Unpaired seta in paradorsal position, on the opposite side of that of segment 5 (Figs. 6B and 9C). Two pairs of setae in laterodorsal position, aligned with the remaining laterodorsal pairs of setae of the odd segments (Figs. 6B and 9C); one pair of setae in ventrolateral and ventromedial positions (Figs. 6A and 9D). Two pairs of sensory spots in subdorsal position (Figs. 6B and 9C); one pair of sensory spots in paradorsal, laterodorsal and ventromedial positions (Figs. 6A, B and 9C, D).

Segment 8 with middorsal process as in the preceding segment (Figs. 6B and 9E). Two pairs of setae in laterodorsal position, aligned with the remaining laterodorsal pairs of setae of the even segments (Figs. 6B and 9E); one pair of setae in paradorsal (not transversally arranged), lateroventral, ventrolateral and ventromedial positions (Figs. 6A, B and 9E, F). Three pairs of sensory spots in subdorsal position (Figs. 6B and 9E); one pair of sensory spots in paradorsal, laterodorsal and ventromedial positions (Figs. 6A, B and 9E, F).

Segment 9 with middorsal process as in the preceding segment (Figs. 6B and 9G). Unpaired seta in paradorsal position, on the opposite side of that of segment 7 (Figs. 6B and 9G). Two pairs of setae in laterodorsal position, aligned with the remaining laterodorsal pairs of setae of the odd segments (Figs. 6B and 9G); one pair of setae in ventrolateral and ventromedial positions (Figs. 6A and 9H). Three pairs of sensory spots in subdorsal position (Figs. 6B and 9G); one pair of sensory spots in paradorsal, laterodorsal and ventromedial positions (Figs. 6A, B and 9G, H). Paired nephridiopores in paralateral position; detailed morphology of nephridiopores not determined.

Segment 10 with slightly pointed, narrow middorsal elevation not surpassing the posterior margin of segment (Figs. 6B and 9I). Unpaired seta in paradorsal position, located on the opposite side of that of the preceding segment (Figs. 6B and 9I). Two pairs of setae in lateroventral position (Figs. 6A, B and 9J). Paired sensory spots in subdorsal, laterodorsal and ventromedial positions (Figs. 6A, B and 9I-J).

Segment 11 with paired type 3 sensory spots in subdorsal position, at the anterior half of segment (Figs. 6B and 9K). Posterior margin of segment of tergal plate straight, softly serrated; sternal plates form a pair of ventral extensions rounded distally (Figs. 6A, B, D and 9K-L). Male with two pairs of stout, thick, hairy penile spines (Figs. 6A, B and 9L). Lateral terminal spines absent.

3.2.5. Remarks on differential characters

H. mazatlanensis sp. nov. agrees well with the diagnosis of the genus (Sánchez et al. 2016), which currently encompasses four species:

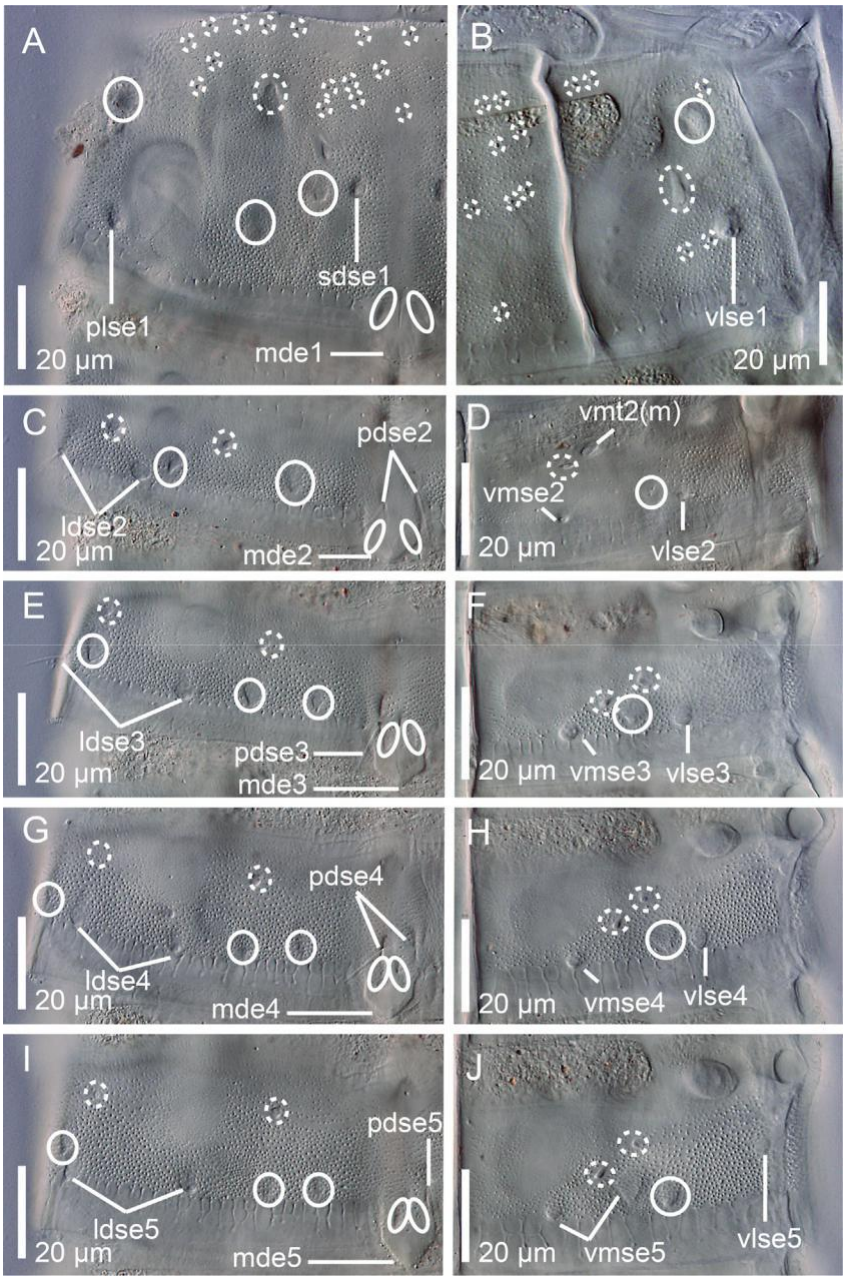

Fig. 8. Light micrographs showing details of cuticular trunk characters of segments 1-5 of male holotype USNM 1558497 of *Higginsium mazatlanensis* sp. nov., with main focus on glandular cell outlets, sensory spots, setae, cuticular elevations and tubes. (A) Left half of tergal plate of segment 1; (B) right half of sternal plates of segment 1; (C) left half of tergal plate of segment 2; (D) right half of sternal plates of segment 2; (E) left half of tergal plate of segment 3; (F) right half of sternal plates of segment 3; (G) left half of tergal plate of segment 4; (H) right half of sternal plates of segment 4; (I) left half of tergal plate of segment 5; (J) right half of sternal plates of segment 5. Abbreviations: ldse, laterodorsal seta; m, male condition of sexually dimorphic character; mde, middorsal elevation; pdse, paradorsal seta; plse, paralateral seta; sdse, subdorsal seta; vlse, ventrolateral seta; vmse, ventromedial seta; vmt, ventromedial tube; sensory spots are marked as closed circles, and glandular cell outlets as dashed circles; numbers after abbreviation indicate the corresponding segment.

Higginsium cataphractum (Higgins, 1961), described from San Juan Archipelago, Washington State (northeastern Pacific); *Higginsium dolichurum* (Sánchez et al., 2011), described from Ares Ria, Spain (northeastern Atlantic), and *Higginsium erismatum* (Higgins, 1983) and *Higginsium trisetosum* (Higgins, 1983), both described from Belize (Caribbean Sea).

H. dolichurum is the species that most differs from *Higginsium mazatlanensis* sp. nov., as lateral terminal spines are present in the former but absent in the latter. Similarly, *H. dolichurum* lacks sexually dimorphic tubes on the male segment 2, which are present in the new species. The remaining species of the genus (*H. cataphractum*, *H. erismatum* and *H. trisetosum*) and *H. mazatlanensis* sp. nov. share the lack of lateral terminal spines and the presence of sexually dimorphic tubes in ventromedial position on the male segment 2.

The available morphological information of *H. cataphractum* is rather scarce (Higgins 1961), and several diagnostic traits that would allow to easier distinction of this species from its congeners could not be observed in the re-examination of the type material by Sánchez et al. (2016) because of the bad preservation of the specimens. However, *H. cataphractum* is characterized

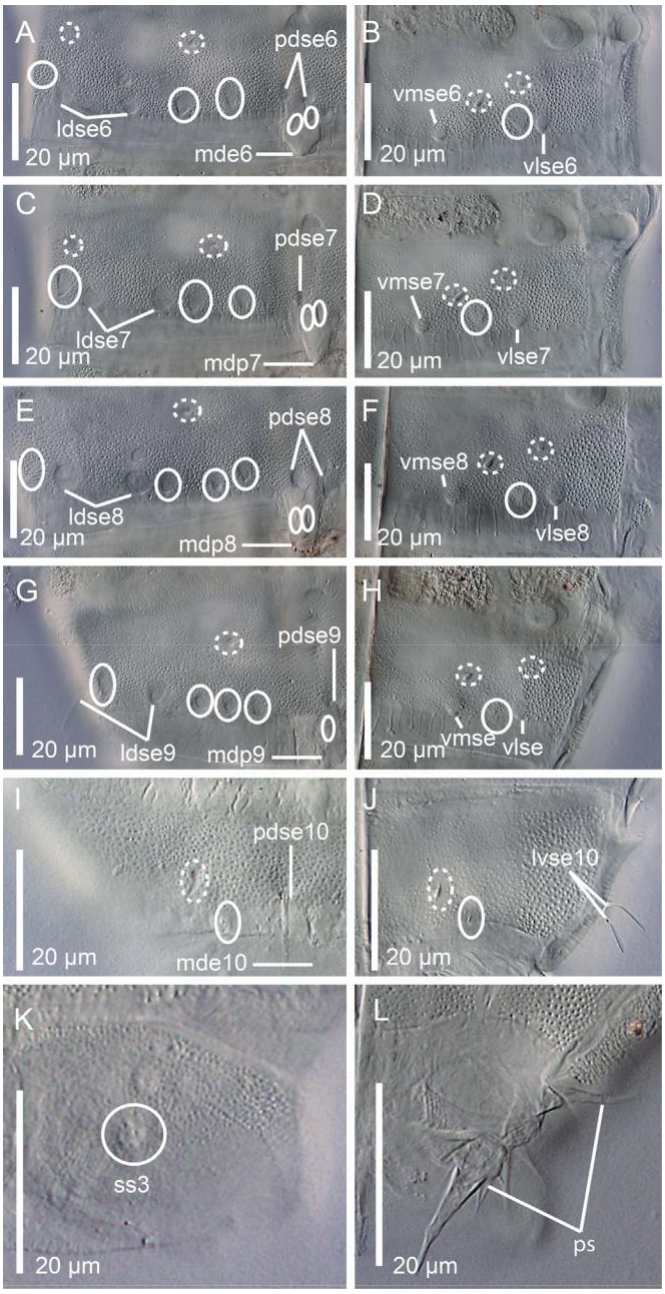

Fig. 9. Light micrographs showing details of cuticular trunk characters of segments 6-11 of male holotype USNM 1558497 of *Higginsium mazatlanensis* sp. nov., with main focus on glandular cell outlets, sensory spots, setae, cuticular elevations and cuticular processes. (A) Left half of tergal plate of segment 6; (B) right half of sternal plates of segment 6; (C) left half of tergal plate of segment 7; (D) right half of sternal plates of segment 7; (E) left half of tergal plate of segment 8; (F) right half of sternal plates of segment 8; (G) left half of tergal plate of segment 9; (H) right half of sternal plates of segment 9; (I) left half of tergal plate of segment 10; (J) right half of tergal and sternal plates of segment 10; (K) left half of tergal plate of segment 11; (L) right half of tergal and sternal plates of segment 11. Abbreviations: ldse, laterodorsal seta; lvse, lateroventral seta; mde, middorsal elevation; mdp, middorsal process; pdse, paradorsal seta; ps, penile spine; ss3, type 3 sensory spot; vlse, ventrolateral seta; vmse, ventromedial seta; sensory spots are marked as closed circles, and glandular cell outlets as dashed circles; numbers after abbreviation indicate the corresponding segment.

by having a single pair of laterodorsal setae on segments 2-9 and lateroventral setae on segments 2, 4, 6-8 and 10, while *H. mazatlanensis* sp. nov. has two pairs of laterodorsal

Table 4

Measurements of adult *Higginsium mazatlanensis* sp. nov. from Mazatlan, including number of measured specimens (*n*), mean of data and standard deviation (SD). There were no remarkable differences in size and/or dimension between the two sexes or sampling locations.

Character	Range	Mean (SD; *n*)
TL (µm)	527.7-581.5	563.9 (25.1; 4)
MSW-6 (µm)	107.5-151.6	133.9 (18.9; 4)
MSW-6/TL (%)	19.0-26.7	23.8 (3.5; 4)
SW-10 (µm)	90.5-104.6	96.7 (7.2; 4)
SW-10/TL (%)	16.0-18.0	17.1 (0.9; 4)
S1 (µm)	60.7-87.9	76.0 (11.3; 4)
S2 (µm)	52.0-57.6	52.6 (6.1; 4)
S3 (µm)	48.4-56.6	54.2 (5.7; 4)
S4 (µm)	53.0-61.4	58.1 (3.7; 4)
S5 (µm)	57.1-64.3	59.2 (3.4; 4)
S6 (µm)	65.4-76.4	68.8 (5.2; 4)
S7 (µm)	62.9-73.1	68.7 (4.3; 4)
S8 (µm)	60.3-84.6	73.3 (11.2; 4)
S9 (µm)	71.4-74.9	73.6 (1.6; 4)
S10 (µm)	39.2-52.7	43.5 (6.2; 4)
S11 (µm)	18.7-26.6	22.8 (3.8; 4)

Abbreviations: MSW-6, maximum sternal width (on segment 6); S, segment lengths; SW-10, standard sternal width (on segment 10); TL, total length of trunk.

setae on segments 2-9, one pair of lateroventral setae on segments 2, 4, 6 and 8 and two pairs on segment 10.

H. erismatum possesses paired, paradorsal setae only on even segments, a single pair of laterodorsal setae on segments 2-9, paired subdorsal setae on segments 2-9, paired ventrolateral setae on segments 1, 5, 7 and 9, whereas *H. mazatlanensis* sp. nov. is characterized by having unpaired paradorsal setae on segments 3, 5, 7 and 9-10, paired paradorsal setae on segments 2, 4, 6 and 8, two pairs of laterodorsal setae on segments 2-9, paired subdorsal setae only on segment 1, paired ventrolateral setae on segments 2-9. Additionally, the arrangement of ventromedial setae of *H. erismatum* is different in both sexes: the females possess these setae on segments 6-9, whereas males have ventromedial setae also on segments 3-5, while both males and females of *H. mazatlanensis* sp. nov. have two pairs on segment 5 and one pair on segments 2-4 and 6-9.

H. trisetosum is the species that resembles *H. mazatlanensis* sp. nov. the most. Both species have two pairs of laterodorsal setae on segments 2-9, midsternal plate of segment 1 with a mushroom-like appearance (due to a lateral constriction near its anterior margin) and secondary pectinate fringes of segments 2-9 composed of three transverse, wavy, softly serrated bands distributed throughout the anterior half of segments. Nevertheless, H. *trisetosum* has subdorsal setae on segments 2-9 and lateroventral setae on segments 1-10, whereas *H. mazatlanensis* sp. nov. has subdorsal setae only on segment 1 and lateroventral setae only on even segments. Moreover, the sternal plates of *H. trisetosum* have ventrolateral setae on segments 1 and 3-9, and ventromedial setae on segment 3-9 (females also on segment 2), while those of *H. mazatlanensis* sp. nov. bear ventrolateral setae on segments 1-9 and ventromedial setae on segments 2-9 (both males and females).

Another morphological feature that allows distinguishing *H. mazatlanensis* sp. nov. from its congeners is the possession of several, minute, rounded glandular cell outlets distributed near the anterior margin of the tergal plate of segment 1 and throughout the surface of the sternal plates of segment 1. These glandular cell outlets are absent in other species of *Higginsium*.

Class **Cyclorhagida** (Zelinka 1896) Sørensen et al. 2015.
Family **Echinoderidae** Zelinka 1894.

Table 5
Summary of nature and arrangement of sensory spots, glandular cell outlets, cuticular processes, cuticular elevations, setae, tubes, nephridiopores and spines in adults of *Higginsium mazatlanensis* sp. nov.

Segment	MD	PD	SD	LD	PL	LV	VL	VM
1	ce	ss	gco, se, ssx2	ss	se	ss	se, ss, gco	
2	ce	se, ss	gco, ss	gco, sex2, ss		se	se, ss, gco	se, gco, tu (m)
3	ce	se:, ss	gco, ssx2	gco, sex2, ss			se, gco	se, ss, gco
4	ce	se, ss	gco, ssx2	gco, sex2, ss		se	se, gco	se, ss, gco
5	ce	se:, ss	gco, ssx2	gco, sex2, ss			sex2, gco	se, ss, gco
6	ce	se, ss	gco, ssx2	gco, sex2, ss		se	se, gco	se, ss, gco
7	cp	se:, ss	gco, ssx2	gco, sex2, ss			se, gco	se, ss, gco
8	cp	se, ss	gco, ssx3	sex2, ss		se	se, gco	se, ss, gco
9	cp	se:, ss	gco, ssx3	sex2, ss	ne		se, gco	se, ss, gco
10	ce	se:	gco, ss	ss		sex2	gco	ss, gco
11			ss3			psx2 (m)		

Abbreviations: ce, cuticular elevation; cp, cuticular process; cpr, cuticular projection; gco, glandular cell outlet; LD, laterodorsal; LV, lateroventral; m, male condition of sexually dimorphic feature; MD, middorsal; ne, nephridiopore; PD, paradorsal; PL, paralateral; ps, penile spine; SD, subdorsal; se, seta; ss, sensory spot; ss3, type 3 sensory spot; tu, tube; VL, ventrolateral; VM, ventromedial; : indicates the presence of unpaired structures.

Genus ***Cephalorhyncha*** Adrianov, 1999 in Adrianov & Malakhov, 1999

3.3. ***Cephalorhyncha teresae*** sp. nov
(Figs. 10-12 and Tables 6 and 7)
urn:lsid:zoobank.org:act:260F18A5-472F-47EE-9EC7-51195C84E66B

3.3.1. Type material

Adult female holotype (USNM 1558501) collected on May 18, 2018 off Mazatlán, Sinaloa State, Mexico, eastern Pacific (L3): 23º05′30″N, 106º 17′45″W; 5 m depth; mounted in Fluoromount G®. Two adult male (USNM 1558502-1558503) and five adult female (USNM 1558504-1558508) paratypes with same collecting data as holotype; mounted in Fluoromount G®.

3.3.2. Diagnosis

Cephalorhyncha with middorsal, acicular spines on segments 4, 6 and 8, in sublateral position on segment 7, and in lateroventral position on segments 8-9. Tubes present in subdorsal position on segment 2 and in lateroventral position on segment 5. Primary pectinate fringe of segments 2-7 with a tuft of elongated spinous projections in middorsal position, whereas straight and not elongated on the sternal plates. Cuticular hairs generally scarce, distributed in one or two straight rows only in the posterior half of the cuticular plates, absent on segments 1 and 11.

3.3.3. Etymology

The species is dedicated to the dear mother of the first author, Mª Teresa Gómez Gómez, who always encouraged and supported him in his biological research.

3.3.4. Description

See Table 6 for measurements and dimensions, and Table 7 for summary of location of spines, tubes, nephridiopores, glandular cell outlets and sensory spots.

Head with retractable mouth cone and introvert (Fig. 11A, B, D, E). Although the holotype and two paratypes had the head partially everted, oral styles and scalids tended to collapse when mounted for LM. There were no available specimens for SEM examination, and only some details of these structures can be provided. Internal part of mouth cone with several rings of inner oral styles; exact number, morphology and arrangement of inner oral styles not determined. External part of mouth cone with a ring of 9 outer oral styles (Fig. 11D). Outer oral styles alternate between longer and shorter ones; five long styles appear anterior to the odd-numbered introvert sections, whereas four shorter ones appear anterior to the even-numbered introvert sections, except in the middorsal section 6 where a style is missing (Fig. 11D). Outer oral styles with two jointed subunits, with a rectangular, smooth basis and a triangular, hook-like, curved inwards, distal piece (Fig. 11D).

Introvert with several rings of cuticular scalids. Ring 01 with ten primary spinoscalids with of a short, quadrangular basal sheath and a distal, elongated end piece; distal piece thick, rounded in cross-section, smooth, hook-like (Fig. 11E). Remaining rings with several scalids also composed of two jointed subunits (Fig. 11E); detailed morphology and arrangement of these scalids not determined.

Neck with sixteen distinct, well-defined, trapezoidal placids, wider at base, with a marked joint between the neck and segment 1 (Figs. 10A, B and 11F, G); midventral one widest (ca. 7 µm wide at base) (Figs. 10A and 11G), remaining ones similar in width (ca. 5 µm wide at base) (Figs. 10A, B and 11F-G). Placids closely situated together at base, separated distally by cuticular folds (Figs. 10A, B and 11F-G). Six trichoscalids attach to the placids of the neck via small, oval trichoscalid plates (Figs. 10A, B and 11F-G).

Trunk slender, markedly tapered towards hind end, composed of eleven trunk segments (Figs. 10A, B and 11A, B). Segment 1 as closed cuticular ring (Figs. 10A, B, 11A, B and 12A, B); segment 2 with one tergal and one sternal cuticular plate (Figs. 10A, B, 11A, B, H and 12A, B); remaining ones with one tergal and two sternal cuticular plates (Figs. 10A, B, 11A, B and 12A, F). Sternal plate of segment 2 incompletely subdivided by an indistinct midventral fissure (Fig. 11H); tergosternal joints well-defined, but joint sites without posteriorly extending projections (Fig. 10A). Tergal anterior plates slightly bulging middorsally; posterior ones more flattened, giving the animal a tapering outline in lateral view. Sternal plates reach their maximum width at segment 6, progressively tapering towards the last trunk segments (Figs. 10A and 11B). Cuticular hairs scarce, distributed in one or two straight, transverse rows on each segment at the posterior half of the cuticular plates, except on segments 1 and 11 where cuticular hairs are absent (except those associated with the sensory spots) (Figs. 10A, B and 12A-F); cuticular hairs relatively long, flexible, emerging from rounded perforation sites (Figs. 12A-F). Most of sensory spots flanked by paired, elongated cuticular hairs (Figs. 10A, B and 12A-F). Posterior margin of segments straight, with well-developed primary pectinate fringes with conspicuously serrated free flaps (Figs. 10A, B and 12A-F); primary pectinate fringes of segments 2-8 forming a middorsal tuft of long, spinous projections (Figs. 10A, B and 12A, C). Secondary pectinate fringes well-developed, slightly extending beyond the limit of the primary pectinate fringes (Figs. 10A, B and 12A-F).

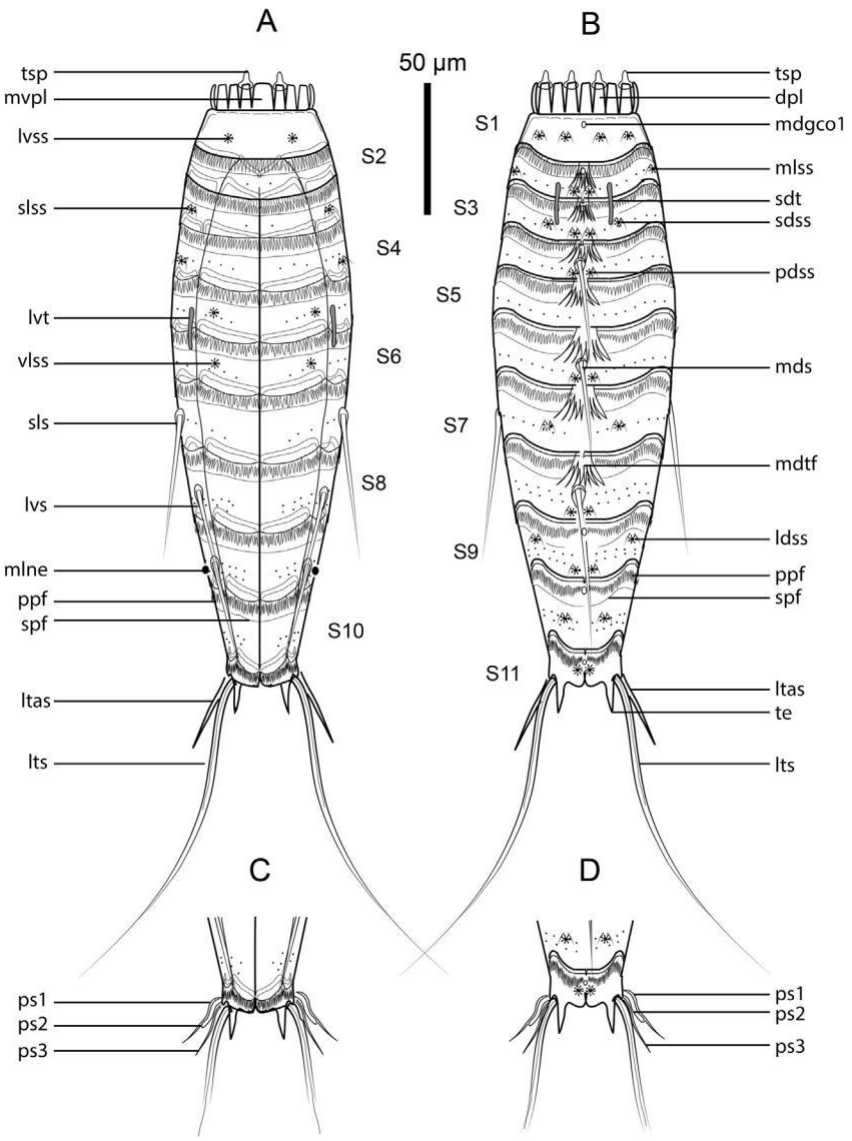

Fig. 10. Line art illustrations of *Cephalorhyncha teresae* sp. nov. (A) Ventral overview of female trunk; (B) dorsal overview of female trunk; (C) ventral view of male segments 10-11; (D) dorsal view of male segments 10-11. Abbreviations: dpl, dorsal placid; ldss, laterodorsal sensory spot; ltas, lateral terminal accessory spine; lts, lateral terminal spine; lvs, lateroventral spine; lvss, lateroventral sensory spot; lvt, lateroventral tube; mdgco1, middorsal type 1 glandular cell outlet; mds, middorsal spine; mdtf, middorsal tuft; mlne, midlateral nephridiopore; mlss, midlateral sensory spot; mvpl, midventral placid; pdss, paradorsal sensory spot; ppf, primary pectinate fringe; ps, penile spine; sdss, subdorsal sensory spot; sdt, subdorsal tube; sls, sublateral spine; slss, sublateral sensory spot; spf, secondary pectinate fringe; te, tergal extension; tsp, trichoscalid plate; vlss, ventrolateral sensory spot.

Segment 1 without spines, tubes or cuticular hairs (except those associated with the sensory spots). Unpaired type 1 glandular cell outlet in middorsal position, near the anterior margin of segment (Figs. 10B and 12A). Paired sensory spots in subdorsal, laterodorsal and lateroventral position, flanked by cuticular hairs, except the lateroventral ones (Figs. 10A, B and 12A, B); detailed morphology of these and remaining sensory spots not determined.

Segment 2 with paired large tubes in subdorsal position (Figs. 10B and 12A). Unpaired type 1 glandular cell outlet in middorsal position near the anterior margin of segment (Figs. 10B and 12A). Paired sensory spots in paradorsal and midlateral positions, flanked by cuticular hairs (Figs. 10B and 12A).

Segment 3 without spines or tubes. Unpaired type 1 glandular cell outlet in middorsal position, near the anterior margin of segment (Figs. 10B and 12A). Paired sensory spots in paradorsal, subdorsal and sublateral positions, flanked by cuticular hairs (Figs. 10A, B and 12A, B).

Segment 4 with a middorsal spine slightly exceeding the posterior edge of the following segment (Figs. 10B and 12A). Paired sensory spots in paradorsal and sublateral positions, the former posterior to the base of the middorsal spine, both laterally flanked by cuticular hairs (Figs. 10A, B and 12A, B).

Segment 5 with paired, thickened, very flexible tubes in lateroventral position (Figs. 10A and 12D). Paired sensory spots in ventrolateral position, near the intersection between the ventrolateral and the ventromedial regions, not flanked by cuticular hairs (Figs. 10A and 12D).

Segment 6 with a middorsal acicular spine exceeding the posterior edge of the following segment, but not reaching the posterior margin of segment 8 (Figs. 10B and 12C). Paired sensory spots in paradorsal and ventrolateral

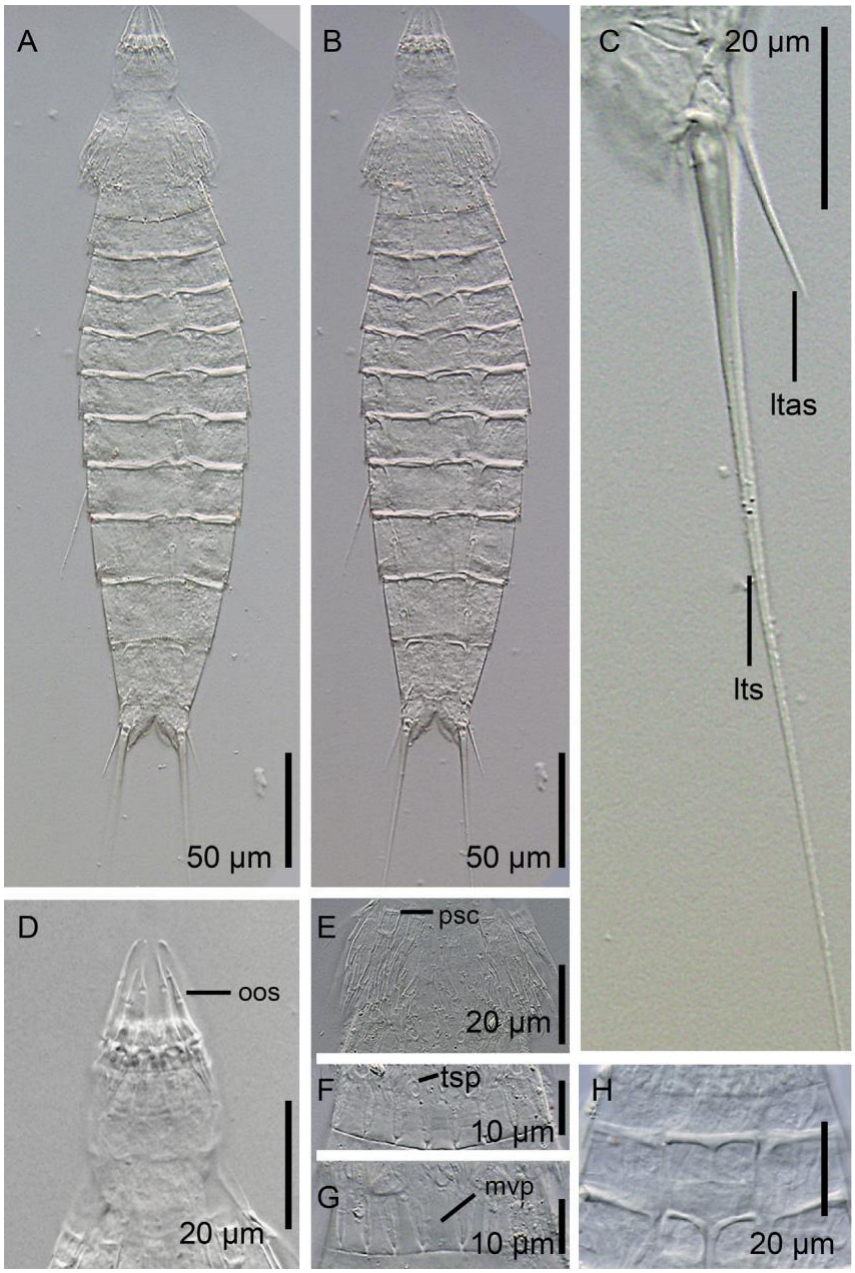

Fig. 11. Light micrographs showing trunk overviews and details in the head, neck, segment 2 and lateral terminal and lateral terminal accessory spines of female holotype USNM 1558501 of *Cephalorhyncha teresae* sp. nov. (A) Dorsal overview of trunk; (B) ventral overview of trunk; (C) ventral view of segment 11, with detail in the lateral terminal and the lateral terminal accessory spines; (D) mouth cone, with detail in the outer oral styles; (E) introvert, with detail in the primary spinoscalids; (F) dorsal view of neck, with detail in the placids and the trichoscalid plates; (G) ventral view of neck, with detail in the placids; (H) ventral view of segment 2. Abbreviations: ltas, lateral terminal accessory spine; lts, lateral terminal spine; mvp, midventral placid; oos, outer oral style; psc, primary spinoscalid; tsp, trichoscalid plate.

regions, the former posterior to the base of the middorsal spine, the latter aligned with those of the previous segment, without lateral cuticular hairs (Figs. 10A, B and 12C, D).

Segment 7 with paired acicular spines in sublateral position, slightly exceeding the posterior edge of the following segment (Figs. 10A, B and 12D). Paired sensory spots in subdorsal position, flanked by cuticular hairs (Figs. 10B and 12C).

Segment 8 with a middorsal acicular spine exceeding the posterior edge of segment 10 but not reaching the posterior end of trunk, and paired acicular spines in lateroventral position, not reaching the posterior edge of the following segment (Figs. 10A, B and 12C, D). Paired sensory spots in paradorsal position, flanked by cuticular hairs (Figs. 10B and 12C).

Segment 9 with paired acicular spines in lateroventral position, slightly exceeding the posterior edge of the following segment (Figs. 10A and 12F). Unpaired type 1 glandular cell outlet in middorsal position, near the anterior margin of segment (Figs. 10B and 12E). Paired sensory spots in paradorsal and laterodorsal positions, flanked by cuticular hairs (Figs. 10B and 12E). Paired nephridiopores in midlateral position (Figs. 10A and 12F); detailed morphology of nephridiopores not determined.

Segment 10 without spines or tubes. Unpaired type 1 glandular cell outlet in middorsal position, near the anterior margin of segment

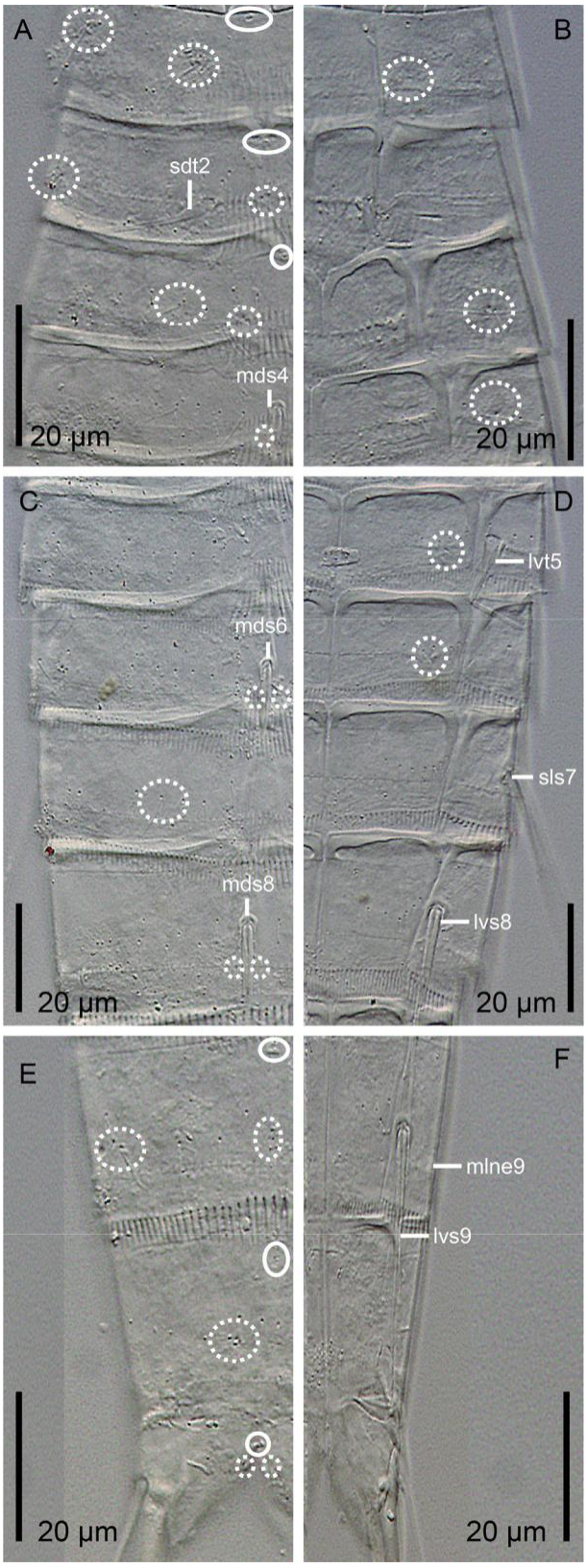

Fig. 12. Light micrographs showing details of cuticular trunk characters of segments 1-11 of female holotype USNM 1558501 of *Cephalorhyncha teresae* sp. nov., with main focus on glandular cell outlets, sensory spots, nephridiopores, tubes and spines. (A) Left half of tergal plate of segments 1-4; (B) right half of sternal plates of segments 1-4; (C) left half of tergal plate of segments 5-8; (D) right half of sternal plates of segments 5-8; (E) left half of tergal plate of segments 9-11; (F) right half of sternal plates of segments 9-11. Abbreviations: lvt, lateroventral tube; lvs, lateroventral spine; mds, middorsal spine; mlne, midlateral nephridiopore; sdt, subdorsal tube; sls, sublateral spine; sensory spots are marked as closed circles, and glandular cell outlets as dashed circles; numbers after abbreviation indicate the corresponding segment.

Table 6

Measurements of adult *Cephalorhyncha teresae* sp. nov. from Mazatlán, including number of measured specimens (*n*), mean of data and standard deviation. Remarkable differences in size and/or dimension between the two sexes were not detected.

Character	Range	Mean (SD; *n*)
TL (µm)	178.5-233.4	204.9 (22.1; 8)
MSW-6 (µm)	30.1-40.4	38.5 (5.9; 5)
MSW-6/TL (%)	14.0-17.8	18.2 (4.1; 5)
SW-10 (µm)	14.4-27.6	21.8 (5.3; 5)
SW-10/TL (%)	7.0-14.9	10.3 (3.0; 5)
S1 (µm)	12.6-19.2	16.2 (2.2; 8)
S2 (µm)	15.3-21.9	19.5 (2.2; 8)
S3 (µm)	18.3-24.9	21.9 (2.3; 8)
S4 (µm)	20.0-28.7	23.4 (2.9; 8)
S5 (µm)	22.7-29.5	26.0 (2.7; 8)
S6 (µm)	22.5-32.6	28.1 (3.3; 8)
S7 (µm)	29.9-34.3	32.6 (2.7; 8)
S8 (µm)	28.9-35.7	32.9 (2.6; 8)
S9 (µm)	32.2-35.9	34.0 (1.1; 8)
S10 (µm)	20.9-32.7	28.3 (4.4; 8)
S11 (µm)	20.7-26.2	22.5 (2.0; 8)
SD2 (tu) (µm)	9.6-15.0	13.1 (2.4; 7)
MD4 (ac) (µm)	28.5-40.3	35.0 (4.7; 7)
MD6 (ac) (µm)	40.1-52.7	48.7 (4.2; 7)
MD8 (ac) (µm)	47.2-73.8	63.4 (8.5; 8)
LV5 (tu) (µm)	9.8-27.0	17.2 (5.4; 8)
SL7 (ac) (µm)	37.8-52.4	48.5 (6.1; 7)
LV8 (ac) (µm)	33.4-40.3	37.0 (2.4; 8)
LV9 (ac) (µm)	37.7-42.5	40.1 (1.6; 8)
LTS (µm)	93.4-130.5	110.3 (13.4; 7)
LTAS (µm)	22.1-23.8	23.0 (0.7; 6)
LTS/TL (%)	46.1-64.5	53.3 (3.3; 7)
LTAS/TL (%)	9.5-13.3	11.5 (1.7; 6)
LTAS/LTS (%)	17.0-25.0	20.4 (3.0; 6)

Abbreviations: ac, acicular spine; LTAS, lateral terminal accessory spine; LTS, lateral terminal spine; LV, lateroventral; MD, middorsal; MSW-6, maximum sternal width (on segment 6); S, segment lengths; SD, subdorsal; SL, sublateral; SW-10, standard sternal width (on segment 10); TL, total length of trunk; tu, tube.

Table 7

Summary of nature and arrangement of spines, tubes, sensory spots, glandular cell outlets and nephridiopores in adults of *Cephalorhyncha teresae* sp. nov.

Segment	MD	PD	SD	LD	ML	SL	LA	LV	VL
1	gco1		ss	ss				ss	
2	gco1	ss	tu		ss				
3	gco1	ss	ss			ss			
4	ac	ss				ss			
5								tu	ss
6	ac	ss							ss
7			ss			ac			
8	ac	ss						ac	
9	gco1	ss		ss	ne			ac	
10	gco1		ss						
11	gco1	ss			psx3 (m)		ltas (f)	lts	

Abbreviations: ac, acicular spine; f, female condition of sexually dimorphic char-acter; gco1, type 1 glandular cell outlet; LA, lateral accessory; LD, laterodorsal; ltas, lateral terminal accessory spine; lts, lateral terminal spine; LV, lateroventral; m, male condition of sexually dimorphic character; MD, middorsal; ML, midlateral; ne, nephridiopore; PD, paradorsal; ps, penile spine; SD, subdorsal; SL, sublateral; ss, sensory spot; tu, tube; VL, ventrolateral.

(Figs. 10B and 12E). Paired sensory spots in subdorsal position near the posterior margin of segment, flanked by cuticular hairs (Figs. 10B and 12E).

Segment 11 with lateral terminal spines long (LTS:TL average ratio = 53.3%), slender, flexible, pointed distally, with a central cavity

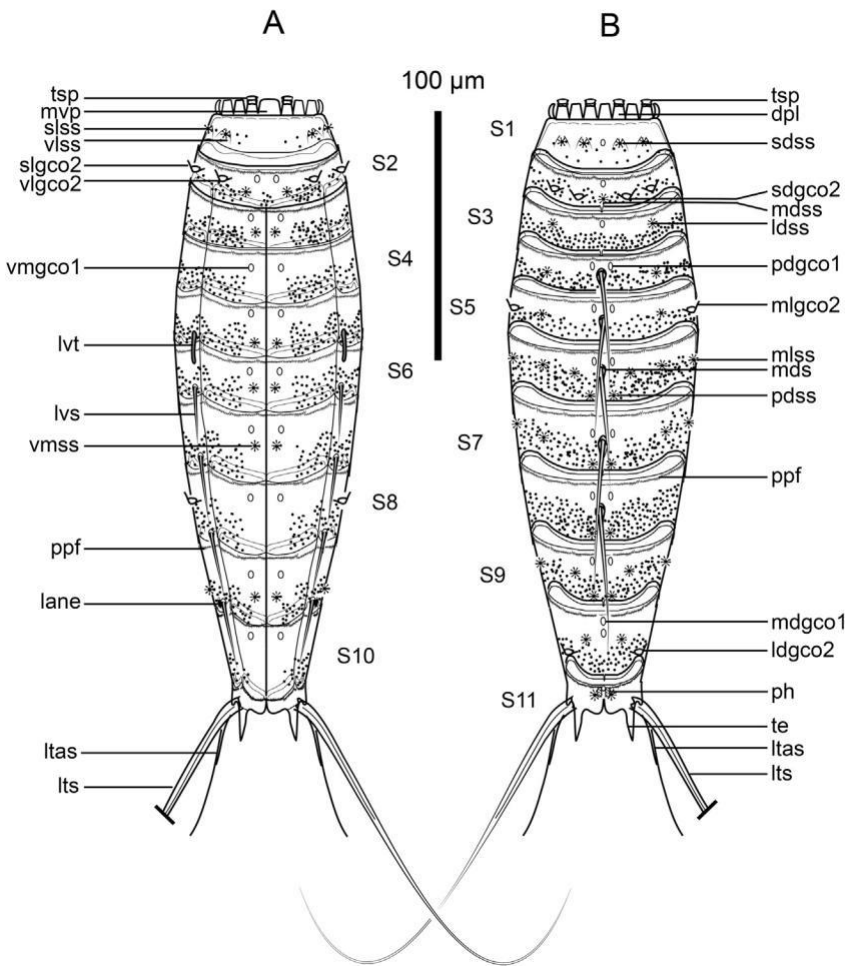

Fig. 13. Line art illustrations of *Echinoderes xalkutaat* sp. nov. (A) Ventral overview of female trunk; (B) dorsal overview of female trunk. Abbreviations: dpl, dorsal placid; lane, lateral accessory nephridiopore; ldgco2, laterodorsal type 2 glandular cell outlet; ldss, laterodorsal sensory spot; ltas, lateral terminal accessory spine; lts, lateral terminal spine; lvs, lateroventral spine; lvt, lateroventral tube; mdgco1, middorsal type 1 glandular cell outlet; mds, middorsal spine; mdss, middorsal sensory spot; mlgco2, midlateral type 2 glandular cell outlet; mlss, midlateral sensory spot; mvp, midventral placid; pdgco1, paradorsal type 1 glandular cell outlet; pdss, paradorsal sensory spot; ph, patch of hairs; ppf, primary pectinate fringe; sdgco2, subdorsal type 2 glandular cell outlet; sdss, subdorsal sensory spot; slgco2, sublateral type 2 glandular cell outlet; slss, sublateral sensory spot; te, tergal extension; tsp, trichoscalid plate; vlgco2, ventrolateral type 2 glandular cell outlet; vlss, ventrolateral sensory spot; vmgco1, ventromedial type 1 glandular cell outlet; vmss, ventromedial sensory spot.

(Figs. 10A, B and 11C). Males with three pairs of penile spines; one pair short, rigid and stubby, the other ones longer, pointed and much more flexible (Figs. 10C, D). Females with paired lateral terminal accessory spines, much shorter than lateral terminal ones (LTAS:LTS average ratio = 11.5%) (Figs. 10A, B and 11C). Unpaired type 1 glandular cell outlet in middorsal position, near the anterior margin of segment (Figs. 10B, D and 12E). Paired sensory spots in paradorsal position, flanked by cuticular hairs, near the posterior margin of segment (Figs. 10B, D and 12E). Tergal plate with tergal extensions long and pointed distally (Figs. 10B, D and 12E). Sternal plates with rounded sternal extensions (Figs. 10A, C and 12F).

3.3.5. Remarks on differential characters

C. teresae sp. nov. agrees well with the diagnosis of the genus (Adrianov & Malakhov 1999; Neuhaus & Blasche 2006). With the description of the new species, the genus is currently composed of six species: *C. asiatica* (Adrianov, 1989), *C. liticola* Sørensen, 2008, *C. flosculosa* Yildiz et al., 2016, *C. nybakkeni* (Higgins, 1986), a newly described species from Pacific polymetallic nodules (see Sánchez et al., 2019), and *C. teresae* sp. nov. The former five species are characterized by having middorsal, acicular spines on segments 4-8 as well as lateral spines and/or tubes on segments 5-9. *C. teresae* sp. nov. possesses middorsal, acicular spines only on segments 4, 6 and 8, and lateral spines on segments 8-9 only. Additionally, the five known species share the presence of paired ventrolateral spines or tubes on segment 2, while *C. teresae* sp. nov. has paired tubes in subdorsal position on this segment. Moreover, *C. teresae* sp. nov. is unique among its congeners in the sublateral position of the spines of segment 6.

Regarding the trunk habitus, *C. teresae* sp. nov. is more similar to *C. asiatica*, with a body outline closer to that of the genus *Echinoderes*, whereas *C. nybakkeni* is a slender species more similar to some species of *Meristoderes*, and *C. flosculosa* and *C. liticola* are characterized by having laterally compressed bodies.

Furthermore, most species of the genus have midventral tufts of elongated, spinous extensions belonging to the primary pectinate fringes on most of the trunk segments, which are absent in the newly described species. However, *C. teresae* sp. nov. is unique also in the middorsal position of these tufts of elongated spinous elongations on segments 2-7.

Genus ***Echinoderes*** Claparède, 1863.

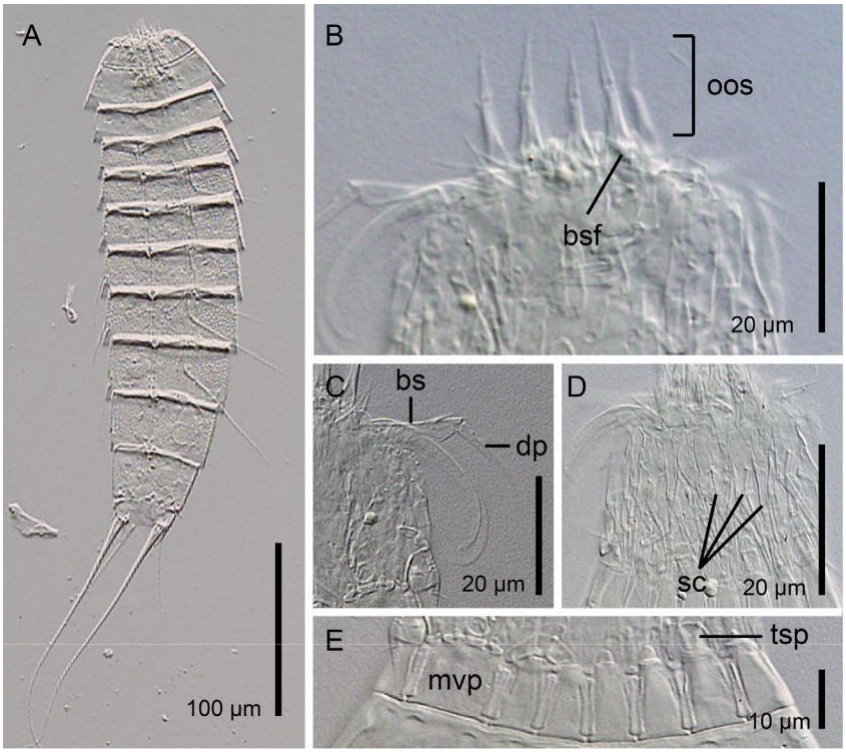

Fig. 14. Light micrographs showing trunk overview and detail in the head and neck of female holotype USNM 1558509 of *Echinoderes xalkutaat* sp. nov. (A) Overview of trunk, showing the lateral and ventral regions of the cuticular plates; (B) mouth cone, with detail of the outer oral styles; (C) introvert, with detail of a primary spinoscalid; (D) overview of introvert, showing the rings of regular scalids; (E) overview of neck, showing some ventral and lateral placids. Abbreviations: bs, basal sheath; bsf, basal sheath's fringe; dp, distal end piece; mvp, midventral placid; oos, outer oral style; sc, scalid; tsp, trichoscalid plate.

3.4. ***Echinoderes xalkutaat*** sp. nov
(Figs. 13-16 and Tables 8 and 9)
urn:lsid:zoobank.org:act:112843D9-15DE-4013-9C00-C2B2445BD537

3.4.1. Type material

Adult female holotype (USNM 1558509) collected on February 11, 2007 at the central Gulf of California, eastern Pacific (St18): 27º09′08″N, 111º39′57″W; 1440 m depth; mounted in Fluoromount G®. Two adult female paratypes (USNM 1558510e1558511) with same collecting data as holotype; mounted in Fluoromount G®.

3.4.2. Diagnosis

Echinoderes with middorsal spines on segments 4-8, lateroventral spines on segments 6-9, and lateroventral tubes on segment 5. Type 2 glandular cell outlets present in subdorsal, laterodorsal, sublateral and ventrolateral positions on segment 2, in midlateral position on segment 5, in sublateral position on segment 8 and laterodorsal position in segment 10. Segment 11 composed of one tergal and two sternal plates, lacking cuticular hairs but with short, tiny hair-like extensions in paradorsal position.

3.4.3. Etymology

The species is named after the myth of the monster "Xalkutaat" of the Paipai people of Santa Catarina, Baja California. According to the legend, Xalkutaat would be a dragon-like creature endowed with fire faced and defeated by a child called "Pies Ligeros" (meaning Light Feet), who gave fire to humanity.

3.4.4. Description

See Table 8 for measurements and dimensions, and Table 9 for summary of the location of spines, tubes, nephridiopores, glandular cell outlets and sensory spots.

Head with retractable mouth cone and introvert (Fig. 14B-D). Although one of the paratypes had the introvert partially everted, oral styles and scalids tended to collapse when mounted for LM. There were no available specimens for SEM examination, and only some details of these structures can be provided. Internal part of mouth cone with several rings of inner oral styles; exact number, arrangement and morphology of inner oral styles not determined. External part of mouth cone with 9 outer oral styles. Outer oral styles alternate between slightly longer and slightly shorter ones (Fig. 14B); five long styles appear anterior to the odd-numbered introvert sections, whereas four sligthly shorter ones appear anterior to the even-numbered introvert sections, except in the middorsal section 6 where a style is missing. Outer oral styles with two jointed subunits, with rectangular basis bearing a short, medial fringe, and a triangular, hook-like, distal structure (Fig. 14B).

Introvert with several rings of scalids. Ring 01 with ten primary spinoscalids with a short, rectangular basal sheath and a distal, long end piece; distal piece wide, rounded to oval in cross-section, smooth, hook-like, with blunt tip (Fig. 14C). Remaining rings with several scalids also composed of two jointed subunits (Fig. 14D); detailed morphology and arrangement of these scalids not determined.

Neck with sixteen trapezoidal placids, wider at base, with a distinct joint between the neck and segment 1 (Figs. 13A and B and 14E); midventral one widest (ca. 12 µm wide at base) (Figs. 13A and 14E), remaining ones alternate between wider and narrower (6-8 µm wide at base) (Figs. 13A, B and 14E). Placids situated closely together at base, separated distally by cuticular folds(Figs. 13A, B and 14E). Six hairy trichoscalids attach to small,

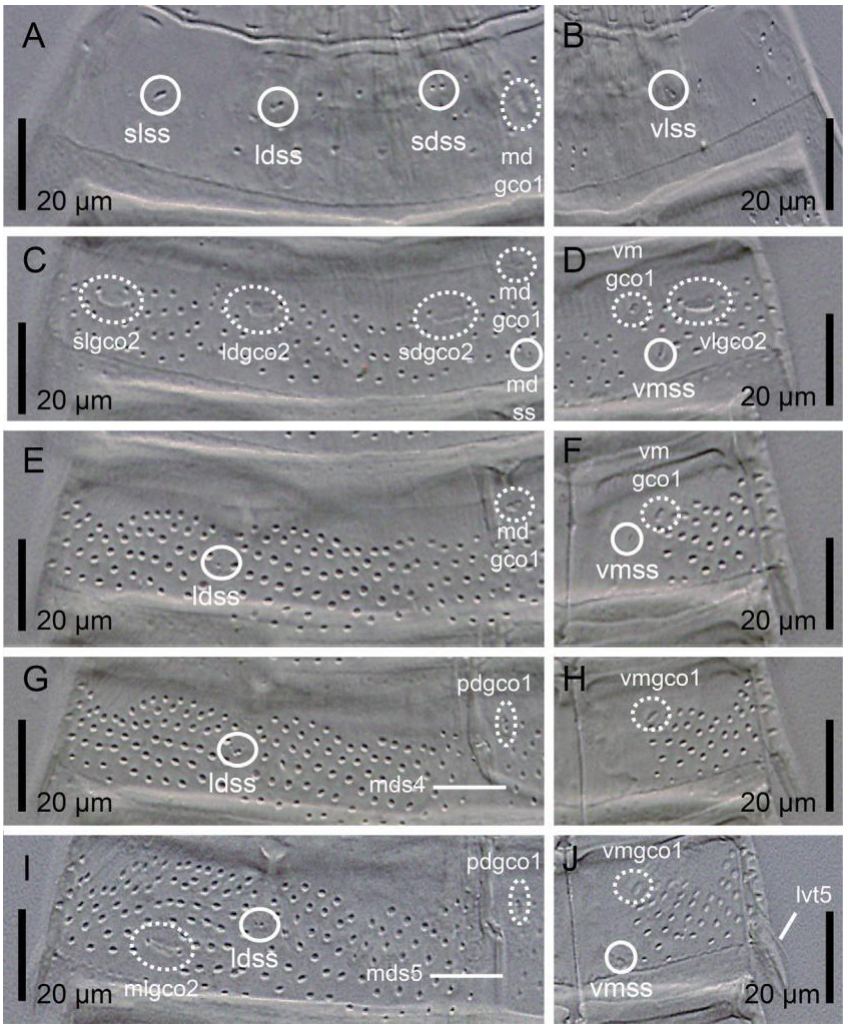

Fig. 15. Light micrographs showing details of cuticular trunk characters of segments 1-5 of female holotype USNM 1558509 of *Echinoderes xalkutaat* sp. nov., with main focus on spines, tubes, sensory spots and glandular cell outlets. (A) Left half of ring plate of segment 1; (B) right half of ring plate of segment 1; (C) left half of ring plate of segment 2; (D) right half of ring plate of segment 2; (E) left half of tergal plate of segment 3; (F) right sternal plate of segment 3; (G) left half of tergal plate of segment 4; (H) right sternal plate of segment 4; (I) left half of tergal plate of segment 5; (J) right sternal plate of segment 5. Abbreviations: ldgco2, laterodorsal type 2 glandular cell outlet; ldss, laterodorsal sensory spot; lvt, lateroventral tube; mdgco1, middorsal type 1 glandular cell outlet; mds, middorsal spine; mdss, middorsal sensory spot; pgco1, paradorsal type 1 glandular cell outlet; sdgco2, subdorsal type 2 glandular cell outlet; sdss, subdorsal sensory spot; slgco2, sublateral type 2 glandular cell outlet; slss, sublateral sensory spot; vlgco2, ventrolateral type 2 glandular cell outlet; vlss, ventrolateral sensory spot; vmgco1, ventromedial type 1 glandular cell outlet; vmss, ventromedial sensory spot; sensory spots are marked as closed circles, and glandular cell outlets as dashed circles; numbers after abbreviation indicate the corresponding segment.

longitudinally compressed trichoscalid plates (Figs. 13A, B and 14E).

Trunk markedly slender, distally tapered, composed of eleven trunk segments (Figs. 13A, B and 14A). Segments 1-2 as closed cuticular rings; remaining ones with one tergal and two sternal plates (Figs. 13A, B, 14A, 15A-J and 16A-H). Tergal anterior plates slightly bulging middorsally; posterior ones more flattened, giving the animal a tapering outline in lateral view (Fig. 14A). Sternal plates reach their maximum width at segment 7, progressively tapering towards the last trunk segments (Figs. 13A and 14A). Cuticular hairs densely distributed all over the trunk in irregular, transverse rows increasing in number towards the posterior end of trunk, plus unpaired midventral patches, except the mesial half of sternal plates of segments 3-10, the anterior half of segment 10 and all of segment 11 where cuticular hairs are absent (Figs. 13A, B, 14A, 15A-J and 16A-H). Posterior margin of segments straight, with well-developed primary pectinate fringes that possess elongated, strongly serrated free flaps; secondary pectinate fringes not detected with LM (Fig. 13A, B).

Segment 1 without spines or tubes. Unpaired type 1 glandular cell outlet in middorsal position (Figs. 13B and 15A). Paired sensory spots in subdorsal, laterodorsal, sublateral and ventrolateral positions (Figs. 13A, B and 15A, B).

Segment 2 without spines or tubes. Unpaired type 1 glandular cell outlet in middorsal position (Figs. 13B and 15C), and paired in ventromedial position (Figs. 13A and 15D). Paired type 2 glandular cell outlets in subdorsal, laterodorsal, sublateral and ventrolateral positions; type 2 glandular cell outlets on this and remaining segments flanked by lateral marginal elongated cuticular hairs (Figs. 13A, B and 15C, D). Unpaired sensory spot in middorsal position, posterior to the middorsal type 1 glandular cell outlet (Figs. 13B and 15C); paired sensory spots in ventromedial position, lateral to the ventromedial type 1 glandular cell outlets, not aligned with those of following segments (Figs. 13A and 15D).

Segment 3 without spines or tubes. Unpaired type 1 glandular cell outlet in middorsal position (Figs. 13B and 15E), and paired in ventromedial position (Figs. 13A and 15F). Paired sensory spots in laterodorsal and ventromedial positions, the latter mesial and posterior to the ventromedial

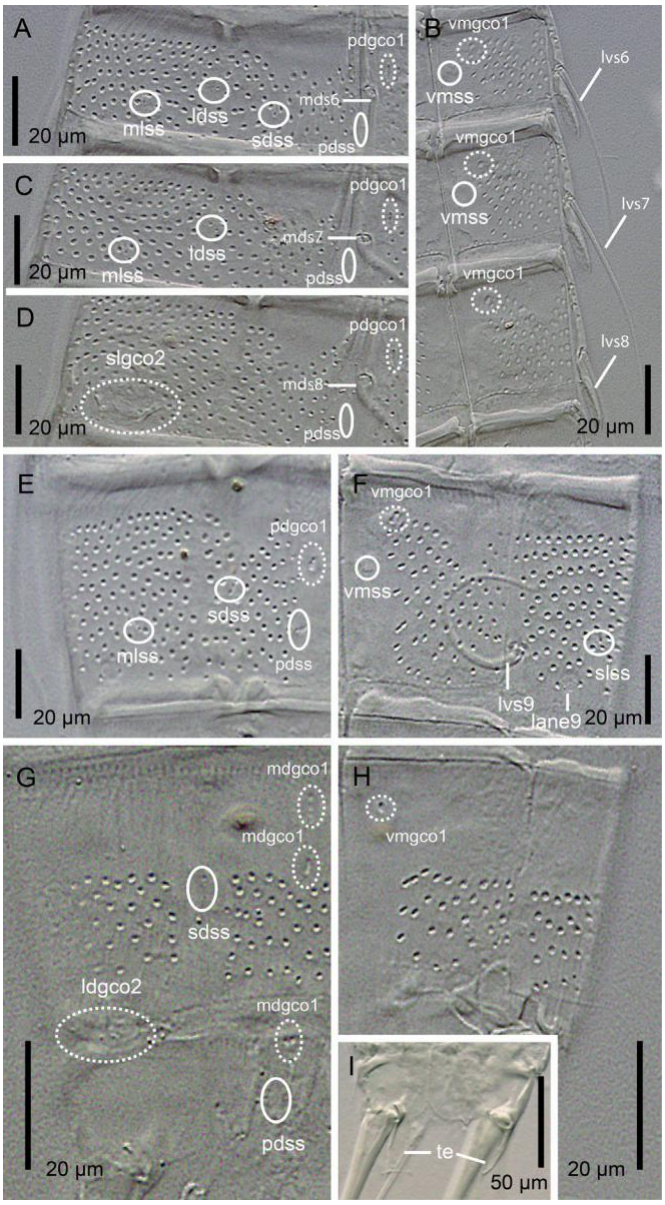

Fig. 16. Light micrographs showing details of cuticular trunk characters of segments 6-11 of female holotype USNM 1558509 of *Echinoderes xalkutaat* sp. nov., with main focus on spines, nephridiopores, sensory spots and glandular cell outlets. (A) Left half of tergal plate of segment 6; (B) right sternal plates of segments 6-8; (C) left half of tergal plate of segment 7; (D) left half of tergal plate of segment 8; (E) left half of tergal plate of segment 9; (F) right sternal plate of segment 9; (G) left half of tergal plates of segments 10-11; (H) right sternal plates of segments 10-11; (I) dorsal view of segment 11, with main focus on tergal extensions. Abbreviations: lane, lateral accessory nephridiopore; ldgco2, laterodorsal type 2 glandular cell outlet; ldss, laterodorsal sensory spot; lvs, lateroventral spine; mdgco1, middorsal type 1 glandular cell outlet; mds, middorsal spine; mlss, midlateral sensory spot; pdgco1, paradorsal type 1 glandular cell outlet; pdss, paradorsal sensory spot; sdss, subdorsal sensory spot; slgco2, sublateral type 2 glandular cell outlet; slss, sublateral sensory spot; te, tergal extension; vmgco1, ventromedial type 1 glandular cell outlet; vmss, ventromedial sensory spot; sensory spots are marked as closed circles, and glandular cell outlets as dashed circles; numbers after abbreviation indicate the corresponding segment.

type 1 glandular cell outlets (Figs. 13A, B and 15E, F).

Segment 4 with a middorsal spine exceeding the posterior edge of the following segment (Figs. 13B and 15G). Paired type 1 glandular cell outlets in paradorsal and ventromedial regions (Figs. 13A, B and 15G, H).

Table 8

Measurements of adult *Echinoderes xalkutaat* sp. nov. from the Gulf of California, including number of measured specimens (*n*), mean of data and standard deviation. Remarkable differences in size and/or dimension between the two sexes unknown, as only females were sampled.

Character	Range	Mean (SD; *n*)
TL (µm)	282.2-303.5	290.2 (11.6; 3)
MSW-7 (µm)	48.4-48.9	48.6 (0.4; 2)
MSW-7/TL (%)	17.1-17.2	17.1 (0.0; 2)
SW-10 (µm)	39.7-39.9	39.8 (0.1; 2)
SW-10/TL (%)	13.9-14.1	14.0 (0.1; 2)
S1 (µm)	26.3-29.8	28.0 (1.7; 3)
S2 (µm)	26.1-32.5	29.5 (3.2; 3)
S3 (µm)	30.1-33.9	32.6 (1.5; 3)
S4 (µm)	29.4-33.2	31.9 (2.1; 3)
S5 (µm)	31.3-36.6	34.7 (2.9; 3)
S6 (µm)	35.0-40.8	37.5 (3.0; 3)
S7 (µm)	39.5-42.0	41.0 (1.3; 3)
S8 (µm)	44.5-46.9	45.4 (1.3; 3)
S9 (µm)	40.9-45	42.6 (2.1; 3)
S10 (µm)	34.5-36.7	35.2 (1.2; 3)
S11 (µm)	23.9-31.9	28.6 (4.2; 3)
MD4 (ac) (µm)	41.9-44.3	43.1 (1.7; 2)
MD5 (ac) (µm)	56.0-56.0	56.0 (0.0; 1)
MD6 (ac) (µm)	65.2-74.9	69.1 (5.1; 3)
MD7 (ac) (µm)	70.2-71.5	70.9 (0.6; 3)
MD8 (ac) (µm)	76.6-83.9	79.6 (3.8; 3)
LV5 (tu) (µm)	7.7-10.3	9.1 (1.3; 3)
LV6 (ac) (µm)	28.0-38.2	33.7 (5.2; 3)
LV7 (ac) (µm)	42.1-43.2	42.7 (0.8; 2)
LV8 (ac) (µm)	45.2-47.4	46.5 (1.1; 3)
LV9 (ac) (µm)	32.1-39.3	35.4 (3.7; 3)
LTS (µm)	171.3-178.6	175.9 (4.0; 3)
LTAS (µm)	50.3-56.2	53.1 (3.0; 3)
LTS/TL (%)	58.9-63.0	60.6 (2.1; 3)
LTAS/TL (%)	17.4-19.7	18.3 (1.3; 3)
LTAS/LTS (%)	28.3-32.8	30.2 (2.3; 3)

Abbreviations: ac, acicular spine; LTAS, lateral terminal accessory spine; LTS, lateral terminal spine; LV, lateroventral; MD, middorsal; MSW-7, maximum sternal width (on segment 7); S, segment lengths; SW-10, standard sternal width (on segment 10); TL, total length of trunk; tu, tube.

Paired sensory spots in laterodorsal position (Figs. 13B and 15G).

Segment 5 with a middorsal spine exceeding the posterior edge of the following segment, but not reaching the posterior margin of segment 7 (Figs. 13B and 15I), and paired, short, narrow tubes in lateroventral position (Figs. 13A and 15J). Paired type 1 glandular cell outlets in paradorsal and ventromedial positions (Figs. 13A, B and 15I, J). Paired type 2 glandular cell outlets in midlateral position (Figs. 13B and 15I). Paired sensory spots in laterodorsal and ventromedial positions, the midlateral pair immediately next to the midlateral type 2 glandular cell outlets and the ventromedial pair posterior to the type 1 glandular cell outlets (Figs. 13A, B and 15I, J).

Segment 6 with a middorsal spine exceeding the posterior edge of the following segment but not reaching the posterior margin of segment 8, and paired spines in lateroventral position (Figs. 13A, B and 16A, B). Paired type 1 glandular cell outlets in paradorsal and ventromedial positions (Figs. 13A, B and 16A, B). Paired sensory spots in paradorsal, subdorsal, laterodorsal, midlateral and ventromedial positions, the paradorsal pair posterior to the paradorsal type 1 glandular cell outlets and the ventromedial pair posterior to the type 1 glandular cell outlets (Figs. 13A, B and 16A, B).

Segment 7 with a middorsal spine exceeding the posterior edge of the following segment but not reaching the posterior margin of segment 9, and paired spines in lateroventral position longer than those of preceding segments (Figs. 13A, B and 16B, C). Paired type 1 glandular cell outlets in paradorsal and ventromedial positions (Figs. 13A, B and 16B, C). Paired sensory spots in paradorsal, laterodorsal, midlateral and ventromedial

Table 9
Summary of nature and arrangement of spines, tubes, sensory spots, glandular cell outlets and nephridiopores in adults of *Echinoderes xalkutaat* sp. nov.

Segment	MD	PD	SD	LD	ML	SL	LA	LV	VL	VM
1	gco1		ss	ss		ss			ss	
2	gco1, ss		gco2	gco2		gco2			gco2	gco1, ss
3	gco1			ss						gco1, ss
4	ac	gco1		ss						gco1
5	ac	gco1		ss	gco2			tu		gco1, ss
6	ac	gco1, ss	ss	ss	ss			ac		gco1, ss
7	ac	gco1, ss		ss	ss			ac		gco1, ss
8	ac	gco1, ss				gco2		ac		gco1
9		gco1, ss	ss		ss	ss	ne	ac		gco1, ss
10	gco1, gco1		ss	gco2						gco1
11	gco1	ss					ltas (f)	lts		

Abbreviations: ac, acicular spine; f, female condition of sexually dimorphic character; gco1/2, type 1/2 glandular cell outlet; LA, lateral accessory; LD, laterodorsal; ltas, lateral terminal accessory spine; lts, lateral terminal spine; LV, lateroventral; MD, middorsal; ML, midlateral; ne, nephridiopore; PD, paradorsal; SD, subdorsal; SL, sublateral; ss, sensory spot; tu, tube; VL, ventrolateral, VM, ventromedial.

positions, the paradorsal pair posterior to the paradorsal type 1 glandular cell outlets, the ventromedial pair posterior to the ventromedial type 1 glandular cell outlets (Figs. 13A, B and 16B, C).

Segment 8 with a middorsal spine exceeding the posterior edge of segment 10 but not reaching the posterior end of trunk, and paired spines in lateroventral position longer than those of the preceding segment (Figs. 13A, B and 16B, D). Paired type 1 glandular cell outlets in paradorsal and ventromedial positions (Figs. 13A, B and 16B, D). Paired type 2 glandular cell outlets in sublateral position (Figs. 13A and 16D). Paired sensory spots in paradorsal position, posterior to the paradorsal type 1 glandular cell outlets (Figs. 13B and 16D).

Segment 9 with paired spines in lateroventral position, shorter than those of the preceding segment (Figs. 13A and 16F). Paired type 1 glandular cell outlets in paradorsal and ventromedial positions (Figs. 13A, B and 16E, F). Paired sensory spots in paradorsal, subdorsal, midlateral, sublateral and ventromedial positions (Figs. 13A, B and 16E, F). Nephridiopore as a very small sieve plate, in lateral accessory position (Figs. 13A and 16F).

Segment 10 without spines or tubes. Two unpaired type 1 glandular cell outlets in middorsal position (Figs. 13B and 16G), and paired in ventromedial position (Figs. 13A and 16H). Paired type 2 glandular cell outlets in laterodorsal position, near the posterior margin of segment (Figs. 13B and 16G). Paired sensory spots in subdorsal position (Figs. 13B and 16G).

Segment 11 with lateral terminal spines long (LTS:TL average ratio = 60.6%), slender, flexible, pointed distally, with a central cavity (Figs. 13A, B and 14A). Females with paired lateral accessory terminal spines, shorter than lateral terminal ones (LTAS:LTS average ratio = 18.3%) (Figs. 13A, B and 14A). Unpaired type 1 glandular cell outlet in middorsal position (Figs. 13B and 16G). Paired sensory spots in paradorsal position (Figs. 13B and 16G). Tergal plate of females with small patches bearing short, tiny hair-like extensions in paradorsal position (Fig. 13B). Tergal extensions long, pointed distally; sternal plates distally rounded (Figs. 13A, B and 16I).

3.4.5. Remarks on differential characters

E. xalkutaat sp. nov. is characterized by possessing middorsal spines on segments 4-8, lateroventral spines on segments 6-9, lateroventral tubes on segment 5, four pairs of type 2 glandular cell outlets on segment 2 and one pair on segments 5, 8 and 10. The general arrangement of spines and tubes in *E. xalkutaat* sp. nov. is one of the most common patterns among species of the genus (Sørensen & Pardos 2008; Neuhaus 2013; Grzelak & Sørensen 2018), but the presence of several pairs of type 2 glandular cell outlets throughout segments 2, 5, 8 and 10 is not as common.

The presence of four pairs of type 2 glandular cell outlets in subdorsal, laterodorsal, sublateral and ventrolateral positions on segment 2, together with the aforementioned arrangement of spines and tubes, is only shared with seven congeners: *Echinoderes angustus* Higgins & Kristensen, 1988, *Echinoderes cernunnos* Sørensen et al., 2012, *Echinoderes drogoni* Grzelak & Sørensen, 2018, *Echinoderes juliae* Sørensen et al., 2018, *Echinoderes obtuspinosus* Sørensen et al., 2012, *Echinoderes romanoi* Landers & Sørensen, 2016 and *Echinoderes tubilak* Higgins & Kristensen, 1988. However, the new species possesses paired type 2 glandular cell outlets in midlateral position on segment 5, in sublateral position on segment 8, and in laterodorsal position on segment 10. This combination is only shared with *E. angustus* and *E. drogoni*, whereas *E. cernunnos* bears these structures on segments 5 and 7-8, *E. juliae* on segments 3-5 and 8, E. obtuspinosus on segments 4 and 8, *E. romanoi* on segments 5 and 8 and *E. tubilak* on segments 4-5 and 8 (Landers & Sørensen 2016; Sørensen et al. 2012, 2018; Grzelak & Sørensen 2018). *E. angustus* can be distinguished from the new species by its type 2 glandular cell outlets on segment 4, and *E. drogoni* has the tubes of segment 5 displaced to a lateral accessory position (Grzelak & Sørensen 2018). Additionally, the female of *E. drogoni* has two tergal plates on segment 11 (Grzelak & Sørensen 2018), while that of *E. xalkutaat* sp. nov. possesses only a single tergal plate on segment 11.

Funding sources

The present study was partially funded by the projects IN-217306-3 and IN-202116, by Programa de Apoyo a Proyectos de Investigación e Innovación Tecnológica (PAPIIT), México, of Dirección General de Asuntos del Personal Académico (DGAPA), México; and the project BIO03/2017, granted by Union Iberoamericana de Universidades (UIU).

Cepeda was supported by a predoctoral fellowship of the Universidad Complutense de Madrid UCM (CT27/16-CT28-16).

References

Adrianov, A.V., 1989. The first report on Kinorhyncha of the Sea of Japan. Zool. Zh. 68 (7), 17-27.

Adrianov, A.V., Malakhov, V.V., 1999. Cephalorhyncha of the World Ocean. KMK Scientific Press, Moscow.

Álvarez-Castillo, L., Hermoso-Salazar, M., Estradas-Romero, A., Prol-Ledesma, R.M., Pardos, F., 2015. First records of Kinorhyncha from the Gulf of California: horizontal and vertical distribution of four genera in shallow basins with CO_2 venting activity. Cah. Biol. Mar. 56 (3), 271-281.

Álvarez-Castillo, L., Hermoso-Salazar, M., Estradas-Romero, A., Prol-Ledesma, R.M., Pardos, F., 2018. New record of *Fissuroderes thermoi* (Kinorhyncha: Cyclo-rhagida) in the Gulf of California. Cah. Biol. Mar. 59, 235-244.

Appeltans, W., Ahyong, S.T., Anderson, G., Angel, M.V., Artois, T., Bailly, N., et al., 2012. The magnitude of global marine species diversity. Curr. Biol. 22, 2189-2202. https://doi.org/10.1016/j.cub.2012.09.036.

Cepeda, D., Pardos, F., Sánchez, N., 2019. Kinorhyncha from the Caribbean, with the description of two new species from Puerto Rico and Barbados. Zool. Anz. 282, 127-139. https://doi.org/10.1016/j.jcz.2019.05.014.

Claparède, A.R.E., 1863. Zur Kenntnis der Gattung *Echinoderes* Duj. Beobachtungen über Anatomie und Entwicklungsgeschichte wirbelloser Thiere an der Küste von Normandie angestellt. Verlag von Wilhelm Engelmann, Leipzig.

Gerlach, S.A., 1971. On the importance of marine meiofauna for benthos communities. Oecologia 6, 176-190.

Grzelak, K., Sørensen, M.V., 2018. New species of *Echinoderes* (Kinorhyncha: Cyclorhagida) from Spitsbergen, with additional information about known arctic species. Mar. Biol. Res. 14, 113-147. https://doi.org/10.1080/17451000. 2017.1367096.

Hakenkamp, C.C., Morin, A., 2001. The importance of meiofauna to lotic ecosystem functioning. Freshw. Biol. 44, 165-175. https://doi.org/10.1046/j.1365-2427. 2000.00589.x.

Higgins, R.P., 1961. Three new homalorhage kinorhynchs from the San Juan Archipelago, Washington. J. Elisha Mitchell Sci. Soc. 77 (1), 81-88.

Higgins, R.P., 1964. Three new kinorhynchs from the North Carolina Coast. Bull. Mar. Sci. 14, 479-493.

Higgins, R.P., 1983. The Atlantic Barrier Reef ecosystem at Carrie Bow Cay, Belize, II: Kinorhyncha. Smithson. Contrib. Mar. Sci. 18, 1-131. https://doi.org/10.5479/si. 01960768.18.1.

Higgins, R.P., 1986. A new species of *Echinoderes* (Kinorhyncha: Cyclorhagida) from a coarse-sand California beach. Trans. Am. Microsc. Soc. 105, 266-273. https://doi.org/10.2307/3226298.

Higgins, R.P., Kristensen, R.M., 1988. Kinorhyncha from Disko Island, west Greenland. Smithson. Contrib. Zool. 458, 1-55. https://doi.org/10.5479/si. 00810282.458.

Landers, S.C., Sørensen, M.V., 2016. Two new species of *Echinoderes* (Kinorhyncha, Cyclorhagida), *E. romanoi* sp n. and *E. joyceae* sp n., from the Gulf of Mexico. ZooKeys 594, 51-71. https://doi.org/10.3897/zookeys.594.8623.

Lang, K., 1953. Reports of the Lund University Chile expedition 1948-1949. 9. Echinoderida. Lunds Universitets Årsskrift N. F. Avd. 2 49, 3-8.

Mokievsky, V., Azovsky, A., 2002. Re-evaluation of species diversity patterns of free-living marine nematodes. Mar. Ecol. Prog. Ser. 238, 101-108. https://doi.org/10. 3354/meps238101.

Neuhaus, B., 2013. Kinorhyncha (=Echinodera). In: Schmidt-Rhaesa, A. (Ed.), Handbook of Zoology, Gastrotricha, Cycloneuralia and Gnathifera, Volume 1 Nematomorpha, Priapulida, Kinorhyncha, Loricifera. De Gruyter, Hamburg, pp. 181-350.

Neuhaus, B., Blasche, T., 2006. *Fissuroderes*, a new genus of Kinorhyncha (Cyclorhagida) from the deep sea and continental shelf of New Zealand and from the continental shelf of Costa Rica. Zool. Anz. 245, 19-52. https://doi.org/10.1016/j. jcz.2006.03.003.

Sánchez, N., Pardos, F., Herranz, M., Benito, J., 2011. *Pycnophyes dolichurus* sp. nov. and *P. aulacodes* sp. nov. (Kinorhyncha, Homalorhagida, Pycnophyidae), two new kinorhynchs from Spain with a reevaluation of homalorhagid taxonomic characters. Helgol. Mar. Res. 65, 319-334. https://doi.org/10.1007/s10152-010-0226-z.

Sánchez, N., Pardos, F., Martínez-Arbizu, P., 2019. Deep-sea Kinorhyncha diversity of the polymetallic nodule fields at the clarion-clipperton Fracture Zone (CCZ). Zool. Anz. 282, 88-105. https://doi.org/10.1016/j.jcz.2019.05.007.

Sánchez, N., Pardos, F., Sørensen, M.V., 2014. Deep-sea Kinorhyncha: two new species from the Guinea Basin, with evaluation of an unusual male feature. Org. Divers. Evol. 14 (4), 349-361. https://doi.org/10.1007/s13127-014-0182-6.

Sánchez, N., Yamasaki, H., Pardos, F., Sørensen, M.V., Martínez, A., 2016. Morphology disentangles the systematics of a ubiquitous but elusive meiofaunal group (Kinorhyncha: Pycnophyidae). Cladistics 32 (5), 479-505. https://doi.org/10. 1111/cla.12143.

Schmid-Araya, J.M., Hildrew, A.G., Robertson, A., Schmid, P.E., Winterbottom, J., 2002. The importance of meiofauna in food webs: evidence from an acid stream. Ecology 83 (5), 1271-1285. https://doi.org/10.2307/3071942.

Schratzberger, M., Ingels, J., 2017. Meiofauna matters: the roles of meiofauna in benthic ecosystems. J. Exp. Mar. Biol. Ecol. 502, 12-25. https://doi.org/10.1016/j. jembe.2017.01.007.

Sørensen, M.V., 2008. A new kinorhynch genus from the Antarctic deep sea and a new species of *Cephalorhyncha* from Hawaii (Kinorhyncha: Cyclorhagida: Echinoderidae). Org. Divers. Evol. 8, 230-232. https://doi.org/10.1016/j.ode. 2007.11.003.

Sørensen, M.V., Dal Zotto, M., Rho, H.S., Herranz, M., Sánchez, N., Pardos, F., Yamasaki, H., 2015. Phylogeny of Kinorhyncha based on morphology and two molecular loci. PLoS One 10 (7), e0133440. https://doi.org/10.1371/journal.pone. 0133440.

Sørensen, M.V., Pardos, F., 2008. Kinorhynch systematics and biology - an introduction to the study of kinorhynchs, inclusive identification keys to the genera. Meiofauna Marina 16, 21-73.

Sørensen, M.V., Rho, H.S., Min, W.G., Kim, D., Chang, C.Y., 2012. An exploration of *Echinoderes* (Kinorhyncha: Cyclorhagida) in Korean and neighboring waters, with the description of four new species and a redescription of *E. tchefouensis* Lou, 1934. Zootaxa 3368, 161-196.

Sørensen, M.V., Rohal, M., Thistle, D., 2018. Deep-sea Echinoderidae (Kinorhyncha: Cyclorhagida) from the northwest Pacific. Eur. J. Taxon. 456, 1-75. https://doi.org/10.5852/ejt.2018.456.

Yildiz, N.O., Sørensen, M.V., Karaytug, S., 2016. A new species of *Cephalorhyncha* Adrianov, 1999 (Kinorhyncha: Cyclorhagida) from the Aegean coast of Turkey. Helgol. Mar. Res. 70, 24. https://doi.org/10.1186/s10152-016-0476-5.

Zelinka, C., 1894. Über die Organisation von *Echinoderes*. Verh. Dtsch. Zool. Ges. 4, 46-49.

Zelinka, C., 1896. Demonstration der Tafeln der *Echinoderes* - monographie. Verh. Dtsch. Zool. Ges. 6, 197-199.

frontiers in Marine Science

ORIGINAL RESEARCH
published: 19 August 2020
doi: 10.3389/fmars.2020.00665

Dragons of the Deep Sea: Kinorhyncha Communities in a Pockmark Field at Mozambique Channel, With the Description of Three New Species

Diego Cepeda[1]*, Fernando Pardos[1], Daniela Zeppilli[2] and Nuria Sánchez[2]

[1] *Departamento de Biodiversidad, Ecología y Evolución, Facultad de Ciencias Biológicas, Universidad Complutense de Madrid, Madrid, Spain,* [2] *Laboratoire Environnement Profond, Institut Français de Recherche pour l'Exploitation de la Mer (IFREMER), Plouzané, France*

Cold seep areas are extremely reduced habitats with spatiotemporal variation of hydrocarbon-rich fluid seepage, low oxygen levels, and great habitat heterogeneity. Cold seeps can create circular to ellipsoid shallow depressions on the seafloor called pockmarks. We investigated two selected pockmarks, characterized by different gas emission, and two sites outside these geological structures at the Mozambique Channel to understand whether and how their environmental conditions affect the kinorhynch fauna in terms of density, richness, and community composition. A total of 11 species have been found living in the studied area, of which three are new species: *Fissuroderes cthulhu* sp. nov., *Fujuriphyes dagon* sp. nov., and *Fujuriphyes hydra* sp. nov. Densities outside the pockmarks are low and regularly decrease from the upper sediment layers, whereas inside the pockmarks, density reaches its highest value at layer 1–2 cm, strongly decreasing along the vertical profile from this depth. Areas under pockmark influence and locations outside pockmarks are similar in terms of species richness, but kinorhynchs showed a significant remarkable higher density at the pockmark sites. Additionally, species composition changes between habitats (inside and outside pockmarks) and between the two sampled pockmarks, with most of the species restricted to one of the studied habitats, except for *Condyloderes* sp. and *Echinoderes unispinosus* present both outside and inside the pockmarks. *Echinoderes hviidarum, E. unispinosus*, and *Fi. cthulhu* sp. nov., present at sites with gas emission, do not only survive under the specific pockmark conditions (characterized by hydrogen sulfide toxicity, methane high concentration, and low availability of dissolved oxygen) but even profit from a habitat with a likely lower competition for space and resources, flourishing and enhancing the density, most likely through the replacement with specialized species. Contrarily, species that only appear outside the pockmarks do not seem to cope with the presence of hydrogen sulfide and methane. Therefore, environmental factors linked to gas emissions have a major role driving the kinorhynch community composition.

Keywords: cold seeps, deep sea, ecology, kinorhynchs, meiofauna, diversity, taxonomy

OPEN ACCESS

Edited by:
Rui Rosa,
University of Lisbon, Portugal

Reviewed by:
Martin Vinther Sørensen,
University of Copenhagen, Denmark
Matteo Dal Zotto,
University of Modena and Reggio Emilia, Italy

****Correspondence:***
Diego Cepeda
diegocepeda@ucm.es

Specialty section:
This article was submitted to Global Change and the Future Ocean, a section of the journal Frontiers in Marine Science

Received: 30 November 2019
Accepted: 21 July 2020
Published: 19 August 2020

Citation:
Cepeda D, Pardos F, Zeppilli D and Sánchez N (2020) Dragons of the Deep Sea: Kinorhyncha Communities in a Pockmark Field at Mozambique Channel, With the Description of Three New Species. Front. Mar. Sci. 7:665. doi: 10.3389/fmars.2020.00665

INTRODUCTION

Worldwide oceans cover about 361.9 million km^2 of the Earth's surface, of which 70% are deep sea plains (Eakins and Sharman, 2010). Nowadays, ocean floor studies have experienced a strong revitalization, showing that the deep sea possesses prosperous, complex biological communities and a huge variety of geochemical environments that host unique species (Levin and Sibuet, 2012; Kennedy et al., 2019). Cold seeps are extreme, reduced habitats on the seafloor where hydrogen sulfide, methane, and other hydrocarbon-rich fluid seepage occurs (Kumar, 2017), causing a fall in oxygen levels and peaks of primary production due to chemoautotrophic organisms (Sibuet and Olu, 1998; Levin, 2005; Zeppilli et al., 2018). Cold seeps generate several geological structures such as pockmarks, circular to ellipsoid shallow depressions on the seafloor where the fluid emission varies spatiotemporally, cones (as mud volcanoes), carbonated structures, and brine pools, oval to rounded-shaped bodies of water that have a salinity higher than the surrounding ocean (Hovland and Judd, 1988; Dando et al., 1991).

Organisms inhabiting cold seeps take advantage of the habitat heterogeneity formed by the variable fluid release intensity and the hydrocarbon-rich fluid concentration of the sediment to occupy extreme, reduced niches that other organisms are unable to inhabit (Levin, 2005; Guillon et al., 2017). These adapted species can reach high levels of abundance and biomass (Rouse and Fauchald, 1997; Levin, 2005; Seitzinger et al., 2010; Vanreusel et al., 2010; Guillon et al., 2017; Sun et al., 2017) as a consequence of few species having evolved the morpho-physiological adaptations required to live in such a challenging habitat (Hourdez and Lallier, 2006; Zeppilli et al., 2018).

Studies of Kinorhyncha from the deep sea have frequently reported unidentified species, mostly from the Indian, Pacific, and Atlantic Oceans (Neuhaus, 2013; Zeppilli et al., 2018). More recently, studies to the species level have received a strong boost, and up to 45 species have recently been described or reported from this environment (Neuhaus and Blasche, 2006; Sørensen, 2008a; Neuhaus and Sørensen, 2013; Sánchez et al., 2014a,b, 2019a; Adrianov and Maiorova, 2015, 2016, 2018a,b; Grzelak and Sørensen, 2018, 2019; Sørensen and Grzelak, 2018; Sørensen et al., 2018, 2019; Yamasaki et al., 2018a,b,c, 2019; Cepeda et al., 2019a). Of these, some species seem to possess wider ranges of distribution than their congeners from the coastal zone. For instance, *Condyloderes kurilensis* Adrianov and Maiorova (2016), and *Fissuroderes higginsi* Neuhaus and Blasche (2006), were originally described from the Kuril-Kamchatka Trench (northwestern Pacific) and New Zealand (southwestern Pacific), respectively, and later found in the deep-sea waters off Oregon and California (northeastern Pacific) and the Clarion-Clipperton Zone (Neuhaus and Blasche, 2006; Adrianov and Maiorova, 2016; Sørensen et al., 2018; Sánchez et al., 2019a). More striking are the cases of *Campyloderes vanhoeffeni* Zelinka, 1913, distributed worldwide in both coastal waters and deep sea (Neuhaus and Sørensen, 2013) and *Echinoderes unispinosus* present in the deep sea of the Atlantic and the Pacific Oceans (Sørensen et al., 2018; Yamasaki et al., 2019; Álvarez-Castillo et al., 2020). This apparent cosmopolitanism might suggest that the deep sea environmental homogeneity promotes much wider distributional ranges than those observed from shallow water species (Sørensen et al., 2018). However, the possibility of having complexes of cryptic species must also be taken into account, since speciation in deep sea environments is not always accompanied by conspicuous morphological changes (Janssen et al., 2015).

Despite these hypotheses, little is known about the main environmental factors that shape the kinorhynch communities in general and particularly in deep sea, extreme environments. Some recent studies performed in the Arctic Ocean and the Gulf of Mexico determined that sediment grain size and trace metals are the variables that most seem to affect the Kinorhyncha species composition (Landers et al., 2018; Grzelak and Sørensen, 2019). Additionally, Álvarez-Castillo et al. (2015) concluded that kinorhynchs are somehow affected by pore water pH in reduced environments such as CO_2 vents. Also, kinorhynch densities have been proven to vary with the sulfide and organic matter concentrations of the seafloor (Sutherland et al., 2007; Mirto et al., 2012; Dal Zotto et al., 2016; Landers et al., 2020). In this context, the main aim of the present paper is to characterize the kinorhynch community associated with pockmarks in the Mozambique Channel deep sea to (1) identify and describe the new species inhabiting the area, (2) report potential kinorhynch species as indicators of cold seep areas, and (3) determine possible differences in richness, density, and species composition inside and outside pockmarks and along the vertical profile.

MATERIALS AND METHODS

Study Area, Sampling, and Processing

A pockmark cluster area was selected for the present study in the deep sea Mozambique Channel, off Mozambique and Madagascar (western Indian Ocean). Samples were collected during the *PAMELA-MOZ01* and *PAMELA-MOZ04* campaigns aboard the R/V *L'Atalante* and *Pourquoi pas?* (Genavir-Ifremer), respectively (Olu, 2014; Jouet and Deville, 2015). Multibeam echosounders and seabed inspection with a deep-towed camera Scampi were used to detect the location of pockmarks obtaining bathymetric data and identifying cold seep macrofauna indicators. Two active pockmarks and two sites outside any pockmark were selected.

MOZ04_MTB2: S 15 21.685; E 45 57.378; 754 m depth.
MOZ01_MTB3: S 15 21.695; E 45 57.388; 757 m depth.
MOZ04_MTB1: S 15 21.812; E 45 57.628; 735 m depth.
MOZ01_MTB6: S 15 31.148; E 45 42.931; 789 m depth.

Samples were obtained with a Barnett-type multi-corer (MTB) with three cores by deployment. Each core of 6.2 cm inner diameter (total surface area of 30.2 cm^2) was horizontally sliced into five layers: layer 1 (0–1 cm depth), layer 2 (1–2 cm depth), layer 3 (2–3 cm depth), layer 4 (3–4 cm depth), and layer 5 (4–5 cm depth). Each subsample was fixed in 4% formalin. Subsequently, the sediment of each slice was sieved on 1-mm and 32-mm sieves at the Ghent laboratory (Belgium) and the IFREMER laboratory (France), and the metazoan meiofauna was separated from the sediment by Ludox centrifugation (Heip et al., 1985) and subsequently fixed in 4% formalin.

Species Identification and Description

Kinorhynchs were separated from the remaining meiofauna using an Irwin loop and washed with distilled water to remove formalin remnants. Kinorhynchs were mounted and identified to species level, except for the juveniles that could be identified only to class level.

For light microscopy (LM), specimens were dehydrated through a graded series of 25, 50, 75, and 100% glycerine to be mounted on glass slides with Fluoromount G®. The mounted specimens were studied, identified, and photographed with a Leica DM2500® LED compound microscope equipped with differential interference contrast (DIC).

For scanning electron microscopy (SEM), specimens were sonically cleaned and transferred to 70% ethanol and progressively dehydrated through a graded series of 80, 90, 95, and 100% ethanol. Hexamethyldisilazane (HMDS) was used for chemical drying through a HMDS-ethanol series. Specimens were coated with gold and mounted on aluminum stubs to be examined with a JSM 6335-F JEOL SEM at the "ICTS Centro Nacional de Microscopía Electrónica" (Universidad Complutense de Madrid, Spain). For species descriptions, line art and image plates composition were done using Adobe Photoshop and Illustrator CC-2014 software. Type and additional material were deposited at the Natural History Museum of Denmark (NHMD).

Environment Characterization

To test the influence of the environment over the kinorhynch communities and detect potential species as indicators of seepages, we selected hydrogen sulfide (H_2S) and methane (CH_4) as a proxy of cold seep activity.

H_2S concentration was quantified by colorimetry (Fonselius, 1983) after precipitation of the sulfide with zinc chloride on board. The concentration was detected in a high level only at the pockmark site MOZ04-MTB1. CH_4 was determined by gas chromatography headspace technique (GC/HSS) (Sarradin and Caprais, 1996), following different sampling techniques between the two cruises. In MOZ-01, 5 ml of pore waters was collected in 10-ml vials by Rhizon samplers (Rhizosphere Research Products R.V., Wageningen), which are thin rods covered by hydrophilic porous polymer designed to extract water from sediment using a vacuum (Seeberg-Elverfeldt et al., 2005); then, 20 ml of a saturated mercuric hydrochloride solution was added to preserve samples. In MOZ-04, 3 ml of sediment was collected in 20-ml vials, where 5 ml of a solution of sodium hydroxide at 1 M was added to avoid any bacterial activity. CH_4 was found at the two study pockmarks. The methodology followed during the cruise MOZ01, using Rhizon samplers, induced a degassing step of dissolved methane in the pore waters, while methane is more preserved by collecting directly the sediment, as done during the cruise MOZ04.

Data Processing and Statistical Analyses

The effect of the environmental conditions on kinorhynch community structure and assemblage was assessed using three community descriptors as response variables: (1) richness, (2) density, and (3) species composition. Richness was measured as number of species, and density as number of individuals per 10 cm^2, including both adults and juveniles.

Kruskal–Wallis analyses (KW) were conducted through R v.6.3.1 software to test differences in kinorhynch richness and density. We assessed changes in community structure through different approaches: along the vertical profile of each habitat (inside and outside pockmarks, considering five layers: 0–1, 1–2, 2–3, 3–4, and 4–5 cm), between habitats (inside vs. outside pockmarks), and between sites sampled at the same habitat.

Differences in adult community composition between habitats and between sites of the same habitat were tested by permutational multivariate analysis of variance (PERMANOVA) calculated with the function "adonis" in the R package *vegan* v. 2.2-1 (Oksanen et al., 2018). Distance matrices were calculated using both Jaccard (incidence) and Ružièka [abundance transformed to $\log_{10}$(abundance C 1)] dissimilarity indices through the function "beta" of the R package *vegan* v. 2.2-1 (Oksanen et al., 2015). In order to further investigate the environmental factors that drive the community composition, H_2S was used as categorical covariate variable (two levels: absence, all layers with concentration of 0 mM; high, layers with concentrations > 200 Mm). CH_4 was detected at both pockmark sites (MOZ01-MTB06 and MOZ04-MTB1), but the concentration was measured following different methods and therefore data cannot be truly comparable. We conducted a principal component analysis (PCA) in abundance using the function "rda" of the R package *vegan* v. 2.2-1 (Oksanen et al., 2015) to visualize community composition variations among sites. Abundance data were transformed in order to use the Hellinger distance among samples using the function "decostand" of the R package *vegan* 2.4-4 (Oksanen et al., 2018), since double absence is not considered as an indicator of similarity and it gives a lower weight to dominant species (Legendre and Gallagher, 2001). A *post hoc* explaining of the PCA axes by adding environmental variables was performed by the function "envfit" of the R package *vegan* 2.4-4 (Oksanen et al., 2018).

RESULTS

Taxonomic Account

Class Allomalorhagida Sørensen et al., 2015.
Family Pycnophyidae Zelinka, 1896.
Genus *Fujuriphyes* Sánchez et al., 2016.

Fujuriphyes dagon sp. nov.
urn:lsid:zoobank.org:act:28C303EF-46AE-4304-887C-9202B7386AB9 (**Figures 1–4**).

Material examined

Holotype, adult female, collected in October 2014 at Mahavavy area, Mozambique Channel, western Indian Ocean (15 31.148^{0}S, 45 42.931^{0}E) at 789 m depth; mounted in Fluoromount G®, deposited at NHMD under accession number: 669762. Paratypes, three adult males, with same collecting data

as holotype; mounted in Fluoromount G®, deposited at NHMD under accession numbers: 669763–669765. Two additional specimens mounted for SEM, same collecting data as type material, deposited at the Meiofauna Collection of the UCM.

Diagnosis

Fujuriphyes without middorsal processes or elevations. Unpaired paradorsal setae on segments 2, 4, 6, and 8. Laterodorsal setae on segments 2–10. Lateroventral setae on even segments. One pair of ventrolateral setae on segments 2–4 and 6–9, and two pairs on segment 5. Males with ventromedial tubes on segment 2. Lateral terminal spines present.

Etymology

The species is named after the fictional deity Dagon (also known as Father Dagon), created by the American writer of horror fiction H.P. Lovecraft (1890–1937) and firstly introduced in the short story "Dagon," published in 1919. In the pantheon of Lovecraftian cosmic entities, Dagon presides over the Deep Ones, an amphibious humanoid race indigenous to Earth's oceans.

Description

See **Supplementary Table 1.1** for measurements and dimensions and **Supplementary Table 1.2** for summary of seta, spine, tube, glandular cell outlet, and sensory spot locations.

Ring 00 of mouth cone with nine equally sized outer oral styles (**Figure 2**) composed of a single, flexible unit, wider at the base, which bears a fringed sheath, progressively tapering toward a distal, pointed tip. Outer oral styles located anterior to each introvert sector, except in the middorsal section 6 where a style is missing (**Figure 2**).

Introvert with six transverse rings of scalids and 10 longitudinal sectors defined by the arrangement of the primary spinoscalids (**Figures 2**, **3H**). Ring 01 with 10 primary spinoscalids, larger than remaining ones, each one composed of a basal, rectangular, wide sheath and a distal, elongated, flexible, distally pointed end piece (**Figures 2**, **3H**). Ring 02 with 10 regular-sized scalids, arranged as one medially in each sector (**Figure 2**). Scalids of this and the following rings are morphologically similar to the primary spinoscalids but smaller (**Figure 3H**). Ring 03 with 20 regular-sized scalids, arranged as 2 in each sector (**Figures 2**, **3H**). Ring 04 with 5 regular-sized scalids, arranged as 1 medially in each odd-numbered sector (**Figures 2**, **3H**). Ring 05 with 15 regular-sized scalids, arranged as 1 medially in each even-numbered sector and 2 in each odd-numbered sector (**Figure 2**). Ring 06 also with 15 regular-sized scalids, arranged as 2 in each even-numbered sector and 1 medially in each odd-numbered sector (**Figure 2**). The location of scalids in rings 01–06 follows a strict pattern around the introvert: each even-numbered sector carries six regular-sized scalids as two chevrons, whereas each odd-numbered sector bears seven regular-sized scalids as a double diamond (**Figures 2**, **3H**).

Neck with four dorsal and two ventral sclerotized placids (**Figures 1A–C**). Dorsal placids rectangular, wide, mesial ones broader (ca. 30–32 µm wide at the base) than lateral ones (ca. 20–23 µm wide at the base), with a notch in the middle region (**Figure 1B**). Ventral placids (ca. 29–31 µm wide at the base) more quadrangular than dorsal ones, with the posterolateral margins curved toward the sternal plates of the first trunk segment (**Figures 1A,C**). A ring of 14 trichoscalids posterior to the scalid rings, arranged as 2 in the odd-numbered sectors (except sector 1 with a single trichoscalid) and 1 in the even-numbered sectors of the introvert (**Figures 2**, **3H**).

Trunk rectangular, stout, triangular in cross-section, composed of 11 segments (**Figures 1A,B**, **3A**, **4A**). Segment 1 with one tergal, two episternal, and one midsternal plate (**Figures 1A–C**, **3A–C**); remaining segments with one tergal and two sternal plates (**Figures 1A–D**, **3A**). Maximum sternal width at segment 6, almost constant throughout the trunk, progressively tapering at the last trunk segments (**Figures 1A,B**, **3A**, **4A**). Sternal cuticular plates relatively narrow in the ratio of maximum sternal width to trunk length (MSW-6:TL interval ratio = 21.9–24.9), giving the animal a slender appearance (**Figures 1A,B**, **3A**, **4A**). Segments 1–10 with oval glandular cell outlets in subdorsal and ventromedial positions (**Figures 1A– C**, **3B–G,I,J**). Segments 2–10 with paired cuticular ridges in laterodorsal and ventrolateral positions, the latter with adjacent, minute glandular cell outlets (**Figures 1A–D**, **3A–G,I,J**). Cuticular hairs acicular, densely covering the cuticular surface of segments 2–10 from paralateral to ventromedial positions (**Figures 4D–G, H–K**). Muscular scars very conspicuous in laterodorsal and ventromedial positions (**Figures 1A–D**, **3B–G,I,J**). Areas with superficially wrinkled cuticle present in ventrolateral position on segments 2–10 and paralateral position on segment 1 (**Figures 1A,C**). Pachycycli and ball-and-socket joints well-developed and thick on segments 2–10 (**Figures 1A–D**, **3A**). Apodemes present on segments 8–10 (**Figures 1A**, **3A**). Posterior margin of segments straight, showing primary pectinate fringes with weakly serrated free flaps; secondary pectinate fringes also straight and finely serrated (**Figures 1A–D**).

Segment 1 without middorsal cuticular process or elevation. Anterolateral margins of the tergal plate as horn-like, distally rounded extensions (**Figures 1A–C**, **3A**, **4A,B**). Anterior margin of tergal plate smooth, followed by a crenulated area (**Figures 1B**, **3B**, **4A,B**). Anterior margin of sternal plates with a wavy median ridge of cuticle (**Figures 1A,C**, **3C**). Midsternal plate trapezoidal, laterally extended at its base, with a lateral constriction near its anterior margin and a straight posterior margin (**Figures 1A,C**, **3C**). Sensory spots in subdorsal (two pairs), laterodorsal (one pair), ventrolateral (two pairs), and ventromedial (one pair) positions (**Figures 1A– C**, **3B,C**, **4B,C**).

Segment 2 without middorsal process or elevation. Unpaired seta in paradorsal position; paired setae in laterodorsal, lateroventral, and ventrolateral positions (**Figures 1A–C**, **3D,E**, **4H,I**). Sensory spots in subdorsal (one pair), laterodorsal (one pair), and ventromedial (two pairs) positions (**Figures 1A– C**, **3D,E**, **4H,I**). Males with sexually dimorphic tubes in ventromedial position (**Figures 1C**, **4I**).

Segment 3 without middorsal process or elevation. Paired setae in laterodorsal and ventrolateral positions (**Figures 1A,B**, **3D,E**). Sensory spots in subdorsal (one pair), laterodorsal (one pair), and ventromedial (two pairs) positions (**Figures 1A,B**, **3D,E**).

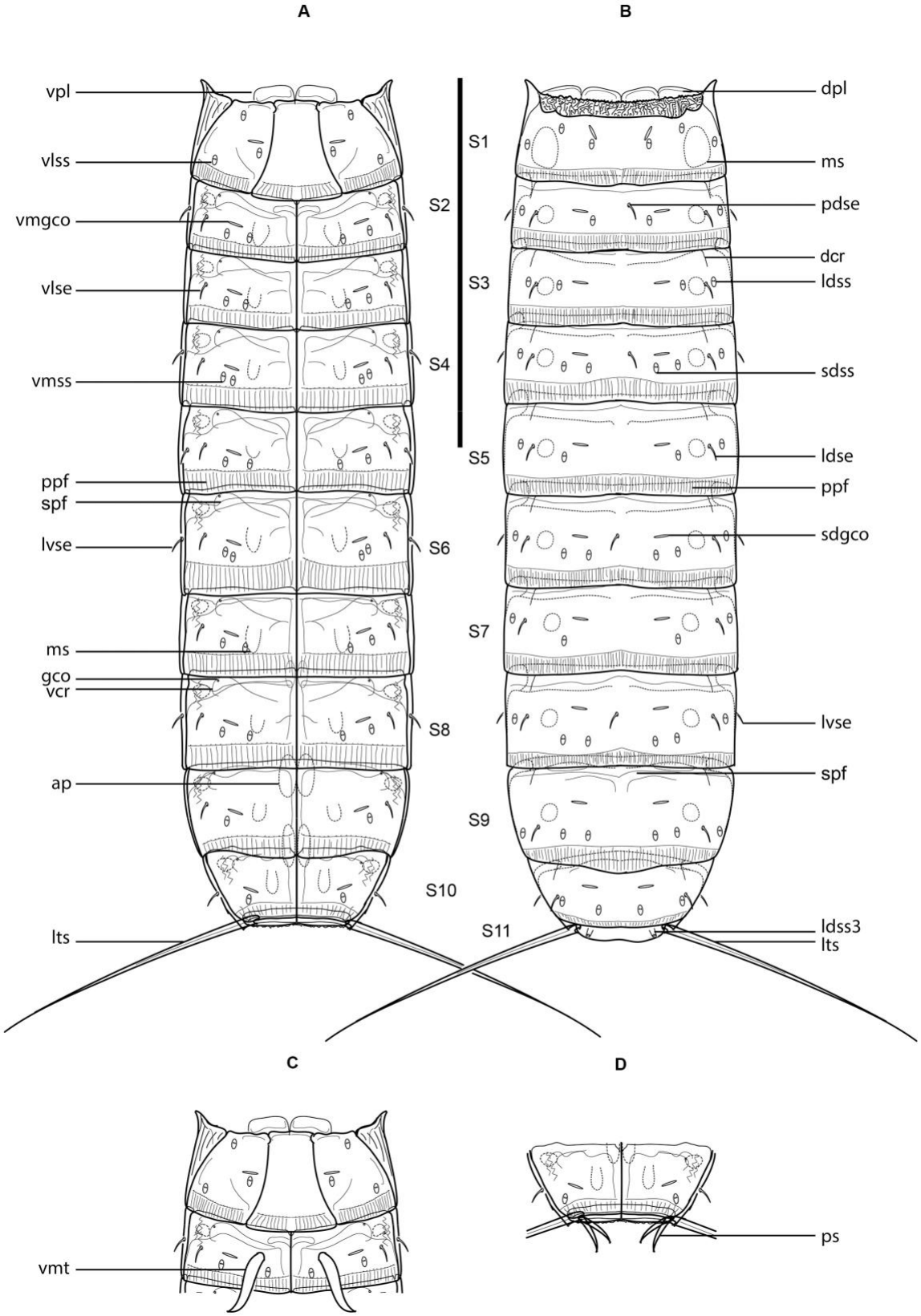

FIGURE 1 | Continued

FIGURE 1 | Line art illustrations of *Fujuriphyes dagon* sp. nov. **(A)** Female, ventral view; **(B)** female, dorsal view; **(C)** male, segments 1–2, ventral view; **(D)** male, segments 10–11, ventral view. Scale bar: 250 µm. Abbreviations: ap, apodeme; dcr, dorsal cuticular ridge; dpl, dorsal placid; gco, glandular cell outlet; ldse, laterodorsal seta; ldss, laterodorsal sensory spot; ldss3, laterodorsal type 3 sensory spot; lts, lateral terminal spine; lvse, lateroventral seta; ms, muscular scar; pdse, paradorsal seta; ppf, primary pectinate fringe; ps, penile spine; sdgco, subdorsal glandular cell outlet; sdss, subdorsal sensory spot; spf, secondary pectinate fringe; vcr, ventral cuticular ridge; vlse, ventrolateral seta; vlss, ventrolateral sensory spot; vmgco, ventromedial glandular cell outlet; vmss, ventromedial sensory spot; vmt, ventromedial tube; vpl, ventral placid.

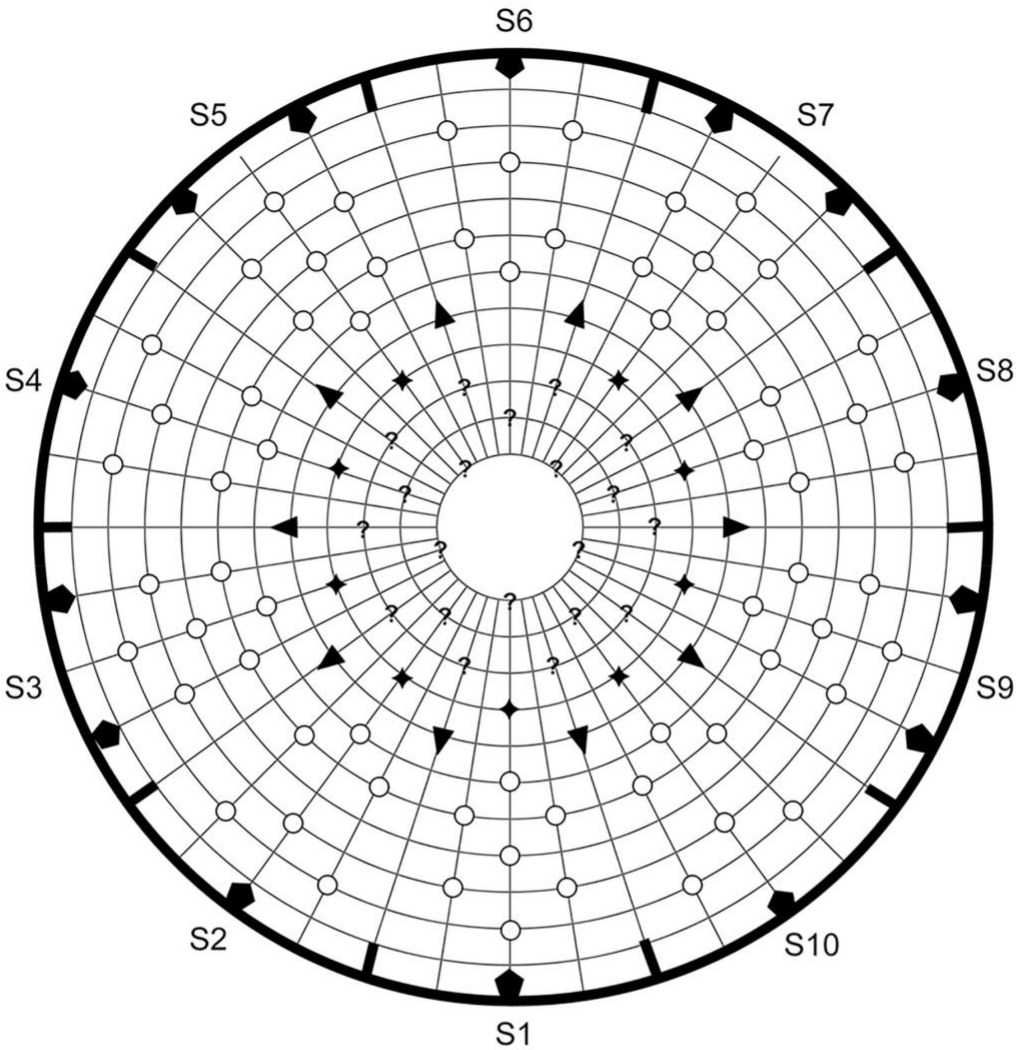

FIGURE 2 | Diagram of mouth cone, introvert, and trichoscalids in *Fujuriphyes dagon* sp. nov., with indication of oral style, scalid, and trichoscalid arrangement.

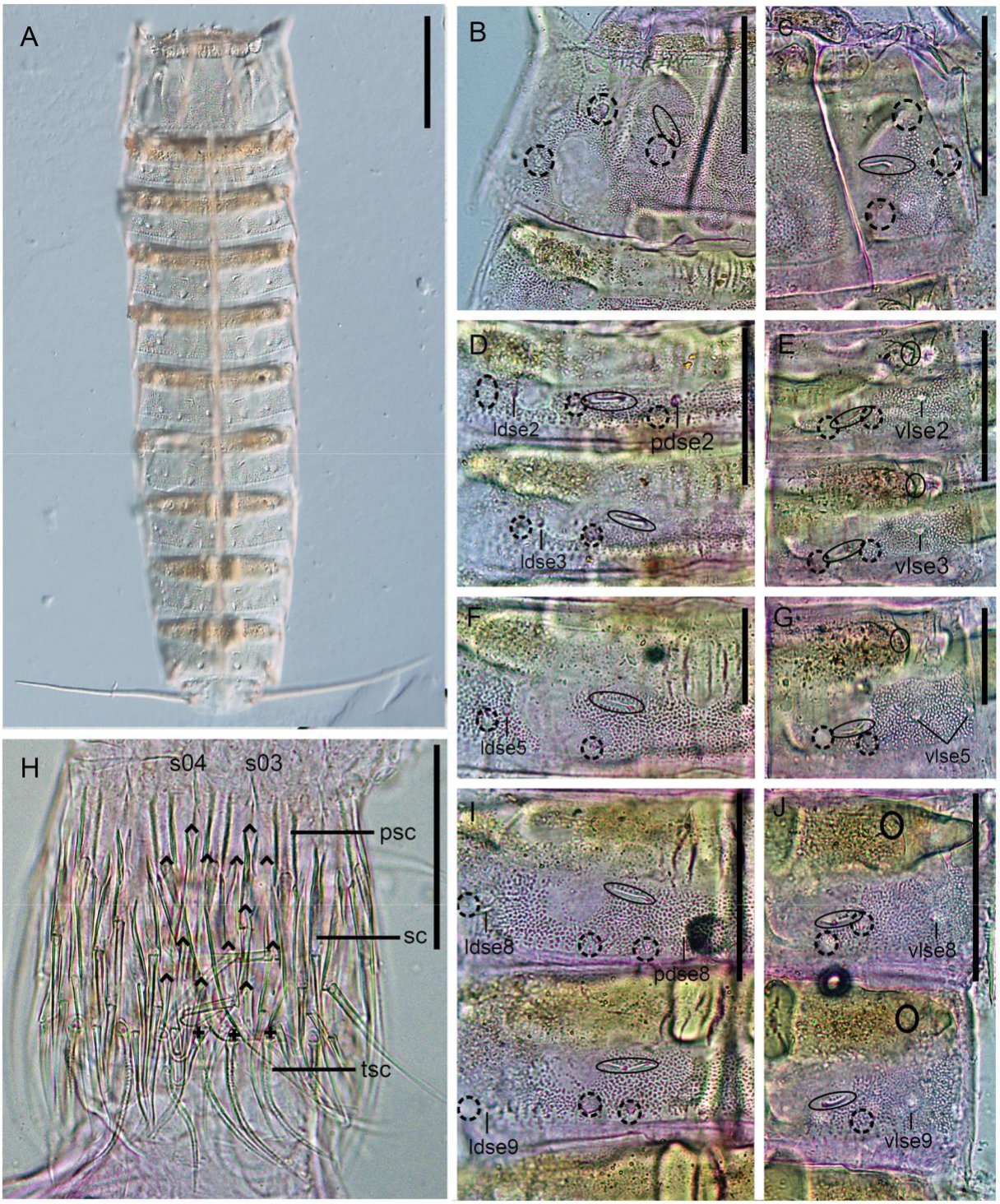

FIGURE 3 | Light micrographs showing trunk overview and details in the head and main trunk cuticular characters of female holotype NHMD 669762 **(B–J)** and male paratype NHMD 669763 **(A)** of *Fujuriphyes dagon* sp. nov. **(A)** Dorsal overview of trunk; **(B)** middorsal to paralateral view on right half of tergal plate of segment 1; **(C)** ventrolateral to ventromedial view on left half of sternal plates of segment 1; **(D)** middorsal to laterodorsal view on right half of tergal plate of segments 2–3; **(E)** left sternal plates of segments 2–3; **(F)** middorsal to laterodorsal view on right half of tergal plate of segment 5; **(G)** left sternal plate of segment 5; **(H)** introvert, with detail of primary spinoscalid, regular-sized scalid, and trichoscalid arrangement of sectors 03–04; **(I)** middorsal to laterodorsal view on right half of tergal plate of segments 8–9; **(J)** left sternal plates of segments 8–9. Scale bars **(A):** 250 µm; **(B–E, H–J)**: 62 µm; **(F)** and **(G):** 31 µm. Abbreviations: ldse, laterodorsal seta; pdse, paradorsal seta; psc, primary spinoscalid; s, sector of introvert; sc, regular-sized scalid; tsc, trichoscalid; vlse, ventrolateral seta; numbers after abbreviations indicate corresponding segment or sector of introvert; carets indicate the arrangement of scalids, and crosses that of trichoscalids; sensory spots are marked as dashed circles, and glandular cell outlets as continuous circles.

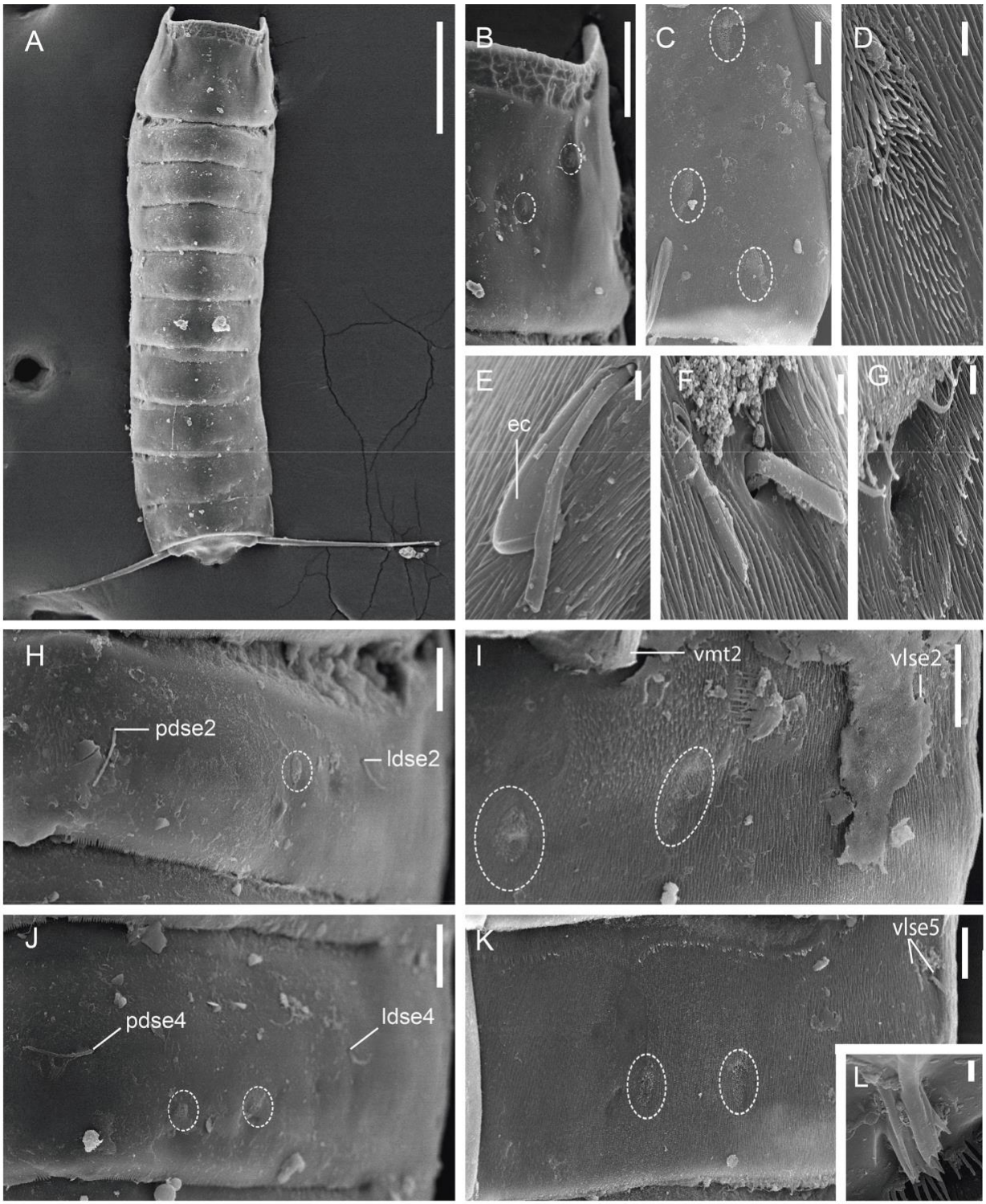

FIGURE 4 | Scanning electron micrographs showing trunk overview and details in the main trunk cuticular appendages of a male of *Fujuriphyes dagon* sp. nov. **(A)** Dorsal overview of trunk; **(B)** middorsal to subdorsal view on left half of tergal plate of segment 1; **(C)** left episternal plate of segment 1; **(D)** ventromedial sensory spot of segment 5; **(E)** lateroventral seta of segment 10; **(F)** ventrolateral setae of segment 5; **(G)** ventral cuticular ridge and associated glandular cell outlet of segment 6; **(H)** middorsal to laterodorsal view on left half of tergal plate of segment 2; **(I)** left sternal plate of segment 2; **(J)** middorsal to laterodorsal view on left half of tergal plate of segment 4; **(K)** left sternal plate of segment 5; **(L)** laterodorsal type 3 sensory spot of segment 11. Scale bars: **(A):** 300 µm; **(B):** 30 µm; **(C,E,H–L)**: 10 µm; **(D,F,G):** 1 mm. Abbreviations: ec, epibiontic Ciliophora; ldse, laterodorsal seta; pdse, paradorsal seta; vlse, ventrolateral seta; vmt, ventromedial tube; numbers after abbreviations indicate corresponding segment; sensory spots are marked as dashed circles.

Segment 4 without middorsal process or elevation. Unpaired seta in paradorsal position; paired setae in laterodorsal, lateroventral, and ventrolateral positions (**Figures 1A,B**, **4J**). Sensory spots in subdorsal (two pairs), laterodorsal (one pair), and ventromedial (two pairs) positions, with the more mesial ventromedial pair laterally shifted compared to those of previous segments (**Figures 1A,B**, **4J**).

Segment 5 without middorsal process or elevation. Two pairs of setae in ventrolateral position; one pair in laterodorsal position (**Figures 1A,B**, **3F,G**, **4F,K**). Sensory spots in subdorsal (one pair), laterodorsal (one pair), and ventromedial (two pairs) positions, the latter aligned with those of segment 3 (**Figures 1A,B**, **3F,G**, **4D,K**).

Segment 6 similar to segment 4 in the arrangement of setae and sensory spots (**Figures 1A,B**, **4G**).

Segment 7 similar to segment 3 in the arrangement of setae and sensory spots (**Figures 1A,B**).

Segment 8 without middorsal process or elevation. Unpaired seta in paradorsal position; paired setae in laterodorsal, lateroventral, and ventrolateral positions (**Figures 1A,B**, **3I,J**). Sensory spots in subdorsal (two pairs), laterodorsal (one pair), and ventromedial (two pairs) positions, the latter aligned with those of the previous segment (**Figures 1A,B**, **3I,J**).

Segment 9 without middorsal process or elevation. Paired setae in laterodorsal and ventrolateral positions (**Figures 1A,B**, **3I,J**). Sensory spots in subdorsal (two pairs), laterodorsal (one pair), and ventromedial (one pair) positions (**Figures 1A,B, 3I,J**). Nephridiopores not observed.

Segment 10 without middorsal process or elevation. Paired setae in laterodorsal and lateroventral positions (**Figures 1A,B,D**, **4E**). One pair of sensory spots in subdorsal, laterodorsal, and ventromedial positions (**Figures 1A,B,D**).

Segment 11 with one pair of type 3 sensory spots in laterodorsal position (**Figures 1B**, **4L**). Males with two pairs of sexually dimorphic penile spines and genital pores (**Figure 1D**). Lateral terminal spines long (LTS:TL interval ratio = 30.1–31.9), robust, widely spread, apparently rigid (**Figures 1A,B**, **3A**, **4A**).

Associated kinorhynch fauna

Fujuriphyes dagon sp. nov. co-occurred with *Condyloderes* sp., *E. unispinosus* and *Fissuroderes cthulhu* sp. nov. in the analyzed samples.

Fujuriphyes hydra sp. nov.

urn:lsid:zoobank.org:act:28E6A464-9534-46AC-A113-16492D6E52BE (**Figures 5**, **6**).

Material examined

Holotype, adult female, collected in November 2015 at Betsiboka area, Mozambique Channel, western Indian Ocean (15 21.695^{0}S, 45 57.388^{0}E) at 757 m depth; mounted in Fluoromount G®, deposited at NHMD under accession number: 669766. Paratypes, two adult males and one adult female, with same collecting data as holotype; mounted in Fluoromount G®, deposited at NHMD under accession numbers: 669767–669769.

Diagnosis

Fujuriphyes with middorsal elevations on segments 1–10, with the elevation of segment 10 appearing smaller and thinner than the others. Unpaired paradorsal setae on segments 2, 4, and 6, and paired on segment 8. Paralateral setae on segment 1. Laterodorsal setae on segments 2–9. One pair of lateroventral setae on segments 2, 4, 6, and 8, and two pairs on segment 10. One pair of ventrolateral setae on segments 3–4 and 6–8, and two pairs on segment 5. Ventromedial setae on segments 2 (only females) and 9. Males with ventromedial tubes on segment 2. Lateral terminal spines present.

Etymology

The species is named after the fictional deity Hydra (also known as Mother Hydra), created by the American writer of cosmic horror fiction H.P. Lovecraft (1890–1937) and firstly introduced in the short story “The Shadow over Innsmouth,” published in 1936. In the pantheon of Lovecraftian cosmic entities, Mother Hydra is the consort of Father Dagon.

Description

See **Supplementary Table 1.3** for measurements and dimensions, and **Supplementary Table 1.4** for summary of cuticular elevation, seta, spine, tube, glandular cell outlet, and sensory spot locations.

The analyzed specimens were not suitable for head examinations; hence, data on morphology, number, and arrangement of scalids and oral styles are not available.

Neck with four dorsal and two ventral, slightly sclerotized placids (**Figures 5A–C**). Dorsal placids rectangular, wide, longitudinally compressed; mesial ones broader (ca. 25–26 µm wide at the base), with the margins closest to the lateral ones more elevated; lateral ones narrower (ca. 20–21 µm wide at the base), with the margins closest to the mesial ones more elevated (**Figure 5B**). Ventral placids also rectangular but much more elongated (ca. 37–40 µm wide at the base), getting narrower toward the lateral sides (**Figures 5A,C**).

Trunk rectangular, stout, strongly sclerotized, triangular in cross-section, composed of 11 segments (**Figures 5A,B**, **6A**). Segment 1 with one tergal, two episternal, and one midsternal plate; remaining segments with one tergal and two sternal plates (**Figures 5A–D**, **6A–J**). Maximum sternal width at segment 6, almost constant throughout the trunk, slightly tapering at the last trunk segments (**Figures 5A,B**, **6A**). Sternal cuticular plates wide in ratio of maximum sternal width to trunk length (MSW-6:TL average ratio = 32.81%), giving the animal a plump appearance (**Figures 5A,B**, **6A**). Middorsal elevations on segments 1–10, with intracuticular, butterfly-like atria of paradorsal sensory spots; middorsal elevation of segment 10 smaller and thinner than previous ones (**Figures 5B**, **6B,D,F,I**). Segments 1–10 with rounded glandular cell outlets in subdorsal and ventromedial positions (**Figures 5A–D**, **6B– J**). Segments 2–10 with paired cuticular ridges in laterodorsal and ventrolateral positions, the latter with adjacent, minute glandular cell outlets (**Figures 5A–D**, **6B–J**). Cuticular hairs not observed. Muscular scars very conspicuous in laterodorsal and ventromedial positions (**Figures 5A–D**, **6B–J**). Pachycycli and

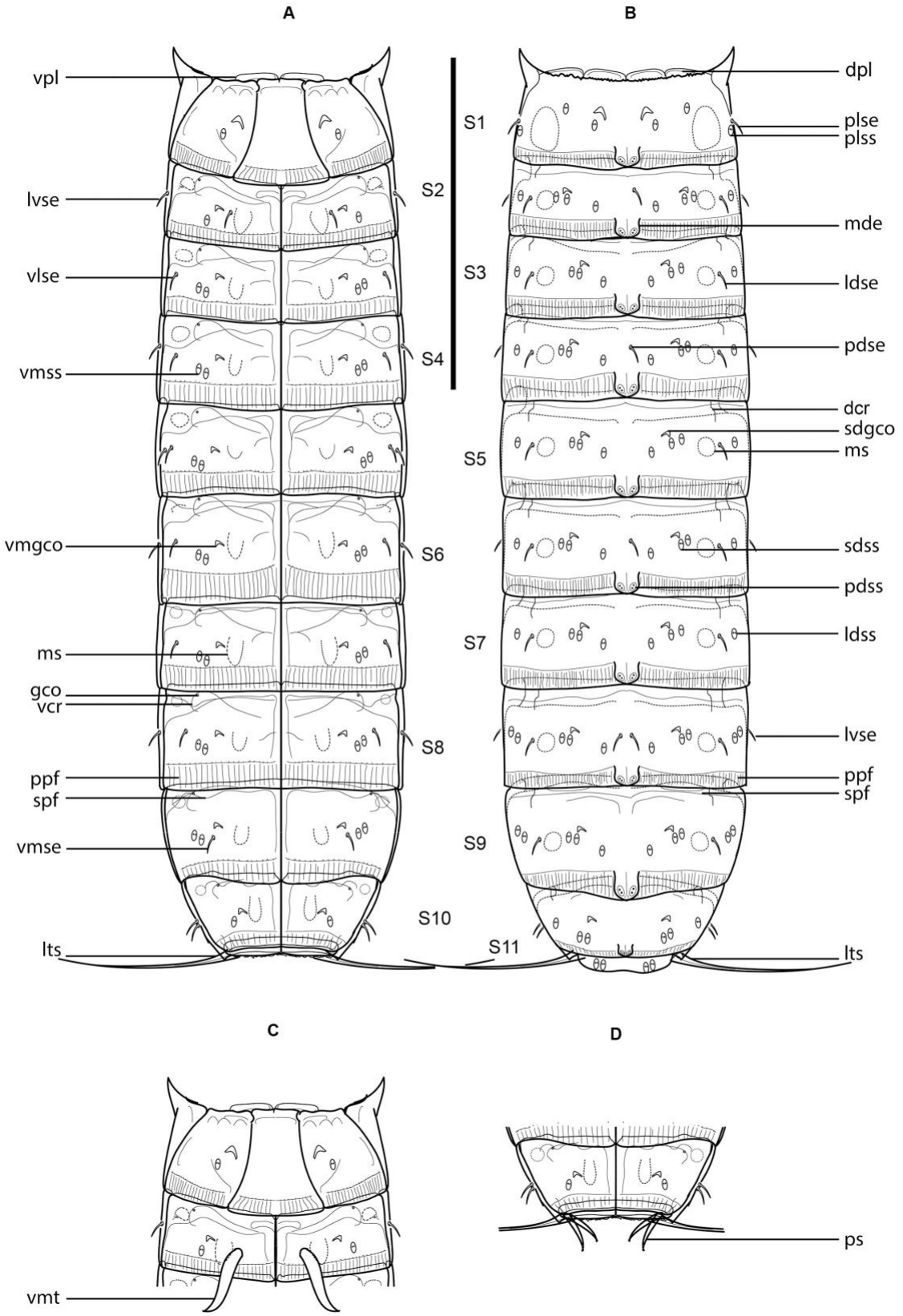

FIGURE 5 | Continued

FIGURE 5 | Line art illustrations of *Fujuriphyes hydra* sp. nov. **(A)** Female, ventral view; **(B)** female, dorsal view; **(C)** male, segments 1–2, ventral view; **(D)** male, segments 10–11, ventral view. Scale bar: 250 µm. Abbreviations: dcr, dorsal cuticular ridge; dpl, dorsal placid; gco, glandular cell outlet; ldse, laterodorsal seta; ldss, laterodorsal sensory spot; lts, lateral terminal spine; lvse, lateroventral seta; mde, middorsal elevation; ms, muscular scar; pdse, paradorsal seta; pdss, paradorsal sensory spot; plse, paralateral seta; plss, paralateral sensory spot; ppf, primary pectinate fringe; ps, penile spine; sdgco, subdorsal glandular cell outlet; sdss, subdorsal sensory spot; spf, secondary pectinate fringe; vcr, ventral cuticular ridge; vlse, ventrolateral seta; vmgco, ventromedial glandular cell outlet; vmse, ventromedial seta; vmss, ventromedial sensory spot; vpl, ventral placid; vmt, ventromedial tube.

ball-and-socket joints well-developed, thick, on segments 2–10 (**Figures 5A–D**, **6A**). Apodemes absent. Posterior margin of segments straight, showing primary pectinate fringes with weakly serrated free flaps (**Figures 5A–D**); secondary pectinate fringes not detectable under LM.

Segment 1 with middorsal elevation and associated butterfly-like intracuticular atria of the paradorsal sensory spots (**Figures 5B**, **6B**). Anterolateral margins of tergal plate as horn-like, distally pointed extensions (**Figures 5A–C**, **6A–C**). Anterior margin of tergal plate finely denticulate (**Figures 5B**, **6B**). Anterior margin of sternal plates with a wavy median ridge of cuticle (**Figures 5A,C**, **6A,C**). Midsternal plate trapezoidal, laterally extended at its base, with a lateral constriction near its anterior margin and a straight posterior margin (**Figures 5A,C**, **6A,C**). Paired setae in paralateral position (**Figures 5B**, **6B**). Sensory spots in paradorsal (one pair), subdorsal (two pairs), paralateral (one pair), and ventromedial (one pair) positions; all of them located at the anterior half of the cuticular plates except the paradorsal and paralateral ones (**Figures 5A–C**, **6B,C**).

Segment 2 with middorsal elevation as on the preceding segment (**Figures 5B**, **6D**). Unpaired seta in paradorsal position, and paired setae in laterodorsal and lateroventral positions; females with paired, sexually dimorphic setae in ventromedial position (**Figures 5A–C**, **6D,E**). Sensory spots in paradorsal (one pair), subdorsal (three pairs), laterodorsal (one pair), and ventromedial (one pair) positions (**Figure 5A–C**, **6D,E**). Males with sexually dimorphic tubes in ventromedial position (**Figure 5C**).

Segment 3 with middorsal elevation as on preceding segments (**Figures 5B**, **6D**). Paired setae in laterodorsal and ventrolateral positions (**Figures 5A,B**, **6D,E**). Sensory spots in paradorsal (one pair), subdorsal (three pairs), laterodorsal (one pair), and ventromedial (two pairs) positions (**Figures 5A,B**, **6D,E**). Subdorsal sensory spots more mesial than those of segment 2; ventromedial sensory spots closely located to each other (**Figures 5A,B**, **6D,E**).

Segment 4 with middorsal elevation as on preceding segments (**Figure 5B**). Unpaired seta in paradorsal position, and paired setae in laterodorsal, lateroventral, and ventrolateral positions, the former aligned with those of segment 3 (**Figures 5A,B**). Sensory spots in paradorsal (one pair), subdorsal (three pairs), laterodorsal (one pair), and ventromedial (two pairs) positions (**Figures 5A,B**).

Segment 5 similar to segment 3 in the arrangement of cuticular elevation, setae, and sensory spots, but with two pairs of ventrolateral setae, situated very close to each other (**Figures 5A,B**, **6F,G**).

Segment 6 similar to segment 4 in the arrangement of cuticular elevation, setae, and sensory spots (**Figures 5A,B**, **6F,G**).

Segment 7 similar to segment 3 in the arrangement of cuticular elevation, setae, and sensory spots (**Figures 5A,B**).

Segment 8 with middorsal elevation as on preceding segments (**Figures 5B**, **6I**). Paired setae in paradorsal, laterodorsal, lateroventral, and ventrolateral positions, the latter more mesial than those of previous segments but still in ventrolateral position (**Figures 5A,B**, **6I,J**). Sensory spots in paradorsal (one pair), subdorsal (three pairs), laterodorsal (two pairs), and ventromedial (two pairs) positions (**Figures 5A,B**, **6I,J**).

Segment 9 with middorsal elevation as on preceding segments (**Figures 5B**, **6I**). Paired setae in laterodorsal and ventromedial positions (**Figure 5A,B**, **6I,J**). Sensory spots in paradorsal (one pair), subdorsal (three pairs), laterodorsal (two pairs), and ventromedial (two pairs) positions (**Figure 5A,B**, **6I,J**). Nephridiopores not observed.

Segment 10 with middorsal elevation smaller and thinner than previous ones (**Figures 5B**, **6H**). Two pairs of setae in lateroventral position (**Figure 5B**). Sensory spots in paradorsal (one pair), subdorsal (two pairs), laterodorsal (one pair), and ventromedial (one pair) positions (**Figures 5A,B**, **6H**).

Segment 11 with two pairs of sensory spots in laterodorsal position (**Figure 5B**). Males with two pairs of sexually dimorphic penile spines and genital pores (**Figure 5D**). Lateral terminal spines long (LTS:TL average ratio = 30.97%), slender, narrow, apparently flexible (**Figures 5A,B**, **6A**).

Associated kinorhynch fauna

Fujuriphyes hydra sp. nov. co-occurred with the species *E. unispinosus* and *Ryuguderes* sp. in the analyzed samples.

Class Cyclorhagida (Zelinka, 1896) Sørensen et al., 2015.
Family Echinoderidae Zelinka, 1894.
Genus *Fissuroderes* Neuhaus and Blasche, 2006.

Fissuroderes cthulhu sp. nov.
urn:lsid:zoobank.org:act:8C27FAF4-0CD2-4767-9FE3-F46DEDDE9147 (**Figures 7–9**).

Material examined

Holotype, adult female, collected in October 2014 at Mahavavy area, Mozambique Channel, western Indian Ocean (15 31.148^{0}S, 45 42.931^{0}E) at 789 m depth; mounted in Fluoromount G®, deposited at NHMD under accession number: 669727. Paratypes, five adult males and four adult females, with same collecting data as holotype; mounted in Fluoromount G®, deposited at NHMD under accession numbers: 669728–669736. Nineteen additional specimens mounted for LM, same collecting data as type material, deposited at NHMD under accession numbers: 669737–669755; one additional specimen mounted for

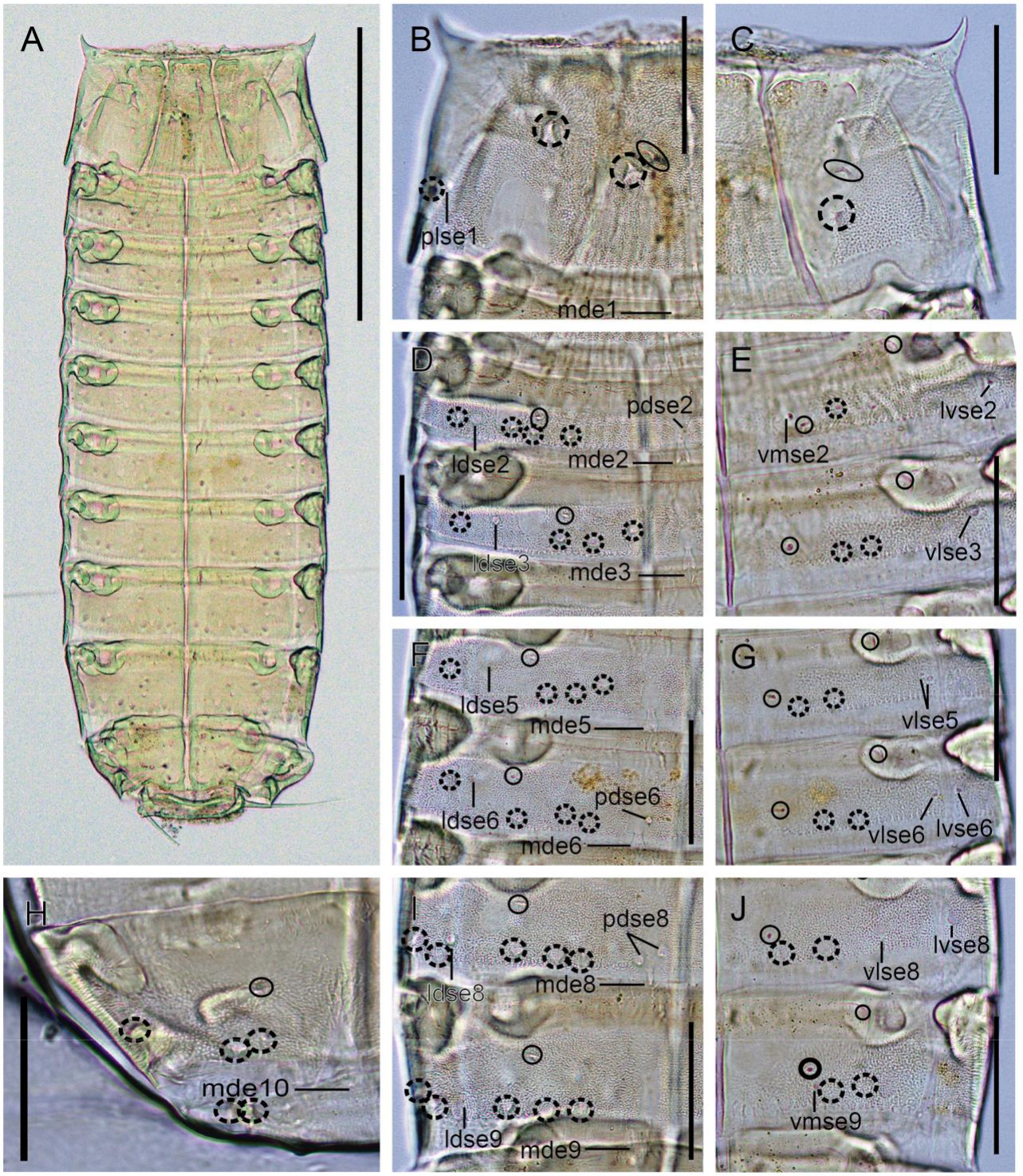

FIGURE 6 | Light micrographs showing trunk overview and details in the main trunk cuticular appendages of female holotype NHMD 669766 of *Fujuriphyes hydra* sp. nov. **(A)** Ventral overview of trunk; **(B)** middorsal to paralateral view on right half of tergal plate of segment 1; **(C)** ventrolateral to ventromedial view on left half of sternal plates of segment 1; **(D)** middorsal to laterodorsal view on right half of tergal plates of segments 2–3; **(E)** left sternal plates of segments 2–3; **(F)** middorsal to laterodorsal view on right half of tergal plates of segments 5–6; **(G)** left sternal plates of segments 5–6; **(H)** middorsal to laterodorsal view on right half of tergal plate of segment 10; **(I)** middorsal to laterodorsal view on right half of tergal plate of segments 8–9; **(J)** left sternal plates of segments 8–9. Scale bars: **(A):** 250 µm; **(B–J)**: 62 µm. Abbreviations: ldse, laterodorsal seta; mde, middorsal elevation; pdse, paradorsal seta; plse, paralateral seta; vlse, ventrolateral seta; vmse, ventromedial seta; numbers after abbreviations indicate corresponding segment; sensory spots are marked as dashed circles (except paradorsal ones), and glandular cell outlets as closed circles.

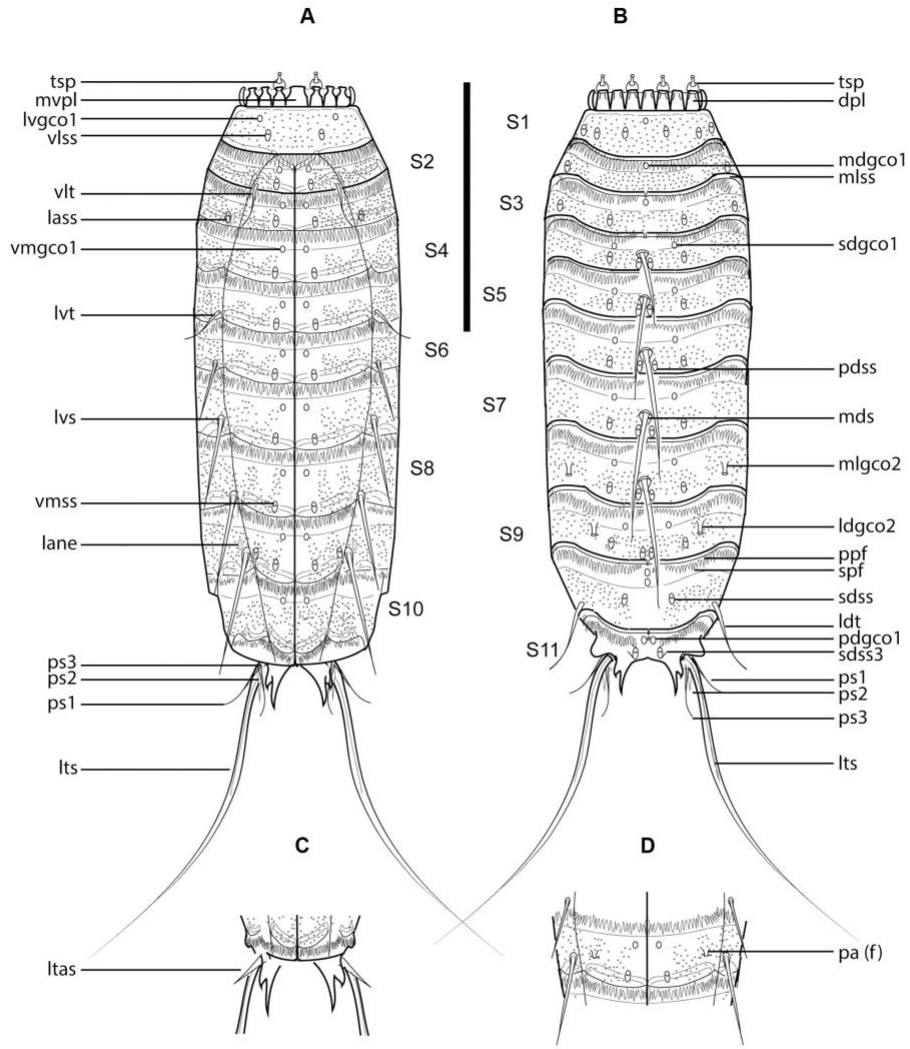

FIGURE 7 | Line art illustrations of *Fissuroderes cthulhu* sp. nov. **(A)** Male, ventral view; **(B)** male, dorsal view; **(C)** female, segments 10–11, ventral view; **(D)** female, segment 7, ventral view. Scale bar: 250 µm. Abbreviations: dpl, dorsal placid; f, female condition of sexually dimorphic character; lane, lateral accessory nephridiopore; lass, lateral accessory sensory spot; ldgco2, laterodorsal type 2 glandular cell outlet; ldss, laterodorsal sensory spot; ldt, laterodorsal tube; ltas, lateral terminal accessory spine; lts, lateral terminal spine; lvgco1, lateroventral type 1 glandular cell outlet; lvs, lateroventral spine; lvt, lateroventral tube; mdgco1, middorsal type 1 glandular cell outlet; mds, middorsal spine; mlgco2, midlateral type 2 glandular cell outlet; mlss, midlateral sensory spot; mvpl, midventral placid; pa, papilla; pdgco1, paradorsal type 1 glandular cell outlet; pdss, paradorsal sensory spot; ppf, primary pectinate fringe; ps, penile spine (followed by number of corresponding pair); sdgco1, subdorsal type 1 glandular cell outlet; sdss, subdorsal sensory spot; sdss3, subdorsal type 3 sensory spot; spf, secondary pectinate fringe; tsp, trichoscalid plate; vlss, ventrolateral sensory spot; vlt, ventrolateral tube; vmgco1, ventromedial type 1 glandular cell outlet; vmss, ventromedial sensory spot.

SEM, same collecting data as type material, deposited at the Meiofauna Collection of the UCM.

Diagnosis

Fissuroderes with spines in middorsal position on segments 4– 8 and in lateroventral position on segments 6–9, increasing progressively in length toward the posterior segments; broad, elongated, and distally pointed tubes in ventrolateral position on segment 2, in lateroventral position on segment 5, and in laterodorsal position on segment 10. Tergal extensions of segment 11 elongated, distally bifurcated, with pointed tips. Type 2 glandular cell outlets in midlateral position on segment 8 and in laterodorsal position of segment 9.

Females with sexually dimorphic papillae in ventrolateral position on segment 7.

Etymology

The species is named after the fictional cosmic entity Cthulhu, created by the American writer of horror fiction H.P. Lovecraft (1890-1937) and firstly introduced in the short story “The Call of Cthulhu,” published in 1928. Considered a Great Old One within the pantheon of Lovecraftian cosmic entities, Cthulhu is a gigantic being of great power described as looking like an octopus or a dragon that lies in a death-like torpor in the sunken city of R’lyeh.

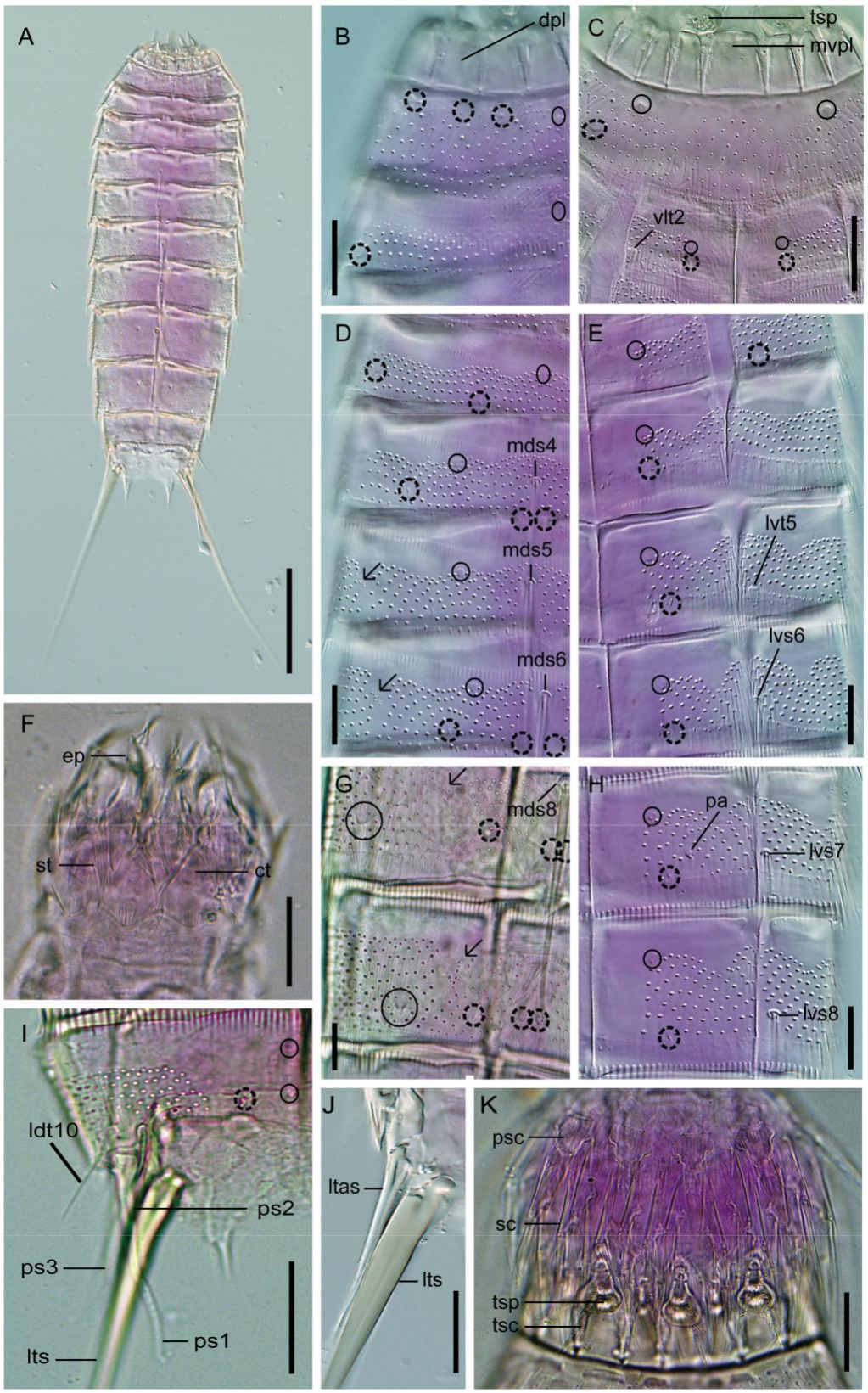

FIGURE 8 | Continued

FIGURE 8 | Light micrographs showing trunk overview and details in the head, neck, and main trunk cuticular characters of female holotype NHMD 669727 **(A–E,H,J)** and male paratype NHMD 669728 **(F,G,I,K)** of *Fissuroderes cthulhu* sp. nov. **(A)** Dorsal overview of trunk; **(B)** neck and middorsal to midlateral view on right half of tergal plates of segments 1–2; **(C)** neck and sublateral to ventromedial view tergal and sternal plates of segments 1–2; **(D)** middorsal to midlateral view on right half of tergal plates of segments 3–6; **(E)** sublateral to ventromedial view on left half of tergal and sternal plates of segments 3–6; **(F)** mouth cone; **(G)** middorsal to midlateral view on right half of tergal plates of segments 8–9; **(H)** sublateral to ventromedial view on left half of tergal and sternal plates of segments 7–8; **(I)** middorsal to midlateral view on right half of tergal plate of segment 10; **(J)** lateral terminal accessory spine; **(K)** introvert. Scale bars: **(A):** 100 µm; **(B–K)**: 20 µm. Abbreviations: ct, cuticular thickening; dpl, dorsal placid; ep, end-piece of outer oral style; ldt, laterodorsal tube; lta*s*, lateral terminal accessory spine; lts, lateral terminal spine; lvs, lateroventral spine; lvt, lateroventral tube; mds, middorsal spine; mvpl, midventral placid; pa, female papilla; ps, penile spine (followed by number of corresponding pair); psc, primary spinoscalid; sc, regular-sized scalid; st, spinous tuft of outer oral style; tsc, trichoscalid; tsp, trichoscalid plate; vlt, ventrolateral tube; numbers after abbreviations indicate corresponding segment; sensory spots are marked as dashed circles, and glandular cell outlets as closed circles; arrows indicate the muscular scars with several perforations as microsculpture.

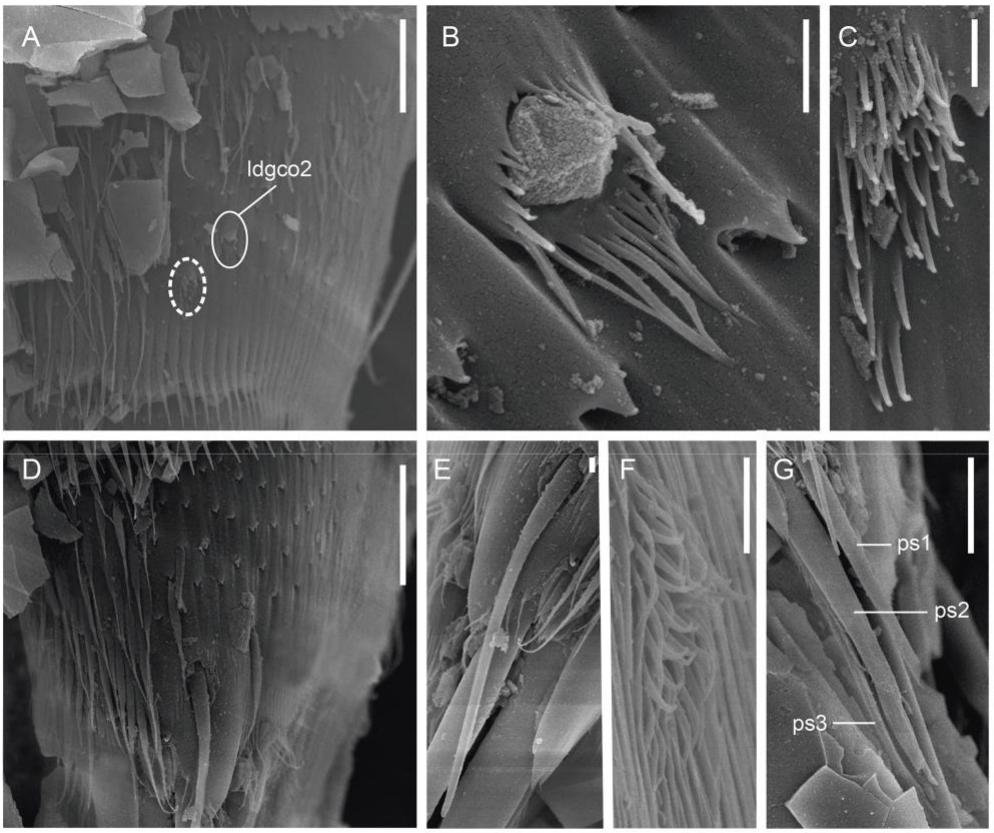

FIGURE 9 | Scanning electron micrographs showing some cuticular characters of segments 9–11 of a male of *Fissuroderes cthulhu* sp. nov. **(A)** Lateral view of segment 9; **(B)** detail of the laterodorsal type 2 glandular cell outlet of segment 9; **(C)** detail of the midlateral sensory spot of segment 9; **(D)** lateral view of segment 10; **(E)** detail of the laterodorsal tube of segment 10; **(F)** detail of the subdorsal sensory spot of segment 10; **(G)** detail of the penile spines of segment 11. Scale bars: **(A,D):** 10 µm; **(B,C,E–G)**: 1 µm. Abbreviations: ldgco2, laterodorsal type 2 glandular cell outlet; ps, penile spine (followed by number of corresponding pair); sensory spots are marked as dashed circles.

Description

See **Supplementary Table 1.5** for measurements and dimensions and **Supplementary Table 1.6** for summary of spine, tube, nephridiopore, glandular cell outlet, and sensory spot locations.

Head with retractable mouth cone and introvert (**Figures 8F,K**). Although some of the specimens have the introvert partially everted, oral styles and scalids tended to be collapsed when mounted for LM; furthermore, specimens for SEM were not suitable for head examination, so only some details on the exact number, arrangement, and morphology of oral styles and scalids can be provided.

Ring 00 of mouth cone with nine outer oral styles alternating in size between slightly larger and smaller ones (**Figure 8F**). Outer oral styles composed of two jointed subunits: a rectangular basal piece with a proximal sheath bearing a long, spinous tuft; and a triangular, curved end piece distally sharped (**Figure 8F**). Triangular, cuticular thickenings flanking the outer oral styles' bases (**Figure 8F**). Outer oral styles located anterior to each introvert sector, except in the middorsal section 6 where a style is missing.

Introvert with six transverse rings of scalids and 10 longitudinal sectors defined by the arrangement of the primary

spinoscalids. Ring 01 with 10 primary spinoscalids, larger than the remaining ones, laterally compressed, composed of a trapezoidal, wide basal sheath and a distal, elongated, flexible, distally blunt end piece (**Figure 8K**). The basal sheath bears two long, thread-like projections laterally and a median fringe of several long and flexible tips (**Figure 8K**). Rings 02–06 with regular-sized, laterally compressed scalids, much smaller than the primary spinoscalids, each one composed of a rectangular basal sheath carrying a median fringe and a distal, pointed end piece (**Figure 8K**). Exact arrangement of these scalids cannot be provided.

Neck with 16 trapezoidal placids, wider at bases, with a distinct joint between the neck and segment 1 (**Figures 7A,B**, **8B,C,K**). Midventral placid widest (ca. 17–19 µm wide at base), remaining ones narrower (ca. 12–13 µm wide at base) (**Figures 7A,B**, **8B,C,K**). Placids closely situated at base, distally separated by cuticular folds (**Figures 7A,B**, **8B,C,K**). A ring of six long, hairy trichoscalids associated with the placids of the neck is present, attached to large, bottle-like trichoscalid plates (**Figures 7A,B**, **8C,K**).

Trunk with 11 segments, triangular in cross-section (**Figures 7A,B**, **8A**). Segment 1 as closed cuticular ring, remaining ones with one tergal and two sternal cuticular plates (**Figures 7A–D**, **8A**). Tergal plates middorsally bulging. Maximum width at segment 6, progressively tapering toward the last trunk segments (**Figures 7A,B**, **8A**). Sternal plates relatively narrow compared to the total trunk length (MSW-6:TL average ratio = 22.3%), giving the animal a rectangular general appearance (**Figures 7A,B**, **8A**). Cuticular hairs present on segments 1–10, acicular, elongated, distally pointed, with rounded to oval-shaped perforation sites (**Figures 7A–D**, **8B–E,G,H**, **9A,D**). Cuticular hairs distributed in 5–7 wavy, transverse rows at the middle part of the plates on segments 2–9; in 6–7 straight, transverse rows almost covering the whole cuticular surface on segment 1; and segment 10 with 5–7 wavy, transverse rows at the middle part of the plates, from subdorsal to ventromedial regions (**Figures 7A–D**, **8B–E,G–I**). Muscular scars with several perforations as microsculpture throughout the trunk (**Figure 8D,G**). Posterior margin of segments 1–10 straight, showing a long, conspicuous primary pectinate fringe with a strong serration with bifid tips (**Figures 7A,B,D**, **8B–E,G,H**, **9A,D**). Secondary pectinate fringes on segments 2–11, with a very weak serration and usually hidden by the primary pectinate fringe of the previous segment (**Figures 7A,B,D**).

Segment 1 without spines and tubes. Unpaired type 1 glandular cell outlet in middorsal position, and paired type 1 glandular cell outlets in lateroventral position (**Figures 7A,B**, **8B,C**). Type 1 glandular cell outlets on this and remaining segments situated at the anterior half of the segment, sometimes hidden under the pectinate fringe of the previous segment. Paired sensory spots in subdorsal, laterodorsal, midlateral, and ventrolateral positions (**Figures 7A,B**, **8B,C**). Sensory spots on this and remaining segments composed of several long micropapillae and sometimes with a single, central cilium (**Figures 9C,F**).

Segment 2 with a pair of wide, flexible tubes in ventrolateral position (**Figures 7A**, **8C**). Tubes on this and remaining segments are composed of a short, rectangular, wide basal-piece and a flexible, elongated, distally pointed end piece that resembles an acicular spine in LM (**Figure 9E**). Unpaired type 1 glandular cell outlet in middorsal position, and paired type 1 glandular cell outlets in ventromedial position (**Figures 7A,B**, **8B,C**). Paired sensory spots in midlateral and ventromedial positions (**Figures 7A,B**, **8B,C**).

Segment 3 without spines and tubes. Unpaired type 1 glandular cell outlet in middorsal position, and paired type 1 glandular cell outlets in ventromedial position (**Figures 7A,B**, **8D,E**). Paired sensory spots in subdorsal, midlateral, lateral accessory, and ventromedial positions (**Figures 7A,B**, **8D,E**).

Segment 4 with a middorsal spine not exceeding the posterior edge of the following segment (**Figures 7B**, **8D**). Spines on this and remaining segments are acicular and flexible, increasing in length toward the end of the trunk throughout both the middorsal and lateroventral series (**Figures 7A,B**, **8D,E,G,H**). Paired type 1 glandular cell outlets in subdorsal and ventromedial positions (**Figures 7A,B**, **8D,E**). Paired sensory spots in paradorsal, laterodorsal, and ventromedial positions (**Figures 7A,B**, **8D,E**).

Segment 5 with a middorsal spine reaching the posterior edge of the following segment, and paired lateroventral tubes (**Figures 7A,B**, **8D,E**). Paired type 1 glandular cell outlets in subdorsal and ventromedial positions (**Figures 7A,B**, **8D,E**). Paired sensory spots in paradorsal, subdorsal, and ventromedial positions (**Figures 7A,B**, **8D,E**).

Segment 6 with a middorsal spine exceeding the posterior edge of the following segment, and paired lateroventral spines (**Figures 7A,B**, **8D,E**). Paired type 1 glandular cell outlets in subdorsal and ventromedial positions (**Figures 7A,B**, **8D,E**). Paired sensory spots in paradorsal, subdorsal, and ventromedial positions (**Figures 7A,B**, **8D,E**).

Segment 7 similar to segment 6 in the arrangement of spines, type 1 glandular cell outlets, sensory spots, and cuticular hairs, as well as in the morphology of the posterior margin of segment, primary and secondary pectinate fringes, except females that have sexually dimorphic papillae in ventrolateral position (**Figures 7A,B,D**, **8H**).

Segment 8 with a middorsal spine exceeding the posterior edge of the following segment, and paired lateroventral spines (**Figures 7A,B**, **8G,H**). Paired type 1 glandular cell outlets in subdorsal and ventromedial positions, and paired type 2 glandular cell outlets in midlateral position (**Figures 7A,B**, **8G,H**). Type 2 glandular cell outlets consist of a big, elevated pore surrounded by a single ring of long micropapillae (**Figure 9B**). Paired sensory spots in paradorsal, subdorsal, and ventromedial positions (**Figures 7A,B**, **8G,H**).

Segment 9 with paired lateroventral spines (**Figure 7A**). Paired type 1 glandular cell outlets in subdorsal and ventromedial positions, and paired type 2 glandular cell outlets in laterodorsal position (**Figures 7A,B**, **8G**, **9B**). Paired sensory spots in paradorsal, subdorsal, and ventromedial positions (**Figures 7A,B**, **8G**, **9C**). Nephridiopores as small sieve plates in lateral accessory position (**Figure 7A**).

Segment 10 with paired laterodorsal tubes (**Figures 7B**, **8I**, **9E**). Two unpaired type 1 glandular cell outlets in middorsal

position, and paired type 1 glandular cell outlets in ventromedial position (**Figures 7A,B**, **8I**). Paired sensory spots in subdorsal position (**Figures 7B**, **8I**, **9F**).

Segment 11 with type 1 glandular cell outlets in paradorsal position and type 3 sensory spots in subdorsal position (**Figure 7B**). Slender, flexible lateral terminal spines (**Figures 7A,B**, **8A,I,J**). Females with paired short, robust lateral accessory spines (LTAS:LTS average ratio = 28.4%) (**Figures 7C**, **8J**). Males with three pairs of penile spines: first and third pairs long, flexible and crenulated, second pair shorter, robust and superficially smooth (**Figures 7A,B**, **8I**, **9G**). Tergal extensions of segment 11 elongated, distally bifurcated, with pointed tips (**Figures 7A–C**, **8I**). Sternal plates distally rounded (**Figures 7A,C**).

Associated kinorhynch fauna

Fissuroderes cthulhu sp. nov. co-occurred with *Condyloderes* sp., *E. unispinosus* and *F. dagon* sp. nov. in the analyzed samples.

Community Structure Along the Vertical Profile and Intra-Habitats Comparison

Densities outside the pockmarks are low and significantly decrease from the upper to the bottom sediment layers (p = 0.0242), varying more gradually than those inside the pockmarks. Densities significantly vary along the vertical profile inside the pockmarks (p = 0.0117), reaching a peak in layer 1– 2 cm (means of ca. 34 specimens per 10 cm^2 at MTB06 and 4 specimens per 10 cm^2 at MTB1), and strongly decreasing from this depth (**Table 1** and **Figures 10**, **11**). Likewise, species richness outside the pockmarks is low and changes significantly with sediment depth (p = 0.0389), having its highest value in the uppermost layer, 0–1 cm (means of ca. 1 species at both MTB2 and MTB03), and no specimens in the deepest layers, 3–4 and 4–5 cm (**Table 1** and **Figure 10**). Species richness is more stable along the vertical profile inside the pockmarks, and no significant differences are observed. The highest values are found in the second sediment layer (means of ca. 3 species at MTB06 and ca. 1 species in MTB1), and kinorhynchs are still present in the bottom layers (highest means at MTB06 of ca. 2 and 1 species at 3–4 and 4–5 cm depth, respectively) (**Table 1** and **Figure 10**).

Considering the whole cores, analyses between sites of the same habitat found no differences comparing sites outside the pockmarks (density, p = 0.5066; richness, p = 0.5002), or between the pockmark sites (density, p = 0.1266; richness, p = 0.0722), except for the species assemblage between the two pockmark sites (see below).

Inter-Habitats Comparison

Both habitats are similar in terms of species richness (p = 0.6831), with means of ca. 1–2 species outside the pockmarks (per site: ca. 2 species at MTB03 and 1 species at MTB2), and means of ca. 2 species inside the pockmarks (per site: ca. 3 species at MTB06 and 1 species at MTB1) (**Table 2** and **Figure 12**). However, kinorhynchs show a significant higher density inside the pockmarks (p = 0.0039), with means of ca. 35–36 specimens per 10 cm^2 inside the pockmarks (per site: 56 specimens at MTB06 and 15 specimens at MTB1) vs.

		OUTSIDE POCKMARK MTB03					OUTSIDE POCKMARK MTB2					INSIDE POCKMARK MTB06					INSIDE POCKMARK MTB1				
	Sediment layer	A	B	C	X	Total	A	B	C	X	Total	A	B	C	X	Total	A	B	C	X	Total
Species Richness	0–1	1	0	2	1 ± 1	3	0	3	1	1.3 ± 1.5	3	-	2	2	2 ± 0	4	0	1	1	0.7 ± 0.6	2
	1–2	4	0	1	1.7 ± 2.1	5	0	0	0	0	0	1	3	4	2.7 ± 1.5	8	2	1	1	1.3 ± 0.6	4
	2–3	1	0	0	0.3 ± 0.6	1	0	0	0	0	0	2	1	2	1.7 ± 0.6	5	0	1	1	0.7 ± 0.6	2
	3–4	0	0	0	0	0	0	0	0	0	0	2	2	2	2 ± 0	6	0	0	1	0.3 ± 0.6	1
	4–5	0	0	0	0	0	0	0	0	0	0	2	1	1	1.3 ± 0.6	4	0	0	1	0.3 ± 0.6	1
Abundance	0–1	2	0	4	2 ± 2	6	0	3	1	1.3 ± 1.5	4	-	44	24	34 ± 14.1	68	0	46	15	20.3 ± 23.5	61
	1–2	11	0	3	4.7 ± 5.7	14	1	1	0	0.7 ± 0.6	2	84	16	210	103.3 ± 98.4	310	7	24	9	13.3 ± 9.3	40
	2–3	2	0	2	1.3 ± 1.2	4	0	0	0	0	0	19	8	68	31.7 ± 31.9	95	6	9	5	6.7 ± 2.1	20
	3–4	0	0	0	0	0	0	0	0	0	0	10	4	10	8 ± 3.5	24	12	1	1	4.7 ± 6.4	14
	4–5	0	0	0	0	0	0	0	0	0	0	2	1	4	2.3 ± 1.5	7	2	0	1	1 ± 1	3
Density (ind/10 cm^2)	0–1	0.7	0	1.3	0.7 ± 0.7		0	1	0.3	0.43 ± 0.51		-	14.6	8	11.3 ± 4.7		0	15.2	5	6.7 ± 7.7	
	1–2	3.6	0	1	1.5 ± 1.8		0.3	0.3	0	0.2 ± 0.17		27.8	5.3	69.6	34.2 ± 32.6		2.3	8	3	4.4 ± 3.1	
	2–3	0.7	0	0.7	0.5 ± 0.4		0	0	0	0		6.3	2.7	22.5	10.5 ± 10.5		2	3	1.7	2.2 ± 0.68	
	3–4	0	0	0	0		0	0	0	0		3.3	1.3	3.3	2.6 ± 1.1		4	0.3	0.3	1.5 ± 2.1	
	4–5	0	0	0	0		0	0	0	0		0.7	0.3	1.3	0.77 ± 0.5		0.7	0	0.3	0.33 ± 0.35	

Data are specified by cores and layers along the vertical profile. Total numbers show the data merging the information of the three cores. X refers to average values ± standard deviation.

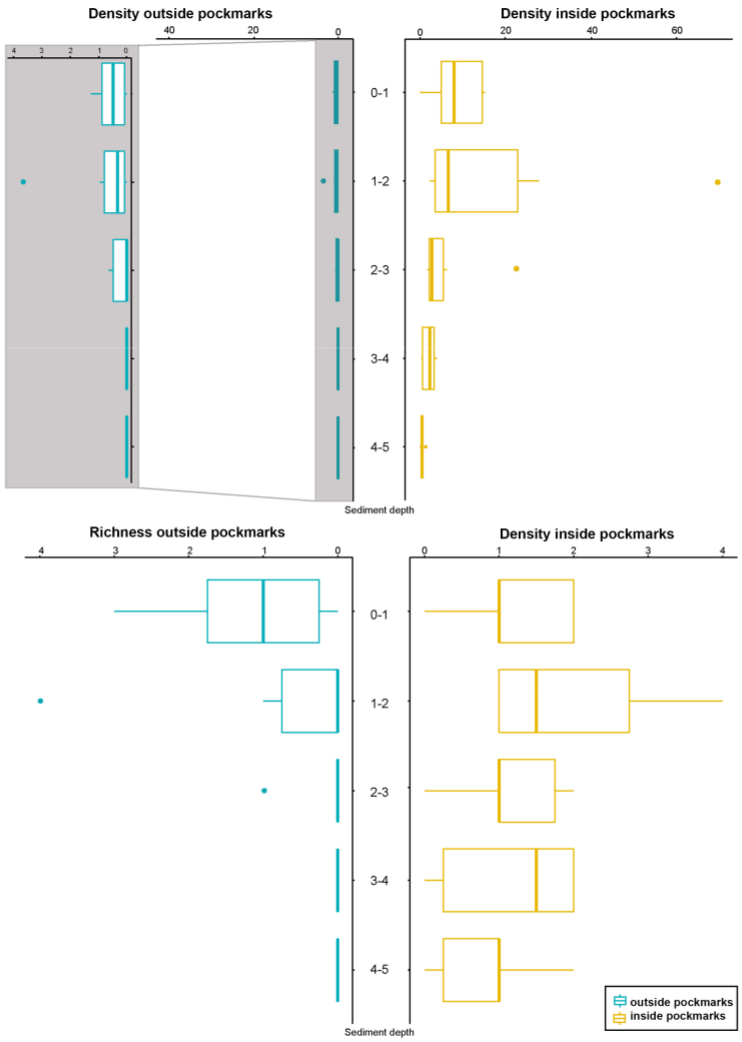

FIGURE 10 | Kinorhynch density and richness along the vertical profile of the two study habitats, inside pockmark (yellow) and outside pockmark (blue). Image enlargement of density outside the pockmark is provided to allow discerning variation of kinorhynch densities along the vertical profile. Boxplots represent the median value (horizontal line within the box), the distributions of 50% of the data (the box), and the highest and lowest values within 95% of the distribution (the whisker).

means of ca. 1–2 specimens per 10 cm^2 outside the pockmarks (per site: ca. 3 specimens per 10 cm^2 at MTB03 and 0 specimens at MTB2) (**Table 2** and **Figures 11**, **12**). Juveniles were always present and relatively abundant both inside and outside the pockmarks, with means of ca. 3–4 specimens per 10 cm^2 outside (per site: ca. 5 specimens, 20.8% of the total kinorhynch abundance at MTB03 and 2 specimens, 33.3% at MTB2) and means of ca. 30–31 specimens per 10 cm^2 inside the pockmarks (per site: ca. 169 specimens, 33.5% of the total kinorhynch abundance at MTB06 and 92 specimens, 65.2% at MTB1) (**Table 2** and **Figure 12**).

It appears that most of the species are restricted to one of the studied habitats, except *Condyloderes* sp. and *E. unispinosus* Yamasaki et al., 2018b that are present both outside and inside the pockmarks. *E. unispinosus* is the dominant species inside the pockmarks (63.1% of the total adult kinorhynch community), followed far behind by *Fi. cthulhu* sp. nov. (15% of the adult community), *Echinoderes hviidarum* Sørensen et al., 2018 (11.8% of the adult community) and *F. dagon* sp. nov. (6.6% of the adult community) (**Table 2** and **Figure 12**). All the referred species were recovered only at the pockmark site MTB06, except for *E. hviidarum* that only appeared at MTB1 (**Table 2** and **Figure 12**). The remaining species were recovered only at one of the sites in low number: *Echinoderes apex* Yamasaki et al. (2018c), *Echinoderes* cf. *dubiosus*, *Echinoderes* sp., *Ryuguderes* sp., and *F. hydra* sp. nov. outside the pockmarks; and *Sphenoderes* cf. *indicus* as a singleton inside the pockmark MTB1 (**Table 2** and **Figure 12**).

Differences in community composition between the two study habitats, inside and outside the pockmarks, were observed (occurrence: $p = 0.005$, *F.Model* = 3.8761, $R^2 = 0.222$; abundance: $p = 0.003$, *F.Model* = 3.8926, $R^2 = 0.235$). Moreover, H_2S was found

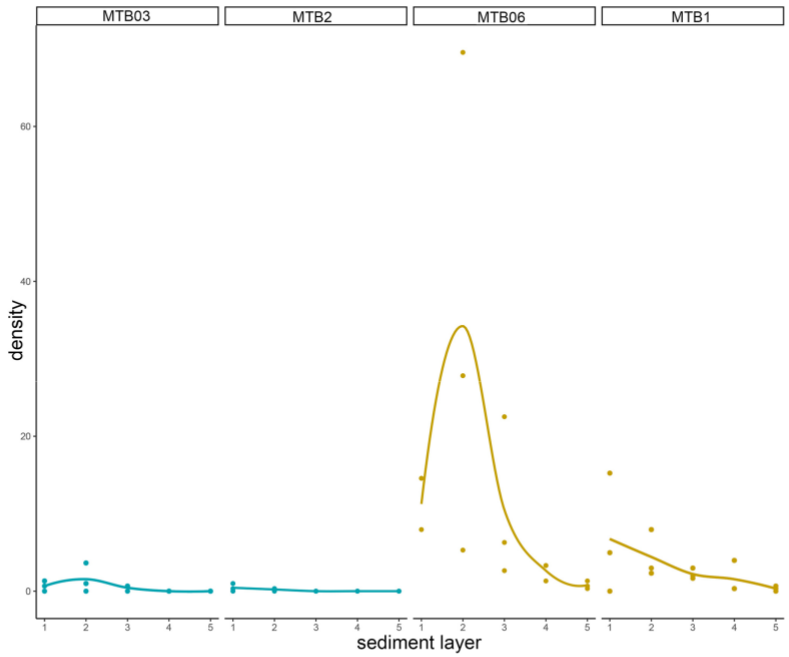

FIGURE 11 | Kinorhynch total density (including both adults and juveniles) along the vertical profile of the four study sites: MTB03 and MTB2 as outside pockmark sites (blue), and MTB06 and MTB1 (purple) as inside pockmark sites (yellow). Layers per core were determined as follows: layer 1 (0–1 cm), layer 2 (1–2 cm), layer 3 (2–3 cm), layer 4 (3–4 cm), and layer 5 (4–5 cm).

as a covariate explanatory variable (occurrence: p = 0.001, *F.Model* = 6.6067, R^2 = 0.3779; abundance: p = 0.001, *F.Model* = 5.6791, R^2 = 0.343). Differences in community composition were found between the two study pockmarks as well (occurrence: p = 0.001, *F.Model* = 44.255, R^2 = 0.678; abundance: p = 0.001, *F.Model* = 18.3670, R^2 = 0.467). None of the analyses showed significant differences to discriminate between sites outside the pockmarks. PCA for illustrating kinorhynch trends in community composition discriminated among sites: PC2 distinguished between sites located inside and outside the pockmarks, whereas PC1 discriminated between the two pockmarks (**Figure 13**). PC1 explained 39.8% of the variance and was mainly affected by the high abundance of *E. hviidarum* at the pockmark site MTB1 (site with the highest concentrations of H_2S and detection of CH_4), whereas *E. unispinosus* followed by *Fi. cthulhu* sp. nov. distinguished the pockmark site MTB06 (site with emission of CH_4 only, H_2S not detected), and PC2 explained 25.7% of the variance, with *Condyloderes* sp., *Echinoderes* cf. *dubious*, and *Ryuguderes* sp. characterizing the sites located outside the pockmarks and *E. unispinosus* and *E. hviidarum* characterizing the sites inside the pockmarks (**Figure 13**). We are aware that a larger total variance explained by the two PCAs would have been desirable and therefore other factors not included in the present study could be responsible for the remaining percentage of variance, but still the studied pockmark conditions explained some differences in the kinorhynch community composition between both pockmarks and between pockmarks and sites outside pockmarks.

DISCUSSION

Remarks on Diagnostic and Taxonomic Features of *F. dagon* sp. nov. and *F. hydra* sp. nov.

The two new species of *Fujuriphyes* agree with the main diagnostic characters of the genus, including the presence of ventrolateral setae on segment 5 and on additional segments from segment 3 to 9 where ventromedial setae are absent, as well as long lateral terminal spines (LTS:TL average ratio > 30%) (Sánchez et al., 2016). Until now, the genus was composed of seven species: three from the Caribbean Sea, *Fujuriphyes dalii* Cepeda et al., 2019b, *F. deirophorus* (Higgins, 1983), and *F. distentus* (Higgins, 1983); one from the Gulf of Mexico, *F. viserioni* Sánchez et al., 2019a,b; one from the East China Sea, *F. longispinosus* Sánchez and Yamasaki, 2016; and two from the Mediterranean Sea, *F. ponticus* (Reinhard, 1881) and *F. rugosus* (Zelinka, 1928).

The presence of lateral terminal spines in both *F. dagon* sp. nov. and *F. hydra* sp. nov. easily allows their differentiation from *F. deirophorus* and *F. distentus* that lack these structures (Higgins, 1983).

The absence of middorsal cuticular specializations (processes or elevations) throughout the trunk in *F. dagon* sp. nov. is only shared with *F. dalii* (Cepeda et al., 2019b). However, both species may be easily distinguished by the arrangement of setae. *F. dalii* has a pair of paralateral setae on segment 1 (Cepeda et al., 2019b), which are absent in *F. dagon* sp. nov. The lateroventral setae of *F. dalii* are

TABLE 2 | Kinorhyncha species identified at study sites.

	OUTSIDE POCKMARK MTB03					OUTSIDE POCKMARK MTB2				
Species	**A**	**B**	**C**	**X**	**Total**	**A**	**B**	**C**	**X**	**Total**
Condyloderes sp.	0	0	0	0	0	0	1	1	0.67 0.58	2
Echinoderes apex	1	0	0	0.33 0.58	1	0	0	0	0	0
Echinoderes cf. dubiosus	0	0	3	1 1.7	3	0	1	0	0.33 0.58	1
Echinoderes hviidarum	0	0	0	0	0	0	0	0	0	0
Echinoderes unispinosus	2	0	1	1 1	3	0	0	0	0	0
Echinoderes sp.	0	0	2	0.67 1.2	2	0	0	0	0	0
Fissuroderes cthulhu sp. nov.	0	0	0	0	0	0	0	0	0	0
Ryuguderes sp.	4	0	0	1.3 2.3	4	0	1	0	0.33 0.58	1
Sphenoderes cf. indicus	0	0	0	0	0	0	0	0	0	0
Fujuriphyes dagon sp. nov.	0	0	0	0	0	0	0	0	0	0
Fujuriphyes hydra sp. nov.	6	0	0	2 3.5	6	0	0	0	0	0
Adult abundance	13	0	6	6.3 6.5	19	0	3	1	1.3 1.5	4
Total abundance	15	0	9	8.0 7.6	24	1	4	1	2 1.7	6
Total density (ind/10 cm^2)	5	0	3	2.6 2.5		0.5	0.2	0.5	0.37 0.15	
Total species richness	4	0	3	2.3 2.1	6	0	3	1	1.3 1.5	3

INSIDE POCKMARK MTB06					INSIDE POCKMARK MTB1				
A	**B**	**C**	**X**	**Total**	**A**	**B**	**C**	**X**	**Total**
0	0	1	0.33 0.58	1	0	0	0	0	0
0	0	0	0	0	0	0	0	0	0
0	0	0	0	0	0	0	0	0	0
0	0	0	0	0	5	24	16	15 9.5	45
77	24	151	84 63.8	252	0	0	0	0	0
0	0	0	0	0	0	0	0	0	0
12	3	42	19 20.4	57	0	0	0	0	0
0	0	0	0	0	0	0	0	0	0
0	0	0	0	0	1	0	0	0.33 0.58	1
0	6	19	8.3 9.7	25	0	0	0	0	0
0	0	0	0	0	0	0	0	0	0
89	33	213	111.7 92.11	335	6	24	16	15.3 9	46
115	73	316	168 129.9	504	27	80	31	46 29.5	138
38.1	24.2	105	55.6 43		8.9	26.5	10.3	15.2 9.8	
2	3	4	3 1	4	2	1	1	1.3 0.6	2

Abundance of each species is specified by cores and merging the data of the three cores in the total. Data are specified by cores and merging the data of the three cores. Total abundance includes adults and juvenile stages. X refers to average values standard deviation.

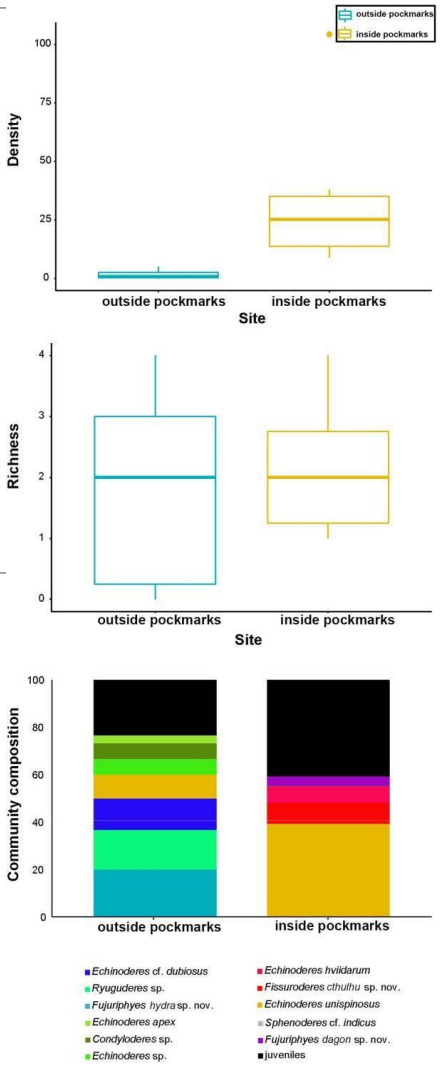

FIGURE 12 | Kinorhynch density, richness, and community composition at the two study habitats, inside pockmark (yellow) and outside pockmark (blue). Boxplots represent the median value (horizontal line within the box), the distributions of 50% of the data (the box), and the highest and lowest values within 95% of the distribution (the whisker). Contribution of each kinorhynchs species to the total community is expressed in percentage in relation to th etotal abundance

only present on segments 2, 4, and 10 (Cepeda et al., 2019b), while those of *F. dagon* sp. nov. are present on all the even-numbered segments. *F. dagon* sp. nov. has ventrolateral setae on segment 2, which are absent in *F. dalii* sp. nov. (Cepeda et al., 2019b). Additionally, *F. dalii* possesses ventromedial setae on segments 8–9 (Cepeda et al., 2019b), whereas *F. dagon* sp. nov. lacks setae in ventromedial position throughout the trunk.

The presence of middorsal elevations throughout segments 1–10 in *F. hydra* is unique within the genus, as the remaining species possess a different arrangement of middorsal elevations. *F. ponticus* and *F. rugosus* bear these structures on segments 1–9; *F. viserioni*, on segment 3; and *F. longispinosus*, on segments 1–6 (Reinhard, 1881; Zelinka, 1928; Sánchez and Yamasaki, 2016; Sánchez et al., 2016, 2019b). Regarding the setae arrangement, *F. hydra* sp. nov. is most similar to *F. dalii* and *F. longispinosus*, as the three species possess two pairs of ventrolateral setae on segment 5 and a relatively low number of ventromedial setae. Thus, *F. dalii* has ventromedial setae on segments 8–9, and *F. longispinosus* bears these structures on segments 2 and 9 in both sexes (Sánchez et al., 2016; Cepeda et al., 2019b). *F. hydra* sp. nov. also has ventromedial setae on segments 2 and 9, but those of segment 2 are only present in females. Moreover, the two pairs of ventrolateral setae of segment 5 of *F. hydra* sp. nov. are situated very close together, a feature that has not been observed in the remaining congeners.

Remarks on Diagnostic and Taxonomic Features of *Fi. cthulhu* sp. nov.

Currently, the genus *Fissuroderes* is morphologically defined by the combination of one tergal and two sternal plates on segment 2 plus paired, sexually dimorphic ventral papillae in females (Herranz and Pardos, 2013), despite the fact that females of one of the species, *Fi. papai* Neuhaus and Blasche, 2006, lack these structures. The newly described species, *Fi. cthulhu* sp. nov., matches the aforementioned condition of sexually dimorphic papillae, as only females bear these structures in ventrolateral position on segment 7. *Polacanthoderes* is the only genus of the family Echinoderidae that shares the arrangement of cuticular plates of segment 2 with *Fissuroderes* (Claparède, 1863; Adrianov and Malakhov, 1999; Neuhaus and Blasche, 2006; Sørensen, 2008a; Herranz et al., 2012), but it is furthermore characterized by possessing unusual morphological features never found in the remaining kinorhynch genera, including acicular spines in subdorsal, laterodorsal, midlateral, ventrolateral, and ventromedial positions (Sørensen, 2008a). This led us to include the new species in the genus *Fissuroderes*. Nevertheless, a total-evidence systematic revision of the family Echinoderidae is needed in order to describe new reliable characters of the different genera (Sørensen, 2008b; Sørensen et al., 2015).

Regarding the spine and tube arrangements, *Fi. cthulhu* sp. nov. is most similar to *Fi. novaezealandia* Neuhaus and Blasche (2006) and *Fi. thermoi* Neuhaus and Blasche (2006), as the three species share the presence of middorsal spines on segments 4–8, lateroventral spines on segments 6–9, ventrolateral tubes on segment 2, and lateroventral tubes on segment 5 (Neuhaus and Blasche, 2006). However, *Fi. novaezealandia* lacks laterodorsal tubes on segment 10, which are present and easily recognizable in *Fi. thermoi* and *Fi. cthulhu* sp. nov. (Neuhaus and Blasche, 2006). The main morphological differences between *Fi. thermoi* and *Fi. cthulhu* sp. nov. are the arrangement of the type 2 glandular cell outlets and female papillae, and the shape of the tergal extensions. *Fissuroderes thermoi* possesses type 2 glandular cell outlets in midlateral position on segments 5, 6, 8, and 9 (females furthermore with papillae in ventromedial position of segment 7), and its tergal extensions are short and distally rounded (Neuhaus and Blasche, 2006), while *Fi. cthulhu* sp. nov. has type 2 glandular cell outlets in midlateral position on segment 8 and in laterodorsal position on segment 9 (females furthermore with papillae in ventrolateral position of segment 7), and its tergal extensions are long, bifurcated, and distally pointed.

New Kinorhynch Records

The species *E. apex*, *E.* cf. *dubiosus*, *E. hviidarum*, *E. unispinosus*, *Ryuguderes* sp., and *Sphenoderes* cf. *indicus* were also reported in the analyzed pockmark field for the first time. In addition, *Condyloderes* sp. and *Echinoderes* sp. were also recorded, but the material was badly preserved and did not allow us to identify them to the species level.

A single specimen of *E. apex* was found at MOZ01-MTB03 (outside pockmarks). The species is characterized by having spines in middorsal position on segments 4, 6, and 8 and in lateroventral position throughout segments 6–9, together with tubes in ventrolateral position on segment 2, lateroventral position on segment 5, and laterodorsal position on segment 10, and type 2 glandular cell outlets in subdorsal position on segment 2, sublateral position on segment 6, and lateral accessory position on segment 8 (Yamasaki et al., 2018c). Moreover, *E. apex* has a relatively short trunk, ranging from 165 to 215 µm, and long lateral terminal spines, ranging from 60.0 to 80.2% of the total trunk length (Yamasaki et al., 2018c). The specimen found in the present study agrees with these diagnostic characters (see **Supplementary Figure 2.1**), except the length of the lateral terminal spines that are slightly shorter than those of the type material, ranging from 54.5 to 56.0% of the total trunk length, but we do not consider this difference important enough to assign the specimen to a different species. *E. apex* has been reported in the Great Meteor Seamount (eastern Atlantic Ocean) at depths of 287–856 m (Yamasaki et al., 2018c). This finding supposes an extension of the distributional range of the species to the Mozambique Channel (Indian Ocean).

Three specimens of *Echinoderes* cf. *dubiosus* were recorded at MOZ01-MTB03 and one was recorded at MOZ04-MTB2 (outside pockmarks). *Echinoderes dubiosus* is characterized by having spines in middorsal position throughout segments 4– 8 and in lateroventral position on segments 6–9 (with those of segment 9 extending beyond segment 11), as well as tubes in lateroventral position on segment 5, sublateral position on

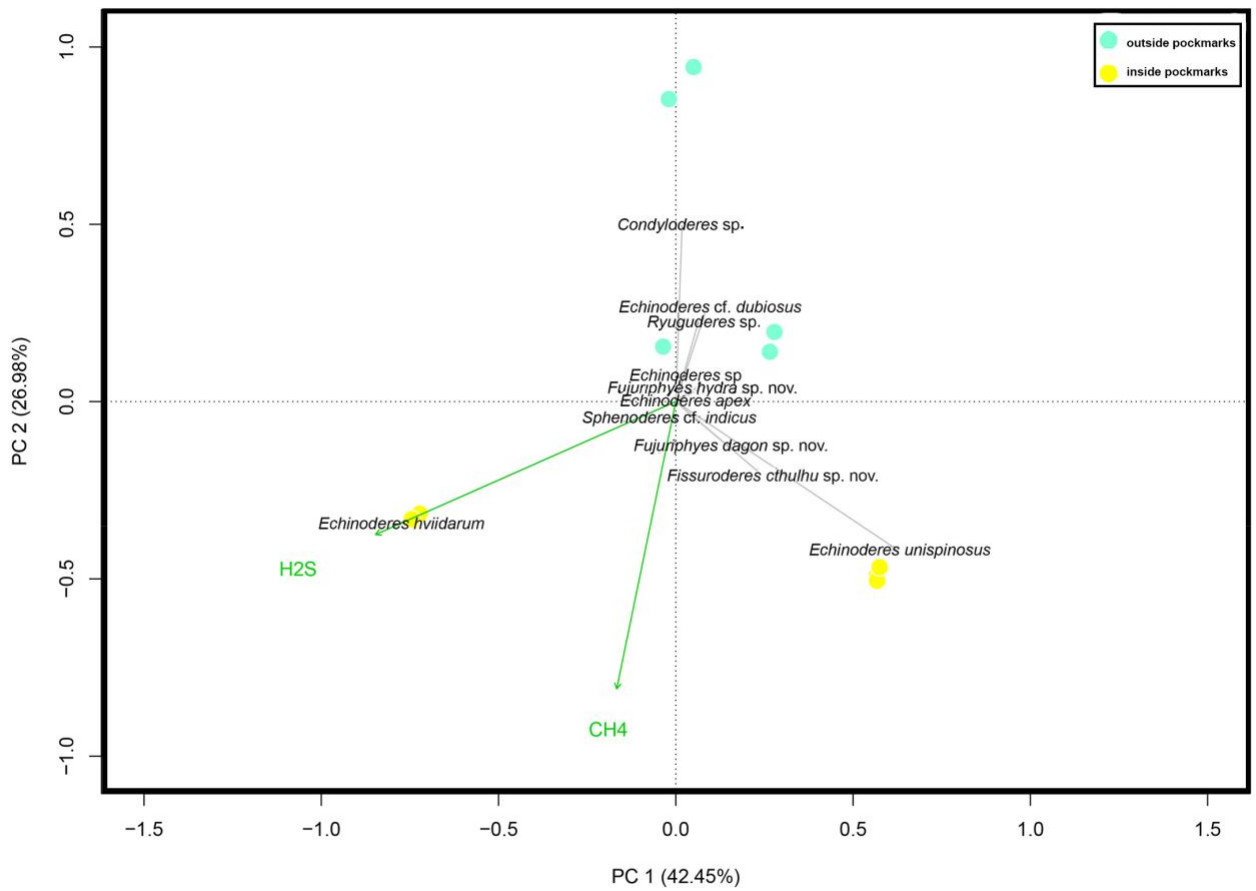

FIGURE 13 | Principal component analysis scaling two bi-plots based on Hellinger-transformed data on kinorhynch species composition considering the four study sites: two sites inside pockmarks (yellow) and two sites outside pockmarks (blue). Passive (post hoc) explanations of axis were conducted using environmental variables (CH_4, methane; and H_2S, hydrogen sulfide concentrations).

segment 8, and laterodorsal position on segment 10, and type 2 glandular cell outlets in midlateral position on segment 2 (Sørensen et al., 2018). The species also has middorsal cuticular structures on segment 9 forming a pore with a posterior papillary flap flanked by paired sensory spots (Sørensen et al., 2018). This last character was not observed in the specimens from the Mozambique Channel (see **Supplementary Figure 2.2**), which led us to tentatively identify them as *E.* cf. *dubiosus*. The species was previously known from the northern California (eastern Pacific Ocean) at 2702–3853 m depth (Sørensen et al., 2018), and this finding increases its bathymetrical and distributional range.

Echinoderes hviidarum was consistently found at MOZ04-MTB1 (within pockmark). The species has spines in middorsal position on segments 6 and 8 and lateroventral position throughout segments 6–9, as well as tubes in lateroventral position on segment 5, lateral accessory position on segment 8, and laterodorsal position on segments 9–10, and a middorsal protuberance on segment 11 (Sørensen et al., 2018). The specimens reported in the Mozambique Channel agree well with the aforementioned diagnostic characters of the species (see **Supplementary Figure 2.3**). *E. hviidarum* was exclusively reported off northern California (eastern Pacific Ocean) at 2702–3853 m depth (Sørensen et al., 2018), but with these findings, the bathymetrical and distributional range of the species is increased.

Echinoderes unispinosus was consistently reported at MOZ01-MTB03 (outside pockmarks) and MOZ01-MTB06 (within pockmark) and can be distinguished from its congeners by possessing spines in middorsal position on segment 4 and lateroventral position on segments 6–7, together with type 2 glandular cell outlets in midlateral position on segment 1; in subdorsal, laterodorsal, sublateral, and ventrolateral positions on segment 2; in lateral accessory position on segment 5; and in sublateral position on segment 8 (Yamasaki et al., 2018b). The species is furthermore characterized by having a narrow primary pectinate fringe with short tips throughout segments 1–10 and tergal extensions long, smoothly pointed (Yamasaki et al., 2018b). The specimens from the Mozambique Channel agree with these diagnostic characters of the species (see

Supplementary Figure 2.4), and the only morphological difference observed was the presence of subdorsal sensory spots on segment 4, which were not detected in the type material. *E. unispinosus* is known to possess a wide distributional range, being present in the northeast Atlantic Ocean, the northeast Pacific Ocean, and the Gulf of Mexico (Sørensen et al., 2018; Yamasaki et al., 2018b; Álvarez-Castillo et al., 2020). Now, its distributional range is furthermore increased to the Indian Ocean.

Three specimens from MOZ01-MTB03 and one from MOZ04-MTB02 (outside pockmarks) were tentatively assigned to *Ryuguderes* sp. This recently established genus of Campyloderidae can be distinguished from *Campyloderes* by having outer oral styles partially fused throughout the basal regions and free distal parts bearing lateral cuticular structures, as well as by the absence of lateroventral spines throughout the first trunk segments (Yamasaki, 2016). Currently, only a single species is known from the Ryukyu Islands (western Pacific Ocean), namely, *Ryuguderes iejimaensis* Yamasaki, 2016. The specimens from the Mozambique Channel seem to possess the diagnostic outer oral styles of *Ryuguderes*, but the lack of SEM material did not allow us to surely confirm this character. In addition, these specimens have important morphological discrepancies with *R. iejimaensis*, including the presence of a middorsal spine on segment 1, lateroventral spines on segment 3, a single pair of lateroventral spines on segment 5, females with middorsal spines on segment 10, and a different arrangement of sensory spots and glandular cell outlets (see **Supplementary Figure 2.5**).

A single specimen of *Sphenoderes* cf. *indicus* was found at MOZ04-MTB01 (within pockmark). *Sphenoderes indicus*, widely reported through the Bay of Bengal (Indian Ocean) at 6–40 m depth, is characterized by having acicular spines in middorsal position throughout segments 1–11 and lateroventral position on segments 3–9, as well as cuspidate spines in lateroventral position on segments 5 and 8–9, with those of segments 5 and 8 located more ventral than the acicular spines (Higgins, 1969). These characters were also found in the specimens from the Mozambique Channel (see **Supplementary Material 9**), but the arrangement of the sensory spots could not be completely determined because of the bad preservation of the specimens, which led us to tentatively identify them as *S.* cf. *indicus*. These findings increase the bathymetrical and distributional range of the species throughout the Indian Ocean.

Kinorhynch Community Structure and Composition

Our results show that kinorhynch density and community composition seem to be influenced by the environmental conditions of each study habitat, whereas similar values of richness were found in the inter-habitat comparison (**Figure 12**).

Kinorhynchs are more abundant inside the pockmarks, where environmental conditions are extreme due to reduced chemical compounds and the shortage of dissolved oxygen (Kumar, 2017; Pastor et al., 2020). Indeed, inside the pockmarks, hydrogen sulfide concentration increases with depth along the vertical profile while the dissolved oxygen plummets (Coull, 1988; Ritt et al., 2011; Ristova et al., 2015; Pastor et al., 2020). Specifically, most of the animals were found in the upper sediment layers (0–1 cm and 1–2 cm) (**Figure 10**). These layers are well-oxygenated (Coull, 1988; Pastor et al., 2020), and in one of the study pockmarks, there is a still relatively low concentration of hydrogen sulfide, a toxic reduced compound (Somero et al., 1989; Bagarinao, 1992; Giere, 2009). These findings agree with the hypothesis of Sánchez et al. (2021) and seem to evidence that the pockmark conditions enhance the abundance of Kinorhyncha, likely through the replacement with opportunistic, specialized species. These species would be able to cope with the pockmark conditions where other meiofaunal organisms cannot live (including other non-adapted species of Kinorhyncha), profiting about this and thriving rapidly (Ritt et al., 2010; Vanreusel et al., 2010; Sánchez et al., 2021). This is also supported by the presence of a relatively high juvenile abundance inside the pockmarks, which shows that these species not only manage to survive under such extreme conditions but also are able to intensely flourish there. Indeed, certain groups of meiofauna, such as nematodes and harpacticoid copepods, can reach high peaks of abundance in extreme environments where competition with other taxa is lower, which makes their prosperity possible (Coull, 1985; Colangelo et al., 2001; Van Gaever et al., 2009; Zeppilli and Danovaro, 2009; Zeppilli et al., 2012, 2018). Alternatively, the elevated kinorhynch density, including the high number of juveniles, may be explained, in the context of pockmarks, as they are considered potential colonizers at sulfide seepages of deep sea vents (Mullineaux et al., 2012).

Additionally, pockmarks are rich in reduced compounds, resulting in higher chemosynthetic microbial densities that live in these habitats as hydrocarbon degraders, acting in the anaerobic oxidation of methane and sulfate reduction processes (Giovannelli et al., 2016). The bacterial mats form a major source of food for meiofauna, including kinorhynchs who likely feed on them (Neuhaus, 2013). Thus, pockmarks may also enhance high kinorhynch densities because of the abundant bacteria, also in those layers where the hydrogen sulfide concentration (formed as a waste product of the anaerobic respiration of reducing microorganisms) is still tolerable. However, as soon as the hydrogen sulfide concentration increases in the subsequent layers, it seems to turn toxic and both kinorhynch density and richness decrease (**Figure 10**).

Cold seeps also increase the spatial heterogeneity of the habitat through geochemical gradients, driving the distribution of the biological communities (Levin, 2005; Guillon et al., 2017). This fact furthermore supports the differences in the community composition between pockmarks and areas outside pockmarks' influence, so the greater availability of geo-chemically heterogeneous microhabitats inside the pockmark may enable the maintenance of a community made up of highly adapted kinorhynch species to the particular conditions of each pockmark.

Thus, even though a similar kinorhynch richness was found in areas under pockmark influence and outside pockmarks,

community composition drastically differs from one habitat to another (**Figures 12**, **13**), suggesting that only certain species are well-adapted and able to tolerate the extreme conditions of this kind of cold seeps, characterized by methane and hydrogen sulfide emissions, as was already confirmed for other meiofaunal groups (Vanreusel et al., 2010; Zeppilli et al., 2012, 2018). The pockmark conditions seem to prevent the survival of non-adapted species, with their consequent fading, as occur for *E. apex*, *E.* cf. *dubiosus*, *Echinoderes* sp., *F. hydra* sp. nov., and *Ryuguderes* sp., only found outside the pockmark sites.

Condyloderes sp., *E. hviidarum*, *E. unispinosus*, *Fi. cthulhu* sp. nov., *F. dagon* sp. nov., and *Sphenoderes* cf. *indicus* characterize the kinorhynch community in the areas under the pockmark's influence. Of these, only *Condyloderes* sp. and *E. unispinosus* seem to be generalistic species capable of living in both habitats, but their abundances are higher inside pockmarks by far. These two species, together with *E. hviidarum* and *Fi. cthulhu* sp. nov., do not simply survive under such harsh conditions but take advantage of a habitat with a likely lower competition for space and resources, flourishing there (Sánchez et al., 2021). Additionally, the dissimilarity in kinorhynch community composition between the two study pockmarks is remarkable as well. *E. hviidarum* seems to be the most tolerant species to hydrogen sulfide as it largely dominated the community at the more active pockmark with higher concentrations of hydrogen sulfide. Indeed, *E. hviidarum* was also present in deep layers where the highest concentrations of hydrogen sulfide were detected. On the other hand, *E. unispinosus*, *Fi. cthulhu* sp. nov., and *F. dagon* sp. nov. only appeared in the pockmark with methane but without hydrogen sulfide emission (**Figure 13**). Therefore, methane and hydrogen sulfide, among other ecological factors, turn out to significantly drive kinorhynch community structure and composition, but we cannot conclude that all the aforementioned species are truthful bioindicators of cold seeps activity, as some of them were originally described from habitats free of seepages influence (Higgins, 1983; Sørensen et al., 2018; Yamasaki et al., 2018b). It remains to be clarified if the species described in the present article, *Fi. cthulhu* sp. nov. and *F. dagon* sp. nov., are only present in cold seepages or not.

CONCLUSION

Despite the fact that data interpretation of the present study must be taken with caution due to the reduced number of sampling sites and the possible effect of spatiotemporal variation among samples, we could make the following conclusions:

- Deep-sea environments host a highly biodiverse community of still undescribed species of Kinorhyncha.
- Kinorhynch richness is similar inside and outside the pockmarks, but the species composition completely changes because of exclusive species at both habitats.
- Contrarily to kinorhynch species richness, abundance is affected by the pockmarks' conditions, being higher within pockmarks than outside them. The extreme conditions of these habitats boost the kinorhynch abundance likely through the replacement with opportunistic specialized species, such as *E. hviidarum*, *E. unispinosus*, and *Fi. cthulhu* sp. nov., able to thrive rapidly under such features where competition is lower by far as hydrogen sulfide is toxic for most metazoans.

DATA AVAILABILITY STATEMENT

All datasets generated for this study are included in the article/**Supplementary Material**.

AUTHOR CONTRIBUTIONS

NS and DZ conceived the general idea of the study. DC, NS, and FP conducted the experimental process, and NS statistically analyzed the results. DC wrote the background and taxonomic part of the manuscript, and NS wrote the methods and the ecological part of the study. All the authors reviewed the manuscript.

FUNDING

This study was done within the framework of the Passive Margin Exploration Laboratories (PAMELA) project, funded by TOTAL and IFREMER. IFREMER furthermore funded the contract of NS to study the meiofauna collected during the PAMELA-MOZ04 campaign. DC was supported by a predoctoral fellowship of the Complutense University of Madrid (CT27/16-CT28-16) and a short-term predoctoral fellowship also of the Complutense University of Madrid (EB14/19).

ACKNOWLEDGMENTS

We would like to thank all the participants and the staff of the R/V *L'Atalante* and *Pour quoi pas?* Vessel, Scampi team and all scientists and students who participated in the PAMELA MOZ1 and MOZ4 cruises, specially to Dr. Karine Olu, chief of the mission, and Lara Macheriotou for processing the cores on board. Moreover, we are grateful to the Ghent meiofauna laboratory for the meiofauna processing and Dr. Lucie Pastor and Christophe Brandily (IFREMER) for the geochemical analyses and advises in the treatment of geo-chemical data. We would also like to thank Dr. Martin V. Sorensen and Dr. Matteo Dal Zotto for their suggestions and comments that kindly improved the present article.

SUPPLEMENTARY MATERIAL

The Supplementary Material for this article can be found online at: https://www.frontiersin.org/articles/10.3389/fmars.2020.00665/full#supplementary-material

REFERENCES

Adrianov, A. V., and Maiorova, A. S. (2015). *Pycnophyes abyssorum* sp. n. (Kinorhyncha: Homalorhagida), the deepest kinorhynch species described so far. *Deep Sea Res. II Top. Stud. Oceanogr.* 111, 49–59. doi: 10.1016/j.dsr2.2014. 08.009

Adrianov, A. V., and Maiorova, A. S. (2016). *Condyloderes kurilensis* sp. nov. (Kinorhyncha: Cyclorhagida)—a new deep water species from the abyssal plain near the Kuril-Kamchatka Trench. *Russ. J. Mar. Biol.* 42, 11–19. doi: 10.1134/ S1063074016010028

Adrianov, A. V., and Maiorova, A. S. (2018a). *Meristoderes okhotensis* sp. nov. – The first deepwater representative of kinorhynchs in the Sea of Okhotsk (Kinorhyncha: Cyclorhagida). *Deep Sea Res. II Top. Stud. Oceanogr.* 154, 99– 105. doi: 10.1016/j.dsr2.2017.10.011

Adrianov, A. V., and Maiorova, A. S. (2018b). *Parasemnoderes intermedius* gen. n., sp. n.—the First Abyssal Representative of the Family Semnoderidae (Kinorhyncha: Cyclorhagida). *Russ. J. Mar. Biol.* 44, 355–362. doi: 10.1134/ S1063074018050024

Adrianov, A. V., and Malakhov, V. V. (1999). *Cephalorhyncha of the World Ocean*. Moscow: KMK Scientific Press.

Álvarez-Castillo, L., Cepeda, D., Pardos, F., Rivas, G., and Rocha-Olivares, Á (2020). *Echinoderes unispinosus* (Kinorhyncha: Cyclorhagida), a new record from deep-sea sediments in the Gulf of Mexico. *Zootaxa* 4821, 196–200.

Álvarez-Castillo, L., Hermoso-Salazar, M., Estradas-Romero, A., Prol-Ledesma, R. M., and Pardos, F. (2015). First records of Kinorhyncha from the Gulf of California: horizontal and vertical distribution of four genera in shallow basins with CO2 venting activity. *Cah. Biol. Mar.* 56, 271–281.

Bagarinao, T. (1992). Sulfide as an environmental factor and toxicant: tolerance and adaptations in aquatic organisms. *Aquat. Toxicol.* 24, 21–62. doi: 10.1016/ 0166-445X(92)90015-F

Cepeda, D., Álvarez-Castillo, L., Hermoso-Salazar, M., Sánchez, N., Gómez, S., and Pardos, F. (2019a). Four new species of Kinorhyncha from the Gulf of California, eastern Pacific Ocean. *Zool. Anz.* 282, 140–160. doi: 10.1016/j.jcz. 2019.05.011

Cepeda, D., Sánchez, N., and Pardos, F. (2019b). First extensive account of the phylum Kinorhyncha from Haiti and the Dominican Republic (Caribbean Sea), with the description of four new species. *Mar. Biodivers.* 49, 2281–2309. doi: 10.1007/s12526-019-00963-x

Claparède, A. R. E. (1863). *Zur Kenntnis der Gattung* Echinoderes *Duj. Beobachtungen über Anatomie und Entwicklungsgeschichte wirbelloser Thiere an der Küste von Normandie angestellt*. Leipzig: Engelmann.

Colangelo, M. A., Bertasi, F., Dall'Olio, P., and Ceccherelli, V. H. (2001). "Meiofaunal biodiversity on hydrothermal seepage off Panarea (Aeolian Islands, Tyrrhenian Sea)," in *Mediterranean Ecosystems: Structures and Processes*, eds F. M. Faranda, L. Guglielmo, and G. Spezie (Berlin: Springer-Verlag), 353–359. doi: 10.1007/978-88-470-2105-1_46

Coull, B. C. (1985). Long-term variability of estuarine meiobenthos: an 11 year study. *Mar. Ecol. Prog. Ser.* 24, 205–218. doi: 10.3354/meps024205

Coull, B. C. (1988). "Ecology of the marine meiofauna," in *Introduction to the Study of Meiofauna*, eds R. P. Higgins and H. Thiel (Washington D.C: Smithsonian Institution Press), 18–38.

Dal Zotto, M., Santulli, A., Simonini, R., and Todaro, M. A. (2016). Organic enrichment effects on a marine meiofauna community, with focus on Kinorhyncha. *Zool. Anz.* 265, 127–140. doi: 10.1016/j.jcz.2016.03.013

Dando, P. R., Austen, M. C., Burke, R. A., Kendall, M. A., Kennicutt, M. C., Judd, A. G., et al. (1991). Ecology of a North Sea pockmark with an active methane seep. *Mar. Ecol. Prog. Ser.* 70, 49–63. doi: 10.3354/meps070049

Eakins, B. W., and Sharman, G. F. (2010). *Volumes of the World's Oceans from ETOPO1*. Boulder, CO: NOAA National Geophysical Data Center.

Fonselius, S. H. (1983). "Determination of hydrogen sulphide," in *Methods of Seawater Analysis*, eds K. Grasshoff, K. Kremling, and M. Ehrhardt (Weinheim: Verlag Chemie), 73–80.

Giere, O. (2009). *Meiobenthology. The Microscopic Motile Fauna of Aquatic Sediments*. Berlin: Springer.

Giovannelli, D., D'Errico, G., Fiorentino, F., Fattorini, D., Regoli, F., Angeletti, L., et al. (2016). Diversity and distribution of prokaryotes within a shallow-water pockmark field. *Front. Microbiol.* 7:941. doi: 10.3389/fmicb.2016. 00941

Grzelak, K., and Sørensen, M. V. (2018). New species of *Echinoderes* (Kinorhyncha: Cyclorhagida) from Spitsbergen, with additional information about known Arctic species. *Mar. Biol. Res.* 14, 113–147. doi: 10.1080/17451000. 2017.1367096

Grzelak, K., and Sørensen, M. V. (2019). Diversity and community structure of kinorhynchs around Svalbard: first insights into spatial patterns and environmental drivers. *Zool. Anz.* 282, 31–43. doi: 10.1016/j.jcz.2019.05.009

Guillon, E., Menot, L., Decker, C., Krylova, E., and Olu, K. (2017). The vesicomyd bivalve habitat at cold-seeps supports heterogeneous and dynamic macrofaunal assemblages. *Deep Sea Res. I Oceanogr. Res. Pap.* 120, 1–13. doi: 10.1016/j.dsr. 2016.12.008

Heip, C. H. R., Vincx, M., and Vranken, G. (1985). The ecology of marine nematodes. *Oceanogr. Mar. Biol.* 23, 399–489.

Herranz, M., and Pardos, F. (2013). *Fissuroderes sorenseni* sp. nov. and *Meristoderes boylei* sp. nov.: first Atlantic recording of two rare kinorhynch genera, with new identification keys. *Zool. Anz.* 2013, 93–111. doi: 10.1016/j.jcz.2013.09.005

Herranz, M., Thormar, J., Benito, J., Sánchez, N., and Pardos, F. (2012). *Meristoderes* gen. nov., a new kinorhynch genus, with the description of two new species and their implications for echinoderid phylogeny (Kinorhyncha: Cyclorhagida, Echinoderidae). *Zool. Anz.* 251, 161–179. doi: 10.1016/j.jcz.2011. 08.004

Higgins, R. P. (1969). Indian Ocean Kinorhyncha: 1. *Condyloderes* and *Sphenoderes*, new cyclorhagid genera. *Smith. Contr. Zool.* 14, 1–13. doi: 10. 5479/si.00810282.14

Higgins, R. P. (1983). The Atlantic barrier reef ecosystem at Carrie Bow Cay, Belize, *II. Kinorhyncha. Smith. Contr. Mar. Sci.* 1, 1–131. doi: 10.5479/si.01960768.18.1

Hourdez, S., and Lallier, F. H. (2006). Adaptations to hypoxia in hydrothermal-vent and cold-seep invertebrates. *Rev. Environ. Sci. Biotechnol.* 6, 143–159. doi: 10.1007/s11157-006-9110-3

Hovland, M., and Judd, A. G. (1988). *Seabed Pockmarks and Seepages: Impact on Geology, Biology and Marine Environment*. London: Grahamand Trotman.

Janssen, A., Kaiser, S., Meibner, K., Brenke, N., Menot, L., and Arbizu, P. (2015). A reverse taxonomic approach to assess macrofaunal distribution patterns in abyssal Pacific polymetallic nodule fields. *PLoS One* 10:e0117790. doi: 10.1371/ journal.pone.0117790

Jouet, G., and Deville, E. (2015). *PAMELA-MOZ04 cruise, R/V Pourquoi pas? Flotte océanographique française opérée par l'Ifremer*. Netherlands: EAGE.

Kennedy, B. R. C., Cantwell, K., Malik, M., Kelley, C., Potter, J., Elliott, K., et al. (2019). The unknown and the unexplored: insights into the Pacific deep-sea following NOAA CAPSTONE expeditions. *Front. Mar. Sci.* 6:480. doi: 10.3389/ fmars.2019.00480

Kumar, A. (2017). "Foreword," in *Investigating Seafloors and Oceans, from Mud Volcanoes to Giant Squid*, ed. A. Joseph (Amsterdam: Elsevier), 9–26.

Landers, S. C., Basshman, R. D., Miller, J. A., Ingels, J., Sánchez, N., and Sørensen, M. V. (2020). Kinorhynch communities from Alabama coastal waters. *Mar. Biol. Res.* doi: 10.1080/17451000.2020.1789660

Landers, S. C., Sørensen, M. V., Beaton, K. R., Jones, C. M., Miller, J. M., and Stewart, P. M. (2018). Kinorhynch assemblages in the Gulf of Mexico continental shelf collected during a two-year survey. *J. Exp. Mar. Biol. Ecol.* 02, 81–90. doi: 10.1016/j.jembe.2017.05.013

Legendre, P., and Gallagher, E. D. (2001). Ecologically meaningful transformations for ordination of species data. *Oecology* 129, 271–280. doi: 10.1007/ s004420100716

Levin, L. A. (2005). Ecology of cold seep sediments: interactions of fauna with flow, chemistry and microbes. *Oceanogr. Mar. Biol.* 43, 1–46. doi: 10.1201/ 9781420037449-3

Levin, L. A., and Sibuet, M. (2012). Understanding continental margin biodiversity: a new imperative. *Annu. Rev. Mar Sci.* 4, 79–112. doi: 10.1146/annurev-marine-120709-142714

Mirto, S., Gristina, M., Sinopoli, M., Maricchiolo, G., Genovese, L., Vizzini, S., et al. (2012). Meiofauna as an indicator for assessing the impact of fish farming at an exposed marine site. *Ecol. Indic.* 18, 468–476. doi: 10.1016/j.ecolind.2011.12. 015

Mullineaux, L. S., Le Bris, N., Mills, S. W., Henri, P., Bayer, S. R., Secrist, R. G., et al. (2012). Detecting the influence of initial pioneers on succession at deep-sea vents. *PLoS One* 7:e50015. doi: 10.1371/journal.pone.0050015

Neuhaus, B. (2013). "Kinorhyncha (=Echinodera)," in *Handbook of Zoology. Gastrotricha, Cycloneuralia and Gnathifera, Volume 1: Nematomorpha,*

Priapulida, Kinorhyncha, Loricifera, ed. A. Schmidt-Rhaesa (Hamburg: De Gruyter), 181–350.

Neuhaus, B., and Blasche, T. (2006). *Fissuroderes*, a new genus of Kinorhyncha (Cyclorhagida) from the deep sea and continental shelf of New Zealand and from the continental shelf of Costa Rica. *Zool. Anz.* 245, 19–52. doi: 10.1016/j. jcz.2006.03.003

Neuhaus, B., and Sørensen, M. V. (2013). Populations of *Campyloderes* sp. (Kinorhyncha, Cyclorhagida): one global species with significant morphological variation? *Zool. Anz.* 252, 48–75. doi: 10.1016/j.jcz.2012.03.002

Oksanen, F. J., Blanchet, F. G., Friendly, M., Kindt, R., Legendre, P., McGlinn, D., et al. (2018). *vegan: Community Ecology Package. R Package Version 2.4-4*. Available online at: https://github.com/vegandevs/vegan (accessed October 02, 2019).

Oksanen, F. J., Blanchet, F. G., Kindt, R., Legendre, P., Minchin, P. R., O'Hara, R. B., et al. (2015). *vegan: Community Ecology Package. R Package Vegan, Version 2.2-1*. Available online at: https://github.com/vegandevs/vegan (accessed October 02, 2019).

Olu, K. (2014). *PAMELA-MOZ01 cruise, R/V L'Atalante. Flotte océanographique française opérée par l'Ifremer*. Netherlands: EAGE.

Pastor, L., Brandily, C., Schmidt, S., Miramontes, E., Péron, M., Apperé, D., et al. (2020). Modern sedimentation and geochemical imprints in sediments from the NW Madagascar margin. *Mar. Geol.* 426:106184. doi: 10.1016/j.margeo.2020. 106184

Reinhard, W. (1881). Über *Echinoderes* und *Desmoscolex* der Umgebung von Odessa. *Zool. Anz.* 4, 588–592.

Ristova, P. P., Wenzhöfer, F., Ramette, A., Felden, J., and Boetius, A. (2015). Spatial scales of bacterial community diversity at cold seeps (eastern Mediterranean Sea). *ISME J.* 9, 1306–1318. doi: 10.1038/ismej.2014.217

Ritt, B., Pierre, C., Gauthier, O., Wenzhöfer, F., Boetius, A., and Sarrazin, J. (2011). Diversity and distribution of cold-seep fauna associated with different geological and environmental settings at mud volcanoes and pockmarks of the Nile deep-sea fan. *Mar. Biol.* 158, 1187–1210. doi: 10.1007/s00227-011-1679-6

Ritt, B., Sarrazin, J., Caprais, J. C., Noël, P., Gauthier, O., Pierre, C., et al. (2010). First insights into the structure and environmental setting of cold-seep communities in the Marmara Sea. *Deep Sea Res. I Oceanogr. Res. Pap.* 57, 1120–1136. doi: 10.1016/j.dsr.2010.05.011

Rouse, G. W., and Fauchald, K. (1997). Cladistics and polychaetes. *Zool. Scr.* 26, 139–204. doi: 10.1111/j.1463-6409.1997.tb00412.x

Sánchez, N., Pardos, F., and Martínez-Arbizu, P. (2019a). Deep-sea Kinorhyncha diversity of the polymetallic nodule fields at the clarion-clipperton fracture zone (CCZ). *Zool. Anz.* 282, 88–105. doi: 10.1016/j.jcz.2019.05.007

Sánchez, N., Pardos, F., and Sørensen, M. V. (2014a). A new kinorhynch genus, *Mixtophyes* (Kinorhyncha: Homalorhagida), from the Guinea Basin deep-sea, with new data on the family Neocentrophyidae. *Helgol. Mar. Res.* 68, 221–239. doi: 10.1007/s10152-014-0383-6

Sánchez, N., Pardos, F., and Sørensen, M. V. (2014b). Deep-sea Kinorhyncha: two new species from the Guinea Basin, with evaluation of an unusual male feature. *Org. Divers. Evol.* 14, 349–361. doi: 10.1007/s13127-014-0182-6

Sánchez, N., Sørensen, M. V., and Landers, S. C. (2019b). Pycnophyidae (Kinorhyncha: Allomalorhagida) from the Gulf of Mexico: *Fujuriphyes viserioni* sp. nov. and a re-description of *Leiocanthus langi* (Higgins, 1964), with notes on its intraspecific variation. *Mar. Biodivers.* 49, 1857–1875. doi: 10.1007/s12526-019-00947-x

Sánchez, N., and Yamasaki, H. (2016). Two new Pycnophyidae species (Kinorhyncha: Allomalorhagida) from Japan lacking ventral tubes in males. *Zool. Anz.* 265, 80–89. doi: 10.1016/j.jcz.2016.04.001

Sánchez, N., Yamasaki, H., Pardos, F., Sørensen, M. V., and Martínez, A. (2016). Morphology disentangles the systematics of a ubiquitous but elusive meiofaunal group (Kinorhyncha: Pycnophyidae). *Cladistics* 32, 479–505. doi: 10.1111/cla. 12143

Sánchez, N., Zeppilli, D., Baldrighi, E., Vanreusel, A., Gasimandova-Lahitsiresy, M., Pastor, L., et al. (2021) A threefold perspective on the role of a pockmark in benthic faunal communities and biodiversity patterns. *Deep Sea Res. Part I Oceanogr. Res. Pap.* 167, e103425. https://doi.org/10.1016/j.dsr.2020.103425.

Sarradin, P. M., and Caprais, J. C. (1996). Analysis of dissolved gases by headspace sampling gas chromatography with column and detector switching. Preliminary results. *Anal. Commun.* 33, 371–373. doi: 10.1039/ac9963300371

Seeberg-Elverfeldt, J., Schlüter, M., Feseker, T., and Koelling, M. (2005). Rhizon sampling of pore waters near the sediment/water interface of aquatic systems. *Limnol. Oceanogr. Meth.* 3, 361–371. doi: 10.4319/lom.2005.3.361

Seitzinger, S. P., Mayorga, E., Bouwman, A. F., Kroeze, C., Beusen, A. H. W., Billen, G., et al. (2010). Global river nutrient export: a scenario analysis of past and future trends. *Glob. Biogeochem. Cycles* 24:GB0A08. doi: 10.1029/ 2009GB003587

Sibuet, M., and Olu, K. (1998). Biogeography, biodiversity and fluid dependence of deep-sea cold-seep communities at active and passive margins. *Deep Sea Res. II Top. Stud. Oceanogr.* 45, 517–567. doi: 10.1016/S0967-0645(97)00074-X

Somero, G. N., Childress, J. J., and Anderson, A. E. (1989). Transport, metabolism and detoxification of hydrogen sulphide in animals from sulphide-rich marine environments. *Aquat. Sci.* 1, 591–614.

Sørensen, M. V. (2008a). A new kinorhynch genus from the Antarctic deep sea and a new species of *Cephalorhyncha* from Hawaii (Kinorhyncha: Cyclorhagida: Echionoderidae). *Org. Divers. Evol.* 8, e1–e232. doi: 10.1016/j.ode.2007.11.003

Sørensen, M. V. (2008b). Phylogenetic analysis of the Echinoderidae (Kinorhyncha: Cyclorhagida). *Org. Divers. Evol.* 8, 233–246. doi: 10.1016/j.ode.2007.11.002

Sørensen, M. V., Dal Zotto, M., Rho, H. S., Herranz, M., Sánchez, N., Pardos, F., et al. (2015). Phylogeny of Kinorhyncha based on morphology and two molecular loci. *PLoS One* 10:e0133440. doi: 10.1371/journal.pone.0133440

Sørensen, M. V., and Grzelak, K. (2018). New mud dragons from Svalbard: three new species of *Cristaphyes* and the first Arctic species of *Pycnophyes* (Kinorhyncha: Allomalorhagida: Pycnophyidae). *PeerJ* 6:e5653. doi: 10.7717/ peerj.5653

Sørensen, M. V., Rohal, M., and Thistle, D. (2018). Deep-sea Echinoderidae (Kinorhyncha: Cyclorhagida) from the Northwest Pacific. *Eur. J. Taxon.* 456, 1–75. doi: 10.5852/ejt.2018.456

Sørensen, M. V., Thistle, D., and Landers, S. C. (2019). North American *Condyloderes* (Kinorhyncha: Cyclorhagida: Kentrorhagata): female dimorphism suggests moulting among adult *Condyloderes*. *Zool. Anz.* 282, 232–251. doi: 10.1016/j.jcz.2019.05.015

Sun, J., Zhang, Y., Xu, T., Zhang, Y., Mu, H., Zhang, Y., et al. (2017). Adaptation to deep-sea chemosynthetic environments as revealed by mussel genomes. *Nat. Ecol. Evol.* 1:0121. doi: 10.1038/s41559-017-0121

Sutherland, T. F., Levings, C. D., Petersen, S. A., Poon, P., and Piercey, B. (2007). The use of meiofauna as an indicator of benthic organic enrichment associated with salmonid aquaculture. *Mar. Poll. Bull.* 54, 1249–1261. doi: 10.1016/j. marpolbul.2007.03.024

Van Gaever, S., Olu, K., Derycke, S., and Vanreusel, A. (2009). Metazoan meiofaunal communities at cold-seeps along the Norwegian margin: influence of habitat heterogeneity and evidence for connection with shallow-water habitats. *Deep Sea Res. I Oceanogr. Res. Pap.* 56, 772–785. doi: 10.1016/j.dsr. 2008.12.015

Vanreusel, A., De Groote, A., Gollner, S., and Bright, M. (2010). Ecology and biogeography of free-living nematodes associated with chemosynthetic environments in the deep-sea: a review. *PLoS One* 5:e12449. doi: 10.1371/ journal.pone.0012449

Yamasaki, H. (2016). *Ryuguderes iejimaensis*, a new genus and species of Campyloderidae (Xenosomata: Cyclorhagida: Kinorhyncha) from a submarine cave in the Ryukyu Islands, Japan. *Zool. Anz.* 265, 69–79. doi: 10.1016/j.jcz.2016. 02.003

Yamasaki, H., Grzelak, K., Sørensen, M. V., Neuhaus, B., and George, K. H. (2018a). *Echinoderes pterus* sp. n. showing a geographically and bathymetrically wide distribution pattern on seamounts and on the deep-sea floor in the Arctic Ocean, Atlantic Ocean, and the Mediterranean Sea (Kinorhyncha, Cyclorhagida). *ZooKeys* 771, 15–40. doi: 10.3897/zookeys.771.25534

Yamasaki, H., Neuhaus, B., and George, K. H. (2018b). New species of *Echinoderes* (Kinorhyncha: Cyclorhagida) from Mediterranean seamounts and from the deep-sea floor in the North-eastern Atlantic Ocean, including notes of two undescribed species. *Zootaxa* 4387, 541–556. doi: 10.11646/zootaxa.4387.3.8

Yamasaki, H., Neuhaus, B., and George, K. H. (2018c). Three new species of Echinoderidae (Kinorhyncha: Cyclorhagida) from two seamounts and the adjacent deep-sea floor in the Northeast Atlantic Ocean. *Cah. Biol. Mar.* 59, 79–106. doi: 10.21411/CBM.A.124081A9

Yamasaki, H., Neuhaus, B., and George, K. H. (2019). Echinoderid mud dragons (Cyclorhagida: Kinorhyncha) from Senghor Seamount (NE Atlantic Ocean) including general discussion of faunistic characters and distribution patterns of seamount kinorhynchs. *Zool. Anz.* 282, 64–87. doi: 10.1016/j.jcz.2019.05.018

Zelinka, K. (1894). Über die Organisation von *Echinoderes*. *Verh. Dtsch. Zool. Ges.* 4, 46–49.

Zelinka, K. (1896). Demonstration der Tafeln der *Echinoderes*-Monographie. *Verh. Dtsch. Zool. Ges.* 6, 197–199.

Zelinka, K. (1913) Die Echinoderen der Deutschen Südpolar-Expedition 1901– 1903. *Deutsche Südpolar Expedition XIV Zoologie* 6, 419–437.

Zelinka, K. (1928). *Monographie der Echinodera*. Leipzig: Engelmann.

Zeppilli, D., Canals, M., Danovaro, R., and Gambi, C. (2012). Meiofauna abundance of westerm Mediterranean Sea seep sediments. *PANGAEA*. doi: 10.1594/PANGAEA.803358

Zeppilli, D., and Danovaro, R. (2009). Meiofaunal diversity and assemblage structure in a shallow-water hydrothermal vent in the Pacific Ocean. *Aquat. Biol.* 5, 75–84. doi: 10.3354/ab00140

Zeppilli, D., Leduc, D., Fontanier, C., Fontaneto, D., Fuchs, S., Gooday, A. J., et al. (2018). Characteristics of meiofauna in extreme marine ecosystems: a review. *Mar. Biodivers.* 48, 35–71. doi: 10.1007/s12526-017-0815-z

Conflict of Interest: The authors declare that the research was conducted in the absence of any commercial or financial relationships that could be construed as a potential conflict of interest.

1. Supplementary Tables.

Supplementary Table 1.1 Measurements of adult *Fujuriphyes dagon* sp. nov. from the Mozambique Channel, including number of measured specimens (*n*), mean of data and standard deviation (SD). There were no remarkable differences in sizes or dimensions between the two sexes. Abbreviations: LTS, lateral terminal spines length; MSW-6, maximum sternal width (on segment 6); S, segment lengths; SW-10, standard sternal width (on segment 10); TL, total trunk length.

Character	Range	Mean (SD; *n*)
TL (µm)	586.3-648.1	611.2 (28.2; 4)
MSW-6 (µm)	129.7-146.5	144.3 (13.1; 4)
MSW-6/TL (%)	21.9-25.0	23.6 (1.6; 4)
SW-10 (µm)	107.0-122.2	112.9 (7.1; 4)
SW-10/TL (%)	18.0-19.5	18.4 (0.9; 4)
S1 (µm)	107.4-121.5	114.2 (5.9; 4)
S2 (µm)	57.9-82.6	71.1 (10.1; 4)
S3 (µm)	62.0-81.2	73.2 (8.l; 4)
S4 (µm)	65.6-90.8	76.8 (10.4; 4)
S5 (µm)	67.8-90.7	78.2 (9.5; 4)
S6 (µm)	63.0-93.4	80.3 (12.7; 4)
S7 (µm)	62.8-92.3	79.3 (12.5; 4)
S8 (µm)	64.6-93.2	81.3 (12.0; 4)
S9 (µm)	62.1-94.0	80.0 (13.6; 4)
S10 (µm)	50.9-71.8	59.8 (8.7; 4)
S11 (µm)	33.2-44.1	38.6 (4.5; 4)
LTS (µm)	183.3-194.9	189.9 (5.1; 4)
LTS/TL (%)	30.1-31.6	31.0 (0.6; 4)

Supplementary Table 1.2 Summary of nature and arrangement of sensory spots, glandular cell outlets, setae, spines and tubes in *Fujuriphyes dagon* sp. nov. Abbreviations: gco, glandular cell outlet; LD, laterodorsal; lts, lateral terminal spine; LV, lateroventral; m, male condition of sexually dimorphic character; PD, paradorsal; ps, penile spine; SD, subdorsal; se, seta; ss, sensory spot; ss3, type 3 sensory spot; t, tube; VL, ventrolateral; VM, ventromedial; * indicates that the structure is unpaired.

Segment	PD	SD	LD	LV	VL	VM
1		ssx2, gco	ss		ssx2	ss, gco
2	se*	ss, gco	se, ss	se	se, gco	t(m), ssx2, gco
3		ss, gco	se, ss		se, gco	ssx2, gco
4	se*	ssx2, gco	se, ss	se	se, gco	ssx2, gco
5		ss, gco	se, ss		sex2, gco	ssx2, gco
6	se*	ssx2, gco	se, ss	se	se, gco	ssx2, gco
7		ss, gco	se, ss		se, gco	ssx2, gco
8	se*	ssx2, gco	se, ss	se	se, gco	ssx2, gco
9		ssx2, gco	se, ss		se, gco	ss, gco
10		ss, gco	se, ss	se	gco	ss, gco
11			ss3	lts, psx2(m)		

Supplementary Table 1.3 Measurements of adult *Fujuriphyes hydra* sp. nov. from the Mozambique Channel, including number of measured specimens (*n*), mean of data and standard deviation (SD). There were no remarkable differences in sizes or dimensions between the two sexes. Abbreviations: LTS, lateral terminal spines length; MSW-6, maximum sternal width (on segment 6); S, segment lengths; SW-10, standard sternal width (on segment 10); TL, total trunk length.

Character	**Range**	**Mean (SD; *n*)**
TL (µm)	649.7-657.7	654.0 (3.3; 4)
MSW-6 (µm)	179.4-270.7	215.6 (39.3; 4)
MSW-6/TL (%)	27.6-41.3	32.8 (5.9; 4)
SW-10 (µm)	127.6-181.4	152.7 (23.1; 4)
SW-10/TL (%)	19.6-27.7	23.3 (3.5; 4)
S1 (µm)	118.6-138.8	131.8 (9.0; 4)
S2 (µm)	61.4-76.5	68.3 (7.3; 4)
S3 (µm)	70.0-78.7	72.9 (3.9; 4)
S4 (µm)	68.6-84.7	74.9 (6.9; 4)
S5 (µm)	73.2-83.5	77.1 (4.5; 4)
S6 (µm)	72.8-80.6	77.3 (3.3; 4)
S7 (µm)	80.0-85.7	82.1 (2.6; 4)
S8 (µm)	76.4-90.8	86.5 (6.9; 4)
S9 (µm)	71.7-91.3	83.1 (8.8; 4)
S10 (µm)	74.2-86.2	79.5 (5.8; 4)
S11 (µm)	27.9-48.9	35.5 (9.5; 4)
LTS (µm)	201.7-202.2	202.0 (0.4; 2)
LTS/TL (%)	30.9-31.0	31.0 (0.1; 2)

Supplementary Table 1.4 Summary of nature and arrangement of sensory spots, glandular cell outlets, cuticular elevations, setae, spines and tubes in *Fujuriphyes hydra* sp. nov. Abbreviations: ce, cuticular elevation; f, female condition of sexually dimorphic character; gco, glandular cell outlet; LD, laterodorsal; lts, lateral terminal spine; LV, lateroventral; m, male condition of sexually dimorphic character; MD, middorsal; PD, paradorsal; PL, paralateral; ps, penile spine; SD, subdorsal; se, seta; ss, sensory spot; t, tube; VL, ventrolateral; VM, ventromedial; * indicates that the structure is unpaired.

Segment	**MD**	**PD**	**SD**	**LD**	**PL**	**LV**	**VL**	**VM**
1	ce	ss	ssx2, gco		se, ss		ss	gco
2	ce	se*, ss	ssx3, gco	se, ss		se	gco	se(f), t(m), ss, gco
3	ce	ss	ssx3, gco	se, ss			se, gco	ssx2, gco
4	ce	se*, ss	ssx3, gco	se, ss		se	se, gco	ssx2, gco
5	ce	ss	ssx3, gco	se, ss			sex2, gco	ssx2, gco
6	ce	se*, ss	ssx3, gco	se, ss		se	se, gco	ssx2, gco
7	ce	ss	ssx3, gco	se, ss			se, gco	ssx2, gco
8	ce	se, ss	ssx3, gco	se, ssx2		se	se, gco	ssx2, gco
9	ce	ss	ssx3, gco	se, ssx2			gco	se, ssx2, gco
10	ce	ss	ssx2, gco	ss		sex2	gco	ss, gco
11				ssx2		lts, psx2(m)		

Supplementary Table 1.5 Measurements of adult *Fissuroderes cthulhu* sp. nov. from the Mozambique Channel, including number of measured specimens (*n*), mean of data and standard deviation (SD). There were no remarkable differences in sizes or dimensions between the two sexes. Abbreviations: ac, acicular spine; LD, laterodorsal; LTAS, lateral terminal accessory spines length; LTS, lateral terminal spines length; LV, lateroventral; MD, middorsal; MSW-6, maximum sternal width (on segment 6); S, segment lengths; SW-10, standard sternal width (on segment 10); t, tube; TL, total trunk length; VL, ventrolateral.

Character	**Range**	**Mean (SD; *n*)**
TL (µm)	327.5-482.8	391.3 (52.1; 9)
MSW-6 (µm)	77.0-84.0	80.6 (3.3; 5)
MSW-6/TL (%)	18.7-25.6	22.3 (3.1; 5)
SW-10 (µm)	61.8-77.3	72.1 (5.7; 7)
SW-10/TL (%)	15.6-23.6	19.5 (3.2; 7)
S1 (µm)	39.9-48.0	42.8 (2.9; 9)
S2 (µm)	34.0-39.6	36.6 (1.9; 9)
S3 (µm)	38.5-46.1	42.0 (2.0; 9)
S4 (µm)	40.3-51.6	46.2 (3.3; 9)
S5 (µm)	46.9-56.5	52.7 (3.2; 9)
S6 (µm)	51.0-65.6	58.1 (4.5; 9)
S7 (µm)	53.3-66.1	60.0 (4.7; 9)
S8 (µm)	53.9-69.2	62.6 (4.2; 9)
S9 (µm)	59.1-65.3	61.8 (2.0; 9)
S10 (µm)	34.7-50.9	47.8 (6.3; 9)
S11 (µm)	45.9-64.2	55.4 (5.3; 9)
VL2 (t) (µm)	10.2-22.0	16.2 (2.0; 4)
MD4 (ac) (µm)	20.6-34.4	27.4 (3.7; 9)
MD5 (ac) (µm)	36.6-65.0	54.2 (10.3; 9)
MD6 (ac) (µm)	47.3-79.2	68.1 (10.9; 9)
MD7 (ac) (µm)	77.0-100.6	80.7 (12.7; 9)
MD8 (ac) (µm)	72.4-105.3	98.4 (10.7; 9)
LD10 (t) (µm)	18.4-30.9	27.3 (3.8; 9)
LV5 (t) (µm)	12.2-24.2	18.3 (4.1; 9)
LV6 (ac) (µm)	18.2-31.1	22.7 (4.1; 9)
LV7 (ac) (µm)	29.8-34.6	33.6 (3.6; 9)
LV8 (ac) (µm)	38.0-45.6	43.0 (2.6; 9)
LV9 (ac) (µm)	51.9-76.6	60.5 (8.1; 9)
LTS (µm)	193.0-234.3	211.0 (17.8; 9)
LTS/TL (%)	47.8-69.8	54.5 (6.8; 9)
LTAS (µm)	48.0-79.9	64.2 (17.9; 4)
LTAS/LTS (%)	21.5-34.3	28.4 (6.6; 4)

Supplementary Table 1.6 Summary of nature and arrangement of acicular spines, tubes, sensory spots, glandular cell outlets and nephridiopores in *Fissuroderes cthulhu* sp. nov. Abbreviations: ac, acicular spine; f, female condition of sexually dimorphic character; gco, glandular cell outlet (followed by number of type); LA, lateral accessory; LD, laterodorsal; ltas, lateral terminal accessory spine; lts, lateral terminal spine; LV, lateroventral; m, male condition of sexually dimorphic character; MD, middorsal; ML, midlateral; ne, nephridiopore; pa, papilla; PD, paradorsal; ps, penile spine; SD, subdorsal; ss, sensory spot; ss3, type 3 sensory spot; tu, tube; VL, ventrolateral; VM, ventromedial; * indicates unpaired structures.

Segment	MD	PD	SD	LD	ML	LA	LV	VL	VM
1	gco1*		ss	ss	ss		gco1	ss	
2	gco1*				ss			tu	ss, gco1
3	gco1*		ss		ss	ss			ss, gco1
4	ac*	ss	gco1	ss					ss, gco1
5	ac*	ss	ss, gco1				tu		ss, gco1
6	ac*	ss	ss, gco1				ac		ss, gco1
7	ac*	ss	ss, gco1				ac	pa (f)	ss, gco1
8	ac*	ss	ss, gco1		gco2		ac		ss, gco1
9		ss	ss, gco1	gco2		ne	ac		ss, gco1
10	gco1*x2		ss	tu					gco1
11		gco1	ss3			psx3 (m), ltas (f)	lts		

2. Supplementary Figures

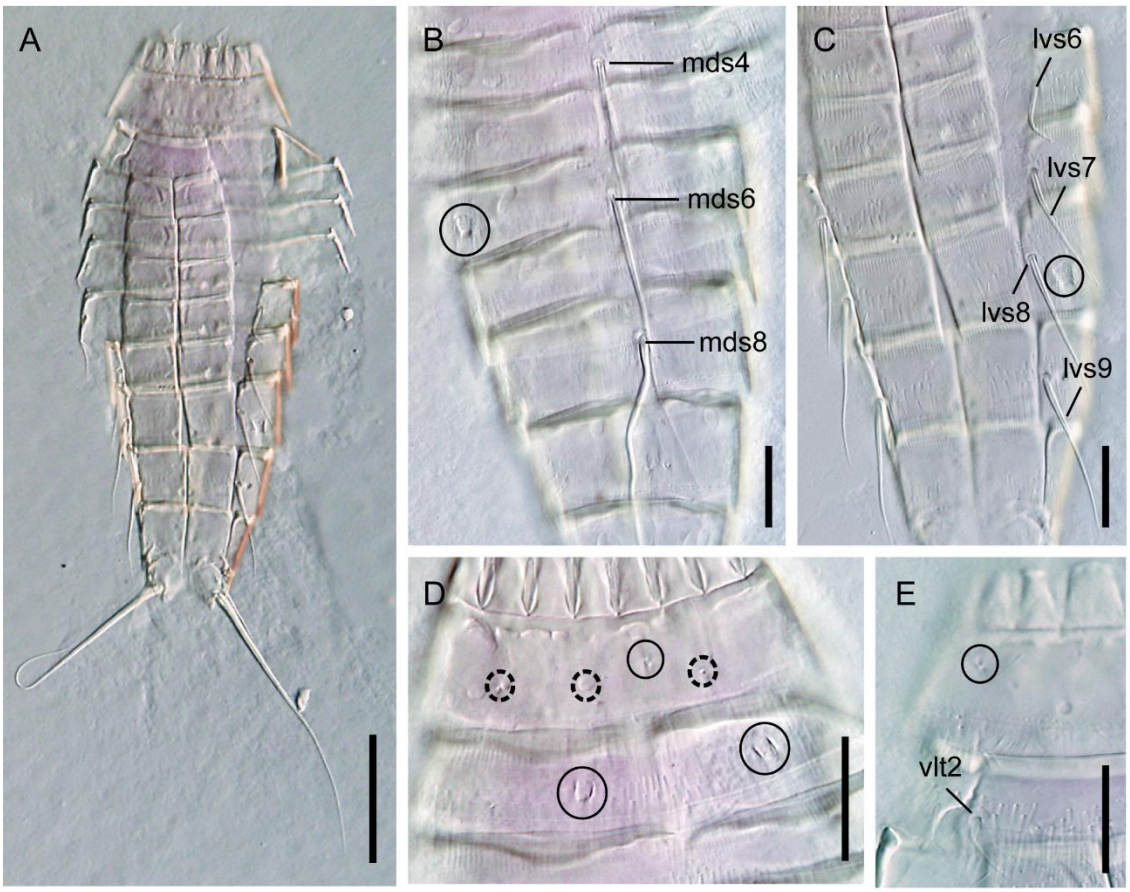

Supplementary Figure 2.1 Diagnostic cuticular characters of a female of *Echinoderes apex* from the station MOZ01-MTB03 (outside pockmark). (A): Ventral trunk overview; (B) Dorsal view of segments 4-9; (C) Ventral view of segments 6-10; (D) Dorsal view of segments 1-2; (E) Lateroventral to ventromedial view on right half of cuticular plates of segments 1-2. Scales: A 50 µm; B-E 20 µm. Abbreviations: lvs, lateroventral spine; mds, middorsal spine; vlt, ventrolateral tube; sensory spots are marked as dashed circles, and glandular cell outlets as closed circles; numbers after abbreviations indicate corresponding segment.

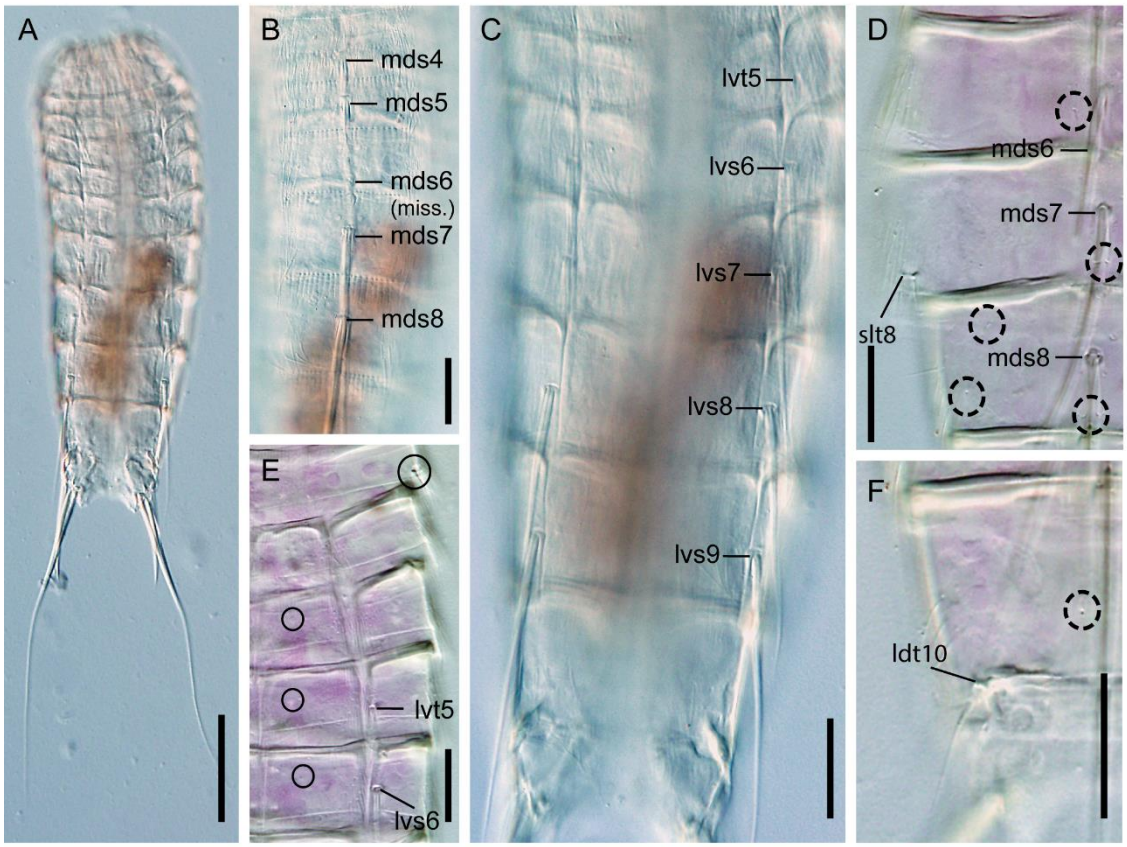

Supplementary Figure 2.2 Diagnostic cuticular characters of a female of *Echinoderes* cf. *dubiosus* from the station MOZ04-MTB02, outside pockmark (A-C) and a male from the station MOZ01-MTB3, outside pockmark (D-F). (A): Ventral trunk overview; (B) Dorsal view of segments 4-8; (C) Ventral view of segments 5-10; (D) Middorsal to sublateral view on right half of tergal plates of segments 6-9; (E) Midlateral to ventromedial view on left half of tergal and sternal plates of segments 2-6; (F) Middorsal to laterodorsal view on right half of tergal plate of segment 10. Scales: A 50 µm; B-F 20 µm. Abbreviations: ldt, laterodorsal tube; lvt, lateroventral tube; lvs, lateroventral spine; mds, middorsal spine; miss, missing (only base detected); slt, sublateral tube; sensory spots are marked as dashed circles, and glandular cell outlets as closed circles; numbers after abbreviations indicate corresponding segment.

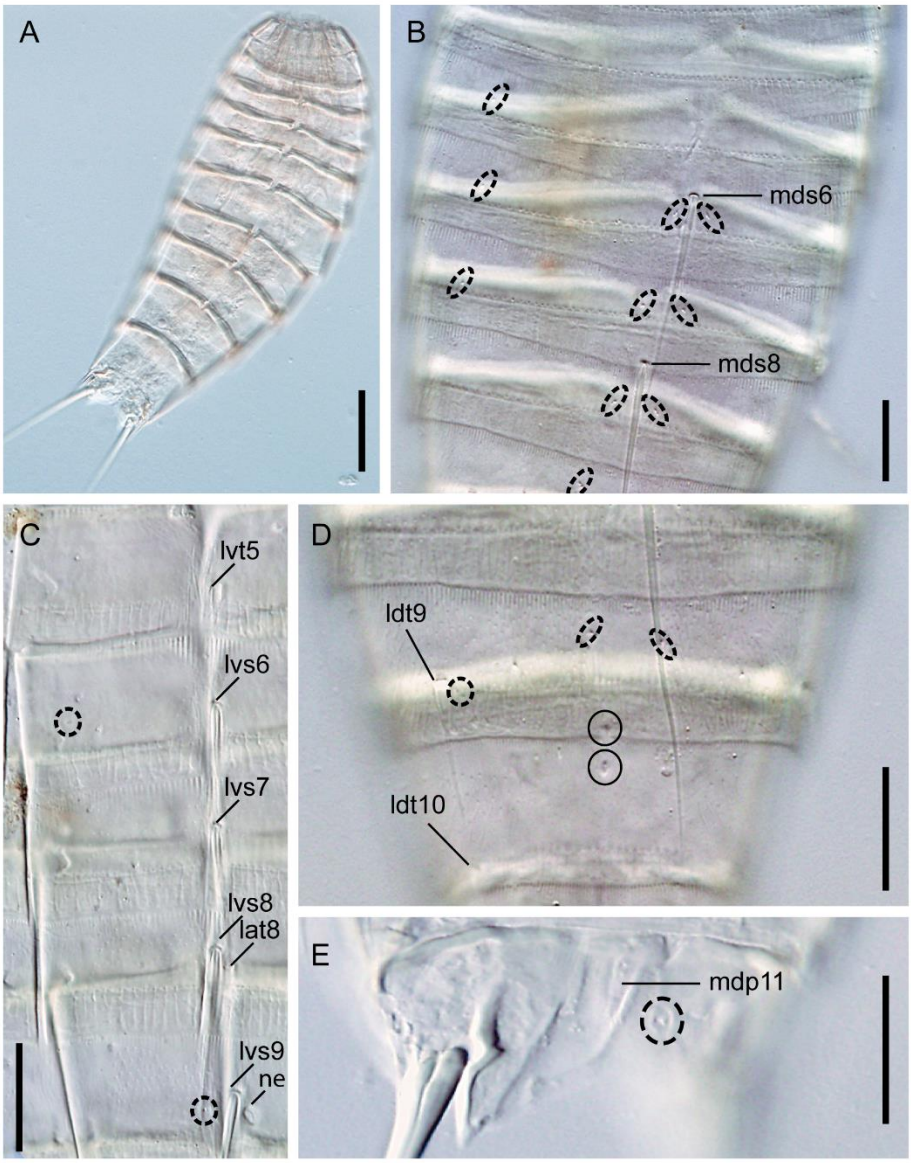

Supplementary Figure 2.3 Diagnostic cuticular characters of a male (A) and a female (B-E) of *Echinoderes hviidarum* from the station MOZ04-MTB1 (within pockmark). (A): Dorsal overview of trunk; (B) Dorsal view of segments 5-9; (C) Lateral accessory to ventromedial view on left half of tergal and sternal plates of segments 5-9; (D) Dorsal view of segments 9-10; (E) Dorsal view of segment 11. Scales: A 50 µm; B-F 20 µm. Abbreviations: lat, lateral accessory tube; ldt, laterodorsal tube; lvs, lateroventral spine; lvt, lateroventral tube; mdp, middorsal protuberance; mds, middorsal spine; ne, nephridiopore; sensory spots are marked as dashed circles, and glandular cell outlets as closed circles; numbers after abbreviations indicate corresponding segment.

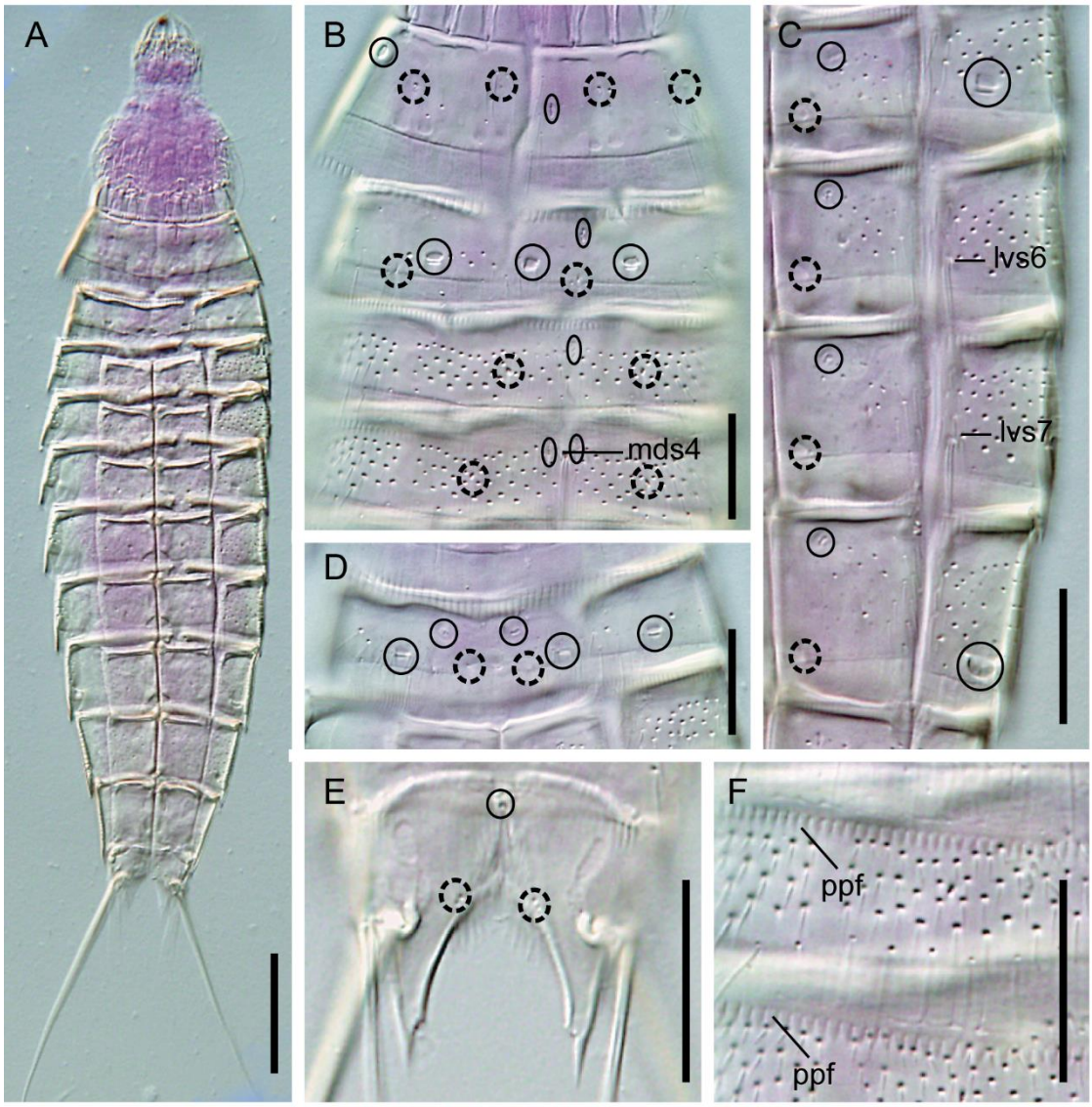

Supplementary Figure 2.4 Diagnostic cuticular characters of a female of *Echinoderes unispinosus* from the station MOZ01-MTB06 (within pockmark). (A): Ventral overview of trunk; (B) Dorsal view of segments 1-4; (C) Sublateral to ventromedial view on left half of tergal and sternal plates of segments 5-8; (D) Ventral view of segment 2; (E) Dorsal view of segment 11; (F) Detail of the primary pectinate fringes of segments 4-5. Scales: A 50 µm; B-F 20 µm. Abbreviations: lvs, lateroventral spine; mds, middorsal spine; ppf, primary pectinate fringe; sensory spots are marked as dashed circles, and glandular cell outlets as closed circles; numbers after abbreviations indicate corresponding segment.

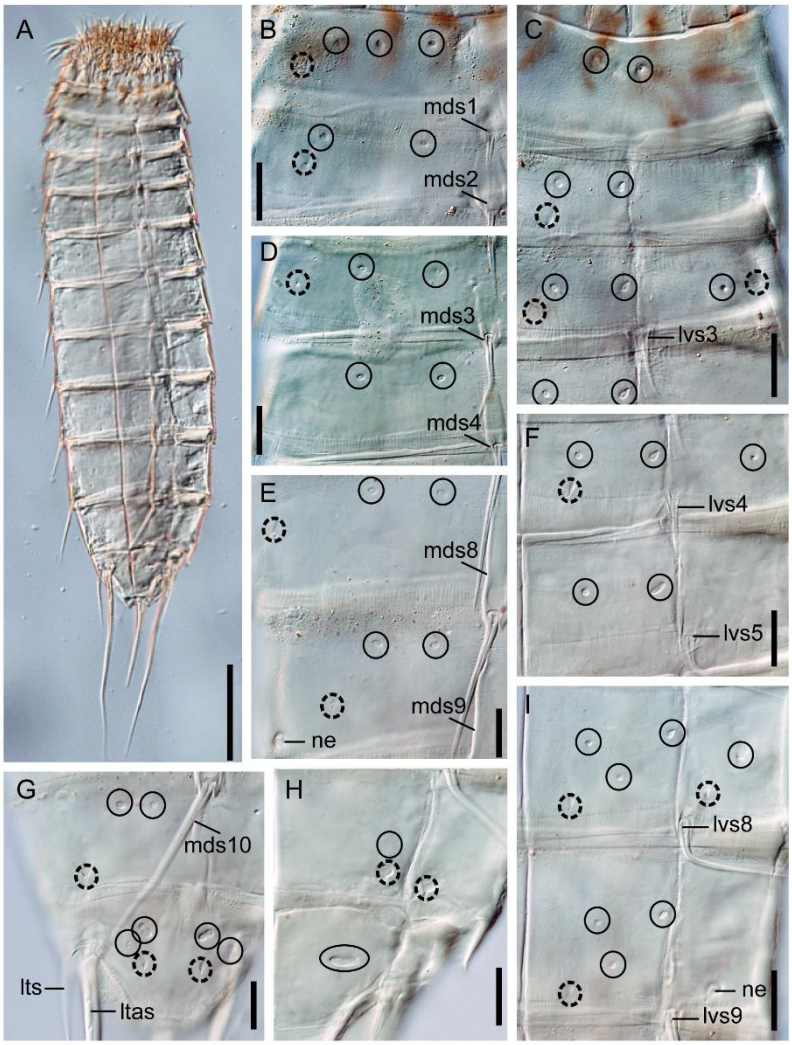

Supplementary Figure 2.5 Diagnostic cuticular characters of a female of *Ryuguderes* sp. from the station MOZ04-MTB02 (outside pockmark). (A) Ventral overview of trunk; (B) Middorsal to laterodorsal view on right half of tergal plates of segments 1-2; (C) Midlateral to ventromedial view on left half of tergal and sternal plates of segments 1-3; (D) Middorsal to laterodorsal view on right half of tergal plates of segments 3-4; (E) Middorsal to laterodorsal view on right half of tergal plates of segments 8-9; (F) Midlateral to ventromedial view on left half of tergal and sternal plates of segments 4-5; (G) Dorsal view of segments 10-11; (H) Midlateral to ventromedial view on left half of tergal and sternal plates of segments 10-11; (I) Midlateral to ventromedial view on left half of tergal and sternal plates of segments 8-9. Scales: A 50 µm; B-F 20 µm. Abbreviations: ltas, lateral terminal accessory spine; lts, lateral terminal spine; lvs, lateroventral spine; mds, middorsal spine; ne, nephridiopore; sensory spots are marked as dashed circles, and glandular cell outlets as closed circles; numbers after abbreviations indicate corresponding segment.

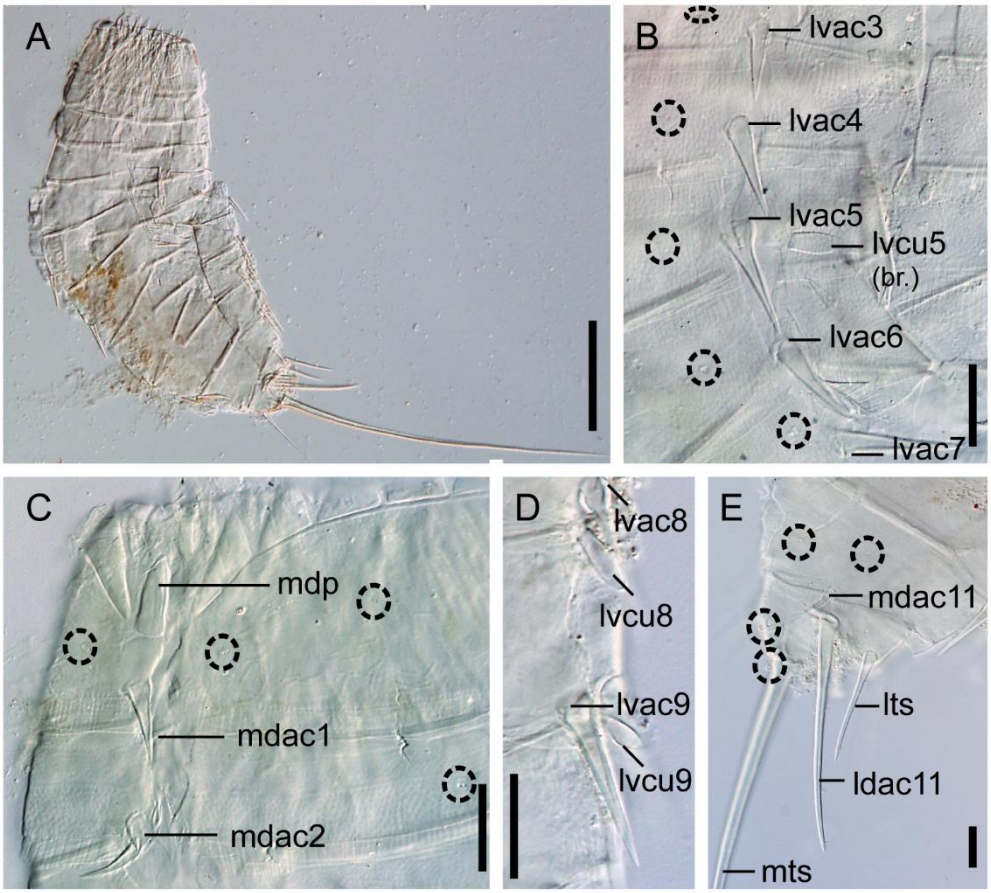

Supplementary Figure 2.6 Diagnostic cuticular characters of a female of *Sphenoderes* cf. *indicus* from the station MOZ04_MTB01 (within pockmark). (A) Lateral overview of trunk; (B) Series of lateroventral spines of segments 3-7; (C) Dorsal view of segments 1-2; (D) Series of lateroventral spines of segments 8-9; (E) Lateral view of segments 10-11. Scales: A 100 µm; B-E 20 µm. Abbreviations: br., broken structure; ldac, laterodorsal acicular spine; lts, lateral terminal spine; lvac, lateroventral acicular spine; lvcu, lateroventral cuspidate spine; mdac, middorsal acicular spine; mdp, middorsal placid; mts, midterminal spine; sensory spots are marked as dashed circles; numbers after abbreviations indicate corresponding segment.

European Journal of Taxonomy 637: 1–15
https://doi.org/10.5852/ejt.2020.637
ISSN 2118-9773
www.europeanjournaloftaxonomy.eu
2020 · Cepeda D. *et al.*

Research article

urn:lsid:zoobank.org:pub:BD1FDE40-F1C4-49C8-BCDB-72AB3EDA9F17

Setaphyes elenae sp. nov., a new species of mud dragon (Kinorhyncha: Allomalorhagida) from Skagerrak (north-eastern Atlantic Ocean)

Diego CEPEDA [1], Alberto GONZÁLEZ-CASARRUBIOS [2,*], Nuria SÁNCHEZ [3] & Fernando PARDOS [4]

[1,2,4] Universidad Complutense de Madrid (UCM), Faculty of Biological Sciences, Department of Biodiversity, Ecology and Evolution. C/ José Antonio Novais 12. 28040 Madrid, Spain. [3] Institut Français de Recherche pour l'Exploitation de la Mer (IFREMER), Deep-sea Laboratory. ZI de la Pointe du Diable. 29280 Plouzané, France.

* Corresponding author: albert23@ucm.es
[1] Email: diegocepeda@ucm.es
[3] Email: Nuria.Sanchez.Santos@ifremer.fr [4]
Email: fpardos@ucm.es

[1] urn:lsid:zoobank.org:author:734A11DE-8E3F-44BB-A0FF-D7341CEE3A83
[2] urn:lsid:zoobank.org:author:E5637211-39C0-4403-8101-1D9BDFC50E41
[3] urn:lsid:zoobank.org:author:878029BD-0D80-4CC5-93ED-F6848744A6EC
[4] urn:lsid:zoobank.org:author:979172E4-7B1D-4E5E-81E9-B530258DDE5D

Abstract. Meiofauna sampling in the proximity of Syd-Hällsö Island (Strömstad, Sweden) revealed a new species of Kinorhyncha from the Skagerrak. The species, *Setaphyes elenae* sp. nov., is distinguished from its congeners by the arrangement of the middorsal cuticular specializations (it has shortened, distally rounded middorsal processes on segments 1 and 9 and middorsal elevations throughout segments 2–8), as well as by the presence of paired laterodorsal setae on segments 3, 5, 7 and 9 and ventromedial setae on segments 3, 5 and 7 in both males and females. The finding of a new species from the north-eastern Atlantic Ocean, provides new valuable information for the recently established genus in the Allomalorhagida.

Keywords. Meiofauna, taxonomy, Scalidophora, biodiversity, invertebrates.

Cepeda D., González-Casarrubios A., Sánchez N. & Pardos F. 2020. *Setaphyes elenae* sp. nov., a new species of mud dragon (Kinorhyncha: Allomalorhagida) from Skagerrak (north-eastern Atlantic Ocean). *European Jopurnal of Taxonomy* 637: 1–15. https://doi.org/10.5852/ejt.2020.637

Introduction

The phylum Kinorhyncha Reinhard, 1887 encompasses a group of meiobenthic, free-living invertebrates that mainly inhabit the upper centimetres of marine and estuarine sediments, although some species have been found living in hard substrata or associated with macroalgae and marine phanerogams (Higgins 1988). Kinorhynchs have been described from shallow to deep-sea waters across the worldwide oceans,

European Journal of Taxonomy 637: 1–15 (2020)

but certain areas have received much more attention to the detriment of others due to the specialists sampling strategies (Sánchez *et al.* 2012; Neuhaus 2013; Sørensen *et al.* 2013; Cepeda *et al.* 2019).

Kinorhynch biodiversity of the North Sea, together with other north-eastern Atlantic areas nearby, has been studied earlier (Neuhaus, 2013). Currently, 20 species are known in this area: *Campyloderes vanhoeffeni* Zelinka, 1913, *Centroderes spinosus* (Reinhard, 1881), *Condyloderes multispinosus* (McIntyre, 1962), *Echinoderes dujardinii* Claparède, 1863, *E. elongatus* (Nyholm, 1947), *E. higginsi* Huys & Coomans, 1989, *E. levanderi* Karling, 1955, *E. peterseni* Higgins & Kristensen, 1988, *E. setiger* (Greeff, 1869), *E. subfuscus* Zelinka, 1928, *E. worthingi* Southern, 1914, *Paracentrophyes quadridentatus* (Zelinka, 1928), *Pycnophyes calmani* (Zelinka in Southern, 1914), *P. communis* Zelinka, 1908, *P. zelinkaei* Southern, 1914, *Semnoderes armiger* Zelinka, 1928, *Setaphyes dentatus* (Reinhard, 1881), *S. flaveolatus* (Zelinka, 1928), *S. kielensis* (Zelinka, 1928) and *Zelinkaderes submersus* (Gerlach, 1969) (Zelinka 1928; Nyholm 1947; McIntyre 1962, 1964; Gerlach 1969; Huys & Coomans 1989; Sørensen *et al.* 2009; Neuhaus *et al.* 2013; Altenburger 2016).

In the context of global change and decreasing studies of taxonomy, especially those of small-sized taxa, there is a need to improve taxonomic information about meiofaunal organisms, even in geographic areas that are supposed to be relatively well-studied (Mora *et al.* 2011; Sørensen & Grzelak 2018). A recent sampling done in the proximities of Syd-Hällsö Island (Strömstad, Sweden) revealed a new species of Kinorhyncha from Skagerrak. Additionally, the species *Echinoderes* cf. *eximus* and *Pycnophyes ancalagon* Sørensen & Grzelak, 2018, the latter recently described from the Svalbard Archipelago (Arctic Ocean), are firstly reported for the boreal area.

Material and methods

Study site

Sampling was undertaken at a single locality near Syd-Hällsö Island (Strömstad, Sweden) during summer 2017, at the eastern-most limit of the North Sea: 58°56.846′ N, 11°4.896′ E (Fig. 1B). This area encompasses the Skagerrak Strait that connects the North Sea with the Kattegat sea region (Fig. 1A).

Skagerrak, with a surface area of about 32 000 km_2, is the deepest area of the North Sea basin, with a maximum depth of 700 m (Weering *et al.* 1993; Rosenberg *et al.* 1996). Skagerrak is dominated by a deep-reaching flow of water from the central and northern North Sea, with a salinity of about 35 psu and to a lesser extent by a weaker inflow from the southern North Sea with a salinity of about 31–34 psu influenced by river inputs (Rosenberg *et al.* 1996). Additionally, the shallowest waters of Skagerrak are also subject of upwelling events that cause low-saline currents along the Swedish and Norwegian coastlines (Rodhe 1996).

Skagerrak forms a natural topographic sediment trap, receiving inputs from the entire north-western European drainage systems and the North Sea shoreline (Weering *et al.* 1993). Thus, Skagerrak has been evidenced as a major depository of fine-grained sediments in the North Sea, with 59% of particles with an average size less than 63 μm (Weering *et al.* 1987). Nevertheless, areas with coarse gravel, sandy coves and sandbars are also present in the area (Curini-Galletti *et al.* 2012).

Sampling and specimen preparation

Sampling was done during the summer of 2017 by dredging. The collected sample was taken at a depth of 55–65 m and mainly consisted of very fine, soft mud. Sediment was kept in large plastic boxes and stored at a constant temperature of 15ºC. Meiofaunal organisms were then extracted by $MgCl_2$-decantation and live material was studied and sorted using stereo microscopes.

Kinorhynchs were preserved in 100% ethanol. For light microscopy (LM), unmounted specimens were dehydrated through a graded series of glycerine. After being kept in 100% glycerine for 24 h, kinorhynchs were mounted on glass slides with Fluoromount G® sealed with Depex®. Mounted specimens were studied with an Olympus© BX51-P microscope with differential interference contrast (DIC) optics equipped with an Olympus© DP-70 camera. Identification to genus level was done using the dichotomous keys provided by Sørensen & Pardos (2008) for cyclorhagids and the genus diagnoses provided by Sánchez *et al.* (2016) for allomalorhagids. For scanning electron microscopy (SEM), some unmounted kinorhynchs were sonically cleaned during 10–15 s and led to chemical point drying using a hexamethyldisilazane-ethanol series. Finally, specimens were coated with gold and mounted on aluminium stubs to be studied with a JSM® 6335-F JEOL SEM at the ICTS Centro Nacional de Microscopía Electrónica (UCM, Spain). Type material was deposited at the Natural History Museum of Denmark (NHMD). Line drawings and image plates composition were done using Adobe® Photoshop and Illustrator CC-2014 software.

Morphometric statistical analyses

Differences in selected morphometric measures (total trunk length, standard width and lateral terminal spines' length) of *Setaphyes elenae* sp. nov. and its congeners were tested. For this, we selected several specimens of *S. dentatus* (n = 18) and *S. flaveolatus* (n = 14), which are the most morphologically similar, and are also distributed through the north-eastern Atlantic Ocean. Specimens of *S. dentatus* and *S. flaveolatus* are from several Atlantic and Mediterranean locations surrounding the Iberian Peninsula, stored at the Meiofauna Collection of the UCM.

Normality and homoscedasticity of the variables were tested using the Saphiro-Wilk's test (together with visual methods of density and Q–Q plots) and the Bartlett's test, respectively. Tukey multiple comparison test and pairwise comparisons between group levels with corrections for multiple testing were used to determine which means amongst the set of means differ from the rest. A one-way analysis of variance (ANOVA) was used to test differences, but when heteroscedasticity was detected, a Welch's

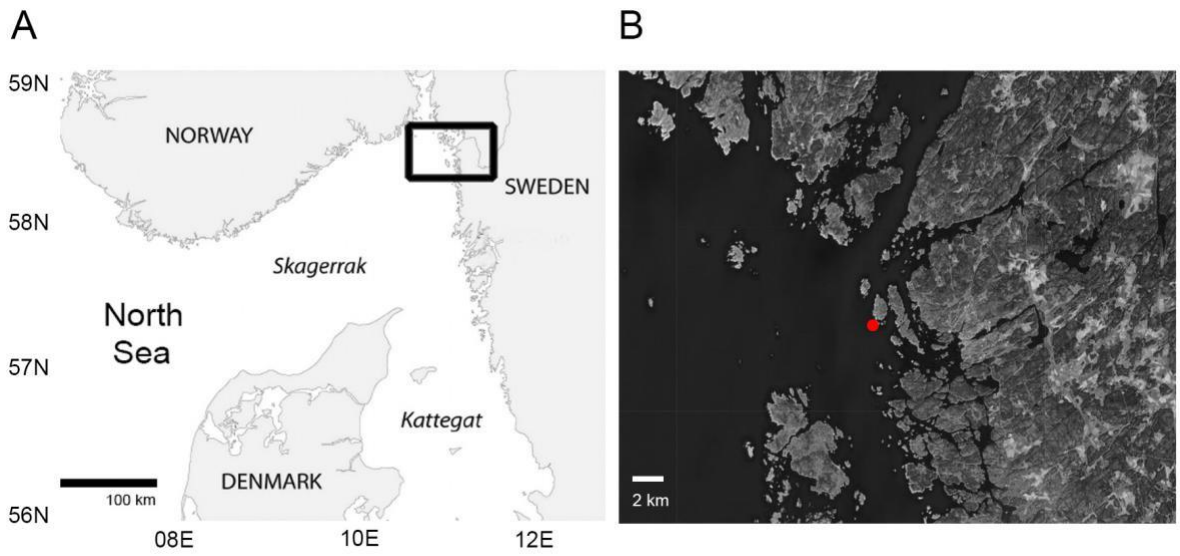

Fig. 1. A. Map showing the sampling area of Syd-Hällsö Island (Strömstad, Sweden). **B**. Detail. Red point shows the specific sampling point.

European Journal of Taxonomy 637: 1–15 (2020)

ANOVA was performed instead. All the statistical analyses were run in R ver. 1.1.453 using the '*stats*' basic package and the '*car*' package ver. 3.0.5 (Fox *et al.* 2019).

Results

Five species co-occurr in the collected sample near Syd-Hällsö Island (Swedish North Sea): *Centroderes spinosus*, *Echinoderes* cf. *eximus*, *Pycnophyes ancalagon*, *Semnoderes armiger* and *Setaphyes elenae* sp. nov.

Class Allomalorhagida Sørensen *et al.*, 2015
Family Pycnophyidae Zelinka, 1896
Genus *Setaphyes* Sánchez *et al.*, 2016

Setaphyes elenae sp. nov.
urn:lsid:zoobank.org:act:6C4FE50F-E39A-451E-B805-60B709B9B9B4
Figs 2–4, Tables 1–3

Diagnosis

Setaphyes with shortened, distally rounded middorsal processes on segments 1 and 9, and middorsal elevations on segments 2–9, superficially covered by tufts of elongated, thick hairs whose tips sometimes surpass the posterior margin of segment. Unpaired setae in paradorsal position on segments 1–9. Laterodorsal setae on segments 3, 5, 7 and 9; paralateral setae absent. Lateroventral setae on segments 2–10. Ventromedial setae on segments 3, 5 and 7. Paired, small, dot-shaped intracuticular structures (maybe outlets of glandular cells) present in several positions throughout the trunk, with a specific arrangement that differs from males to females. Males with paired, sexually dimorphic ventromedial tubes on segment 2, and females with paired, sexually dimorphic ventrolateral setae on segment 2. Lateral terminal spines present, relatively short, slender. Segment 11 retractable into segment 10.

Etymology

The species is dedicated to Ms Elena González, sister of the second author.

Material examined

Holotype

ATLANTIC OCEAN • ♀ adult (mounted in Fluoromount G®); near Syd-Hällsö Island, Skagerrak (Fig. 1B); 58°56.846′ N, 11°4.896′ E; 55–65 m depth; Ulf Jondelius and Fredrik Pleijel leg.; very fine mud; NHMD 655358.

Paratypes

ATLANTIC OCEAN • 3 adult ♂♂, 2 adult ♀♀ (all mounted in Fluoromount G®); same collection data as for holotype; NHMD 655359 to 655363.

Additional non-type material

ATLANTIC OCEAN • 8 specs (four mounted for LM and four mounted for SEM); same collection data as for holotype; Meiofauna Collection UCM.

Description

See Table 1 for measurements and dimensions, Table 2 for summary of cuticular elevation, process, seta, tube, nephridiopore and sensory spot locations, and Table 3 for summary of intracuticular, dot-shaped structure locations.

Table 1. Measurements of nine adult specimens of *Setaphyes elenae* sp. nov. (four males and five females) from Skagerrak. Abbreviations: LTS = lateral terminal spines; MSW = maximum sternal width (measured at segment 5); S = segments' length (followed by number of corresponding segment); Sd = standard deviation; SSW = standard sternal width (measured at segment 10); TL = total length.

Character	Range ♀	Mean ♀	Range ♂	Mean ♂	Total range	Total mean	Sd
TL (µm)	612.67–722.64	679.192	614.32–647.86	625.51	612.67–722.64	655.33	44.06
MSW–5 (µm)	179.55–188.89	183.422	168.06–176.25	170.72	168.06–188.89	177.78	7.61
MSW–5/TL (%)	26–29.5	27	26.2–28.4	27.3	26–29.5	27.2	1.22
SSW (µm)	141.41–152.44	144.178	124.68–133.65	131.065	124.68–152.44	138.35	8.23
SSW/TL (%)	19.7–23	21.3	19.2–21.9	21	19.2–23	21.1	1.14
S1 (µm)	87.74–108.41	96.584	89.16–96.28	91.548	87.74–108.41	94.35	6.31
S2 (µm)	59.74–82.08	69.712	62.45–68.07	65.068	59.74–82.08	67.65	6.42
S3 (µm)	57.56–79.22	70.068	63.54–68.8	66.655	57.56–79.22	68.55	6.04
S4 (µm)	70.27–79.51	74.618	68.79–81.68	74.51	68.79–81.68	74.57	4.48
S5 (µm)	69.77–83.01	77.1	69.3–76.08	74.438	69.3–83.01	75.92	5.84
S6 (µm)	73.96–81.58	78.504	73.81–83.53	77.013	73.81–83.53	77.84	3.51
S7 (µm)	74.47–85.94	80.752	73.33–80.37	75.385	73.33–85.94	78.37	4.70
S8 (µm)	69.57–86.82	80.846	77.08–79.98	78.138	69.57–86.82	79.64	5.31
S9 (µm)	70.24–84.44	79.61	68.76–78.56	74.463	68.76–84.44	77.32	5.43
S10 (µm)	64.87–77.97	73.66	60.93–71.98	67.165	60.93–77.97	70.77	5.92
S11 (µm)	27.93–39.81	32.3	27.49–34.23	30.615	27.49–39.81	31.55	3.74
LTS (µm)	90.64–105.7	100.9	149.06–168.74	158.928	90.64–168.74	126.69	31.29
LTS/TL (%)	13.9–15.8	14.9	24–26	25.4	13.9–26	19.6	5.60

Head with retractable mouth cone and introvert. The collected specimens were not suitable for head examinations, hence data on number and arrangement of scalids and oral styles are not available.

Neck with four dorsal and two ventral sclerotized placids (Fig. 2A–B, D). Dorsal placids rectangular, with a slightly convex anterior margin; mesial ones broader than lateral ones (Fig. 2B). Ventral placids morphologically similar to dorsal ones but much more elongated, getting thinner towards the lateral sides (Fig. 2A, D).

Trunk with eleven segments (Figs 2A–B, 3A, H, 4A). Segment 1 with one tergal, two episternal and one sub-trapezoidal, midsternal plate; remaining ones with one tergal and two sternal cuticular plates (Figs 2A–D, 3A, H). Tergal cuticular plates slightly bulging middorsally. Sternal plates reach their maximum width at segment 5, but are almost constant in width across the trunk, slightly tapering at the last three trunk segments (Figs 2A–B, 3A, H). Sternal cuticular plates are relatively narrow in the ratio maximum width to total trunk length (MSW-5: TL average ratio = 27.2%), giving the animal a slender appearance (Figs 2A–B, 3A, H, 4A). Middorsal processes on segments 1 and 9, shortened and distally rounded (Figs 2B, 3B, M, 4G, I); middorsal elevations on segments 2–8, pentagonally-shaped, distally rounded, with intracuticular, butterfly-like atria of paradorsal sensory spots (Figs 2B, 3D, F, I, K, 4B, E). Middorsal elevations superficially covered by tufts of elongated, thick cuticular hairs whose tips

European Journal of Taxonomy 637: 1–15 (2020)

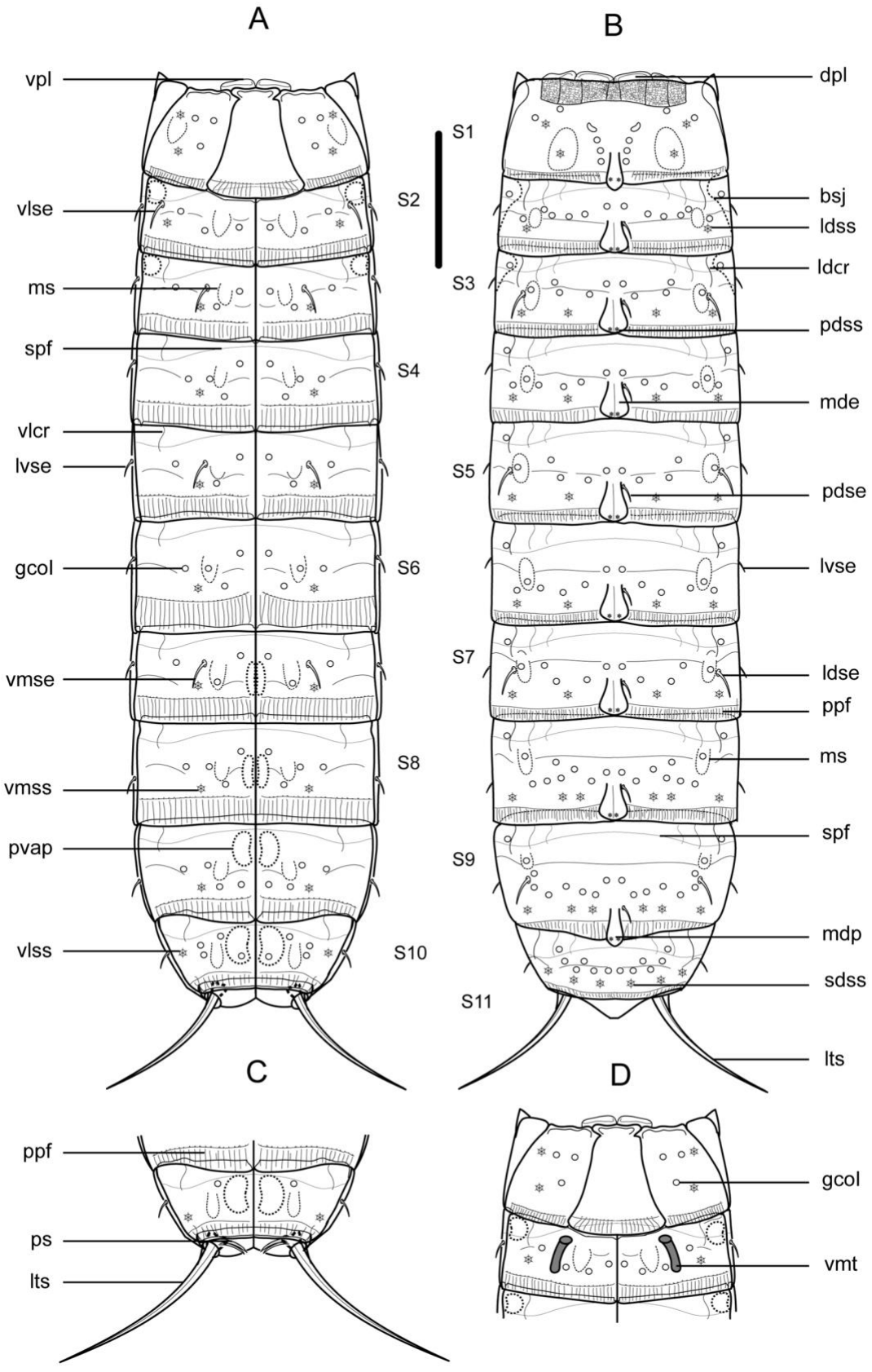

Table 2. Summary of nature and arrangement of cuticular elevations, processes, spines, tubes, setae, sensory spots and nephridiopores in *Setaphyes elenae* sp. nov. Abbreviations: ce = cuticular elevation; cp = cuticular process; LD = laterodorsal; lts = lateral terminal spine; LV = lateroventral; MD = middorsal; ne = nephridiopore; PD = paradorsal; SD = subdorsal; se = seta; ss = sensory spot; tu = tube; VL = ventrolateral; VM = ventromedial. * indicates unpaired structures.

Segment	MD	PD	SD	LD	LV	VL	VM
1	cp*	ss	ss	ss		ss, ss	
2	ce*	se*, ss		ss	se	se (♀)	ss, tu (♂)
3	ce*	se*, ss	ss	ss, se	se		se, ss
4	ce*	se*, ss	ss	ss	se		ss
5	ce*	se*, ss	ss	ss, se	se		se, ss
6	ce*	se*, ss	ss	ss	se		ss
7	ce*	se*, ss	ss	ss, se	se		se, ss
8	ce*	se*, ss	ss, ss	ss	se		ss
9	cp*	se*, ss	ss, ss	ss, se	se, ne		ss
10			ss, ss	ss	se	ss	
11					lts		

sometimes surpass the posterior margin of the segments (Fig. 4B, E). Intracuticular, minute, dot-shaped, rounded to oval structures (maybe outlets of glandular cells) throughout the cuticle on segments 1–10 (Figs 2A–D, 3B–G, I–N). Location and pairs of these structures per segment differ from males to females (Table 3), and deviations from the bilateral symmetry of their arrangement have been observed in some specimens. Up to three pairs of conspicuous laterodorsal cuticular ridges on segments 2–10 (Figs 2A– B, 3D–G, I–N). Cuticular hairs acicular, elongated, emerging from oval perforation sites, distributed all over the trunk cuticle. Pachycycli and ball-and-socket joints only conspicuous on segments 2–3, reduced on posterior segments (Fig. 2A–B, D). Apodemes on segments 7–10 (Fig. 2A–C). Primary pectinate fringe finely serrated; secondary pectinate fringe as a double tranverse, hairy-like, wavy row; free flaps covering the anterior part of subsequent segment (Figs 2A–D, 4D). Muscular scars as rounded to oval, hairless areas in laterodorsal and ventromedial positions on segments 1–10 (those of segment 1 in subdorsal and ventrolateral positions), quite inconspicuous (Fig. 2A–D).

Segment 1 with shortened, distally rounded middorsal process still extending beyond the posterior margin of segment (Figs 2B, 3B, 4G). Anterolateral margins of the tergal plate as horn-shaped, short, wide, distally curved and pointed extensions (Figs 2A–B, D, 3A–C, H, 4A). Anterior margin of segment with a reticule-like ornamentation dorsally (Figs 2B, 3B, 4C). Setae absent. Two pairs of sensory spots

Fig. 2 (opposite page)**.** Line art illustrations of adult *Setaphyes elenae* sp. nov. **A**. ♀, ventral overview. **B**. ♀, dorsal overview. **C**. ♂, segments 10–11, ventral view. **D**. ♂, segments 1–2, ventral view. Abbreviations: bsj = ball-and-socket joint; dpl = dorsal placid; gcoI = type I glandular cell outlet; ldcr = laterodorsal cuticular ridge; ldse = laterodorsal seta; ldss = laterodorsal sensory spot; lts = lateral terminal spine; lvse = lateroventral seta; mde = middorsal elevation; mdp = middorsal process; ms = muscular scar; pdse = paradorsal seta; pdss = paradorsal sensory spot; ppf = primary pectinate fringe; ps = penil spine; pvap = paraventral apodeme; sdss = subdorsal sensory spot; spf = secondary pectinate fringe; vlcr = ventrolateral cuticular ridge; vlse = ventrolateral seta; vlss = ventrolateral sensory spot; vmse = ventromedial seta; vmss = ventromedial sensory spot; vmt = ventromedial tube; vpl = ventral placid. Scale bar = 100 µm.

European Journal of Taxonomy 637: 1–15 (2020)

Table 3. Summary of nature and arrangement of intracuticular structures (maybe outlets of glandular cells) in *Setaphyes elenae* sp. nov., including sexually dimorphic differences. Abbreviations: LD = laterodorsal; PD = paradorsal; PL = paralateral; PV = paraventral; SD = subdorsal; VL = ventrolateral; VM = ventromedial.

Segment	PD	SD	LD	PL	VL	VM	PV
1	3× (♀), 2× (♂)	2× (♀), 1× (♂)	1× (♀), 2× (♂)		3×		
2	1×	2×	3× (♀), 1× (♂)			2× (♀), 3× (♂)	1×
3	1×	3× (♀), 2× (♂)	1×	1×		2× (♀), 3× (♂)	1×
4	1×	2×	3× (♀), 1×(♂)	1×		3×	1×
5	1×	3× (♀), 2× (♂)	2×	1×		2× (♀), 3× (♂)	1×
6	1×	2×	3× (♀), 1× (♂)	1×		3×	1×
7	1×	3× (♀), 2× (♂)	1×	1×		2× (♀), 3× (♂)	1×
8	1×	5× (♀), 3× (♂)	2×	1×		3×	1×
9	1×	4× (♀), 2× (♂)	3× (♀), 1× (♂)	1×		3×	1×
10	1×	2× (♀), 3× (♂)	3× (♀), 1× (♂)			3× (♀), 1× (♂)	1× (♀)
11							

in ventrolateral position longitudinally arranged, and one pair in paradorsal, subdorsal and laterodorsal positions (Figs 2A–B, D, 3B–C, 4G). Sensory spots on this and subsequent segments as oval areas with several rows of cuticular micropapillae surrounding a single pore (Fig. 4B, G, J).

Segment 2 with middorsal elevation not projecting beyond the posterior margin of segment (Figs 2B, 3D, 4E). Unpaired seta in paradorsal position, on this and following segments indifferently located to the right or to the left of the middorsal cuticular specialization, not following any particular pattern, near the anterior margin of the segment (Figs 2B, 3D, 4E); paired setae in lateroventral position (Figs 2A–B, D, 3E); females furthermore with paired, sexually dimorphic setae in ventrolateral position (Figs 2A, 3E). Sexually dimorphic male tubes in ventromedial position (Fig. 2D); detailed morphology of these tubes not determined. Paired sensory spots in paradorsal, laterodorsal and ventrolateral position, the latter near the ventrolateral-ventromedial limit, not longitudinally aligned with the following ventromedial sensory spots (Figs 2A–B, D, 3D–E).

Fig. 3 (opposite page)**.** Light micrographs showing trunk overviews and details of cuticular trunk characters of ♀, holotype (NHMD 655358) (A–L, N) and ♂, paratype (NHMD 655361) (M) of *Setaphyes elenae* sp. nov. **A**. Dorsal overview. **B**. Dorsal view on right half of segment 1. **C**. Ventral view on left half of segment 1. **D**. Dorsal view on right half of segment 2. **E**. Ventral view on left half of segment 2. **F**. Dorsal view on right half of segment 3. **G**. Ventral view on left half of segment 3. **H**. Ventral overview. **I**. Dorsal view on right half of segment 4. **J**. Ventral view on left half of segment 4. **K**. Dorsal view on right half of segment 8. **L**. Ventral view on left half of segment 8. **M**. Dorsal view on right half of segment 9. **N**. Ventral view on left half of segment 9. Abbreviations: ldse = laterodorsal seta; lts = lateral terminal spine; lvse = lateroventral seta; mde = middorsal elevation; mdp = middorsal process; pdse = paradorsal seta; vlse = ventrolateral seta; vmse = ventromedial seta. Numbers after abreviations indicate correspong segment; sensory spots are marked as dashed circles, and glandular cell outlets as continuous circles. Scale bars: A, H = 100 µm; B–G, I–N = 20 µm.

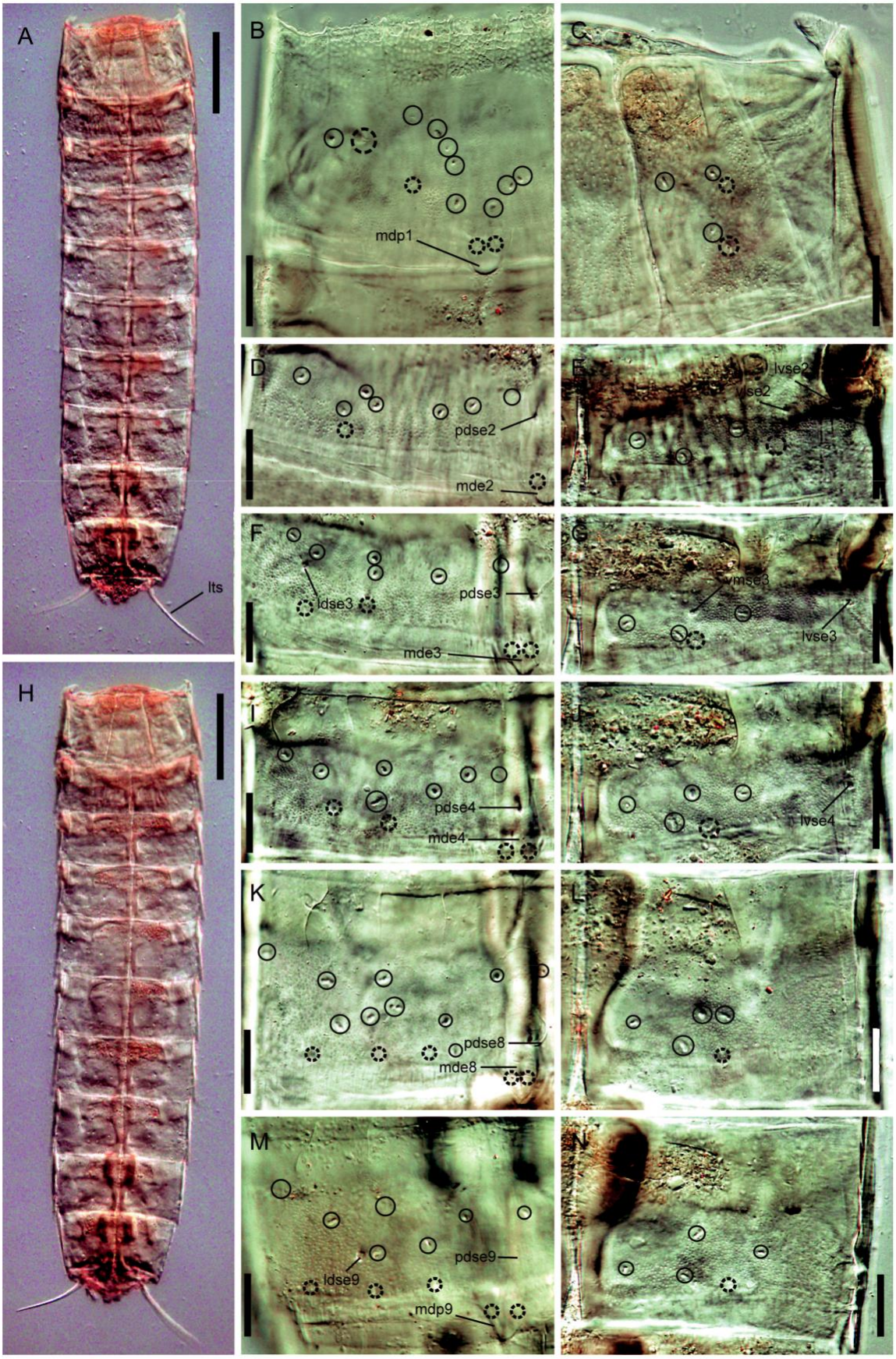
A
lts
B
mdp1
C
D
pdse2
mde2
E
lvse2
vse2
F
ldse3
pdse3
mde3
G
vmse3
lvse3
H
I
pdse4
mde4
J
lvse4
K
pdse8
mde8
L
M
pdse9
ldse9
mdp9
N

European Journal of Taxonomy 637: 1–15 (2020)

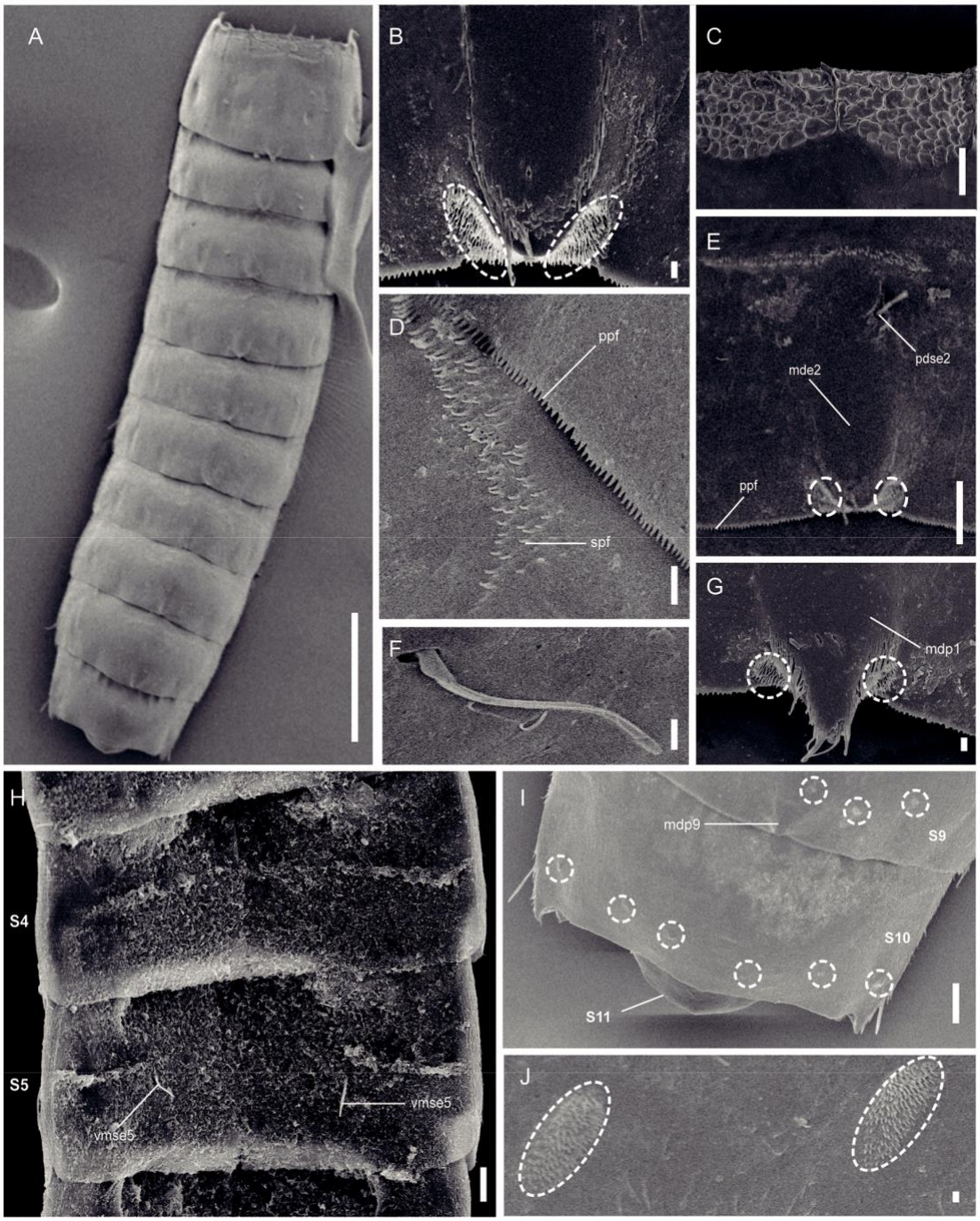

Fig. 4. Scanning electron micrographs showing general overview and details of the cuticular trunk morphology of a non-type specimen of *Setaphyes elenae* sp. nov. **A**. Dorsal overview. **B**. Middorsal elevation of segment 4. **C**. Cuticular ornamentation of anterior margin of segment 1. **D**. Detail of primary and secondary pectinate fringes of segment 5. **E**. Middorsal to paradorsal view of segment 2. **F**. Laterodorsal seta of segment 5. **G**. Middorsal process of segment 1. **H**. Ventral view of segments 4–5. **I**. Dorsal view of segment 10. **J**. Subdorsal sensory spots of segment 8. Abbreviations: mde = middorsal elevation; mdp = middorsal process; pdse = paradorsal seta; ppf = primary pectinate fringe; s = segment; vmse = ventromedial seta. Numbers after abbreviations indicate corresponding segment; sensory spots are marked as dashed circles. Scale bars: A = 100 µm; B, D, F–G, J = 1 µm; C, E, H–I = 10 µm.

Segment 3 with middorsal elevation as on the preceding segment (Figs 2B, 3F). Unpaired seta in paradorsal position (Figs 2B, 3F); paired setae in laterodorsal, lateroventral and ventromedial positions (Figs 2A–B, 3F–G). Paired sensory spots in paradorsal, subdorsal, laterodorsal and ventromedial positions, the latter mesially shifted compared to the previous ones, aligned with those of the following segments (Figs 2A–B, 3F–G).

Segment 4 with middorsal elevation as on the preceding segment (Figs 2B, 3I, 4B). Unpaired seta in paradorsal position (Figs 2B, 3I); paired setae in lateroventral position (Figs 2A–B, 3J). Paired sensory spots in paradorsal, subdorsal, laterodorsal and ventromedial positions (Figs 2A–B, 3I–J).

Segment 5 similar to segment 3 in the arrangement of the cuticular elevation, setae and sensory spots (Figs 2A–B, 4F, H).

Segment 6 similar to segment 4 in the arrangement of the cuticular elevation, setae and sensory spots (Fig. 2A–B).

Segment 7 similar to segments 3 and 5 in the arrangement of the cuticular elevation, setae and sensory spots (Fig. 2A–B).

Segment 8 with middorsal elevation as on the preceding segment (Figs 2B, 3K). Unpaired seta in paradorsal position (Figs 2B, 3K); paired setae in lateroventral position (Fig. 2A–B). Two pairs of sensory spots in subdorsal position, and one pair in paradorsal, laterodorsal and ventromedial positions (Figs 2A–B, 3K–L, 4J).

Segment 9 with middorsal process as that of segment 1 (Figs 2B, 3M, 4I). Unpaired seta in paradorsal (Figs 2B and 3M); paired setae in laterodorsal and lateroventral positions (Fig. 2A–B). Two pairs of sensory spots in subdorsal position, and one pair in paradorsal, laterodorsal and ventromedial positions (Figs 2A–B, 3M–N, 4I). Nephridiopores in lateroventral position.

Segment 10 without middorsal cuticular specialization. Paired setae in lateroventral position (Figs 2A– C, 4I). Two pairs of sensory spots in subdorsal position, and one pair in laterodorsal and ventrolateral positions, the latter near the tergosternal junction (Figs 2A–C, 4I).

Segment 11 without cuticular appendages, partly retractable into segment 10 (Fig. 4A, I). Tergal plate triangular, with a concave and distally pointed posterior margin; sternal plates form a pair of ventral extensions rounded distally (Figs 2A–C, 4I). Males with two sexually dimorphic pairs of stout, thick penile spines (Fig. 2C). Lateral terminal spines' length differs from males (relatively longer, LTS average ratio = 158.93 μm) to females (relatively shorter, LTS average ratio = 100.9 μm)

Discussion

Setaphyes elenae sp. nov. clearly agrees with the main diagnostic characters of the genus, including the absence of ventrolateral setae on segment 5, the presence of unpaired paradorsal setae on segments 2–9 and paired lateroventral setae on segments 2–10, ball-and-socket joints only conspicuous at segments 2–3 (reduced on posterior segments), and the presence of scattered, dot-shaped, intracuticular structures (sometimes called as cuticular scars) at both tergal and sternal plates (Sánchez *et al.* 2016). However, it can easily be distinguished from the remaining species of the genus by the unique arrangement of setae and middorsal cuticular specializations.

Regarding the seta arrangements, *Setaphyes elenae* sp. nov. has paired laterodorsal setae on segments 3, 5, 7 and 9, a pattern similar to that of *S. dentatus* and *S. flaveolatus* (Reinhard 1881; Zelinka 1928; Sánchez *et al.* 2016), with the exception that these congeners lack the setae on segment 9. The remaining

European Journal of Taxonomy 637: 1–15 (2020)

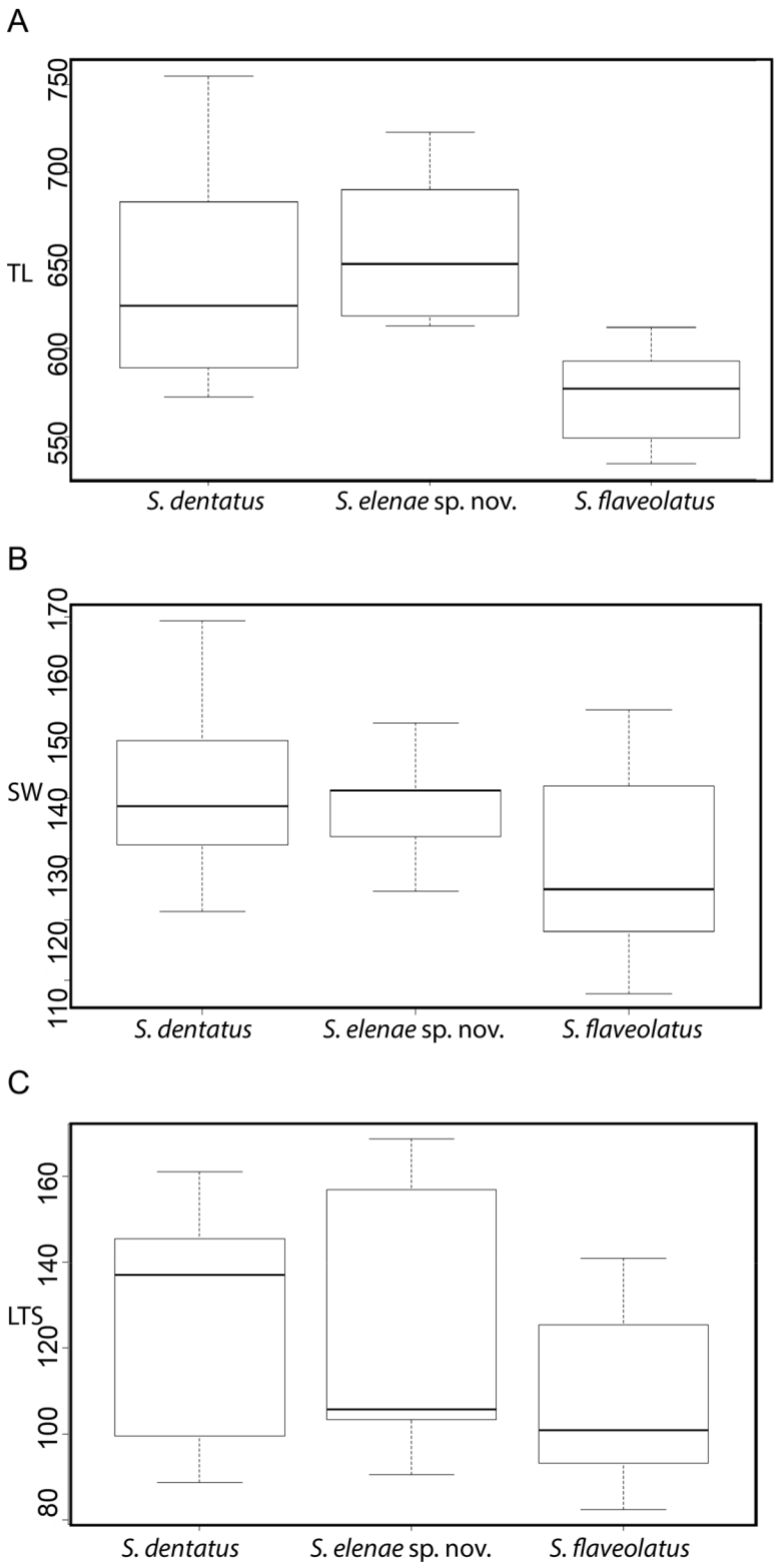

Fig. 5. Boxplots showing the ranges of different body measurements of *Setaphyes elenae* sp. nov., *S. dentatus* (Reinhard, 1881) and *S. flaveolatus* (Zelinka, 1928). **A**. Total trunk length. **B**. Standard sternal width. **C**. Lateral terminal spines' length.

species of the genus also possess laterodorsal setae also even segments. In addition, *S. elenae* sp. nov. is characterized by bearing shortened, distally rounded middorsal processes on segments 1 and 9 exclusively, while both *S. dentatus* and *S. flaveolatus* have middorsal processes on segments 1 and 7–9. The pattern of ventromedial setae also differs between *S. dentatus* (on segments 4–5 and 7–9, females furthermore on segment 3), *S. flaveolatus* (on segments 5 and 7–8, females furthermore on segment 3) and *S. elenae* sp. nov. (on segments 3, 5 and 7).

Setaphyes cimarensis Sánchez *et al.*, 2018, *S. dentatus*, *S. elenae* sp. nov. and *S. flaveolatus* are also characterized by having patterns of cuticular ornamentation that can be used to discriminate congeners (Sánchez *et al.* 2018). Longitudinal, parallel, fold-like cuticular thickenings are present on segment 10 in *S. dentatus* and *S. cimarensis*, which are absent in *S. elenae* sp. nov. and *S. flaveolatus*. Moreover, *S. flaveolatus* has a continuous, reticule-like ornamentation only present in the middle region of the tergal plate, whereas *S. dentatus* and *S. elenae* sp. nov. possess a similar ornamentation extended throughout the anterior margin of the plate, and *S. cimarensis* is characterized by having small, rounded, isolated depressions near the anterior margin of the plate with a net-like structure (Sánchez *et al.* 2018).

The only statistically significant differences were found in the total trunk length (TL) between *Setaphyes elenae* sp. nov. and *S. flaveolatus* (p = 0.00042), so we can conclude that these two morphologically similar species may be also distinguished by the total trunk length (Fig. 5A). Oppositely, *S. dentatus* and *S. elenae* sp. nov. overlap, and statistically significant differences were not found (p = 0.51153) (Fig. 5A). *Setaphyes flaveolatus* is the smallest of the tested species, with a total trunk length of 500– 600 µm, followed by *S. dentatus* and *S. elenae* sp. nov. with a total trunk length of 600–800 µm (Fig. 5A). The remaining analysed morphometric measurements were not significantly different between *S. elenae* sp. nov. and the aforementioned congeners (Fig. 5B–C).

Acknowledgements

We would like to thank Dr Ulf Jondelius from the Swedish Museum of Natural History (Stockholm) and Dr Fredrik Pleijel from the University of Gothenburg for organising the sampling expedition and taking the meiofaunal samples, and also to Nuria Rico Seijo for providing us the kinorhynch specimens for the present study. D. Cepeda was supported by a predoctoral fellowship of the Complutense University of Madrid (CT27/16-CT28/16).

References

Altenburger A. 2016. The neuromuscular system of *Pycnophyes kielensis* (Kinorhyncha: Allomalorhagida) investigated by confocal laser scanning microscopy. *EvoDevo* 7: 25. https://doi.org/10.1186/s13227-016-0062-6

Cepeda D., Sánchez N. & Pardos F. 2019. First extensive account of the phylum Kinorhyncha from Haiti and the Dominican Republic (Caribbean Sea), with the description of four new species. *Marine Biodiversity* 49*:* 2281–2309. https://doi.org/10.1007/s12526-019-00963-x

Curini-Galletti M., Artois T., Delogu V., De Smet W.H., Fontaneto D., Jondelius U., Leasi F., Martínez A., Meyer-Wachsmuth I., Nilsson K.S., Tongiorgi P., Worsaae K. & Todaro, M.A. 2012. Patterns of diversity in soft-bodied meiofauna: dispersal ability and body size matter. *PLoS ONE* 7: e33801. https://doi.org/10.1371/journal.pone.0033801

Fox J., Weisberg S., Price B., Adler D., Bates D., Baud-Bovy G., Bolker B., Ellison S., Firth D., Friendly M., Gorjanc G., Graves S., Heiberger R., Krivitsky P., Laboissiere R., Maechler M., Monette G., Murdoch D., Nilsson H., Ogle D., Ripley B., Venables W., Walker S., Winsemius D., Zeileis A. & R Core Team. 2019. Package 'car'. Ver. 3.0-5. https://r-forge.r-project.org/projects/car/

Gerlach S.A. 1969. *Cateria submersa* sp. n., ein cryptorhager Kinorhynch aus dem sublitoralen Mesopsammal der Nordsee. *Veröffenlichungen des Instituts für Meeresforschung in Bremerhaven* 12: 161–168.

Higgins R.P. 1988. Kinorhyncha. *In*: Higgins R.P. & Thiel H. (eds) *Introduction to the Study of Meiofauna*: 328–331. Smithsonian Institution Press, Washington D.C.

Huys R. & Coomans A. 1989. *Echinoderes higginsi* sp.n. (Kinorhyncha, Cyclorhagida) from the southern North Sea with a key to the genus *Echinoderes* Claparède. *Zoologica Scripta*: 18: 211–221. https://doi.org/10.1111/j.1463-6409.1989.tb00446.x

McIntyre A.D. 1962. The class Kinorhyncha (Echinoderida) in British waters. *Journal of the Marine Biological Association of the United Kingdom* 42: 503–509. https://doi.org/10.1017/S0025315400054217

McIntyre, A.D. 1964. Meiobenthos of sub-littoral muds. *Journal of the Marine Biological Association of the United Kingdom* 44 (3): 665–674. https://doi.org/10.1017/S0025315400027843

Mora C., Tittensor D.P., Adl S., Simpson A.G.B. & Worm B. 2011. How many species are there on Earth and in the Ocean? *PLoS Biology* 9: e1001127. https://doi.org/10.1371/journal.pbio.1001127

Neuhaus B. 2013. Kinorhyncha (= Echinodera). *In*: Schmidt-Rhaesa A. (ed.) *Handbook of Zoology. Gastrotricha, Cycloneuralia and Gnathifera. Volume 1: Nematomorpha, Priapulida, Kinorhyncha, Loricifera*: 1–69. De Gruyter, Göttingen. https://doi.org/10.1515/9783110272536

Neuhaus B., Pardos F. & Sørensen M.V. 2013. Redescription, morphology and biogeography of *Centroderes spinosus* (Reinhard, 1881) (Kinorhyncha, Cyclorhagida) from Europe. *Cahiers de Biologie Marine* 54: 109–131. https://doi.org/10.21411/CBM.A.8E3FD0CA

Nyholm K.G. 1947. Studies in the Echinoderida. *Arkiv för Zoologi* 39: 1–36.

Reinhard W. 1881. Über *Echinoderes* und *Desmoscolex* der Umgebung von Odessa. *Zoologischer Anzeiger* 4: 588–592.

Rodhe J. 1996. On the dynamics of the large-scale circulation of the Skagerrak. *Journal of Sea Research* 35: 9–21. https://doi.org/10.1016/S1385-1101(96)90731-5

Rosenberg R., Cato I., Förlin L., Grip K. & Rodhe J. 1996. Marine environment quality assessment of the Skagerrak-Kattegat. *Journal of Sea Research* 35: 1–8. https://doi.org/10.1016/S1385-1101(96)90730-3

Sánchez N., Herranz M., Benito J. & Pardos F. 2012. Kinorhyncha from the Iberian Peninsula: new data from the first intensive sampling campaigns. *Zootaxa* 3402: 24–44. https://doi.org/10.11646/zootaxa.3402.1.2

Sánchez N., Yamasaki H., Pardos F., Sørensen M.V. & Martínez A. 2016. Morphology disentangles the systematics of a ubiquitous but elusive meiofaunal group (Kinorhyncha: Pycnophyidae). *Cladistics* 32: 479–505. https://doi.org/10.1111/cla.12143

Sánchez N., García-Herrero A., García-Gómez G. & Pardos F. 2018. A new species of the recently established genus *Setaphyes* (Kinorhyncha, Allomalorhagida) from the Mediterranean with an identification key. *Marine Biodiversity* 48 (1): 249–258. https://doi.org/10.1007/s12526-017-0651-1

Sørensen M.V. & Grzelak K. 2018. New mud dragons from Svalbard: three new species of *Cristaphyes* and the first Arctic species of *Pycnophyes* (Kinorhyncha: Allomalorhagida: Pycnophyidae). *PeerJ* 28: e5653. https://doi.org/10.7717/peerj.5653

Sørensen M.V. & Pardos F. 2008. Kinorhynch systematics and biology – an introduction to the study of kinorhynchs, inclusive identification keys to the genera. *Meiofauna Marina* 16: 21–73.

Sørensen M.V., Heiner I. & Hansen J.G. 2009. A comparative morphological study of the kinorhynch genera *Antygomonas* and *Semnoderes* (Kinorhyncha, Cyclorhagida). *Helgoland Marine Research* 63: 129–147. https://doi.org/10.1007/s10152-008-0132-9

Sørensen M.V., Rho H.S., Min W.G., Kim D. & Chang S.Y. 2013. Occurrence of the newly described kinorhynch genus *Meristoderes* (Cyclorhagida: Echinoderidae) in Korea, with the description of four new species. *Helgoland Marine Research* 67 (2): 291–319. https://doi.org/10.1007/s10152-012-0323-2

Weering T.C.E., Berger G.W. & Kalf J. 1987. Recent sediment accumulation in the Skagerrak, Northeastern North Sea. *Netherlands Journal of Sea Research* 21: 177–189. https://doi.org/10.1016/0077-7579(87)90011-1

Weering T.C.E., Rumohr J. & Liebezeit G. 1993. Holocene sedimentation in the Skagerrak: a review. *Marine Geology* 111: 379–391. https://doi.org/10.1016/0025-3227(93)90142I

Zelinka C. 1928. *Monographie der Echinodera.* Engelmann, Leipzig.

Manuscript received: 4 December 2019
Manuscript accepted: 16 March 2020
Published on: 29 April 2020
Topic editor: Rudy Jocqué
Desk editor: Pepe Fernández

Zoological Journal of the Linnean Society, 2019, **187**, 1041–1060. With 8 figures.

Allometric growth in meiofaunal invertebrates: do all kinorhynchs show homogeneous trends?

DIEGO CEPEDA*, DAVID ÁLAMO, NURIA SÁNCHEZ and FERNANDO PARDOS

Department of Biodiversity, Ecology and Evolution, Faculty of Biological Sciences, Complutense University, José Antonio Novais Street, 12, Madrid 28040, Spain

Received 10 January 2019; revised 23 May 2019; accepted for publication 2 August 2019

Allometry determines relevant modifications in metazoan morphology and biology and is affected by many different factors, such as ontogenetic constraints and natural selection. A linear mixed model approach and reduced major axis regression were used to explore evolutionary interspecific allometric trends between the total trunk length and the lengths of the segments and spines in the phylum Kinorhyncha at three taxonomic levels: the whole phylum, the class and the family. Statistically significant results were found in all the trunk segments, meaning that these body units grow proportionally correlated with the body, contrary to the results obtained for the spines. Developmental and morphophysiological constraints could lead to negative allometry in the first and last segments, because these body regions in kinorhynchs are essential to the implementation of some of the main biological functions, such as feeding and locomotion. The differential arrangement of cuticular appendages between the taxonomic groups considered seems to cause different evolutionary trends, because positive allometry may appear if a segment requires more space to accommodate a large number of organs and appendages, and vice versa. The presence of sexual dimorphism could also define positive allometry of a segment, owing to the need to harbour the sexually dimorphic appendages and their associated structures.

ADDITIONAL KEYWORDS : biodiversity – ecology – evolutionary trends – growth – morphology – morphometrics.

INTRODUCTION

The shape of animals varies by changes in the proportions of their body regions and structures relative to body dimensions as a whole (Shingleton, 2010; Anzai *et al.*, 2017). These variations reflect relevant modifications of animal function, biology and life-history traits (Calder, 1984; Schmidt-Nielsen, 1984; Banavar *et al.*, 2013). Usually, the growth of a body part covaries with that of another body region or the entire body through exponential scaling, which is known as allometry (Huxley & Tessier, 1936; Gayon, 2000). Allometric relationships are expressed mathematically by the following formula: $Y = a \times X^b$, where Y represents a body part whose allometry is of interest, X represents another body region or the body as a whole that is used as reference for comparison, and a and b are constants (Huxley, 1924, 1932). Huxley (1924) and Huxley & Tessier (1936) recognized that many scaling relationships, when plotted on a logarithmic scale, become linear and are consequently easier to interpret: $\log(Y) = \log(a) + b \times \log(X)$, where $\log(a)$ represents the intercept and b the slope of the line. The slope, also called the allometric coefficient, defines negative allometry if $0 < b < 1$, isometry if $b \approx 1$ and positive allometry if $b > 1$ (Huxley, 1932; White & Gould, 1965). The structure of interest will proportionally grow faster, more slowly or at the same speed as the structure of reference when positive allometry, negative allometry or isometry is present, respectively (Huxley, 1932).

Three types of allometry are usually considered: ontogenetic, static and evolutionary (Cheverud, 1970; Pélabon *et al.*, 2014). Ontogenetic allometry analyses changes in the proportional growth between a body structure of interest and the body as a whole during the development of an individual (*e.g.* Shea, 1985; Garland & Else, 1987), whereas static allometry defines the correlation in growth of a body part between individuals belonging to a population or species at identical developmental stages (*e.g.* Pélabon *et al.*, 2013; Freidline *et al.*, 2015), and evolutionary allometry is the study of the correlated rates of growth between the

*Corresponding author. E-mail: diegocepeda@ucm.es

means of populations or species (*e.g.* Anzai *et al.*, 2017; Bidau & Martínez, 2018). Variation in selection pressures and genetic constraints usually configure the evolutionary allometric relationships between body regions (Tidière *et al.*, 2017). If evolutionary pressures influence body size, the correlated growth relationships that the body maintains with the remaining body parts constrain the direction of phenotypic evolution, meaning that these body regions will evolve in the same way as the allometry of the ancestral population (Lande, 1979, 1985). Conversely, if selection pressures affect the size of a body part, the allometric relationship with body size could increase or decrease compared with the allometry of the ancestral population (Zeng, 1988; Voje *et al.*, 2014). A third scenario may occur when a non-linear increase or decrease in the selection of a trait size with increasing body size produces a non-linear evolutionary allometry (Higginson *et al.*, 2015).

Kinorhyncha encompasses a group of exclusively marine, benthic, free-living, meiofaunal species, with an elongated body divided into an introvert, a neck and a trunk (Sørensen & Pardos, 2008). The trunk is composed of 11 segments, both externally and internally divided into cuticular plates, cuticular appendages, muscles, gland cells, sensory cells and the central nervous system (Neuhaus, 2013). The most remarkable kinorhynch cuticular appendages are tubes, spines and setae, whose function still remains unknown, although they are attributed a possible relationship with secretory functions and/or reception of sensory stimuli (Zelinka, 1928; GaOrdóñez *et al.*, 2000; Neuhaus, 2013). Two types of spines are usually recognized: acicular and cuspidate. Acicular spines are articulated, elongated spines with pointed tips, whereas cuspidate spines are articulated, hirsute, bottle-like spines, with a widened base and a tapered distal portion bearing a terminal pore (Higgins, 1990; Sørensen & Pardos, 2008; Neuhaus, 2013). Traditionally, all original descriptions of new kinorhynch species have been accompanied by standard measurements of the body trunk, body segments and cuticular appendages (*e.g.* Higgins, 1977b; Sánchez *et al.*, 2013; Neuhaus *et al.*, 2014; Sørensen *et al.*, 2016) carried out by a few specialists, which minimizes bias and error when taking the measurements. Thus, kinorhynchs are an ideal model for the study of allometric relationships, owing to their conserved morphology and the high standardization of metric data from descriptions of new taxa.

The main aim of the present study was to analyse kinorhynch evolutionary allometry of body segments and spines in a large collection of species spanning the full range of sizes and habitats of both extant classes, Cyclorhagida and Allomalorhagida. This work is the first example of this type of study for the phylum Kinorhyncha.

MATERIAL AND METHODS

Data collection

A dataset of 160 kinorhynch species belonging to both extant classes, Cyclorhagida (N = 101) and Allomalorhagida (N = 59), was constructed (see Supporting Information, Data S1). The sample encompasses representative species of four families [cyclorhagid families Centroderidae (N = 10) and Echinoderidae (N = 91); allomalorhagid families Neocentrophyidae (N = 7) and Pycnophyidae (N = 52)] and 16 genera distributed worldwide, from shallow waters to deep sea in all types of marine substrata. The remaining families and genera were discarded because of the low sample size and/or a lack of measures.

Kinorhynch cuticular appendages are given different names depending on their position on the body. The most frequent are the middorsal spines, the lateroventral spines and the lateral terminal spines (Sørensen & Pardos, 2008; Neuhaus, 2013). The mean total body length (TL), mean length of individual segments (S1– S11), mean length of middorsal spines of segments 4–8 (MDS4–MDS8), mean length of lateroventral spines of segments 6–9 (LVS6–LVS9) and mean length of lateral terminal spines (LTS) were recorded for every species from the literature concerning the original descriptions of the species or from the redescription when available (see Supporting Information, Data S1). We calculated the mean of the original data when it was not provided in the data source. We have selected those spines that are present in the middorsal position of segments 4–8 and in the lateroventral position of segments 6–9 because they are the most common throughout the analysed cyclorhagids (Neuhaus, 2013). Although sexual dimorphism exists in most kinorhynch species regarding the presence of certain cuticular appendages, no differences were considered in the present study between males and females because the total length and lengths of segments do not usually vary significantly between sexes, and the spines considered in the present study are not affected by dimorphism in the selected species (Neuhaus, 2013).

Middorsal and lateroventral spines are present only within Cyclorhagida, because allomalorhagids possess different types of cuticular appendages, such as tubes and setae, whereas the lateral terminal spines are present in all cyclorhagids and most of the extant allomalorhagids (Neuhaus, 2013; Sánchez *et al.*, 2016). The middorsal and lateroventral spines may appear on different segments along the trunk, from segment 1 to 11, but the great majority are located on segments 4–8 (middorsal) and 6–9 (lateroventral) (Neuhaus, 2013). Moreover, some of the species that we considered possess a midterminal spine (MTS), but we decided to exclude it from the analyses

because of the low sample size. Despite the highly standardized kinorhynch measurements, a few older studies followed other criteria for measurement (*e.g.* Zelinka, 1928; Omer-Cooper, 1957); therefore, here we considered only those studies in which body length was measured from the anterior edge of segment 1 to the tip of tergal extensions and segments lengths were measured from the edge of the anterior pachycyclus to the tip of the pectinate fringe. A graphical summary of the external morphology of the two extant kinorhynch classes, with their main cuticular appendages used in the present study, is shown in Figure 1. All the variables considered were $\log_{10}$-transformed to perform the allometric analyses and normalize the data (see Supporting Information, Data S1).

Statistical analysis

Allometric studies were conducted separately at different taxonomic levels (phylum, class and family). A series of linear mixed models (LMMs) were performed in order to control the phylogenetic dependence of the considered species, using the *nlme* package (Pinheiro *et al.*, 2017) in the R software environment. Linear mixed models allow both fixed and random effects and are particularly useful

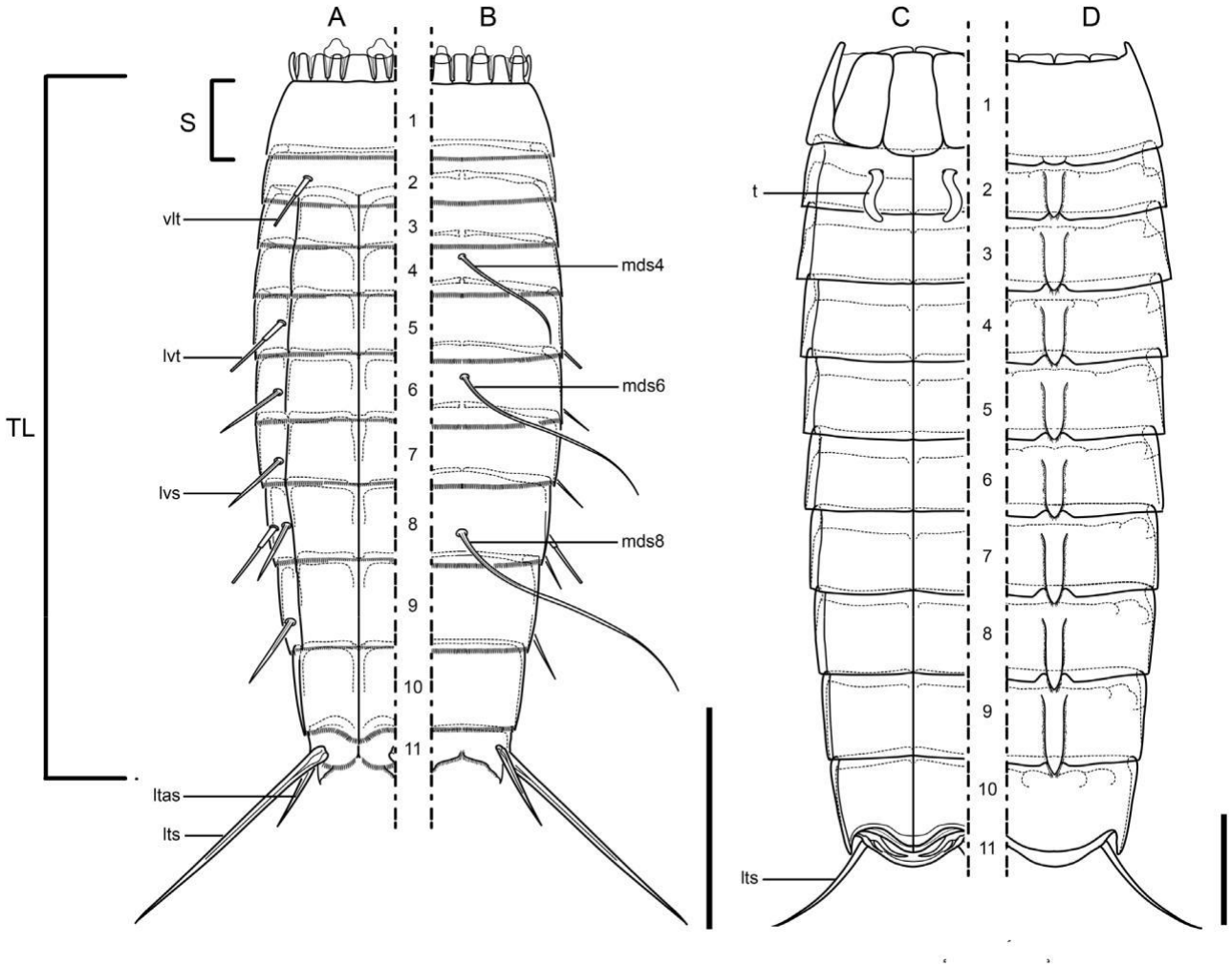

Figure 1. Line art illustrations of generalized external cuticular morphology of both extant kinorhynch classes, Cyclorhagida and Allomalorhagida, showing the morphological features studied in the present paper. A, ventral overview of left half of Cyclorhagida. B, dorsal overview of right half of Cyclorhagida. C, ventral overview of left half of Allomalorhagida. D, dorsal overview of right half of Allomalorhagida. Scale bars: 100 μm. Abbreviations: mds4, middorsal spine of segment 4; mds6, middorsal spine of segment 6; mds8, middorsal spine of segment 8; ltas, lateral terminal accessory spine; lts, lateral terminal spine; lvs, lateroventral spine; lvt, lateroventral tube; S, segment length; t, male sexually dimorphic ventromedial tube; TL, total trunk length; vlt, ventrolateral tube.

when there is no independence of the data, such as arises from a hierarchical structure (McCullagh & Nelder, 1989). Our data, obtained from species, are hierarchized by Linnean taxonomy; therefore, the observations are not independent, because within a particular taxonomic category the data are likely to be more similar. Although the best approach to eliminate the phylogenetic correlation of a dataset is phylogenetic generalized least squares, this tool requires a solid phylogenetic tree (Freckleton *et al.*, 2002; Tidière *et al.*, 2017). However, many parts of the kinorhynch phylogeny currently remain unresolved, making the application of phylogenetic generalized least squares unsuitable. Instead, LMMs use phylogenetic information extracted from Linnaean taxonomy, using a nested structure in the random-effect component of the model, which provides a good solution to the lack of solid and extensive molecular phylogenies (Winter, 2013; Holt & Jønsson, 2014). Results of LMMs were shown graphically using the *ggplot2* package (Wickham *et al.*, 2018) in the R software environment. Calculation of 95% confidence intervals using the *lmmfit* package (Maj, 2011) in the R environment allowed assessment of the significance of the regression slopes, considering isometry when $0.95 < b < 1.05$.

Taking into account that reduced major axis (RMA) regressions are the ideal tool when working with means and that a possible bias could have been introduced in the measurements (Smith, 2009), RMA regressions were also performed to analyse the aforementioned allometric relationships. Our data were obtained by different researchers, and sometimes obtaining an accurate measurement from a collection of specimens can be difficult; therefore, measurement error may have been introduced. Reduced major axis regression is a method specifically orientated to handle errors in the variables, minimizing the sum of the areas, with both vertical and horizontal distances of the data points from the resulting line, rather than the least squares sum of squared vertical distances (Harper, 2014). Phylogenetic RMA regression was not used for the same reasons explained above, and the phylogenetic correlation of the data was not tested by these analyses. As a result, we followed the results of the RMA regressions only when the independence of the data was tested by the LMMs (in other words, when the random factors of LMMs were practically zero and there was no need to carry out an LMM instead of a simple linear model). Reduced major axis regressions were performed using the *lme4* package (Bates *et al.*, 2018) in the R environment.

List of abbreviations

LMM	Linear mixed model
LTS	(Mean length of) lateral terminal spine
LVS6	(Length of) lateroventral spine of segment 6
LVS7	(Length of) lateroventral spine of segment 7
LVS8	(Length of) lateroventral spine of segment 8
LVS9	(Length of) lateroventral spine of segment 9
MDS4	(Length of) middorsal spine of segment 4
MDS5	(Length of) middorsal spine of segment 5
MDS6	(Length of) middorsal spine of segment 6
MDS7	(Length of) middorsal spine of segment 7
MDS8	(Length of) middorsal spine of segment 8
MTS	Midterminal spine
RMA	Reduced major axis regression
S1	(Length of) segment 1
S2	(Length of) segment 2
S3	(Length of) segment 3
S4	(Length of) segment 4
S5	(Length of) segment 5
S6	(Length of) segment 6
S7	(Length of) segment 7
S8	(Length of) segment 8
S9	(Length of) segment 9
S10	(Length of) segment 10
S11	(Length of) segment 11
TL	Total trunk length

RESULTS

Results of linear regression analysis of $\log_{10}$(segment length) vs. $\log_{10}$(total trunk length) are represented graphically for Kinorhyncha (Fig. 2), Cyclorhagida (Fig. 3), Allomalorhagida (Fig. 4), Echinoderidae (Fig. 5), Centroderidae (Fig. 6), Pycnophyidae (Fig. 7) and Neocentrophyidae (Fig. 8). The statistical results are shown in the Supporting Information (Data S2 and S3).

Evolutionary allometry of segment 1

A statistically significant, negative allometry was revealed by the allometric coefficient b = 0.0778 in the LMM analysis for the whole phylum, whereas this evolutionary allometry became positive in the RMA analysis, with b = 1.298. In both cases, the body structure used as reference (TL) showed a strong correlation with segment 1, as expressed by the coefficients of determination (r^2_{LMM} = 0.916, r^2_{RMA} = 0.907). The phylogenetic dependence also showed an important contribution to the mixed model, as shown by the percentage explained by random factors ($\%_{EXP}$) = 76.74.

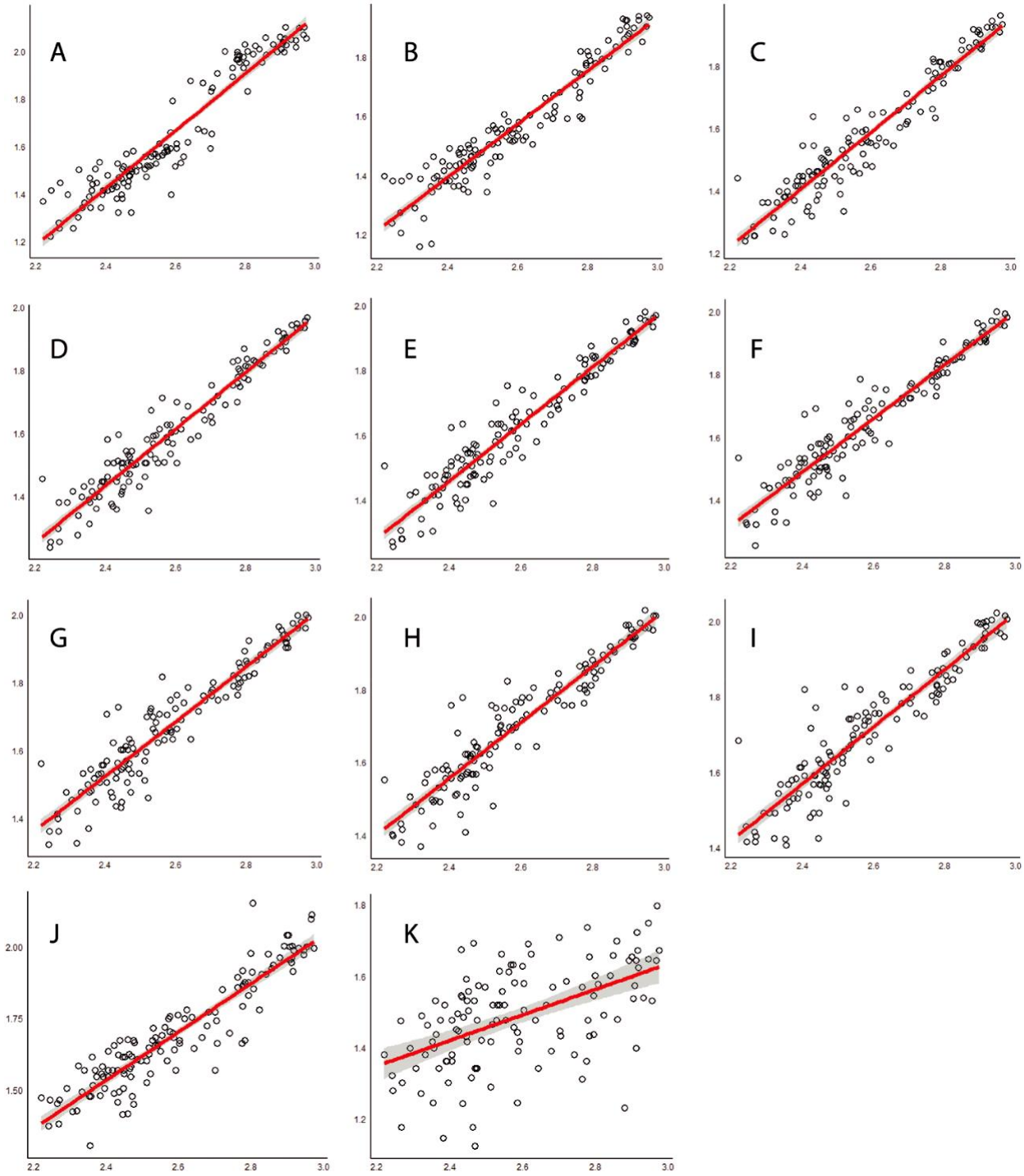

Figure 2. Results of linear regression analyses of Kinorhyncha. A, segment 1. B, segment 2. C, segment 3. D, segment 4. E, segment 5. F, segment 6. G, segment 7. H, segment 8. I, segment 9. J, segment 10. K, segment 11. The *x*-axis represents the independent variable (TL), and the *y*-axis represents the dependent variable (S1–S11); grey shading represents the confidence band.

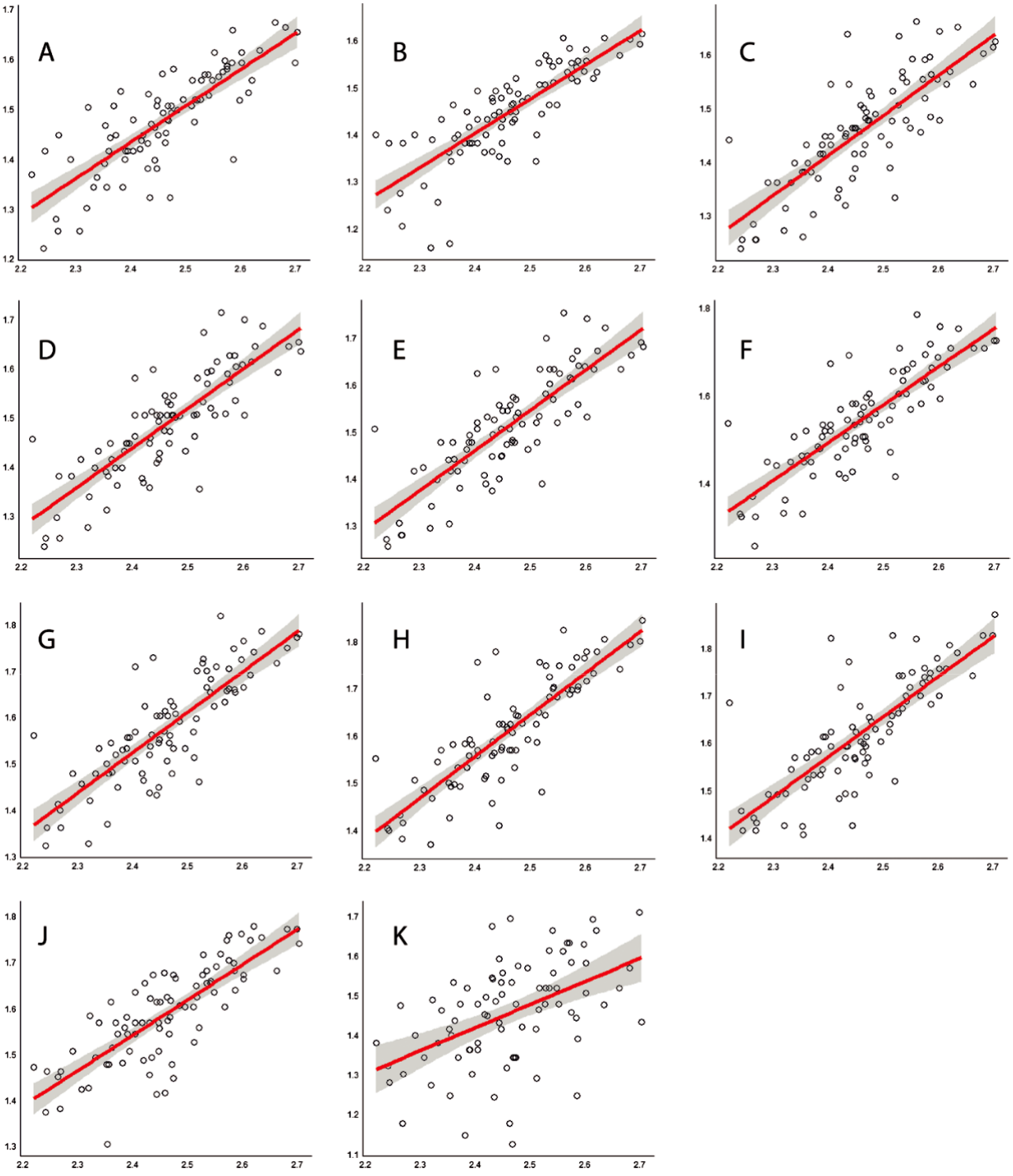

Figure 3. Results of linear regression analyses of Cyclorhagida. A, segment 1. B, segment 2. C, segment 3. D, segment 4. E, segment 5. F, segment 6. G, segment 7. H, segment 8. I, segment 9. J, segment 10. K, segment 11. The *x*-axis represents the independent variable (TL), and the *y*-axis represents the dependent variable (S1–S11); grey shading represents the confidence band.

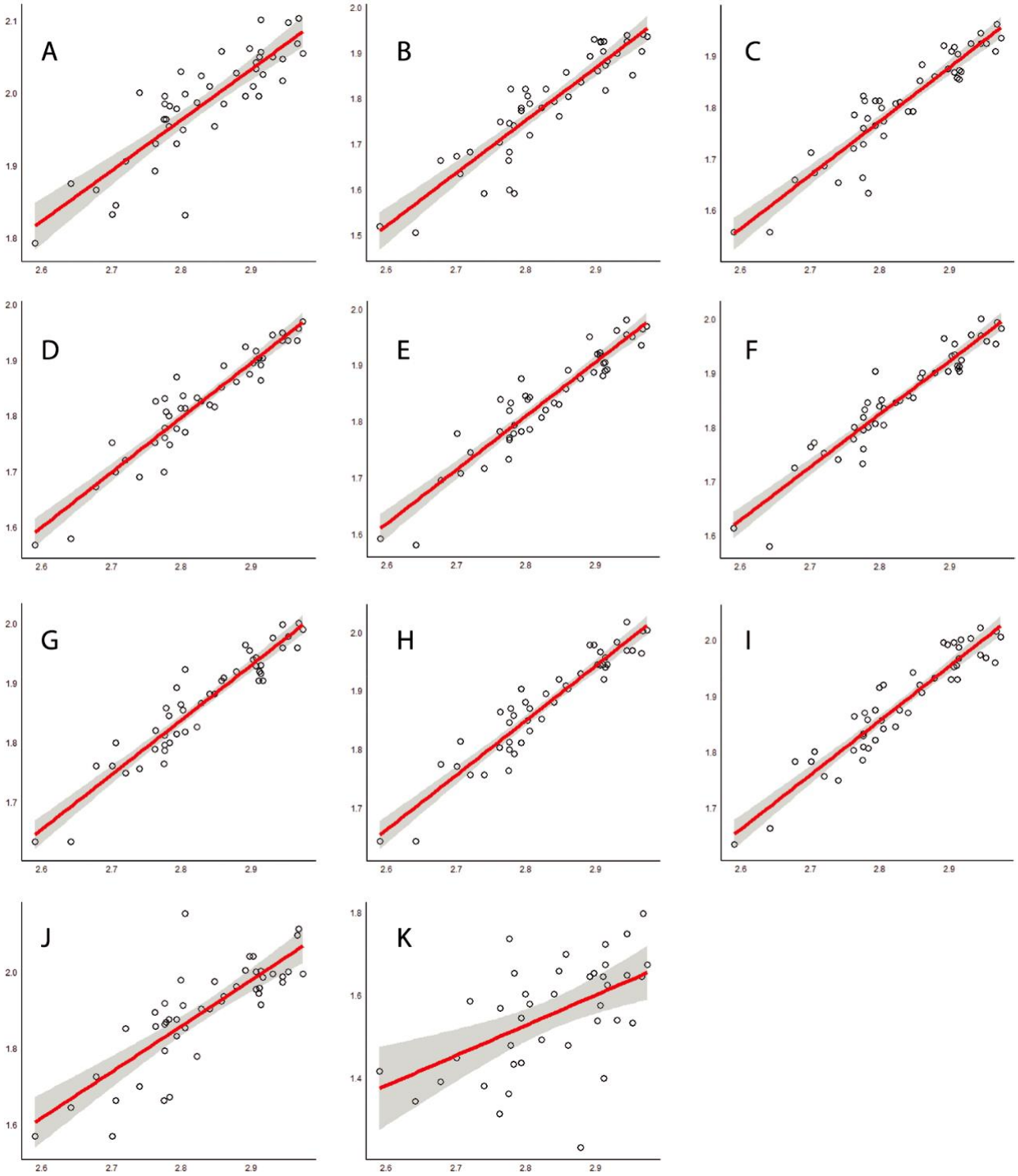

Figure 4. Results of linear regression analyses of Allomalorhagida. A, segment 1. B, segment 2. C, segment 3. D, segment 4. E, segment 5. F, segment 6. G, segment 7. H, segment 8. I, segment 9. J, segment 10. K, segment 11. The *x*-axis represents the independent variable (TL), and the *y*-axis represents the dependent variable (S1–S11); grey shading represents the confidence band.

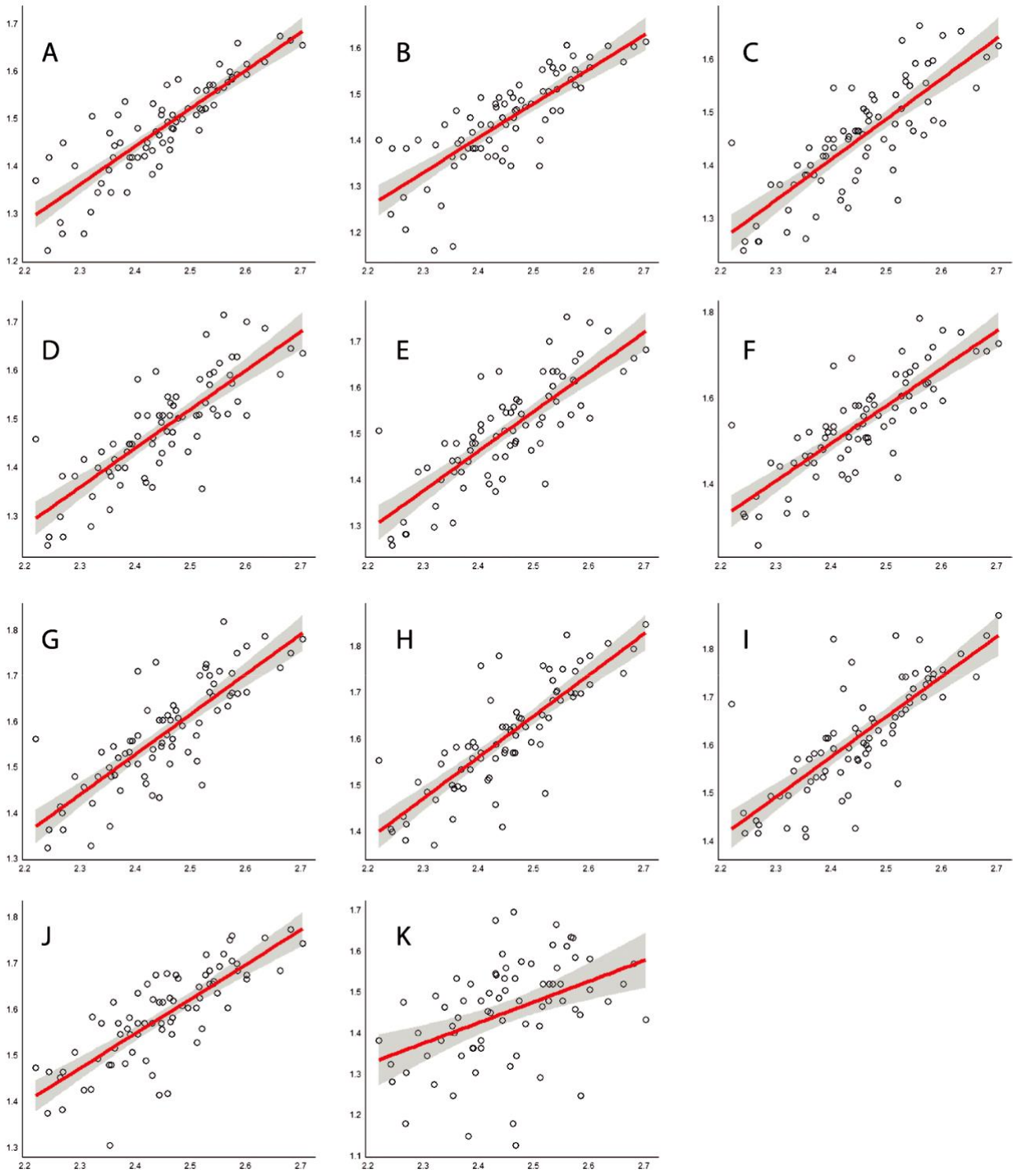

Figure 5. Results of linear regression analyses of Echinoderidae. A, segment 1. B, segment 2. C, segment 3. D, segment 4. E, segment 5. F, segment 6. G, segment 7. H, segment 8. I, segment 9. J, segment 10. K, segment 11. The *x*-axis represents the independent variable (TL), and the *y*-axis represents the dependent variable (S1–S11); grey shading represents the confidence band.

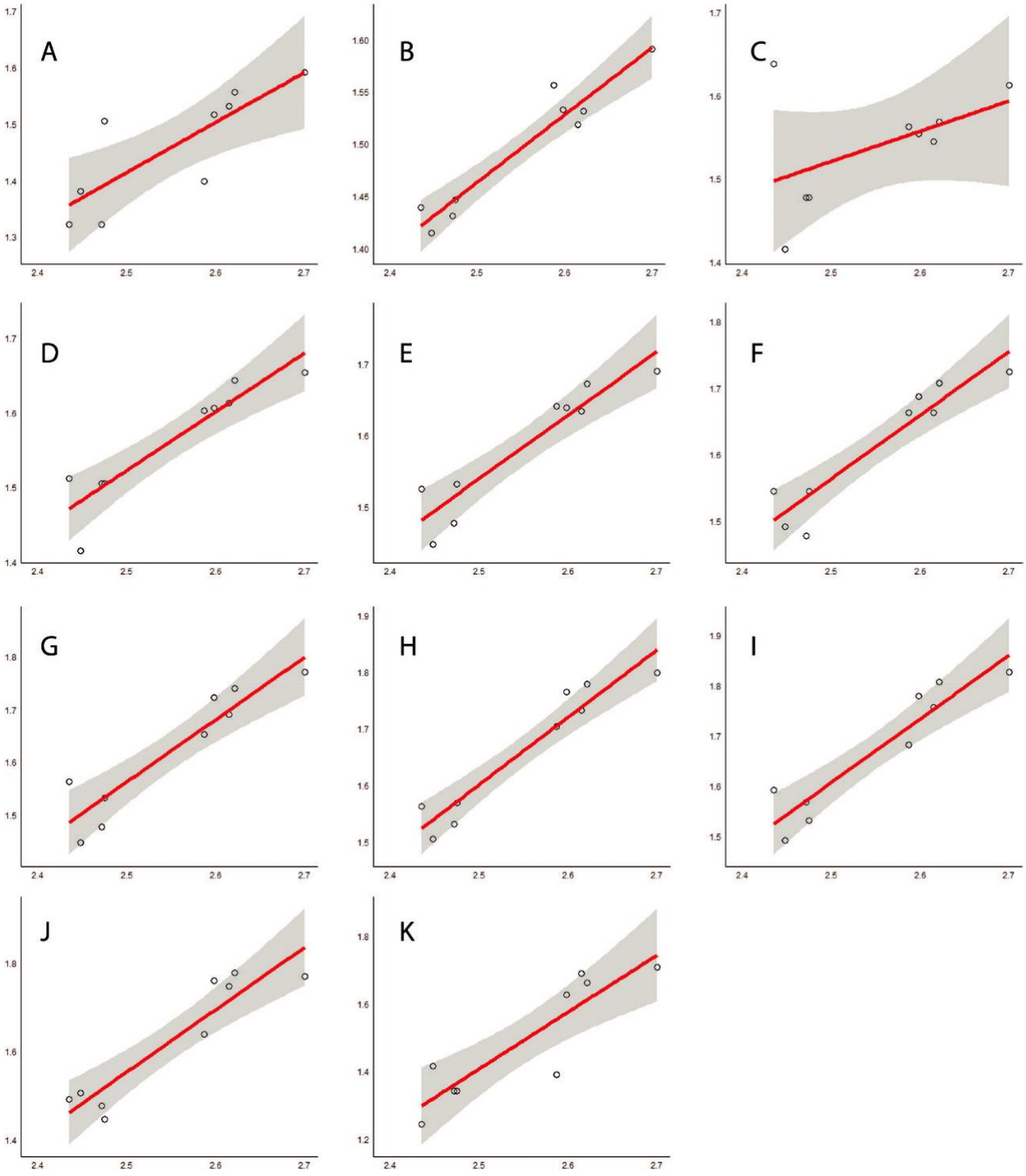

Figure 6. Results of linear regression analyses of Centroderidae. A, segment 1. B, segment 2. C, segment 3. D, segment 4. E, segment 5. F, segment 6. G, segment 7. H, segment 8. I, segment 9. J, segment 10. K, segment 11. The *x*-axis represents the independent variable (TL), and the *y*-axis represents the dependent variable (S1–S11); grey shading represents the confidence band.

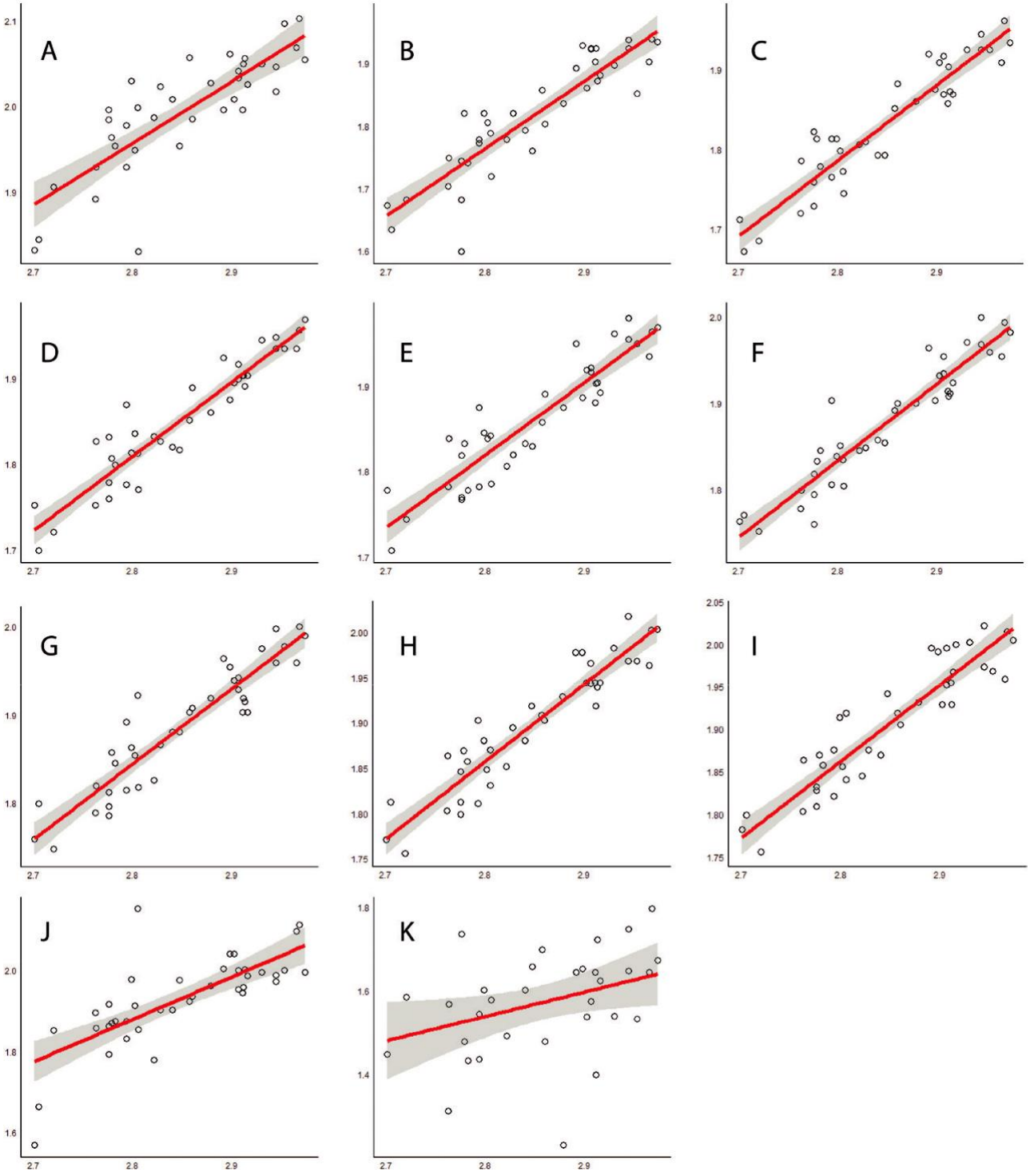

Figure 7. Results of linear regression analyses of Pycnophyidae. A, segment 1. B, segment 2. C, segment 3. D, segment 4. E, segment 5. F, segment 6. G, segment 7. H, segment 8. I, segment 9. J, segment 10. K, segment 11. The *x*-axis represents the independent variable (TL), and the *y*-axis represents the dependent variable (S1–S11); grey shading represents the confidence band.

When considering the classes separately, different results were obtained. For Cyclorhagida, a statistically significant, negative allometry was demonstrated (b = 0.725) in the LMM analysis and isometry (b = 0.981) in the RMA test. In both cases, TL also showed a relatively high correlation with segment 1 (r^2_{LMM} = 0.647, r^2_{RMA} = 0.651), albeit

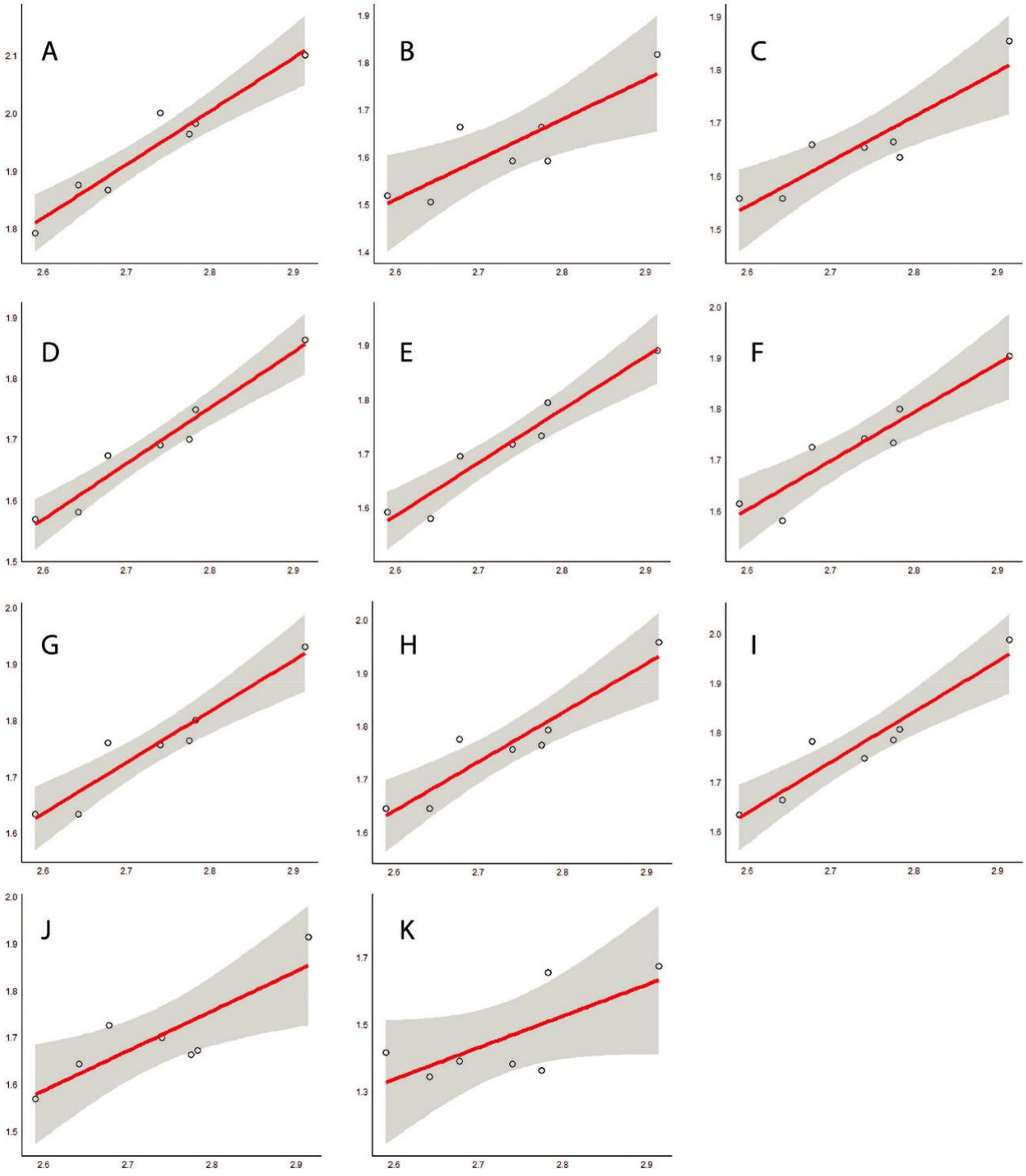

Figure 8. Results of linear regression analyses of Neocentrophyidae. A, segment 1. B, segment 2. C, segment 3. D, segment 4. E, segment 5. F, segment 6. G, segment 7. H, segment 8. I, segment 9. J, segment 10. K, segment 11. The *x*-axis represents the independent variable (TL), and the *y*-axis represents the dependent variable (S1–S11); grey shading represents the confidence band.

lower than that observed for the whole phylum. Random factors contributed greatly to the LMM, as showed by $\%_{EXP}$ = 58.55. For Allomalorhagida, both statistical tests yielded a negative, statistically significant allometry (b_{LMM} = 0.705, b_{RMA} = 0.833), with a relatively high relationship between S1 and TL (r^2_{LMM} = 0.560, r^2_{RMA} = 0.737) and

a relatively low contribution of the random factors of the LMM ($\%_{EXP}$ = 13.33).

Echinoderidae constitutes most of the Cyclorhagida sample size (N = 76), and the statistical tests performed individually for the family showed similar results. Centroderidae showed a statistically significant allometry, negative for the LMM analysis (b = 0.385) and positive for the RMA test (b = 1.235). The coefficients of determination showed similar values to those of Echinoderidae (r^2_{LMM} = 0.705, r^2_{RMA} = 0.658), and the contribution of random factors was significantly large ($\%_{EXP}$ = 79.67).

Pycnophyidae represents most of the allomalorhagid sample size (N = 52), and similar results to those of Allomalorhagida were obtained for Pycnophyidae. A statistically significant isometry was proved for Neocentrophyidae in both tests (b_{LMM} = 0.997, b_{RMA} = 0.967), with a high correlation between S1 and TL (r^2_{LMM} = 0.837, r^2_{RMA} = 0.932) and an important contribution for the LMM by the random effects ($\%_{EXP}$ = 71.11).

Evolutionary allometry of segment 2

The evolutionary allometry of segment 2 was negative (b = 0.863) in the LMM, whereas the RMA determined approximate isometry (b = 0.963) for the whole phylum. The trend towards isometry of segment 2 compared with segment 1 is remarkable, as shown by the upper value of the confidence intervals. The coefficients of determination demonstrated an important correlation between the growth of segment 2 and trunk growth as a whole (r^2_{LMM} = 0.848, r^2_{RMA} = 0.908), and the contribution of random effects to the mixed model was significantly lower than that for S1, as expressed by $\%_{EXP}$ = 32.93.

Cyclorhagida maintained the general phylum trend towards the S2 negative allometry (b = 0.726) in the LMM and the isometry (b = 0.980) in the RMA when analysing the classes separately, whereas Allomalorhagida possessed a positive allometry in both statistical tests (b_{LMM} = 1.105, b_{RMA} = 1.355). Similar coefficients of determination were obtained for both classes, demonstrating the high correlation between the growth of S2 and that of the trunk. The contribution of random effects to the LMM was substantial only in Allomalorhagida ($\%_{EXP}$ = 36.61) and was insignificant in Cyclorhagida.

The cyclorhagid family Echinoderidae showed negative allometry in the LMM (b = 0.748) and isometry in the RMA (b = 1.040), in agreement with the results obtained for the whole phylum and the class Cyclorhagida. Centroderidae yielded a strong, statistically significant, negative allometry in both statistical tests (b_{LMM} = 0.667, b_{RMA} = 0.676). Pycnophyidae was also in agreement with the positive allometry obtained for the class Allomalorhagida, whereas Neocentrophyidae displayed a negative allometry in the LMM (b = 0.848), although the contribution of random effects was practically nil and the upper value of the confidence interval was less than the values of the positive allometry. Moreover, the coefficients of determination were considerable for Echinoderidae (r^2_{LMM} = 0.513, r^2_{RMA} = 0.640), Centroderidae (r^2_{LMM} = 0.659, r^2_{RMA} = 0.919), Pycnophyidae (r^2_{LMM} = 0.655, r^2_{RMA} = 0.814) and the Neocentrophyidae RMA (r_2 = 0.733), but not so much for the Neocentrophyidae LMM (r_2 = 0.253). The contributions of random effects to the LMMs were relatively considerable only for Centroderidae ($\%_{EXP}$ = 29.62) and Pycnophyidae ($\%_{EXP}$ = 20.00).

Evolutionary allometries of segments 3–9

The allometric results obtained for segments 3–9 were homogeneous when compared with those of the distal segments. For the whole Kinorhyncha, the LMMs yielded statistically significant, negative allometries for all the segments considered, in agreement with the results shown in the RMAs, except for segments 3 and 4, which displayed isometric relationships. The coefficients of determination were high, implying that there was a strong evolutionary correlation between the length of segments and total length of the trunk. Moreover, the percentage of variance explained owing to random effects in the LMMs varied from 0 (e.g. segments 4 and 5) to nearly 30% (e.g. segment 3), indicating that phylogenetic relationship has an extremely variable influence on the allometric correlations.

For cyclorhagids, the LMMs yielded similar results to those of the phylum as a whole, although the upper values of the confidence intervals were closer to isometry, whereas the RMAs determined isometry (segment 3) or positive allometries (segments 4–9). For allomalorhagids, the general trend was maintained, although all the values were closer to isometry than those of Cyclorhagida and Kinorhyncha. Again, the coefficients of determination were high, defining a strong evolutionary relationship in the growth of the segments and the body as a whole. The random effects made an important contribution to the LMMs for Allomalorhagida, whereas in Cyclorhagida their influence was extremely variable.

Regarding the separate analysis of the families, Echinoderidae yielded similar results to those of the cyclorhagids, whereas Centroderidae gave different results depending on the segment. The length of segment 3 did not maintain a statistically significant correlation with the TL (P_{LMM} = 1.1932, P_{RMA} = 0.06), whereas negative

allometries were determined in segments 4 and 5, isometry in segment 6 and positive allometries in segments 7–9. Despite this apparent disparity, it seemed that the central segments of Centroderidae tended towards isometry, as determined by the confidence intervals. Concerning the allomalorhagid families, both Pycnophyidae and Neocentrophyidae showed similar results to those of Allomalorhagida and Kinorhyncha, with slightly negative allometries for all the segments considered. The coefficients of determination were again high, consecutively determining a strong correlation between the evolutionary allometries of the central segments and the TL. Random effects showed a relatively conspicuous contribution to the LMMs only for some segments of Pycnophyidae and were almost insignificant in the remaining families.

Evolutionary allometry of segment 10

A statistically significant, negative allometry was obtained for segment 10 in both LMM and RMA analysis (b_{LMM} = 0.844, b_{RMA} = 0.936). The allometric growth of S10 was highly dependent on TL, as expressed by the coefficients of determination (r^2_{LMM} = 0.779, r^2_{RMA} = 0.850). Additionally, random effects had a strong influence on the phylogenetic history ($\%_{EXP}$ = 39.63).

Cyclorhagida seemed to follow the phylum trend, showing a negative allometry in the LMM (b = 0.767) and an isometry in the RMA (b = 1.054), whereas Allomalorhagida yielded a positive allometry in both statistical tests (b_{LMM} = 1.173, b_{RMA} = 1.703). In both classes, a strong correlation between S10 and TL was demonstrated by the coefficients of determination. The random effects had a much stronger influence in Allomalorhagida ($\%_{EXP}$ = 40.33) than in Cyclorhagida ($\%_{EXP}$ = 14.66).

Similar results to those of class Cyclorhagida were obtained for Echinoderidae. Conversely, Centroderidae yielded a positive allometry of S10 in both LMM and RMA analysis (b_{LMM} = 1.414, b_{RMA} = 1.598). The coefficients of determination showed an important correlation in the growth of S10 with respect to the TL, contrary to the random effects. Pycnophyidae, in addition to Centroderidae, yielded a positive allometry in both LMM and RMA tests (b_{LMM} = 1.102, b_{RMA} = 1.679), with a significant correlation between S10 and TL found only in the RMA analysis (r^2_{LMM} = 0.365, r^2_{RMA} = 0.562), and a relatively low influence of random effects ($\%_{EXP}$ = 23.40). Neocentrophyidae showed a negative allometry in the LMM (b = 0.849) and a positive allometry in the RMA (b = 1.075), with a strong correlation between S10 and TL Demonstrated only in the RMA test (r^2_{LMM} = 0.227, r^2_{RMA} = 0.717) and a practically negligible phylogenetic influence in the LMM ($\%_{EXP}$ = 0.008).

Evolutionary allometry of segment 11

A statistically significant, strong, negative allometry was obtained for growth of S11 in both statistical tests (b_{LMM} = 0.481, b_{RMA} = 0.755) when considering the whole phylum dataset. However, the coefficients of determination demonstrated a low correlation between S11 and TL (r^2_{LMM} = 0.245, r^2_{RMA} = 0.279). Conversely, random effects had an important influence of the phylogeny in the LMM ($\%_{EXP}$ = 38.95).

In both Cyclorhagida and Allomalorhagida, a negative allometry was obtained for S11 in the LMMs (b = 0.579 and b = 0.730, respectively) but a positive allometry in the RMAs (b = 1.921 and b = 2.274, respectively). The coefficients of determination were again low, and random effects had a considerable phylogenetic influence only in Cyclorhagida.

Regarding the separate analysis of families, Echinoderidae and Pycnophyidae yielded similar results to those obtained for their respective class, whereas a statistically significant, strong, positive allometry was demonstrated for Centroderidae in both LMM and RMA tests (b_{LMM} = 1.463, b_{RMA} = 2.095). The coefficients of determination were again low, and random effects had a considerable influence only in the cyclorhagid families. The results obtained for Neocentrophyidae were statistically significant only for the RMA test (P = 0.03) and showed a strong, positive allometry (b = 1.693).

Evolutionary allometries of spines

No statistically significant allometric relationships were determined between most of the spines considered and the TL. In the rare cases when a statistically significant correlation was obtained, the coefficients of determination were very low (r_2 < 0.01), meaning that the TL was not allometrically correlated with the growth of the spines. Additionally, the lengths of the spines were also compared with the total lengths of the segments to which they belonged, but again no statistically significant allometric correlations were obtained. The allometric relationships regarding the lateral terminal spines were not statistically significant.

DISCUSSION

Evolutionary allometry of segment 1

The LMM analyses determined an important phylogenetic correlation of the data, meaning that the general negative allometry obtained for all the taxonomic ranks cannot be ignored in favour of the results of the RMA regressions. The only family that exhibited isometry in the growth of segment 1 was Neocentrophyidae, but the lower endpoint of the confidence interval was inside the range of negative allometry.

The first trunk segment defines an anatomical, functionally essential body region for the biology of the kinorhynch. It connects through the neck with the head, composed of a mouth cone and an introvert and accommodating organs such as a pharyngeal bulb and the brain. The head is a protruding, telescopic structure, with a complex muscular system that is attached, in part, to the cuticle of the first segment, and is responsible for feeding and locomotion (Sørensen & Pardos, 2008; Neuhaus, 2013). In some allomalorhagids, the dorsal and ventral placid retractors and the neck muscle, which allow closure of the neck when the introvert and the mouth cone are retracted inside the body, are attached basally to segment 1 (Altenburger, 2016). In both Cyclorhagida and Allomalorhagida, the pharyngeal bulb protractors and the introvert circular muscle retractors are also anchored to the posterior cuticle of segment 1 (Kristensen & Higgins, 1991; Herranz *et al.*, 2014; Altenburger, 2016). The dorsoventral muscles are specially developed in the first trunk segment, and the contraction of this segment causes an increase in the internal pressure to push the introvert out (Kristensen & Higgins, 1991; Herranz *et al.*, 2014; Altenburger, 2016). Moreover, there are additional lateral longitudinal muscles that connect the first two segments (Altenburger, 2016). Though there are some other muscles related to the introvert attached to more central trunk segments (Herranz *et al.*, 2014), most of them are associated with this one as explained above, and the head itself is directly connected to the first trunk segment. Additionally, the head and first segment are developed completely from the first postembryonic stages, with fully functional structures (Kozloff, 1972; Higgins, 1977a, b; Neuhaus, 1993, 1995, 2017; Sørensen *et al.*, 2000, 2010; Schmidt-Rhaesa & Rothe, 2006; Neuhaus & Kegel, 2015). Thus, there is a need for these structures to be developed completely from the early ontogenetic phases.

This early development of the anterior region of the body seems to be responsible for the generalized negative allometry observed in the first trunk segment. Despite its greater length, S1 would grow proportionally more slowly compared with the general trunk growth driven by morphophysiological restrictions, because an increase in its relative growth rate could cause dysfunction of the head in relationship to feeding, locomotion and nervous coordination, which are the main functions of the head. Given that this negative allometry was observed in all kinorhynch groups studied, the pattern is likely to reflect an ancestral developmental pathway shared by all kinorhynchs, independent of their body size and adaptations to different habitats. This hypothesis is also supported by the more pronounced negative trend observed in Allomalorhagida. Most of the allomalorhagid species are found at the upper limit of the possible body size for a kinorhynch to be functional (Giere, 2009). A greater body size could mean the impossibility of retaining a meiofaunal way of life, and this would impose a phylogenetic restriction on the growth of the first trunk segment.

Evolutionary allometry of segment 2

The analyses of the segment 2 allometric trends yielded more heterogeneous results than those obtained for the first trunk segment. For the whole phylum, an important phylogenetic correlation of the data was shown, and the generalized negative allometry yielded by the LMM must be taken into account. In a similar way to the first segment, the second segment is associated with the complex neuromuscular system of the head. As mentioned in the previous subsection, there is an extra pair of lateral longitudinal muscles posteriorly attached to the second segment (Altenburger, 2016), in addition to ~14–16 short longitudinal muscles, called introvert circular muscle retractors, whose posterior ends extend towards the pachycyclus of the second trunk segment (Kristensen & Higgins, 1991; Herranz *et al.*, 2014). This association with the head could explain the negative allometry of S2, in a similar manner to S1, as a need to maintain these structures completely developed from the early ontogenetic stages owing to their functional importance. Hence, the allometric trend of S2 would be imposed, in part, by that of S1, because both support much of the neuromuscular system attached to the head.

When performing separate analysis for the classes, Cyclorhagida lacked phylogenetic correlation in its data, and the RMA analysis yielded isometry, whereas Allomalorhagida exhibited phylogenetic correlation, and the LMM showed positive allometry. Thus, differential selection pressures affecting the growth of S2 might increase the generalized negative allometry of the phylum. In most of the cyclorhagid species included in this analysis, the second trunk segment may possess a pair of ventrolateral or lateroventral tubes in both sexes (Sørensen & Pardos, 2008). Tubes are usually short, thin-walled, flexible, tubule-like, articulated cuticular appendages, with a blunt tip and a

pore whose function still remains doubtful (Neuhaus, 2013). However, it has been hypothesized that these structures might be associated with sensory cells and/or secretive glandular cells (Zelinka, 1928; Higgins, 1983; GaOrdóñez *et al.*, 2008). Despite the lack of morphological studies in this regard, it can be assumed that the need to harbour these cuticular appendages and their associated secretive and/or sensorial structures might have caused an increase in the relative growth rate of the second trunk segment, leading to isometry.

Likewise, males of most of the Pycnophyidae species possess a pair of ventromedial tubes (Sørensen & Pardos, 2008; Sánchez *et al.*, 2016; Sánchez & Yamasaki, 2016). These tubes are proportionally thicker and stouter than those of the cyclorhagids and constitute a sexually dimorphic character (Neuhaus, 2013). Their function remains open, but given that only males possess these conspicuous appendages in most species, a possible sexual function may be attributed, and indeed, a process of sexual selection could be acting. A link between positive allometry and sexual selection has been proved when exaggerated traits are present in many different animal taxa, such as vertebrates and arthropods (Tomkins *et al.*, 2010; Calabuig *et al.*, 2013; Ramírez-Ponce *et al.*, 2017). This could explain the positive allometry observed for the class Allomalorhagida in the second trunk segment, although it cannot be assumed that the ventrolateral tubes of the males are subject to sexual selection. Empirical data separating sexes and a phylogenetic framework are essential to clarify the possible causes of this positive allometric trend of S2.

When performing separate analysis for the families, similar results were obtained to those for the corresponding classes. Nevertheless, the cyclorhagid family Centroderidae yielded a negative allometric trend for the second trunk segment despite the presence of proportionally longer ventrolateral tubes (Neuhaus *et al.*, 2014). In this family, the selection pressure towards retaining a negative allometric trend in the anterior segments seemed to be stronger and counteracted that of favouring the positive allometry because of the presence of ventrolateral tubes.

Evolutionary allometry of segments 3–9

The central segments showed little phylogenetic correlation of the data, and isometry or a slight negative allometry for the posterior-most segments were shown by the RMA regression analysis for the whole phylum. However, when performing separate analysis for the classes, Cyclorhagida showed isometry for segment 3 and positive allometries for segments 4–9, whereas Allomalorhagida exhibited a strong phylogenetic correlation of the data, and the LMM analysis yielded isometry for segments 3, 5, 6 and 9 and slight negative allometries for segments 4, 7 and 8. The results of the tests separated by families yielded similar results to those for the corresponding class.

Cyclorhagids, specifically Echinoderidae, usually possess a higher number of cuticular appendages (spines and tubes) on segments 4–9 (Sørensen & Pardos, 2008; Neuhaus, 2013). Spines have been suggested to be mechanoreceptors, associated with sensory cells (Zelinka, 1928; Nebelsick, 1991). The need to harbour these appendages might have driven the selective pressure to increase the proportional growth rate of segments 4–9 towards positive allometry. On the contrary, most of allomalorhagids lack these types of cuticular appendages, and when present, they are not arranged through the central trunk segments (Neuhaus, 2013; Sánchez *et al.*, 2016). Setae are the most common cuticular appendages in the allomalorhagid Pycnophyidae and Neocentrophyidae, and these structures are also associated with sensory and/or glandular cells (Zelinka, 1928; Neuhaus, 2013; Sánchez *et al.*, 2016). Setae are proportionally shorter and have a much weaker cuticular articulation support than the cyclorhagid spines and tubes, and there would not be much need to increase the proportional growth rates of the central trunk segments to carry the setae themselves. These differences could explain the unequal selective pressures observed between cyclorhagids and allomalorhagids.

Additionally, the excretory system of kinorhynchs is based on paired protonephridia located laterodorsally in segment 8, with openings to the outside sublaterally in segment 9 (Reinhard, 1885; Zelinka, 1908; 1928; Neuhaus, 1988; Kristensen & Hay-Schmidt, 1989). The need to develop a larger space to accommodate the excretory system could explain the positive allometry observed for segment 9 in Cyclorhagida and the isometry yielded in Allomalorhagida, despite this segment usually lacking cuticular appendages.

Evolutionary allometry of segment 10

The phylogenetic correlation of the whole phylum data was considerable, as reported by the LMM, which yielded a negative allometric trend for segment 10. This segment usually lacks cuticular appendages (Neuhaus, 2013). The absence of body structures that require extra space could mark an evolutionay trend towards negative allometry and explain the results observed.

When analysing the classes separately, both Cyclorhagida and Allomalorhagida showed an important phylogenetic correlation of the data. The LMM for Cyclorhagida yielded a negative allometry, following the general phylum trend, whereas the LMM

for Allomalorhagida resulted in positive allometry. Most of the Pycnophyidae included in the present analysis, which represent the majority of the class, possess conspicuous apodemes inside segment 10 and sometimes also in segment 9. Apodemes are paraventral cuticular thickenings, where dorsal and ventral longitudinal muscles attach basally (Altenburger, 2016; Sánchez *et al.*, 2016). Although these muscles are also present in the remaining segments, they are more developed in segment 10, because apodemes are absent in other regions of the trunk where the muscles attach basally only to the pachycyclus (Altenburger, 2016). Thus, the need to harbour the apodemes could explain the observed positive allometric trend of the allomalorhagid segment 10. Moreover, as previously mentioned, segment 9 can also possess conspicuous apodemes, and this segment showed isometry opposite to the other central segments, which exhibited negative allometry, reinforcing this hypothesis. Additionally, females of the allomalorhagid family Pycnophyidae possess a dorsal gut-opening muscle in segment 10, which is absent in males (Altenburger, 2016). In a similar way to the sexually dimorphic ventrolateral tubes of Pycnophyidae males, this character could determine the positive allometric trend observed in segment 10 of allomalorhagids, because only females possess the aforementioned muscle.

The analyses for the families separately were very similar to those for the class; hence, we follow the same hypothesis mentioned above to explain the results observed.

Evolutionary allometry of segment 11

The LMMs showed an important phylogenetic correlation of the data, with the exceptions of the class Allomalorhagida and the allomalorhagid family Neocentrophyidae, for which the results of the RMAs were considered. The whole phylum, the class Cyclorhagida and the cyclorhagid family Echinoderidae yielded the most negative allometries of all those obtained in the present study. As in the case of the anterior-most trunk segments, segment 11 is functionally essential for the biology of kinorhynchs. Usually, this segment bears a pair of wide, relatively long (compared with the remaining trunk cuticular appendages) lateral terminal spines (Sørensen & Pardos, 2008; Neuhaus, 2013). Unlike the other spines, lateral terminal spines possess a pair of terminal spine elevator muscles and a pair of terminal spine depressor muscles that are attached to the ventral side of the segment 11 pachycyclus (Kristensen & Higgins, 1991; Herranz *et al.*, 2014; Altenburger, 2016). In echinoderid Cyclorhagida, segment 11 possesses the dorsal cuticular plates extended to form the tergal extensions (Sørensen & Pardos, 2008; Neuhaus, 2013), and there are paired tergal extension muscles associated with the basal part of these extensions and anteriorly attached to the segment 11 pachycyclus (Herranz *et al.*, 2014). The lateral terminal spines start their development from the earlier juvenile stages (Higgins, 1974; Neuhaus, 2013, 2017; Neuhaus & Sørensen, 2013; Neuhaus *et al.*, 2014; Neuhaus & Kegel, 2015). In a similar way to the first trunk segments, the early development of the posterior body region could be responsible for the negative allometric trends observed for S11. Morphophysiological restrictions associated with the muscles that allow the movement of the tergal extensions and the lateral terminal spines would lead to a proportionally slower growth of S11 compared with the general body size.
&

However, some exceptions to the observed negative allometries must be mentioned. The class Allomalorhagida showed a strong positive allometric trend in S11. Generally, Allomalorhagida and, in particular, Pycnophyidae juveniles develop lateral terminal spines from the latest juvenile stages, contrary to cyclorhagids (Higgins, 1974, 1990; Brown, 1985; Neuhaus, 1993; 1995; Lemburg, 2002; Sørensen *et al.*, 2010). This difference could lead to the observed positive allometry of allomalorhagid S11, because the need to harbour the lateral terminal spines (and their associated structures) would appear in the last postembryonic stages, which would have to grow proportionally more rapidly in this class than in Cyclorhagida. Nevertheless, the available postembryonic information must be regarded carefully, because these studies were based exclusively on a limited number of preserved specimens and were not representative of the biodiversity of the whole phylum (Neuhaus, 2013). Additionally, the families Centroderidae and Neocentrophyidae also showed positive allometry in S11. These two families are characterized by having a midterminal spine (Zelinka, 1907; Higgins, 1969; Martorelli & Higgins, 2004; Sørensen & Pardos, 2008; Sørensen *et al.*, 2010; Neuhaus, 2013; Adrianov & Maiorova, 2016). Although the existence of muscles associated with this structure still remains unexplored, it is assumed that at least one muscle is connected to its base in order to control its movement, as in other kinorhynch families with a midterminal spine, such as Antygomonidae (Müller & Schmidt-Rhaesa, 2003). The need to harbour this structure, with the associated musculature, could lead to the positive allometric trends observed for S11 in the families Centroderidae and Neocentrophyidae.

Conclusion

1. Statistically significant evolutionary allometric trends were found in all the trunk segments compared with the total length of the trunk,

meaning that these body units grow proportionally, correlated with body growth.

2. The influence of the phylogeny in the data, explained as random effects in the LMM analyses, varied from 0% (*e.g.* segments 4 and 5 of Kinorhyncha) to almost 80% (*e.g.* segment 1 of Centroderidae), indicating that phylogenetic relationships have an extremely variable effect on the allometric trends.
3. Developmental constraints seem to define negative allometric trends if an increase in the length of a body structure might lead to disturbances and alterations that affect morphophysiological functioning and the way of life of kinorhynchs as components of meiofaunal communities. These developmental constraints seem to act most intensely in the distal segments of the body that define essential regions to carry out all the main kinorhynch functions.
4. Sexually dimorphic traits, especially if they are exaggerated and conspicuous in only one sex, could define positive allometric trends in the correlated body structures, because an increase in their size has a logical basis in adaptive terms.
5. Differences in the number and diversity of body structures in a segment might influence the emergence of positive allometric trends if a segment requires more space to accommodate a large number of organs and appendages.
6. Correlated growth between the spines and the body, or between the spines and the corresponding trunk segments, has not been observed at any taxonomic level. Thus, the development of these cuticular appendages might be influenced by environmental factors rather than by phylogenetic and evolutionary trends.
7. Sexually dimorphic differences could also explain the differential allometric trends observed between classes and families. Therefore, these conclusions must be drawn with some reservation, because separate analyses in males and females would need to be performed in order to determine the possible role of sexual dimorphism in the allometry of Kinorhyncha.

ACKNOWLEDGEMENTS

D.C. was supported by a predoctoral fellowship of the Complutense University of Madrid (CT27/16–CT28/16).

REFERENCES

Adrianov AV, **Maiorova AS. 2016.** *Condyloderes kurilensis* sp. nov. (Kinorhyncha: Cyclorhagida) – a new deep water species from the abyssal plain near the Kuril-Kamchatka Trench. *Russian Journal of Marine Biology* **42:** 11–19.

Altenburger A. 2016. The neuromuscular system of *Pycnophyes kielensis* (Kinorhyncha: Allomalorhagida) investigated by confocal laser scanning microscopy. *EvoDevo* **7**: 25.

Anzai H, **Oishi K**, **Kumagai H**, **Hosoi E**, **Nakanishi Y**, **Hirooka H. 2017.** Interspecific comparison of allometry between body weight and chest girth in domestic bovids. *Scientific Reports* **7:** 4817.

Banavar JR, **Cooke TJ**, **Rinaldo A**, **Maritan A. 2013.** Form, function, and evolution of living organisms. *Proceedings of the National Academy of Sciences of the United States of America* **111:** 3332–3337.

Bates D, **Maechler M**, **Bolker B**, **Walker S**, **Bojensen-Christensen RH**, **Singmann H**, **Green P. 2018.** Linear mixed-effects models using 'Eigen' and S4. R package version 3.1-114. Available at: https://github.com/lme4/lme4/ (last accessed date, 4 September 2019).

Bidau CJ, **Martínez PA. 2018.** Evolutionary negative allometry of orthopteran hind femur length is a general phenomenon. *Zoomorphology* **137:** 291–304.

Brown R. 1985. *Developmental and taxonomic studies of Sydney harbour Kinorhyncha*. Unpublished Ph.D. Thesis, Macquarie University.

Calabuig CP, **Green AJ**, **Muriel R**, **Katzenberger M**, **Patino-Martínez J**, **Moreira HM. 2013.** Allometry as evidence of sexual selection in monochromatic birds: the case of the Coscoroba swan (Anseriformes: Anatidae). *Zoologia (Curitiba)* **30:** 424–429.

Calder WA. 1984. *Size, function and life history*. Cambridge: Harvard University Press.

Cheverud JM. 1970. Relationships among ontogenetic, static, and evolutionary allometry. *American Journal of Physical Anthropology* **59:** 139–149.

Freckleton RP, **Harvey PH**, **Pagel M. 2002.** Phylogenetic analysis and comparative data: a test and review of the evidence. *The American Naturalist* **160:** 712–726.

Freidline SE, **Gunz P**, **Hublin JJ. 2015.** Ontogenetic and static allometry in the human face: contrasting Khoisan and Inuit. *American Journal of Physical Anthropology* **158:** 116–131.

G-Ordóñez D, **Pardos F**, **Benito J. 2000.** Cuticular structures and epidermal glands of *Echinoderes cantabricus* and *E. hispanicus* (Kinorhyncha, Cyclorhagida) with special reference to their taxonomic value. *Journal of Morphology* **246:** 161–178.

G-Ordóñez D, **Pardos F**, **Benito J. 2008.** Three new *Echinoderes* (Kinorhyncha, Cyclorhagida) from north Spain, with new evolutionary aspects in the genus. *Zoologischer Anzeiger – a Journal of Comparative Zoology* **247:** 95–111.

Garland T, **Else PL. 1987.** Seasonal, sexual, and individual variation in endurance and activity metabolism in lizards. *American Journal of Physiology* **252:** 439–449.

Gayon J. 2000. History of the concept of allometry. *American Zoologist* **40:** 748–758.

Giere O. 2009. *Meiobenthology. The Microscopic Motile Fauna of Aquatic Sediments*. Berlin: Springer.

Harper WV. 2014. Reduced major axis regression: teaching alternatives to least squares. In: Makar K, DeSousa B, Gould R, eds. *Sustainability in statistics education. Proceedings of the Ninth International Conference on Teaching Statistics (ICOTS9, July 2014), Flagstaff, Arizona, USA*. Voorburg: International Statistical Institute Press, 1–4.

Herranz M, **Boyle MJ**, **Pardos F**, **Neves RC. 2014.** Comparative myoanatomy of *Echinoderes* (Kinorhyncha): a comprehensive investigation by CLSM and 3D reconstruction. *Frontiers in Zoology* **11:** 31.

Higgins RP. 1969 . Indian Ocean Kinorhyncha: 2. Neocentrophyidae, a new homalorhagid family. *Proceedings of the Biological Society of Washington* **82:** 113–128.

Higgins RP. 1974. Chapter 11. Kinorhyncha. In: Giese AC, Pearce JS, eds. *Reproduction of marine invertebrates, volume I. Acoelomate and pseudocoelomate metazoans*. New York: Academic Press, 507–518.

Higgins RP. 1977a. Redescription of *Echinoderes dujardinii* (Kinorhyncha) with descriptions of closely related species. *Smithsonian Contributions to Zoology* **248:** 01–26.

Higgins RP. 1977b. Two new species of *Echinoderes* (Kinorhyncha) from South Carolina. *Transactions of the American Microscopical Society* **96:** 340–354.

Higgins RP. 1983. The Atlantic barrier reef ecosystem at Carrie Bow Cay, Belize, II: Kinorhyncha. *Smithsonian Contributions to Marine Science* **18:** 1–131.

Higgins RP. 1990. Zelinkaderidae, a new family of cyclorhagid Kinorhyncha. *Smithsonian Contributions to Zoology* **500:** 1–26.

Higginson DM, **Badyaev AV**, **Segraves KA**, **Pitnick S. 2015.** Causes of discordance between allometries at and above species level: an example with aquatic beetles. *The American Naturalist* **186:** 176–186.

Holt BJ, **Jønsson KA. 2014.** Reconciling hierarchical taxonomy with molecular phylogenies. *Systematic Biology* **63:** 1010–1027.

Huxley JS. 1924. Constant differential growth-ratios and their significance. *Nature* **114:** 895–896.

Huxley JS. 1932. *Problems of relative growth.* London: Methuen and Company Limited.

Huxley JS, **Tessier G. 1936.** Terminology of relative growth. *Nature* **137:** 780–781.

Kozloff EN. 1972. Some aspects of development in *Echinoderes* (Kinorhyncha). *Transactions of the American Microscopical Society* **91:** 119–130.

Kristensen RM, **Hay-Schmidt A. 1989.** The protonephridia of the arctic kinorhynch *Echinoderes aquilonius* (Cyclorhagida, Echinoderidae). *Acta Zoologica* **70:** 13–27.

Kristensen RM, **Higgins RP. 1991.** Chapter 10. Kinorhyncha. In: Harrison FW, Ruppert EE, eds. *Microscopic anatomy of invertebrates, volume 4: Aschelminthes.* New York: Wiley-Liss Press, 377–404.

Lande R. 1979. Quantitative genetic analysis of multivariate evolution applied to brain:body size allometry. *Evolution* **33:** 402–416.

Lande R. 1985. Genetic and evolutionary aspects of allometry. In: Jungers WL, ed. *Size and scaling in primate biology*. Boston: Springer-Verlag, 21–32.

Lemburg C. 2002. A new kinorhynch *Pycnophyes australensis* sp. n. (Kinorhyncha: Homalorhagida: Pycnophyidae) from Magnetic Island, Australia. *Zoologischer Anzeiger – a Journal of Comparative Zoology* **241:** 1–4.

Maj A. 2011. Lmmfit: goodness-of-fit-measures for linear mixed models with one-level-grouping. *R package version v.1.0*. Available at: https://github.com/mi2-warsaw/lmmfit/ (last accessed date, 4 September 2019).

Martorelli S, **Higgins RP. 2004.** Kinorhyncha from the stomach of the shrimp *Pleoticus muelleri* (Bate, 1888) from Comodoro Rivadavia, Argentina. *Zoologischer Anzeiger – a Journal of Comparative Zoology* **243:** 85–98.

McCullagh P, **Nelder JA. 1989.** *Generalized linear models*. London: Chapman & Hall/CRC Press.

Müller MCM, **Schmidt-Rhaesa A. 2003.** Reconstruction of the muscle system in *Antygomonas* sp. (Kinorhyncha, Cyclorhagida) by means of phalloidin labelling and cLSM. *Journal of Morphology* **256:** 103–110.

Nebelsick M. 1991. Ultrastructural investigations of three taxonomic characters in the trunk region of *Echinoderes capitatus* (Kinorhyncha, Cyclorhagida). *Zoologica Scripta* **21:** 335–345.

Neuhaus B. 1988. Ultrastructure of protonephridia in *Pycnophyes kielensis* (Kinorhyncha, Homalorhagida). *Zoomorphology* **108:** 245–253.

Neuhaus B. 1993. Postembryonic development of *Pycnophyes kielensis* and *P. dentatus* (Kinorhyncha) from the North Sea. *Microfauna Marina* **8:** 163–193.

Neuhaus B. 1995. Postembryonic development of *Paracentrophyes praedictus* (Homalorhagida): neoteny questionable among the Kinorhyncha. *Zoologica Scripta* **24:** 179–192.

Neuhaus B. 2013. 5. Kinorhyncha (=Echinodera). In: Schmidt-Rhaesa A, ed. *Handbook of zoology. Gastrotricha, Cycloneuralia and Gnathifera. Volume 1: Nematomorpha, Priapulida, Kinorhyncha, Loricifera.* Göttingen: De Gruyter, 181–348.

Neuhaus B. 2017. Redescription of *Tubulideres seminoli* Sørensen *et al*., 2007 and notes on *Wollunquaderes majkenae* Sørensen & Thormar, 2010 (Kinorhyncha, Cyclorhagida): morphology, postembryonic development, life cycle and new characters. *Zoologischer Anzeiger – a Journal of Comparative Zoology* **270:** 123–154.

Neuhaus B, **Kegel A. 2015.** Redescription of *Cateria gerlachi* (Kinorhyncha, Cyclorhagida) from Sri Lanka and of *C. styx* from Brazil, with notes on *C. gerlachi* from India and *C. styx* from Chile, and the ground pattern of the genus. *Zootaxa* **3965:** 1–77.

Neuhaus B, **Pardos F**, **Sørensen MV**, **Higgins RP. 2014.** New species of *Centroderes* (Kinorhyncha: Cyclorhagida) from the northwest Atlantic Ocean, life cycle and ground pattern of the genus. *Zootaxa* **3901:** 1–69.

Neuhaus B, **Sørensen MV. 2013.** Populations of *Campyloderes* sp. (Kinorhyncha, Cyclorhagida): one global species with significant morphological variation? *Zoologischer Anzeiger – a Journal of Comparative Zoology* **252:** 48–75.

Omer-Cooper J. 1957. Deux nouvelles espèces de Kinorhyncha en provenance de l'Afrique du Sud. *Bulletin Mensuel de la Société Linnéenne de Lyon* **26:** 213–216.

Pélabon C, **Bolstad GH**, **Egset CK**, **Cheverud JM**, **Pavlicev M**, **Rosenqvist G. 2013.** On the relationship between ontogenetic and static allometry. *The American Naturalist* **181:** 195–212.

Pélabon C, **Firmat C**, **Bolstad GH**, **Voje KL**, **Houle D**, **Cassara J**, **Hansen TF. 2014.** Evolution of morphological allometry. *Annals of the New York Academy of Sciences* **1320:** 58–75.

Pinheiro J, **Bates D**, **DebRoy S**, **Sarkar D**, **R Core Team**. **2017.** Nlme: linear and nonlinear mixed effects model. R package version 3.1-131. Available at: https://CRAN.R-project.org/package=nlme (last accessed date, 4 September 2019).

Ramírez-Ponce A, **Garfias-Lozano G**, **Contreras-Ramos A. 2017.** The nature of allometry in an exaggerated trait: the postocular flange in *Platyneuromus* Weele (Insecta: Megaloptera). *PLoS One* **12:** e0172388.

Reinhard W. 1885. Kinorhyncha (*Echinoderes*), leur structure anatomique et leur place dans le système. *Travaux de la Société des Naturalistes à l'Université Impériale de Kharkow* **19:** 205–305.

Sánchez N, **Rho HS**, **Min WG**, **Kim D**, **Sørensen MV. 2013.** Four new species of *Pycnophyes* (Kinorhyncha: Homalorhagida) from Korea and the East China Sea. *Scientia Marina* **77:** 353–380.

Sánchez N, **Yamasaki H. 2016.** Two new Pycnophyidae species (Kinorhyncha: Allomalorhagida) from Japan lacking ventral tubes in males. *Zoologischer Anzeiger – a Journal of Comparative Zoology* **265:** 80–89.

Sánchez N, **Yamasaki H**, **Pardos F**, **Sørensen MV**, **Martínez A. 2016.** Morphology disentangles the systematics of a ubiquitous but elusive meiofaunal group (Kinorhyncha: Pycnophyidae). *Cladistics* **32:** 479–505.

Schmidt-Nielsen K. 1984. *Why is animal size so important?* Cambridge: Cambridge University Press.

Schmidt-Rhaesa A, **Rothe BH. 2006.** Postembryonic development of dorsoventral and longitudinal musculature in *Pycnophyies kielensis* (Kirnohyncha, Homalorhagida). *Integrative and Comparative Biology* **46:** 144–150.

Shea BT. 1985. 9. Ontogenetic allometry and scaling. A discussion based on the growth and form of the skull in African apes. In: Jungers WL, ed. *Size and scaling in primate biology*. Boston: Springer-Verlag, 175–205.

Shingleton A. 2010. Allometry: the study of biological scaling. *Nature Education Knowledge* **3:** 2.

Smith RJ. 2009. Use and misuse of the reduced major axis for line-fitting. *American Journal of Physical Anthropology* **14:** 476–486.

Sørensen MV, **Accogli G**, **Hansen JG. 2010.** Postembryonic development of *Antygomonas incomitata* (Kinorhyncha: Cyclorhagida). *Journal of Morphology* **271:** 863–882.

Sørensen MV, **Herranz M**, **Landers SC. 2016.** A new species of *Echinoderes* (Kinorhyncha: Cyclorhagida) from the Gulf of Mexico, with the redescription of *Echinoderes bookhouti* Higgins, 1964. *Zoologischer Anzeiger – a Journal of Comparative Zoology* **265:** 48–68.

Sørensen MV, **Jørgensen A**, **Boesgaard TM. 2000.** A new *Echinoderes* (Kinorhyncha: Cyclorhagida) from a submarine cave in New South Wales, Australia. *Cahiers de Biologie Marine* **41:** 167–179.

Sørensen MV, **Pardos F. 2008.** Kinorhynch systematics and biology – an introduction to the study of kinorhynchs, inclusive identification keys to the genera. *Meiofauna Marina* **16:** 21–73.

Sørensen MV, **Rho HS**, **Kim D. 2010.** A new species of *Condyloderes* (Cyclorhagida, Kinorhyncha) from Korea. *Zoological Science* **27:** 234–242.

Tidière M, **Lemaître JF**, **Pélabon C**, **Gimenez O**, **Gaillard JM. 2017.** Evolutionary allometry reveals a shift in selection pressure on male horn size. *Journal of Evolutionary Biology* **30:** 1826–1835.

Tomkins JL, **LeBas NR**, **Witton MP**, **Martill DM**, **Humphries S. 2010.** Positive allometry and the prehistory of sexual selection. *The American Naturalist* **176**: 141-148.

Voje KL, **Hansen TF**, **Egset CK**, **Bolstad GH**, **Pélabon C. 2014.** Allometic constraints and the evolution of allometry. *Evolution* **68:** 866–885.

White JF, **Gould SJ. 1965.** Interpretation of the coefficient in the allometric equation. *The American Naturalist* **99:** 5–18.

Wickham H, **Chang W**, **Henry L**, **Pedersen TL**, **Takahashi K**, **Wilke C**, **R Core Team**. **2018.** Create elegant data visualisations using the grammar of graphics. R package version 3.1-216. New York: Springer-Verlag. Available at: https://ggplot2.tidyverse.org/ (last accessed date, 4 September 2019).

Winter B. 2013. Linear models and linear mixed effects models in R with linguistic applications. *ArXiv:1308.5499*. Available at: https://arxiv.org/abs/1308.5499 (last accessed date, 4 September 2019).

Zelinka K. 1907. Zur Kenntnis der Echinoderen. *Zoologischer Anzeiger – a Journal of Comparative Zoology* **32:** 120–136.

Zelinka K. 1908. Zur Anatomie der Echinoderen. *Zoologischer Anzeiger – a Journal of Comparative Zoology* **33:** 629–647.

Zelinka K. 1928. *Monographie der Echinodera.* Leipzig: Verlag von Wilhelm Engelmann.

Zeng ZB. 1988. Long-term correlated response, interpopulation covariation, and interspecific allometry. *Evolution* **42:** 363–374.

SUPPORTING INFORMATION

Additional Supporting Information may be found in the online version of this article at the publisher's web-site:

Data S1. Dataset of 160 kinorhynch species belonging to both extant classes, Cyclorhagida (N = 101) and Allomalorhagida (N = 59), with the data source, the original data and the $\log_{10}$-transformed measures that were considered for the study. Abbreviations: LTS, length of lateral terminal spines; LVS, lateroventral spine length (followed by number of corresponding segment); MDS, middorsal spine length (followed by number of corresponding segment); S, segment length (followed by number of corresponding segment); TL, total trunk length (see online at https://academic.oup.com/zoolinnean/article/187/4/1041/5601088#supplementary-data).

Data S2. Results of the linear mixed model (LMM) analyses of the evolutionary, allometric relationship between body segment length with respect to total trunk length (S~TL) in Kinorhyncha at phylum, class and family levels (Table 1) and the spine length with respect to total trunk length and the corresponding segment (Table 2). Abbreviations: *b*, allometric coefficient; 95% CI, 95% confidence intervals; *N*, sample size; *P*, *P*-value; r_2, coefficient of determination; *t*, *t*-value; $\%_{EXP}$, percentage explained by random factors.

Data S3. Results of the reduced major axis (RMA) regression analyses of the evolutionary, allometric relationship between body segment length with respect to total trunk length (S~TL) in Kinorhyncha at phylum, class and family levels. Abbreviations: *b*, allometric coefficient; 95% CI, 95% confidence intervals; *N*, sample size; *P*, *P*-value; r_2, coefficient of determination.

Data S2, Table 1. Results of the LMMs analyses of the evolutionary, allometric relationship between body segments' length with respect to total trunk length (S~TL) in Kinorhyncha at phylum, class and family levels. Abbreviations: *n*, sample size; *b*, allometric coefficient; 95%CI, 95% confidence intervals; *t*, t-value; *p*, p-value; r^2, coefficient of determination; $\%_{EXP}$, % explained by random factors.

Model	Taxon	*n*	*b*	95%CI	*t*	*p*	r^2	$\%_{EXP}$
S1~TL	Kinorhyncha	131	0.778	0.69-0.86	17.99	<0.00001	0.916	76.74
S2~TL		132	0.863	0.79-0.94	23.17	<0.00001	0.848	32.93
S3~TL		132	0.875	0.81-0.94	25.15	<0.00001	0.853	29.11
S4~TL		132	0.902	0.84-1.01	39.98	<0.00001	0.869	0.00
S5~TL		132	0.884	0.84-0.93	36.62	<0.00001	0.850	0.00
S6~TL		132	0.859	0.81-0.91	33.46	<0.00001	0.844	9.68
S7~TL		132	0.830	0.77-0.89	28.37	<0.00001	0.830	18.84
S8~TL		132	0.794	0.74-0.85	27.44	<0.00001	0.820	18.51
S9~TL		132	0.762	0.70-0.82	26.57	<0.00001	0.784	10.14
S10~TL		132	0.844	0.75-0.94	17.12	<0.00001	0.779	39.63
S11~TL		123	0.481	0.33-0.63	6.19	<0.00001	0.245	38.95
S1~TL	Cyclorhagida	85	0.725	0.62-0.83	14.16	<0.00001	0.647	58.55
S2~TL		85	0.726	0.61-0.84	12.58	<0.00001	0.540	0.003
S3~TL		85	0.746	0.62-0.87	11.82	<0.00001	0.510	0.002
S4~TL		85	0.803	/	13.37	<0.00001	0.571	0.002
S5~TL		85	0.860	0.73-0.99	13.06	<0.00001	0.561	0.002
S6~TL		85	0.869	0.74-1.00	13.32	<0.00001	0.571	0.008
S7~TL		85	0.870	0.74-1.00	13.02	<0.00001	0.567	18.51
S8~TL		85	0.885	/	14.01	<0.00001	0.595	0.005
S9~TL		85	0.843	/	11.92	<0.00001	0.517	0.002
S10~TL		85	0.767	0.64-0.89	11.96	<0.00001	0.522	14.66
S11~TL		83	0.579	0.36-0.80	5.28	<0.00001	0.235	46.80
S1~TL	Allomalorhagida	46	0.705	0.57-0.84	10.91	<0.00001	0.560	13.33
S2~TL		47	1.105	0.92-1.29	12.28	<0.00001	0.702	36.61
S3~TL		47	0.984	0.85-1.11	15.43	<0.00001	0.794	49.12
S4~TL		47	0.947	0.84-1.05	18.74	<0.00001	0.835	54.16
S5~TL		47	0.959	0.85-1.07	17.84	<0.00001	0.811	45.65
S6~TL		47	0.963	0.85-1.07	18.06	<0.00001	0.814	39.53
S7~TL		47	0.919	0.82-1.02	18.17	<0.00001	0.791	26.31
S8~TL		47	0.924	0.82-1.03	17.91	<0.00001	0.796	30.76
S9~TL		47	0.972	0.86-1.08	18.45	<0.00001	0.783	18.42
S10~TL		47	1.173	0.88-1.47	8.00	<0.00001	0.523	40.33
S11~TL		40	0.730	0.34-1.12	3.84	<0.00001	0.086	0.002
S1~TL	Echinoderidae	76	0.761	0.65-0.87	14.23	<0.00001	0.654	42.68

S2~TL		76	0.748	0.62-0.88	11.43	<0.00001	0.513	0.001
S3~TL		76	0.761	/	11.29	<0.00001	0.530	0.001
S4~TL		76	0.800	/	11.78	<0.00001	0.571	0.001
S5~TL		76	0.862	0.71-1.01	11.54	<0.00001	0.522	0.001
S6~TL		76	0.872	0.72-1.02	11.84	<0.00001	0.534	0.001
S7~TL		76	0.872	0.73-1.02	11.98	<0.00001	0.544	11.84
S8~TL		76	0.888	/	12.70	<0.00001	0.568	0.001
S9~TL		76	0.836	0.68-0.99	10.77	<0.00001	0.486	0.001
S10~TL		76	0.748	/	11.32	<0.00001	0.509	0.001
S11~TL		74	0.523	0.29-0.75	4.54	<0.00001	0.178	46.84
S1~TL	Centroderidae	9	0.385	0.09-0.69	3.17	0.0194	0.705	79.67
S2~TL		9	0.667	0.48-0.86	8.60	0.0001	0.659	29.62
S3~TL		9	0.363	0.01-0.97	1.46	0.1932	0.368	0.003
S4~TL		9	0.787	/	6.38	0.0007	0.526	0.001
S5~TL		9	0.890	/	7.16	0.0004	0.606	0.001
S6~TL		9	0.960	0.63-1.28	7.23	0.0004	0.622	0.005
S7~TL		9	1.183	0.77-1.61	6.71	0.0005	0.620	0.004
S8~TL		9	1.192	0.87-1.52	8.97	0.0001	0.733	0.005
S9~TL		9	1.267	/	7.20	0.0004	0.660	0.004
S10~TL		9	1.414	/	6.71	0.0005	0.646	0.003
S11~TL		9	1.463	0.57-2.35	4.03	0.0069	0.567	41.30
S1~TL	Pycnophyidae	39	0.728	0.56-0.89	8.98	<0.00001	0.479	15.56
S2~TL		40	1.089	0.91-1.27	12.40	<0.00001	0.655	20.00
S3~TL		40	0.999	0.88-1.12	16.48	<0.00001	0.763	28.57
S4~TL		40	0.906	0.80-1.01	16.87	<0.00001	0.768	33.33
S5~TL		40	0.900	0.77-1.02	14.81	<0.00001	0.723	17.57
S6~TL		40	0.901	0.79-1.01	11.84	<0.00001	0.770	23.33
S7~TL		40	0.855	0.74-0.97	15.39	<0.00001	0.716	10.00
S8~TL		40	0.859	0.75-0.97	16.28	<0.00001	0.739	13.79
S9~TL		40	0.900	/	15.09	<0.00001	0.707	0.001
S10~TL		40	1.102	0.77-1.43	6.83	<0.00001	0.365	23.40
S11~TL		33	0.508	0.01-1.07	1.84	<0.00001	0.032	18.44
S1~TL	Neocentrophyidae	7	0.997	0.78-1.22	14.48	0.0007	0.837	71.11
S2~TL		7	0.848	0.12-1.57	3.71	0.0341	0.253	0.005
S3~TL		7	0.847	0.29-1.40	4.86	0.0166	0.429	0.004
S4~TL		7	0.917	0.62-1.21	9.85	0.0022	0.771	0.012
S5~TL		7	0.982	0.61-1.36	8.36	0.0036	0.730	37.78
S6~TL		7	0.956	0.46-1.45	6.09	0.0089	0.588	20.00
S7~TL		7	0.906	/	7.10	0.0057	0.647	0.006
S8~TL		7	0.928	0.44-1.41	6.10	0.0088	0.582	0.005
S9~TL		7	1.021	0.54-1.50	6.82	0.0064	0.654	0.005

S10~TL		7	0.849	0.09-1.61	3.56	0.0378	0.227	0.008
S11~TL		7	0.938	/	2.27	0.1083	0.032	78.18

Data S2, Table 2. Results of the LMMs analyses of the evolutionary, allometric relationship between spines length with respect to total trunk length and corresponding segment length in Kinorhyncha at phylum, class and family levels.
Abbreviations: LTS, lateral terminal spine; LV, lateroventral spine (followed by number of corresponding segment); MD, middorsal spine (followed by number of corresponding segment); *n*, sample size; *b*, allometric coefficient; 95%CI, 95% confidence intervals; *t*, t-value; *p*, p-value; r^2, coefficient of determination; S, segment (followed by number of segment); TL, total trunk length; $\%_{EXP}$, % explained by random factors.

Model	**Taxon**	***n***	***b***	**95%CI**	***t***	***p***	r^2	$\%_{EXP}$
LTS~TL	Kinorhyncha	147	0.123	-0.20-0.45	0.76	0.4523	0.07	43.34
LTS~S11		116	0.053	-0.28-0.39	0.31	0.7538	0.08	45.52
MD4~ TL		89	0.083	-0.56-0.36	0.48	0.6716	0.01	29.66
MD4~ S4		77	0.013	-0.33-0.60	0.58	0.5635	0.02	28.57
MD5~ TL		50	0.269	-0.41-0.95	1.59	0.4310	0.02	34.88
MD5~ S5		43	0.797	0.30-1.29	3.26	0.0024	0.01	48.08
MD6~ TL		78	0.247	-0.28-0.77	0.94	0.3504	0.01	36.34
MD6~ S6		66	0.504	0.07-0.94	2.31	0.0245	0.01	44.31
MD7~ TL		48	0.145	/	0.438	0.6634	0.03	0.000
MD7~ S7		41	0.864	0.35-1.37	3.43	0.0016	0.02	43.71
MD8~ TL		74	0.045	-0.49-0.58	0.17	0.8672	0.02	36.67
MD8~ S8		62	0.362	-0.12-0.84	1.51	0.1376	0.01	45.79
LV6~ TL		73	0.478	0.13-0.83	2.73	0.0081	0.02	28.22
LV6~ S6		62	0.556	0.22-0.89	3.31	0.0016	0.02	26.50
LV7~ TL		75	0.459	0.10-0.82	2.56	0.0126	0.01	28.97
LV7~ S7		64	0.436	0.07-0.80	2.38	0.0207	<0.01	27.65
LV8~ TL		89	0.028	-0.34-0.39	0.15	0.8802	0.01	32.68
LV8~ S8		77	0.084	-0.28-0.45	0.46	0.6491	0.02	30.35
LV9~ TL		80	0.196	-0.17-0.56	1.07	0.2874	0.01	35.92
LV9~ S9		69	0.389	0.01-0.76	2.07	0.0425	0.01	33.76
LTS ~ TL	Cyclorhagida	99	-0.024	-0.50-0.46	-0.097	0.9225	0.02	44.39
LTS ~ S11		81	-0.009	-0.46-0.44	-0.040	0.9680	0.03	45.13
MD4~ TL		89	-0.099	-0.56-0.36	-0.425	0.6716	0.01	28.26
MD4~ S4		77	0.136	-0.33-0.60	0.58	0.5635	0.03	28.66
MD5~ TL		50	0.269	-0.41-0.95	0.80	0.4310	0.03	34.78
MD5~ S5		43	0.797	0.30-1.29	3.26	0.0024	0.02	48.08
MD6~ TL		78	0.247	-0.28-0.77	0.94	0.3504	0.02	36.33
MD6~ S6		66	0.504	0.07-0.94	2.31	0.0245	0.02	44.17
MD7~ TL		48	0.145	/	0.438	0.6634	0.05	0.003
MD7~ S7		41	0.864	0.35-1.37	3.43	0.0016	0.04	43.70

MD8~ TL		74	0.045	-0.49-0.58	0.17	0.8672	0.03	36.66
MD8~ S8		62	0.362	-0.12-0.84	1.51	0.1376	0.01	45.79
LV6~ TL		73	0.478	0.13-0.83	2.73	0.0081	0.02	28.22
LV6~ S6		62	0.556	0.22-0.89	3.31	0.0016	0.04	26.50
LV7~ TL		75	0.459	0.10-0.82	2.56	0.0126	0.02	28.97
LV7~ S7		64	0.436	0.07-0.80	2.38	0.0207	<0.01	27.65
LV8~ TL		89	0.028	-0.34-0.39	0.15	0.8802	0.02	32.68
LV8~ S8		77	0.084	-0.28-0.45	0.46	0.6491	0.04	30.62
LV9~ TL		80	0.196	-0.17-0.56	1.07	0.2874	0.02	36.17
LV9~ S9		69	0.389	0.01-0.76	2.07	0.0425	0.02	34.03
LTS ~ TL	Allomalorhagida	48	0.342	-0.46-1.15	0.86	0.3963	0.12	50.93
LTS ~ S11		35	-0.083	-0.48-0.31	-0.43	0.6716	0.16	64.45
LTS ~ TL	Echinoderidae	91	0.027	-0.48-0.53	0.11	0.9152	0.020	30.08
LTS ~ S11		74	0.030	-0.46-0.52	0.12	0.9016	0.020	31.81
MD4~ TL		80	-0.085	-0.60-0.43	-0.33	0.7420	0.001	28.26
MD4~ S4		68	0.196	-0.32-0.71	0.76	0.4479	0.02	31.73
MD5~ TL		41	0.424	-0.40-1.25	1.04	0.3054	0.01	40.04
MD5~ S5		34	0.891	0.33-1.46	3.22	0.0031	0.04	44.41
MD6~ TL		69	0.354	-0.23-0.94	1.20	0.2335	0.001	33.79
MD6~ S6		57	0.594	0.11-1.08	2.47	0.0169	0.02	35.19
MD7~ TL		39	0.400	-0.44-1.24	0.97	0.3395	0.04	16.27
MD7~ S7		32	1.038	0.46-1.62	3.65	0.0010	0.06	16.20
MD8~ TL		65	0.179	-0.42-0.78	0.60	0.5500	0.03	28.31
MD8~ S8		53	0.478	-0.06-1.01	1.80	0.0786	0.02	24.80
LV6~ TL		69	0.454	0.09-0.81	2.52	0.0142	0.01	23.31
LV6~ S6		58	0.543	0.19-0.89	3.12	0.0029	0.02	20.94
LV7~ TL		71	0.436	0.06-0.81	2.35	0.0219	<0.01	28.24
LV7~ S7		60	0.436	0.05-0.82	2.28	0.0264	0.01	25.46
LV8~ TL		80	0.030	-0.37-0.43	0.15	0.8802	0.03	32.57
LV8~ S8		68	0.093	-0.31-0.50	0.46	0.6475	0.04	29.65
LV9~ TL		71	0.178	-0.23-0.58	0.88	0.3833	<0.01	38.16
LV9~ S9		60	0.456	0.03-0.88	2.14	0.0365	0.01	33.33
LTS ~ TL	Centroderidae	8	0.434	-0.49-1.36	1.21	0.2810	0.696	84.55
LTS ~ S11		7	0.168	-0.64-0.98	0.57	0.5963	0.526	46.55
MD4~ TL		9	0.571	-0.54-1.68	1.25	0.2562	0.165	60.58
MD4~ S4		9	0.081	-1.33-1.49	0.14	0.8931	0.230	48.32
MD5~ TL		9	0.534	-0.39-1.46	1.41	0.2090	0.068	65.93
MD5~ S5		9	0.257	-0.83-1.34	0.58	0.5841	0.162	58.37
MD6~ TL		9	0.432	-0.32-1.18	1.41	0.2081	0.099	67.01
MD6~ S6		9	0.294	-0.50-1.09	0.90	0.4019	0.172	47.75
MD7~ TL		9	0.430	-0.23-1.09	1.60	0.1599	0.021	69.94

MD7~ S7		9	0.142	-0.47-0.76	0.56	0.5932	0.200	62.79
MD8~ TL		9	0.252	-0.41-0.92	0.92	0.3904	0.152	65.43
MD8~ S8		9	0.088	-0.50-0.67	0.37	0.7270	0.228	61.29
LV6~ TL		4	0.510	-1.18-2.20	1.30	0.3236	0.330	57.27
LV6~ S6		4	0.357	-1.19-1.91	0.99	0.4261	0.382	56.91
LV7~ TL		4	0.929	/	1.83	0.2087	0.139	57.04
LV7~ S7		4	0.464	-1.81-2.74	0.88	0.4722	0.287	50.07
LV8~ TL		9	0.959	0.05-1.87	2.57	0.0423	0.333	75.64
LV8~ S8		9	0.861	0.15-1.57	2.97	0.025	0.364	78.12
LV9~ TL		9	0.603	-0.63-1.84	1.19	0.2781	0.172	58.75
LV9~ S9		9	0.153	-0.83-1.14	0.38	0.7170	0.287	40.84
LTS ~ TL	Pycnophyidae	43	0.503	-0.36-1.36	1.19	0.2422	0.073	41.31
LTS ~ S11		30	0.055	-0.33-0.44	0.30	0.7694	0.076	58.73
LTS ~ TL	Neocentrophyidae	5	-1.154	-6.05-3.74	-1.01	0.4171	0.374	78.18
LTS ~ S11		5	-1.089	-3.81-1.63	-1.72	0.2274	0.389	81.52

Data S3. Results of the RMAs analyses of the evolutionary, allometric relationship between body segments' length with respect to total trunk length (S~TL) in Kinorhyncha at phylum, class and family levels. Abbreviations: *n*, sample size; *b*, allometric coefficient; 95%CI, 95% confidence intervals; *p*, p-value; r^2, coefficient of determination.

Model	**Taxon**	***n***	***b***	**95%CI**	***p***	***r²***
S1~TL	Kinorhyncha	131	1.298	1.23-1.37	0.01	0.907
S2~TL		132	0.963	0.91-1.02	0.01	0.908
S3~TL		132	0.972	0.92-1.03	0.01	0.912
S4~TL		132	0.951	0.90-1.00	0.01	0.925
S5~TL		132	0.940	0.89-0.99	0.01	0.912
S6~TL		132	0.909	0.86-0.96	0.01	0.907
S7~TL		132	0.867	0.82-0.92	0.01	0.895
S8~TL		132	0.826	0.78-0.88	0.01	0.888
S9~TL		132	0.825	0.77-0.88	0.01	0.862
S10~TL		132	0.936	0.87-1.01	0.01	0.850
S11~TL		123	0.755	0.57-1.02	0.01	0.279
S1~TL	Cyclorhagida	85	0.981	0.84-1.16	0.01	0.651
S2~TL		85	0.980	0.84-1.15	0.01	0.656
S3~TL		85	1.044	0.89-1.25	0.01	0.628
S4~TL		85	1.056	0.91-1.23	0.01	0.683
S5~TL		85	1.154	1.00-1.35	0.01	0.673
S6~TL		85	1.152	1.00-1.35	0.01	0.681
S7~TL		85	1.157	1.00-1.35	0.01	0.675
S8~TL		85	1.141	1.00-1.32	0.01	0.703
S9~TL		85	1.175	1.00-1.40	0.01	0.631
S10~TL		85	1.054	0.90-1.25	0.01	0.637

S11~TL		83	1.921	1.36-3.09	0.01	0.242
S1~TL	Allomalorhagida	46	0.833	0.70-1.00	0.01	0.737
S2~TL		47	1.355	1.18-1.57	0.01	0.824
S3~TL		47	1.163	1.04-1.31	0.01	0.870
S4~TL		47	1.062	0.96-1.18	0.01	0.898
S5~TL		47	1.037	0.94-1.16	0.01	0.889
S6~TL		47	1.052	0.96-1.16	0.01	0.903
S7~TL		47	0.990	0.90-1.10	0.01	0.896
S8~TL		47	1.004	0.91-1.11	0.01	0.898
S9~TL		47	1.052	0.95-1.17	0.01	0.892
S10~TL		47	1.703	1.39-2.15	0.01	0.659
S11~TL		40	2.274	1.47-4.68	0.01	0.279
S1~TL	Echinoderidae	76	0.977	0.86-1.12	0.01	0.751
S2~TL		76	1.040	0.88-1.25	0.01	0.640
S3~TL		76	1.063	0.90-1.28	0.01	0.632
S4~TL		76	1.093	0.93-1.30	0.01	0.652
S5~TL		76	1.202	1.02-1.44	0.01	0.643
S6~TL		76	1.197	1.02-1.43	0.01	0.654
S7~TL		76	1.183	1.01-1.41	0.01	0.663
S8~TL		76	1.169	1.00-1.38	0.01	0.685
S9~TL		76	1.196	1.00-1.45	0.01	0.610
S10~TL		76	1.024	0.86-1.23	0.01	0.633
S11~TL		74	2.039	1.35-3.82	0.01	0.192
S1~TL	Centroderidae	9	1.235	0.70-3.03	0.01	0.658
S2~TL		9	0.676	0.52-0.89	0.01	0.919
S3~TL		9	0.930	0.01-1.10	0.06	0.235
S4~TL		9	0.875	0.61-1.32	0.01	0.853
S5~TL		9	0.974	0.71-1.40	0.01	0.880
S6~TL		9	1.052	0.77-1.51	0.01	0.882
S7~TL		9	1.328	0.96-1.99	0.01	0.865
S8~TL		9	1.272	0.99-1.70	0.01	0.920
S9~TL		9	1.404	1.04-2.04	0.01	0.881
S10~TL		9	1.598	1.16-2.41	0.01	0.865
S11~TL		9	2.095	1.41-3.82	0.01	0.786
S1~TL	Pycnophyidae	39	0.898	0.72-1.13	0.01	0.693
S2~TL		40	1.267	1.09-1.50	0.01	0.814
S3~TL		40	1.033	0.92-1.17	0.01	0.881
S4~TL		40	0.936	0.84-1.05	0.01	0.890
S5~TL		40	0.939	0.82-1.08	0.01	0.856
S6~TL		40	0.954	0.85-1.07	0.01	0.895
S7~TL		40	0.938	0.82-1.07	0.01	0.864

S8~TL		40	0.929	0.82-1.05	0.01	0.879
S9~TL		40	0.999	0.88-1.15	0.01	0.856
S10~TL		40	1.679	1.29-2.33	0.01	0.562
S11~TL		33	3.662	1.89-35.61	0.01	0.140
S1~TL	Neocentrophyidae	7	0.967	0.71-1.35	0.01	0.932
S2~TL		7	1.063	0.56-2.75	0.04	0.733
S3~TL		7	0.966	0.59-1.81	0.02	0.825
S4~TL		7	0.949	0.74-1.25	0.01	0.951
S5~TL		7	1.030	0.76-1.45	0.01	0.930
S6~TL		7	1.045	0.70-1.70	0.01	0.881
S7~TL		7	0.965	0.68-1.44	0.01	0.909
S8~TL		7	1.011	0.68-1.63	0.01	0.881
S9~TL		7	1.098	0.77-1.68	0.01	0.902
S10~TL		7	1.075	0.55-2.92	0.03	0.717
S11~TL		7	1.693	0.01-1.71	0.03	0.507

SCIENTIFIC REPORTS
nature research

OPEN

Does sediment composition sort kinorhynch communities? An ecomorphological approach through geometric morphometrics

Diego Cepeda[1*], Dolores Trigo[1], Fernando Pardos[1,3] & Nuria Sánchez[2,3]

Ecomorphology studies the relationship between organisms' morphology and environment features. To better understand whether the shape of the body and the appendages involved in the movement is correlated to sediment composition in meiofaunal organisms, we study the evolved morphological adaptations to environment in selected taxa of the phylum Kinorhyncha: the allomalorhagid families Dracoderidae and Pycnophyidae, and the cyclorhagid genus *Echinoderes*. The selected taxa include the most diverse groups of Kinorhyncha worldwide, representing the 75.5% of the total phylum diversity. Widened, plump bodies and lateral terminal spines may be adaptive for species living in coarse, more heterogeneous sediments, as they could maintain a more powerful musculature to actively displace the sediment grains applying a greater force. Conversely, slender, vermiform bodies and lateral terminal spines would represent an adaptation of species inhabiting fine, more homogeneous sediments where there would not be much need to exert a high force to displace the sediment particles, and a more vermiform shape would even favour the burrowing of the animal through the smaller interstices. The studied kinorhynch taxa would also be adapted to the higher velocity of the sea-water and the intense erosion and transportation of heterogeneous sediments by possessing more robust bodies, avoiding getting laid off substratum under these conditions. These findings provide evolutionary evidence that body shape in the studied kinorhynch groups is adapted to environment.

[1]Universidad Complutense, Department of Biodiversity, Ecology and Evolution, Madrid, 28040, Spain. [2]Institut Français de Recherche pour l'Exploitation de la Mer, Deep-sea Laboratory, Plouzané, 29280, France. [3]These authors contributed equally: Fernando Pardos and Nuria Sánchez. *email: diegocepeda@ucm.es

Morphological adaptations are frequently a response of ecological pressures and changes in environmental variables[1,2]. Ecomorphology can be defined as the study of the relationship between organisms' morphology and ecological features[3,4]. Indeed, environmental heterogeneity is one of the main promoters of morphological variation in animals that inhabit changeable habitats[5,6]. In the context of marine ecosystems, meiobenthic habitats possess complex, dynamic interactions that are intricately combined and influenced by numerous abiotic factors[7]. The structure of the sediment is one of the main meiobenthic abiotic parameters, performing a leading role in meiobenthic ecology since its features influence the degree of accessibility of meiofaunal organisms[8,9].

Soft sediments are composed of inorganic particles, organic matter and pore water, so meiobenthic organisms are strongly affected by their variations[10]. As for instance, the grain size of the sediment inhabited by the organisms determines the relative availability of interstitial spaces and subsequently influences the abundance and composition of the meiofaunal communities[11]. Morphological and size adaptations of meiofauna to grain size have been evidenced in different groups. Meiofauna can be divided in several categories regarding the different way of movement through the sediment particles: interstitial forms, burrowers, epibenthic organisms and hyperbenthic taxa. Interstitial meiofauna moves among sedimentary grains without displacing them, whereas burrowing meiofauna actively displace the particles, usually with body structures acting as spades and moved by muscles[10]. Most interstitial taxa (*e.g.* tardigrades, some harpacticoid copepods and nematodes, a few ostracods such as Xestoleberididae, and most gastrotrichs and annelids) are stouter and plumper in finer sediments where they need to dig through the sediment particles or live as sediment dwellers near the surface, whereas slender, vermiform species tend to inhabit in coarser sediments where they can move more easily through the interstitial space[12–15]. However, some exceptions to this can be found, as certain interstitial taxa (*e.g.* the gastrotrich genus

Musellifer Hummon, 1969, or even some kinorhynchs such as the genera *Cateria* Gerlach, 1956 and *Franciscideres* Dal Zotto *et al*., 2013, or some species of *Cephalorhyncha* Adrianov in Adrianov and Malakhov, 1999) live in fine sediments and are rather slender and vermiform. Burrowing meiofauna (*e.g*. loriciferans, most kinorhynchs and ostracods, and some annelids, harpacticoid copepods and nematodes), that moves by active displacement of the sediment, is more frequent in finer sediments, and relationships between grain size and body shape are much more uncharted[16–18]. Other categories of meiofaunal organisms must also be mentioned, such as the epibenthic forms (*e.g*. gastropods, some foraminiferans such as the *Symbiodinium* Freudenthal, 1962 group), which live on top of other meiofaunal organisms or algae, or the hyperbenthic taxa (most copepods, nauplii, some annelids, nematodes and bivalves) that are able to swim through the water column, having both a more reduced relationship with sediment features[7,14].

On the other hand, the influence of organic matter on meiofaunal communities has been widely studied from a trophic point of view as it is fundamental for the productivity of meiobenthic communities[19], but its possible role in the organism shapes still remains unexplored. The carbon-to-nitrogen ratio (C/N) is a good measure of the quality of detritus whose accumulation over sediment usually changes the physical properties of the latter, acting as a cementing agent[20]. Moreover, the C/N ratio also gives information on the state of the decomposition processes, as it depends on several factors including sedimentary features, rate of microbial degradation, column water productivity and terrestrial inputs[21,22]. Finally, the hydrogen ion concentration (pH) is also of relevance in meiobenthic ecology as it can induce morphological deformations and act as limiting factor for many organisms[8,23].

In this regard, kinorhynchs are an ideal model to study morphology-sediment relationships since this phylum is mainly composed of burrowing meiofaunal species that inhabit a wide variety of oceanic soft sediments[24,25]. The main aim of the present paper is to determine whether and how sediment features (grain size, content of organic matter and pH) affect body shape and size of kinorhynchs, through a geometric morphometrics approach using selected kinorhynch taxa: the allomalorhagid families Dracoderidae (2.3% of the total phylum diversity) and Pycnophyidae (31% of the total phylum diversity), and the cyclorhagid genus *Echinoderes* Claparède, 1863 (42.2% of the total phylum diversity). Likewise, we test if shape and size of two kinds of cuticular appendages are also affected by sediment: lateral terminal spines (LTS) and primary spinoscalids. Primary spinoscalids are used by kinorhynchs to actively move through the sediment[24,25], whereas the LTS, of still unclear function, are in constant contact with the sediment, being very conspicuous and large in most of the groups and thus forced to move through the sediment particles.

Results

Sediments composition. Most of the analysed sediment samples ($n = 16$) consisted in sand, with an average size of 49.44–327.8 μm. Seven samples were defined as mud, with an average size of 9.5–27.52 μm, and only two were dominated by gravel, with an average size of 56.96–1353.9 μm. Values of sorting (σ) were generally low (mean of $\sigma = 4.085$), and hence most of the sediment samples were poorly sorted, with the sediment spread over a large range of size classes (*i.e*. more heterogeneity). However, some samples had high values of sorting and were well sorted (σ up to 16.54), with most of the sediment confined to a few size classes. Values of skewness (*Sk*) indicated a general trend to the asymmetry in the spread of the particle sizes towards low diameters (mean of $Sk = -0.243$), meaning that the samples contain more categories of particles with sizes under the average value (*i.e*. more categories of finer particles). Nevertheless, some samples had positive values of *Sk* with more categories of coarser particles above the average size. Finally, values of kurtosis (*K*) revealed that most of the samples are leptokurtic, with a low concentration of the particles relative to the average size (mean of $K = 1.704$). Some samples were determined as platykurtic ($K < 1$), with particles very concentrated relative to the average size, as well as mesokurtic ($K \approx 1$). In summary, though there is a majority of sandy, quite heterogeneous, leptokurtic sediments, the set of samples are of relative variability.

Regarding the content in organic matter, range of C/N ratio was wide, from 7.71 to 61.26. Most of the analysed samples were poor or very poor in organic carbon content ($\%_C < 2.0$), except the samples 4 and 5 from Algeciras Bay ($\%_C = 2.2821$ and 2.2356, respectively; see Supplementary Information). Regarding the content in nitrogen, the samples were also poor or very poor ($\%_N < 0.15$), except the samples 4 and 5 from Algeciras Bay again ($\%_N = 0.1821$ and 0.1649, respectively; see Supplementary Information). The generally low C/N ratio values seem to be consequence of the poor content in nitrogen of most of the analysed samples. Moreover, an important input of terrestrial organic matter was detected in most of the sampled localities, with high values of C/N ratio (>10)[26]. A single exception was found at one locality of Jamaica (locality 2) where organic matter of marine origin seemed to be dominant, showing a low value of C/N ratio (between 4 and 10) (see Supplementary Information). pH varied from 6.677 to 8.883, with most of sediment samples showing alkaline values.

Body shape. The two first axes of the principal component analysis (PCA) explained a total of 78.374% of the symmetric (50.044% by PC_1 and 28.330% by PC_2) and 75.504% of the asymmetric (65.833% by PC_1 and 9.671% by PC_2) components of the variation in shape across specimens (Fig. 1A,B). Regarding the symmetric component, specimens with positive PC_1 and PC_2 values tended to have a body shape that was more widened and plumper, whereas those specimens with negative PC_1 and PC_2 values had a tendency towards a slender, more narrowed (vermiform) body shape, as showed by the wireframe graphs (Fig. 2A,B). Here, we will refer to these two body shape extremes as "stouter and plumper" and "vermiform and slender", respectively.

Linear mixed models (LMMs) and generalized linear mixed models (GLMMs) yielded that the variance in body shape by the symmetric component was 27.66% explained by PC_1 and 21.95% by PC_2, as determined by the coefficients of determination (Table 1). Average size, skewness and kurtosis were the only sediment variables that contributed to explain the shape variance of the model (Table 1). According with the model, stouter and plumper specimens are more likely found in sediments with a coarse average size of particles with more representation of

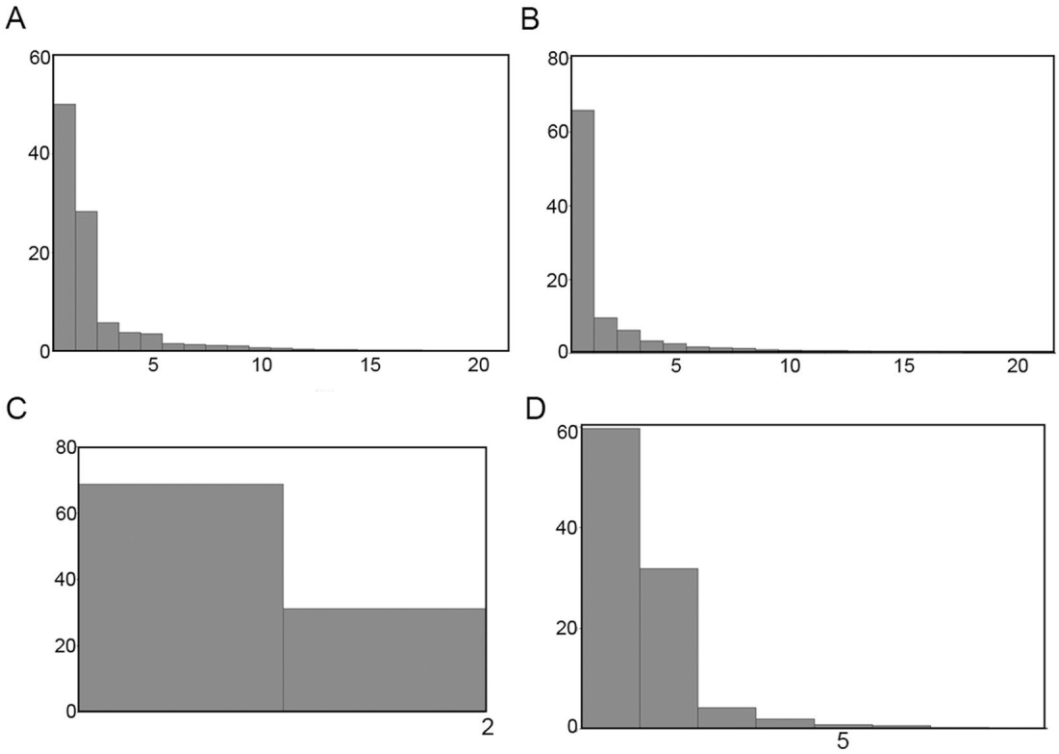

Figure 1. Principal component axes that explain the variance in the symmetrical component of the body shape (**A**), the asymmetrical component of the body shape (**B**), the LTS shape (**C**) and the primary spinoscalids shape (**D**). X axis represents number of principal components, Y axis represents % explained by principal components.

coarser categories (as indicated by the positive values of skewness) and a relatively high value of heterogeneity in particle sizes (as indicated by the positive values of kurtosis). On the opposite, vermiform and slender specimens are more abundant in sediments with a fine average size of particles with more representation of finer categories (as indicated by the negative values of skewness) and a relatively low value of heterogeneity in particle sizes (as indicated by the negative values of kurtosis).

Additionally, vermiform and slender kinorhynchs were mainly found in the samples from Jamaica, whereas samples from the Iberian Peninsula resulted in a wide range of shapes but usually more robust than the former ones (Fig. 3A,B). However, this result has to be taken with caution, since the Jamaican specimens are represented only by three localities around the same bay.

Phylogeny resulted of high influence, with 58.96% for PC_1 and 27.55% for PC_2 of the variance not explained by the fixed-effect component of the models (Table 1). These results showed an important genetic effect in body shape, as also showed by the boxplots (Fig. 3C,D). Thus, the cyclorhagid genus *Echinoderes* was characterized by a slender, more vermiform shape, with a mean value of PC_1 lower than the allomalorhagid families Dracoderidae and Pycnophyidae (Fig. 3C). The allomalorhagid genera *Dracoderes* Higgins & Shirayama, 1990 and *Leiocanthus* Sánchez *et al*., 2016 showed the most robust and plumpest body shape (Fig. 3C).

Concerning the asymmetrical component, specimens with positive or negative PC_1 and PC_2 values tended to suffer different kinds of deviations (slight twists and zigzags on sternal plates) from the bilateral symmetry (Fig. 2C,D). Only the sediment pH seemed to influence these deviations of the symmetrical pattern, affecting the PC_1 and explaining 46.85% of the total variance (Table 1). We found a positive correlation between pH and PC_1, with more alkaline values causing deviations from bilateral symmetry. Phylogeny did not show any influence on the asymmetrical component of body shape, as the random-effect component of the model was not found as an explicative factor.

LTS shape. Variation in shape of LTS is mainly explained by the first PCA axis (68.715%) (Fig. 1C). Positive values of PC_1 defined widened and stout spines, while negative values tended to define slender and narrowed spines (Fig. 2E).

The only sediment variables that influenced in modelling LTS shape were skewness, kurtosis and C/N ratio, explaining a 20.66% of the total variance of PC_1 (Table 1). Stouter and more widened spines tended to be correlated with sediments with more heterogeneity of particle sizes, with special abundance of coarser categories, and with lower C/N ratios (more content in organic nitrogen), and vice versa. Regarding the localities, we found a huge variety of LTS shapes with no apparent differences between the Iberian Peninsula and Jamaica (Fig. 4A). The random-effect component only had a high influence in LTS shape regarding the PC_1 ($\%_{EXP} = 32.12$). Indeed, the cyclorhagid genus *Echinoderes* showed the trend of more elongated, slender spines than the allomalorhagid families Dracoderidae and Pycnophyidae, whose mean values determined the presence of stouter, more widened structures (Fig. 4C).

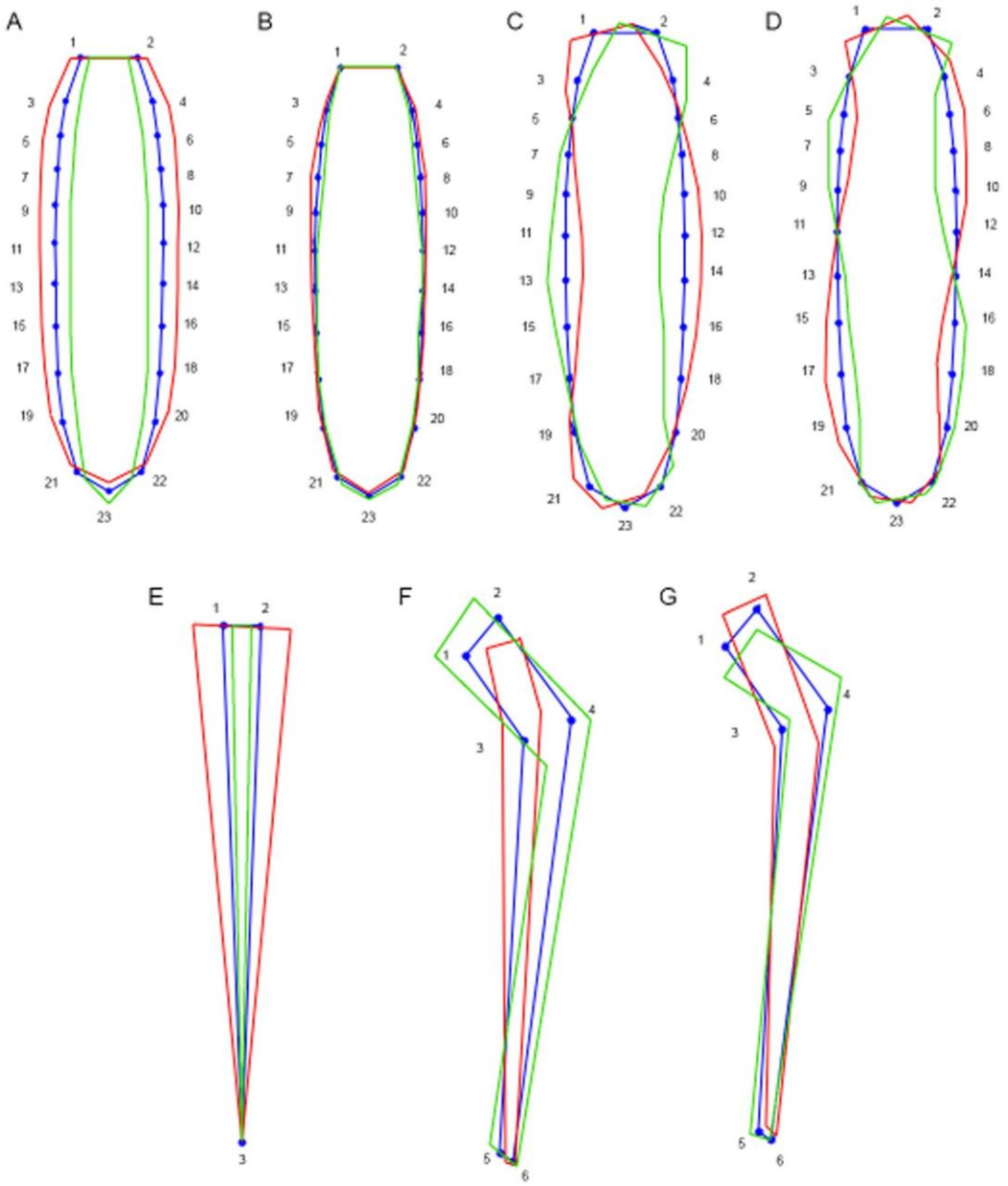

Figure 2. Wireframe representations of the variation in shape of sternal plates (**A–D**), LTS (**E**) and primary spinoscalids (**F,G**) along the principal components that explain most of the variance. Blue wireframes represent the mean shape observed across all sample individuals, and red and green wireframes represent the most extreme shapes. (**A**) PC1 of symmetrical component of sternal plates; (**B**) PC2 of symmetrical component of sternal plates; (**C**) PC1 of asymmetrical component of sternal plates; (**D**) PC2 of asymmetrical component of sternal plates; (**E**) PC1 of LTS; (**F**) PC1 of primary spinoscalids; (**G**) PC2 of primary spinoscalids.

Primary spinoscalids shape. Variation in shape of primary spinoscalids was explained in a 91.605% by the first two PCA axes (PC_1 = 59.68% and PC_2 = 31.925%) (Fig. 1D). Positive values of PC_1 defined scalids with a proportionally shortened and narrow basal sheath and a more acicular tip, whereas negative values were related to scalids with a proportionally elongated and wide basal sheath with a distally rounded tip (Fig. 2F). Variation of PC_2 defined scalids with more elongated but still wider basal sheaths and a more acicular tip with positive values, and proportionally shortened but narrower basal sheaths and a rounded distal tip with negative values (Fig. 2G).

None of the sediment variables showed a significant influence on the shape variation.

Size. Centroid size (CS) of sternal plates varied between 147.99 and 1136.57 (653.08 ± 301.12), *i.e.* the largest kinorhynchs were almost eight times larger than the smallest ones. The smallest kinorhynch belonged to the species *Leiocanthus lageria* (Sánchez *et al*., 2013), and the largest one to the species *Setaphyes dentatus* (Reinhard, 1881). There was no significant influence of sediment variables on body CS.

Model	Variable	Estimate	StdE	*t*	R^2	$\%_{EXP}$
PC_{1Sym}	Intercept	1.66e-01	1.09e-01	1.52	0.2766	58.96
	X	1.01e-04	5.46e-05	1.85		
	Sk	3.46e-02	1.95e-02	1.78		
	K	1.31e-02	4.68e-03	2.79		
PC_{2Sym}	Intercept	−7.289e-02	7.33e-02	−0.994	0.2195	27.55
	X	5.986e-05	1.807e-05	3.312		
	Sk	6.747e-02	1.132e-02	5.962		
	K	7.652e-03	3.315e-03	2.308		
PC_{1Asym}	Intercept	−1.037e-01	5.744e-02	−1.805	0.4685	0
	pH	1.327e-02	7.161e-03	1.853		
PC_{2Asym}	Intercept	6.739e-03	2.188e-02	0.308	0.5218	0
PC_{1lts}	Intercept	7.17e-02	5.76e-02	0.213	0.2066	32.12
	Sk	1.52e-02	8.97e-03	0.090		
	C/N	−5.03e-04	2.06e-04	0.015		

Table 1. Coefficients of linear mixed models and generalized linear mixed models of body and LTS shape analyses. Only variables with significant results ($p < 0.05$) are included. Abbreviations: C/N, carbon-nitrogen ratio; *K*, kurtosis; R^2, coefficient of determination; *Sk*, skewness; StdE, standard error; *t*, t-value; *X*, average size; $\%_{EXP}$, % explained by random-effect component.

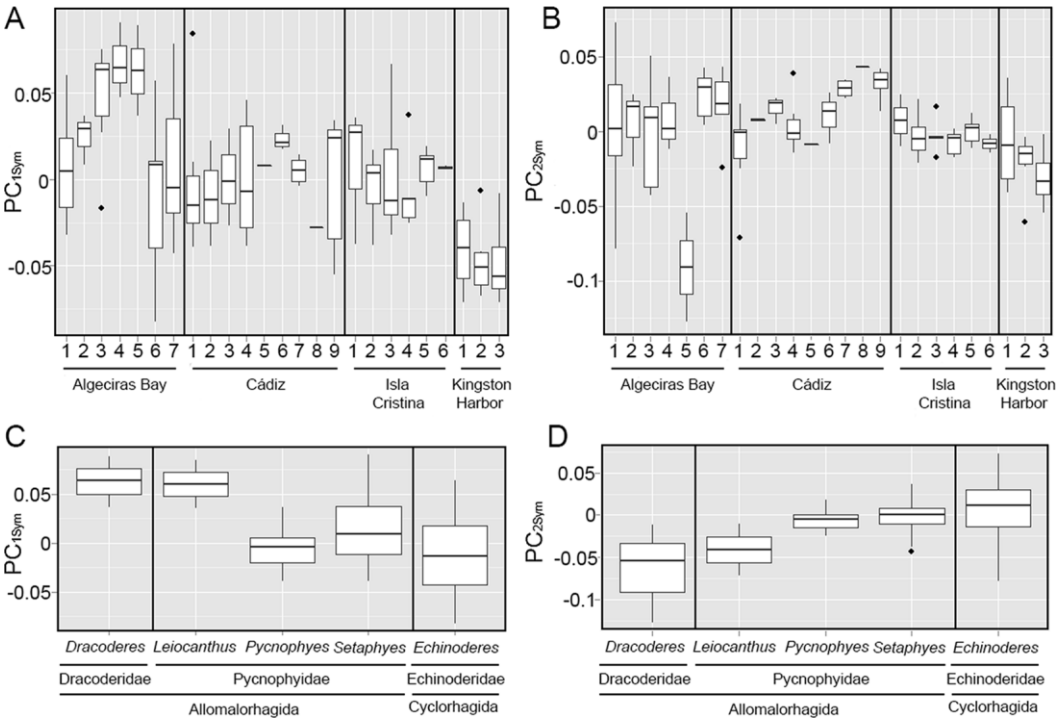

Figure 3. Box-and-whisker plots of variation in symmetric body shape between localities (**A,B**) and random-effect (*i.e.* phylogenetic influence) component (**C,D**). The boxplots show the median (middle line), quartiles (boxes), 1.5 times the interquartile range (whiskers) and extreme values (dots).

CS of LTS varied between 62.11 and 207.94 (113.73 ± 29.49), meaning that the biggest LTS were more than three times larger than the smallest ones. *Pycnophyes communis* Zelinka, 1908 was the species with the smallest LTS, while *Dracoderes gallaicus* Sørensen *et al.*, 2012 possessed the largest ones (Fig. 4D). We found influence of sorting, skewness and kurtosis on LTS CS, as the fixed-effect component of the model explained together a 23.53% of the total observed variance (Table 2). Additionally, phylogeny resulted of high influence as the random-effect component of the model explained 65.44% of the variance. We did not found any particular difference between samples from the Iberian Peninsula and the sample from Jamaica (Fig. 4B). In summary, we found specimens with larger LTS in sediments with high heterogeneity of particle sizes and more content of finer sediments.

CS of primary spinoscalids varied between 27.17 and 76.25 (43.35 ± 11.87), meaning that the largest primary spinoscalids were almost three times larger than the smallest ones. *Echinoderes hispanicus* Pardos *et al.*, 1998 was

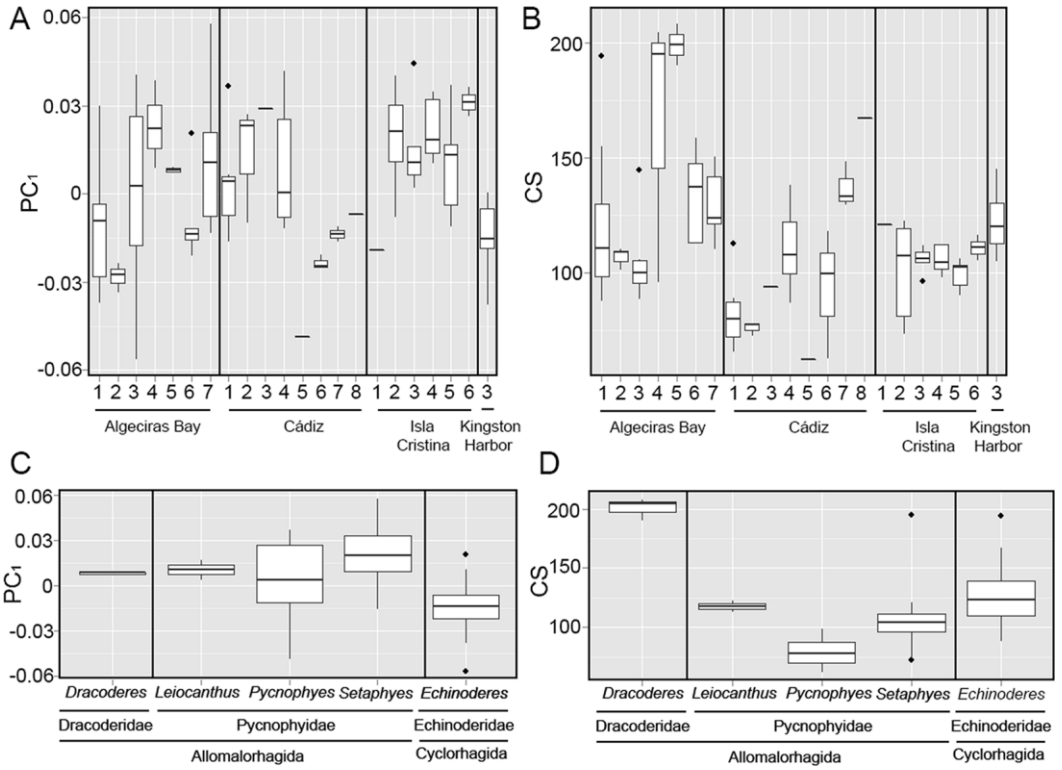

Figure 4. Box-and-whisker plots of variation in LTS shape between localities (**A**) and random-effect (*i.e.* phylogenetic influence) component (**C**), and variation in LTS size between localities (**B**) and random-effect (*i.e.* phylogenetic influence) component (**D**). The boxplots show the median (middle line), quartiles (boxes), 1.5 times the interquartile range (whiskers) and extreme values (dots).

Variable	Estimate	StdE	*t*	R^2	$\%_{EXP}$
Intercept	−0.0039	0.0051	−0.7605	0.2353	65.44
σ	0.00008	0.0001	0.7833		
Sk	−0.0022	0.0008	−2.9397		
K	0.0004	0.0002	1.8871		

Table 2. Coefficients of generalized linear mixed models of LTS size analyses. Only variables with significant results ($p < 0.05$) are included. Abbreviations: *K*, kurtosis; R^2, coefficient of determination; *Sk*, skewness; StdE, standard error; *t*, t-value; $\%_{EXP}$, % explained by random-effect component.

the species with the smallest primary spinoscalids, whereas *Dracoderes gallaicus* had the largest ones. There was no significant influence of sediment variables on primary spinoscalids CS.

Discussion

Meiofaunal organisms are tremendously dependent of sediment and therefore reveal the effect of sediment structure and composition on morphology as crucial to better understand animals-habitat interactions. For our group of study, the allomalorhagid families Dracoderidae and Pycnophyidae and the cyclorhagid genus *Echinoderes* (phylum Kinorhyncha), we found relationships between body and LTS shape with some of the analysed sediment variables. Additionally, the phylogeny contributed to the variation in shape of kinorhynchs as well.

Body shape adaptations of meiofauna to grain size have been mainly explored in interstitial taxa. Sediments with coarser size of particles usually host slender, more vermiform species as they have to move through tight interstitial spaces, whereas finer sediments are inhabited by stouter species whose body enables them to penetrate more easily through the particles, acquiring a movement similar to that of burrowers[12–15]. However, relationships between body shape and sediment composition still remains unexplored for burrowing meiofauna. Kinorhynchs, as meiofaunal burrowers mainly, use the introvert scalids to move through the sediment[17,25,27].

We found statistically significant influence of average size, skewness and kurtosis of sedimentary particles over body shape of the analysed kinorhynch taxa. The analyses showed that kinorhynch species inhabiting coarser sediments with a high variety of different particles' sizes tended to be stouter and plumper compared to those inhabiting finer, more homogeneous sediments, whose bodies were slender and more vermiform. These results seem to go, at first sight, against those above mentioned for the interstitial meiofauna. However, the analysed kinorhynch taxa are representatives of the burrowing meiofauna that move actively through the sediment displacing the

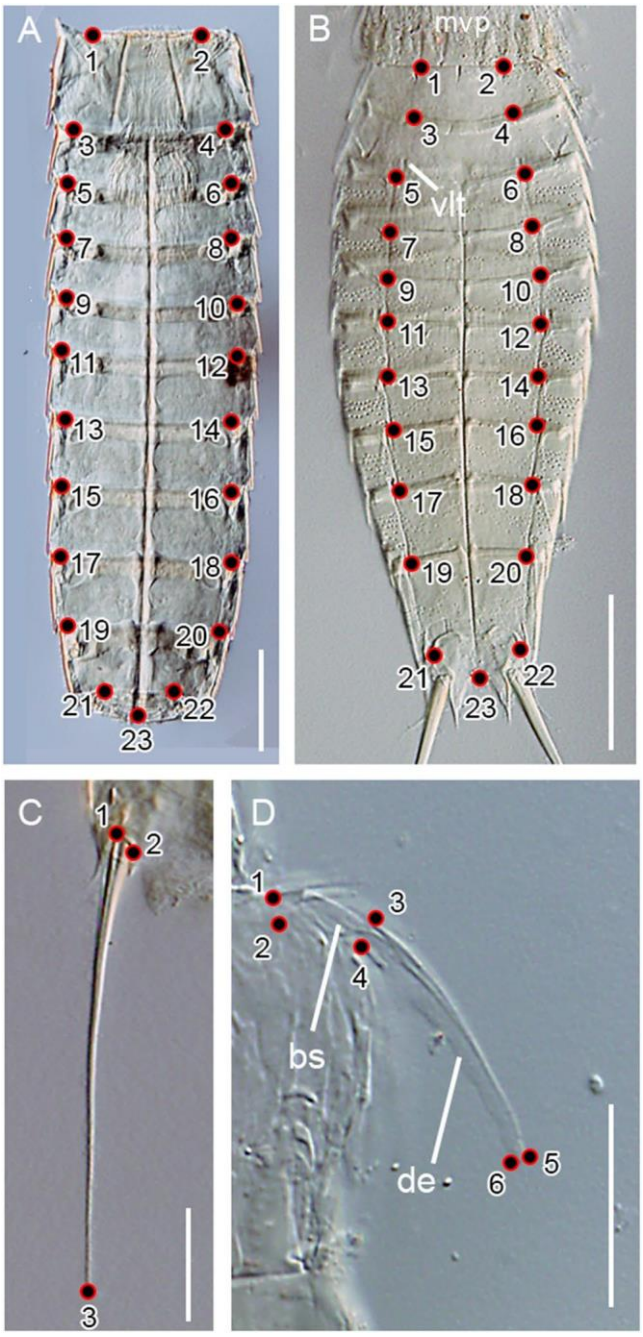

Figure 5. Position of landmarks used on digital micrographs. (**A**) Sternal plates of an adult male of *Pycnophyes communis* (Allomalorhagida); (**B**) sternal plates of an adult male of *Echinoderes* sp. 1 (Cyclorhagida); (**C**) right lateral terminal spine of an adult male of *Echinoderes* sp. 2 (Cyclorhagida); (**D**) primary spinoscalid of an adult male of *Echinoderes* sp. 1 (Cyclorhagida) in lateral view. Scales: A, 100 µm; B,C, 50 µm; D, 20 µm. Abbreviations: bs, basal sheath; de, distal end; mvp, midventral placid; vlt, ventrolateral tube.

grains with the introvert scalids[24,25]. In this context, a more robust and plumper body may suppose an adaptive advantage for the species that live in coarser sediments, allowing to maintain a more powerful musculature to displace the sediment particles by generating a greater force. Indeed, for the interstitial taxa that act to some extent as burrowers in finer sediments, plump and robust bodies suppose an adaptation for this active movement through the sediment, as previously explained. In parallel, the possession of a slender, vermiform body in species inhabiting finer sediments would also be adaptive, since it would not be necessary to apply much force to move the finer sediment particles, and this body morphology would even facilitate the burrowing through the smallest interstices by simple movements of the body combined with that of the introvert scalids. Indeed, fine-grained sediments of moderate to high water content show the phenomenon of thixotropy, where a small force against the sediment is enough to allow sediment displacement[10]. It remains to be seen if other kinorhynch taxa not included

in the present study (*e.g*. Franciscideridae, Kentrorhagata, Xenosomata) agree with the results herein obtained for Dracoderidae, Pycnophyidae and *Echinoderes*, or if they contrarily exhibit different patterns of body morphological adaptations to sediment.

Heterogeneity of grain sizes, very different from those of the average (kurtosis), also seems to favour the presence of more robust, plump species. These sediments correspond to gravel and gravelly sand, reflecting the presence of many different categories of coarser sizes. This result seems to also support the previously proposed hypothesis. Heterogeneity of inorganic particles dominated by coarse sediments also reflects a heterogeneity of sedimentary processes, with variable and strong depositional currents[10,27–29]. In these areas of high current velocity, with intense erosion and transportation, meiofaunal organisms must be capable of rapid reburial, favouring the presence of stout and plump burrowing species in coarser sediments.

Regarding the phylogenetic component of the models, body shape differences among classes and families are strongly influenced by genetics. In this context, some kinorhynch taxa with slender and more vermiform bodies, such as the allomalorhagid genera *Franciscideres* Dal Zotto *et al*., 2013 and *Gracilideres* Yamasaki, 2019, or the cyclorhagid genera *Cateria* Gerlach, 1956, *Triodontoderes* Sørensen and Rho, 2009 and *Zelinkaderes* Higgins, 1990 have been found inhabiting relatively coarse sediments, except *Triodontoderes lagahoo* Cepeda *et al*., 2019 and *Zelinkaderes floridensis* Higgins, 1990. This could be due to the existence of different adaptation patterns in the remaining kinorhynch taxa not included in the present study. Although the allomalorhagid families Dracoderidae and Pycnophyidae plus the cyclorhagid genus *Echinoderes* constitute an extensive part of the total phylum diversity (75.5%), still another great part of kinorhynch morphological diversity is not included herein., which could possess different morphological adaptations to sediment.

It has been also hypothesized that slender, vermiform kinorhynchs tend to inhabit coarser sediments as an adaptation to the interstitial environment[30]. However, this hypothesis is mostly based in the presence of a thin and flexible cuticle that would make the animal more bendable when moving through the sediment particles, rather than in the shape of the body. Thus, it is likely that a combination of morphological features, including body shape and flexibility of the cuticle, among others, are responsible from defining the adaptive process of kinorhynchs to the different types of substrata.

Fluctuating asymmetry (*i.e*. departures from perfect bilateral symmetry) usually occurs due to the incapacity of the organisms to contain disorders from environment or endogenous conditions during its development, leading to a lesser reproductive success and survival rate[31]. According to our results, body asymmetry of analysed kinorhynchs is affected by pH, reflecting the largest deviations from the bilateral pattern of the sternal plates under values of pH below 7.0 (acidic) and above 8.5 (strongly alkaline) as well (see Supplementary Information). In marine sediments, pH between 7.5–8.5 is well-buffered against pH oscillations, but lower or higher values, combined with other stress factors (*e.g*. high temperatures, extreme salinity, etcetera) may be detrimental for meiofauna[7]. Indeed, previous studies have shown that meiofauna experiences episodes of high mortality after exposure to recurrent pH changes[32–35].

On the other hand, animals with exoskeletons containing chitin, such as crustaceans and molluscs, suffer a significant loss of chitin under acidic pH values[36,37]. Kinorhynchs also possess an external cuticle with a chitinous basal layer[25], and deformations in body morphology could be induced under acidic conditions. As for the possible effect of alkaline pH, it is likely that too alkaline (>8.5) values are not able by themselves to cause deviations from the bilateral symmetry of kinorhynchs. However, combined with other environmental factors such as episodes of increasing temperature and salinity, alkaline pH could induce deformations of kinorhynch sternal plates, leading to asymmetrical patterns.

The lack of genetic basis of the observed asymmetry in kinorhynchs is in accordance with the aforementioned idea about deviations from the bilateral symmetry, as these deviations usually lead to low rates of fitness and biological success in animals.

LTS are elongate, basally articulated, distally pointed cuticular appendages present in lateroventral position on segment 11 of most kinorhynch species[25]. The function of these spines still remains unknown, but they are the most conspicuous cuticular structures as they tend to be the largest ones compared to other appendages, projecting well beyond the end of the trunk. Another conspicuous cuticular appendage is the midterminal spine, present in some kinorhynch taxa such as the cyclorhagid orders Kentrorhagata and Xenosomata, or the allomalorhagid families Franciscideridae and Neocentrophyidae. In any case, LTS are forced to move through the sediment interstices accompanying the general movement of the animal.

According to our results, species with more shortened and widened LTS seem to occur in sediments with a wide range of different coarse particles (*i.e*. dominated by coarse sediments), whilst species with slender and more narrowed LTS tend to inhabit in substrata with a wide range of different fine particles (*i.e*. dominated by fine sediments). These results are similar to those obtained for kinorhynchs' body shape. More robust and widened LTS could allow kinorhynchs of the analysed taxa better moving through the sediment particles in coarser sediments, actively moving and displacing the grains by exerting a greater force. In fact, LTS are the only cuticular appendages of Kinorhyncha (together with the midterminal spines) that are linked to internal muscles, meaning that the animals are able to move them[38–40]. Additionally, coarser sediments are usually a result of strong currents, so the presence of more robust, widened LTS could allow kinorhynchs clinging more tightly to the sediment particles under episodes of high hydrodynamics. It is important to note that the obtained results for the LTS adaptive shape are not necessarily applicable to kinorhynch taxa bearing an also conspicuous midterminal spine, which have not been included in the present study. Most of these kinorhynchs with a midterminal spine, also linked to internal muscles, inhabit fine sediments (Neuhaus, 2013), and a possible morphological adaptation to sediment of this cuticular appendage remains to be explored.

Moreover, species with shortened and widened LTS were mostly found in sediments with more content in organic nitrogen and more likely of marine origin, whereas species with slender and narrowed LTS were mainly found in sediments with more content in organic carbon and a significant input of terrestrial organic matter. The different proportions of carbon and nitrogen influence the abundance and composition of the micro and meiobenthos communities, influencing in the possible food sources for kinorhynchs and the complex biological

interactions between the different taxa, and this could lead to the observed differences in LTS shape, rather than carbon and nitrogen affecting the physical properties of the sediment[8].

Finally, a relationship between LTS' size and three sediment variables (sorting, skewness and kurtosis) was found. Thus, larger LTS are related to sediments with many different size categories (heterogeneous) and a certain dominance of finer categories, while species with smaller LTS inhabit more homogeneous sediments with a certain dominance of coarser categories. Heterogeneous grain size distributions in marine sediments is usually linked to dynamic, intensely eroded areas, as mentioned above, or influenced by processes of bioturbation[41]. Additionally, heterogeneous sediments possess a more efficient grain packing than homogeneous sediments of similar size[42]. Sediment packing influences the amount of water that can be stored in sediment and its ease of circulation, the degree to which dissolved materials can be hosted and the strength of the sediment under shearing load[43]. In this context, the presence of larger LTS in such heterogeneous sediments, with more dynamism of sea-water circulation and bioturbation processes together with a larger amount of organic matter and other dissolved materials that may hinder movements, could facilitate the displacement of the animal through the interstices and furthermore favour its anchoring to the sediment particles if needed.

None of the sediment variables showed a significant influence on the primary spinoscalids shape. This result is striking taking into account that scalids are the main kinorhynch appendages used for displacement[25] and consequently they should be influenced by sediment structure and composition. However, this could be explained by the lower sample size of primary spinoscalids' micrographs ($n = 22$) compared to that of body shape ($n = 127$) and LTS ($n = 99$).

Methods

Sampling and dataset. Samplings were done using a meiobenthic dredge in two different campaigns: one around the Iberian Peninsula, from February to November 2011 (22 localities), and one off Jamaica, in March 1976 (three localities). Samples from the Iberian Peninsula were collected by Dr J. Benito, Dr M. Herranz, Dr F. Pardos and Dr N. Sánchez in three main regions: Algeciras Bay (western Mediterranean Sea), Cádiz and Isla Cristina, Huelva (north-eastern Atlantic Ocean), whereas samples from Jamaica were collected by Dr R. P. Higgins in Kingston Harbor (Caribbean Sea). For a complete list of species, number of specimens per species and data on sampling localities see Supplementary Information. Dredges are really useful for collecting large samples of meiofaunal organisms rather than more quantitative methods such as corers that usually collect too low numbers of specimens, but they may present some problems when applying granulometric methods in the collected sediment. Meiobenthic dredges cannot be always related to sediment area, because they usually mix the different patches of sediment that are in a certain area, but we tried to minimize this bias by getting the dredge in circles around the same area of sediment and selecting the sampled areas following nautical charts of bottom sea sediments to only sample in those locations with a rather homogeneous sediment (not split into patches).

Each sediment sample was firstly used to extract meiofaunal organisms by the bubble-and-blot method, then fixed and preserved in a neutralised formalin solution to prevent the organic matter from decaying, for granulometric, organic matter and pH analyses. A total of 127 kinorhynch specimens of the two extant classes (Allomalorhagida, $n = 62$; Cyclorhagida, $n = 65$) were obtained and studied, including representatives of three families (allomalorhagid Dracoderidae, $n = 3$, and Pycnophyidae, $n = 59$; cyclorhagid Echinoderidae, $n = 65$) accommodated into five genera (*Dracoderes*, $n = 3$; *Echinoderes*, $n = 65$; *Leiocanthus*, $n = 2$; *Pycnophyes*, $n = 16$; *Setaphyes*, $n = 41$). It must be noticed the lack of part of the diversity of the phylum Kinorhyncha in the studied samples, including the allomalorhagid families Franciscideridae and Neocentrophyidae, and the cyclorhagid orders Kentrorhagata and Xenosomata. Indeed, the results herein obtained are only applicable to the allomalorhagid families Dracoderidae and Pycnophyidae, and the cyclorhagid order Echinorhagata, which are, on the other hand, the species-richest taxa within Kinorhyncha.

Photography. Light micrographs of kinorhynch specimens were obtained using an Olympus DP-70 camera attached to an Olympus BX51-P microscope with differential interference contrast (DIC) optics. We followed the subsequent cautions to avoid different kind of biases. Firstly, only adult males were photographed to eliminate morphological variance due to sex and/or developmental stage. We selected males instead of females to have a higher number of sediment samples.

Regarding photographic distortions, we minimized measurement shape errors due to 2D photographs limitations by selecting only those specimens that were as flattened as possible[44]. 2D photographs obscure the variance of a dataset as they eliminate the Z dimension of depth variability[45–48]. The referred flattening does not influence the structures whose morphological variation we wanted to analyse (*i.e.* sternal plates, LTS and primary spinoscalids), since they are in themselves quite flattened (for further information see below *Geometric morphometrics* subsection). Therefore, those specimens that had not been sufficiently flattened during the mounting process for light microscopy (LM) were discarded. Furthermore, barrel and pincushion distortions may appear when taking a photograph, causing the centre of straight lines to bow out toward or bend inward the edges of the image respectively[49]. We avoided the use of different cameras and lenses as well as changing the camera settings and the placement of the specimens near the margins of the photograph to evade the aforementioned distortions.

Sediment structure and composition. Sediment samples, originally preserved in a neutralized formalin solution, were air-dried to remove remains of formalin. Sediment granulometry and pH in H_2O were determined following the methods of Guitián & Carballas[50]. Particle size scales applied in the present study follow those adopted by Blott & Pye[51]. According to this criteria, gravel is defined as particles >2 mm diameter, sand as particles from 2 mm to 63 µm, and silt (*i.e.* mud) as particles from 63 µm to 4 µm[51]. Particles defined as clay (<4 µm) were not found in any of the analysed samples, so the term mud used hereinafter refers to silt particles. In each of these main categories of

sediment, a series of subclasses were defined to cover the different grain size intervals[51], which are frequently used in marine sediment works. Four parameters were used to describe grain size distribution: average size, sorting, skewness and kurtosis. Sorting is the spread of the sizes around the average, skewness describes the preferential spread to one side of the average and kurtosis analyses the degree of concentration of the grains relative to the average. The software Gradistat v.8[52] was used to obtain the aforementioned parameters by the Folk & Ward method[53]. The method of moments for calculation of average, sorting, skewness and kurtosis was disregarded as it is enormously affected by outliers and should not be used unless the complete size distribution of sediment grains is fully known[54].

Total nitrogen content (N) was determined using the Kjeldahl method as described by Page *et al*.[55], and that of organic carbon (C) by the method of Anne[56] adapted for a microplate reader. Finally, the C/N ratio was calculated. For a summary of granulometry, organic matter content and pH values per sample see Supplementary Information.

Geometric morphometrics. Body, LTS and primary spinoscalids shape and size were analysed independently through geometric morphometrics. The software tpsUtil v.3.2 was used to build the tps files[57]. Placing of landmarks was done using the software tpsDig v.2.31[57]. For body shape, a total of 23 Cartesian landmarks were placed to extract the sternal plates morphology as reflection of body shape. When kinorhynchs are mounted for LM, the final shape of the body can be strongly biased by the force used to flatten the specimens in order to make the taxonomic characters more visible[25]. However, sternal plates' morphology is not affected by this process, and hence they turn out as the best suitable feature to study general body shape in kinorhynchs. Landmarks 1–22 were positioned in each segment at the anterior margin of the pachycycli where tergal and sternal plates joint, whereas landmark 23 was placed at the posterior joint of the sternal plates of segment 11 (Fig. 5A,B). For species with a single, ring-like cuticular plate at the first trunk segment (*e.g*. genera *Echinoderes* and *Dracoderes*), landmarks were placed at the base of the two placids that are closest to the midventral placid (Fig. 5B). For species with a single, ring-like cuticular plate also at the second trunk segment (*e.g*. genus *Echinoderes*), landmarks were placed at the anterior margin of the pachycycli that is immediately above the lateroventral/ventrolateral tubes (Fig. 5B). For LTS' shape, a total of three Cartesian landmarks were used to extract their morphology. Two landmarks were placed at the base of the spine, while the third one was positioned at the tip (Fig. 5C). For primary spinoscalids' shape, six Cartesian landmarks were used: two at the base of the scalid, two at the junction between the basal sheath and the tip, and two at the tip of the scalid (Fig. 5D). Only primary spinoscalids laterally placed (Fig. 5D) were used in order to have all the photographs equally oriented.

MorphoJ v.1.07a software[58] was used to superimpose the resulting landmark configuration by Generalized Procrustes analysis and to compute CS as the square root of the summed squared distances of each Cartesian landmark from the centroid of the landmark configuration. CS values are the only measurement independent of shape and represent the overall size of each studied structure[59]. For body shape, the Generalized Procrustes analysis was run taking into account the bilateral symmetry of kinorhynchs, defining a symmetric and an asymmetric component of the variation[58]. A prior series of multiple linear regression of Procrustes coordinates onto CS were used to test for allometry (*i.e*. influence of size on shape) as defined by Monteiro[60]. Influence of allometry was found in the symmetric component of body shape ($r^2 = 0.2501$; $p < 0.001$) and in the LTS' analysis ($r^2 = 0.4228$; $p < 0.001$). Therefore, residuals of the regression were used instead of the raw coordinates in the subsequent analyses to correct for the allometric influence[61]. Principal component analyses (PCA) and wireframe graphs were performed to visualize the patterns of shape changes for each component.

Statistical analyses. All the statistical analyses were implemented in R v.3.0.1. We firstly tested for correlation of sediment variables using the Kendall rank correlation coefficient[62] with the *ggpubr* package[63]. Percentages of the three main categories of size particles were removed from the variables because of correlation: % of gravel correlated with average size (*tau* = 0.51; p = 0.01), % of sand with average size (*tau* = 0.47; p = 0.02), sorting (*tau* = −0.43; p = 0.03) and pH (*tau* = −0.40; p = 0.05), and % of mud with average size (*tau* = 0.57; p < 0.001), sorting (*tau* = 0.42; p = 0.03) and C/N (*tau* = 0.57; p = 0.03).

A series of linear mixed models (LMM) were used to assess the effect of the sediment structure and composition on body, LTS and primary spinoscalids shape. To control the effect of the phylogeny in our species dataset, we extract the phylogenetic information from Linnaean taxonomy using a nested structure in the random-effect component of the LMMs[64]. PC scores of the main PCA axes that define the variation in shape among individuals in geometric morphometrics were used as the response variables of the LMMs, whereas the sediment variables (average size, sorting, skewness and kurtosis) were set as the fixed-effect component. LMMs were performed using the *nlme* and *lme4* packages[65,66]. Marginal and conditional R^2 were calculated for each LMM using the *MuMIn* package[67].

When the assumptions of the LMMs were violated (*i.e*. absence of correlation in the residuals, homoscedasticity and normal distribution of the residuals), a series of generalized linear mixed models (GLMMs) were run. The Durbin-Watson, Breusch-Pagan and Shapiro-Wilk tests were used to check for correlation in the residuals, homoscedasticity and normal distribution of the residuals respectively, using the *lmtest* package[68]. GLMMs were run using the *glmmADMB* package[69].

Data availability

All data generated or analysed during this study are available from the corresponding author on reasonable request or included in this published article (and its Supplementary Information Files).

Received: 25 September 2019; Accepted: 28 January 2020;
Published online: 13 February 2020

References

1. Pigliucci, M. Phenotypic plasticity in *Evolutionary ecology: concepts and case studies* (eds. Fox, C.W., Roff, D.A. & Fairbairn, D.J.) 58–69 (Oxford University Press, 2001).
2. Kelly, S. A., Panhuis, T. M. & Stoehr, A. M. Phenotypic plasticity: molecular mechanisms and adaptive significance. *Compr. Physiol.* **2**, 1417–1439, https://doi.org/10.1002/cphy.c110008 (2012).
3. Karr, J. R. & James, F. C. *Eco-morphological configurations and convergent evolution in species and communities*. *Ecology and evolution of communities*. (Harvard University Press, 1975).
4. Bock, W. J. Concepts and methods in ecomorphology. *J. Biosci*. **19**, 403–413, 0.1007/BF02703177 (1994).
5. Pigliucci, M. Evolution of phenotypic plasticity: where are we going now? *Trends in Ecol. Evol.* **20**, 481–486, https://doi.org/10.1016/j.tree.2005.06.001 (2005).
6. Marques, N. C. S., Rattis, L. & Nomura, F. Local environmental conditions affecting anural tadpoles' microhabitat choice and morphological adaptation. *Mar. Freshwater Res.* **70**, 395–401, https://doi.org/10.1071/MF18106 (2018).
7. Giere, O. Habitat, habitat conditions and their study methods in *Meiobenthology: the microscopic fauna in aquatic sediments* (ed. Giere, O.) 5–43 (Springer-Verlag, 2009).
8. Giere, O., Eleftheriou, A. & Murison, D. J. Abiotic Factors in *Introduction to the study of meiofauna* (eds. Higgins, R. P. & Thiel, H.) 61–78 (Smithsonian Institution Press, 1988).
9. Fonseca, G. *et al*. Testing for nematode-granulometry relationships. *Mar. Biodivers.* **44**, 435–443, https://doi.org/10.1007/s12526-014-0241-4 (2014).
10. Levinton, J. S. Benthic life habitats in *Marine biology: function, biodiversity, ecology* (ed. Levinton, J. S.) 245–267 (Oxford University Press, 2017).
11. Wieser, W. The effect of grain size on the distribution of small invertebrates inhabiting the beaches of Puget Sound. *Limnol. Oceanogr.* **4**, 181–194, https://doi.org/10.4319/lo.1959.4.2.0181 (1959).
12. Hicks, G. R. F. & Coull, B. C. The ecology of marine meiobenthic harpacticoid copepods. *Oceanogr. Mar. Biol.* **21**, 67–175 (1983).
13. Heip, C. H. R., Vincx, M. & Vranken, G. The ecology of marine nematodes. *Oceanogr. Mar. Biol.* **23**, 399–489 (1985).
14. Tita, G., Vincx, M. & Desrosiers, G. Size spectra, body width and morphotypes of intertidal nematodes: an ecological interpretation. *J. Mar. Biol. Ass. U. K.* **79**, 1007–1015, https://doi.org/10.1017/S0025315499001241 (1999).
15. Vanaverbeke, J., Merckx, B., Degraer, S. & Vincx, M. Sediment-related distribution patterns of nematodes and macrofauna: two sides of the benthic coin? *Mar. Environ. Res.* **71**, 31–40, https://doi.org/10.1016/j.marenvres.2010.09.006 (2011).
16. Martens, P. M. & Schockaert, E. R. The importance of turbellarians in the marine meiobenthos: a review. *Hydrobiologia* **132**, 295–303 (1986).
17. Urban-Malinga, B. Meiobenthos in marine coastal sediments in *Sedimentary coastal zones from high to low latitudes: similarities and differences* (eds. Martini, I. P. & Wanless, H. R.) 59–78 (Berforts Information, 2014).
18. Traunspurger, W. & Majdi, N. Meiofauna in *Methods in Stream Ecology* (eds. Hauer, F. & Lamberti G.) 273-295 (Elsevier, 2017).
19. Greiser, N. & Faubel, A. Biotic Factors in *Introduction to the study of meiofauna* (eds. Higgins, R. P. & Thiel, H.) 79–114 (Smithsonian Institution Press, 1988).
20. Dainez-Filho, M. S. *et al*. Role of sediment structuring by detritus on colonization and interspecific competition of one native and one invasive submerged macrophyte. *Hydrobiologia* **834**, 63–74, 0.1007/s10750-019-3909-8 (2019).
21. Graf, G. *et al*. The importance of the spring phytoplankton bloom for the benthic system of Kiel Bight. *Rapp. P.-V. Réun. Cons. Int. Explor. Mer* **183**, 136–143 (1984).
22. Burone, L., Muniz, P., Pires-Vanin, A. M. S. & Rodrigues, M. Spatial distribution of organic matter in the surface sediments of Ubatuba Bay (Southeastern Brazil). *An. Acad. Bras. Ciênc.* **75**, 77–90, https://doi.org/10.1590/S0001-37652003000100009 (2003).
23. LeCadre, V., Debenay, J. P. & Lesourd, M. Low pH effects on *Ammonia beccarii* test deformation: implications for using test deformations as a pollution indicator. *J. Foramin. Res.* **33**, 1–9, https://doi.org/10.2113/0330001 (2003).
24. Sørensen, M. V. & Pardos, F. Kinorhynch systematics and biology – An introduction to the study of kinorhynchs, inclusive identification keys to the genera. *Meiofauna Marina* **16**, 21–73 (2008).
25. Neuhaus, B. Kinorhyncha (=Echinodera) in *Handbook of Zoology, Gastrotricha, Cycloneuralia and Gnathifera, Volume 1: Nematomorpha, Priapula, Kinorhyncha, Loricifera* (ed. Schmidt-Rhaesa, A.) 181–348 (De Gruyter, 2013).
26. Faganelli, J., Malej, A., Pezdic, J. & Malacic, V. C: N:P ratios and stable C isotopic ratios as indicator of sources of organic matter in the Gulf of Trieste (northern Adriatic). *Oceanologia* **11**, 377–382 (1988).
27. McCave, I. & Hall, I. R. Size sorting in marine muds: processes, pitfalls, and prospects for paleoflow-speed proxies. *Geochem. Geophys. Geosy.* **7**, Q10N05, https://doi.org/10.1029/2006GC001284 (2006).
28. Thomsen, L. & Gust, G. Sediment erosion thresholds and characteristics of re-suspended aggregates on the western European continental margin. *Deep-Sea Res. Pt. I* **47**, 1881–1897, https://doi.org/10.1016/S0967-0637(00)00003-0 (2000).
29. Bao, R., Blattmann, T. M., McIntyre, C., Zhao, M. & Eglinton, T. I. Relationships between grain size and organic carbon ^{14}C heterogeneity in continental marine sediments. *Earth Planet. Sc. Lett.* **505**, 76–85, https://doi.org/10.1016/j.epsl.2018.10.013 (2019).
30. Yamasaki, H. *Gracilideres mawatarii*, a new genus and species of Franciscideridae (Allomalorhagida: Kinorhyncha) – A kinorhynch with thin body cuticle, adapted to the interstitial environment. *Zool. Anz.* **282**, 176–188, https://doi.org/10.1016/j.jcz.2019.05.010 (2019).
31. Daloso, D. M. The ecological context of bilateral symmetry of organ and organisms. *Nat. Sci.* **6**, 1–7, https://doi.org/10.4236/ns.2014.64022 (2014).
32. Barry, J. P. *et al*. Effects of direct ocean CO_2 injection on deep-sea meiofauna. *J. Oceanogr.* **60**, 759–766, https://doi.org/10.1007/s10872-004-5768-8 (2004).
33. Carman, K. R., Thistle, D., Fleeger, J. W. & Barry, J. P. Influence of introduced CO_2 on deep-sea metazoan meiofauna. *J. Oceanogr.* **60**, 767–772, https://doi.org/10.1007/s10872-004-5769-7 (2004).
34. Thistle, D. *et al*. Simulated sequestration of industrial carbon dioxide at a deep-sea site: effects on species of harpacticoid copepods. *J. Exp. Mar. Biol. Ecol.* **330**, 151–158, https://doi.org/10.1016/j.jembe.2005.12.023 (2006).
35. Zeppilli, D. *et al*. Is the meiofauna a good indicator for climate change and anthropogenic impacts? *Mar. Biodivers.* **45**, 505–535, https://doi.org/10.1007/s12526-015-0359-z (2015).
36. Bhadury, P. Effects of ocean acidification on marine invertebrates – a review. *Indian J. Mar. Sci.* **44**, 454–464 (2015).
37. Mustafa, S., Kharudin, S. N. & Kian, A. Y. S. Effect of simulated ocean acidification on chitin content in the shell of white shrimp. *Litopenaeus vannamei. Iran. J. Fish. Sci.* **9**, 6–9 (2015).
38. Kristensen, R. M. & Higgins, R. P. Kinorhyncha in *Microscopic Anatomy of Invertebrates, Volume 4:* Aschelminthes (eds. Harrison, F.W. & Ruppert, E.E.), 377–404 (Wiley-Liss Press, 1991).
39. Herranz, M., Boyle, M.J., Pardos, F. & Neves, R.C. Comparative myoanatomy of *Echinoderes* (Kinorhyncha): a comprehensive investigation by CLSM and 3D reconstruction. *Front. Zool.* **11**, 31, 10.1186/1742-9994-11-31 (2014).
40. Altenburger, A. The neuromuscular system of *Pycnophyes kielensis* (Kinorhyncha: Allomalorhagida) investigated by confocal laser scanning microscopy. *EvoDevo* **7**, 25, https://doi.org/10.1186/s13227-016-0062-6 (2016).
41. Cozzoli, F. *et al*. The combined influence of body size and density on cohesive sediment resuspension by bioturbators. *Sci. Rep.* **8**, 3831, https://doi.org/10.1038/s41598-018-22190-3 (2018).
42. Parker, S. P. *et al*. Effect of particle size and heterogeneity on sediment biofilm metabolism and nutrient uptake scaled using two approaches. *Ecosphere* **9**, e02137, https://doi.org/10.1002/ecs2.2137 (2018).

43. Allen, J. R. L. Packing of sedimentary particles in *Sedimentary Structures Their Character and Physical Basis Volume I* (ed. Allen,J.R.L.), 137–177 (Elsevier, 1982).
44. Bakkes, D. K. Evaluation of measurement error in rotational mounting of larval *Rhipicephalus* (Acari: Ixodida: Ixodidae) species in geometric morphometrics. *Zoomorphology* **136**, 403–410, https://doi.org/10.1007/s00435-017-0357-8 (2017).
45. Arnqvist, G. & Martensson, T. Measurement error in geometric morphometrics: empirical strategies to assess and reduce its impact on measures of shape. *Acta Zool. Acad. Sci. H.* **44**, 73–96 (1998).
46. Palmer, A. R. Fluctuating asymmetry analyses: A Primer in *Developmental Instability: Its Origins and Evolutionary Implications. Contemporary Issues in Genetics and Evolution Volume 2* (ed. Markow, T. A.), 543–548 (Springer, 1994).
47. Cardini, A. Missing the third dimension in geometric morphometrics: how to assess if 2D images really are a good proxy for 3D structures? *Hystrix* **25**(73), 81, https://doi.org/10.4404/hystrix-25.2-10993 (2014).
48. Fruciano, C. Measurement error in geometric morphometrics. *Dev. Genes Evol.* **226**, 139–158, https://doi.org/10.1007/s00427-016- 0537-4 (2016).
49. Collins, K. S. & Gazley, M. F. Does my posterior look big in this? The effect of photographic distortion on morphometric analyses.
Paleobiology **43**, 508–520, https://doi.org/10.1017/pab.2016.48 (2017).
50. Guitián, F. & Carballas, T. *Técnicas de análisis de suelos* (Pico Sacro, 1976).
51. Blott, S. J. & Pye, K. Particle size scales and classification of sediment types based on particle size distributions: review and recommended procedures. *Sedimentology* **59**, 2071–2096, https://doi.org/10.1111/j.1365-3091.2012.01335.x (2012).
52. Blott, S. J. & Pye, K. Gradistat: A grain size distribution and statistics package for the analysis of unconsolidated sediments. *Earth Surf. Proc. Land.* **26**, 1237–1248, https://doi.org/10.1002/esp.261 (2001).
53. Folk, R. L. & Ward, W. C. Brazos River bar: a study in the significance of grain size parameters. *J. Sediment. Petrol.* **27**, 3–26 (1957).
54. McManus, J. Grain size determination and interpretation in *Techniques in Sedimentology* (ed. Tucker, M.), 63–85 (Blackwell, 1988).
55. Page, A. L., Miller, R. K. & Keeney, D. R. *Methods in soil analysis. Part 2: Chemical and microbiological properties* (Madison, 1982).
56. Anne, P. Sur le dosage rapid du carbone organique des sols. *Annales de Agronomie* **2**, 162–172 (1945).
57. Rohlf, F. J. The tps series of software. *Hystrix* **26**, 9–12, https://doi.org/10.4404/hystrix-26.1-11264 (2015).
58. Klingenberg, C. P. MorphoJ: an integrated software package for geometric morphometrics. *Mol. Ecol. Res.* **11**, 353–357, https://doi. org/10.1111/j.1755-0998.2010.02924.x (2011).
59. Verhaegen, G., Neiman, M. & Haase, M. Ecomorphology of a generalist freshwater gastropod: complex relations of shell morphology, habitat, and fecundity. *Org. Divers. Evol*. **18**, 425-441, 10.1007s13127-018-0377-3 (2018).
60. Monteiro, L. R. Multivariate regression models and geometric morphometrics: the search for casual factors in the analysis of shape.
Syst. Biol. **48**, 192–199 (1999).
61. Klingenberg, C. P. Size, shape, and form: concepts of allometry in geometric morphometrics. *Develop. Genes Evol.* **226**, 113–137, https://doi.org/10.1007/s00427-016-0539-2 (2016).
62. Kendall, M. A New Measure of Rank Correlation. *Biometrika* **30**, 81–89, https://doi.org/10.1093/biomet/30.1-2.81 (1938).
63. Kassambara, A. & R Core Team. *The Comprehensive R Archive Network*, https://cran.r-project.org/web/packages/ggpubr/ (2019).
64. Holt, B. J. & Jønsson, K. A. Reconciling hierarchical taxonomy with molecular phylogenies. *Syst. Biol.* **63**, 1010–1027, https://doi. org/10.1093/sysbio/syu061 (2014).
65. Bates, D., Maechler, M., Bolker, B. & Walker, S. Fitting Linear Mixed-Effects Models Using lme4. *J. Stat. Softw.* **67**, 1–48, https://doi.org/10.18637/jss.v067.i01 (2015).
66. Pinheiro, J., Bates, D., DebRoy, S., Sarkar, D. & R Core Team. *The Comprehensive R Archive Network*, https://CRAN.R-project.org/ package=nlme (2019).
67. Bartoń, K. & R Core Team (2019) *The Comprehensive R Archive Network*, https://cran.r-project.org/web/packages/MuMIn/ (2019).
68. Hothorn, T. *et al*. *The Comprehensive R Archive Network*, https://CRAN.R-project.org/package=lmtest (2019).
69. Bolker, B., Skaug, H., Magnusson, A. & Nielsen, A. *The glmmADMB package – R*, http://glmmadmb.r-forge.r-project.org/ glmmADMB (2012).

Acknowledgements

D.C. was supported by a predoctoral fellowship of the Complutense University of Madrid (CT27/16-CT28/16).

Author contributions

D.C., F.P. and N.S. conceived the general idea of the study, D.C. and D.T. conducted the experimental process and D.C. analysed the results. All authors reviewed the manuscript.

Competing interests

The authors declare no competing interests.

Additional information

Supplementary information is available for this paper at https://doi.org/10.1038/s41598-020-59511-4.

Correspondence and requests for materials should be addressed to D.C.

Reprints and permissions information is available at www.nature.com/reprints.

Publisher's note Springer Nature remains neutral with regard to jurisdictional claims in published maps andinstitutional affiliations.

Supplementary Information.

Supplementary Material 1. Information on sampling stations and species and number of specimens per species found in each locality that were used in the present study. Abbreviations: *n*, number of specimens per species.

Locality	Date	Coordinates	Depth	Species	*n*
Algeciras Bay 1	11.02.07	36º05.805'N 5º26.284'W	30	*Echinoderes cantabricus*	1
				Echinoderes hispanicus	4
				Echinoderes sp. 1	6
Algeciras Bay 2	11.02.07	36º07.229'N 5º25.114'W	24	*Echinoderes sp. 1*	3
Algeciras Bay 3	11.02.08	36º09.272'N 5º26.296'W	12	*Echinoderes hispanicus*	1
				Setaphyes dentatus	8
Algeciras Bay 4	11.02.08	36º10.348'N 5º26.464'W	16	*Dracoderes gallaicus*	3
Algeciras Bay 5	11.02.08	36º10.583'N 5º24.620'W	25	*Echinoderes cantabricus*	2
Algeciras Bay 6	11.02.08	36º10.741'N 5º23.243'W	8	*Echinoderes dujardinii*	1
				Echinoderes hispanicus	1
				Setaphyes dentatus	3
Algeciras Bay 7	11.02.08	36º09.630'N 5º22.256'W	12	*Echinoderes dujardinii*	2
				Echinoderes hispanicus	6
Isla Cristina 1	11.04.11	37º11.940'N 7º21.236'W	2	*Echinoderes dujardinii*	2
				Setaphyes dentatus	1
Isla Cristina 2	11.04.11	37º10.963'N 7º16.549'W	11	*Pycnophyes communis*	2
				Setaphyes dentatus	6
Isla Cristina 3	11.04.11	37º11.527'N 7º14.601'W	12	*Setaphyes dentatus*	5
Isla Cristina 4	11.04.11	37º12.320'N 7º20.534'W	4	*Setaphyes dentatus*	5
Isla Cristina 5	11.04.11	37º11.887'N 7º13.019'W	7	S*etaphyes dentatus*	6
Isla Cristina 6	11.04.12	37º08.324'N 7º20.308'W	15	*Pycnophyes communis*	2
Cádiz 1	11.11.10	36º33.755'N 6º18.500'W	13	*Leiocanthus lageria*	1
				Pycnophys communis	7
				Setaphyes dentatus	2
Cádiz 2	11.11.10	36º35.791'N 6º17.888'W	10	*Setaphyes dentatus*	3

Cádiz 3	11.11.10	36º34.117'N	7	*Echinoderes dujardinii*	1
		6º15.141'W		*Pycnophyes communis*	1
				Setaphyes dentatus	1
Cádiz 4	11.11.10	36º32.761'N	11	*Echinoderes hispanicus*	2
		6º15.141'W		*Pycnophyes almansae*	1
				Pycnophyes communis	3
				Setaphyes dentatus	1
Cádiz 5	11.11.10	36º32.310'N	4	*Echinoderes worthingi*	1
		6º14.245'W			
Cádiz 6	11.11.10	36º31.930'N	4	*Echinoderes dujardinii*	2
		6º12.960ºW		*Echinoderes worthingi*	1
Cádiz 7	11.11.11	36º31.124'N	11	*Echinoderes dujardinii*	2
		6º15.692'W		*Echinoderes hispanicus*	1
				Echinoderes sp. 1	1
Cádiz 8	11.11.11	36º28.304'N	4	*Echinoderes hispanicus*	1
		6º10.936'W			
Cádiz 9	11.11.11	36º29.798'N	1	*Echinoderes cantabricus*	4
		6º12.871'W		*Echinoderes hispanicus*	1
				Leiocanthus lageria	1
Kingston	76.03.10	17º56.24'N	2	*Echinoderes imperforatus*	1
Harbor 1		76º50.00'W		*Echinoderes parahorni*	1
				Echinoderes sp. 2	2
Kingston	76.03.10	17º56.30'N	1	*Echinoderes parahorni*	3
Harbor 2		76º49.12'W		*Echinoderes sp. 2*	3
Kingston	76.03.11	17º57.18'N	4	*Echinoderes astridae*	6
Harbor 3		76º50.24'W		*Echinoderes parahorni*	3

Supplementary Material 2

Table 1. Granulometry of sediment samples. Abbreviations: *K*, kurtosis; *Sk*, skewness; *X*, average size; σ, sorting.

Sample	**Textural group**	**%Gravel**	**%Sand**	**%Mud**	**X**	***σ***	***Sk***	***K***
Algeciras Bay 1	Slightly gravelly sand	0.6	91.,6	7.8	229.5	3.488	-0.262	2.103
Algeciras Bay 2	Muddy sandy gravel	66.8	23.5	9.8	1353.9	3.699	-1.644	4.463
Algeciras Bay 3	Slightly gravelly sand	0	93.1	6.9	133.7	3.007	-0.301	2.536
Algeciras Bay 4	Sligthly gravelly sandy mud	0	31.2	68.8	10.42	7.011	0.286	0.557
Algeciras Bay 5	Sligthly gravelly sandy mud	0	49.9	50.1	23.56	7.072	-0.566	0.519
Algeciras Bay 6	Sligthly gravelly sand	0.1	94.9	5	210.5	1.918	-0.273	0.869
Algeciras Bay 7	Gravelly sand	9.5	82.5	7.9	292.3	4.313	0.024	2.254
Cádiz 1	Sligthly gravelly muddy sand	0	88.6	11.4	126.3	1.712	-0.325	0.923
Cádiz 2	Sligthly gravelly muddy sand	0	82.7	17.3	99.54	2.725	-0.269	2.679
Cádiz 3	Sligthly gravelly muddy sand	0	82.6	17.4	101.9	2.735	-0.268	2.674
Cádiz 4	Sligthly gravelly sand	0	95.8	4.2	199.4	1.863	-0.081	0.954
Cádiz 5	Sligthly gravelly sand	0	92.8	7.1	140.9	2.531	-0.373	2.22
Cádiz 6	Gravelly sand	7.2	88.6	4.1	327.8	2.638	0.038	2.368
Cádiz 7	Sligthly gravelly sand	2.4	90.5	7.1	305.2	2.798	-0.415	3.384
Cádiz 8	Sligthly gravelly sandy mud	0	41.8	58.1	16.06	8.372	0.181	0.537
Cádiz 9	Sligthly gravelly mud	3.2	4.7	92.1	19.85	3.146	-0.389	2.152
Isla Cristina 1	Muddy gravel	38.9	11.1	50	56.96	16.54	-0.088	0.594

Isla Cristina 2	Sligthly muddy sand	gravelly	3.2	80.9	15.9	108.6	2.658	-0.164	2.301
Isla Cristina 3	Sligthly muddy sand	gravelly	0	86.7	13.3	114.3	1.677	-0.005	0.778
Isla Cristina 4	Sligthly sand	gravelly	0	93.5	6.5	163.9	2.238	-0.15	1.103
Isla Cristina 5	Sligthly muddy sand	gravelly	0	86.6	13.4	122.7	1.901	0.138	0.913
Isla Cristina 6	Gravelly mud		7.2	15.7	77.1	19.52	7.639	-0.036	1.541
Kingston Harbor 1	Sligthly sandy mud	gravelly	0	11	89	9.502	4.639	-0.225	0.609
Kingston Harbor 2	Sligthly mud	gravelly	0	2.8	97.2	27.52	2.09	-0.437	2.367
Kingston Harbor 3	Sligthly muddy sand	gravelly	0	59.9	40	49.44	3.715	-0.468	1.198

Table 2. Organic matter content and pH of sediment samples. Abbreviations: *C*, carbon; C/N, carbon-nitrogen ratio, *N*, nitrogen; *NC*, not calculated.

Sample	**%$_C$**	**%$_N$**	**C/N**	**pH**
Algeciras Bay 1	0.8624	0.0423	20.39	8.311
Algeciras Bay 2	1.0984	0.0849	12.94	8.883
Algeciras Bay 3	0.3722	0.0204	18.25	8.084
Algeciras Bay 4	2.2821	0.1821	12.53	6.691
Algeciras Bay 5	2.2356	0.1649	13.56	6.677
Algeciras Bay 6	0.3397	0.0141	24.09	8.311
Algeciras Bay 7	0.6805	0.0646	10.53	8.883
Cádiz 1	0.4309	0.0359	12	8.349
Cádiz 2	0.4633	0.0193	24.01	8.432
Cádiz 3	0.7522	0.0246	30.58	8.027
Cádiz 4	0.5392	0.0157	34.34	8.293
Cádiz 5	0.5452	0.0089	61.26	8.403
Cádiz 6	0.8622	0.0171	50.42	8.219
Cádiz 7	0.6309	0.0377	18.72	8.252
Cádiz 8	1.8445	0.0789	23.38	7.419
Cádiz 9	*NC*	*NC*	*NC*	7.681
Isla Cristina 1	1.2274	0.0758	16.19	7.543
Isla Cristina 2	0.6058	0.0312	19.42	7.942

Isla Cristina 3	0.3232	0.0158	20.46	7.775
Isla Cristina 4	0.4708	0.0195	24.14	8.081
Isla Cristina 5	0.3717	0.0234	15.88	8.3
Isla Cristina 6	1.5441	0.1415	10.91	6.84
Kingston Harbor 1	*NC*	*NC*	*NC*	7.53
Kingston Harbor 2	5.3474	0.6932	7.71	*NC*
Kingston Harbor 3	4.3655	0.2906	15.02	7.877

Organisms Diversity & Evolution (2021) 21:43–58
https://doi.org/10.1007/s13127-020-00471-y

ORIGINAL ARTICLE

From biggest to smallest mud dragons: size-latitude trends in a group of meiobenthic animals worldwide

Diego Cepeda[1] & Fernando Pardos[1] & Nuria Sánchez[1]

Received: 25 June 2020 / Accepted: 19 November 2020 / Published online: 6 January 2021

Abstract

Size-latitude trends in the meiobenthic phylum Kinorhyncha, commonly known as mud dragons, have been explored in oceans worldwide. Generalized least squares regression was used to assess relationships between size and latitude, as well as between size, latitude, and two selected environmental variables that exhibit latitudinal gradation: the sea surface temperature and the net primary productivity. Different structures of spatial autocorrelation and potential confounding factors, such as the species richness and the number of kinorhynch records that could affect latitudinal gradients, were also addressed. In addition, generalized mixed models were used to determine the influence of the phylogeny on body size. Size-latitude relationships of Kinorhyncha were commonly found globally, as well as for particular geographic regions (hemispheres and/or coastlines), with important differences between taxonomic groups. These size-latitude trends were heterogeneous and implied the influence of the latitude itself, environmental variables, and phylogeny. These facts indicate that a single underlying process is not likely to explain the observed relationships but a complex interaction of several macroecological patterns both present and past. Perhaps, the inclusion of future new reports, conducted in undersampled areas, may shed some light on the matter and reveal more generalized size-latitude patterns. Nevertheless, it is also likely that broadly generalizable size-latitude relationships may not exist in meiofaunal communities.

Keywords Meiofauna · Kinorhyncha · Macroecological patterns · Biogeography · Sea surface temperature · Net primary productivity

Introduction

Metazoan body size is a relevant biological feature due to its ecological implications on metabolism, physiology, life history traits, and population dynamics (Peters 1983; Brown 1995; McClain and Rex 2001; Smith and Brown 2002). Ecological patterns in body size have been studied for a wide variety of taxa, with special focus on terrestrial and freshwater ecosystems (Lindsey 1966; Belk and Houston 2002; Ashton and Feldman 2003; Rodríguez et al. 2008; Alho et al. 2010; Zamora-Camacho et al. 2014; Rollinson and Locke 2018; Sargis et al. 2018). However, marine environments have received less attention and these patterns still remain scarcely documented, particularly on small-sized invertebrates (Roy 2002; Young et al. 2006; Cepeda et al. 2020).

Latitude is thought to be one of the main forces modelling body size trends in animals (Bergmann 1848; Allen 1877; Partridge and Coyne 1997; McDowall 2007; Stillwell 2010). Although meiofaunal organisms are frequently disregarded concerning size-latitude relationships (Hillebrand and Azovsky 2001; Fenchel and Finlay 2004; Azovsky and Mazei 2013), a few previous studies showed that they can actually exhibit latitudinal trends (e.g. Armenteros & Ruiz-Abierno 2015; Brun et al. 2016; Bartels et al. 2019). Different hypotheses have been proposed to explain size-latitude trends, which are not necessarily exclusive. Bergmann (1848) postulated that mammal body size positively increases with latitude because larger bodies imply smaller surface area to volume ratios, being metabolically more efficient. This rule has also been proved to agree with size-latitude trends in several ectotherm taxa (Lindsey 1966; Defeo and Cardoso 2002; Ashton and Feldman 2003; Chown and Gaston 2010; Berke et al. 2013; Zamora-Camacho et al.

* Diego Cepeda
diegocepeda@ucm.es

1 Department of Biodiversity, Ecology and Evolution, Complutense University of Madrid (UCM), C/José Antonio Novais, 12, 28040 Madrid, Spain

2014; Saunders and Tarling 2018) in which development may increase more rapidly than somatic growth at higher temperatures, resulting in smaller body sizes at lower latitudes such as the equatorial ones (Chown and Gaston 2010; Arendt 2011; Escribano et al. 2014). Another hypothesis to explain size-latitude trends is based on resource availability (Rosenzweig 1968; Blackburn et al. 1999; Blackburn and Hawkins 2004; Virgós et al. 2011). It postulates that more productive habitats possess greater resources, which could be linked to larger body sizes (Blackburn and Hawkins 2004; McNab 2010). Thus, if productivity shows a latitudinal gradient, this may also drive latitudinal changes in organisms' body size (Cushman et al. 1993; Arnett and Gotelli 2003; Bartels et al. 2019). Thereby, body size may be linked to several biological traits that directly respond to particular environmental variables that change with latitude, showing a masked, indirect latitudinal trend (Blackburn et al. 1999).

Body size is furthermore influenced by genetics and evolutionary trade-offs, which may play a key role in size determination (Crickmore and Mann 2009). Therefore, the observed body size-latitude relationships could be mainly a result of these genetic constraints (Berke et al. 2013). In summary, body size trends are influenced by a complex mix of macroecological patterns, species genetics and evolutionary history.

The main aim of the present paper is to explore these topics by analysing size-latitude trends for a whole phylum of meiofaunal invertebrates, the Kinorhyncha. Kinorhynchs, commonly known as mud dragons, are a group of holobenthic, free-living species whose body size ranges from ca. 200 µm up to 1000 µm, and they inhabit the upper layers of oceanic sediments from polar to equatorial latitudes and from intertidal to hadal depths (Higgins 1988; Neuhaus, 2013; Adrianov and Maiorova 2019; Sørensen and Pardos 2020). Kinorhynchs are characterized by having a body divided into three sections: head, neck and trunk. The head is composed of a mouth cone and an introvert related to feeding and locomotion, and they are retractable structures that can be completely everted or retracted into the body trunk; the neck provides a closure system when the head is fully retracted; the trunk houses the remaining organs and structures of the animal and is typically divided into eleven segments (Higgins 1988; Sørensen and Pardos 2020). The present study supposes a further step in our understanding of macroecological patterns in the latitudinal distribution of exclusive, marine meiofaunal invertebrates using kinorhynchs as a model.

Materials and methods

Occurrence and body size dataset

The geographic occurrence dataset for worldwide kinorhynchs belonging to two classes (Allomalorhagida and Cyclorhagida) and ten families (Antygomonidae, Campyloderidae, Cateriidae, Centroderidae, Dracoderidae, Echinoderidae, Neocentrophyidae, Pycnophyidae, Semnoderidae and Zelinkaderidae) plus two incertae sedis taxa (*Tubulideres* Sørensen, Heiner, Ziemer and Neuhaus, 2017; and *Wollunquaderes* Sørensen and Thormar, 2010) was compiled using the available bibliography with records of Kinorhyncha identified to species level. For each publication, geographical coordinates were extracted and included in the dataset. When two or more records of the same species were found at the same geographical point but in substantially different depths (more than or equal to 10 m of difference) and/or environments, all of them were included in the dataset. We are aware that differences in about 10 m are not necessar-ily substantial in some regions such as the deep sea, but taking into account that most of kinorhynch records are from shallow waters (less than 200 m), we decided to err in favour of coastal reports. The resulting dataset gathered 1371 occurrences of 279 kinorhynch species (Fig. 1, Appendix S1).

Body size value per species was obtained from the following formula: $[\log_2 (\text{length} \times \text{width})^{0.5}]$, where length refers to the mean total length of the trunk and width to the mean width measured at the widest sternal trunk cuticular plates (Fig. 2, Appendix S1). The total trunk length is measured from the anterior margin of the first trunk segment to the final tip of the segment 11 tergal extensions (Fig. 2), which excludes the head and the neck. Even in the few cases when the head is fully everted, this is not taken into consideration while measuring the total trunk length. The maximum sternal width is measured from one edge to another of the widest sternal plates (Fig. 2), whose value is not artificially altered in mounted specimens for light microscopy. Currently, no data on the maximum cross-section height of kinorhynchs is available, because when mounted for light microscopy, kinorhynchs are artificially flattened in order to make the taxonomic characters easily visible. Although some kinorhynch taxa, especially those of the class Cyclorhagida, have a certain natural dorso-ventral compression of the body, others, such as most allomalorhagids, are conspicuously triangular in cross section (Kristensen and Higgins 1991; Sánchez et al. 2011). Nevertheless, the lack of truly reliable and measurable height in most kinorhynchs does not allow us to include it. In addition, the aforementioned formula is thought to reflect well the real body size as it calculates an approximation of the body surface (Fig. 2) and correlates well with biomass (Roy et al. 2000; Kosnik et al. 2006). A similar formula has been used to calculate body size in other benthic organisms that are also quite compressed, such as bivalves (Roy et al. 2000; Kosnik et al. 2006). The logarithmic base 2 transformation is applied to normalize the size-frequency distributions (Roy 2002; Berke et al. 2013). Body size values for each species were calculated for the present study by the authors, but the measures necessary for their calculation were extracted from the

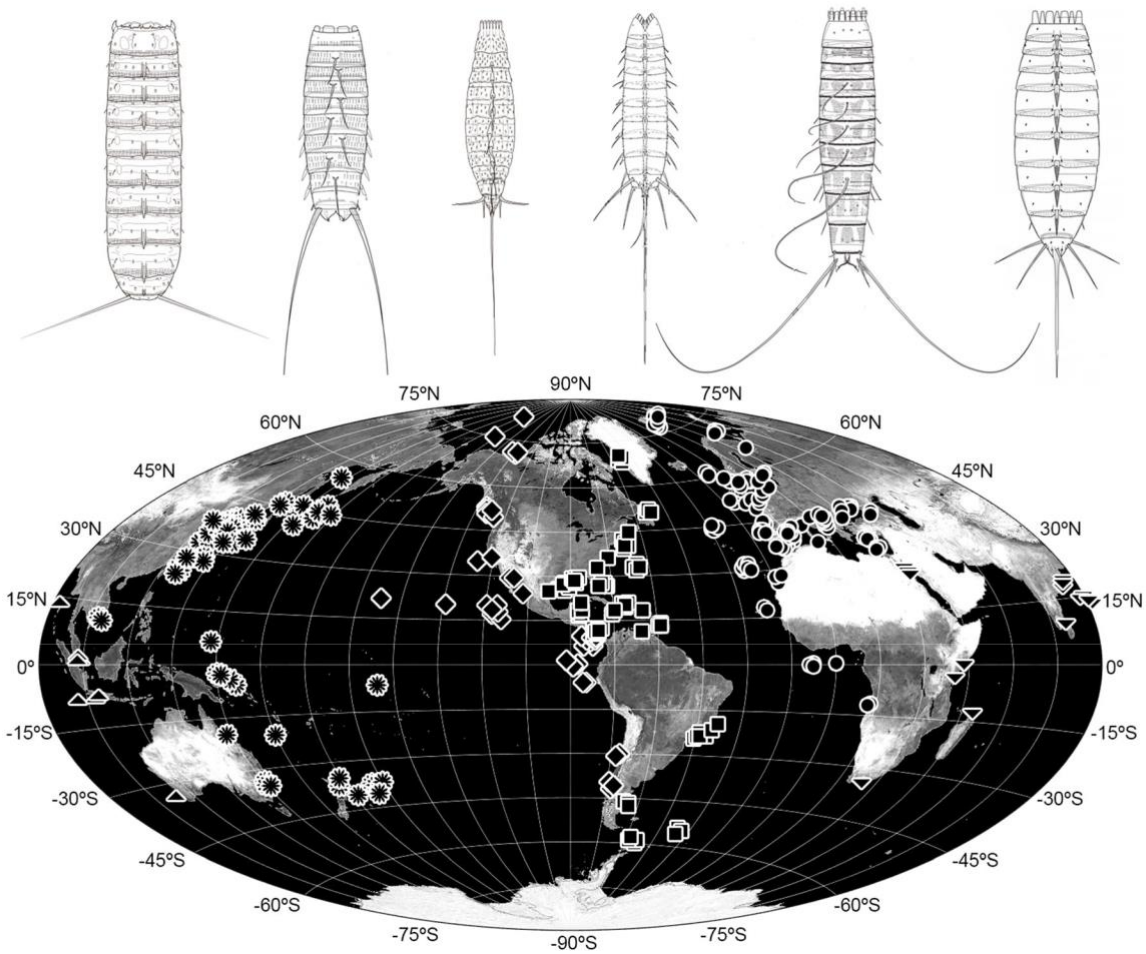

Fig. 1 World map with Hammer-Aitoff projection, showing all occurrence records of the phylum Kinorhyncha. Different symbols were used for each coastline (squares = western Atlantic, circles = eastern Atlantic, asterisks = western Pacific, diamonds = eastern Pacific, down-triangles = western Indian, up-triangles = eastern Indian). Drawings at the top represent some of the diversity of kinorhynchs (from left to right: *Cristaphyes cornifrons*, *Dracoderes gallaicus*, *Triodontoderes lagahoo*, *Semnoderes armiger*, *Echinoderes muricatus*, *Centroderes spinosus*); drawings are modified from Cepeda et al. 2019a, 2019b; Sørensen et al. 2008, 2012; Neuhaus et al. 2013; Pardos et al. 2016

literature, including the original descriptions or redescriptions of the species (Appendix S1). Minimum and maximum values of total trunk length and width were also compiled (Appendix S1), because even in the absence of latitudinal differences in mean values, the effect of latitude could be to reduce maximum or to increase minimum body size.

All data on length and width were only based on adult specimens, as juveniles grow with each moult (Neuhaus 2013). We did not build two separate datasets for males and females, even knowing that sexual dimorphism sometimes affects kinorhynch body size, because we wanted to manage a dataset as big as possible, and because we are analysing general trends acting over species.

Geographical units

The dataset contained single point records from all over the world, and we grouped them in geographical units represented by grids of 1° latitude and longitude (Appendix 1). The spatial resolution reported in the bibliography varied enormously from one publication to another, reflecting different sampling methodologies, and 1° latitude/longitude was the finest possible spatial resolution. Additionally, as most records come from continental slopes and could be consequently connected along the continents' edges, we grouped the occurrence data following six major coastlines: western and eastern Atlantic, western and eastern Pacific, and western and eastern Indian (Fig. 1, Appendix S1). Although this division of six major coastlines is arguable, it allows grouping the reports in geographically close and connected areas. In addition, this division into north-to-south coasts provides a large amount of latitudinal information.

Response, explanatory and confounding variables

The mean, maximum and minimum body size were determined as response variables, whereas latitude was used as explanatory variable. Latitudinal information was

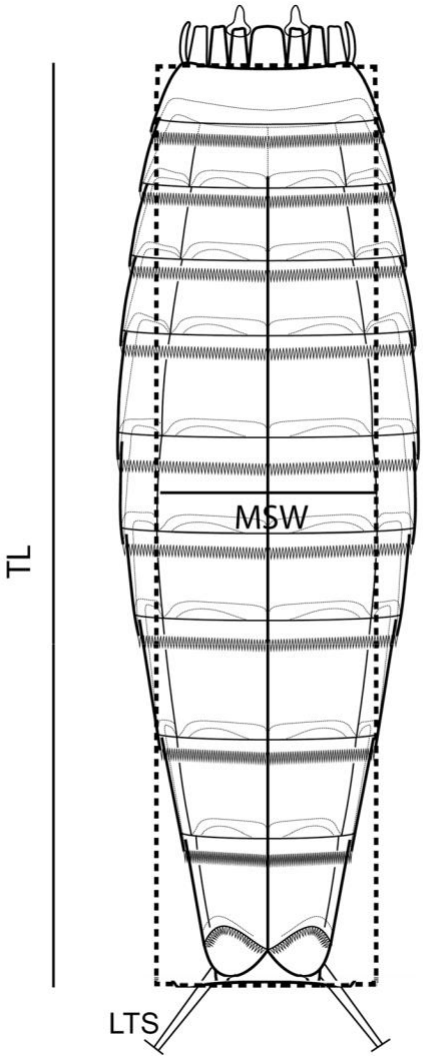

Fig. 2 Line art drawing representing a generalized external morphology of a specimen of cyclorhagid Kinorhyncha. Measures used to calculate an approximation of kinorhynch body size are indicated. Abbreviations: LTS, lateral terminal spine; MSW, maximum sternal width; TL; total trunk length

entered with both absolute and squared values to test for linear and U-shaped trends. As latitude does not influence body size by itself alone, two environmental factors were additionally included as explanatory variables: the mean sea surface temperature (SST) and the net primary productivity (NPP). SST data were obtained from the US National Oceanic and Atmospheric Administration (NOAA) for the years 1990–2018 (Reynolds et al. 2002) and NPP data from the Guillaume Maze's ocean productivity data site for the years 1997–2007 (Maze 2011). SST and NPP mean values were extracted and calculated in each 1° grid.

SST offers fundamental information on the global climate system and is an essential parameter in marine model predictions and simulators, and also very important for marine ecosystem studies. Our organisms under study, the phylum Kinorhyncha, are meiofaunal and consequently inhabit the ocean floor. Some studies have previously proved that the SST is strongly correlated with the sea bottom temperature (SBT) up to a certain depth extension (Cheung et al. 2013a, b), and that using SST instead of SBT (not arbitrarily, but because in most cases only SST is available) has no effect on the analysis. On the other hand, ocean temperature progressively decreases throughout the mixed upper layer of seawater until it reaches the thermocline at ca. 200 m depth, getting there much colder; below 1000 m depth, the temperature remains almost constant (Tomczak 2019). Thus, the difference in temperature between shallow waters and points located below 200 m is substantial. The thermocline is semi-permanent and varies from season to season and year to year, and most importantly, from latitude to latitude, being practically non-existent in the polar regions (> 60°) (Tomczak 2019). A total of 196 out of 1370 kinorhynch records are below 60° latitude and 200 m depth (Appendix S1). We are aware that using the SST for these points, as an approximation of temperature, can introduce a bias in the analyses, but it is the only temperature measurement available for the latitudinal range and the resolution managed in the present study throughout enough years at global scale. In addition, similar studies also used the SST as an approximation of temperature for latitudinal worldwide analyses (Berke et al. 2013; Bartels et al. 2019).

Also, two likely confounding factors that could be affecting body size were included as explanatory variables: the species richness and the number of occurrence records per 1° latitudinal band (Appendix 1). Another potential confounding factor included in the analysis was the phylogenetic influence on body size, *i.e.* the observed data could be more similar to each other because they are phylogenetically related and not due to a latitudinal trend.

Confounding variables, based on count data, were log-transformed to correct for their geometric behaviour (Crawley 2012), while the remaining continuous variables (independent, environmental and latitudinal variables) were also log-transformed and scaled to remove the effect of differences in scale and sampling units between variables (Zuur et al. 2009).

Statistical analyses

A series of generalized least squares regression models (GLS), fitted by maximum likelihood, were conducted to include spatial autocorrelation for analysing size-latitude trends. Addressing spatial autocorrelation is not necessarily compulsory for this kind of study, given that the occurrence of a taxon at multiple latitudes is likely a consequence of its biology rather than a data-quality problem (Hawkins 2011). However, data autocorrelation is frequently considered as an important source of bias (Berke et al. 2013), so we wanted to follow the most conservative approach by addressing potential

non-spatial and spatial correlation patterns in the models, including exponential, Gaussian, spherical, linear and rational quadratic correlation structures (Zuur et al. 2009). The Akaike information criterion (AIC) was used to select the best model among the set because this value is useful when comparing identical models with different link functions. In case of selecting a spatial model in the previous step, a likelihood ratio test on AIC was performed to decide whether the best spatial models explained significantly better the response variable (Appendix S3). When the models with spatial structures were not significantly better than the non-spatial ones, *i.e.* no improvement attributable to the attachment of a spatial structure, we relied on the results of the linear models without spatial structure, given that they are more easily interpretable. Once the best model was selected, we expressed the contribution of each variable by calculating the relative importance (RI) as the sum of the Akaike weights of the submodels in which the variable appeared, from the whole set of submodels including all combinations of explanatory variables (Burnham and Anderson 2002). If the non-spatial model was selected, we additionally calculated the partial coefficients of determination (R^2).

Moreover, as latitude does not influence body size by itself, we performed another series of models including the aforementioned environmental variables (SST and NPP). We also followed the above mentioned considerations for the selection of size-latitude models.

Phylogenetic generalized least squares are the best approach to address the phylogenetic influence in the analyses, but these models require a solid and extensive phylogenetic tree (Freckelton et al. 2002; Tidière et al. 2017), which does not exist currently for the phylum Kinorhyncha at the species level. Instead, we addressed the phylogenetic effect performing a series of generalized mixed models (GMMs). These models contain both fixed and random effects, and are particularly useful when analysing data that are not truly independent, in other words, when a hierarchical, multilevel correlation structure is present (Holt and Jønsson 2014). Our dataset contains body size data that is hierarchically organized in taxonomic categories depending on the phylogenetic relationships of the different kinorhynch taxa. This means that the species included in a particular taxonomic category are likely to be more similar in terms of body size than species belonging to phylogenetically more distant taxa. In broad terms, the fixed effects of the GMMs evaluate the levels of our main variable (*i.e.* body size) using data from all its levels (in our case, we are interested in evaluating how latitude can influence kinorhynch body size). Contrarily, the random effects are categorical, grouping factors that can potentially affect our main variable (in our case, the taxonomic categories that depend on the phylogenetic relationships between the different kinorhynch taxa). Marginal (mR^2) and conditional (cR^2) r-squared values were reported for the GMMs to explain both the fixed and the sum of the fixed and random effect contribution, respectively.

Finally, given that latitudinal trends may appear in only one hemisphere, models were also repeated in each hemisphere alone. Similarly, models were also repeated in each major coastline, except those of the Indian Ocean because of the low sample size.

A strictly restrictive approach was determined to identify the significance of the considered variables in all the models of the present study (α-level < 0.001), given the large number of different models fitted on the same dataset (Bartels et al. 2019). Models were conducted using the nlme package (Pinheiro et al. 2020), and their results were reported as a type II ANOVA table using the car package (Fox and Weisberg 2019), in R v.3.6.2 (R Core Team 2020).

Results

The present section only includes the summarized results for the global analysis in tables, whilst results per hemisphere and coastline can be found in the Supporting Information files.

Latitudinal trends in kinorhynch body size

Squared values of latitude were found as a statistically significant variable modelling the mean, minimum and maximum body size of kinorhynchs in the global analysis (Tables 1 and 3). For the GLS, the RI of the squared latitude was high (RI = 0.89 for mean and maximum body size, RI = 0.98 for minimum body size) (Table 1), and the variability explained by this variable in the GMMs was also considerable, as indicated by the mR^2 value (5.66% for mean body size, 4.37% for minimum body size and 5.50% for maximum body size) (Table 3). These results represent a U-shaped, latitudinal increase in mean body size (Fig. 3a). Additionally, as the effect of latitude also influenced minimum and maximum body size (Tables 1 and 3), smaller species tended to disappear at higher latitudes and larger species tended to be absent at lower latitudes (Fig. 3c, e).

When considering the hemispheres separately, latitude was only found as statistically significant in the GMM for the minimum body size in the northern hemisphere, explaining near 4.74% of the variability together with the coastline (Supporting Information Appendix S2: Table 3). In this case, a linear relationship was found, as indicated by the absolute values of latitude (Fig. 3d and Supporting Information Appendix S2: Table 3), with smaller species regularly disappearing from the equator to the north pole. The remaining size-latitude relationships per hemisphere, although quite heterogeneous (Fig. 3b, d, f and Supporting Information Appendix S2: Tables 1–8), were not found as statistically significant.

Table 1 Results of the generalized least squares models of latitudinal gradients in mean, minimum and maximum body size, accounting for absolute and squared values of latitude, species richness and subdivision into six main geographical areas.

	χ^2	*p*	*RI*
Mean body size			
Latitude	1.41	0.2346	0.09
Latitude (squared)	16.80	*0.0002*	0.89
Species richness	0.01	0.9353	0.03
Records	0.18	0.6724	0.04
Coastline	23.44	*0.0001*	0.97
Minimum body size			
Latitude	0.62	0.4280	0.06
Latitude (squared)	16.18	*0.0001*	0.98
Species richness	0.02	0.8968	0.03
Records	0.35	0.5534	0.04
Coastline	20.45	*0.0010*	0.89
Maximum body size			
Latitude	2.30	0.1295	0.15
Latitude (squared)	18.02	*< 0.0001*	0.89
Species richness	< 0.01	0.9837	0.04
Records	0.08	0.7764	0.04
Coastline	22.84	*0.0004*	0.97

Statistically significant *p* values with an α level < 0.001 are in italics

p, *p*-value; *RI*, relative importance of a variable

The coastline strongly influenced the kinorhynchs' body size and was found statistically significant at all the analysed levels (Tables 1, 2, 3 and 4). Different latitudinal trends were detected per coastline:

- The western Atlantic and Pacific coasts showed similar trends, with squared values (*i.e.* U-shaped relationship) of latitude statistically significant in the linear and mixed models for mean, minimum and maximum body size (for the western Atlantic, Supporting Information Appendix S2: Table 10 and Appendix S4: Fig. S1a–c; for the western Pacific, Appendix S2: Tables 17 and 19 and Appendix S4: Fig. S2a–c).
– In the eastern Atlantic, absolute values of latitude were statistically significant in the mixed models for mean, minimum and maximum body size, and squared values for maximum body size, meaning that a linear or a U-shaped relationship was found differing per taxonomic group (Supporting Information Appendix S2: Tables 15 and 16 and Appendix S4: Fig. S1d–f).
– In the eastern Pacific, both absolute and squared values of latitude were statistically significant in the GLS for mean, minimum and maximum body size, although the squared ones had higher importance (Supporting Information Appendix S2: Table 21, and Appendix S4: Fig. S2d–f). Squared values of latitude were also found marginally significant in the mixed models for mean body size (Supporting Information Appendix S2: Table 23).

Environmental variables in latitudinal trends

The analyses including two environmental variables, namely SST and NPP, yielded heterogeneous results between the global dataset and those performed per hemisphere and coastline, determining a differential influence of these variables on kinorhynch body size. Most statistically significant results were generated by the GMMs, once the effect of the phylogeny was controlled. For the global analysis, the SST was found as a driver of change in mean and minimum body size, while the NPP was not a statistically significant predictor, with a marginal importance in all the performed models (Tables 2 and 4, Fig. 4a and Supporting Information Appendix S4: Fig. S3a).

Regarding the hemispheres, the SST was found again as an important predictor of mean, minimum and maximum body size for the northern one (Supporting Information Appendix S2: Table 4), whereas none of the selected environmental features were significant for the southern hemisphere (Supporting Information Appendix S2: Tables 6 and 8). On the other hand, the western Atlantic and the western Pacific were the two coastlines with higher influence of NPP over mean, minimum and maximum body size (Fig. 4c–d, Supporting Information Appendix S2: Tables 12 and 20 and Appendix S4: Fig. S3b– d), whereas the SST was only found as an important driver of body size for the eastern Atlantic (over maximum body size) (Fig. 4b and Supporting Information Appendix S2: Table 16).

Phylogenetic influence in kinorhynch body size

The random-effect component of the GMMs allowed the extraction and control of the phylogenetic influence in kinorhynch body size. For almost all the analyses, phylogeny was found as an important factor determining similarities between taxonomic congeners, in most cases with higher influence than latitude and environmental variables (Tables 3 and 4 and Supporting Information Appendix S2: Tables 3, 4, 7, 8, 19, 20, 23 and 24). The only exception to this was the analyses for the eastern Atlantic, with zero effect of the phylogeny over body size (Supporting Information Appendix S2: Tables 15 and 16).

Yet, the fixed-effect component of the models, which determined the effect of the latitude (and the environmental variables), also showed a certain degree of variance in kinorhynch body size throughout the latitudinal gradient. The latitudinal influence is, in most cases, much less than that

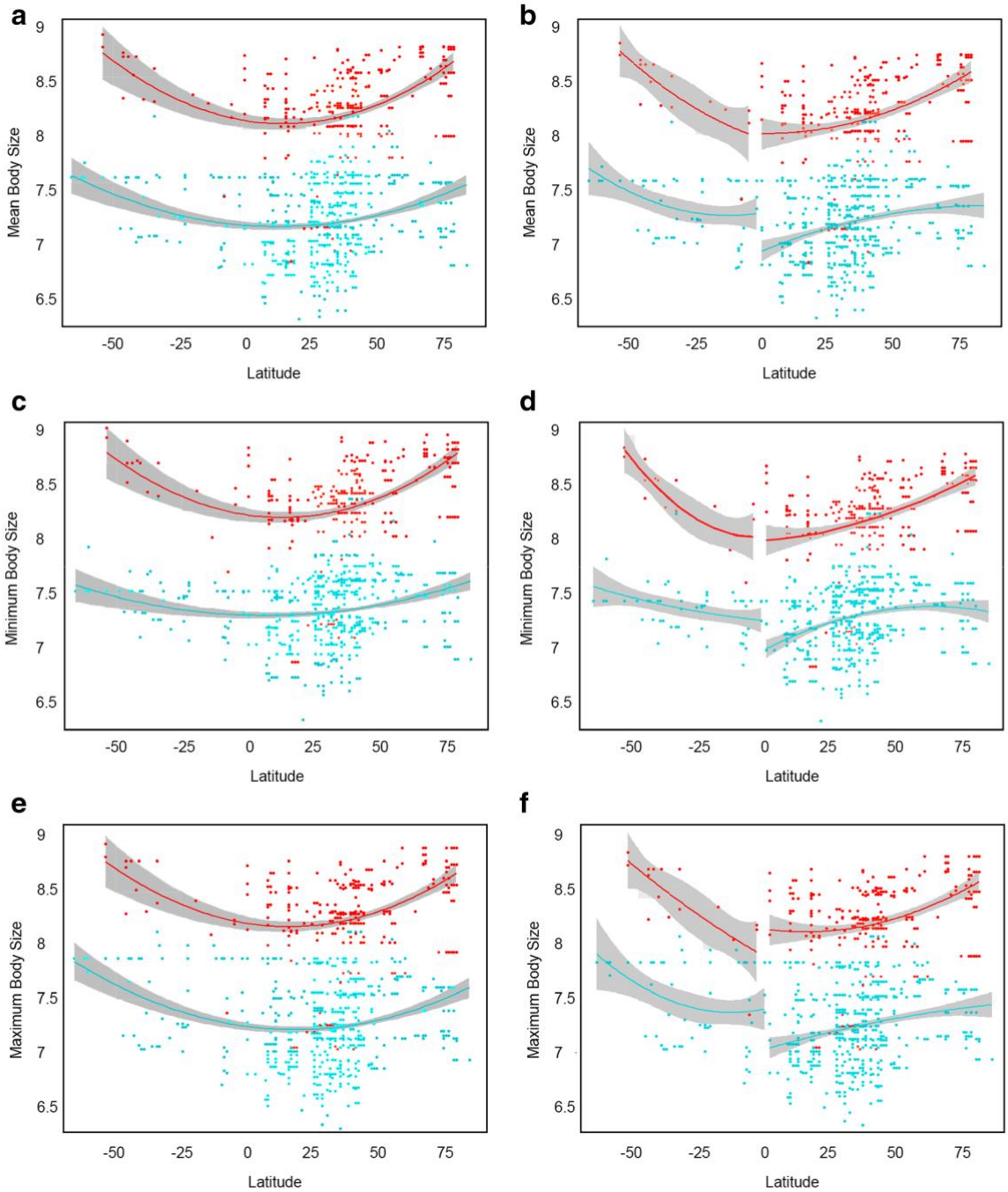

Fig. 3 Representation of size-latitude trends between mean (a, b), minimum (c, d) and maximum (e, f) body size and raw values of latitude for the global analysis (left) and the hemisphere analyses (right), depicted separately for allomalorhagids (red dots and lines) and cyclorhagids (cyan dots and lines)

given by the phylogenetic effect, but still significant enough to take it into account.

Discussion

Is Kinorhyncha body size correlated to latitude?

The global analyses showed a U-shaped relationship between body size (mean, minimum and maximum) and latitude, with the body size lowest at latitudes of ca. 10–25°, then increasing towards the poles (Fig. 3a, c, e). This also indicates that the largest species tend to be scarcer at latitudes of 10–25° and vice versa (Fig. 3a, e). The pattern was consistently found for both Allomalorhagida and Cyclorhagida.

As both tropics have similar environmental conditions, it is striking to find this asymmetric pattern with kinorhynchs of smaller sizes around the Tropic of Cancer but not in the Tropic of Capricorn. The most likely situation is that the observed pattern is suffering from sampling biases, slightly

Table 2 Results of the generalized least squares models of latitudinal gradients in body size (mean, minimum and maximum) including the environmental variables: the mean sea surface temperature (SST) and the mean net primary productivity (NPP), accounting for absolute and squared values of latitude, species richness, species records and subdivi-sion into six main geographical areas

	χ^2	*p*	*RI*
Mean body size			
Latitude	1.27	0.2588	0.08
Latitude (squared)	2.06	0.1512	0.64
Species richness	0.01	0.9381	0.03
Records	0.13	0.7187	0.04
SST	0.48	0.4906	0.39
NPP	0.19	0.6592	0.03
Coastline	23.02	*0.0003*	0.97
Minimum body size			
Latitude	0.53	0.4668	0.06
Latitude (squared)	1.72	0.1901	0.62
Species richness	0.01	0.9038	0.03
Records	0.28	0.5980	0.04
SST	0.68	0.4110	0.05
NPP	0.56	0.4550	0.04
Coastline	20.15	*0.0012*	0.84
Maximum body size			
Latitude	2.24	0.1348	0.15
Latitude (squared)	2.05	0.1517	0.71
Species richness	< 0.01	0.9951	0.04
Records	0.05	0.8282	0.04
SST	0.62	0.4324	0.39
NPP	0.17	0.6796	0.03
Coastline	22.31	*0.0005*	0.98

Statistically significant *p* values with an α level < 0.001 are in italics *p*, *p* value; *RI*, relative importance of a variable

shifting the curve towards positive latitudes as almost no records of kinorhynchs are currently known for the southern hemisphere at latitudes of ca. − 10 to − 25° (Figs. 1 and 3). If this were the case, kinorhynchs would be smaller at the equator, slightly increasing in size towards tropic latitudes and faster towards higher latitudes. Similar results of size-latitude trends have also been found in other marine groups of invertebrates, such as certain families of bivalves (Berke et al. 2013), tardigrades (Bartels et al. 2019), copepods (Lonsdale and Levinton, 1985; Brun et al. 2016) and plankton species (San Martín et al. 2006; Boyce et al. 2015). Thus, size-latitude relationships seem to be relatively common in marine ectotherm invertebrates, though immensely variable between geographic areas and taxonomic groups.

Nevertheless, this sampling bias prevents the complete discarding of a bimodal distribution of size-latitude trends, as it has also been previously observed for other marine taxa (Chaudhary et al. 2016). Under this bimodal distribution, kinorhynch species at tropic latitudes would be the smallest species, with those of the equatorial regions of intermediate sizes between those and the polar ones.

Are there differences between hemispheres and coastlines?

Size-latitude relationships in Kinorhyncha seem to strongly depend on the coastline rather than the hemisphere, although some differences between hemispheres were also found. For the northern hemisphere, only the minimum body size was affected by latitude once the phylogenetic effect was controlled (Supporting Information Appendix S2: Table 3). The class Allomalorhagida, at this hemisphere, showed an almost linear increase in minimum body size from the equator towards the poles, which suggests that the smallest species tend to be distributed at lower latitudes (Fig. 3d). The class Cyclorhagida exhibited a hump-shaped size-latitude relationship, with the smallest species near the equator and the northern pole (Fig. 3d). This disparity of results again suggests an underlying heterogeneous variability for size-latitude relationships in Kinorhyncha, which agrees with the results obtained for other marine ectotherm taxa (Lindsey 1966; Ashton and Feldman 2003; Chown and Gaston 2010; Berke et al. 2013). On the other hand, size-latitude trends were not found in the southern hemisphere. The most likely explanation is the lower number of kinorhynch records available for this hemisphere (almost absent at latitudes of ca. − 10 to − 25°, as already referred above), together with the much less land mass compared to the northern one, since most samplings are carried out at the continental margins.

Kinorhynchs also exhibited heterogeneous size-latitude trends between coastlines. U-shaped relationships were the most common in the eastern and western Pacific and the western Atlantic, as well as for Allomalorhagida in the eastern Atlantic (Supporting Information Appendix S4: Figs. S1a-f and S2a-f). However, Cyclorhagida in the eastern Atlantic showed a slightly hump-shaped relationship (Supporting Information Appendix S4: Fig. S1d-f) as that obtained for the northern hemisphere. Again, these results clearly indicate that the macroecological patterns influencing size-latitude trends are driven by many diverse processes, likely both present and past, in different regions and for different lineages, resulting in heterogeneous size-latitude trends. It is also possible that, since the vast majority of the available reports are coastal, the influence of the coastline in the models is reflected instead of that of the hemisphere.

What are the environmental drivers modelling size-latitude trends in Kinorhyncha?

Our results showed that both temperature and productivity seemed to drive some variation of kinorhynch body size

Table 3 Results of the generalized mixed models of latitudinal gradients in mean, minimum and maximum body size, accounting for absolute and squared values of latitude, species richness, records and subdivision into six main geographical areas

	Estimate	StdE	*t*	*p*	mR^2	cR^2
Mean body size						
Latitude	− 0.0361	0.0214	− 1.68	0.0911	0.0566	0.6766
Latitude (squared)	0.1834	0.0209	− 8.79	*< 0.0001*		
Species richness	− 0.0445	0.0245	− 1.81	0.0685		
Records	0.0205	0.0246	0.83	0.404		
Coastline	/	/	/	*< 0.0001*		
Minimum body size						
Latitude	− 0.0329	0.0212	− 1.55	0.1197	0.0437	0.7142
Latitude (squared)	0.1684	0.0206	8.15	*< 0.0001*		
Species richness	− 0.0311	0.0242	− 1.28	0.1980		
Records	0.0117	0.0243	0.48	0.6295		
Coastline	/	/	/	*< 0.0001*		
Maximum body size						
Latitude	− 0.0195	0.0224	− 0.87	0.3827	0.0550	0.6427
Latitude (squared)	0.1701	0.0229	7.43	*< 0.0001*		
Species richness	− 0.0352	0.0264	− 1.33	0.1807		
Records	0.0217	0.0264	0.82	0.4086		
Coastline	/	/	/	*< 0.0001*		

Statistically significant *p* values with an α level < 0.001 are in italics

cR^2, conditional effects measure; mR^2, marginal effects measure; *p*, *p*-value; StdE, standard error; *t*, *t*-value

Table 4 Results of the generalized mixed models of latitudinal gradients in mean, minimum and maximum body size, accounting for absolute and squared values of latitude, species richness, species records, sea surface temperature (SST), net primary productivity (NPP) and subdivision into six main geographical areas

	Estimate	StdE	*t*	*p*	mR^2	cR^2
Mean body size						
Latitude	− 0.0384	0.0212	− 1.81	0.0690	0.0664	0.6815
Latitude (squared)	0.0186	0.0353	0.53	0.5978		
Species richness	− 0.0096	0.0248	− 0.39	0.6967		
Records	− 0.0182	0.0251	− 0.73	0.4651		
SST	− 0.2015	0.0333	− 6.04	*<0.0001*		
NPP	0.0153	0.0116	1.32	0.1852		
Coastline	/	/	/	*<0.0001*		
Minimum body size						
Latitude	− 0.0361	0.0209	− 1.73	0.0822	0.0552	0.7202
Latitude (squared)	− 0.0098	0.0348	− 0.28	0.7781		
Species richness	0.0081	0.0244	0.33	0.7384		
Records	− 0.0314	0.0246	− 1.27	0.2006		
SST	− 0.2207	0.0328	− 6.72	*<0.0001*		
NPP	0.0237	0.0115	2.07	0.0374		
Coastline	/	/	/	*<0.0001*		
Maximum body size						
Latitude	− 0.0250	0.0302	− 0.83	0.4046	0.1015	0.6352
Latitude (squared)	0.1075	0.0856	1.26	0.2072		
Species richness	− 0.0243	0.0283	− 0.86	0.3891		
Records	0.0051	0.0245	0.21	0.8348		
SST	− 0.0914	0.0760	− 1.20	0.2269		
NPP	0.0218	0.0138	1.57	0.1135		
Coastline	/	/	/	*<0.0001*		

Statistically significant p values with an α level < 0.001 are in italics

cR^2, conditional effects measure; mR^2, marginal effects measure; *p*, *p*-value; StdE, standard error; *t*, *t*-value

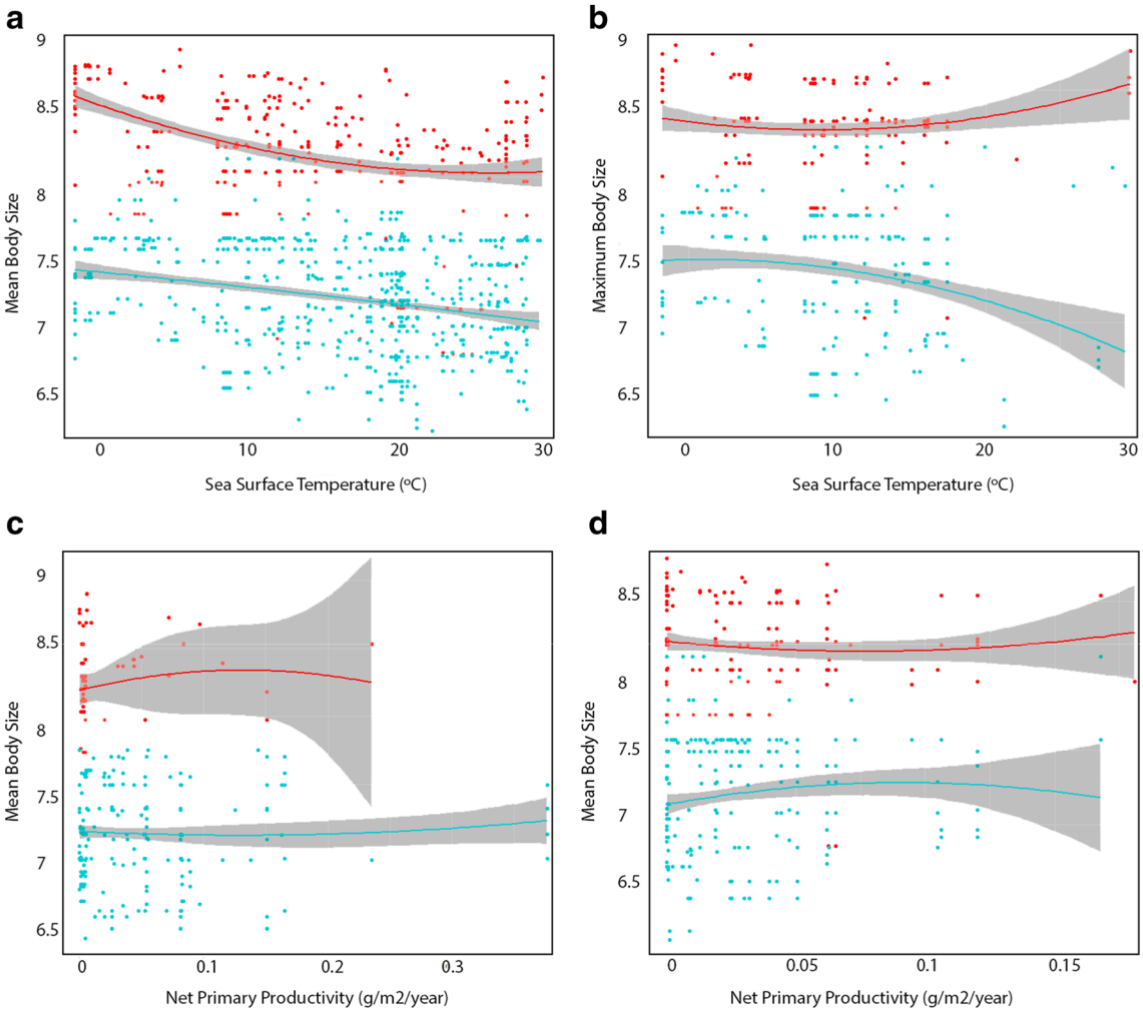

Fig. 4 Representation of selected size-temperature and size-productivity trends: mean body size and temperature for the global analysis (a), maximum body size and temperature for the eastern Atlantic (b), mean body size and productivity for the western Atlantic (c), and mean body size and productivity for the western Pacific (d). Results are depicted separately for allomalorhagids (red dots and lines) and cyclorhagids (cyan dots and lines)

throughout the latitudinal gradient. The effect of the sea temperature was found as a consistent driver of mean and minimum body size in the global analysis, as long as the phylogenetic effect was included in the models. Furthermore, the temperature also significantly affected maximum body size trends in the eastern Atlantic.

It is well known that body size and temperature are inversely correlated in many terrestrial and aquatic taxa, with larger bodies at lower temperatures and vice versa (Forster et al. 2012). Although temperature is not a common factor in influencing ectotherm, small-sized taxa, because these organisms rapidly adjust their temperature depending on the environment (Blackburn et al. 1999; Blanckenhorn and Demont 2004; Bartels et al. 2019), a temperature-size relationship has been found in some cases, e.g. some species of estuarine copepods (Lonsdale and Levinton 1985), beach isopods (Cardoso and Defeo 2003) and crabs (Defeo and Cardoso 2002). These studies are based on intraspecific patterns of body size changes. However, the same hypotheses that explain intraspecific size-latitude relationships may apply to interspecific studies if most species within a family or genus are governed by the same mechanism (Berke et al. 2013), or if extinction and speciation work differently on smaller and larger species at community level (Bartels et al. 2019). This has been established to explain size-temperature gradients in marine copepods through the so-called temperature-size rule (Horne et al. 2016). This hypothesis may be applied to our results: kinorhynch species inhabiting low latitudes (with higher sea temperature) would accelerate development more rapidly than somatic growth, leading to smaller adult body size (Chown and Gaston 2010; Arendt 2011) (Fig. 4a and Supporting Information Appendix S4: Fig. S3a). However, this hypothesis has a strong limitation, as it remains still unknown which physiological mechanisms of ectotherms rule the ability to increase the amount of resources allocated to development at the expense of final body size (Kingsolver

and Huey 2008), or even if this response supposes an adaptation rather than a physiological limitation (Walters and Hassall 2006). Indeed, we cannot be sure that kinorhynch species within a particular family or genus respond equally to temperature-size relationships, although these relationships were more evident by including the phylogenetic effect in the mixed models.

Another hypothesis proposed to explain the reduced body size of ectotherm taxa at higher temperatures is the risk of predation by other ectotherms. Predation pressure determines an increased predation risk favouring earlier maturation at the expense of growing, leading to smaller final body sizes near the equator (Williams 1966; Sibly and Atkinson 1994; Atkinson 1995). The distribution pattern on size-latitude observed in our results seems to be in line with this hypothesis (Fig. 3a, c, d, e and Supporting Information Appendix S2: Table 3), despite several studies having ruled out this effect for ectotherm organisms (Lindsey 1966; Atkinson 1994; Vinarski 2014). Kinorhynchs are likely included in the diet of many marine invertebrates such as decapods and snails (Martorelli and Higgins 2004; Margulis and Chapman 2009). These predators show a latitudinal gradient of species richness and abundance, decreasing both towards high latitudes (Roy et al. 1998; Boschi 2000; Dworschak 2000; Boschi 2002; Rex et al. 2005; Barnes 2010). This fact supports the aforementioned hypothesis of the sampling bias affecting a hypothetical linear size-latitude trend in kinorhynchs, with smaller sizes at the equator and increasing towards higher latitudes. More recent studies, however, have shown that most marine taxa actually exhibit bimodal distributions of species richness, being more abundant at the tropics then decreasing towards the equator and the poles (Chaudhary et al. 2016; Saeedi et al. 2017, 2019). The differential predation risk between the tropics and the remaining geographical zones could explain the alternative bimodal distribution on kinorhynch size-latitude relationship, which still cannot be discarded as stated above, with kinorhynch species of reduced minimum body size more concentrated around the Tropic of Cancer and absent at both the equator and the poles (see first subsection of the "Discussion").

The marine productivity was correlated with mean and minimum body size in the western Atlantic and with the mean, minimum and maximum body size in the western Pacific, once taken into account the phylogeny in the mixed models (Supporting Information Appendix S2: Tables 12 and 20). Marine productivity is known to be positively correlated with body size in both terrestrial and aquatic taxa. This is called the resource availability hypothesis, which establishes that species are able to reach larger body size at areas with higher resource abundance (Ho et al. 2009; Huston and Wolverton 2011), areas with strong seasonal fluctuations of resources (Blackburn et al. 1999) and/or areas with lower inter-specific competition owing to increased access to resources (Moran and Woods 2012). This trend has been found in marine fishes and copepods cultured in laboratory conditions (Berggreen et al. 1988; Huston and Wolverton 2011), though an inverse correlation has been found in field copepods (Brun et al. 2016). Our results of the western Atlantic showed that mean body size of Cyclorhagida progressively increases with productivity, and that of Allomalorhagida reaches a peak at medium values and then decreases with the highest productivity values (hump-shaped relationship) (Fig. 4c). In the western Pacific, mean, minimum and maximum values of Cyclorhagida follow the same pattern of Allomalorhagida in the western Atlantic, whilst those of Allomalorhagida are U-shaped, meaning that body size increases with the lowest and the highest values of productivity (Fig. 4d and Supporting Information Appendix S4: Fig. S3b-c).

The resource availability hypothesis seems to agree with the results obtained for Cyclorhagida in the western Atlantic, whereas the remaining results are quite heterogeneous. Latitudes with the highest values of productivity are likely to favour the existence of species with larger body size, but it should not be forgotten that many other environmental factors, in some cases with more influence than productivity, may be responsible for the observed heterogeneous responses between kinorhynch body size and marine productivity (Huston and Wolverton 2011). For instance, dissolved oxygen has been proposed as an important limiting factor for meiofauna body size, especially combined with temperature (Atkinson 1994; Kennish 2017; Neira et al. 2018). In lower latitudes (with higher temperatures), the dissolved oxygen is scarcer, which would act favouring smaller body size to increase gas exchange.

Are there potential sampling biases masking latitude-size trends in Kinorhyncha?

Given the different shapes, spatial distributions and phylogenetic effects of the observed kinorhynch size-latitude relationships, it could be the case that sampling biases may be the cause of this strong variability of patterns. In this context, it must be taken into account that large regions of the world still remain poorly sampled, especially the Indian Ocean, the African waters and the southern hemisphere.

Undersampling is considered one of the main biases when detecting biogeographical trends (Whittaker and Fernández-Palacios 2006; Finlay and Esteban 2007; Ashton-Acton 2013), especially for small-sized organisms (Foissner 2006; Azovsky and Mazei 2013; Meyer et al. 2018). Actually, kinorhynch species richness is not mainly determined by latitude but species records; in other words, the current known distribution of kinorhynch species reflects a map of researcher sampling efforts rather than natural distribution patterns. This has been previously proposed to explain the currently limited knowledge on the geographic distribution of Kinorhyncha

(Sánchez et al. 2012, 2013; Neuhaus 2013; Grzelak and Sørensen 2018; Cepeda et al. 2019) and other meiofaunal organisms, such as rotifers and tardigrades (Fontaneto et al. 2012; Bartels et al. 2019). The results obtained in the present study are relatively strong, as latitudinal trends were repeatedly detected despite the relatively low number of observations and the inclusion of several confounding factors such as species richness, records, spatial autocorrelation and phylogenetic influence. However, if our knowledge on kinorhynch distribution was more similar to the real pattern, a more consistent global trend could emerge due to an improved sampling.

Another bias frequently linked to biogeographical trends is the differential sampling effort by body size, as smaller species tend to be undersampled compared to larger ones (Wyatt and Carlton 2002; Guillera-Arroita et al. 2019). However, such bias is unlikely to substantially influence our analyses, given that kinorhynchs are all small-sized, meiofaunal organisms with a rather homogeneous body size which ranges from ca. 200 μm up to 1000 μm (Neuhaus 2013). Moreover, recently described species are not disproportionately small, and a relationship between kinorhynch body size and date of species description seems to be absent.

Finally, it must be taken into account the possibility of sediment features in kinorhynch size-latitude relationships. Although sediment properties seem to influence kinorhynch body shape, no evidence was found between sediment properties and body size (Cepeda et al. 2020). Nevertheless, the previous work was carried out with a limited sample size from two main geographic regions (the Iberian Peninsula and the Caribbean Sea), and perhaps sediment features could influence kinorhynch body size at a larger geographical (*i.e.* latitudinal) scale.

Is there a phylogenetic effect on Kinorhyncha body size?

Almost all the performed mixed models showed that phylogeny has a strong effect on body size; in other words, congeners are more similar in size to each other than to phylogenetically distant species. This becomes especially evident when discriminating size-latitude trends between classes (Figs. 3 and 4 and Supporting Information Appendix S4: Figs. S1, S2 and S3). Despite this, the phylogenetic effect does not eliminate the size-latitude trend because even in the mixed models, latitude and environmental variables were also found as relatively important predictors of body size variability. Indeed, only the mixed models found significant size-latitude trends in some cases, indicating different patterns between the two kinorhynch classes. This unequal response to latitude between the phylogenetic groups is likely due to different evolutionary histories acting in body size modelling.

Nevertheless, it must always be taken into account that body size is a complex biological feature influenced by many different ecological, historical and evolutionary trade-offs (Berke et al. 2013). As mentioned above, the mixed models showed that the variation explained by the fixed-effect component (*i.e.* variation explained by latitude, environmental variables and confounding factors) is lower than that explained by the phylogeny by far, which supports this idea. Analysis of such complex biological characteristics usually yields low values of variability determination, because many different factors that also model body size are disregarded in the models (other environmental factors such as dissolved oxygen, pH or organic matter; interspecific competition, predation, historical events, local patterns associated to certain geographic areas, etcetera).

Conclusions

Kinorhynch size-latitude trends showed a huge variety of patterns throughout hemispheres, coastlines and taxonomic groups, revealing a complex interaction of several factors. These results agree with those obtained for other marine ectotherm taxa, such as copepods, bivalves or tardigrades, which indicates that, contrarily to endotherms, ectotherm organisms do not respond to a single particular factor but to a network of multiple variables that configure a high heterogeneity in size-latitude relationships. It is likely that the inclusion of new records and the discovery of new kinorhynchs will clarify the observed latitudinal trends in the present study.

Supplementary Information The online version contains supplementary material available at https://doi.org/10.1007/s13127-020-00471-y.

Authors' contribution FP, NS and DC conceived together the general idea of the study. DC created the dataset and conducted the whole exper-imental and statistical process. FP, NS and DC discussed the results and defined the main conclusions of the study. DC wrote the manuscript. All the authors reviewed the manuscript.

Funding DC was supported by a predoctoral fellowship from the University Complutense of Madrid (CT27/16-CT28/16). NS was funded by the Community of Madrid and the University Complutense of Madrid in the framework of the Research Talent Attraction Programme for incorporation into research groups in the Community of Madrid (2019) (2019-T2/AMB-13328).

Data availability The original data used in this study are available within the article (Supporting Information Appendix S1). Data on environmental variables used in the present study are available in the following public domains: US National Oceanic and Atmospheric Administration (NOAA) (http://noaa.gov/) and Guillaume Maze's data site (http://data. guillaumemaze.org/). Geographic occurrences of all the species were extracted from the literature, which are referenced in the Supporting Information Appendix S1.

Compliance with ethical standards

Conflicts of interest The authors declare that they have no conflict of interest.

Code availability Software code is available via formal application to the authors.

References

Adrianov, A. V., & Maiorova, A. S. (2019). *Echinoderes ultraabyssalis* sp. nov. from the Kuril-Kamchatka Trench – the first hadal representative of the Kinorhyncha (Kinorhyncha: Cyclorhagida). Progress in Oceanography, 178, e102142. https://doi.org/10.1016/ j.pocean.2019.102142.

Alho, J. S., Herczeg, G., Laugen, A. T., Räsänen, K., Laurila, A., & Merilä, J. (2010). Allen's rule revisited: quantitative genetics of extremity length in the common frog along a latitudinal gradient. Journal of Evolutionary Biology, 24(1), 59–70. https://doi.org/10. 1111/j.1420-9101.2010.02141.x.

Allen, J. A. (1877). The influence of physical conditions in the genesis of species. Radical Review, 1, 108–140.

Arendt, J. D. (2011). Size-fecundity relationships, growth trajectories, and the temperature-size rule for ectotherms. Evolution, 65, 43–51. https://doi.org/10.1111/j.1558-5646.2010.01112.x.

Arnett, A. E., & Gotelli, N. J. (2003). Bergmann's rule in larval ant lions: testing the starvation resistance hypothesis. Ecological Entomology, 28, 645–650. https://doi.org/10.1111/j.1365-2311.2003.00554.x.

Armenteros, M., & Ruiz-Abierno, A. (2015). Body size distribution of free-living marine nematodes from a Caribbean coral reef. Nematology, 17, 1153–1164 https://doi.org/10.1163/15685411-00002930.

Ashton, K. G., & Feldman, C. R. (2003). Bergmann's rule in non-avian reptiles: turtles follow it, lizards and snakes reverse it. Evolution, 57, 1151–1163. https://doi.org/10.1111/j.0014-3820.2003.tb00324.x.

Ashton-Acton, Q. (2013). Issues in global environment – globalization and global change research (3rd edn.). Atlanta: ScholarlyEditions.

Atkinson, D. (1994). Temperature and organism size: a biological law of ectotherms? Advances in Ecological Research, 25, 1–58. https://doi. org/10.1016/S0065-2504(08)60212-3.

Atkinson, D. (1995). Effects of temperature on the size of aquatic ectotherms: exceptions to the general rule. Journal of Thermal Biology, 20(1/2), 61–74. https://doi.org/10.1016/0306-4565(94)00028-H.

Azovsky, A., & Mazei, Y. (2013). Large-scale patterns in the diversity and distribution of marine benthic ciliates: do microbes have macroecology? Global Ecology and Biogeography, 22, 163–172. https://doi.org/10.1111/j.1466-8238.2012.00776.x.

Barnes, R. S. K. (2010). Regional and latitudinal variation in the diversity, dominance and abundance of microphagous microgastropods and other benthos in intertidal beds of dwarf eelgrass, *Nanozostera* spp. Marine Biodiversity, 40, 95–106. https://doi.org/10.1007/ s12526-010-0036-1.

Bartels, P. J., Fontaneto, D., Roszkowska, M., Nelson, D. R., & Kaczmarek, Ł. (2019). Latitudinal gradients in body size in marine tardigrades. Zoological Journal of the Linnean Society. https://doi. org/10.1093/zoolinnean/zlz080.

Belk, M. C., & Houston, D. D. (2002). Notes and comments Bergmann's rule in ectotherms: a test using freshwater fishes. American Naturalist, 160(6), 83–88. https://doi.org/10.1086/343880.

Berggreen, U., Hansen, B., & Kiørboe, T. (1988). Food size spectra, ingestion and growth of the copepod *Acartia tonsa* during development: implications for determination of copepod production. Marine Biology, 99, 341–352. https://doi.org/10.1007/BF02112126.

Bergmann, C. (1848). Über die Verhältnisse der Wärmeökonomie der Thiere zu ihrer Grösse. Göttinger Studien, 3, 595–708.

Berke, S. K., Jablonski, D., Krug, A. Z., Roy, K., & Tomasovych, A. (2013). Beyond Bergmann's rule: size-latitude relationships in marine Bivalvia worldwide. Global Ecology and Biogeography, 22, 173–183. https://doi.org/10.1111/j.1466-8238.2012.00775.x.

Blackburn, T. M., Gaston, K. J., & Loder, N. (1999). Geographic gradients in body size: a clarification of Bergmann's rule. Diversity and Distributions, 5, 165–174. https://doi.org/10.1046/j.1472-4642. 1999.00046.x.

Blackburn, T. M., & Hawkins, B. A. (2004). Bergmann's rule and the mammal fauna of northern North America. Ecography, 27, 715–724. https://doi.org/10.1111/j.0906-7590.2004.03999.x.

Blanckenhorn, W. U., & Demont, M. (2004). Bergmann and converse Bergmann latitudinal clines in arthropods: two ends of a continuum? Integrative and Comparative Biology, 44, 413–424. https://doi.org/ 10.1093/icb/44.6.413.

Boschi, E. E. (2000). Species of decapod crustaceans and their distribution in the American marine zoogeographic provinces. Revista de Investigación y Desarrollo Pesquero, 13, 1–136.

Boschi, E. E. (2002). Distribution of continental shelf decapod crustaceans along the American Pacific Coast. In E. Escobar-Briones & F. Álvarez (Eds.), Modern approaches to the study of Crustacea (pp. 235–239). New York: Springer.

Boyce, D. G., Frank, K. T., & Leggett, W. C. (2015). From mice to elephants: overturning the "one size fits all" paradigm in marine plankton food chains. Ecology Letters, 18(6), 504–515. https://doi. org/10.1111/ele.12434.

Brown, J. H. (1995). Macroecology. Chicago: University of Chicago Press.

Brun, P. G., Payne, M. R., & Kiørboe, T. (2016). Trait biogeography of marine copepods – an analysis across scales. Ecology Letters, 19(12), 1403–1413. https://doi.org/10.1111/ele.12688.

Burnham, K. P., & Anderson, D. R. (2002). Model selection and multimodel inference: a practical information-theoretic approach. New York: Springer.

Cardoso, R., & Defeo, O. (2003). Geographical patterns in reproductive biology of the pan-American sandy beach isopod Excirolana braziliensis. Marine Biology, 143, 573–581. https://doi.org/10. 1007/s00227-003-1073-0.

Cepeda, D., Álvarez-Castillo, L., Hermoso-Salazar, M., Sánchez, N., Gómez, S., & Pardos, F. (2019a). Four new species of Kinorhyncha from the Gulf of California, eastern Pacific Ocean. Zoologischer Anzeiger, 282, 140–160. https://doi.org/10.1016/j.jcz.2019.05.011.

Cepeda, D., Sánchez, N., & Pardos, F. (2019b). First report of the family Zelinkaderidae (Kinorhyncha: Cyclorhagida) for the Caribbean Sea, with the description of a new species of *Triodontoderes* Sørensen & Rho, 2009 and an identification key for the family. Zoologischer Anzeiger, 282, 116–126. https://doi.org/10.1016/j.jcz.2019.05.017.

Cepeda, D., Trigo, D., Pardos, F., & Sánchez, N. (2020). Does sediment composition sort kinorhynch communities? An ecomorphological approach through geometric morphometrics. Scientific Reports, 10, e2603. https://doi.org/10.1038/s41598-020-59511-4.

Chaudhary, C., Saeedi, H., & Costello, M. J. (2016). Bimodality of latitudinal gradients in marine species richness. Trends in Ecology & Evolution, 31, 670–676. https://doi.org/10.1016/j.tree.2016.06.001.

Cheung, W. L., Pauly, D., & Sarmiento, J. L. (2013a). How to make progress in projecting climate change impacts. ICES Journal of Marine Science, 70, 1069–1074. https://doi.org/10.1093/icesjms/fst133.

Cheung, W. L., Sarmiento, J. L., Dunne, J., Frolicher, T. L., Lam, V. W. Y., Deng-Palomares, M. L., Watson, R., & Pauly, D. (2013b). Shrinking of fishes exacerbates impacts of global ocean changes on marine ecosystems. Nature Climate Change, 3, 254–258. https://doi.org/10.1038/nclimate1691.

Chown, S. L., & Gaston, K. J. (2010). Body size variation in insects: a macroecological perspective. Biological Reviews, 85, 139–169. https://doi.org/10.1111/j.1469-185X.2009.00097.x.

Crawley, M. J. (2012). The R book (2nd ed.). Chichester: Wiley.

Crickmore, M. A., & Mann, R. S. (2009). The control of size in animals: insights from selector genes. Bioessays, 30(9), 843–853. https://doi.org/10.1002/bies.20806.

Cushman, J. H., Lawton, J. H., & Manly, B. F. J. (1993). Latitudinal patterns in European ant assemblages: variation in species richness and body size. Oecologia, 95, 30–37. https://doi.org/10.1007/ BF00649503.

Defeo, O., & Cardoso, R. S. (2002). Macroecology of population dynamics and life history traits of the mole crab *Emerita brasiliensis* in Atlantic sandy beaches of South America. Marine Ecology Progress Series, 239, 169–179. https://doi.org/10.3354/meps239169.

Dworschak, P. C. (2000). Global diversity in the Thalassinidea (Decapoda). Journal of Crustacean Biology, 20(2), 238–245. https://doi.org/10.1163/1937240X-90000025.

Escribano, R., Hidalgo, P., Valdés, V., & Frederick, L. (2014). Temperature effects on development and reproduction of copepods in the Humboldt Current: the advantage of rapid growth. Journal of Plankton Research, 36(1), 104–116. https://doi.org/10.1093/plankt/ fbt095.

Fenchel, T., & Finlay, B. J. (2004). The ubiquity of small species: patterns of local and global diversity. BioScience, 54(8), 777–784. https://doi.org/10.1641/0006-3568(2004)054[0777:TUOSSP]2.0.CO;2.

Finlay, B. J., & Esteban, G. F. (2007). Body size and biogeography. In A. G. Hildrew, D. G. Raffaelli, & R. Edmonds-Brown (Eds.), Body size: the structure and function of aquatic ecosystems (pp. 167– 185). Cambridge: Cambridge University Press.

Foissner, W. (2006). Biogeography and dispersal of microorganisms: a review emphasizing protists. Acta Protozoologica, 45(2), 111–136.

Fontaneto, D., Barbosa, A. M., Segers, H., & Pautasso, M. (2012). The "rotiferologist" effect and other global correlates of species richness in monogonont rotifers. Ecography, 35, 174–182. https://doi.org/10. 1111/j.1600-0587.2011.06850.x.

Forster, J., Hirst, A. G., & Atkinson, D. (2012). Warming-induced reductions in body size are greater in aquatic than terrestrial species. PNAS, 109(47), 19310–19314. https://doi.org/10.1073/pnas. 1210460109.

Fox, J., & Weisberg, S. (2019). An R companion to applied regression (3rd ed.). Thousand Oaks: Sage.

Freckelton, R. P., Harvey, P. H., & Pagel, M. (2002). Phylogenetic analysis and comparative data: a test and review of the evidence. The American Naturalist, 160, 712–726. https://doi.org/10.1086/343873.

Grzelak, K., & Sørensen, M. V. (2018). Diversity and distribution of Arctic *Echinoderes* species (Kinorhyncha: Cyclorhagida), with the description of one new species and a redescription of *E. arlis* Higgins 1966. Marine Biodiversity, 49, 1131–1150. https://doi.org/10.1007/s12526-018-0889-2.

Guillera-Arroita, G., Kéry, M., & Lahoz-Monfort, J. J. (2019). Inferring species richness using multispecies occupancy modelling: estimation performance and interpretation. Ecology and Evolution, 9(2), 780–792. https://doi.org/10.1002/ece3.4821.

Hawkins, B. A. (2011). Eight (and a half) deadly sins of spatial analysis. Journal of Biogeography, 39, 1–9. https://doi.org/10.1111/j.1365-2699.2011.02637.x.

Hillebrand, H., & Azovsky, A. I. (2001). Body size determines the strength of the latitudinal diversity gradient. Ecography, 24, 251–256. https://doi.org/10.1034/j.1600-0587.2001.240302.x.

Higgins, R. P. (1988). Kinorhyncha. In R. P. Higgins & H. Thiel (Eds.), Introduction to the study of meiofauna (pp. 328–331). Washington, DC: Smithsonian Institution Press.

Ho, C. K., Pennings, S. C., & Carefoot, T. H. (2009). Is diet quality an overlooked mechanism for Bergmann's rule? The American Naturalist, 175, 269–276. https://doi.org/10.1086/649583.

Holt, B., & Jønsson, K.A. (2014) Reconciling hierarchical taxonomy with molecular phylogenies. Systematic Biology, 63, 1010–1017. https:// doi.org/10.1093/sysbio/syu061

Horne, C. R., Hirst, A. G., Atkinson, D., Neves, A., & Kiørbe, T. (2016). A global synthesis of seasonal temperature-size responses in copepods. Global Ecology and Biogeography, 25(8), 988–999. https:// doi.org/10.1111/geb.12460.

Huston, M. A., & Wolverton, S. (2011). Regulation of animal size by eNPP, Bergmann's rule and related phenomena. Ecological Monographs, 81, 349–405. https://doi.org/10.1890/10-1523.1.

Kennish, M. J. (2017). Ecology of estuaries, volume II: biological aspects. Boca Ratón: CRC Press.

Kingsolver, J. G., & Huey, R. B. (2008). Size, temperature, and fitness: three rules. Evolutionary Ecology Research, 10(2), 251–268.

Kosnik, M. A., Jablonski, D., Lockwood, R., & Novack-Gottshall, P. M. (2006). Quantifying molluscan body size in evolutionary and ecological analyses: maximizing the return on data-collection efforts. Palaios, 21(6), 588–597. https://doi.org/10.2110/palo.2006.p06-012r.

Kristensen, R. M., & Higgins, R. P. (1991). Kinorhyncha. In R. W. Harrison & E. E. Ruppert (Eds.), Microscopic anatomy of invertebrates, Vol. 4 (pp. 377–404). New York: John Wiley and Sons.

Lindsey, C. C. (1966). Body sizes of poikilotherm vertebrates at different latitudes. Evolution, 20, 456–465.

Lonsdale, D. J., & Levinton, J. S. (1985). Latitudinal differentiation in copepod growth: an adaptation to temperature. Ecology, 66, 1397– 1407. https://doi.org/10.2307/1938002.

Margulis, L., & Chapman, M. (2009). Kingdom and domains: an illustrated guide to the phyla of life on Earth. Boston: Academic Press.

Martorelli, S., & Higgins, R. P. (2004). Kinorhyncha from the stomach of the shrimp *Pleoticus muelleri* (Bate, 1888) from Comodoro Rivadavia, Argentina. Zoologischer Anzeiger, 243, 85-98.https:// doi.org/10.1016/j.jcz.2004.07.003

Maze, G. (2011). 1997-2007 SeaWIFS based monthly standard estimate of NPP. Available at: http://www.ifremer.fr/lpo/files/gmaze/data/standard_vgpm.seawifs.global.nc.gz (accessed 1 November 2018).

McClain, C. R., & Rex, M. (2001). The relationship between dissolved oxygen concentration and maximum size in deep-sea turrid gastropods: an application of quantile regression. Marine Biology, 139, 681–685. https://doi.org/10.1007/s002270100617.

McDowall, R. M. (2007). Jordan's and other ecogeographical rules, and the vertebral number in fishes. Journal of Biogeography, 35(3), 501–508. https://doi.org/10.1111/j.1365-2699.2007.01823.x.

McNab, B. K. (2010). Geographic and temporal correlations of mammalian size reconsidered: a resource rule. Oecologia, 164, 13–23. https://doi.org/10.1007/s00442-010-1621-5.

Meyer, K. M., Memiaghe, H., Korte, L., Kenfack, D., Alonso, A., & Bohannan, B. J. M. (2018). Why do microbes exhibit weak biogeographic patterns? The Multidisciplinary Journal of Microbial Ecology, 12(6), 1404–1413. https://doi.org/10.1038/s41396-018-0103-3.

Moran, A. L., & Woods, H. A. (2012). Why might they be giants? Towards an understanding of polar gigantism. The Journal of Experimental Biology, 215, 1995–2002. https://doi.org/10.1242/jeb.067066.

Neira, C., Ingels, J., Mendoza, G., Hernández-López, E., & Levin, L. A. (2018). Distribution of meiofauna in bathyal sediments influenced by the oxygen minimum zone off Costa Rica. Frontiers in Marine Science, 5, e448. https://doi.org/10.3389/fmars.2018.00448.

Neuhaus, B. (2013). Kinorhyncha (= Echinodera). In A. Schmidt-Rhaesa (Ed.), Handbook of Zoology. Gastrotricha, Cycloneuralia and Gnathifera. Volume 1: Nematomorpha, Priapulida, Kinorhyncha, Loricifera (pp. 181–348). Göttingen: De Gruyter.

Neuhaus, B., Pardos, F., Sørensen, M. V., & Higgins, R. P. (2013). Redescription, morphology and biogeography of *Centroderes spinosus* (Reinhard, 1881) (Kinorhyncha, Cyclorhagida) from Europe. Cahiers de Biologie Marine, 54(1), 109–131. https://doi.org/10.21411/CBM.A.8E3FD0CA.

Pardos, F., Herranz, M., & Sánchez, N. (2016). Two sides of a coin: the phylum Kinorhyncha in Panama (II). Pacific Panama. Zoologischer Anzeiger, 265(26-47), 26–47. https://doi.org/10.1016/j.jcz.2016.06. 006.

Partridge, L., & Coyne, L. A. (1997). Bergmann's rule in ectotherms: is it adaptative? Evolution, 51, 632–635.

Peters, R. H. (1983). The ecological implications of body size. Cambridge: Cambridge University Press.

Pinheiro, J., Bates, D., DebRoy, S., Sarkar, D., & R Core Team (2020). nlme: linear and nonlinear mixed effects models. R package version 3.1–145, https://CRAN.R-project.org/package=nlme. Accessed 1 Feb 2020

R Core Team. (2020). R: a language and environment for statistical computing. Vienna: R Foundation for Statistical Computing http:// www.R-project.org/. Accessed 1 Feb 2020

Rex, M. A., Crame, J. A., Stuart, C. T., & Clarke, A. (2005). Large-scale biogeographic patterns in marine mollusk: a confluence of history and productivity? Ecology, 86, 2288–2297. https://doi.org/10.1890/ 04-1056.

Reynolds, R. W., Rayner, N. A., Smith, T. M., Stokes, D. C., & Wang, W. (2002). An improved in situ and satellite SST analysis for climate. Journal of Climate, 15, 1609–1625. https://doi.org/10.1175/1520-0442(2002)015<609:AIISAS>2.0.CO;2.

Rollinson, N., & Locke, R. (2018). Temperature-dependent oxygen lim-itation and the rise of Bergmann's rule in species with aquatic respiration. Evolution, 2018, 977–988. https://doi.org/10.1111/evo. 13458.

Rodríguez, A., Olalla-Tárraga, M. A., & Hawkins, B. A. (2008). Bergmann's rule and the geography of mammal body size in the Western Hemisphere. Global Ecology and Biogeography, 17, 274–283. https://doi.org/10.1111/j.1466-8238.2007.00363.x.

Rosenzweig, M. L. (1968). The strategy of body size in mammalian carnivores. The American Midland Naturalist, 80(2), 299–315. https://doi.org/10.2307/2423529.

Roy, K. (2002). Bathymetry and body size in marine gastropods: a shallow water perspective. Marine Ecology Progress Series, 237, 143–149. https://doi.org/10.3354/meps237143.

Roy, K., Jablonski, D., & Martien, K. K. (2000). Invariant size-frequency distributions along a latitudinal gradient in marine bivalves. PNAS, 97, 13150–13155. https://doi.org/10.1073/pnas.97.24.13150.

Roy, K., Jablonski, D., Valentine, J. W., & Rosenberg, G. (1998). Marine latitudinal diversity gradients: tests of casual hypotheses. PNAS, 95(7), 3699–3702. https://doi.org/10.1073/pnas.95.7.3699.

Saeedi, H., Costello, M. J., Warren, D., & Brandt, A. (2019). Latitudinal and bathymetrical species richness patterns in the NW Pacific and adjacent Arctic Ocean. Scientific Reports, 9, e9303. https://doi.org/ 10.1038/s41598-019-45813-9.

Saeedi, H., Dennis, T. E., & Costello, M. J. (2017). Bimodal latitudinal species richness and high endemicity of razor clams (Mollusca). Journal of Biogeography, 44, 592–604. https://doi.org/10.1111/jbi. 12903.

San Martín, E., Harris, R. P., & Irigoien, X. (2006). Latitudinal variation in plankton size spectra in the Atlantic Ocean. Deep Sea Research Part II: Topical Studies in Oceanography, 53, 1560–1572. https:// doi.org/10.1016/j.dsr2.2006.05.006.

Sánchez, N., Herranz, M., Benito, J., & Pardos, F. (2012). Kinorhyncha from the Iberian Peninsula: new data from the first intensive sampling campaigns. Zootaxa, 3402, 24–44. https://doi.org/10.11646/ zootaxa.3402.1.2.

Sánchez, N., Pardos, F., Herranz, M., & Benito, J. (2011). *Pycnophyes dolichurus* sp. nov. and *P. aulacodes* sp. nov. (Kinorhyncha, Homalorhagida, Pycnophyidae), two new kinorhynchs from Spain with a reevaluation of homalorhagid taxonomic characters. Helgoland Marine Research, 65, 319–334. https://doi.org/10.1007/ s10152-010-0226-z.

Sánchez, N., Rho, H. S., Min, W. G., Kim, D., & Sørensen, M. V. (2013). Four new species of *Pycnophyes* (Kinorhyncha: Homalorhagida) from Korea and the East China Sea. Scientia Marina, 77(2), 353–380. https://doi.org/10.3989/scimar.03769.15A.

Sargis, E. J., Millien, V., Woodman, N., & Olson, L. E. (2018). Rule reversal: ecogeographical patterns of body size variation in the common treeshrew (Mammalia, Scandentia). Ecology and Evolution, 8(3), 1634–1645.

Saunders, R. A., & Tarling, G. A. (2018). Southern Ocean mesopelagic fish comply with Bergmann's rule. The American Naturalist, 191(3), 343–351.

Sibly, R. M., & Atkinson, D. (1994). How rearing temperature affects optimal adult size in ectotherms. Functional Ecology, 8, 486–493. https://doi.org/10.2307/2390073.

Smith, K. F., & Brown, J. H. (2002). Patterns of diversity, depth range and body size among pelagic fishes along a gradient of depth. Global Ecology and Biogeography, 11, 313–322. https://doi.org/ 10.1046/j.1466-822X.2002.00286.x.

Sørensen, M. V., Heiner, I., & Hansen, J. G. (2008). A comparative morphological study of the kinorhynch genera *Antygomonas* and *Semnoderes* (Kinorhyncha: Cyclorhagida). Helgoland Marine Research, 63, 129–147. https://doi.org/10.1007/s10152-008-0132-9.

Sørensen, M. V., Herranz, M., Rho, H. S., Min, W. G., Yamasaki, H., Sánchez, N., & Pardos, F. (2012). On the genus *Dracoderes* Higgins & Shirayama, 1990 (Kinorhyncha: Cyclorhagida) with a redescription of its type species, *D. abei*, and a description of a new species from Spain. Marine Biology Research, 8(3), 210–232. https://doi. org/10.1080/17451000.2011.615328.

Sørensen, M. V., & Pardos, F. (2020). Kinorhyncha. In A. Schmidt-Rhaesa (Ed.), Guide to the identification of marine meiofauna (pp. 391–414). Munich: Verlag Dr. Friedrich Pfeil.

Stillwell, R. C. (2010). Are latitudinal clines in body size adaptive? Oikos, 119, 1387–1390. https://doi.org/10.1111/j.1600-0706.2010.18670. x.

Tidière, M., Lemaître, J. F., Pélabon, C., Gimenez, O., & Gaillard, J. M. (2017). Evolutionary allometry reveals a shift in selection pressure on male horn size. Journal of Evolutionary Biology, 30, 1826–1835. https://doi.org/10.1111/jeb.13142.

Tomczak, M. (2019). Upper ocean mean horizontal structure. In J. K. Cochran, H. J. Bokuniewicz, & P. L. Yager (Eds.), Encyclopedia of ocean sciences (3rd edition), volume 1: Marine biogeochemistry (pp. 60–70). Cambridge: Elsevier Academic Press.

Vinarski, M. V. (2014). On the applicability of Bergmann's rule to ectotherms: the state of the art. Biology Bulletin Reviews, 4, 232–242. https://doi.org/10.1134/S2079086414030098.

Virgós, E., Kowalczyk, R., Trua, A., De Marinis, A., Mangas, J. G., Barea-Azcón, J. M., & Geffen, E. (2011). Body size clines in the European badger and the abundant centre hypothesis. Journal of Biogeography, 38, 1546–1556. https://doi.org/10.1111/j.1365-2699.2011.02512.x.

Walters, R. J., & Hassall, M. (2006). The temperature-size rule in ectotherms: may a general explanation exist after all? The American Naturalist, 167(4), 510–523. https://doi.org/10.1086/501029.

Whittaker, R. J., & Fernández-Palacios, J. M. (2006). Island biogeography; ecology, evolution and conservation (1st ed.). Oxford: Oxford University Press.

Williams, G. C. (1966). Adaptation and natural selection. Princeton: Princeton University Press.

Wyatt, T., & Carlton, J. T. (2002). Phytoplankton introductions in European coastal waters: why are so few invasions reported? CIESM Workshop Monographs, 20, 41–46.

Young, C. M., Arellano, S. M., Hamel, J. F., & Mercier, A. (2006). Chapter 16. Ecology and evolution of larval dispersal in the deep sea. In T. Carrier, A. Reitzel, & A. Heyland (Eds.), Evolutionary ecology of marine invertebrate larvae (pp. 229–250). Oxford: Oxford University Press Scholarship Online.

Zamora-Camacho, F. J., Reguera, S., & Moreno-Rueda, G. (2014). Bergmann's rules body size in an ectotherm: heat conservation in a lizard along a 2200-metre elevational gradient. Journal of Evolutionary Biology, 27(12), 2820–2828. https://doi.org/10.1111/jeb.12546.

Zuur, A. F., Ieno, E. N., Walker, N. J., & Savelieve, A. A. (2009). Mixed effects models and extensions in ecology with R (1st ed.). New York: Springer.

Supplementary Information

Appendix S1 Dataset containing original measures used to extract body size per kinorhynch species, latitude and longitude values defining grids of 1° latitude/longitude, and body size values. Abbreviations: BS, body size; LAT, latitude; LON, longitude; MSW, maximum sternal width; TL, total trunk length. Body measurements are indicated in μm and depth in metres (see https://link.springer.com/article/10.1007/s13127-020-00471-y#additional-information to access to it).

Appendix S2 Supporting tables with the results of the generalized least squares, linear and mixed models analysing size-latitude trends per hemisphere and coastline.

Supporting Table 1. Results of the generalized least squares models of latitudinal gradients in the mean, minimum and maximum body size, accounting for absolute and squared values of latitude, species richness, records and subdivision into six main geographical areas in the northern hemisphere. Abbreviations: *p*, *p*-value; RI, relative importance of a variable; χ^2, chi-squared value. Statistically significant *p*-values with an α-level<0.001 are reported in bold.

Mean body size	χ^2	***p***	**RI**
Latitude	0.08	0.7781	0.43
Latitude (squared)	1.99	0.1584	0.71
Species richness	0.06	0.8067	0.03
Records	0.31	0.5783	0.03
Coastline	27.89	**<0.0001**	1.00
Minimum body size	χ^2	***p***	**RI**
Latitude	<0.01	0.9507	0.34
Latitude (squared)	1.57	0.2108	0.43
Species richness	0.11	0.7393	0.03
Records	0.52	0.4703	0.05
Coastline	25.06	**<0.0001**	1.00
Maximum body size	χ^2	***p***	**RI**
Latitude	0.14	0.7030	0.35
Latitude (squared)	2.17	0.1407	0.44
Species richness	0.04	0.8430	0.03
Records	0.22	0.6383	0.04
Coastline	28.01	**<0.0001**	1.00

Supporting Table 2. Results of the generalized least squares models of latitudinal gradients in the mean, minimum and maximum body size, accounting for absolute and squared values of latitude, species richness, records, sea surface temperature (SST). net primary productivity (NPP) and subdivision into six main geographical areas in the northern hemisphere. Abbreviations: *p*, *p*-value; RI, relative importance of a variable; χ^2, chi-squared value. Statistically significant p-values with an α-level<0.001 are reported in bold.

Mean body size	χ^2	***p***	**RI**
Latitude	2.31	0.1282	0.31
Latitude (squared)	2.48	0.1151	0.43
Species richness	0.02	0.8905	0.03
Records	0.26	0.6108	0.04
SST	4.08	0.0434	0.57
NPP	0.06	0.8070	0.03
Coastline	29.13	**<0.0001**	1.00
Minimum body size	χ^2	***p***	**RI**
Latitude	1.79	0.1805	0.31
Latitude (squared)	1.99	0.1585	0.46
Species richness	0.04	0.8339	0.03
Records	0.49	0.4828	0.04
SST	3.96	0.0467	0.58
NPP	0.23	0.6293	0.03
Coastline	26.74	**<0.0001**	0.99
Maximum body size	χ^2	***p***	**RI**
Latitude	2.77	0.0960	0.31
Latitude (squared)	2.78	0.0955	0.44
Species richness	0.01	0.9249	0.03
Records	0.19	0.6622	0.03
SST	4.39	0.0360	0.56
NPP	0.11	0.7425	0.03
Coastline	29.29	**<0.0001**	1.00

Supporting Table 3. Results of the generalized mixed models of latitudinal gradients in the mean, minimum and maximum body size, accounting for absolute and squared values of latitude, species richness, records and subdivision into six main geographical areas for the northern hemisphere. Abbreviations: cR^2, conditional effects measure; mR^2, marginal effects measure; *p*, *p*-value; StdE, standard error; *t*, *t*-value. Statistically significant p-values with an α-level<0.001 are reported in bold.

Mean body size	**Estimate**	**StdE**	***t***	***p***	mR^2	cR^2
Latitude	0.1634	0.0562	2.91	0.0035	0.0545	0.6951
Latitude (squared)	0.0095	0.0557	0.17	0.8645		
Species richness	-0.0245	0.0224	-1.09	0.2731		
Records	-0.0014	0.0223	-0.06	0.9478		
Coastline	/	/	/	**<0.0001**		
Minimum body size	**Estimate**	**StdE**	***t***	***p***	mR^2	cR^2
Latitude	0.2444	0.0512	4.77	**<0.0001**	0.0474	0.7298
Latitude (squared)	-0.0792	0.0503	-1.57	0.1139		
Species richness	-0.0162	0.0213	-0.76	0.4453		
Records	-0.0097	0.0211	-0.46	0.6455		
Coastline	/	/	/	**<0.0001**		
Maximum body size	**Estimate**	**StdE**	***t***	***p***	mR^2	cR^2
Latitude	0.1580	0.0528	2.99	0.0027	0.0548	0.6729
Latitude (squared)	0.0107	0.0519	0.21	0.8356		
Species richness	-0.0333	0.0220	-1.51	0.1289		
Records	0.0094	0.0217	0.43	0.6647		
Coastline	/	/	/	**<0.0001**		

Supporting Table 4. Results of the generalized mixed models of latitudinal gradients in the mean, minimum and maximum body size, accounting for absolute and squared values of latitude, species richness, species records, sea surface temperature (SST), net primary productivity (NPP) and subdivision into six main geographical areas for the northern hemisphere. Abbreviations: cR^2, conditional effects measure; mR^2, marginal effects measure; *p*, *p*-value; StdE, standard error; *t*, *t*-value. Statistically significant *p*-values with an α-level<0.001 are reported in bold.

Mean body size	**Estimate**	**StdE**	***t***	***p***	mR^2	cR^2
Latitude	-0.1663	0.0821	-2.03	0.0418	0.0645	0.6992
Latitude (squared)	0.0649	0.0557	1.17	0.2415		
Species richness	0.0027	0.0227	0.12	0.9066		
Records	-0.0146	0.0222	-0.66	0.5091		
SST	-0.3038	0.0565	-5.38	**<0.0001**		
NPP	0.0131	0.0122	1.08	0.2793		
Coastline	/	/	/	**<0.0001**		
Minimum body size	**Estimate**	**StdE**	***t***	***p***	mR^2	cR^2
Latitude	-0.0892	0.0762	-1.17	0.2598	0.0559	0.7317
Latitude (squared)	-0.0154	0.0508	-0.30	0.7613		
Species richness	0.0149	0.0217	0.68	0.4917		
Records	-0.0255	0.0210	-1.21	0.2237		
SST	-0.2978	0.0517	-5.75	**<0.0001**		
NPP	0.0192	0.0119	1.61	0.1058		
Coastline	/	/	/	**<0.0001**		
Maximum body size	**Estimate**	**StdE**	***t***	***p***	mR^2	cR^2
Latitude	-0.1949	0.0846	-2.30	0.0207	0.064	0.6771
Latitude (squared)	0.0861	0.0577	1.49	0.1336		
Species richness	0.0001	0.0232	0.01	0.9968		
Records	-0.0101	0.0227	-0.44	0.6554		
SST	-0.3040	0.0583	-5.21	**<0.0001**		
NPP	0.0167	0.0124	1.35	0.1763		
Coastline	/	/	/	**<0.0001**		

Supporting Table 5. Results of the linear models of latitudinal gradients in the mean, minimum and maximum body size, accounting for absolute and squared values of latitude, species richness, records and subdivision into six main geographical areas in the southern hemisphere. Abbreviations: *F*, *F*-value; p, *p*-value; R^2, coefficient of determination; RI, relative importance of a variable. Statistically significant p-values with an α-level<0.001 are reported in bold.

Median body size	***F***	***p***	**Partial R^2**	**RI**
Latitude	1.53	0.2191	0.0195	0.24
Latitude (squared)	0.10	0.7543	0.1186	0.24
Species richness	10.36	0.0019	0.1186	0.23
Records	8.69	0.0042	0.1014	0.16
Coastline	3.53	0.0063	0.1864	0.27
Minimum body size	***F***	***p***	**Partial R^2**	**RI**
Latitude	2.33	0.1309	0.0294	0.22
Latitude (squared)	0.01	0.9160	0.1363	0.21
Species richness	12.15	**0.0008**	0.1363	0.27
Records	11.17	**0.0013**	0.1267	0.19
Coastline	3.15	0.0122	0.1699	0.14
Maximum body size	***F***	***p***	**Partial R^2**	**RI**
Latitude	0.96	0.3298	0.0294	0.28
Latitude (squared)	0.40	0.5274	0.1363	0.32
Species richness	10.18	0.0021	0.1267	0.24
Records	9.05	0.0035	0.0928	0.17
Coastline	3.28	0.0097	0.1699	0.29

Supporting Table 6. Results of the linear models of latitudinal gradients in the mean, minimum and maximum body size, accounting for absolute and squared values of latitude, species richness, records, sea surface temperature (SST), net primary productivity (NPP) and subdivision into six main geographical areas in the southern hemisphere. Abbreviations: *F*, *F*-value; *p*, *p*-value; R^2, coefficient of determination; RI, relative importance of a variable. Statistically significant *p*-values with an α-level<0.001 are reported in bold.

Mean body size	***F***	***p***	**Partial R^2**	**RI**
Latitude	0.49	0.4873	0.0064	0.25
Latitude (squared)	0.64	0.4274	0.0084	0.27
Species richness	10.59	0.0017	0.1237	0.23
Records	7.83	0.0065	0.0946	0.16
SST	2.26	0.1365	0.0293	0.26
NPP	1.57	0.2144	0.0205	0.12
Coastline	3.45	0.0073	0.1872	0.27
Minimum body size	***F***	***p***	**Partial R^2**	**RI**
Latitude	1.03	0.3133	0.0136	0.24
Latitude (squared)	1.32	0.2535	0.0173	0.25
Species richness	12.55	**0.0007**	0.1433	0.20
Records	10.52	0.0018	0.1230	0.15
SST	2.47	0.1205	0.0318	0.25
NPP	0.89	0.3495	0.0117	0.11
Coastline	2.98	0.0164	0.1659	0.27
Maximum body size	***F***	***p***	**Partial R^2**	**RI**
Latitude	0.15	0.6996	0.0020	0.33
Latitude (squared)	0.29	0.5903	0.0039	0.39
Species richness	10.35	0.0019	0.1213	0.80
Records	7.88	0.0064	0.0951	0.79
SST	2.23	0.1396	0.0289	0.65
NPP	2.69	0.1052	0.0346	0.72
Coastline	3.09	0.0136	0.1710	0.70

Supporting Table 7. Results of the generalized mixed models of latitudinal gradients in the mean, minimum and maximum body size, accounting for absolute and squared values of latitude, species richness, records and subdivision into six main geographical areas for the southern hemisphere. Abbreviations: cR^2, conditional effects measure; mR^2, marginal effects measure; *p*, *p*-value; StdE, standard error; *t*, *t*-value. Statistically significant *p*-values with an α-level<0.001 are reported in bold.

Mean body size	**Estimate**	**StdE**	***t***	***p***	mR^2	cR^2
Latitude	-0.1947	0.1768	-1.10	0.2418	0.0844	0.8426
Latitude (squared)	0.0743	0.1806	0.41	0.6618		
Species richness	0.1103	0.1134	0.97	0.3009		
Records	-0.0184	0.1186	-0.15	0.8687		
Coastline	/	/	/	**0.0010**		
Minimum body size	**Estimate**	**StdE**	***t***	***p***	mR^2	cR^2
Latitude	-0.2269	0.1727	-1.31	0.1625	0.0985	0.8473
Latitude (squared)	0.0359	0.1764	0.20	0.8286		
Species richness	0.1335	0.1108	1.20	0.2000		
Records	-0.0184	0.1159	-0.74	0.4258		
Coastline	/	/	/	**0.0004**		
Maximum body size	**Estimate**	**StdE**	***t***	***p***	mR^2	cR^2
Latitude	-0.1961	0.1859	-1.05	0.2622	0.0913	0.7969
Latitude (squared)	0.0723	0.1898	0.38	0.6854		
Species richness	0.1150	0.1190	0.97	0.3043		
Records	-0.0171	0.1244	-0.14	0.8835		
Coastline	/	/	/	0.0044		

Supporting Table 8. Results of the generalized mixed models of latitudinal gradients in the mean, minimum and maximum body size, accounting for absolute and squared values of latitude, species richness, species records, sea surface temperature (SST), net primary productivity (NPP) and subdivision into six main geographical areas for the southern hemisphere. Abbreviations: cR^2, conditional effects measure; mR^2, marginal effects measure; *p*, *p*-value; StdE, standard error; *t*, *t*-value. Statistically significant *p*-values with an α-level<0.001 are reported in bold.

Mean body size	**Estimate**	**StdE**	***t***	***p***	mR^2	cR^2
Latitude	-0.1371	0.1838	-0.95	0.4217	0.0876	0.8478
Latitude (squared)	-0.1418	0.2522	-0.56	0.5449		
Species richness	0.1383	0.1159	1.19	0.1987		
Records	-0.0571	0.1228	-0.46	0.6166		
SST	-0.2780	0.2263	-1.23	0.1858		
NPP	-0.0269	0.0526	-0.51	0.5814		
Coastline	/	/	/	**0.0004**		
Minimum body size	**Estimate**	**StdE**	***t***	***p***	mR^2	cR^2
Latitude	-0.1740	0.1799	-0.97	0.2974	0.1040	0.8495
Latitude (squared)	-0.1641	0.2468	-0.66	0.4740		
Species richness	0.1593	0.1134	1.40	0.1303		
Records	-0.1226	0.1202	-1.02	0.1720		
SST	-0.2571	0.2215	-1.16	0.2112		
NPP	-0.0253	0.0515	-0.49	0.5963		
Coastline	/	/	/	**0.0002**		
Maximum body size	**Estimate**	**StdE**	***t***	***p***	mR^2	cR^2
Latitude	-0.1382	0.1933	-0.71	0.4413	0.0960	0.8015
Latitude (squared)	-0.1510	0.2656	-0.57	0.5403		
Species richness	0.1429	0.1216	1.17	0.2057		
Records	-0.0565	0.1288	-0.44	0.6366		
SST	-0.2861	0.2379	-1.20	0.1929		
NPP	-0.0306	0.0553	-0.55	0.5504		
Coastline	/	/	/	**0.0019**		

Supporting Table 9. Results of the generalized least squares models of latitudinal gradients in the mean, minimum and maximum body size, accounting for absolute and squared values of latitude, species richness and records in the western Atlantic coastline. Abbreviations: *F*, *F*-value; *p*, *p*-value; R^2, coefficient of determination; RI, relative importance of a variable; χ^2, chi-squared value. Statistically significant *p*-values with an α-level<0.001 are reported in bold.

Mean body size	***F***	***p***	**Partial R^2**	**RI**
Latitude	4.22	0.0406	0.0104	0.10
Latitude (squared)	43.89	**<0.0001**	0.0987	0.27
Species richness	23.36	**<0.0001**	0.0534	0.16
Records	22.62	**<0.0001**	0.0550	0.16
Minimum body size	**χ2**	***p***	**RI**	
Latitude	0.48	0.4894	0.09	
Latitude (squared)	3.13	0.0770	0.27	
Species richness	5.52	0.0183	0.20	
Records	6.11	0.0134	0.19	
Maximum body size	***F***	***p***	**Partial R^2**	**RI**
Latitude	5.33	0.0215	0.0131	0.14
Latitude (squared)	41.98	**<0.0001**	0.0948	0.27
Species richness	21.57	**<0.0001**	0.0475	0.13
Records	20.00	**<0.0001**	0.0510	0.15

Supporting Table 10. Results of the generalized least squares and linear models of latitudinal gradients in the mean, minimum and maximum body size, accounting for absolute and squared values of latitude, species richness, records, sea surface temperature (SST) and net primary productivity (NPP) in the western Atlantic coastline. Abbreviations: *F*, *F*-value; *p*, *p*-value; R^2, coefficient of determination; RI, relative importance of a variable; χ^2, chi-squared value. Statistically significant *p*-values with an α-level<0.001 are reported in bold.

Mean body size	***F***	***p***	**Partial R^2**	**RI**
Latitude	4.54	0.0337	0.0112	0.85
Latitude (squared)	16.80	**<0.0001**	0.0404	1.00
Species richness	16.93	**<0.0001**	0.0434	1.00
Records	18.11	**<0.0001**	0.0407	1.00
SST	1.85	0.1744	0.0046	0.57
NPP	0.22	0.6427	0.0005	0.41
Minimum body size	**χ^2**	***p***	**RI**	
Latitude	0.46	0.4985	0.09	
Latitude (squared)	1.04	0.3082	0.29	
Species richness	5.21	0.0225	0.19	
Records	5.87	0.0154	0.19	
SST	<0.01	0.9445	0.25	
NPP	0.14	0.7071	0.06	
Maximum body size	***F***	***p***	**Partial R^2**	**RI**
Latitude	5.70	0.0174	0.0141	0.85
Latitude (squared)	16.84	**<0.0001**	0.0405	1.00
Species richness	14.48	**0.0002**	0.0363	1.00
Records	15.03	**0.0001**	0.0350	1.00
SST	2.22	0.1372	0.0055	0.57
NPP	0.93	0.3348	0.0023	0.41

Supporting Table 11. Results of the generalized mixed models of latitudinal gradients in the mean, minimum and maximum body size, accounting for absolute and squared values of latitude, species richness and records for the western Atlantic coastline. Abbreviations: cR^2, conditional effects measure; mR^2, marginal effects measure; *p*, *p*-value; StdE, standard error; *t*, *t*-value. Statistically significant *p*-values with an α-level<0.001 are reported in bold.

Mean body size	**Estimate**	**StdE**	***t***	***p***	mR^2	cR^2
Latitude	-0.0922	0.0392	-2.35	0.0180	0.0823	0.7298
Latitude (squared)	0.2929	0.0412	7.11	**<0.0001**		
Species richness	0.0298	0.0629	0.47	0.6338		
Records	-0.0070	0.0587	0.12	0.9050		
Minimum body size	**Estimate**	**StdE**	***t***	***p***	mR^2	cR^2
Latitude	-0.1174	0.0429	-2.74	0.0059	0.0723	0.7298
Latitude (squared)	0.3135	0.0450	6.96	**<0.0001**		
Species richness	0.0700	0.0683	1.02	0.7010		
Records	-0.0244	0.0640	-0.38	0.3025		
Maximum body size	**Estimate**	**StdE**	***t***	***p***	mR^2	cR^2
Latitude	-0.0795	0.0378	-2.10	0.0344	0.0757	0.7422
Latitude (squared)	0.2645	0.0397	6.66	**<0.0001**		
Species richness	0.0011	0.0607	0.02	0.8849		
Records	-0.0283	0.0566	-0.50	0.6144		

Supporting Table 12. Results of the generalized mixed models of latitudinal gradients in the mean, minimum and maximum body size, accounting for absolute and squared values of latitude, species richness, species records, sea surface temperature (SST) and net primary productivity (NPP) for the western Atlantic coastline. Abbreviations: cR^2, conditional effects measure; mR^2, marginal effects measure; *p*, *p*-value; StdE, standard error; *t*, *t*-value. Statistically significant p-values with an α-level<0.001 are reported in bold.

Mean body size	**Estimate**	**StdE**	***t***	***p***	mR^2	cR^2
Latitude	-0.0939	0.0388	-2.42	0.0146	0.0909	0.7428
Latitude (squared)	0.2362	0.0913	2.59	0.0090		
Species richness	0.0744	0.0639	1.16	0.2401		
Records	-0.0420	0.0605	-0.69	0.4838		
SST	-0.0905	0.0859	-1.05	0.2878		
NPP	0.0766	0.0229	3.34	**0.0007**		
Minimum body size	**Estimate**	**StdE**	***t***	***p***	mR^2	cR^2
Latitude	-0.1212	0.0419	-2.89	0.0035	0.0825	0.7431
Latitude (squared)	0.2499	0.0994	2.51	0.0112		
Species richness	0.1163	0.0684	1.70	0.0862		
Records	-0.0753	0.0650	-1.16	0.2419		
SST	-0.1009	0.0932	-1.08	0.2747		
NPP	0.0874	0.0253	3.45	**0.0005**		
Maximum body size	**Estimate**	**StdE**	***t***	***p***	mR^2	cR^2
Latitude	-0.0822	0.0377	-2.18	0.0278	0.0801	0.7503
Latitude (squared)	0.2537	0.0887	2.86	0.0039		
Species richness	0.0296	0.0621	0.48	0.6305		
Records	-0.0022	0.0588	-0.04	0.9701		
SST	-0.0345	0.0835	-0.41	0.6768		
NPP	0.0590	0.0223	2.65	0.0074		

Supporting Table 13. Results of the generalized least squares models of latitudinal gradients in the mean, minimum and maximum body size, accounting for absolute and squared values of latitude, species richness and records in the eastern Atlantic coastline. Abbreviations: *p*, *p*-value; RI, relative importance of a variable; χ^2, chi-squared value. Statistically significant *p*-values with an α-level<0.001 are reported in bold.

Mean body size	χ^2	***p***	**RI**
Latitude	0.71	0.4003	0.16
Latitude (squared)	2.24	0.1343	0.23
Species richness	0.01	0.9292	0.06
Records	1.44	0.2308	0.19
Minimum body size	χ^2	***p***	**RI**
Latitude	1.49	0.2216	0.42
Latitude (squared)	1.77	0.1829	0.78
Species richness	0.05	0.8303	0.34
Records	0.43	0.5101	0.7
Maximum body size	**χ2**	***P***	**RI**
Latitude	1.84	0.1753	0.15
Latitude (squared)	2.60	0.1070	0.2
Species richness	<0.01	0.9600	0.06
Records	1.76	0.1844	0.28

Supporting Table 14. Results of the generalized least squares models of latitudinal gradients in the mean, minimum and maximum body size, accounting for absolute and squared values of latitude, species richness, records, sea surface temperature (SST) and net primary productivity (NPP) in the eastern Atlantic coastline. Abbreviations: *p*, *p*-value; RI, relative importance of a variable; χ^2, chi-squared value. Statistically significant *p*-values with an α-level<0.001 are reported in bold.

Mean body size	χ^2	***p***	**RI**
Latitude	2.63	0.1050	0.42
Latitude (squared)	1.55	0.2125	0.53
Species richness	0.01	0.9037	0.06
Records	0.32	0.5725	0.3
SST	0.59	0.4441	0.51
NPP	0.56	0.4542	0.84
Minimum body size	χ^2	***p***	**RI**
Latitude	1.54	0.2143	0.19
Latitude (squared)	0.16	0.6926	0.28
Species richness	0.01	0.9194	0.06
Records	0.02	0.8807	0.13
SST	0.14	0.7053	0.22
NPP	0.37	0.5416	0.09
Maximum body size	χ^2	***p***	**RI**
Latitude	2.60	0.1066	0.33
Latitude (squared)	1.51	0.2171	0.48
Species richness	<0.01	0.9571	0.06
Records	0.97	0.3254	0.20
SST	0.52	0.5168	0.35
NPP	0.82	0.3662	0.11

Supporting Table 15. Results of the generalized mixed models of latitudinal gradients in the mean, minimum and maximum body size, accounting for absolute and squared values of latitude, species richness and records for the eastern Atlantic coastline. Abbreviations: cR^2, conditional effects measure; mR^2, marginal effects measure; *p*, *p*-value; StdE, standard error; *t*, *t*-value. Statistically significant *p*-values with an α-level<0.001 are reported in bold.

Mean body size	**Estimate**	**StdE**	***t***	***p***	mR^2	cR^2
Latitude	-0.4239	0.0808	-5.24	**<0.0001**	0.0296	0.0296
Latitude (squared)	0.4574	0.1811	2.53	0.0112		
Species richness	0.0069	0.0253	0.27	0.0923		
Records	-0.0630	0.0376	-1.68	0.7845		
Minimum body size	**Estimate**	**StdE**	***t***	***p***	mR^2	cR^2
Latitude	-0.4317	0.0755	-5.72	**<0.0001**	0.0316	0.0316
Latitude (squared)	0.4903	0.1718	2.85	0.0041		
Species richness	0.0087	0.0243	0.36	0.7174		
Records	-0.0581	0.0352	-1.65	0.0973		
Maximum body size	**Estimate**	**StdE**	***t***	***p***	mR^2	cR^2
Latitude	-0.3041	0.0834	-3.64	**0.0002**	0.0365	0.6484
Latitude (squared)	0.3073	0.1090	2.82	0.0046		
Species richness	0.0050	0.0274	0.18	0.8538		
Records	-0.0961	0.0406	-2.37	0.0174		

Supporting Table 16. Results of the generalized mixed models of latitudinal gradients in the mean, minimum and maximum body size, accounting for absolute and squared values of latitude, species richness, species records, sea surface temperature (SST) and net primary productivity (NPP) for the eastern Atlantic coastline. Abbreviations: cR^2, conditional effects measure; mR^2, marginal effects measure; *p*, *p*-value; StdE, standard error; *t*, *t*-value. Statistically significant *p*-values with an α-level<0.001 are reported in bold.

Mean body size	**Estimate**	**StdE**	***t***	***p***	mR^2	cR^2
Latitude	-0.4432	0.0862	-5.14	**<0.0001**	0.0211	0.0211
Latitude (squared)	0.2887	0.2444	1.18	0.2345		
Species richness	0.0090	0.0256	0.35	0.7246		
Records	-0.0531	0.0395	-1.34	0.1766		
SST	-0.1775	0.1635	-1.08	0.2745		
NPP	0.0107	0.0269	0.40	0.6892		
Minimum body size	**Estimate**	**StdE**	***t***	***p***	mR^2	cR^2
Latitude	-0.4545	0.0790	-5.76	**<0.0001**	0.0194	0.0194
Latitude (squared)	0.3245	0.2265	1.43	0.2345		
Species richness	0.0098	0.0243	0.40	0.7246		
Records	-0.0638	0.0360	-1.77	0.1766		
SST	-0.1491	0.1368	-1.09	0.2745		
NPP	-0.0056	0.0246	-0.23	0.6891		
Maximum body size	**Estimate**	**StdE**	***t***	***p***	mR^2	cR^2
Latitude	-0.4450	0.0836	-5.32	**<0.0001**	0.0409	0.0409
Latitude (squared)	0.2315	0.0685	3.38	**0.0007**		
Species richness	0.0594	0.0308	1.93	0.0522		
Records	-0.1149	0.0319	-3.61	**0.0003**		
SST	-0.2665	0.0562	-4.74	**<0.0001**		
NPP	0.0385	0.0207	1.85	0.6146		

Supporting Table 17. Results of the linear models of latitudinal gradients in the mean, minimum and maximum body size, accounting for absolute and squared values of latitude, species richness and records in the western Pacific coastline. Abbreviations: *F*, *F*-value; *p*, *p*-value; R^2, coefficient of determination; RI, relative importance of a variable. Statistically significant *p*-values with an α-level<0.001 are reported in bold.

Mean body size	***F***	***p***	**Partial R^2**	**RI**
Latitude	0.14	0.7100	0.0007	0.27
Latitude (squared)	31.83	**<0.0001**	0.1292	1.00
Species richness	12.16	**0.0006**	0.0537	0.98
Records	11.81	**0.0007**	0.0522	0.98
Minimum body size	***F***	***p***	**Partial R^2**	**RI**
Latitude	1.27	0.2603	0.0060	0.41
Latitude (squared)	23.91	**<0.0001**	0.1003	1.00
Species richness	10.50	**0.0014**	0.0467	0.96
Records	9.32	0.0025	0.0416	0.96
Maximum body size	***F***	***p***	**Partial R^2**	**RI**
Latitude	0.18	0.7380	0.0008	0.27
Latitude (squared)	37.69	**<0.0001**	0.1494	1.00
Species richness	12.30	**0.0006**	0.0543	0.99
Records	13.52	**0.0003**	0.0593	0.99

Supporting Table 18. Results of the linear models of latitudinal gradients in the mean, minimum and maximum body size, accounting for absolute and squared values of latitude, species richness, records, sea surface temperature (SST) and net primary productivity (NPP) in the western Pacific coastline. Abbreviations: *F*, *F*-value; *p*, *p*-value; R^2, coefficient of determination; RI, relative importance of a variable. Statistically significant *p*-values with an α-level<0.001 are reported in bold.

Mean body size	***F***	***p***	**Partial R^2**	**RI**
Latitude	0.34	0.5627	0.0016	0.33
Latitude (squared)	4.35	0.0381	0.0201	0.95
Species richness	8.58	0.0038	0.0389	0.95
Records	9.28	0.0026	0.0420	0.97
SST	0.06	0.8113	0.0003	0.31
NPP	5.11	0.0247	0.0236	0.81
Minimum body size	***F***	***p***	**Partial R^2**	**RI**
Latitude	1.63	0.2029	0.0076	0.53
Latitude (squared)	3.07	0.0812	0.0143	0.88
Species richness	7.24	0.0077	0.0330	0.89
Records	7.12	0.0082	0.0325	0.89
SST	0.02	0.8789	0.0001	0.37
NPP	3.86	0.0509	0.0179	0.69
Maximum body size	***F***	***p***	**Partial R^2**	**RI**
Latitude	0.02	0.8922	<0.0001	0.27
Latitude (squared)	5.12	0.0246	0.0236	0.96
Species richness	8.65	0.0036	0.0392	0.96
Records	10.73	**0.0012**	0.0482	0.98
SST	0.07	0.7911	0.0003	0.30
NPP	6.65	0.0106	0.0304	0.92

Supporting Table 19. Results of the generalized mixed models of latitudinal gradients in the mean, minimum and maximum body size, accounting for absolute and squared values of latitude, species richness and records for the western Pacific coastline. Abbreviations: cR^2, conditional effects measure; mR^2, marginal effects measure; *p*, *p*-value; StdE, standard error; *t*, *t*-value. Statistically significant *p*-values with an α-level<0.001 are reported in bold.

Mean body size	**Estimate**	**StdE**	***t***	***p***	mR^2	cR^2
Latitude	0.0143	0.0407	0.35	0.7214	0.1611	0.8487
Latitude (squared)	0.2356	0.0348	6.77	**<0.0001**		
Species richness	-0.2828	0.0619	-4.56	**<0.0001**		
Records	0.2268	0.0638	3.56	**0.0003**		
Minimum body size	**Estimate**	**StdE**	***t***	***p***	mR^2	cR^2
Latitude	0.0322	0.0414	0.78	0.4311	0.1167	0.8537
Latitude (squared)	0.1985	0.0354	5.61	**<0.0001**		
Species richness	-0.2346	0.0629	-3.73	**0.0002**		
Records	0.1822	0.0648	2.81	**0.0044**		
Maximum body size	**Estimate**	**StdE**	***t***	***p***	mR^2	cR^2
Latitude	-0.0130	0.0415	-0.31	0.7510	0.1707	0.8439
Latitude (squared)	0.2589	0.0355	7.30	**<0.0001**		
Species richness	-0.3016	0.0632	-4.77	**<0.0001**		
Records	0.2615	0.065	4.02	**<0.0001**		

Supporting Table 20. Results of the generalized mixed models of latitudinal gradients in the mean, minimum and maximum body size, accounting for absolute and squared values of latitude, species richness, species records, sea surface temperature (SST) and net primary productivity (NPP) for the western Pacific coastline. Abbreviations: cR^2, conditional effects measure; mR^2, marginal effects measure; *p*, *p*-value; StdE, standard error; *t*, *t*-value. Statistically significant *p*-values with an α-level<0.001 are reported in bold.

Mean body size	**Estimate**	**StdE**	***t***	***p***	mR^2	cR^2
Latitude	0.0598	0.0409	1.46	0.1374	0.1784	0.8618
Latitude (squared)	-0.0050	0.0808	-0.06	0.9494		
Species richness	-0.1624	0.0696	-2.33	0.0177		
Records	0.1196	0.0725	1.65	0.0936		
SST	-0.2017	0.0747	-2.70	0.0060		
NPP	-0.0860	0.0245	-3.51	**0.0003**		
Minimum body size	**Estimate**	**StdE**	***t***	***p***	mR^2	cR^2
Latitude	0.0779	0.0418	1.86	0.0582	0.1294	0.8661
Latitude (squared)	-0.0484	0.0826	-0.59	0.5513		
Species richness	-0.1112	0.0711	-1.56	0.1122		
Records	0.0692	0.0741	0.93	0.3425		
SST	-0.2132	0.0763	-2.79	0.0045		
NPP	-0.0761	0.025	-3.04	**0.0019**		
Maximum body size	**Estimate**	**StdE**	***t***	***p***	mR^2	cR^2
Latitude	0.0330	0.0415	0.80	0.4181	0.1934	0.8573
Latitude (squared)	0.0203	0.0819	0.25	0.8013		
Species richness	-0.1821	0.0706	-2.58	0.0087		
Records	0.1587	0.0735	2.16	0.0281		
SST	-0.1930	0.0757	-2.55	0.0096		
NPP	-0.0990	0.0248	-4.00	**<0.0001**		

Supporting Table 21. Results of the generalized least squares models of latitudinal gradients in the mean, minimum and maximum body size, accounting for absolute and squared values of latitude, species richness and records in the eastern Pacific coastline. Abbreviations: *p*, *p*-value; RI, relative importance of a variable; χ^2, chi-squared value. Statistically significant *p*-values with an α-level<0.001 are reported in bold.

Mean body size	χ^2	***p***	**RI**
Latitude	11.99	**0.0005**	0.67
Latitude (squared)	16.05	**<0.0001**	0.77
Species richness	<0.01	0.9564	0.13
Records	0.29	0.5891	0.14
Minimum body size	χ^2	***p***	**RI**
Latitude	12.50	**0.0004**	0.74
Latitude (squared)	19.78	**<0.0001**	0.86
Species richness	0.02	0.6579	0.18
Records	1.15	0.2833	0.22
Maximum body size	**χ2**	***p***	**RI**
Latitude	11.63	**0.0006**	0.74
Latitude (squared)	14.87	**0.0001**	0.80
Species richness	0.06	0.8106	0.10
Records	0.39	0.5339	0.11

Supporting Table 22. Results of the generalized least squares models of latitudinal gradients in the mean, minimum and maximum body size, accounting for absolute and squared values of latitude, species richness, records, sea surface temperature (SST) and net primary productivity (NPP) in the eastern Pacific coastline. Abbreviations: *p*, *p*-value; RI, relative importance of a variable; χ^2, chi-squared value. Statistically significant p-values with an α-level<0.001 are reported in bold.

Mean body size	χ^2	***p***	**RI**
Latitude	10.43	**0.0012**	0.67
Latitude (squared)	5.77	0.0163	0.67
Species richness	0.01	0.9222	0.12
Records	0.30	0.5839	0.13
SST	0.09	0.7624	0.33
NPP	0.14	0.7105	0.10
Minimum body size	χ^2	***p***	**RI**
Latitude	10.47	**0.0012**	0.71
Latitude (squared)	5.62	0.0177	0.70
Species richness	<0.01	0.9416	0.17
Records	0.61	0.4335	0.19
SST	<0.01	0.9704	0.38
NPP	0.04	0.8506	0.10
Maximum body size	χ^2	***p***	**RI**
Latitude	9.52	0.0020	0.74
Latitude (squared)	4.33	0.0373	0.68
Species richness	0.05	0.8226	0.10
Records	0.38	0.5371	0.10
SST	0.01	0.9315	0.34
NPP	<0.01	0.8389	0.10

Supporting Table 23. Results of the generalized mixed models of latitudinal gradients in the mean, minimum and maximum body size, accounting for absolute and squared values of latitude, species richness and records for the eastern Pacific coastline. Abbreviations: cR^2, conditional effects measure; mR^2, marginal effects measure; *p*, *p*-value; StdE, standard error; *t*, *t*-value. Statistically significant *p*-values with an α-level<0.001 are reported in bold.

Mean body size	**Estimate**	**StdE**	***t***	***p***	mR^2	cR^2
Latitude	-0.1293	0.0822	-1.57	0.1103	0.0884	0.7067
Latitude (squared)	0.2684	0.0855	3.14	**0.0014**		
Species richness	-0.0717	0.1192	-0.60	0.3821		
Records	0.0958	0.1114	0.86	0.5410		
Minimum body size	**Estimate**	**StdE**	***t***	***p***	mR^2	cR^2
Latitude	-0.0730	0.0646	-1.13	0.2510	0.0979	0.7337
Latitude (squared)	0.1755	0.0665	2.64	0.0073		
Species richness	-0.3180	0.0968	-3.28	**0.0014**		
Records	0.3047	0.0971	3.13	**0.0008**		
Maximum body size	**Estimate**	**StdE**	***t***	***p***	mR^2	cR^2
Latitude	-0.0804	0.0680	-1.18	0.2293	0.1707	0.8439
Latitude (squared)	0.1514	0.0702	2.15	0.0284		
Species richness	-0.3223	0.1124	-2.87	0.0035		
Records	0.2776	0.1100	2.52	0.0103		

Supporting Table 24. Results of the generalized mixed models of latitudinal gradients in the mean, minimum and maximum body size, accounting for absolute and squared values of latitude, species richness, records, sea surface temperature (SST) and net primary productivity (NPP) for the eastern Pacific coastline. Abbreviations: cR^2, conditional effects measure; mR^2, marginal effects measure; *p*, *p*-value; StdE, standard error; *t*, *t*-value. Statistically significant *p*-values with an α-level<0.001 are reported in bold.

Mean body size	**Estimate**	**StdE**	***t***	***p***	mR^2	cR^2
Latitude	-0.1648	0.0835	-1.97	0.0435	0.0831	0.7157
Latitude (squared)	0.3170	0.1464	2.16	0.0268		
Species richness	-0.0602	0.1172	-0.51	0.5993		
Records	0.0998	0.1092	0.91	0.3499		
SST	0.0477	0.1544	0.31	0.7519		
NPP	-0.0769	0.0446	-1.72	0.0777		
Minimum body size	**Estimate**	**StdE**	***t***	***p***	mR^2	cR^2
Latitude	-0.1686	0.0893	-1.89	0.0534	0.1192	0.1356
Latitude (squared)	0.2133	0.1842	1.16	0.2363		
Species richness	-0.1827	0.1175	-1.56	0.1116		
Records	0.2010	0.1122	1.87	0.0557		
SST	-0.1177	0.1709	-0.69	0.4813		
NPP	-0.0549	0.0469	-1.17	0.2311		
Maximum body size	**Estimate**	**StdE**	***t***	***p***	mR^2	cR^2
Latitude	-0.1166	0.0677	-1.72	0.0780	0.0704	0.7803
Latitude (squared)	0.1819	0.1134	1.60	0.1010		
Species richness	0.2606	0.1074	-2.77	0.0046		
Records	-0.2974	0.1056	2.47	0.0116		
SST	0.0329	0.1070	0.31	0.7531		
NPP	-0.1074	0.0433	-2.48	0.0112		

Appendix S3 Supporting tables with the results of the comparisons between generalized least squares models, including five different spatial structures (exponential, Gaussian, spherical, linear and rational quadratic), and the linear models without spatial structure testing the effect of latitude (both raw and squared values), environmental and confounding variables on kinorhynch body size, also including the subdivision into six major coastlines.

Supporting Table 1. Results of the comparison between generalized least squares models including five different spatial structures and the linear models without spatial structure testing the effect of latitude (both absolute and squared values), species richness, number of records and subdivision into six major coastlines on body size (mean, minimum and maximum values). The Akaike Information Criterion (AIC), the likelihood ratios (logLik) and the degrees of freedom (dF) of each model are reported. The results of a likelihood ratio test (lrt) between the non-spatial and the spatial generalized least squares model with the lowest AIC value is also reported. Selected models are highlighted in red.

Model		AIC	dF	logLik	lrt
Mean Body Size	Non-spatial	3750.51	1360	-1864.25	χ^2=310.80 p<0.0001
	Exponential	3443.70	1360	-1708.85	
	Gaussian	3754.51	1360	-1864.25	
	Spherical	3754.50	1360	-1864.25	
	Linear	3754.48	1360	-1864.24	
	Rational quadratic	3451.03	1360	-1712.51	
Minimum Body Size	Non-spatial	3747.59	1360	-1862.79	χ^2=302.06 p<0.0001
	Exponential	3449.53	1360	-1711.76	
	Gaussian	3751.59	1360	-1862.79	
	Spherical	3751.59	1360	-1862.79	
	Linear	3751.59	1360	-1862.79	
	Rational quadratic	3458.01	1360	-1761.01	
Maximum Body Size	Non-spatial	3766.22	1360	-1872.11	χ^2=300.59 p<0.0001
	Exponential	3469.63	1360	-1721.82	
	Gaussian	3770.22	1360	-1872.11	
	Spherical	3770.22	1360	-1872.11	
	Linear	3770.22	1360	-1872.12	
	Rational quadratic	3478.64	1360	-1726.32	

Supporting Table 2. Results of the comparison between generalized least squares models including five different spatial structures and the linear models without spatial structure testing the effect of latitude (both absolute and squared values), species richness, number of records, sea surface temperature, net primary productivity and subdivision into six major coastlines on body size (mean, minimum and maximum values). The Akaike Information Criterion (AIC), the likelihood ratios (logLik) and the degrees of freedom (dF) of each model are reported. The results of a likelihood ratio test (lrt) between the non-spatial and the spatial generalized least squares model with the lowest AIC value is also reported. Selected models are highlighted in red.

Model		AIC	dF	logLik	lrt
Mean Body Size	Non-spatial	3739.78	1358	-1856.89	χ^2=297.22 p<0.0001
	Exponential	3446.56	1358	-1708.28	
	Gaussian	3743.78	1358	-1856.89	
	Spherical	3743.78	1358	-1856.89	
	Linear	3743.78	1358	-1856.89	
	Rational quadratic	3454.44	1358	-1712.22	
Minimum Body Size	Non-spatial	3735.96	1358	-1854.98	χ^2=288.19 p<0.0001
	Exponential	3451.77	1358	-1710.88	
	Gaussian	3739.96	1358	-1854.98	
	Spherical	3739.96	1358	-1854.98	
	Linear	3739.96	1358	-1854.98	
	Rational quadratic	3461.04	1358	-1715.52	
Maximum Body Size	Non-spatial	3757.24	1358	-1865.62	χ^2=288.27 p<0.0001
	Exponential	3472.96	1358	-1721.48	
	Gaussian	3761.24	1358	-1865.62	
	Spherical	3761.24	1358	-1865.62	
	Linear	3761.24	1358	-1865.62	
	Rational quadratic	3482.29	1358	-1726.15	

Supporting Table 3. Results of the comparison between generalized least squares models including five different spatial structures and the linear models without spatial structure testing the effect of latitude (both absolute and squared values), species richness, number of records and subdivision into six major coastlines on body size (mean, minimum and maximum values) in the northern hemisphere. The Akaike Information Criterion (AIC), the likelihood ratios (logLik) and the degrees of freedom (dF) of each model are reported. The results of a likelihood ratio test (lrt) between the non-spatial and the spatial, generalized least squares model with the lowest AIC value is also reported. Selected models are highlighted in red.

Model		AIC	dF	logLik	lrt
Mean Body Size	Non-spatial	3545.83	1273	-1761.91	χ^2=336.53 p<0.0001
	Exponential	3213.29	1273	-1593.65	
	Gaussian	3513.58	1273	-1743.79	
	Spherical	3513.65	1273	-1743.82	
	Linear	3513.58	1273	-1743.79	
	Rational quadratic	3218.61	1273	-1596.30	
Minimum Body Size	Non-spatial	3506.80	1273	-1742.40	χ^2=336.53 p<0.0001
	Exponential	3220.10	1273	-1597.05	
	Gaussian	3507.17	1273	-1740.59	
	Spherical	3507.28	1273	-1740.64	
	Linear	3507.22	1273	-1740.61	
	Rational quadratic	3226.26	1273	-1600.13	
Maximum Body Size	Non-spatial	3530.49	1273	-1754.24	χ^2=296.40 p<0.0001
	Exponential	3238.09	1273	-1606.05	
	Gaussian	3532.24	1273	-1753.12	
	Spherical	3237.03	1273	-1605.52	
	Linear	3263.50	1273	-1618.75	
	Rational quadratic	3244.86	1273	-1609.43	

Supporting Table 4. Results of the comparison between generalized least squares models including five different spatial structures and the linear models without spatial structure testing the effect of latitude (both absolute and squared values), species richness, number of records, sea surface temperature, net primary productivity and subdivision into six major coastlines on body size (mean, minimum and maximum values) in the northern hemisphere. The Akaike Information Criterion (AIC), the likelihood ratios (logLik) and the degrees of freedom (dF) of each model are reported. The results of a likelihood ratio test (lrt) between the non-spatial and the spatial, generalized least squares model with the lowest AIC value is also reported. Selected models are highlighted in red.

Model		AIC	dF	logLik	lrt
Mean Body Size	Non-spatial	3493.55	1271	-1733.77	χ^2=283.78 p<0.0001
	Exponential	3213.77	1271	-1591.89	
	Gaussian	3494.66	1271	-1732.33	
	Spherical	3494.72	1271	-1732.36	
	Linear	3494.66	1271	-1732.33	
	Rational quadratic	3220.11	1271	-1595.05	
Minimum Body Size	Non-spatial	3490.11	1271	-1732.05	χ^2=273.67 p<0.0001
	Exponential	3220.43	1271	-1595.22	
	Gaussian	3490.35	1271	-1730.18	
	Spherical	3490.46	1271	-1730.23	
	Linear	3490.40	1271	-1730.20	
	Rational quadratic	3227.45	1271	-1598.72	
Maximum Body Size	Non-spatial	3513.06	1271	-1743.53	χ^2=278.77 p<0.0001
	Exponential	3238.29	1271	-1604.15	
	Gaussian	3514.74	1271	-1742.37	
	Spherical	3514.76	1271	-1742.38	
	Linear	3514.31	1271	-1618.15	
	Rational quadratic	3246.24	1271	-1608.12	

Supporting Table 5. Results of the comparison between generalized least squares models including five different spatial structures and the linear models without spatial structure testing the effect of latitude (both absolute and squared values), species richness, number of records and subdivision into six major coastlines on body size (mean, minimum and maximum values) in the southern hemisphere. The Akaike Information Criterion (AIC), the likelihood ratios (logLik) and the degrees of freedom (dF) of each model are reported. The results of a likelihood ratio test (lrt) between the non-spatial and the spatial, generalized least squares model with the lowest AIC value is also reported. Selected models are highlighted in red. * indicates that the result is marginally significant.

Model		AIC	dF	logLik	lrt
Mean Body Size	Non-spatial	235.61	77	-106.81	/
	Exponential	239.61	77	-106.81	
	Gaussian	239.61	77	-106.81	
	Spherical	239.61	77	-106.81	
	Linear	239.61	77	-106.81	
	Rational quadratic	239.61	77	-106.81	
Minimum Body Size	Non-spatial	235.52	77	-106.76	/
	Exponential	239.52	77	-106.76	
	Gaussian	239.52	77	-106.76	
	Spherical	239.52	77	-106.76	
	Linear	239.52	77	-106.76	
	Rational quadratic	239.52	77	-106.76	
Maximum Body Size	Non-spatial	234.33	77	-106.16	/
	Exponential	238.33	77	-106.16	
	Gaussian	238.33	77	-106.16	
	Spherical	238.33	77	-106.16	
	Linear	238.33	77	-106.16	
	Rational quadratic	238.33	77	-106.16	

Supporting Table 6. Results of the comparison between generalized least squares models including five different spatial structures and the linear models without spatial structure testing the effect of latitude (both absolute and squared values), species richness, number of records, sea surface temperature, net primary productivity and subdivision into six major coastlines on body size (mean, minimum and maximum values) in the southern hemisphere. The Akaike Information Criterion (AIC), the likelihood ratios (logLik) and the degrees of freedom (dF) of each model are reported. The results of a likelihood ratio test (lrt) between the non-spatial and the spatial, generalized least squares model with the lowest AIC value is also reported. Selected models are highlighted in red.

Model		AIC	dF	logLik	lrt
Mean Body Size	Non-spatial	234.29	75	-104.15	/
	Exponential	238.29	75	-104.15	
	Gaussian	238.29	75	-104.15	
	Spherical	238.29	75	-104.15	
	Linear	238.29	75	-104.15	
	Rational quadratic	238.29	75	-104.15	
Minimum Body Size	Non-spatial	234.93	75	-104.46	/
	Exponential	238.93	75	-104.46	
	Gaussian	238.93	75	-104.46	
	Spherical	238.93	75	-104.46	
	Linear	238.93	75	-104.46	
	Rational quadratic	238.93	75	-104.46	
Maximum Body Size	Non-spatial	231.55	75	-102.78	/
	Exponential	235.55	75	-102.78	
	Gaussian	235.55	75	-102.78	
	Spherical	235.55	75	-102.78	
	Linear	235.55	75	-102.78	
	Rational quadratic	235.55	75	-102.78	

Supporting Table 7. Results of the comparison between generalized least squares models including five different spatial structures and the linear models without spatial structure testing the effect of latitude (both absolute and squared values), species richness and number of records on body size (mean, minimum and maximum values) in the western Atlantic coastline. The Akaike Information Criterion (AIC), the likelihood ratios (logLik) and the degrees of freedom (dF) of each model are reported. The results of a likelihood ratio test (lrt) between the non-spatial and the spatial, generalized least squares model with the lowest AIC value is also reported. Selected models are highlighted in red.

Model		AIC	dF	logLik	lrt
Mean Body Size	Non-spatial	1101.66	401	-544.83	/
	Exponential	1105.66	401	-544.83	
	Gaussian	1105.66	401	-544.83	
	Spherical	1105.66	401	-544.83	
	Linear	1105.66	401	-544.83	
	Rational quadratic	1105.66	401	-544.83	
Minimum Body Size	Non-spatial	1104.59	401	-546.29	χ^2=23.50 p<0.0001
	Exponential	1108.59	401	-546.29	
	Gaussian	1108.59	401	-546.29	
	Spherical	1108.59	401	-546.29	
	Linear	1108.59	401	-546.29	
	Rational quadratic	1085.09	401	-534.55	
Maximum Body Size	Non-spatial	1102.58	401	-545.29	/
	Exponential	1106.58	401	-545.29	
	Gaussian	1106.58	401	-545.29	
	Spherical	1106.58	401	-545.29	
	Linear	1106.58	401	-545.29	
	Rational quadratic	1106.58	401	-545.29	

Supporting Table 8. Results of the comparison between generalized least squares models including five different spatial structures and the linear models without spatial structure testing the effect of latitude (both absolute and squared values), species richness, number of records, sea surface temperature and net primary productivity on body size (mean, minimum and maximum values) in the western Atlantic coastline. The Akaike Information Criterion (AIC), the likelihood ratios (logLik) and the degrees of freedom (dF) of each model are reported. The results of a likelihood ratio test (lrt) between the non-spatial and the spatial, generalized least squares model with the lowest AIC value is also reported. Selected models are highlighted in red.

Model		AIC	dF	logLik	lrt
Mean Body Size	Non-spatial	1103.17	399	-543.59	/
	Exponential	1107.17	399	-543.59	
	Gaussian	1107.17	399	-543.59	
	Spherical	1107.17	399	-543.59	
	Linear	1107.17	399	-543.59	
	Rational quadratic	1107.17	399	-543.59	
Minimum Body Size	Non-spatial	1106.51	399	-545.26	χ^2=21.56 p<0.0001
	Exponential	1110.51	399	-545.26	
	Gaussian	1110.51	399	-545.26	
	Spherical	1110.51	399	-545.26	
	Linear	1110.51	399	-545.26	
	Rational quadratic	1088.95	399	-543.47	
Maximum Body Size	Non-spatial	1102.59	399	-543.29	/
	Exponential	1106.59	399	-543.29	
	Gaussian	1106.59	399	-543.29	
	Spherical	1106.59	399	-543.29	
	Linear	1106.59	399	-543.29	
	Rational quadratic	1106.59	399	-543.29	

Supporting Table 9. Results of the comparison between generalized least squares models including five different spatial structures and the linear models without spatial structure testing the effect of latitude (both absolute and squared values), species richness and number of records on body size (mean, minimum and maximum values) in the eastern Atlantic coastline. The Akaike Information Criterion (AIC), the likelihood ratios (logLik) and the degrees of freedom (dF) of each model are reported. The results of a likelihood ratio test (lrt) between the non-spatial and the spatial, generalized least squares model with the lowest AIC value is also reported. Selected models are highlighted in red.

Model		AIC	dF	logLik	lrt
Mean Body Size	Non-spatial	1590.37	556	-789.18	χ^2=124.03 p<0.0001
	Exponential	1594.37	556	-789.18	
	Gaussian	1594.23	556	-789.11	
	Spherical	1594.25	556	-789.13	
	Linear	1496.74	556	-726.87	
	Rational quadratic	1594.36	556	-789.18	
Minimum Body Size	Non-spatial	1592.62	556	-790.31	χ^2=126.85 p<0.0001
	Exponential	1596.62	556	-790.31	
	Gaussian	1596.40	556	-790.20	
	Spherical	1596.50	556	-790.25	
	Linear	1469.77	556	-726.88	
	Rational quadratic	1596.24	556	-790.12	
Maximum Body Size	Non-spatial	1591.09	556	-789.55	χ^2=142.48 p<0.0001
	Exponential	1595.09	556	-789.55	
	Gaussian	1594.98	556	-789.49	
	Spherical	1594.99	556	-789.49	
	Linear	1452.62	556	-718.31	
	Rational quadratic	1595.11	556	-789.55	

Supporting Table 10. Results of the comparison between generalized least squares models including five different spatial structures and the linear models without spatial structure testing the effect of latitude (both absolute and squared values), species richness, number of records, sea surface temperature and net primary productivity on body size (mean, minimum and maximum values) in the eastern Atlantic coastline. The Akaike Information Criterion (AIC), the likelihood ratios (logLik) and the degrees of freedom (dF) of each model are reported. The results of a likelihood ratio test (lrt) between the non-spatial and the spatial, generalized least squares model with the lowest AIC value is also reported. Selected models are highlighted in red.

Model		AIC	dF	logLik	lrt
Mean Body Size	Non-spatial	1567.13	554	-775.57	χ^2=114.80 p<0.0001
	Exponential	1571.13	554	-775.57	
	Gaussian	1571.04	554	-775.52	
	Spherical	1571.05	554	-775.52	
	Linear	1456.33	554	-718.17	
	Rational quadratic	1571.13	554	-775.57	
Minimum Body Size	Non-spatial	1571.38	554	-777.69	χ^2=96.67 p<0.0001
	Exponential	1575.37	554	-777.69	
	Gaussian	1575.14	554	-777.57	
	Spherical	1575.25	554	-777.63	
	Linear	1478.70	554	-729.35	
	Rational quadratic	1575.24	554	-777.62	
Maximum Body Size	Non-spatial	1570.71	554	-777.36	χ^2=119.33 p<0.0001
	Exponential	1574.71	554	-777.36	
	Gaussian	1574.66	554	-777.32	
	Spherical	1574.64	554	-777.32	
	Linear	1455.38	554	-717.69	
	Rational quadratic	1574.71	554	-777.36	

Supporting Table 11. Results of the comparison between generalized least squares models including five different spatial structures and the linear models without spatial structure testing the effect of latitude (both absolute and squared values), species richness and number of records on body size (mean, minimum and maximum values) in the western Pacific coastline. The Akaike Information Criterion (AIC), the likelihood ratios (logLik) and the degrees of freedom (dF) of each model are reported. The results of a likelihood ratio test (lrt) between the non-spatial and the spatial, generalized least squares model with the lowest AIC value is also reported. Selected models are highlighted in red.

Model		AIC	dF	logLik	lrt
Mean Body Size	Non-spatial	522.93	214	-255.47	/
	Exponential	526.93	214	-255.47	
	Gaussian	526.93	214	-255.47	
	Spherical	526.93	214	-255.47	
	Linear	526.93	214	-255.47	
	Rational quadratic	526.93	214	-255.47	
Minimum Body Size	Non-spatial	529.03	214	-258.52	/
	Exponential	533.03	214	-258.52	
	Gaussian	533.03	214	-258.52	
	Spherical	533.03	214	-258.52	
	Linear	533.03	214	-258.52	
	Rational quadratic	533.03	214	-258.52	
Maximum Body Size	Non-spatial	524.49	214	-256.25	/
	Exponential	528.49	214	-256.25	
	Gaussian	528.49	214	-256.25	
	Spherical	528.49	214	-256.25	
	Linear	528.49	214	-256.25	
	Rational quadratic	528.49	214	-256.25	

Supporting Table 12. Results of the comparison between generalized least squares models including five different spatial structures and the linear models without spatial structure testing the effect of latitude (both absolute and squared values), species richness, number of records, sea surface temperature and net primary productivity on body size (mean, minimum and maximum values) in the western Pacific coastline. The Akaike Information Criterion (AIC), the likelihood ratios (logLik) and the degrees of freedom (dF) of each model are reported. The results of a likelihood ratio test (lrt) between the non-spatial and the spatial, generalized least squares model with the lowest AIC value is also reported. Selected models are highlighted in red.

Model		AIC	dF	logLik	lrt
Mean Body Size	Non-spatial	521.70	212	-252.85	/
	Exponential	525.70	212	-252.85	
	Gaussian	525.70	212	-252.85	
	Spherical	525.70	212	-252.85	
	Linear	525.70	212	-252.85	
	Rational quadratic	525.70	212	-252.85	
Minimum Body Size	Non-spatial	529.09	212	-256.54	/
	Exponential	533.09	212	-256.54	
	Gaussian	533.09	212	-256.54	
	Spherical	533.09	212	-256.54	
	Linear	533.09	212	-256.54	
	Rational quadratic	533.09	212	-256.54	
Maximum Body Size	Non-spatial	521.71	212	-252.86	/
	Exponential	525.71	212	-252.86	
	Gaussian	525.71	212	-252.86	
	Spherical	525.71	212	-252.86	
	Linear	525.71	212	-252.86	
	Rational quadratic	525.71	212	-252.86	

Supporting Table 13. Results of the comparison between generalized least squares models including five different spatial structures and the linear models without spatial structure testing the effect of latitude (both absolute and squared values), species richness and number of records on body size (mean, minimum and maximum values) in the eastern Pacific coastline. The Akaike Information Criterion (AIC), the likelihood ratios (logLik) and the degrees of freedom (dF) of each model are reported. The results of a likelihood ratio test (lrt) between the non-spatial and the spatial, generalized least squares model with the lowest AIC value is also reported. Selected models are highlighted in red.

Model		AIC	dF	logLik	lrt
Mean Body Size	Non-spatial	384.95	154	-186.47	χ^2=87.89 p<0.0001
	Exponential	301.98	154	-142.99	
	Gaussian	301.21	154	-142.60	
	Spherical	301.05	154	-142.53	
	Linear	301.56	154	-142.78	
	Rational quadratic	301.10	154	-142.55	
Minimum Body Size	Non-spatial	370.87	154	-179.44	χ^2=87.98 p<0.0001
	Exponential	288.97	154	-136.49	
	Gaussian	286.89	154	-135.45	
	Spherical	287.09	154	-135.55	
	Linear	296.15	154	-140.08	
	Rational quadratic	334.77	154	-159.38	
Maximum Body Size	Non-spatial	388.68	154	-188.34	χ^2=72.81 p<0.0001
	Exponential	319.87	154	-151.94	
	Gaussian	320.30	154	-152.15	
	Spherical	320.47	154	-152.23	
	Linear	320.47	154	-152.24	
	Rational quadratic	358.18	154	-171.09	

Supporting Table 14. Results of the comparison between generalized least squares models including five different spatial structures and the linear models without spatial structure testing the effect of latitude (both absolute and squared values), species richness, number of records, sea surface temperature and net primary productivity on body size (mean, minimum and maximum values) in the eastern Pacific coastline. The Akaike Information Criterion (AIC), the likelihood ratios (logLik) and the degrees of freedom (dF) of each model are reported. The results of a likelihood ratio test (lrt) between the non-spatial and the spatial, generalized least squares model with the lowest AIC value is also reported. Selected models are highlighted in red.

Model		AIC	dF	logLik	lrt
Mean Body Size	Non-spatial	386.13	152	-185.06	χ^2=85.31 p<0.0001
	Exponential	305.88	152	-142.94	
	Gaussian	305.19	152	-142.59	
	Spherical	304.82	152	-142.41	
	Linear	305.11	152	-142.56	
	Rational quadratic	351.36	152	-165.66	
Minimum Body Size	Non-spatial	369.09	152	-176.54	χ^2=82.30 p<0.0001
	Exponential	292.93	152	-136.47	
	Gaussian	290.83	152	-135.42	
	Spherical	291.06	152	-135.53	
	Linear	290.78	152	-135.39	
	Rational quadratic	336.70	152	-158.35	
Maximum Body Size	Non-spatial	389.83	152	-186.91	χ^2=70.00 p<0.0001
	Exponential	323.82	152	-151.91	
	Gaussian	324.25	152	-152.13	
	Spherical	324.26	152	-152.13	
	Linear	328.46	152	-154.23	
	Rational quadratic	361.22	152	-170.61	

Appendix S4 Supporting figures representing graphically size-latitude trends and relationships between body size and environmental variables for the global analyses, and the analyses conducted separately per hemisphere and coastline (only those of statistically significant results are included).

Supporting Figure 1. Size-latitude trends in the western (A-C) and the eastern Atlantic (C-F), depicted separately for allomalorhagids (red dots and lines) and cyclorhagids (cyan dots and lines).

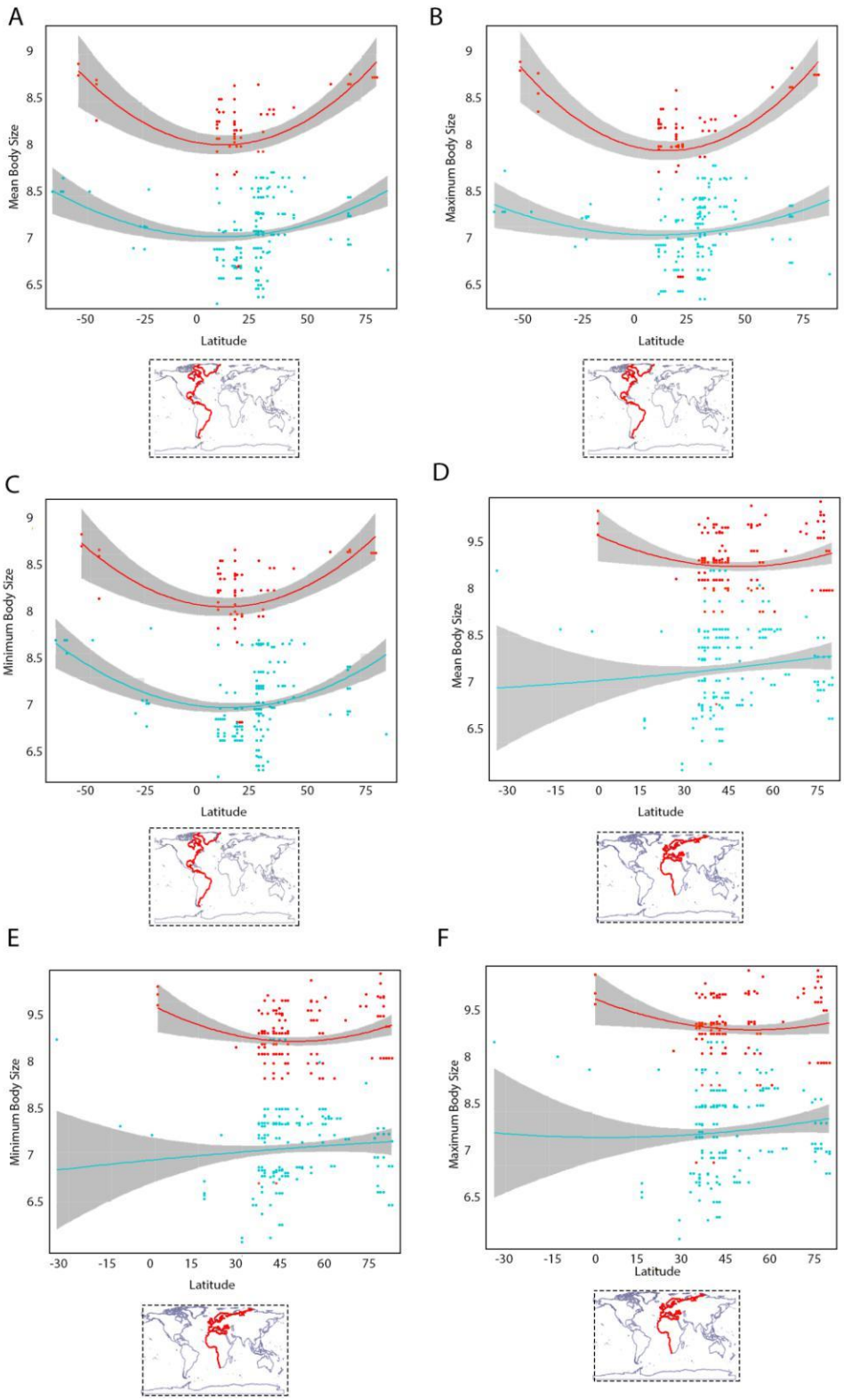

Supporting Figure 2. Size-latitude trends in the western (A-C) and the eastern Pacific (D-F), depicted separately for allomalorhagids (red dots and lines) and cyclorhagids (cyan dots and lines).

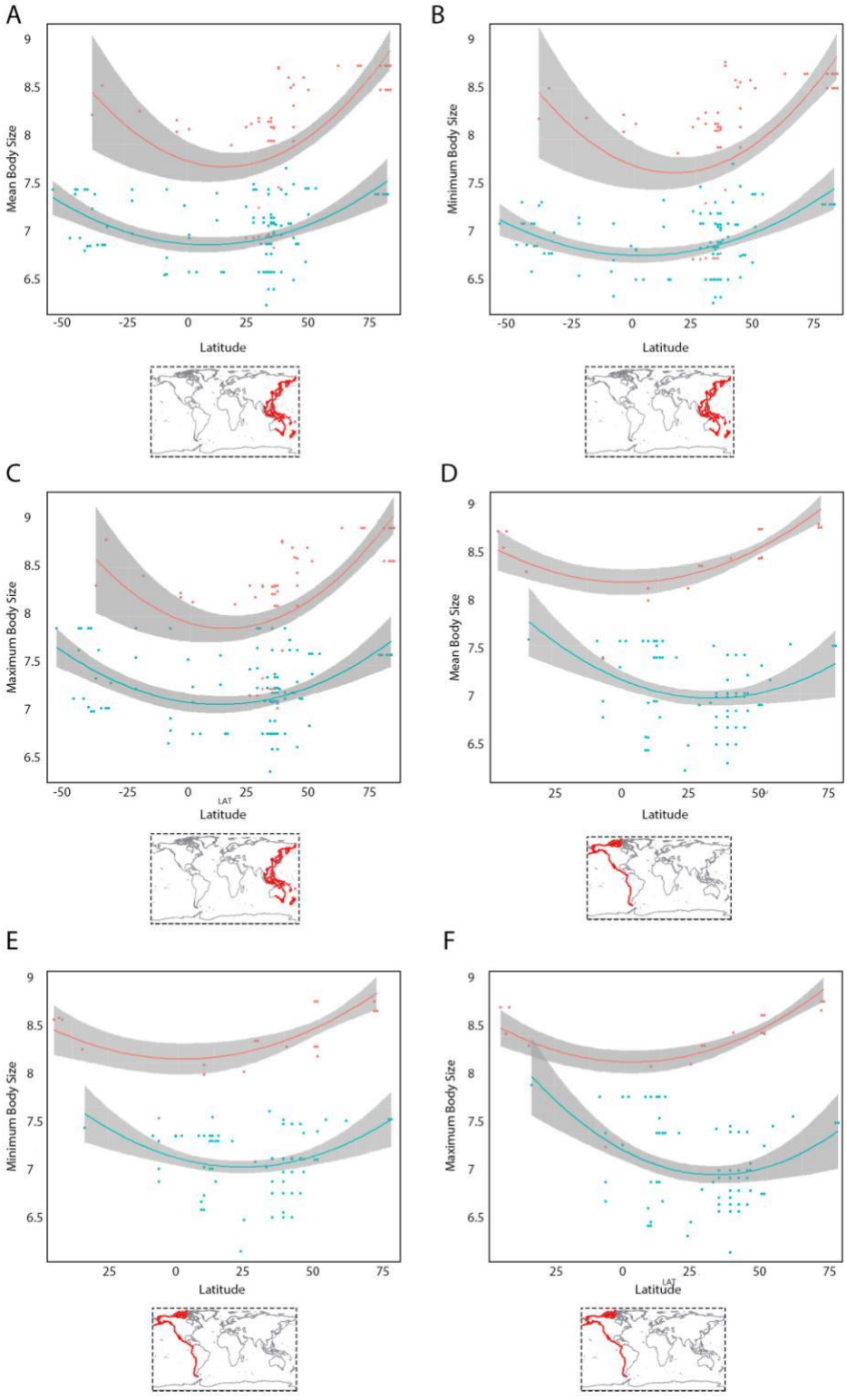

Supporting Figure 3. Selected trends between environmental variables and body size: minimum body size and temperature for the global analysis (A), minimum body size and productivity for the western Pacific (B), maximum body size and productivity for the western Pacific (C), and minimum body size and productivity for the western Atlantic (D).

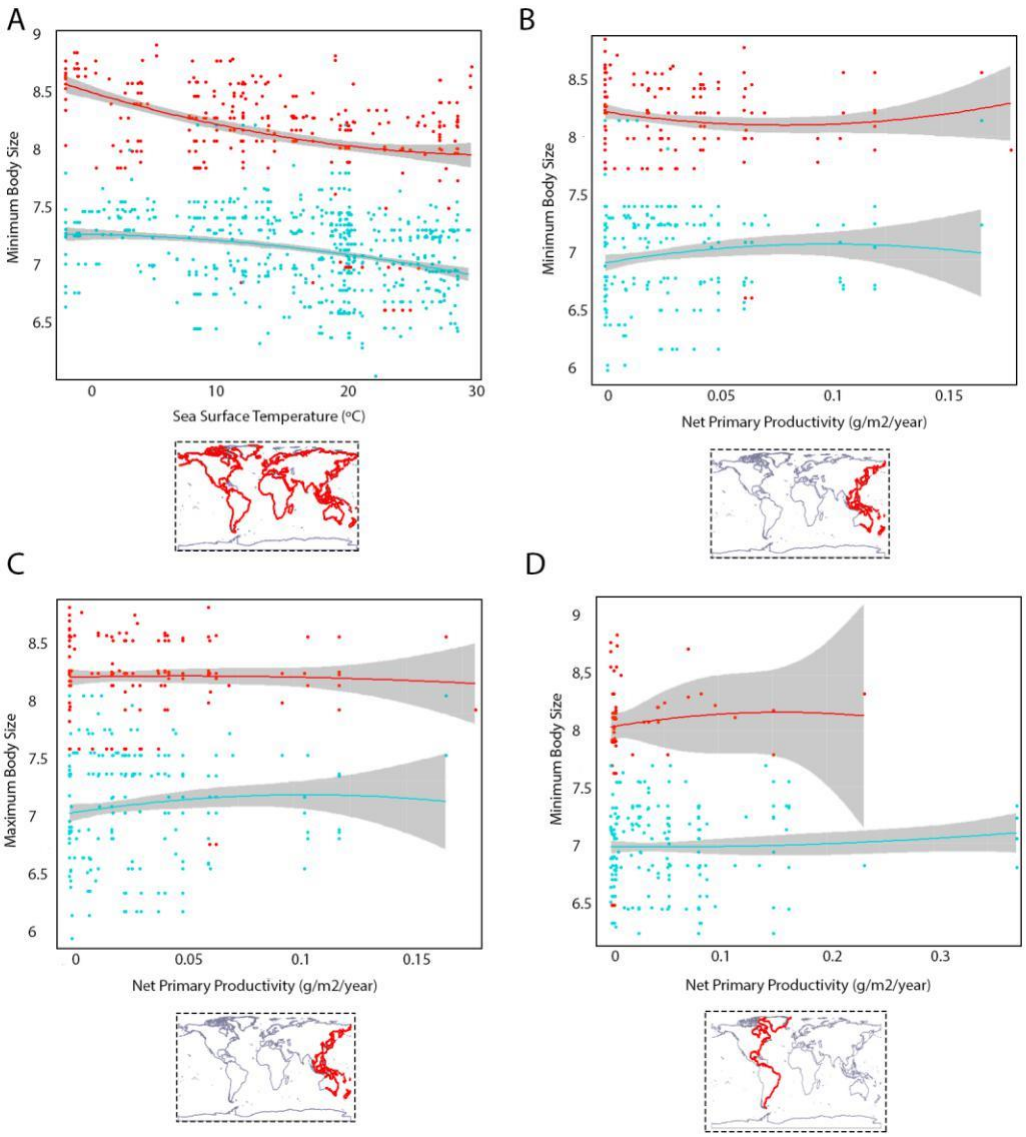

APPENDIX II. NEW SPECIES OF *SETAPHYES* FROM PORTUGAL.

González-Casarrubios, A.; Cepeda, D.; Pardos, F.; Neves, R.; Sánchez, N.

A new species of the allomalorhagid genus *Setaphyes* Sánchez *et al.*, 2016 has been found inhabiting the intertidal zone of a large muddy beach with communities of *Zostera marina* L. in Alvor, Portugal (north-eastern Atlantic Ocean) (see Table 3 of Material and Methods). The new species fits well into the genus *Setaphyes* as it lacks ventrolateral setae on segment 5 and possesses paradorsal setae throughout segments 2-9, lateroventral setae throughout segments 2-10 and numerous dot-shaped glandular cell outlets scattered on the cuticle's surface (Sánchez *et al*., 2016).

This species may be unequivocally distinguished from the remaining congeners by the arrangement of the dorsal setae and the absence of a particular pattern of cuticular ornamentation on segments 1 and 10. This lack of ornamentations is only shared with *S. australensis* (Lemburg, 2002), *S. iniorhaptus* (Higgins, 1983) and *S. kielensis* (Zelinka, 1928). Additionally, the new species has paired paradorsal setae on segments 2-7 and 9 and unpaired seta on segment 8, a pattern only shared with *S. kielensis.* Nevertheless, the pattern of dorsal setae shows a high intraspecific variation in *S. kielensis*. The new species from Portugal and *S. kielensis* furthermore greatly differ in the total trunk length and the standard sternal width.

APPENDIX III. NEW SPECIES OF KINORHYNCHS FROM THE CLARION-CLIPPERTON DEEP-SEA ZONE.

Sánchez, N.; González-Casarrubios, A.; Cepeda, D.; Pardos, F.; Martínez-Arbizu, P.

Three new species of the cyclorhagid genus *Echinoderes* Claparède, 1863 have been discovered at the Clarion-Clipperton zone (north-eastern Pacific Ocean) in a deep-sea manganese nodule field (see Table 3 of Material and Methods). Despite these species have the most common pattern of spines and tubes found in the genus *Echinoderes*, they are also characterized by possessing numerous type 2 glandular cell outlets on most trunk segments.

Echinoderes sp. I has laterodorsal type 2 glandular cell outlets throughout segments 1-9. The only species that resembles this pattern is *E. ohtsukai* Yamasaki and Kajihara, 2012, which bears these structures throughout segments 2-9. In addition, *E. ohtsukai* has a single middorsal spine on segment 4 (*Echinoderes* sp. I throughout segments 4-8) and lacks lateroventral spines on segment 9, which are present in *Echinoderes* sp. I.

Echinoderes sp. II possesses laterodorsal type 2 glandular cell outlets on segments 2 and 4-9, and a similar pattern has been observed in *E. multiporus* Yamasaki *et al.*, 2018 (in Yamasaki *et al.*, 2018b), *E. hwiizaa* Yamasaki and Fujimoto, 2014, *E. serratulus* Yamasaki, 2016 and *E. schwieringae* Yamasaki *et al.*, 2019. However, all of them can be unequivocally distinguished from *Echinoderes* sp. II by the arrangement of the dorsal spines: absent in *E. hwiizaa*, on segment 4 in *E. serratulus* and on segments 4, 6 and 8 in *E. multiporus* and *E. schwieringae* (vs. segments 4-8 in *Echinoderes* sp. II). Additionally, *E. hwiizaa* and *E. serratulus* have ventral type 2 glandular cell outlets on segment 2, which are replaced by tubes in *Echinoderes* sp. II.

Echinoderes sp. III is characterized by having laterodorsal type 2 glandular cell outlets on segments 2, 5 and 7-9, and a similar pattern may be found in *E. cernunnos* Sørensen *et al.*, 2012, *E. drogoni* Grzelak and Sørensen, 2018, *E. romanoi* Landers and Sørensen, 2016 and *E. xalkutaat* Cepeda *et al.*, 2019. Nevertheless, none of these congeners possess type 2 glandular cell outlets on segment 9, as *Echinoderes* sp. III does. In addition to this, all the aforementioned congeners have more than one pair of type 2

glandular cell outlets on segment 2 (including ventral ones), which are absent in *Echinoderes* sp. III.

APPENDIX IV. NEW SPECIES OF *LEIOCANTHUS* FROM THE GULF OF MEXICO.

Cepeda, D.[*]; Sánchez, N.[*], Sørensen, M.V.; Landers, S.C.

[*] equal contributions

Two new species of the allomalorhagid genus *Leiocanthus* Sánchez *et al.*, 2016 have been revealed at the Gulf of Mexico (western Atlantic Ocean) (see Table 3 of Material and Methods). The genus is morphologically characterized by the absence of middorsal cuticular specializations on posterior segments (7 onwards) and the absence of ventrolateral setae on both anterior (3-4) and posterior (6-9) segments (Sánchez *et al.*, 2016; 2019b). The discovery of the two new species significantly increases the kinorhynch fauna of the Gulf of Mexico, following the prior contributions in the Gulf of Mexico of Sørensen and Landers (2014; 2017a; 2017b; 2018), Landers and Sørensen (2016; 2018), Sørensen *et al.* (2016; 2019), Sánchez *et al.* (2019b) and Álvarez-Castillo *et al.* (2020).

Leiocanthus sp. I lacks lateral terminal spines, a feature only shared by *L. langi* (Higgins, 1964) and *L. mainensis* (Blake, 1930). *Leiocanthus mainensis* can be easily distinguished from *Leiocanthus* sp. I by the presence of laterodorsal setae throughout segments 2-9, as the latter only possesses laterodorsal setae on segments 3, 5, 7 and 9. The main morphological discrepancies between *L. langi* and *Leiocanthus* sp. I are the number of paired sensory spots throughout the sternal plates (two pairs in *L. langi* vs. a single pair in *Leiocanthus* sp. I), the distribution of the paradorsal setae (segments 4, 6 and 8 in *L. langi* vs. segments 4 and 6 in *Leiocanthus* sp. I), the position of the sternal setae of segments 3 and 8 (ventromedial position in *L. langi* vs. paraventral position in *Leiocanthus* sp. I) and the cuticular ornamentation of segment 1 (anterior margin smooth with poorly extended, triangular, anterolateral enlargements in *L. langi* vs. anterior margin strongly denticulate with strikingly extended, recurved, horn-shaped, anterolateral enlargements in *Leiocanthus* sp. I).

Leiocanthus sp. II may be unambiguously distinguished from its congeners by the absence of ventromedial setae on segment 5, which is a unique feature within the genus. *Leiocanthus chalgap* (Sánchez *et al.*, 2013) is the most similar species to *Leiocanthus* sp. II, but several, morphological differences are present, including the distribution of

laterodorsal setae (segments 2-5 and 9 in *L. chalgap* vs. segments 3, 5, 7 and 9 in *Leiocanthus* sp. II), the distribution of the middorsal elevations (segments 2-4 in *L. chalgap* vs. segments 2-6 in *Leiocanthus* sp. II), the shape of the midsternal plate and the distribution of the apodemes.

APPENDIX V. USE OF ISOTOPES FOR DETERMINATION OF FEED INTAKE IN KINORHYNCHS – PRELIMINARY RESULTS.

Cepeda, D.[*]; Sánchez, N.[*]; Zeppilli, D.; Pardos, F.; Michel, L. N.

[*] equal contributions

Stable isotope ratios are frequently used to describe metazoan feeding ecology, as the animal soft tissues are composed of roughly 40% carbon and 10% nitrogen obtained through diet (McCormack *et al.*, 2019). The most common stable isotopes for this purpose are $\delta^{13}C$ and $\delta^{15}N$. Metazoans acquire their isotopic composition from the food they consume with a small isotopic enrichment, so the isotopic ratios become higher compared to diet (McCormack *et al.*, 2019). This feature allows us to determine the level of the food web where a species is located as well as the most likely food sources.

Kinorhynchs are part of the marine, meiofaunal communities, and as such, they have been reported as a food source for macrofaunal organisms, including bivalves, annelids, shrimps and gobiid fishes (Martorelli and Higgins, 2004; Neuhaus, 2013), but it is still unclear whether these predators feed on them accidentally. On the other hand, little is known about the food sources of kinorhynchs. It has been hypothesized that kinorhynchs usually feed on detritus, algae, diatoms and bacteria using the mouth cone oral styles (Neuhaus, 2013). Ciliary sensory cells have been described on these structures, and they could play an important role in determining food quality (Neuhaus, 2013). Moreover, the complex muscle system associated with the mouth cone would be responsible for protracting it as far forward as possible, then contracting it to suck water and food (Neuhaus, 2013).

The content of the digestive tract of selected species of Kinorhyncha has been mainly studied by Zelinka (1928), Higgins (1990), Adrianov (1991) and Adrianov and Malakhov (1994), evidencing the presence of bacteria, diatoms and/or sediment with detritus and microorganisms. Additionally, Adrianov and Malakhov (1994), furthermore supported by personal observations of Neuhaus (2013), hypothesized that kinorhynchs are able to manipulate diatoms by the mouth cone oral styles and to do food gardening by producing mucus through some cuticular appendages (mainly spines, setae, tubes and glandular cell outlets) in order to trap bacteria, diatoms and detritus on their body. Yushin *et al.* (1990) and Adrianov *et al.* (1993) revealed the presence of some kind of modified

epithelial cells inside the digestive tract likely hosting endosymbiotic, chemolithoautotroph, sulphur-oxidizer bacteria, but this has been discarded by further research of Neuhaus (1994), who demonstrated undigested individual bacteria surrounded by vesicles.

To furthermore explore the Kinorhyncha feeding ecology, selected species of this phylum were collected off Vigo and Bayona (Galicia, Spain), and Roscoff (Brittany, France). Detailed information on these species, sampling locations, number of specimens per species and isotopic analyses may be found in Table 1. Kinorhynch specimens and possible food sources, including nematods, shrimps, algae and sediment (with bacteria, detritus and diatoms) were frozen at -80ºC. Posteriorly, specimens were rinsed in distilled Milli-Q water, freeze-dried and ground into a homogeneous powder using a ball mill. Tissues were weighed in tin capsules and analysed on a Delta V Plus stable isotope ratio mass spectrometer. Result values are expressed in δ (‰) notation with respect to VPDB ($\delta_{13}C$) and atmospheric air ($\delta_{15}N$).

Table 1. Analysed species of kinorhynchs and possible food sources, with data on sampling locations and results of the $\delta_{13}C$ and $\delta_{15}N$.

Species/sample	Station	*N*	Analysed mass (mg)	$\delta_{13}C$ (‰)	$\delta_{15}N$ (‰)
Antygomonas sp.	Bayona	18	0.010	-21.1	-
Echinoderes cantabricus	Vigo	91	0.028	-16.9	-
Echinoderes dujardinii	Roscoff	29	0.017	-13.4	-
Pycnophyes aulacodes	Vigo	51	0.083	-16.6	7.2
Ampelisca brevicornis	Roscoff	1	1.000	-11.0	13.2
Neomysis integer	Roscoff	2	1.000	-12.2	12.0
Oncholaimidae	Vigo	20	0.032	-19.1	-
Oncholaimidae	Roscoff	43	0.047	-14.5	-
Sphaerolaimidae	Roscoff	25	0.015	-15.1	-
Cladophora sp.	Roscoff	1	2.486	-14.8	6.9
Ectocarpus sp.	Roscoff	1	2.804	-16.3	8.5
Enteromorpha sp.	Roscoff	1	2.451	-15.0	8.4
Fucus spiralis	Roscoff	1	2.978	-18.4	7.0
Ulva lactuca	Roscoff	1	2.484	-19.7	6.8
Sediment	Bayona	-	24.405	-19.2	4.6
Sediment	Vigo	-	26.444	-23.0	5.3
Sediment	Roscoff	-	26.608	-20.6	-

The results show that many of the analysed taxa (including cyclorhagid Kinorhyncha and nematods) or samples (sediment from Roscoff) did not have a sufficient sample size to yield a value of $\delta_{15}N$. This exposes the difficulty to apply this methodology to meiofaunal organisms compared to macrofaunal ones. However, a new line of research is opened, which undoubtedly requires many more samplings, including a higher number of specimens per selected species, and of course a greater variety of sampling locations to elucidate the food sources of this enigmatic metazoan phylum.

4 – Discussion

"Now is the time to understand more,

so that we may fear less" (Marie Curie)

This thesis comprehends a large contribution to the knowledge of the phylum Kinorhyncha to date including a synthesis of different methodological approaches and biological disciplines to better understand the diversity, functioning and way-of-life of these meiofaunal organisms, using an integrative view. The core of the thesis is, therefore, the phylum Kinorhyncha, where every new finding or report of a kinorhynch species leads to a new question regarding these animals, which, like a stone in a pond, generates a new line (or circle) of knowledge around the aforementioned core to be developed. Thus, questions and hypothesis about the systematics, ecology, biogeography and biology of the kinorhynch species are brought and proposed, ready to be tested by the scientific method, and also starting new paths for future research in the field.

The present discussion offers a holistic vision of all the topics covered in the thesis on the phylum Kinorhyncha, although further details and specific information of a certain line of research may be found in the discussion subsections of the different articles included in the Results section.

4.1 Taxonomy and biodiversity (sections 3.1-3.7 and Appendix I of Results).

One of the most important approaches in zoology is the study, identification, classification and description of species. Thus, taxonomy, the science of classification of living organisms, stands crucial and must become one of the most important priorities taken into account the current diversity crisis facing the planet (Pinto *et al.*, 2021). We must not forget that the ultimate intention of any researcher is to elucidate how their preferred organisms function, live and evolve, and how they are adapted to their environment, something that cannot be explained without the recognition of the morphology and the classification of the species (Giribet, 2015). Going further,

descriptive taxonomy is more than an inventory of diversity but a pioneering exploration of life in a poorly known planet, and the needed foundation for other biological disciplines (Wilson, 2004), especially if we want to shed light into the patterns that explain the current diversity and adaptations of a particular animal phylum. This fact becomes even more important taking into account that more than 80 % of the oceans is still unexplored.

In this context, the first aim that was set for this thesis was to expand the limited knowledge of the kinorhynch species inhabiting scarcely documented areas. The current knowledge of Kinorhyncha species is strongly biased by the specialists sampling strategies (Sørensen and Pardos, 2008; Neuhaus, 2013). Certain areas of the oceans have been extensively explored in terms of Kinorhyncha biodiversity, including the European waters, the North American coastline, and the Sea of Japan and adjacent waters (Neuhaus, 2013). Extensive, more local studies have also been carried out in Belize, the Gulf of Mexico, the Arctic Ocean, the Russian Pacific coast and New Zealand (Neuhaus, 2013). Thus, entire areas of the world suffer from a lack of knowledge on the kinorhynch species that inhabit their waters. It has been proposed that we only know about the 9-15% of the worldwide Kinorhyncha biodiversity (Appeltans *et al.*, 2012), and though a considerable amount of species have already been described since the year of the publication of the aforementioned paper (ca. 130 species), it is still necessary to promote basic, taxonomic studies in the phylum to better know which species inhabit the different seas and oceans (sections **3.1-3.7**, **3.10** and **Appendix I** of Results).

While selecting the appropriate locations for this, geographical areas that constitute important hotspots of biodiversity for marine fauna in general and meiofaunal in particular, and/or have ecological and biogeographical relevance, were taken into account. Nevertheless, we did not want to forget about other geographic areas of which, though there are enough taxonomic studies to place them in some of the best known locations, they still continue providing taxonomic novelties. Thus, three areas and/or environments were selected to develop this first branch of the thesis: the Caribbean Sea, the deep-sea, and the North Sea (sections **3.1-3.7** and **Appendix I** of Results).

4.1.1 BIODIVERSITY OF KINORHYNCHA IN THE CARIBBEAN SEA (sections **3.1-3.4** and **Appendix I** of Results).

4.1.1.1 OVERVIEW.

The Caribbean Sea is a biodiversity hotspot (Myers *et al.*, 2000; Mittermeier *et al.*, 2004) in terms of number of species but also very relevant for marine ecological processes and interactions between organisms (Marchese, 2015).

The first reported kinorhynch species from the Caribbean Sea was *Echinoderes caribiensis* at the Bahía de Mochima, Venezuela (Kirsteuer, 1964). Lately, Higgins (1983) published a detailed study of the coral reef kinorhynch fauna of Carrie Bow Cay, Belize, including the description of eighteen new species: *Cristaphyes belizensis*, *C. longicornis*, *Echinoderes abbreviatus*, *E. horni*, *E. imperforatus*, *E. truncatus*, *E. wallaceae*, *Fujuriphyes deirophorus*, *F. distentus*, *Higginsium erismatum*, *H. trisetosum*, *Leiocanthus corrugatus*, *L. ecphantor*, *L. emarginatus*, *Paracentrophyes praedictus*, *Pycnophyes apotomus*, *P. stenopygus* and *Setaphyes iniorhaptus*. Posteriorly, the Caribbean Panama kinorhynchs were studied by Sørensen (2006), whose samples yielded the description of two new species, *Echinoderes collinae* and *E. intermedius*, and the first report of *E. spinifurca*, *Pycnophyes beaufortensis*, *Semnoderes* cf. *pacificus* and two still undescribed species (*Cephalorhyncha* sp. and *Echinoderes* sp.). This work was latter supplemented by Neuhaus et al. (2014) with the description of *Centroderes barbanigra* from La Española and Panama, and Pardos *et al.* (2016a) with the description of *Cristaphyes panamensis*, *Echinoderes rociae*, *E. orestauri* and *Pycnophyes alexandroi*, and reporting *Antygomonas* cf. *paulae* and *Campyloderes* sp. from the region for the first time. Finally, Sánchez and Martínez (2019) explored the kinorhynch fauna from a Caribbean anchialine cave in the Caribbean Mexico, which yielded the description of a new species, *Pycnophyes kukulkan*, and the report of an undescribed species of *Paracentrophyes* sp.

Thus, before the beginning of the present thesis, the Caribbean Sea hosted 32 species of Kinorhyncha belonging to 12 genera and seven families (Kirsteuer, 1964; Higgins, 1983; Sørensen, 2006; Pardos et al., 2016a; Sánchez and Martínez, 2019). The papers published to date related to the thesis increased this number to 52 species belonging to 15 genera and nine families, which represents an increase of ca. 37 % of the total Caribbean Kinorhyncha biodiversity (sections **3.1-3.4** and **Appendix I** of Results). A total of nine species have been described as new to science, namely *Cristaphyes cornifrons*, *C. retractilis*, *Dracoderes spyro*, *Echinoderes barbadensis*, *E. brevipes*, *E. jesusi*, *E. parahorni*, *Fujuriphyes dalii* and *Triodontoderes lagahoo* (sections **3.1-3.4** and **Appendix I** of Results). This high number of new species had not been repeated for the

Caribbean since the exhaustive sampling of the coral reef habitat of Carrie Bow Cay (Belize) by Higgins (1983), who described 18 new species. Furthermore, several kinorhynch species previously known from other geographic areas were newly reported for the Caribbean Sea, including *E. astridae* (originally described from Araçá Bay, São Sebastião, Brazil), *E. augustae* and *Semnoderes lusca* (originally described from the nearby Gulf of Mexico), and *E. sublicarum* (originally described from South Carolina) (Higgins, 1977b; Sørensen, 2014; Sørensen and Landers, 2014). Finally, the distribution range of several Caribbean species have been expanded, as they were found in new Caribbean locations. This is the case of *C. longicornis*, *E. horni*, *E. imperforatus*, *E. wallaceae*, *F. deirophorus*, *F. distentus*, *Higginsium erismatum* and *Leiocanthus corrugatus* (previously known only from Carrie Bow Cay, Belize), and *E. intermedius* and *E. orestauri* (previously known only from Bocas del Toro, Panama) (Higgins, 1983; Sørensen, 2006; Pardos et al., 2016b) (sections **3.1-3.4** and **Appendix I** of Results).

In summary, the Caribbean Sea seems to host a rich fauna of Kinorhyncha, and this thesis has greatly helped to know its hidden kinorhynch biodiversity, making this area one of the best known nowadays for the phylum, together with the Mediterranean Sea, the North Atlantic American and European shorelines (including the Gulf of Mexico) and the Sea of Japan and adjacent waters (Neuhaus, 2013).

4.1.1.2 Is the Caribbean Sea a Kinorhyncha hotspot of biodiversity?

As previously mentioned, prior to the study of the Caribbean samples that are part of the present thesis, works on Kinorhyncha in the Caribbean Basin were rather scarce and reduced to very specific locations, *e.g.* Caribbean Panama and the coral reef ecosystem at Carrie Bow Cay (Belize) (Neuhaus, 2013). After our study, the Kinorhyncha richness of the Caribbean Sea was increased by ca. 37 % with the description and/or report of 20 new species for the area, yielding a total of 52 valid species (sections **3.1-3.4** and **Appendix I** of Results). Moreover, the description of two new species, *Dracoderes spyro* and *Triodontoderes lagahoo*, represented the first report of the corresponding genera for the Atlantic American coast in general and the Caribbean Basin in particular (sections **3.3-3.4** of Results). In summary, the Caribbean seems to host a rich Kinorhyncha fauna, as ca. 16 % of the worldwide species are present in this area, as well as ca. 48 % of the worldwide genera (Neuhaus, 2021).

Concerning the obtained data, it would be tempting to designate the Caribbean Sea as a new Kinorhyncha hotspot of biodiversity. However, the observed species richness could just be the result of a more intensive sampling effort. Similar studies also yielded a high number of Kinorhyncha species in other areas, such as the Arctic Ocean (Higgins, 1966; 1991; Higgins and Korczynski, 1989; Adrianov, 1995; Grzelak and Sørensen, 2018; 2019; Sørensen and Grzelak, 2018; Yamasaki et al., 2018a), the Iberian Peninsula (Pardos et al., 1998; GªOrdóñez et al., 2008; Sørensen et al., 2010a; 2012a; Sánchez et al., 2011; 2012; Herranz et al., 2012; Neves *et al.*, 2016), the Sea of Japan and adjacent waters (Adrianov, 1989; Higgins and Shirayama, 1990; Song and Chang, 2001; Adrianov *et al.*, 2002; Lundbye *et al.*, 2010; Sánchez and Yamasaki, 2016; Sánchez *et al.*, 2013; Sørensen *et al.*, 2010a; 2010b; 2010c; 2012a; 2012b; 2013; Yamasaki, 2016; 2019; Yamasaki and Kahijara, 2012; Yamasaki *et al.*, 2012; 2020), or the north-western Atlantic coast of USA (Higgins, 1964; 1965; 1977b; 1982; 1990; Sørensen *et al.*, 2005; 2007; 2016; 2019; Herranz and Pardos, 2013; Herranz *et al.*, 2014; Neuhaus *et al.*, 2014; Sørensen and Landers, 2014; 2017a; 2017b; Landers and Sørensen, 2016; 2018). Accordingly, with the current available data and until more regions are explored with equivalent sampling efforts, it would not be acceptable to consider the Caribbean Sea as a hotspot of Kinorhyncha biodiversity but just a relatively well sampled area.

4.1.1.3 Are there differences in species richness between the main marine Caribbean ecoregions and do we currently know a significant representativeness of the Caribbean Kinorhyncha biodiversity?

Relevant differences in species richness between the main marine Caribbean ecoregions (as defined by Spalding *et al.*, 2007) have been observed. Thus, the Western Caribbean hosts the highest number of kinorhynchs, as up to 21 species have been reported (Higgins, 1983; Sánchez and Martínez, 2019). On the opposite side, the Eastern Caribbean, based on the studied samples from Barbados and Guadeloupe of the present thesis, has only two kinorhynch species. The remaining areas, *i.e.* Southwestern Caribbean, Southern Caribbean and Greater Antilles, show similar values of species richness (14, 15 and 16 species, respectively) (Kirsteuer, 1964; Sørensen, 2006; Neuhaus *et al.*, 2014; Pardos *et al.*, 2016; samples of the present thesis). However, it must be taken into account that the observed differences in the number of species do not reflect the real distribution of the kinorhynch richness in the Caribbean, but rather (again) the sampling strategies of the

specialists. For instance, having a single sample from Cuba cannot be considered equal to having multiple samples collected at different points throughout Twin Cays and Carrie Bow Cay in Belize; without any doubt, there will be a very significant difference in species richness, but this will not necessarily have to be real, but simply the result of the differential sampling effort applied in the considered areas. Therefore, the observed differences in the kinorhynch species richness of the considered marine Caribbean ecoregions should be taken with caution, offering a pioneer information, but without forgetting that it is necessary to promote new, more equitable samplings in the most uncharted areas.

Following in the line with the above, sampled-based rarefaction curves were applied to determine whether or not the sampling effort applied so far for the different Caribbean regions has been enough (**Appendix I** of Results). As a result, a large difference can be seen between the species richness estimators and the real species richness values, both for the samples studied *de novo* for the present thesis, and for the entire set of Caribbean areas sampled up to date (**Appendix I** of Results). Furthermore, none of the curves has reached its asymptote. In this way, we can conclude that, nowadays, we still do not know a realistic representation of the kinorhynch biodiversity throughout the Caribbean Sea. Although this thesis has significantly contributed to increase the known number of kinorhynch species in the area, it is necessary to promote new studies in the Caribbean to discover the hidden Kinorhyncha biodiversity inhabiting its waters.

4.1.1.4 ARE THERE SIMILARITIES BETWEEN THE KINORHYNCH CARIBBEAN FAUNA AND THAT OF ADJACENT REGIONS?

The majority of the Caribbean Kinorhyncha species (36 out of 52 taxa, ca. 69 %) are restricted to this sea, reinforcing the idea of the Caribbean as one of the world's greatest centres of endemic biodiversity (Miloslavich *et al.*, 2010). Despite this, several species may be found both inside and outside the Caribbean Basin.

Most of these kinorhynchs species are also distributed through the Gulf of Mexico and adjacent waters (Atlantic coast of Florida, Bermuda and/or North and South Carolina). It is the case of *Antygomonas paulae*, *Centroderes barbanigra*, *Echinoderes augustae*, *E. parahorni*, *E. spinifurca*, *E. sublicarum*, *E. truncatus*, *Leiocanthus*

corrugatus, *Pycnophyes beaufortensis*, *P. alexandroi* and *Semnoderes lusca* (Sørensen *et al.*, 2005; 2016; Sørensen, 2007; Neuhaus *et al.*, 2014; Sørensen and Landers, 2014; 2018; Landers and Sørensen, 2016; Landers *et al.*, 2018; 2019; 2020; Sánchez *et al.*, 2019) (sections **3.1**-**3.4** and **Appendix I** of Results). The Caribbean Basin connects to the Gulf of Mexico through the Yucatan Canal, making these two bodies of water dynamically interdependent (Oey *et al.*, 2005; Escobar-Briones, 2008). Certainly, several marine species are shared between them (Miloslavich *et al.*, 2010), and kinorhynchs, as the other taxa in common, could use the Yucatan Canal as a passageway, explaining the presence of shared species (sections **3.1** and **Appendix I** of Results).

Another two water entities, the Caribbean and the Pacific coastline of Panama, harbour some shared kinorhynch species, including *E. intermedius* and *P. alexandroi* (Pardos *et al.*, 2016a; 2016b) (sections **3.1** and **Appendix I** of Results). As pointed by Pardos *et al.* (2016a), three hypotheses may be raised to explain their presence at both sides of the Panama Isthmus:

- The species shared by the Caribbean Basin and the Pacific coastline of Panama possess wide geographic distribution ranges, reinforcing the idea that, in meiofaunal communities, everything is everywhere (EiE hypothesis) (Finlay, 2002; Fenchel and Finlay, 2004).
- Both species were distributed through the old Central American Seaway before the rising of the Panama Isthmus, which posteriorly yielded the isolation of the Caribbean and the Pacific populations of the species but without conspicuous, evolutionary changes (Pardos *et al.*, 2016a).
- The Panama Isthmus is acting as passageway for fauna exchange between the two water entities, allowing these kinorhynchs to migrate from one to another. This idea has also been proposed for other taxa (*e.g.* Menzies, 1968; McCosker and Dawson, 1975; Miloslavich *et al.*, 2011).

Although our current knowledge on genetics and biogeography in the phylum Kinorhyncha is rather scarce, some points regarding the aforementioned hypotheses may be highlighted. Firstly, kinorhynchs from shallow coastal waters generally seem to possess restricted distribution areas, frequently to a single or very few locations (Sørensen and Pardos, 2008; Neuhaus, 2013), making the EiE hypothesis hardly applicable for *E. intermedius* and *P. alexandroi*. The possibility of having isolated populations due to the Panama Isthmus raising, without any perceptible evolutionary change in ca. 12 million

years, makes the second hypothesis unlikely, even in the most favourable scenario with the lowest evolutionary rate (Pardos *et al.*, 2016a). Finally, kinorhynchs would face several difficulties while migrating through the Panama Canal, including the presence of freshwater, and the fact that the Canal is not sea-level (Pardos *et al.*, 2016a). Migration through ships would make the trip more suitable for kinorhynchs; indeed, Herranz and Leander (2016) reported the first case of possible human-vectored migration of a kinorhynch between Japan and British Columbia (Canada) due to the transport of oysters for cultivation (however, without direct evidence).

Finally, other three species seem to possess even more wide distributions: *E. astridae* has been also reported in Brazil (Sørensen, 2014); *E. horni* in Hawaii (Dunn *et al.*, 2008); and *S. pacificus* in California, New Caledonia and the Clarion-Clipperton Fracture Zone (Higgins, 1967; Sánchez *et al.*, 2019) (sections **3.1**-**3.4** and **Appendix I** of Results). In any case, the application of molecular techniques, including DNA sequencing for the identification and study of kinorhynchs populations, could shed some light into the degree of connectivity of these geographical areas in terms of kinorhynch species.

The presence of some kinorhynch affinities between the Caribbean Sea and the Pacific Central America, as well as the supposedly wide distribution of *E. horni* and *S. pacificus* through the Caribbean and the Pacific Ocean, led us to the study of several meiofaunal samples from the lower Gulf of California during the workshop "Muestreo, morfología, taxonomía y análisis genético en meiofauna: copépodos harpacticoides (Crustacea, Copepoda) y dragones del fango (Kinorhyncha)", hosted by the Instituto de Ciencias del Mar y Limnología (Mazatlán, Mexico) in 2018 (section **3.5** of Results). Our aim was to determine if both the Caribbean and the Gulf of California could also share some species. However, the studied samples from the lower Gulf of California yielded two new kinorhynch species, namely *Cephalorhyncha teresae* and *E. xalkutaat*, but no shared species were found whatsoever.

In summary, it seems likely that the Caribbean fauna is mainly represented by endemisms and some species also shared with the nearby Gulf of Mexico, whilst other few species may also possess wider geographic distributions through the Pacific Ocean, but no affinities between the Caribbean and the Gulf of California were established.

4.1.1.5 FUTURE PERSPECTIVE.

Most of the analysed Caribbean samples for the present thesis were obtained by Dr R. P. Higgins and colleagues during the 60-90s, which had been stored at the Smithsonian Institution of Washington Invertebrate Zoology collection as unprocessed samples. These samples were the result of a series of more or less extensive samplings that Dr R. P. Higgins carried out in Caribbean locations that, at that time, were geographically and politically accessible to him. The samplings were usually performed by a meiobenthic dredge, which is a qualitative sampling method, since a fixed sediment volume cannot be obtained this way (Fleeger *et al.*, 1988). Thus, it is not possible to make an accurate quantification of the sampling effort used in each locality, much less compare the data obtained between locations in terms of abundance.

Accordingly, it cannot be ensured that, in the localities for which samples are available, a complete representation of the real Kinorhyncha richness is reflected in our data. It is possible that new samplings in the same areas reveal the existence of still unknown species for the Caribbean. But even more important than this, the random nature of Dr R. P. Higgins' sampling depending on the accessibility of the different Caribbean regions at that time makes certain Caribbean areas still uncharted. One of the clearest examples can be seen in Cuba, where a single sampling from the Bahía de Guantánamo was available. Due to the Cuban-American Treaty of Relations of 1903, the USA assumed the territorial control of the south area at the Bahía de Guantánamo, making it more accessible for American citizens. It is unlikely that the current Cuban knowledge on Kinorhyncha species truly reflects the real biodiversity of the island, taking into account that it is based on this singe sampling and Cuba represents the largest island in the Caribbean Basin. Similarly, the Lesser Antilles are quite unexplored in terms of Kinorhyncha biodiversity, as only occasional samples from Guadeloupe, Barbados and Tobago were available.

Apart from certain Caribbean territories being more or less extensively sampled, it must be taken into consideration that the Caribbean Basin possesses an average depth of 2200 m, and its deepest point at the Cayman Trench reaches up to 7686 m (Lemenkova, 2020). Despite this, all the samples studied in the present thesis were collected in shallow coastal waters less than 100 m depth, and usually within the first 20 m. Again, this fact reflects the available sampling capacity of Dr R. P. Higgins at the time the samples were obtained, as meiobenthic dredges can be only used though the first depth metres. The

current knowledge on Caribbean Kinorhyncha is strongly biased in terms of bathymetry, and the kinorhynch Caribbean fauna from deeper waters remains to be studied.

In summary, this thesis has considerably updated the Kinorhyncha knowledge of the Caribbean Basin. However, new paths are open to the future, as still several Caribbean areas need to be studied in terms of geography and bathymetry.

4.1.2 BIODIVERSITY OF KINORHYNCHA IN THE DEEP-SEA (sections **3.5-3.6** of Results).

4.1.2.1 OVERVIEW.

Deep-sea ecosystems, which include waters and marine sediments from 200 m depth, cover more than 65 % of the Earth's surface (Danovaro *et al.*, 2010) and are essential to life because of the functions and services they provide (Jones *et al.*, 2014). However, because of the vastness and remoteness of these habitats, the study and management of deep-sea ecosystems is not an easy task, bringing significant methodological impediments that make this environment a great unknown in general terms (Ramírez-Llodra *et al.*, 2010; Marchese, 2015).

In recent years, up to 47 kinorhynch species have been described or reported from this environment, with focus on the Atlantic and the Pacific Oceans (Neuhaus and Blasche, 2006; Sørensen, 2008a; Neuhaus and Sørensen, 2013; Sánchez *et al.*, 2014a, b; Adrianov and Maiorova, 2015, 2016, 2018a, b; 2019, 2020; Grzelak and Sørensen, 2018, 2019; Sørensen and Grzelak, 2018; Sørensen *et al.*, 2018, 2019; Yamasaki *et al.*, 2018a, b, c, 2019). *Echinoderes ultraabyssalis* Adrianov and Maiorova, 2019, found at 9541 m depth at the Kuril-Kamchatka Trench, represents the deepest record of an identified kinorhynch up to date (Adrianov and Maiorova, 2019).

The present thesis furthermore contributed to increase the knowledge on deep-sea Kinorhyncha fauna with the exploration of a pockmark field at the Mozambique Channel, and also several deep-sea points at the central Gulf of California; these two works yielded the description of five new species, namely *Cristaphyes fortis*, *Echinoderes xalkutaat*, *Fujuriphyes dagon*, *F. hydra* and *Fissuroderes cthulhu* (sections **3.5-3.6** of Results). But even more relevant, several, previously known deep-sea kinorhynchs species were also reported for the Mozambique Channel, including *E. apex*, *E. dubiosus*, *E. hviidarum*, *E. unispinosus* and *Sphenoderes indicus* (sections **3.5-3.6** of Results).

4.1.2.2 ARE DEEP-SEA KINORHYNCH SPECIES MORE WIDELY DISTRIBUTED THAN THEIR CONGENERS FROM SHALLOWER WATERS?

As mentioned above, the present thesis reports previously known deep-sea kinorhynchs species at the Mozambique Channel (section **3.6** of Results). Indeed, deep-sea kinorhynchs seem somehow to possess wider distributional ranges compared to the congeners from shallower waters (Sørensen *et al.*, 2018; Yamasaki *et al.*, 2019). For example, *Condyloderes kurilensis* and *F. higginsi* were originally described from the Kuril-Kamchatka Trench (northwest Pacific Ocean) and New Zealand (southwest Pacific Ocean) respectively, but they also have been reported in the deep-sea waters off Oregon and California, northeast Pacific Ocean, and the Clarion-Clipperton Zone (Neuhaus and Blasche, 2006; Adrianov and Maiorova, 2016; Sørensen *et al.*, 2018; Sánchez *et al.*, 2019); even more striking is the case of *Campyloderes vanhoeffeni*, distributed worldwide in both coastal and deep waters (Neuhaus and Sørensen, 2013). Regarding the previously deep-sea known species recovered at the Mozambique Channel in the present thesis, *Echinoderes apex* had been reported in the Great Meteor Seamount (eastern Atlantic Ocean) up to 856 m depth (Yamasaki *et al.*, 2018c), *E. dubiosus* and *E. hviidarum* in northern California (eastern Pacific Ocean) up to 3853 m depth (Sørensen *et al.*, 2018), and *E. unispinosus* in the northeast Atlantic Ocean, the northeast Pacific Ocean and the Gulf of Mexico up to 3708 m depth (Sørensen *et al.*, 2018; Yamasaki *et al.*, 2018b; Álvarez-Castillo *et al.*, 2020).

Two main hypotheses are managed when trying to explain the wider distribution ranges of deep-sea Kinorhyncha:

- More homogeneous, environmental conditions of deep-sea (compared to those of coastal environments) promote wider distributional patterns. A majority of evidence suggests that many deep-sea taxa are broadly distributed, indicating that broad geographical distributions may be more frequent at greater depths (McClain and Hardy, 2010). In case of kinorhynchs, this has been proposed by Sørensen *et al.* (2018).
- Deep-sea complexes of cryptic species are common, since speciation is not always accompanied by conspicuous morphological changes (*e.g.* Janssen *et al.*, 2015; Cerca *et al.*, 2018; Van Steenkiste *et al.*, 2018; Vakati *et al.*, 2019). Lack of phenotypic divergence in metazoans may occur under extreme environmental

conditions (as those of deep-sea) when stabilizing selection prevents morphological changes, *i.e.* morphological stasis (Bickford *et al.*, 2007). In other cases, there are other non-morphological differences between the species of a cryptic complex, such as ethological (Knowlton, 2000; Bickford *et al.*, 2007).

Currently, there is no enough information on whether these supposedly widely distributed deep-sea species are truly the same species or we are facing complexes of cryptic species. Although the two hypotheses could agree with the reported deep-sea kinorhynchs at the Mozambique Channel (section **3.6** of Results), both have their limitations.

The deep-sea, once considered as a dark, homogeneous, unchangeable wasteland, actually possesses a great variety of geological and hydrological conditions, generating a wide range of different, heterogeneous habitats that allow more species to co-exist (Vanreusel *et al.*, 2009; Zeppilli *et al.*, 2016). It seems unlikely, therefore, to speak of a general environmental homogeneity in the deep-sea, making the first hypothesis only applicable to those species that inhabit more or less homogeneous habitats, such as certain zones of the abyssal plains. In our case of study at the Mozambique Channel, two main habitats were detected: one defined by high concentrations of methane and hydrogen sulphide (pockmarks), and other characterized by very low levels (or absence) of the aforementioned substances (outside pockmarks), defining a certain grade of environmental heterogeneity (Levin, 2005; Guillon *et al.*, 2017). In fact, our results showed that kinorhynchs density and community composition seem to be influenced by these two abiotic factors. Most of the reported species were restricted to one of the two habitats, except *Condyloderes* sp. and *E. unispinosus* that were present both inside and outside pockmarks, though the latter was more abundant inside these structures. These findings seem to evidence that the extreme environmental conditions of the pockmarks enhance the abundance of Kinorhyncha, likely through the replacement with opportunistic, specialized species (Sánchez *et al.*, 2021). Moreover, the species only present inside pockmarks not only would be able to cope with the extreme environmental conditions but also would profit, thriving there (Ritt *et al.*, 2010; Vanreusel *et al.*, 2010; Sánchez *et al.*, 2021). Thus, the first hypothesis does not seem to quite fit for the observed widely distributed kinorhynchs at the Mozambique Channel since most of the species inhabiting within the pockmarks were also reported in the abyssal plains and the surrounding seamounts, habitats with very different environmental conditions.

The second hypothesis seems to be more likely. It could be that the populations inside and outside pockmarks have exclusively ethological differences, understood as the interaction of such populations with their environment, *e.g.* with the differential available resources, as pockmarks are richer in methanotrophic bacteria, which likely represent a food source for kinorhynchs inhabiting pockmarks. Because of that, it is extremely vital to continue exploring the vast ocean depths combining traditional and novel techniques in order to obtain new information, material and reports that can shed some light in the aforementioned aspects of the deep-sea kinorhynch biogeography.

4.1.2.3 FUTURE PERSPECTIVE.

It is also essential to highlight the need to continue exploring the deep-sea kinorhynch communities to better understand the unknown biodiversity that these waters harbour, and to establish the distribution patterns and dispersal mechanisms of kinorhynchs in this peculiar environment. Particularly, molecular techniques of characterization and identification of species must be applied in order to clarify the taxonomic status of the deep-sea kinorhynchs.

4.1.3 BIODIVERSITY OF KINORHYNCHA IN THE NORTH SEA (section **3.7** of Results).

The North Sea is part of the north-eastern Atlantic Ocean and connects to it through the English Channel and to the Norwegian Sea in the north. It is, perhaps, one of the most known areas worldwide in terms of Kinorhyncha biodiversity, together with the adjacent European waters (Neuhaus, 2013). However, an occasional sampling done in the proximities of Syd-Hällsö Island (Strömstad, Sweden), in the Skagerrak area, revealed the presence of a new species of the genus *Setaphyes*, that was formally described as part of the thesis project as *S. elenae* (section **3.7** of Results). Moreover, the previously known species *Centroderes spinosus*, *Echinoderes* cf. *eximus*, *Pycnophyes ancalagon* and *Semnoderes armiger* were found co-occurring with *S. elenae* (section **3.7** of Results).

Thus, relatively well-known areas may still mask the existence of undescribed kinorhynch species. This was also the case of Yamasaki *et al.* (2020), whose sampling yielded the description of three new species of *Echinoderes* in other of the best well-known areas: the Sea of Japan and adjacent waters (Neuhaus, 2013). However, in this case, the study explored a very specific environment, a submarine cave, which usually

host different, specific fauna (Martínez and Fontaneto, 2018; Mammola *et al.*, 2019). Another remarkable case was that of Varney *et al.* (2019) that revisited one of the first sampling locations in the prolific career of Dr R. P. Higgins, the San Juan Archipelago (Higgins, 1960; 1961; 1977a; Adrianov and Higgins, 1996), describing a new species, *Echinoderes kohni* Varney *et al.*, 2019.

We strongly need to explore both unknown and supposedly well sampled areas in order to continue describing the still hidden Kinorhyncha biodiversity that undoubtedly will contribute to better understand this phylum in a future.

4.1.4 CAN TAXONOMICAL FEATURES OF THE DESCRIBED SPECIES IN THE PRESENT THESIS BE RELEVANT FOR SYSTEMATICS? (sections **3.1-3.7** and **Appendix I** of Results)

Although the phylum Kinorhyncha has been included in several metazoan phylogenies, the internal, phylogenetic relationships of kinorhynch taxa remained quite unknown, in terms of Henningian analysis, until the first attempts done by Sørensen (2008b) and Yamasaki *et al.* (2013). These studies supported some of the traditional kinorhynch groups that had been postulated by Zelinka (1907), Higgins (1964; 1990) and Adrianov and Malakhov (1996; 1999b), whilst evidenced new internal relationships never proposed before. It was not until Sørensen *et al.* (2015) that the first comprehensive, and up to date the only systematic study on the whole phylum Kinorhyncha was done, based on morphology and two molecular loci (18S and 28S rRNA). This study divided the phylum into the two main classes currently recognized, Allomalorhagida and Cyclorhagida (see Introduction for further information), the former accommodating the prior class Homalorhagida plus *Dracoderes* and *Franciscideres* that had been previously considered as cyclorhagids, whereas the latter included the classic cyclorhagid Kinorhyncha except the aforementioned genera (Sørensen *et al.*, 2015). However, the internal relationships in the main clades generated by this phylogeny (*e.g.* families Echinoderidae and Pycnophyidae, which are the most diverse families accommodating ca. 49% and 31% respectively of the total phylum biodiversity), as well as between them, remained unresolved. Sánchez *et al.* (2016) did, in the next year, a systematic revision of the family Pycnophyidae, based on both morphological and molecular data, synonymizing *Kinorhynchus* with *Pycnophyes* (the only pycnophyid genera described up to then) and erecting six new genera.

Several species of Pycnophyidae have been described for the present thesis, including *Cristaphyes cornifrons, C. fortis, C. retractilis, Fujuriphyes dagon, F. dalii, F. hydra, Higginsium mazatlanensis* and *Setaphyes elenae* (sections **3.1-3.2** and **3.5-3.7** of Results). These descriptions have reinforced the proposed diagnostic characters of the new genera erected by Sánchez *et al.* (2016), including the middorsal cuticular specializations, the arrangement of the paradorsal, lateroventral and ventrolateral setae, the pachycycli development, the morphology and arrangement of the glandular cell outlets (previously known as cuticular scars), the total trunk length, and the relative length of the lateral terminal spines (if present). The pycnophyid clades supported by both morphological and molecular characters seem to be well established according to the present knowledge on this family.

The description of *Dracoderes spyro* from La Española (Greater Antilles, Caribbean Sea) represented the first record of the genus in the western Atlantic Ocean, since most of its congeners had been described for the western Pacific Ocean, except *D. gallaicus* known from the eastern Atlantic Ocean and the Mediterranean Sea (section **3.3** of Results). With the discovery of *D. spyro*, an attempt to perform a total-evidence phylogeny for the family Dracoderidae was made, since the only available phylogeny up to date was exclusively based on molecular data (Yamasaki, 2015). However, the results were not very informative, as reflected by the generalized low support values for the clades, and minimal modifications in the data matrix caused large changes in the tree topologies. Thus, although enough morphological information was available for almost all species of Dracoderidae (except *D. orientalis*), the low number of known species up to date along with molecular data being only available for half of the species may have caused this lack of support.

Another interesting finding was the description of *Triodontoderes lagahoo* from Tobago (Lesser Antilles, Caribbean Sea), reporting the genus in the western Atlantic Ocean for the first time (section **3.4** of Results). The only known congener up to now, *T. anulap*, was described from the Chuuk Archipelago, western Pacific Ocean (Sørensen and Rho, 2009). *Triodontoderes*, together with *Zelinkaderes*, belongs to the family Zelinkaderidae, considered as monophyletic by Sørensen *et al.* (2015). This family is characterized by possessing an introvert with one ring of primary spinoscalids followed by three or four rings of regular scalids (Sørensen and Rho, 2009). The introvert of Zelinkaderidae is, therefore, characterized by the reduction of, at least, one ring of scalids

when compared with other kinorhynch families (Higgins, 1990; Bauer-Nebelsick, 1995; Sørensen *et al.*, 2007; Sørensen and Rho, 2009; Altenburger *et al.*, 2015). The description of *T. lagahoo* is in line with these previous findings, which seem to evidence a stronger reduction of introvert scalids in *Zelinkaderes* rather than in *Triodontoderes*, as this reduction involves more than one ring in the former genus but only the last ring in the latter genus. Another two kinorhynch genera are also characterized by a strong reduction of introvert scalids, namely *Cateria* and *Gracilideres*, which share with *Triodontoderes* the reduction of scalids in the last introvert ring (Neuhaus and Kegel, 2015; Herranz *et al.*, 2019a; Yamasaki, 2019). The reduction of scalids could have occurred independently in the four genera, as also proposed by Herranz *et al.* (2019), but this hypothesis cannot be tested until a more complete systematic analysis is performed. The presence of distally tripartite neck placids in *T. lagahoo* moreover supports the idea of this character being a synapomorphy of Zelinkaderidae (Sørensen and Rho, 2009); it is likely that the plesiomorphic condition for placid morphology in the family is the possession of distally tripartite placids, then *Z. yong* would have suffered a reversion of the character state through the placid reduction as an autapomorphy of the species. Again, this hypothesis cannot be correctly tested until more morphological, and especially molecular data is available. Finally, the description of *T. lagahoo* also seemed to evidence a greater number of spines throughout the dorsal and lateral series in *Triodontoderes* compared to *Zelinkaderes*; however, it is still too early to infer an evolutionary trend towards increasing or decreasing the number of spines in Zelinkaderidae.

Several species of Echinoderidae, the richest family in terms of species, have also been described for the present thesis, including *Cephalorhyncha teresae, Echinoderes barbadensis, E. brevipes, E. jesusi, E. parahorni, E. xalkutaat* and *Fissuroderes cthulhu* (sections **3.1-3.2** and **3.5-3.6** of Results). One of the pending tasks in Kinorhyncha systematics, as evidenced by Sørensen *et al.* (2015), is to resolve the Echinoderidae internal relationships, as phylogenetically relevant characters have been traditionally neglected in the Echinoderidae phylogenetic scenario to favour the cuticular composition of the second trunk segment, in a similar way that what occurred with Pycnophyidae and the presence of lateral terminal spines (Sánchez *et al.*, 2016). Undoubtedly, the more known species of Echinoderidae, the greater the data matrix (with both morphological and molecular) that can be used for future phylogenetic analyses.

4.2 Evolutionary morphology, ecology and morpho-ecology (sections 3.6 and 3.8-3.9 of Results).

Once the diversity of a certain group is known through the classification and description of the species, new questions may emerge in our minds. How do these organisms live? How are they adapted to their environment? How has its evolutionary history been? What are the main environmental factors that determine their distribution? In the present section, we will discuss the obtained results for some of these questions in the frame of the phylum Kinorhyncha.

Metazoans exhibit a wide variety of forms and shapes, which are essential to define the features of the different phyla. These morphological traits may vary by changes in the proportions of certain body regions and structures relative to body dimensions as a whole (*i.e.* allometric growth), implying relevant variations in animal function and biology (Shingleton, 2010; Anzai *et al.*, 2017). Kinorhynchs are characterized by having a somehow preserved body shape and dimension that though varies from one taxonomic group to another, this variation is not as evident as in other animal phyla (Sørensen and Pardos, 2020). In addition, the fact of permanently being part of meiofaunal communities imposes a body size limit that rarely exceeds 1000 µm of body length (Neuhaus, 2013). Additionally, kinorhynchs exhibit a wide variety of body structures on the cuticular surface, such as spines, setae and tubes, whose function is still controversial, but whose shape and arrangement are frequently used for systematic purposes (Neuhaus, 2013; Sørensen and Pardos, 2020).

At this point, after the description of multiple new species for the present thesis, we wondered if the different body regions (segments) and main cuticular structures (spines) of Kinorhyncha, despite their apparent homogeneity, could be subject to evolutionary patterns or rather be mainly adapted to environmental conditions. To test the first hypothesis, we focused on the concept of evolutionary allometry to know whether these kinorhynch body regions and cuticular appendages show any evolutionary particular trend and whether the allometric growth could be used to support the current Kinorhyncha systematics.

4.2.1 THE EVOLUTIONARY CONSTRAINTS IMPOSED ON THE MOST DISTAL BODY SEGMENTS (section **3.8** of Results).

Our results showed that the first, second and last trunk segments (S1, S2 and S11 henceforth) are affected by generalized negative allometric growth in the whole phylum Kinorhyncha (section **3.8** of Results). We hypothesized that developmental constraints seem to define negative allometry when an increase in the size of a body segment may lead to severe morpho-physiological alterations (section **3.8** of Results). The most distal body segments (S1, S2 and S11) define essential regions since they are of important functions such as feeding, locomotion and nervous coordination.

S1 and S2 define an anatomical body region that connects to the head and the neck, accommodating important organs such as the pharyngeal bulb and the brain (Neuhaus, 2013; Sørensen and Pardos, 2020). The head, responsible for feeding, locomotion and sensorial and nervous coordination, is a protruding, telescopic structure capable of completely retracting inside the body (Neuhaus, 2013; Sørensen and Pardos, 2020). For this reason, the head is attached to the S1 and S2 through a complex net of muscles (Kristensen and Higgins, 1991; Herranz *et al.*, 2014; Altenburger, 2016). In addition, the S1 and S2 are completely developed from the first postembryonic stages with fully functional structures (Kozloff, 1972; Higgins, 1977a; 1977b; Neuhaus, 1993; 1995; 2017; Sørensen *et al.*, 2000; 2010b; Schmidt-Rhaesa and Rothe, 2006; Neuhaus and Kegel, 2015), evidencing the tremendous importance of this body region for the kinorhynch life. Thus, the S1 and S2 would proportionally grow more slowly (compared to the general trunk growth) due to morpho-physiological restrictions, as an increase in its relative growth rate could lead to fatal head dysfunctions. Given that this negative allometry was obtained in all the studied kinorhynchs taxa, the pattern is likely to reflect an ancestral developmental pathway shared by all Kinorhyncha, independent of their body size and adaptations to different habitats. The only exception to the rule was observed in the positive allometric growth of Allomalorhagida regarding the S2, a fact that will be dealt in the next section.

In a similar way, the S11 usually bears a pair of wide, relatively long (compared with the remaining cuticular appendages) lateral terminal spines (Neuhaus, 2013; Sørensen and Pardos, 2020) that, unlike the other spines, have their own associated muscles (Kristensen and Higgins, 1991; Herranz *et al.*, 2014; Altenburger, 2016). In addition, the lateral terminal spines start their development from the earlier juvenile stages (Higgins, 1974; Neuhaus, 2013; 2017; Neuhaus and Sørensen, 2013; Neuhaus *et al.*, 2014; Neuhaus and Kegel, 2015). Again, morpho-physiological restrictions associated

with the muscles that allow the movement of the lateral terminal spines would lead to a proportionally slower growth of the S11 compared with the general body growth. The only exception was found in the class Allomalorhagida and the cyclorhagid family Centroderidae. Typically, allomalorhagid juveniles develop the lateral terminal spines from the latest juvenile stages, contrarily to cyclorhagids (Higgins, 1974; 1990; Brown, 1985; Neuhaus, 1993; 1995; Lemburg, 2002; Sørensen *et al.*, 2010d). This difference could lead to the observed positive allometry of allomalorhagid S11, as the need to harbour the lateral terminal spines, and their associated structures, would appear in the last postembryonic stages, which would have to grow propotionally more rapidly. In the case of Centroderidae, this family is characterized by having a midterminal spine (in addition to the lateral terminal spines) on S11, and the need to harbour this spine (together with its associated structures such as muscles) could lead to the observed positive allometry in this group.

4.2.2 THE PRESENCE OF EXAGGERATED SEXUAL DIMORPHIC CHARACTERS CAN CAUSE POSITIVE ALLOMETRIC TRENDS (section **3.8** of Results).

Positive allometry has been linked to sexual selection when exaggerated, sexually dimorphic features are present in different metazoan phyla (Tomkins *et al.*, 2010; Calabuig *et al.*, 2013; Ramírez-Ponce *et al.*, 2017). If a sexually dimorphic character is under sexual selection, an increased relative size of the structure could yield to increased reproductive success, resulting in positive allometry (Bonduriansky, 2007).

This could be applied to the observed positive allometry of S2 in Allomalorhagida (section **3.8** of Results), as most allomalorhagid species included in the analysis are characterized by males possessing a pair of ventrolateral tubes that are absent in females (Neuhaus, 2013; Sánchez *et al.*, 2016). The need to bear a relative increased in size pair of tubes could yield to a positive allometric growth of S2. However, the function of these male tubes is currently unknown, and we cannot be sure that this trait is under directional sexual selection.

4.2.3 MAKE IT BIGGER: I NEED SOME EXTRA SPACE FOR MY CUTICULAR STRUCTURES! (section **3.8** of Results)

One of the most disparate results between Kinorhyncha classes was obtained for the central trunk segments (S3-S10), as cyclorhagids exhibited isometry to positive allometric growth whilst allomalorhagids showed isometry to negative allometry (section **3.8** of Results). Cyclorhagids, and specifically Echinoderidae (most representatives of the class) usually have a higher number of cuticular appendages, such as spines and tubes, throughout the segments that exhibited a positive allometric trend, and these structures have different associated glandular and/or sensory cells (Zelinka, 1928; Nebelsick, 1991; Neuhaus, 2013; Sørensen and Pardos, 2020). Contrarily, allomalorhagids lack of spines and tubes, possessing setae instead, which are tube-like appendages proportionally smaller and have a weaker cuticular insertion than the previous ones (Zelinka, 1928; Neuhaus, 2013; Sánchez *et al.*, 2016).

These differences could explain the unequal selective pressures observed between cyclorhagids and allomalorhagids, as the former would need some extra cuticular space to harbour a higher number of cuticular appendages (and their associated structures) and a more strongly cuticular articulation at their bases, leading to the observed evolutionary, positive allometry of central trunk segments (section **3.8** of Results). This hypothesis may be reinforced by some observed facts concerning S9-10. The S9 bears paired protonephridial openings in both Allomalorhagida and Cyclorhagida (Reinhard, 1885; Zelinka, 1908; 1928; Neuhaus, 1988; Kristensen and Hay-Schmidt, 1989), and the need to develop a larger space to accommodate the excretory system could furthermore explain the observed positive allometric trend of cyclorhagid S9 and the isometry in Allomalorhagida despite S9 usually lacking cuticular appendages. The Allomalorhagida S10 usually possesses a pair of apodemes (paraventral cuticular thickenings where dorsal and ventral longitudinal muscles are attached) (Altenburger, 2016; Sánchez *et al.*, 2016) which are absent in Cyclorhagida, agreeing with the opposite allometric trends observed between the clases. Furthermore, Cyclorhagida S10 usually lacks cuticular appendages, supporting the observed generalized, negative allometric growth yielded by this segment in the analyses.

Despite the previous considerations, no statistically significant allometric relationships were determined between most of the spines considered and the total trunk length nor the total length of the corresponding segment. Although spines are considered an essential systematic character to distinguish between genera and species, specially in Cyclorhagida, these structures do not seem to be subject of evolutionary, allometric

trends. From this last observation, we thought that the spines could respond to adaptation patterns to the environment rather than possessing an evolutionary trend imposed by the phylogenetic history.

4.2.4 SEDIMENT GRAIN COMPOSITION (section **3.9** of Results).

As previously introduced, little is known about the Kinorhyncha ecology that concerns the relationships of kinorhynchs to their environments, including both abiotic and biotic factors, and the consequences of these relationships for evolution, morphological adaptation, population growth and regulation, interaction between species and populations, the composition of biological communities, and energy flow and nutrient cycling through the ecosystem.

In the present thesis, the first steps to elucidate some of these questions are taken, mainly focusing on studying whether the most relevant abiotic factors of certain meiofaunal ecosystems have a significant influence on the kinorhynchs most conspicuous cuticular structures (spines), their external morphology (body shape) and, finally, on their community composition.

The structure of the sediment is one of the main meiobenthic abiotic parameters, as its features (type of particles, content in organic matter, pore water, etc.) strongly influence the degree of accessibility of meiofaunal organisms and, in consequence, the composition of the meiofaunal communities (Giere *et al.*, 1988; Fonseca *et al.*, 2014). However, no information is available on whether the sediment type influences the kinorhynch morphological adaptations to the environment (and hence, if sediment composition sorts kinorhynch communities), as it has been evidenced for different meiofaunal groups, including harpacticoid copepods, turbellarians and nematodes (see, for instance, Hicks and Coull, 1983; Heip *et al.*, 1985; Martens and Schockaert, 1986; Tita *et al.*, 1999; Vanaberbeke *et al.*, 2011).

Our analyses evidenced that the lateral terminal spines (elongate, basally articulated, distally pointed, cuticular appendages present in lateroventral position on segment 11 of most kinorhynchs species), despite their function still remaining unknown, are somehow adapted to sediment composition (section **3.9** of Results). These cuticular appendages are the most conspicuous, as they project well beyond the trunk end, being forced to move through the sediment particles accompanying the general movement of

the animal. Kinorhynch species with stouter and plumper spines (more similar to an equilateral triangle) seem to occur in sediments with a wide variety of coarse particles (*i.e.* dominated by coarse grains), while species with slender spines (more similar to an isosceles triangle) tend to inhabit substrata with a wide variety of fine grains (*i.e.* dominated by fine particles) (section **3.9** of Results). The possession of stouter and plumper lateral terminal spines could allow kinorhynchs more efficiently moving through the sediment particles in coarser sediments, by the active displacement of the grains exerting a greater force. Actually, these spines are the only cuticular appendages of Kinorhyncha that are linked to internal muscles, meaning that the animals are able to move them (Kristensen and Higgins, 1991; Herranz *et al.*, 2014; Altenburger, 2016). Additionally, coarser sediments are usually a result of stronger currents, so the presence of stout and plump spines could allow kinorhynchs clinging more tightly to the sediment particles under episodes of high hydrodynamics. At the same time, the presence of slender lateral terminal spines (which are linked to more flexible structures) in kinorhynchs inhabiting finer sediments would facilitate the movement of the animal through the smaller interstices and particles.

We also obtained similar results for body size, which seems to go against the general hypothesis for meiofaunal interstitial organisms according to which species inhabiting fine sediments usually possess stouter and plumper bodies, whereas species that live in coarse sediments generally have slender and vermiform bodies (section **3.9** of Results). However, it must be taken into account that kinorhynchs are part of the so-called burrowing meiofaunal that actively move through the sediment displacing the particles. In this context, a more robust and plumper body may suppose an adaptive advantage when living in coarse sediments as it can generate a greater force to displace those sediment grains (section **3.9** of Results). Contrarily, a slender and more vermiform body of those species inhabiting fine sediments would be adaptive since it would not be necessary to apply much force to move the finer particles, and this body morphology would even facilitate the burrowing through the smallest interstices by simple body movements (section **3.9** of Results). This explanation is supported by the phenomenon of thixotropy, which explains that a smaller force against the sediment is enough to allow grains displacement in fine sediments (Levinton, 2017). Moreover, sediments with a heterogeneous composition of particles are a reflection of variable, strong depositional currents (Thomsen and Gust, 2000; McCave and Hall, 2006; Levinton, 2017; Bao *et al.*,

2019). In these areas of high current velocity, with intense erosion and transportation of sediment, meiofaunal organisms must be capable of burrowing rapidly, favouring the presence of stouter and plumper bodies in coarser sediments.

4.2.5 OTHER ABIOTIC FACTORS OF THE SEDIMENT (sections **3.6** and **3.9** of Results)

Organic matter concentration and pH are frequently considered relevant abiotic factors for meiofaunal organisms. However, just a few studies have explored their role in the morphological adaptations of meiofaunal to their environment. The C/N ratio, which includes information on the relative proportion of carbon and nitrogen in the organic matter, can explain relevant features of marine sediments that may be influential in defining the morphological adaptations of the meiofaunal organisms, such as terrestrial inputs or column water productivity. On the other hand, extreme values of pH may induce morphological deformations in meiofauna with exocuticle.

Our studies showed that kinorhynch species with stouter and plumper lateral terminal spines (more similar to an equilateral triangle) are more abundant in sediments with higher content in organic nitrogen (more likely of marine origin), whereas species with slender and elongated lateral terminal spines (more similar to an isosceles triangle) dominate in sediments with higher content in organic carbon (more likely of terrestrial origin) (section **3.9** of Results). The different proportions of organic carbon and nitrogen, and their origin, likely affect the composition of the micro- and meiobenthos communities, leading to strong fluctuations between the different marine sediments. The morphological changes in the lateral terminal spines observed between the kinorhynch species are unlikely due to the changing proportions of organic carbon and nitrogen but a possible adaptation to the different environments that these proportions create limiting the micro- and meiobenthos accessibility (Giere *et al.*, 1988) (section **3.9** of Results).

Fluctuating asymmetry in body shape was observed in those kinorhynch species inhabiting sediments with extreme values of pH (section **3.9** of Results). It has been proved that marine invertebrates with chitin-based exoskeletons may suffer a significant chitin loss, leading to body deformations, while exposed to recurrent pH changes, or under extreme acidic conditions (Badhury, 2015; Mustafa *et al.*, 2015). This could be related to the observed deviations from the bilateral symmetry observed in some of the analysed kinorhynch specimens inhabiting sediments with extreme values of pH.

The study of certain deep-sea, extreme habitats (cold seep pockmarks) at the Mozambique Channel allowed us to analyze the environmental variables of these habitats that drive the composition of the kinorhynch communities (section **3.6** of Results). We selected hydrogen sulphide (H_2S) and methane (CH_4) concentrations as environmental variables, knowing that these gases are the most abundant in active pockmarks (section **3.6** of Results).

Kinorhynchs were more abundant inside the pockmarks, where environmental conditions are extreme due to the aforementioned reduced compounds and the shortage of dissolved oxygen (Kumar, 2017; Pastor *et al.*, 2020) (section **3.6** of Results). The pockmark conditions seem to enhance the Kinorhyncha abundance likely through the replacement with opportunistic, specialized species, as also hypothesized by Sánchez *et al.* (2021). These species would be able to cope with the extreme pockmark conditions under which other meiofaunal species cannot live, taking advantage of this and thriving rapidly (Ritt *et al.*, 2010; Vanreusel *et al.*, 2010; Zeppilli *et al.*, 2011; 2018; Sánchez *et al.*, 2021). This was furthermore supported by the presence of a high number of juveniles inside pockmarks, which shows that these species are not only able to cope with the environmental conditions but also survive and flourish there (section **3.6** of Results). Actually, kinorhynchs have been proposed to be potential colonizers of deep-sea sulphide seepages due to these characteristics (Mullineaux *et al.*, 2012).

The dissimilar composition of the kinorhynch communities inside and outside pockmarks again suggests that only certain, well-adapted species are able to cope with the extreme environmental conditions of the pockmarks (section **3.7** of Results). These conditions seemed to prevent the survival of the non-adapted species, with their consequent fading, as occurred for *Echinoderes apex, E.* cf. *dubiosus, Echinoderes* sp., *Fujuriphyes hydra* and *Ryuguderes* sp. that were exclusively found outside the pockmarks (section **3.7** of Results). Contrarily, *Condyloderes* sp., *E. hviidarum, E. unispinosus, Fissuroderes cthulhu, Fu. dagon* and *Sphenoderes* cf. *indicus* characterized the kinorhynch community inside pockmarks (section **3.6** of Results). Of these, only *Condyloderes* sp. and *E. unispinosus* were generalistic species that inhabited both kinds of habitats, although their abundances were higher inside the pockmarks (section **3.7** of Results). Therefore, H_2S and CH_4 turned out to significantly drive the kinorhynch community structure and composition in deep-sea pockmarks.

4.2.6 FUTURE PERSPECTIVE

These studies have considerably increased the knowledge of the biology, evolutionary trends, ecology and morpho-ecology of the phylum Kinorhyncha. In fact, they can be considered pioneers in this field, as they had no precedent. However, it is still necessary to expand these research lines by studying new samples and kinorhynch populations. It is unknown whether there is a preference for certain types of sediment by the different kinorhynch species, or how the sediment influences the kinorhynch communities beyond the body morphological adaptations.

Moreover, some of the proposed hypotheses on the evolutionary allometric growth of the trunk segments must be tested, including those related to sexual dimorphism, or the presence of a greater or lesser number of cuticular appendages.

4.3 Macroecology and biogeography (section 3.10 of Results).

Macroecology studies the relationships between organisms and their environment at a large spatial scale to characterize and define diversity patterns (Brown, 1995). In this context, latitude is considered one of the main factors influencing different aspects of metazoans biology, distribution, abundance, richness and community dynamics. One of the most relevant metazoan features is body size due to its ecological implications on metabolism, physiology, life history traits, and population subtleties, as mentioned in previous sections of this discussion (Peters, 1983; Brown, 1995; McClain and Rex, 2001; Smith and Brown, 2002). This fact becomes even more relevant in meiofaunal organisms due to these organisms living in the small interstices of the sediment, where body size may be a limiting factor.

Latitude frequently defines body size-latitude trends (Bergmann, 1848; Allen, 1877; Partridge and Coyne, 1997; McDowall, 2007; Stillwell, 2010), including in some meiofaunal taxa such as copepods, nematodes and tardigrades (Armenteros and Ruiz-Abierno, 2015; Brun *et al.*, 2016; Bartels *et al.*, 2019). In this context, we explored size-latitude relationships in the phylum Kinorhyncha at a broad spatial scale (worldwide) to determine if these organisms are influenced by latitude (or by environmental variables that show a latitudinal change, including the sea surface temperature and the net primary productivity).

We obtained a U-shaped relationship between body size and latitude, being the body size lower at latitudes of ca. 10-25º then increasing towards the poles (section **3.10** of Results). Moreover, the largest species tended to be scarcer at latitudes of ca. 10-25º and vice versa (section **3.10** of Results). The pattern was consistently found for both Allomalorhagida and Cyclorhagida (section **3.10** of Results). In addition to this, temperature and primary productivity seemed to drive some variation of Kinorhyncha body size throughout the latitudinal gradient (section **3.10** of Results).

Temperature and body size correlate inversely under specific scenarios, and in the case of small-sized, marine ectotherms that rapidly adjust their body temperature depending on that of the environment, species inhabiting lower latitudes (with higher sea temperature) would accelerate development faster than somatic growth, leading to a smaller body size in the adult (Chown and Gaston, 2010; Arendt, 2011; Forster *et al.*, 2012). This hypothesis, however, has a strong limitation, as we do not currently know if ectotherms may increase the amount of resources allocated to development at the expense of final body size through physiological mechanisms, of even if this response would be adaptive rather than just a physiological limitation (Walters and Hassall, 2006; Kingsolver and Huey, 2008). Another hypothesis frequently proposed to explain why body size of marine ectotherms is sometimes smaller at low latitudes (*i.e.* higher sea temperature) is the predation risk, which could favour earlier maturation of organisms at the expense of growing, leading to smaller body sizes (Williams, 1966; Sibly and Atkinson, 1994; Atkinson, 1995). Kinorhynchs are likely included in the diet of many marine invertebrates, including decapods and snails (Martorelli and Higgins, 2004; Margulis and Chapman, 2009). These potential predators show a latitudinal gradient of species richness and abundance, decreasing both towards high latitudes (Roy *et al.*, 1998; Boschi, 2000; 2002; Dworschak, 2000; Rex *et al.*, 2005; Barnes, 2010), which means that the predation risk is higher at lower latitudes. This fact agrees with the aforementioned hypothesis of the predation risk and could apply for the observed patterns in Kinorhyncha. More recent studies, however, have shown a bimodal distribution of the mentioned predators, being these taxa more abundant and the tropics, then decreasing both towards the equator and the poles (Chaudhary *et al.*, 2016; Saeedi *et al.*, 2017; 2019). In fact, we showed that the smallest kinorhynch species were accumulated at the Tropic of Cancer, and taking into account that both tropics possess similar environmental conditions, and that Kinorhyncha records are missing at the Tropic of Capricorn, the size-latitude

distribution of Kinorhyncha could also agree with a bimodal distribution, with the smallest species located around the tropics, and those from the equator being intermediate between the tropical and the polar ones. If this were the case, the predation risk hypothesis could explain even better the observed trends.

The effect of the net primary productivity on kinorhynch body size seemed to be more discrete, since a positive correlation was only observed throughout the western Pacific and the western Atlantic coastlines. The so-called source availability hypothesis determines that metazoans are able to reach larger body size at areas with higher resource abundance (Ho *et al.*, 2009; Huston and Wolverton, 2011), areas with strong seasonal fluctuations of resources (Blackburn *et al.*, 1999), and/or areas with lower interspecific competition owing to increased access to resources (Moran and Woods, 2012). The resource availability hypothesis seems to agree with the results obtained for Cyclorhagida through the western Atlantic, whereas the remaining results are more heterogeneous. Latitudes with the highest values of productivity are likely to favour the occurrence of species with larger body size, but it should not be forgotten that many other environmental factors, sin some cases with more influence than primary productivity, may be responsible for the observed heterogeneous responses between kinorhynch body size and marine productivity.

Kinorhyncha size-latitude relationships showed, in general terms, a great variety of patterns throughout hemispheres, coastlines and taxonomic groups, revealing a complex interaction of several factors (section **3.10** of Results). These results agree with those obtained for other marine, ectotherm taxa such as copepods, bivalves and tardigrades, indicating that, contrarily to endotherms, ectotherm organisms do not respond to a single particular factor but to a network of multiple variables that configure a high heterogeneity in size-latitude trends. It is likely that the inclusion of new records and the discovery of new species will clarify the observed latitudinal trends in the present study. Furthermore, these results could suggest possible coevolution scenarios, at least in shallow waters, between the interstitial fauna (biological process, including the phyologenetic evolution and diversity and body changes; at this point, and due to their habitat, meiofaunal organisms would represent a good study model) and deposition phenomena of marine sediments (geological process) (Boyd *et al.*, 1992).

4.4 Synthesis.

More than 170 years have passed since the first discovery of a mud dragon at Saint Malo (France, eastern Atlantic Ocean) by the French biologist Félix Dujardin, with his study entitled "*Sur un petit animal marin, l'Echinodère, formant un type intermédiaire entre les Crustacés et les Vers*" (Dujardin, 1851). In the course of all those years, many discoveries have been made around this enigmatic metazoan phylum. The publications in systematics, and especially in classic taxonomy, have been particularly noteworthy, generating an essential foundation of knowledge as part of basic science.

With the present thesis, we continued this path by studying and describing the uncharted kinorhynch fauna from different places worldwide. Through the discovery of new taxa and their description, the knowledge basis is expanded and allow us generating and testing new hypotheses about aspects that had never been explored in the phylum Kinorhyncha, such as its biology, ecology and biogeography. We must not forget the value that some biological disciplines have for others, so that they provide feedback and allow us developing integrative studies with a broader approach with the ultimate goal of better understanding this mysterious animal phylum.

5 - Conclusions / Conclusiones

"All truths are easy to understand once they are discovered;

the point is to discover them" (Galileo Galilei)

Taxonomy and biodiversity.

- The Caribbean Sea hosts a rich kinorhynch fauna, representing ca. 16 % of the worldwide Kinorhyncha species, and is currently considered as one of the best known places in the world in terms of Kinorhyncha biodiversity.
- The knowledge on the kinorhynch biodiversity of the Caribbean Sea has been significantly increased (ca. 37 %) through the study of the numerous meiofaunal samples collected by Dr R. P. Higgins and his collegues and that were stored at the Smithsonian Institution of Washington facilities.
- A total of nine species have been found as new to science in the area belonging to five genera and four families.
- A total of four previously known species have been reported in the Caribbean Sea for the first time, increasing their distribution range.
- The Caribbean distribution range of ten species previously described and/or reported in the Caribbean Sea have been expanded with their report in new Caribbean areas.
- The current sampling effort applied in the Caribbean Sea is not exhaustive, as the asymptotes of the corresponding rarefaction curves were not reached. Specifically, the Antilles suffer more from a lack of sampling effort compared to the continental Caribbean.
- The deep-sea, taken as a whole, harbours a much richer meiofaunal than previously thougth. Specifically, five new species have been described from two independent, deep-sea samplings in the Gulf of California and the Mozambique Channel.
- Several, previously known kinorhynch species from the deep-sea have been also found at the Mozambique Channel, reinforcing the idea that deep-sea

Kinorhyncha species possess more widely distributions than their congeners from shallow waters.

- Some relatively well known and sampled ocean areas, in terms of Kinorhyncha biodiversity, still have undescribed species. This was verified with the description of a new species of *Setaphyes* from the North Sea.
- The identification and description of these kinorhynch fauna from multiple sampling sites reinforce the recently established diagnostic characters of the new erected pycnophyid genera and potentially represent key aspects to resolve the Kinorhyncha internal phylogenetic relationships in the future.

Taxonomía y biodiversidad.

- El mar Caribe alberga una fauna de kinorrincos rica en especies (aproximadamente el 16 % de las especies conocidas a nivel mundial se encuentran en esta área), y es considerado actualmente como uno de los mares mejor conocidos en términos de biodiversidad del filo Kinorhyncha.
- Se ha incrementado considerablemente el conocimiento sobre la fauna de kinorrincos del mar Caribe (aproximadamente en un 37 %) gracias al estudio de las numerosas muestras de meiofauna recogidas por el Dr. R. P. Higgins y sus colaboradores y que se encontraban almacenadas en el Instituto Smithsoniano de Washington.
- Se ha descubierto un total de nueve especies nuevas en esta área, pertenecientes a cinco géneros y cuatro familias diferentes.
- Se han registrado cuatro especies previamente conocidas por primera vez en el mar Caribe, lo que ha incrementado sus rangos conocidos de distribución.
- Se ha aumentado el rango de distribución de diez especies previamente conocidas en el mar Caribe, gracias a nuevos registros de las mismas en diferentes localidades caribeñas.
- El esfuerzo de muestreo aplicado en el mar Caribe no resulta suficiente para conocer la verdadera biodiversidad de kinorrincos, ya que las curvas de rarefacción no alcanzan su asíntota. Concretamente, las Antillas precisan de un mayor esfuerzo de muestreo comparado con el Caribe continental.

- El mar profundo, como conjunto, alberga comunidades de meiofauna mucho más ricas en especies de lo que una vez se pensó. Concretamente, se han descrito cinco nuevas especies de kinorrincos en dos localidades distintas: el golfo de California y el canal de Mozambique.
- Se han registrado por primera vez varias especies de kinorrincos del mar profundo previamente conocidas en el canal de Mozambique, reforzando la idea de que dichas especies del mar profundo poseen rangos de distribución mucho más amplios que los de sus parientes de aguas someras.
- Algunas áreas marinas relativamente bien conocidas y muestreadas, en términos de biodiversidad del filo Kinorhyncha, todavía tienen especies sin describir. Esto se demostró con la descripción de una nueva especie del género *Setaphyes* en el mar del Norte.
- La identificación y descripción de la fauna de kinorrincos de los lugares previamente mencionados refuerza los caracteres diagnósticos recientemente establecidos en los nuevos géneros de la familia Pycnophyidae y representan potenciales aspectos clave para continuar el estudio de las relaciones filogenéticas internas del filo en un futuro.

Evolutionary morphology, ecology and morpho-ecology.

- The body segments of selected Kinorhyncha taxa exhibit patterns of evolutionary allometric growth when compared to the total trunk growth.
- The first, second and eleventh body segments (which define important body regions as they are responsible for essential functions such as feeding, locomotion and nervous coordination) show a generalized, negative allometric growth likely due to developmental constraints, as an increase in the relative size of such segments could lead to severe morpho-physiological dysfunctions.
- The mid-body segments display a more variable allometric trend, mostly depending on the number and type of cuticular appendages (and their associated structures and/or organs). Thus, if a segment is characterized by possessing a greater number of cuticular appendages throughout the different kinorhynch taxa, it will likely exhibit a positive allometric growth, and vice versa.

- The cuticular spines of selected Kinorhynch taxa do not exhibit patterns of evolutionary allometric growth when compared to the total trunk growth or the growth of the corresponding body segment.
- The granulometric properties of the marine sediment stand as one of the main abiotic factors filtering the composition of the kinorhynch communities. Specifically, selected Kinorhyncha taxa are morphologically adapted to the different grain size of their habitats.
- Kinorhynch species with stouter and plumper body and lateral terminal spine shapes tend to inhabit coarser sediments, or sediments with a relatively heterogeneous variety of grain particles. This morphology would allow these species to move more efficiently through the coarse sediment grains by exerting a greater force to actively displace the grains. The more robust lateral terminal spines would also facilitate these species to cling more tightly to the sediment particles under episodes of strong currents and disturbations.
- Kinorhynch species with slender and more vermiform body and lateral terminal spine shapes tend to inhabit finer sediments, or sediments with a more homogeneous variety of particles. This morphology would facilitate the movement of these species through the smaller interstices and particles of these sediments.
- Extreme values and fluctuations of pH may induce asymmetry in the body shape of the kinorhynchs, as the chitin-based exoskeleton may suffer a significant chitin loss, leading to fluctuating asymmetry and body deformations.
- In extreme deep-sea habitats, such as cold seep pockmarks, the concentration of reduced substances (methane and hydrogen sulphide) configures the composition of the kinorhynch communities. The more extreme environmental conditions within the pockmarks enhance the abundance of the few species that are not only able to cope with such conditions but even profit from the absence of competitors, flourishing there.

Morfología evolutiva, ecología y morfoecología.

- Los segmentos corporales de taxones seleccionados de kinorrincos muestran patrones de crecimiento alométrico evolutivos cuando se comparan con el tamaño total del cuerpo.
- El primer, segundo y undécimo segmentos corporales (los cuales constituyen regiones esenciales encargadas de funciones como la toma de alimento, la locomoción y la coordinación nerviosa) exhiben patrones generalizados de crecimiento alométrico negativo evolutivo debido a restricciones durante la ontogenia, ya que un aumento en su tasa relativa de crecimiento podría causar alteraciones morfofisiológicas graves.
- Los segmentos corporales intermedios poseen un rango mucho más heterogéneo de patrones de crecimiento alométrico evolutivo, dependiendo del número y tipo de apéndices cuticulares (y sus estructuras y/o órganos asociados). Así, si un segmento se caracteriza por tener un mayor número de apéndices cuticulares entre los diferentes taxones de kinorrincos, probablemente exhiba una tendencia de crecimiento alométrico positivo, y viceversa.
- Las espinas cuticulares de taxones seleccionados del filo Kinorhyncha no mostraron ningún tipo de tendencia de crecimiento alométrico evolutivo cuando se compararon con el tamaño total del tronco o con el tamaño de los segmentos correspondientes.
- Las propiedades granulométricas del sedimento marino se erigen como uno de los principales factores abióticos a la hora de configurar la composición de las comunidades de kinorrincos. Concretamente, taxones seleccionados de kinorrincos se encuentran morfológicamente adaptados a la diferente granulometría de sus hábitats.
- Especies de kinorrincos con cuerpos y espinas laterales terminales más robustos y rechonchos tienen a vivir en sedimentos más gruesos, o sedimentos con una mayor heterogeneidad de tamaños de partícula. Esta morfología permite a dichas especies moverse eficientemente a través de los granos de sedimento gruesos gracias a que pueden ejercer una fuerza mayor a la hora de desplazar dichos granos. Las espinas laterales terminales más robustas también les posibilitan anclarse más fuertemente a los granos de sedimento bajo condiciones de fuertes corrientes y/o perturbaciones.

- Especies de kinorrincos con cuerpos y espinas laterales terminales más vermiformes suelen vivir en sedimentos finos, o sedimentos con una mayor homogeneidad de tamaños de partícula. Esta morfología permite a dichas especies moverse más fácilmente a través de los intersticios y granos de sedimento de menor tamaño.
- Valores extremos de pH y fluctuaciones constantes del mismo pueden causar asimetría en el cuerpo de los kinorrincos, ya que su exoesqueleto, basado en quitina, puede sufrir una pérdida importante de este compuesto, derivando en desviaciones del patrón de simetría bilateral y deformaciones corporales.
- En ambientes extremos del mar profundo, como los pockmarks de las zonas de emanación frías, la concentración de sustancias reductoras (metano y ácido sulfhídrico) cobra especial importancia a la hora de configurar la composición de las comunidades de kinorrincos. Estas condiciones ambientales tan extremas dentro de los pockmarks favorecen la abundancia de las pocas especies de kinorrincos que no solo son capaces de aguantarlas sino incluso de proliferar bajo las mismas gracias a una menor presión de competidores.

Macroecology and biogeography.

- Body size of kinorhynchs is influenced by latitude at a global, worldwide scale, showing a U-shaped relationship with the lowest sizes at latitudes of ca. 10-25º and the greatest sizes at the poles. It is likely that the lack of samplings at latitudes of -10 to -25º prevents finding the smallest species at the equator.
- However, the sampling worldwide biases prevent the complete discarding of a bimodal distribution of size-latitude trends, with kinorhynchs being smaller at the tropics, larger at the poles and intermediate in size at the equator.
- Heterogeneous, size-latitude relationships were found between hemispheres, coastlines and taxonomic groups, evidencing that a single underlying factor does not exclusively explain the observed latitudinal trends but rather a complex mix of different variables.
- Temperature and primary productivity, which vary latitudinally, explain part of the observed size-latitude trends in the phylum through the resource availability, the predation risk and the differential development-somatic growth hypotheses.

Macroecología y biogeografía.

- El tamaño corporal de los kinorrincos se ve influenciado por la latitud a escala global, mostrando una relación en forma de "U" donde encontramos a las especies de menor tamaño en latitudes de aproximadamente 10-25º y las de mayor tamaño en los polos. Es probable que la falta de muestreos en latitudes de aproximadamente -10 a -25º haga que no encontremos a las especies más pequeñas en el ecuador.
- Sin embargo, los sesgos de muestreo existentes a nivel mundial no nos permiten descartar que exista una distribución bimodal en la relación tamaño corporal-latitud, de modo que habría kinorrincos más pequeños en los trópicos, más grandes en los polos, y de tamaño intermedio en el ecuador.
- Se comprobó una alta variabilidad en los patrones existentes entre tamaño corporal y latitud cuando se estudiaron diferenciando por hemisferios, líneas de costa y grupos taxonómicos. Esto evidencia que probablemente no haya un único factor que explique esto, sino una compleja mezcla de variables.
- La variación latitudinal en la temperatura y los valores de productividad primaria explica parte de las relaciones observadas entre el tamaño corporal y la latitud del filo Kinorhyncha, a través de las hipótesis de la disponibilidad de recursos, del riesgo de depredación y del desfase entre el desarrollo y el crecimiento somático.

6 – References

"We live in a society exquisitely dependent on science and technology, in which hardly anyone knows anything about science and technology" (Carl Sagan)

Adrianov AV. 1989. The first report on Kinorhyncha of the Sea of Japan. *Zoologichesky Zhurnal* **68(7)**: 17-27.

Adrianov AV. 1991. Some peculiarities of biology of Cephalorhyncha, Kinorhyncha. *Ekologiya Morya* **39**: 57-61.

Adrianov AV. 1995. The first description of kinorhynchs from the Spitsbergen Archipelago (Greenland Sea), with a key to the genus *Pycnophyes* (Homalorhagida, Kinorhyncha). *Canadian Journal of Zoology* **73**: 1554-1566. https://doi.org/10.1139/z95-184.

Adrianov AV, Higgins RP. 1996. *Pycnophyes parasanjuanensis*, a new kinorhynch (Kinorhyncha: Homalorhagida: Pycnophyidae) from San Juan Island, Washington, U.S.A. *Proceedings of the Biological Society of Washington* **109(2)**: 236-247.

Adrianov AV, Maiorova AS. 2015. *Pycnophyes abyssorum* sp. n. (Kinorhyncha: Homalorhagida), the deepest kinorhynch species described so far. *Deep-sea Research Part II: Topical Studies in Oceanography* **111**: 49-59. https://doi.org/10.1016/j.dsr2.2014.08.009.

Adrianov AV, Maiorova AS. 2016. *Condyloderes kurilensis* sp. nov. (Kinorhyncha: Cyclorhagida)—a new deep water species from the abyssal plain near the Kuril-Kamchatka Trench. *Russian Journal of Marine Biology* **42**: 11-19. https://doi.org/10.1134/S1063074016010028.

Adrianov AV, Maiorova AS. 2018a. *Meristoderes okhotensis* sp. nov. – The first deepwater representative of kinorhynchs in the Sea of Okhotsk (Kinorhyncha: Cyclorhagida). *Deep-sea Research Part II: Topical Studies in Oceanography* **154**: 99-105. https://doi.org/10.1016/j.dsr2.2017.10.011.

Adrianov AV, Maiorova AS. 2018b. *Parasemnoderes intermedius* gen. n., sp. n.—the First Abyssal Representative of the Family Semnoderidae (Kinorhyncha: Cyclorhagida). *Russian Journal of Marine Biology* **44**: 355-362. https://doi.org/10.1134/S1063074018050024.

Adrianov AV, Maiorova AS. 2019. *Echinoderes ultraabyssalis* sp. nov. from the Kuril-Kamchatka Trench – the first hadal representative of the Kinorhyncha (Kinorhyncha: Cyclorhagida). *Progress in Oceanography* **178**: e102142. https://doi.org/10.1016/j.pocean.2019.102142.

Adrianov AV, Maiorova AS. 2020. *Echinoderes vulcanicus* sp. nov. from the active marine volcano Piip – the first representative of the Kinorhyncha in the Bering Sea (Kinorhyncha: Cyclorhagida). *Zoologischer Anzeiger* **289**: 35-49. https://doi.org/10.1016/j.jcz.2020.08.006.

Adrianov AV, Malakhov VV. 1990. Sense organs of Kinorhyncha using the example of the order Homalorhagida (Cephalorhyncha, Kinorhyncha). *Zoologichesky Zhurnal* **69(4)**: 5-14.

Adrianov AV, Malakhov VV. 1991. Fine structure of the reproductive system in Cephalorhyncha, Kinorhyncha. *Zoologischesky Zhurnal* **70(5):** 28-38.

Adrianov AV, Malakhov VV. 1994. Kinorhyncha: structure, development, phylogeny and taxonomy. Nauka Publishing, Moscow. 1st ed., 262 pp.

Adrianov AV, Malakhov VV. 1996. The phylogeny and classification of the class Kinorhyncha. *Zoosystematica Rossica* **4(1)**: 23-44.

Adrianov AV, Malakhov VV. 1999a. Kinorhyncha. In: Adiyodi KG, Adiyodi RG (eds.) *Reproductive biology of invertebrates. Volume IX, Part A: Progress in male gamete ultrastructure and phylogeny.* John Wiley and Sons, Chichester, pp. 193-211.

Adrianov AV, Malakhov VV. 1999b. *Cephalorhyncha of the world ocean*. KMK Scientific Press, Moscow. 1st ed., 328 pp.

Adrianov AV, Malakhov VV, Yushin VV. 1990. Fine structure of the cuticle of *Pycnophyes kielensis* (Kinorhyncha, Homalorhagida). *Zoologichesky Zhurnal* **69(1):** 5-11.

Adrianov AV, Malakhov VV, Yushin VV. 1993. Intracellular endosymbionts and parasites in the gut epithelium of kinorhynchs. *Russian Journal of Marine Biology* **17(5)**: 271-278.

Adrianov AV, Murakami C, Shirayama Y. 2002. *Echinoderes aureus* n. sp. (Kinorhyncha: Cyclorhagida) from Tanabe Bay (Honshu Island), Japan, with a key to the genus *Echinoderes*. *Species Diversity* **7**: 47-66. https://doi.org/10.12782/specdiv.7.47.

Adrianov AV, Rybakov AV. 1991. *Kinorhynchospora japonica* gen. n., sp. n. (Microsporidia) from the intestine ephitelium of *Kinorhynchus yushini* (Homalorhagida, Pycnophyidae), from the Sea of Japan. *Zoologichesky Zhurnal* **70(10)**: 5-11.

Allen JA. 1877. The influence of physical conditions in the genesis of species. *Radical Review* **1**: 108-140.

Altenburger A. 2016. The neuromuscular system of *Pycnophyes kielensis* (Kinorhyncha: Allomalorhagida) investigated by confocal laser scanning microscopy. *EvoDevo* **7**: e25. https://doi.org/ 10.1186/s13227-016-0062-6.

Altenburger A, Rho HS, Chang CY, Sørensen MV. 2015. *Zelinkaderes yong* sp. nov. from Korea - the first recording of *Zelinkaderes* (Kinorhyncha: Cyclorhagida) in Asia. *Zoological Studies* **54**: e25. https://doi.org/ 10.1186/s40555-014-0103-6.

Álvarez-Castillo L, Cepeda D, Pardos F, Rivas G, Rocha-Olivares Á. 2020. *Echinoderes unispinosus* (Kinorhyncha: Cyclorhagida), a new record from deep-sea sediments in the Gulf of Mexico. *Zootaxa* **4821(1)**: e13. https://doi.org/10.11646/zootaxa.4821.1.13.

Ansari ZA, Chatterji A, Parulekar AH. 1984. Effect of domestic sewage on sand beach meiofauna at Goa, India. *Hydrobiologia* **111**: 229-233. https://doi.org/10.1007/BF00007203.

Anzai H, Oishi K, Kumagai H, Hosoi E, Nakanishi Y, Hirooka H. 2017. Interspecific comparison of allometry between body weight and chest girth in domestic bovids. *Scientific Reports* **7**: e4817. https://doi.org/10.1038/s41598-017-04976-z.

Appeltans W, Ahyong ST, Anderson G, Angel MV, Artois T, Bailly N, *et al.* 2012. The magnitude of global marine species diversity. *Current Biology* **22(23)**: 2189-2202. https://doi.org/10.1016/j.cub.2012.09.036.

Arendt JD. 2011. Size-fecundity relationships, growth trajectories, and the temperature-size rule for ectotherms. *Evolution* **65**: 43-51. https://doi.org/10.1111/j.1558-5646.2010.01112.x.

Armenteros M, Ruiz-Abierno A. 2015. Body size distribution of free-living marine nematodes from a Caribbean coral reef. *Nematology* **17**: 1153-1164. https://doi.org/10.1163/15685411-00002930.

Atkinson D. 1995. Effects of temperature on the size of aquatic ectotherms: exceptions to the general rule. *Journal of Thermal Biology* **20(1&2)**: 61-74. https://doi.org/10.1016/0306-4565(94)00028-H.

Badhury P. 2015. Effects of ocean acidification on marine invertebrates – a review. *Indian Journal of Marine Science* **44**: 454-464.

Bao R, Blattmann TM, McIntyre C, Zhao M, Eglinton TI. 2019. Relationships between grain size and organic carbon ^{14}C heterogeneity in continental marine sediments. *Earth and Planetary Science Letters* **505**: 76-85. https://doi.org/10.1016/j.epsl.2018.10.013.

Barnes RSK. 2010. Regional and latitudinal variation of in the diversity, dominance and abundance of microphagous microgastropods and other benthos in intertidal beds of dwarf eelgrass, *Nanozostera* spp. *Marine Biodiversity* **40**: 95-106. https://doi.org/10.1007/s12526-010-0036-1.

Bartels PJ, Fontaneto D, Rozskowska M, Nelson DR, Kaczmarek Ł. 2019. Latitudinal gradients in body size in marine tardirgades. *Zoological Journal of the Linnean Society* **188(3)**: 820-838. https://doi.org/10.1093/zoolinnean/zlz080.

Bauer-Nebelsick M. 1995. *Zelinkaderes klepali* sp. nov. from shallow water sands of the Red Sea. *Annalen des Naturhistorischen Museums in Wien, Serie B Botanik und Zoologie* **97**: 57-74.

Bergmann C. 1848. Über die Verhältnisse der Wärmeökonomie der Thiere zu ihrer Grösse. *Göttinger Studien* **3**: 595-708.

Bickford D, Lohman DJ, Sodhi NS, Ng PKL, Meier R, Winker K, *et al.* 2007. Cryptic species as a window on diversity and conservation. *Trends in Ecology & Evolution* **22(3)**: 148-155. https://doi.org/10.1016/j.tree.2006.11.004.

Blackburn TM, Gaston KJ, Loder N. 1999. Geographic gradients in body size: a clarification of Bergmann's rule. *Diversity and Distributions* **5(4):** 165-174. https://doi.org/10.1046/j.1472-4642.1999.00046.x.

Blake CH. 1930. Three new species of worms belonging to the order Echinodera. *Biological Survey of the Mount Desert Region* **4**: 3-10.

Bonduriansky R. 2017. Sexual selection and allometry: a critical reappraisal of the evidence and ideas. *Evolution* **61(4)**: 838-849. https://doi.org/10.1111/j.1558-5646.2007.00081.x.

Boschi EE. 2000. Species of decapod crustaceans and their distribution in the American marine zoogeographic provinces. *Revista de Investigación y Desarrollo Pesquero* **13**: 1-136.

Boschi EE. 2002. Distribution of continental shelf decapod crustanceans along the American Pacific Coast. In: Escobar-Briones E, Álvarez F (eds.) *Modern Approaches to the Study of Crustacea*. Springer, New York, pp. 235-239.

Boyd R, Darlymple R, Zaitlin BA. 1992. Classification of clastic coastal depositional environments. *Sedimentary Geology* **80(3-4):** 139-150. https://doi.org/10.1016/0037-0738(92)90037-R.

Brown JH. 1995. *Macroecology*. The University of Chicago Press, Chicago. 1st ed., 270 pp.

Brown R. 1983. Spermatophore transfer and subsequent sperm development in a homalorhagid kinorhynch. *Zoologica Scripta* **12(4):** 257-266. https://doi.org/10.1111/j.1463-6409.1983.tb00509.x.

Brown R. 1985. *Developmental and taxonomic studies of Sydney harbour Kinorhyncha*. Ph.D. Thesis, Macquarie University, Sydney, 193 pp.

Brown R. 1989. Morphology and ultrastructure of the sensory appendages of a kinorhynch introvert. *Zoologica Scripta* **18(4):** 471-482. https://doi.org/10.1111/j.1463-6409.1989.tb00141.x.

Brun PG, Payne MR, Kiørboe T. 2016. Trait biogeography of marine copepods – an analysis across scales. *Ecology Letters* **19(2)**: 1403-1413. https://doi.org/10.1111/ele.12688.

Brusca RC, Moore W, Shuster SM. 2016. *Invertebrates.* Oxford University Press, Oxford. 3rd ed., 1104 pp.

Calabuig CP, Green AJ, Muriel R, Katzenberger M, Patino-Martínez J, Moreira HM. 2013. Allometry as evidence of sexual selection in monochromatic birds: the case of the Coscoroba swan (Anseriformes: Anatidae). *Zoologia (Curitiba)* **30(4)**: 424-429. https://doi.org/10.1590/S1984-46702013000400008.

Castro P., Huber M.E. 2007. *Biología marina.* McGraw Hill Interamericana de España, Madrid. 6th ed., 514 pp.

Cepeda D, Pardos F, Sánchez N. 2019b. A new species and first record of *Dracoderes* (Kinorhyncha: Allomalorhagida: Dracoderidae) from American waters, with an identification key of the genus. *Zoologischer Anzeiger* **282**: 106-115. https://doi.org/10.1016/j.jcz.2019.05.019.

Cepeda D, Sánchez N, Pardos F. 2019a. First report of the family Zelinkaderidae (Kinorhyncha: Cyclorhagida) for the Caribbean Sea, with the description of a new species of *Triodontoderes* Sørensen & Rho, 2009 and an identification key for the family. *Zoologischer Anzeiger* **282**: 116-126. https://doi.org/10.1016/j.jcz.2019.05.017.

Cepeda D, Sánchez N, Pardos F. 2019c. First extensive account of the phylum Kinorhyncha from Haiti and the Dominican Republic (Caribbean Sea), with the description of four new species. *Marine Biodiversity* **49(5):** 2281-2309. https://doi.org/10.1007/s12526-019-00963-x.

Cerca J, Purschke G, Struck TH. 2018. Marine connectivity dynamics: clarifying cosmopolitan distributions of marine interstitial invertebrates and the meiofaunal paradox. *Marine Biology* **165**: e123. https://doi.org/10.1007/s00227-018-3383-2.

Chang CY, Song YH. 2002. *Echinoderes lanceolatus*, a new kinorhynch from Korea (Kinorhyncha, Cyclorhagida, Echinoderidae). *The Korean Journal of Systematic Zoology* **18(2)**: 203-2011.

Chaudhary C, Saeedi H, Costello MJ. 2016. Bimodality of latitudinal gradients in marine species richness. *Trends in Ecology & Evolution* **31**: 670-676. https://doi.org/10.1016/j.tree.2016.06.001.

Chown SL, Gaston KJ. 2010. Body size variation in insects: a macroecological perspective. *Biological Reviews* **85**: 139-169. https://doi.org/10.1111/j.1469-185X.2009.00097.x.

Claparède ARE. 1863. *Beobachtungen über Anatomie und Entwicklungsgeschichte wirbelloser Thiere: an der Küste von Normandie angestellt.* Verlag von Wilhelm Engelmann, Leipzig. 1st ed, 120 pp.

Costello MJ, Chaudhary C. 2017. Marine biodiversity, biogeography, deep-sea gradients, and conservation. *Current Biology* **27(11)**: R511–R527. https://doi.org/10.1016/j.cub.2017.04.060.

Dal Zotto M. 2015. *Antygomonas caeciliae*, a new kinorhynch from the Mediterranean Sea, with report of mitochondrial genetic data for the phylum. *Marine Biology Research* **11(7)**: 1-14. https://doi.org/10.1080/17451000.2015.1007872.

Dal Zotto M, Neuhaus B, Yamasaki H, Todaro MA. 2019. The genus *Condyloderes* (Kinorhyncha: Cyclorhagida) in the Mediterranean Sea, including the description of two new species with novel characters. *Zoologischer Anzeiger* **282**: 206-231. https://doi.org/10.1016/j.jcz.2019.05.006.

Danovaro R, Company JB, Corinaldesi C, D'Onghia G, Galil B, Gambi C, *et al.* 2010. Deep-sea biodiversity in the Mediterranean Sea: the known, the unknown, and the unknowable. *PLoS ONE* **5**: e11832. https://doi.org/10.1371/journal.pone.0011832.

De Bovée F, Soyer J. 1974. Cycle anual quantitatif du méiobenthos des vases terrigènes côtières distribution verticale. *Vie et Milieu, Série B* **24(1)**: 141-157.

Dovgal I, Chatterjee T, Ingole BS, Nanajkar M. 2008. First report of *Limnoricus ponticus* Dovgal and Lozowskiy (Ciliophora, Suctorea) as epibionts on *Pycnophyes* (Kinorhyncha) from Indian Ocean with key to species of the genus *Limnoricus*. *Cahiers de Biologie Marine* **49:** 381-385.

Dujardin F. 1851. Sur un petit animal marin, l'Echinodère, formant un type intermédiaire entre les Crustacés et les Vers. *Annales des Sciences Naturelles, Zoologie* **15**: 158-160.

Dunn CW, Giribet G, Edgecombe GD, Hejnol A. 2014. Animal phylogeny and its evolutionary implications. *Annual Review of Ecology, Evolution and Systematics* **45:** 371-395. https://doi.org/10.1146/annurev-ecolsys-120213-091627.

Dunn CW, Hejnol A, Matus DQ, Pang K, Browne WE, Smith SA, *et al.* 2008. Broad phylogenomic sampling improvesresolution of the animal tree of life. *Nature* **452**: 745-749. https://doi.org/10.1038/nature06614.

Dworschak PC. 2000. Global diversity in the Thalassinidea (Decapoda). *Journal of Crustacean Biology* **20(2)**: 238-245. https://doi.org/10.1163/1937240X-90000025.

Escobar-Briones E. 2008. Current knowledge on benthic communities in the Gulf of Mexico. In: Withers K, Nippers M (eds.) *Environmental Analysis of the Gulf of Mexico*. Texas A&M University Press, Corpus Christi, pp. 115-133.

Fenchel T, Finlay BJ. 2004. The ubiquity of small species: patterns of local and global diversity. *BioScience* **54**: 777-784. https://doi.org/10.1641/0006-3568(2004)054[0777:TUOSSP]2.0.CO;2.

Finlay BJ. 2002. Global dispersal of free-living microbial eukaryote species. *Science* **296**: 1061-1063. https://doi.org/10.1126/science.1070710.

Fleeger JW, Thistle D, Thiel H. 1988. Sampling equipment. In: Higgins RP, Thiel H (eds.) *Introduction to the Study of Meiofauna*. Smithsonian Institution Press, Washington DC, pp. 115-133.

Fonseca G, Maria TF, Kandratavicius N, Venekey V, Gheller PF, Gallucci F. 2014. Testing for nematode-granulometry relationships. *Marine Biodiversity* **44(3)**: 435-443. 10.1007/s12526-014-0241-4.

Forster J, Hirst AG, Atkinson D. 2012. Warming-induced reductions in body size are greater in aquatic than terrestrial species. *PNAS* **109(47)**: 19310-19314. https://doi.org/10.1073/pnas.1210460109.

Freckelton RP, Harvey PH, Pagel M. 2002. Phylogenetic analysis and comparative data: a test and review of the evidence. *The American Naturalist* **160**: 712-726. https://doi.org/10.1086/343873.

Frithsen JB, Elmgren R, Rudnick DT. 1985. Responses of benthic meiofauna to long-term, low-level additions of No. 2 fuel oil. *Marine Ecology Progress Series* **23**: 1-14. https://doi.org/ 10.3354/meps023001.

GªOrdóñez D, Pardos F, Benito J. 2000. Cuticular structures and epidermal glands of *Echinoderes cantabricus* and *E. hispanicus* (Kinorhyncha, Cyclorhagida) with special

reference to their taxonomic value. *Journal of Morphology* **246**: 161-178. https://doi.org 10.1002/1097-4687(200012)246:3<161::AID-JMOR1>3.0.CO;2-R.

GªOrdóñez D, Pardos F, Benito J. 2008. Three new *Echinoderes* (Kinorhyncha, Cyclorhagida) from North Spain, with new evolutionary aspects in the genus. *Zoologischer Anzeiger* **247**: 95-111. https://doi.org/10.1016/j.jcz.2007.07.001.

Gerlach SA. 1969. *Cateria submersa* sp. n., ein cryptorhager Kinorhynch aus dem sublitoralen Mesopsammal der Nordsee. *Veröffenlichungen des Instituts für Meeresforschung in Bremerhaven* **12**: 161-168.

Giere O. 2009. Habitat, habitat conditions and their study methods. In: Giere O (ed.) *Meiobenthology: the microscopic fauna in aquatic sediments*. Springer-Verlag, Berlin, pp. 5-43.

Giere O, Eleftheriou A, Murison DJ. 1988. Abiotic factors. In: Higgins RP, Thiel H (eds.) *Introduction to the Study of Meiofauna*. Smithsonian Institution Press, Washington DC, pp. 61-78.

Giribet G. 2015. Morphology should not be forgotten in the era of genomics – a phylogenetic perspective. *Zoologischer Anzeiger* **256**: 96-103. https://doi.org/10.1016/j.jcz.2015.01.003.

Grego M, De Tronch M, Forte J, Malej A. 2009. Main meiofauna taxa as indicator for assessing the spatial and seasonal impact of fish farming. *Marine Pollution Bulletin* **58**: 1178-1186. https://doi.org/10.1016/j.marpolbul.2009.03.020.

Grzelak K, Sørensen MV. 2018. New species of *Echinoderes* (Kinorhyncha: Cyclorhagida) from Spitsbergen, with additional information about known Arctic species. *Marine Biology Research* **14(2)**: 113-147. https://doi.org/10.1080/17451000.2017.1367096.

Grzelak K, Sørensen MV. 2019. Diversity and community structure of kinorhynchs around Svalbard: First insights into spatial patterns and environmental drivers. *Zoologischer Anzeiger* **282**: 31-43. https://doi.org/10.1016/j.jcz.2019.05.009.

Guillon E, Menot L, Decker C, Krylova E, Olu K. 2017. The vesicomyd bivalve habitat at cold-seeps supports heterogeneous and dynamic macrofaunal assemblages. *Deep-sea*

Research Part I: Oceanographic Research Papers **120**: 1-13. https://doi.org/10.1016/j.dsr.2016.12.008.

Hajduk G. 2019. *Introduction to Linear Mixed Models.* I Workshop Introduction to Linear Mixed Models [Accessed at https://ourcodingclub.github.io/tutorials/mixed-models/#explore-the-data on 2021-04-14].

Heip CHR, Vincx M, Vranken G. 1985. The ecology of marine nematodes. *Oceanography and Marine Biology* **23**: 399-489.

Herman RI, Dahms HU. 1992. Meiofauna communities along a depth transect off Halley Bay (Weddell Sea – Antarctica). *Polar Biology* **12**: 313-320. https://doi.org/10.1007/978-3-642-77595-6_36.

Herranz M, Boyle MJ, Pardos F, Neves RC. 2014. Comparative myoanatomy of *Echinoderes* (Kinorhyncha): a comprehensive investigation by CLSM and 3D reconstruction. *Frontiers in Zoology* **11**: e31. https://doi.org/ 10.1186/1742-9994-11-31.

Herranz M, Di Domenico M, Sørensen MV, Leander BS. 2019a. The enigmatic kinorhynch *Cateria styx* Gerlach, 1956 – a sticky son of a beach. *Zoologischer Anzeiger* **282**: 10-30. https://doi.org/10.1016/j.jcz.2019.05.016.

Herranz M, Leander BS. 2016. Redescription of *Echinoderes ohtsukai* Yamasaki and Kajihara, 2012 and *E. kozloffi* Higgins, 1977 from the northeastern Pacific coast, including the first report of a potential invasive species of kinorhynchs. *Zoologischer Anzeiger* **265**: 108-126. https://doi.org/10.1016/j.jcz.2016.02.004.

Herranz M, Leander BS, Pardos F, Boyle MJ. 2019b. Neuroanatomy of mud dragons: a comprehensive view of the nervous system in *Echinoderes* (Kinorhyncha) by confocal laser scanning microscopy. *BMC Evolutionary Biology* **19**: e86. https://doi.org/10.1186/s12862-019-1405-4.

Herranz M, Pardos F. 2013. *Fissuroderes sorenseni* sp. nov. and *Meristoderes boylei* sp. nov.: First Atlantic recording of two rare kinorhynch genera, with new identification keys. *Zoologischer Anzeiger* **253(2)**: 93-111. https://doi.org/10.1016/j.jcz.2013.09.005.

Herranz M, Sánchez N, Pardos F, Higgins RP. 2014. New Kinorhyncha from Florida coastal waters. *Helgoland Marine Research* **68**: 59-87. https://doi.org/10.1007/s10152-013-0369-9.

Herranz M, Sørensen MV, Park T, Leander BS, Worsaae K. 2020. Insights into mud dragon morphology (Kinorhyncha, Allomalorhagida): myoanatomy and neuroanatomy of *Dracoderes abei* and *Pycnophyes ilyocryptus*. *Organisms Diversity & Evolution* **20**: 467-493. https://doi.org/10.1007/s13127-020-00447-y.

Herranz M, Thormar J, Benito J, Sánchez N, Pardos F. 2012. *Meristoderes* gen. nov., a new kinorhynch genus, with the description of two new species and their implications for echinoderid phylogeny (Kinorhyncha: Cyclorhagida, Echinoderidae). *Zoologischer Anzeiger* **251(3)**: 161-179. https://doi.org/10.1016/j.jcz.2011.08.004.

Herranz M, Yangel E, Leander BS. 2017. *Echinoderes hakaiensis* sp. nov.: a new mud dragon (Kinorhyncha, Echinoderidae) from the northeastern Pacific Ocean with the redescription of *Echinoderes pennaki* Higgins, 1960. *Marine Biodiversity* **48(1)**: 303-325. https://doi.org/10.1007/s12526-017-0726-z.

Hicks GRF, Coull BC. 1983. The ecology of marine meiobenthic harpacticoid copepods. *Oceanography and Marine Biology* **21**: 67-175.

Higgins RP. 1960. A new species of *Echinoderes* (Kinorhyncha) from Puget Sound. *Transactions of the American Microscopical Society* **79(1):** 85-91. https://doi.org/10.2307/3223976.

Higgins RP. 1961. Three new homalorhage kinorhynchs from the San Juan Archipelago, Washington. *Journal of the Elisha Mitchell Scientific Society* **77(1):** 81-88.

Higgins RP. 1964. Three new kinorhynchs from the North Carolina coast. *Bulletin of Marine Science* **14(3)**: 479-493.

Higgins RP. 1965. The homalorhagid Kinorhyncha of northeastern US coastal waters. *Transactions of the Microscopical American Society* **84**: 65-72.

Higgins RP. 1966. *Echinoderes arlis*, a new kinorhynch from the Arctic Ocean. *Pacific Science* **20:** 518-520.

Higgins RP. 1967. The Kinorhyncha of New Caledonia. *Expédition Française sur Recifs Coralliens de la Nouvelle Calédonie. Éditions de la Fondation Singer-Polignac, Paris* **2**: 75-90.

Higgins RP. 1969. *Condyloderes* and *Sphenoderes*, new cyclorhagid genera. *Smithsonian Contributions to Zoology* **14**: 1-13. https://doi.org/10.5479/si.00810282.14.

Higgins RP. 1974. Kinorhyncha. In: Giese AC, Pearce JS (eds.) *Reproduction of marine invertebrates. Volume I: Acoelomate and pseudocoelomate metazoans*. Academic Press, New York, pp. 507-518.

Higgins RP. 1977a. Redescription of *Echinoderes dujardinii* (Kinorhyncha) with descriptions of closely related species. *Smithsonian Contributions to Zoology* **248:** 1-26. https://doi.org/10.5479/si.00810282.248.

Higgins RP. 1977b. Two new species of *Echinoderes* (Kinorhyncha) from South Carolina. *Transactions of the American Microscopical Society* **96(3)**: 340-354. https://doi.org/ 10.2307/3225864.

Higgins RP. 1978. *Echinoderes gerardi* n. sp. and *E. riedli* (Kinorhyncha) from the Gulf of Tunis. *Transactions of the American Microscopical Society* **97(2)**: 171-180. https://doi.org/ 10.2307/3225589.

Higgins RP. 1982. Three new species of Kinorhyncha from Bermuda. *Transactions of the American Microscopical Society* **104**: 305-316.

Higgins RP. 1983. The Atlantic Barrier Reef Ecosystem at Carrie Bow Cay, Belize, II. Kinorhyncha. *Smithsonian Contributions to Marine Science* **1**: 1-131. https://doi.org/10.5479/si.01960768.18.1.

Higgins RP. 1985. The genus *Echinoderes* (Kinorhyncha: Cyclorhagida) from the English Channel. *Journal of the Marine Biological Association of the United Kingdom* **65(3)**: 785-800.

Higgins RP. 1986. A new species of *Echinoderes* (Kinorhyncha: Cyclorhagida) from a coarse-sand California beach. *Transactions of the American Microscopical Society* **105(3)**: 266-273. https://doi.org/ 10.2307/3226298.

Higgins RP. 1990. Zelinkaderidae, a new family of cyclorhagid Kinorhyncha. *Smithsonian Contributions to Zoology* **500**: 1-26. https://doi.org/10.5479/si.00810282.500.

Higgins RP. 1991. *Pycnophyes chukchiensis*, a new homalorhagid kinorhynchs from the Arctic Sea. *Proceedings of the Biological Society of Washington* **104(1)**: 184-188.

Higgins RP, Korcynski RE. 1989. Two new species of *Pycnophyes* (Homalorhagida, Kinorhyncha) from the Canadian coast of the Beaufort Sea. *Canadian Journal of Zoology* **67**: 2056-2064. https://doi.org/10.1139/z89-293.

Higgins RP, Kristensen RM. 1988. Kinorhyncha from Disko Island, west Greenland. *Smithsonian Contributions to Zoology* **438**: 1-70. https://doi.org/10.5479/si.00810282.458.

Higgins RP, Shirayama Y. 1990. Dracoderidae, a new family of the cyclorhagid Kinorhyncha from the Inland Sea of Japan. *Zoological Science* **7**: 939-946.

Higgins RP, Thiel H. 1988. *Introduction to the study of meiofauna*. Smithsonian Institution Press, Washington D.C. 1st ed., 488 pp.

Ho CK, Pennings SC, Carefoot TH. 2009. Is diet quality an overlooked mechanism for Bergmann's rule? *The American Naturalist* **175**: 269-276. https://doi.org/10.1086/649583.

Hua E, Zhang ZN, Yu ZS, Zhang Y. 2010. Preliminary study on the immediate response of the nematode community to typhoon Soudelor. *Deep-sea Research Part II: Topical Studies in Oceanography* **57**: 1064-1070. https://doi.org/10.1016/j.dsr2.2010.02.008.

Hummon WD. 1975. Respiratory and osmoregulatory physiology of a meiobenthic marine gastrotrich, *Turbanella ocellata* Hummon, 1974. *Cahiers de Biologie Marine* **16**: 255-268.

Huston MA, Wolverton S. 2011. Regulation of animal size by eNPP, Bergmann's rule and related phenomena. *Ecological Monographs* **81**: 349-405. https://doi.org/10.1890/10-1523.1.

Huys R, Coomans A. 1989. *Echinoderes higginsi* n. sp. (Kinorhyncha, Cyclorhagida) from the southern North Sea with a key to the genus *Echinoderes* Claparède. *Zoologica Scripta* **18(2)**: 211-221. https://doi.org/ 10.1111/j.1463-6409.1989.tb00446.x.

Janssen A, Kaiser S, Meiβner K, Brenke N, Menot L, Martínez-Arbizu P. 2015. A reverse taxonomic approach to assess macrofaunal distribution patterns in abyssal Pacific polymetallic nodule fields. *PLoS ONE* **10**: e0117790. https://doi.org/10.1371/journal.pone.0117790.

Jensen P. 1983. Meiofaunal abundance and vertical zonation in a sublittoral soft bottom, with a test of the Haps corer. *Marine Biology* **74**: 319-326. https://doi.org/10.1007/BF00403458.

Jeuniaux C. 1975. Principes de systématique biochimique et application a quelques problems particuliers concernant les Aschelminthes, les polychétes et les tardigrades. *Cahiers de Biologie Marine* **16**: 597-612.

Jones DO, Yool A, Wei CL, Henson SA, Ruhl HA, Watson RA, *et al*. 2014. Global reductions in seafloor biomass in response to climate change. *Global Change Biology* **20(6):** 1861-1872. https://doi.org/10.1111/gcb.12480.

Karling TG. 1955. *Echinoderes levanderi* n. sp. (Kinorhyncha) aus der Ostsee. *Arkiv för Zoologi* **7(10)**: 189-192.

Kingsolver JG, Huey RB. 2008. Size, temperature, and fitness: three rules. *Evolutionary Ecology Research* **10(2)**: 251-268.

Kirsteuer E. 1964. Zur Kenntnis der Kinorhynchen Venezuelas. *Zoologischer Anzeiger* **173**: 388-393.

Knowlton N. 2000. Molecular genetic analyses of species boundaries in the sea. *Hydrobiologia* **420**: 73-90. https://doi.org/10.1023/A:1003933603879.

Kozloff EN. 1972. Some aspects of development in *Echinoderes* (Kinorhyncha). *Transactions of the American Microscopical Society* **91(2)**: 119-130.

Kozloff EN. 2007. Stages of development, from first cleavage to hatching, of an *Echinoderes* (phylum Kinorhyncha: class Cyclorhagida). *Cahiers de Biologie Marine* **48**: 199-206.

Kristensen RM, Hay-Schmidt A. 1989. The protonephridia of the arctic kinorhynch *Equinoderes aquilonius* (Cyclorhagida, Echinoderidae). *Acta Zoologica* **70**: 13-27.

Kristensen RM, Higgins RP. 1991. Kinorhyncha. In: Harrison FW, Ruppert EE (eds.) *Microscopic anatomy of invertebrates, Volume 4: Aschelmintes.* Wiley-Liss Press, New York. pp. 377-404.

Kumar A. 2017. Foreword. In: Joseph A (ed.) *Investigating Seafloors and Oceans, from Mud Volcanoes to Giant Squid.* Elsevier, Amsterdam, pp. 9-26.

Landers SC, Bassham RD, Miller JM, Ingels J, Sánchez N, Sørensen MV. 2020. Kinorhynch communities from Alabama coastal waters. *Marine Biology Research* **16(6&7)**: 494-505. https://doi.org/10.1080/17451000.2020.1789660.

Landers SC, Sørensen MV. 2016. Two new species of *Echinoderes* (Kinorhyncha, Cyclorhagida), *E. romanoi* sp. n. and *E. joyceae* sp. n., from the Gulf of Mexico. *ZooKeys* **594**: 51-71. https://doi.org/10.3897/zookeys.594.8623.

Landers SC, Sørensen MV. 2018. *Echinoderes sylviae* n. sp. (Kinorhyncha, Cyclorhagida) from the Gulf of Mexico, with comparative notes on a similar species *E. spinifurca*. *Bulletin of Marine Science* **94(4)**: 1499-1514. https://doi.org/10.5343/bms.2017.1167.

Landers SC, Sørensen MV, Beaton KR, Jones CM, Miller JM, Stewart PM. 2018. Kinorhynch assemblages in the Gulf of Mexico continental shelf collected during a two-year survey. *Journal of Experimental Marine Biology and Ecology* **502**: 81-90. https://doi.org/10.1016/j.jembe.2017.05.013.

Landers SC, Sørensen MV, Sánchez N, Beaton KR, Miller JM, Ingels J. 2019. Kinorhynch communities on the Louisiana continental shelf. *Proceedings of the Biological Society of Washington* **132(1)**: 1-14. https://doi.org/10.2988/18-00008.

Lang K. 1963. The relation between the Kinorhyncha and Priapulida and their connection with the Aschelmintes. In: Dougherty EC (ed.) *The lower Metazoa. Comparative biology and phylogeny*. University of California Press, Berkeley, pp. 256-262.

Lee HJ, Gerdes D, Vanhove S, Vincx M. 2001a. Meiofauna response to iceberg disturbance on the Antarctic continental shelf at Kapp Norvegia (Eweddell Sea). *Polar Biology* **24**: 926-933. https://doi.org/10.1007/s003000100301.

Lee HJ, Vanhove S, Peck LS, Vincx M. 2001b. Recolonisation of meiofauna after catastrophic iceberg scouring in shallow Antarctic sediments. *Polar Biology* **24**: 918-925. https://doi.org/10.1007/s003000100300.

Lemburg C. 2002. A new kinorhynch *Pycnophyes australensis* sp. n. (Kinorhyncha: Homalorhagida: Pycnophyidae) from Magnetic Island, Australia. *Zoologischer Anzeiger* **241(2)**: 173-189. https://doi.org/10.1078/S0044-5231(04)70072-8.

Lemenkova P. 2020. Geomorphology of the Puerto Rico Trench and Cayman Through in the context of the geological evolution of the Caribbean Sea. *Annales Universitatis Mariae Curie-Sklodowska Sectio B – Geographia Geologia Mineralogia et Petrographia* **75**: 115-141. https://doi.org/10.17951/b.2020.75.115-141.

Levin IA. 2005. Ecology of cold seep sediments: interactions of fauna with flow, chemistry and microbes. *Oceanography and Marine Biology* **43**: 1-46. https://doi.org/10.1201/9781420037449-3.

Levinton JS. 2017. Benthic life habitats. In: Levinton JS (ed.) *Marine Biology: Function, Biodiversity, Ecology*. Oxford University Press, Oxford, pp. 245-267.

Lundbye H, Rho HS, Sørensen MV. 2011. *Echinoderes rex* n. sp. (Kinorhyncha: Cyclorhagida), the largest *Echinoderes* species found so far. *Scientia Marina* **75(1)**: 41-51. https://doi.org/10.3989/scimar.2011.75n1041.

Lysykh NM. 2005. The taxonomic composition and quantitative development of the soft bottom meiobenthos under mariculture of *Mytilus galloprovincialis* Lam., 1819 (the Black Sea). *Morskoj Ekologiceskij Zhurnal* **4(1)**: 61-68.

Mammola S, Cardoso P, Culver DC, Deharveng L, Ferreira R, Fiŝer C, *et al*. 2019. Scientists' warning on the conservation of subterranean ecosystems. *BioScience* **69(8)**: 641-650. https://doi.org/ 10.1093/biosci/biz064.

Marchese C. 2015. Biodiversity hotspots: a shortcut for a more complicated concept. *Global Ecology and Conservation* **3**: 297-309. https://doi.org/10.1016/j.gecco.2014.12.008.

Margulis L, Chapman M. 2009. *Kingdoms and Domains: An Illustrated Guide to the Phyla of Life on Earth.* Academic Press, Boston. 1st ed., 659 pp.

Martens PM, Schockaert ER. 1986. The importance of turbellarians in the marine meiobenthos: a review. *Hydrobiologia* **132**: 295-303.

Martínez A, Fontaneto D. 2018. Global correlates of diversity in aquatic subterranean fauna. *ARPHA Conference Abstracts* **1:** e29513. https://doi.org/10.3897/aca.1.e29513.

Martorelli S, Higgins RP. 2004. Kinorhyncha from the stomach of the shrimp *Pleoticus muelleri* (Bate, 1888) from Comodoro Rivadavia, Argentina. *Zoologischer Anzeiger* **243(1&2)**: 85-98. https://doi.org/10.1016/j.jcz.2004.07.003.

McCave I, Hall IR. 2006. Size sorting in marine muds: processes, pitfalls, and prospects for paleoflow-speed proxies. *Geochemistry, Geophysics, Geosystems* **7(10)**: eQ10N05. https://doi.org/10.1029/2006GC001284.

McClain C, Hardy SM. 2010. The dynamics of biogeographic ranges in the deep-sea. *Proceedings of the Royal Society B Biological Sciences* **277(1700)**: e1057. https://doi.org/10.1098/rspb.2010.1057.

McClain CR, Rex M. 2001. The relationship between dissolved oxygen concentration and maximum size in deep-sea turrid gastropods: an application of quantile regression. *Marine Biology* **139**: 681-685. https://doi.org/10.1007/s002270100617.

McCormack SA, Trebilco R, Melbourne-Thomas J, Blanchard JL, Fulton EA, Constable A. 2019. Using stable isotope data to advance marine food web modelling. *Reviews in Fish Biology and Fisheries* **29**: 277-296. https://doi.org/10.1007/s11160-019-09552-4.

McCosker JE, Dawson CE. 1975. Biotic passage through the Panama Canal, with particular reference to fishes. *Marine Biology* **30**: 343-351. https://doi.org/10.1007/BF00390639.

McCullagh P, Nelder JA. 1989. *Generalized Linear Models*. London: Chapman & Hall/CRC Press.

McDowall RM. 2007. Jordan's and other ecogeographical rules, and the vertebral number in fishes. *Journal of Biogeography* **35(3)**: 501-508. https://doi.org/10.1111/j.1365-2699.2007.01823.x.

Menzies RJ. 1968. Transport of marine life between oceans through the Panama Canal. *Nature* **220**: 802-803. https://doi.org/10.1038/220802a0.

Miloslavich P, Díaz JM, Klein E, Alvarado JJ, Díaz C, Gobin J, *et al.* 2010. Marine biodiversity in the Caribbean: regional estimates and distribution patterns. *PLoS ONE* **5(8)**: e0011916. https://doi.org/10.1371/journal.pone.0011916.

Miloslavich P, Klein E, Díaz JM, Hernández CE, Bigatti G, Campos L, *et al.* 2011. Marine biodiversity in the Atlantic and Pacific Coasts of South America: knowledge and gaps. *PLoS ONE* **6**: e14631. https://doi.org/10.1371/journal.pone.0014631.

Mittermeier RA, Robles-Gil P, Hoffmann M, Pilgrim J, Brooks T, Mittermeier CG, *et al*. 2004. *Hotspots revisited: Earth's biologically richest and most endangered terrestrial ecoregions.* CEMEX, Mexico City.

Modig H, Ólafsson E. 1998. Responses of Baltic benthic invertebrates to hypoxic events. *Journal of Experimental Marine Biology and Ecology* **229**: 133-148. s://doi.org/10.1016/S0022-0981(98)00043-4.

Moran AL, Woods HA. 2012. Why might they be giants? Towards an understanding of polar gigantism. *The Journal of Experimental Biology* **215**: 1995-2002. https://doi.org/10.1242/jeb.067066.

Moritz K, Storch V. 1972. Über den ultrastrukturellen Bau der Skaliden von *Trachydemus giganteus* (Kinorhyncha). *Marine Biology* **16(1):** 81-89. https://doi.org/10.1007/BF00347852.

Mullineaux LS, Le Bris N, Mills SW, Henri P, Bayer SR, Scrist RG, *et al*. 2012. Detecting the influence of initial pioneers on succession at deep-sea vents. *PLoS ONE* **7**: e50015. https://doi.org/10.1371/journal.pone.0050015.

Murrell MC, Fleeger JW. 1989. Meiofauna abundance on the Gulf of Mexico continental shelf affected by hypoxia. *Continental Shelf Research* **9(12)**: 1049-1062. https://doi.org/10.1016/0278-4343(89)90057-5.

Müller MCM, Schmidt-Rhaesa A. 2003. Reconstruction of the muscle system in *Antygomonas* sp. (Kinorhyncha, Cyclorhagida) by means of phalloidin labelling and CLSM. *Journal of Morphology* **256(2)**: 103-110. https://doi.org/10.1002/jmor.10058.

Mustafa S, Kharudin SN, Kian AYS. 2015.Effect of simulated ocean acidification on chitin content in the shell of white shrimp *Litopenaeus vannamei*. *Iran Journal of Fisheries Sciences* **9**: 6-9.

Myers N, Mittermeier RA, Mittermeier CG, Da Fonseca GA, Kent J. 2000. Biodiversity hotspots for conservation priorities. *Nature* **403**: 853-858. https://doi.org/10.1038/35002501.

Nascimento FJA, Karlson AML, Elmgren R. 2008. Settling blooms of filamentous cyanobacteria as food for meiofauna assemblages. *Limnology and Oceanography* **53(6)**: 2636-2643. https://doi.org/10.4319/lo.2008.53.6.2636.

Nebelsick M. 1990. *Antygomonas incomitata* gen. et sp. n. (Cyclorhagida, Kinorhyncha) and its phylogenetic relationships. *Zoologica Scripta* **19(2):** 143-152. https://doi.org/10.1111/j.1463-6409.1990.tb00248.x.

Nebelsick M. 1992. Ultrastructural investigations of three taxonomic characters in the trunk region of *Echinoderes capitatus* (Kinorhyncha, Cyclorhagida). *Zoologica Scripta* **21(4):** 335-345. https://doi.org/10.1111/j.1463-6409.1992.tb00335.x.

Nebelsick M. 1993. Introvert, mouth cone, and nervous system of *Echinoderes capitatus* (Kinorhyncha, Cyclorhagida) and implications for the phylogenetic relationships of Kinorhyncha. *Zoomorphology* **113**: 211-232. https://doi.org/10.1007/BF00403313.

Neuhaus B. 1988. Ultrastructure of protonephridia in *Pycnophyes kielensis* (Kinorhyncha, Homalorhagida). *Zoomorphology* **108**: 245-253. https://doi.org/10.1007/BF00312224.

Neuhaus B. 1991. *Zur Ultrastruktur, Postembryonalentwicklung und phylogenetischen Verwandtschaft der Kinorhyncha*. Ph.D. Thesis, University of Göttingen, 190 pp.

Neuhaus B. 1993. Postembryonic development of *Pycnophyes kielensis* and *P. dentatus* (Kinorhyncha) from the North Sea. *Microfauna Marina* **8**: 163-193.

Neuhaus B. 1994. Ultrastructure of alimentary canal and body cavity, ground pattern, and phylogenetic relationships of the Kinorhyncha. *Microfauna Marina* **9**: 61-156.

Neuhaus B. 1995. Postembryonic development of *Paracentrophyes praedictus* (Homalorhagida): neoteny questionable among the Kinorhyncha. *Zoologica Scripta* **24(3)**: 179-192.

Neuhaus B. 1997. Ultrastructure of head sensory organs in *Pycnophyes kielensis* and *P. dentatus* (Homalorhagida, Kinorhyncha). *Zoomorphology* **117**: 33-40.

Neuhaus B. 2013. Kinorhyncha (=Echinodera). In: Schmidt-Rhaesa A (ed.) *Handbook of Zoology, Gastrotricha, Cycloneuralia and Gnathifera, Volume 1: Nematomorpha, Priapula, Kinorhyncha, Loricifera*. De Gruyter, Hamburg. pp. 181-348.

Neuhaus B. 2017. Redescription of *Tubulideres seminoli* Sørensen *et al.*, 2017, and notes on *Wollunquaderes majkenae* Sørensen and Thormar, 2010 (Kinorhyncha, Cyclorhagida): morphology, postembryonic development, life cycle and new characters. *Zoologischer Anzeiger* **270**: 123-154. https://doi.org/10.1016/j.jcz.2017.09.004.

Neuhaus B. 2021. World Kinorhyncha Database [Accessed at http://www.marinespecies.org/kinorhyncha on 2021-04-09]. https://doi.org/10.14284/457.

Neuhaus B, Blasche T. 2006. *Fissuroderes*, a new genus of Kinorhyncha (Cyclorhagida) from the deep-sea and continental shelf of New Zealand and from the continental shelf of Costa Rica. *Zoologischer Anzeiger* **245**: 19-52. https://doi.org/10.1016/j.jcz.2006.03.003-

Neuhaus B, Higgins RP. 2002. Ultrastructure, biology, and phylogenetic relationships of Kinorhyncha. *Integrative and Comparative Biology* **42**: 619-632. https://doi.org/10.1093/icb/42.3.619.

Neuhaus B, Kegel A. 2015. Redescription of *Cateria gerlachi* (Kinorhyncha, Cyclorhagida) from Sri Lanka and of *C. styx* from Brazil, with notes on *C. gerlachi* from India and *C. styx* from Chile, and the ground pattern of the genus. *Zootaxa* **3965**: 1-77. https://doi.org/10.11646/zootaxa.3965.1.1.

Neuhaus B, Pardos F, Sørensen MV, Higgins RP. 2014. New species of *Centroderes* (Kinorhyncha: Cyclorhagida) from the Northwest Atlantic Ocean, life cycle, and ground pattern of the genus. *Zootaxa* **3901(1)**: 1-69. https:/doi.org/10.11646/zootaxa.3901.1.1.

Neuhaus B, Sørensen MV. 2013. Populations of *Campyloderes* sp. (Kinorhyncha, Cyclorhagida): One global species with significant morphological variation? *Zoologischer Anzeiger* **252**: 48-75. https://doi.org/10.1016/j.jcz.2012.03.002.

Neves R, Sørensen MV, Herranz M. 2016. First account on kinorhynchs from Portugal, with the description of two new species: *Echinoderes lusitanicus* sp. nov. and *E. reicherti* sp. nov. *Marine Biology Research* **12(5)**: 455-470. https://doi.org/10.1080/17451000.2016.1154973.

Nicholls AG. 1935. Copepods from the interstitial fauna of a sandy beach. *Journal of the Marine Biological Association of the United Kingdom* **20**: 379-405. https://doi.org/10.1017/S0025315400045306.

Nyholm KG. 1947. Studies in the Echinoderida. *Arkiv för Zoologi* **39A(14)**: 1-36.

Nyholm KG. 1976. Ultrastructure of the spermatozoa in Homalorhaga Kinorhyncha. *Zoon* **4**: 11-18.

Nyholm KG, Nyholm PG. 1976a. Ultrastructure of the pharyngeal muscles of Homalorhaga Kinorhyncha. *Zoon* **4**: 121-130.

Nyholm KG, Nyholm PG. 1976b. Z-bodies and supercontraction in the integumental muscles of homalorhaga Kinorhyncha. *Zoon* **4**: 131-136.

Nyholm KG, Nyholm PG. 1982. Spermatozoa and spermatogenesis in Homalorhaga Kinorhyncha. *Journal of Ultrastructure Research* **78(1):** 1-12.

Oey LY, Ezer T, Lee HC. 2005. Loop current, rings and related circulation in the Gulf of Mexico: a review of numerical models and future challenges. *Geophysical Monograph Series* **161**: 31-56. https://doi.org/10.1029/161GM04.

Ostmann A, Nordhaus I, Sørensen MV. 2012. First recording of kinorhynchs from Java, with the description of a new brackish water species from a mangrove-fringed lagoon. *Marine Biodiversity* **42**: 79-91. https://doi.org/10.1007/s12526-011-0094-z.

Palmer MA, Strayer DL. 1996. Meiofauna. In: Hauer RR, Lamberti GA (eds.) *Methods in stream ecology*. Elsevier, Amsterdam. pp. 315-337.

Pardos F, Herranz M, Sánchez N. 2016b. Two sides of a coin: the phylum Kinorhyncha in Panama. II) Pacific Panama. *Zoologischer Anzeiger* **265**: 26-47. https://doi.org/10.1016/j.jcz.2016.06.006.

Pardos F, Higgins RP, Benito J. 1998. Two new *Echinoderes* (Kinorhyncha, Cyclorhagida) from Spain, including a reevaluation of kinorhynch taxonomic characters. *Zoologischer Anzeiger* **237**: 195-208. https://doi.org/ 10.1016/j.jcz.2007.07.001.

Pardos F, Sánchez N, Herranz M. 2016a. Two sides of a coin: the phylum Kinorhyncha in Panama. I) Caribbean Panama. *Zoologischer Anzeiger* **265**: 3-25. https://doi.org/10.1016/j.jcz.2016.06.005.

Partridge L, Coyne LA. 1997. Bergmann's rule in ectotherms: is it adaptive? *Evolution* **51**: 632-635.

Pastor L, Brandily C, Schmidt S, Miramontes E, Péron M, Apperé D, *et al*. 2020. Modern sedimentation and geochemical imprints in sediments from the NW Madagascar margin. *Marine Geology* **426**: e106184. https://doi.org/10.1016/j.margeo.2020.106184.

Peters RH. 1983. *The Ecological Implications of Body Size*. Cambridge University Press, Cambridge. 1st ed., 65 pp.

Pinto AP, Mejdalani G, Mounce R, Silveira LF, Marinoni L, Rafael JA. 2021. Are publications on zoological taxonomy under attack? *Royal Society Open Science* **8(2)**: online first. https://doi.org/10.1098/rsos.201617.

R Core Team. 2021. R: a language and environment for statistical computing. Vienna: R Foundation for Statistical Computing [Accessed at http://www.R-project.org/ on 2021-04-14].

Ramírez-Llodra E, Brandt A, Danovaro R, De Mol B, Escobar E, German CR, *et al*. 2010. Deep, diverse and definitely different: unique attributes of the world's largest ecosystem. *Biogeosciences* **7**: 2851-2899. https://doi.org/10.5194/bg-7-2851-2010.

Ramírez-Ponce A, Garfias-Lozano G, Contreras-Ramos A. 2017. The nature of allometry in an exaggerated trait: the postocular flange in *Platyneuromus* Weele (Insecta: Megaloptera). *PLoS ONE* **12**: e0172388. https://doi.org/10.1371/journal.pone.0172388.

Reimer L. 1963. Zur Verbreitung der Kinorhyncha in der mittleren Ostsee. *Zoologischer Anzeiger* **171(11/12)**: 440-447.

Reinhard W. 1881. Über *Echinoderes* und *Demoscolex* der Umgegend von Odessa. *Zoologischer Anzeiger* **4(97)**: 588-592.

Reinhard W. 1885. Kinorhyncha (*Echinoderes*), leur structure anatomique et leur place dans le système. *Travaux de la Société des naturalistes à l'Université Impériale de Kharkow* **19:** 205-305.

Remane A. 1940. Einführung in die zoologische Ökologie der Nordund Ostsee, Volume 1a. In: Grimpe G, Wagler E (eds.) *Die Tierwelt der Nord- und Ostsee.* Akademische Verlagsgesellschaft, Leipzig. pp. 1-238.

Rex MA, Crame JA, Stuart CT, Clarke A. 2005. Large-scale biogeographic patterns in marine mollusks: a confluence of history and productivity? *Ecology* **86**: 2288-2297. https://doi.org/10.1890/04-1056.

Ritt B, Pierre C, Gauthier O, Wenzhöfer F, Boetius A, Sarrazin J. 2011. Diversity and distribution of cold-seep fauna associated with different geological and environmental

settings at mud volcanoes and pockmarks of the Nile deep-sea fan. *Marine Biology* **158**: 1187-1210. https://doi.org/10.1007/s00227-011-1679-6.

Rothe BH, Schmidt-Rhaesa A. 2004. Probable development from continuous to segmental longitudinal musculature in *Pycnophyes kielensis* (Kinorhyncha, Homalorhagida). *Meiofauna Marina* **13**: 21-28.

Roy K, Jablonski D, Valentine JW, Rosenberg G. 1998. Marine latitudinal diversity gradients: tests of casual hypotheses. *PNAS* **95(7)**: 3699-3702. https://doi.org/10.1073/pnas.95.7.3699.

Saeedi H, Costello MJ, Warren D, Brandt A. 2019. Latitudinal and bathymetrical species richness in the NW Pacific and adjacent Arctic Ocean. *Scientific Reports* **9**: e9303. https://doi.org/10.1038/s41598-019-45813-9.

Saeedi H, Dennis TE, Costello MJ. 2017. Bimodal latitudinal species richness and high endemicity of razor clams (Mollusca). *Journal of Biogeography* **44**: 592-604. https://doi.org/10.1111/jbi.12903.

Sánchez N, García-Herrero Á, García-Gómez G, Pardos F. 2017. A new species of the recently established genus *Setaphyes* (Kinorhyncha, Allomalorhagida) from the Mediterranean with an identification key. *Marine Biology Research* **48(1)**: 249-258. https://doi.org/10.1007/s12526-017-0651-1.

Sánchez N, Herranz M, Benito J, Pardos F. 2012. Kinorhyncha from the Iberian Peninsula: new data from the first intensive sampling campaigns. *Zootaxa* **3402**: 24-44. https://doi.org/10.11646/zootaxa.3402.1.2.

Sánchez N, Herranz M, Benito J, Pardos F. 2014c. *Pycnophyes almansae* sp. nov. And *Pycnophyes lageria* sp. nov., two new homalorhagid kinorhynchs (Kinorhyncha, Homalorhagida) from the Iberian Peninsula, with special focus on introvert features. *Marine Biology Research* **10(1)**: 17-36. https://doi.org/ 10.1080/17451000.2013.793804.

Sánchez N, Martínez A. 2019. Dungeons and dragons: Two new species and records of Kinorhyncha from anchialine cenotes and marine lava tubes. *Zoologischer Anzeiger* **282**: 161-175. https://doi.org/10.1016/j.jcz.2019.05.012.

Sánchez N, Pardos F, Herranz M, Benito J. 2011. *Pycnophyes dolichurus* sp. nov. and *P. aulacodes* sp. nov. (Kinorhyncha, Homalorhagida, Pycnophyidae), two new kinorhynchs

from Spain with a reevaluation of homalorhagid taxonomic characters. *Helgoland Marine Research* **65**: 319-334. https://doi.org/10.1007/s10152-010-0226-z.

Sánchez N, Pardos F, Martínez-Arbizu P. 2019a. Deep-sea Kinorhyncha diversity of the polymetallic nodule fields at the Clarion-Clipperton Fracture Zone (CCZ). *Zoologischer Anzeiger* **282:** 88-105. https://doi.org/10.1016/j.jcz.2019.05.007.

Sánchez N, Pardos F, Sørensen MV. 2014a. A new kinorhynch genus, *Mixtophyes* (Kinorhyncha: Homalorhagida), from the Guinea Basin deep-sea, with new data on the family Neocentrophyidae. *Helgoland Marine Research* **68**: 221-239. https://doi.org/10.1007/s10152-014-0383-6.

Sánchez N, Pardos F, Sørensen MV. 2014b. Deep-sea Kinorhyncha: two new species from the Guinea Basin, with evaluation of an unusual male feature. *Organisms Diversity and Evolution* **14**: 349-361. https://doi.org/10.1007/s13127-014-0182-6.

Sánchez N, Rho HS, Min WG, Kim D, Sørensen MV. 2013. Four new species of *Pycnophyes* (Kinorhyncha: Homalorhagida) from Korea and the East China Sea. *Scientia Marina* **77(2)**: 353-380.

Sánchez N, Sørensen MV, Landers SC. 2019b. Pycnophyidae (Kinorhyncha: Allomalorhagida) from the Gulf of Mexico: *Fujuriphyes viserioni* sp. nov. and a redescription of *Leiocanthus langi* (Higgins, 1964), with notes on its intraspecific variation. *Marine Biodiversity* **49(4)**: 1857-1875. https://doi.org/10.1007/s12526-019-00947-x.

Sánchez N, Yamasaki H. 2016. Two new Pycnophyidae species (Kinorhyncha: Allomalorhagida) from Japan lacking ventral tubes in males. *Zoologischer Anzeiger* **265**: 80-89. https://doi.org/10.1016/j.jcz.2016.04.001.

Sánchez N, Yamasaki H, Pardos F, Sørensen MV, Martínez A. 2016. Morphology disentangles the systematics of a ubiquitous but elusive meiofaunal group (Kinorhyncha: Pycnophyidae). *Cladistics* **32(5)**: 479-505. https://doi.org/10.1111/cla.12143.

Sánchez N, Zeppilli D, Baldrighi E, Vanreusel A, Lahitsiresy MS, Brandily C, *et al.* 2021. A threefold perspective on the role of a pockmark in benthic faunal communities and biodiversity patterns. *Deep-sea Research Part I Oceanographic Research Papers* **167**: e013425. https://doi.org/10.1016/j.dsr.2020.103425.

Santos PJP, Botter-Carvalho M, Do Nascimento AB, Marinho JR, Carvalho PVVC, Valebça, APMC. 2009. Response of estuarine meiofauna assemblage to effects of fertilizer enrichment in the sugar cane monoculture, Pernambuco, Brazil. *Brazilian Journal of Oceanography* **57(1)**: 43-55. http://dx.doi.org/10.1590/S1679-87592009000100005.

Schmidt-Rhaesa A, Rothe BH. 2006. Postembryonic development of dorsoventral and longitudinal musculature in *Pycnophyes kielensis* (Kinorhyncha, Homalorhagida). *Integrative and Comparative Biology* **46**: 155-150. https://doi.org/10.1093/icb/icj019.

Seibold E, Berger WH. 1993. *The sea floor – An introduction to marine geology*. Springer, Berlin. 2nd ed., 356 pp. https://doi.org/10.1007/978-3-662-22519-6.

Sergeeva NG, Gooday AJ, Mazlumyan SA. Kolesnikova EA, Lichtschlag A, Kosheleva TN, *et al*. 2012. Meiobenthos of the oxic/anoxic interface in the southwestern region of the Black Sea: abundance and taxonomic composition. *Cellular Origin, Life in Extreme Habitats and Astrobiology* **21(5)**: 369-401.

Sheremetevskij AM. 1974. Kinorhyncha of the Black Sea. *Zoologichesky Zhurnal* **53(7)**: 974-987.

Shingleton A. 2010. Allometry: the study of biological scaling. *Nature Education Knowledge* **3(10)**: e2.

Sibly RM, Atkinson D. 1994. How rearing temperatures affects optimal adult size in ectotherms. *Functional Ecology* **8**: 486-493. https://doi.org/10.2307/2390073.

Smith KF, Brown JH. 2002. Patterns of diversity, depth range and body size among pelagic fishes along a gradient of depth. *Global Ecology and Biogeography* **11**: 313-322. https://doi.org/10.1046/j.1466-822X.2002.00286.x.

Snelgrove PVR. 1997. The importance of marine sediment biodiversity in ecosystem processes. *Ambio* **26(8)**: 578-583.

Song YH, Chang CY. 2001. First record of *Campyloderes macquariae* Johnston (Kinorhyncha, Cyclorhagida, Centroderidae) from the North Pacific. *Korean Journal of Systematic Zoology* **17**: 207-216.

Sørensen MV. 2006. New kinorhynchs from Panama, with a discussion of some phylogenetically significant cuticular structures. *Meiofauna Marina* **15**: 51-77.

Sørensen MV. 2007. A new species of *Antygomonas* (Kinorhyncha: Cyclorhagida) from the Atlantic coast of Florida, U.S.A. *Cahiers de Biologie Marine* **48**: 155-168.

Sørensen MV. 2008a. A new kinorhynch genus from the Antarctic deep-sea and a new species of *Cephalorhyncha* from Hawaii (Kinorhyncha: Cyclorhagida: Echinoderidae). *Organisms Diversity and Evolution* **8**: 1-18. https://doi.org/10.1016/j.ode.2007.11.003.

Sørensen MV. 2008b. Phylogenetic analysis of the Echinoderidae (Kinorhyncha: Cyclorhagida). *Organisms Diversity and Evolution* **8(3)**: 233-246. https://doi.org/10.1016/j.ode.2007.11.002.

Sørensen MV. 2014. First account of echinoderid kinorhynchs from Brazil, with the description of three new species. *Marine Biodiversity* **44(3)**: 251-274. https://doi.org/10.1007/s12526-013-0181-4.

Sørensen MV, Accogli G, Hansen JG. 2010d. Postembryonic development of *Antygomonas incomitata* (Kinorhyncha: Cyclorhagida). *The Journal of Morphology* **271**: 863-882. https://doi.org/10.1002/jmor.10844.

Sørensen MV, Dal Zotto M, Rho HS, Herranz M, Sánchez N, Pardos F, *et al*. 2015. Phylogeny of Kinorhyncha based on morphology and two molecular loci. *PLoS ONE* **10(7)**: e0133440. https://doi.org/10.1371/journal.pone.0133440.

Sørensen MV, Grzelak K. 2018. New mud dragons from Svalbard: three new species of *Cristaphyes* and the first Arctic species of *Pycnophyes* (Kinorhyncha: Allomalorhagida: Pycnophyidae). *PeerJ* **6**: e5653. https://doi.org/10.7717/peerj.5653.

Sørensen MV, Heiner I, Ziemer O. 2005. A new species of *Echinoderes* from Florida (Kinorhyncha: Cyclorhagida). *Proceedings of the Biological Society of Washington* **118(3)**: 499-508. https://doi.org/ 10.2988/0006-324X(2005)118[499:ANSOEF]2.0.CO;2.

Sørensen MV, Heiner I, Ziemer O, Neuhaus B. 2007. *Tubulideres seminoli* gen. et sp. nov. and *Zelinkaderes brightae* sp. nov. (Kinorhyncha, Cyclorhagida) from Florida. *Helgoland Marine Research* **61**: 247-265. https://doi.org/ 10.1007/s10152-007-0073-8.

Sørensen MV, Herranz M, Landers SC. 2016. A new species of *Echinoderes* (Kinorhyncha: Cyclorhagida) from the Gulf of Mexico, with a redescription of *E.*

bookhouti Higgins, 1964. *Zoologischer Anzeiger* **265**: 48-68. https://doi.org/10.1016/j.jcz.2016.04.004.

Sørensen MV, Herranz M, Rho HS, Min WG, Yamasaki H, Sánchez N, *et al*. 2012a. On the genus *Dracoderes* Higgins and Shirayama, 1990 (Kinorhyncha: Cyclorhagida) with a redescription of its type species, *D. abei*, and a description of a new species from Spain. *Marine Biology Research* **8**: 210-232. https://doi.org/10.1080/17451000.2011.615328.

Sørensen MV, Jorgensen A, Boesgaard TM. 2000. A new *Echinoderes* (Kinorhyncha: Cyclorhagida) from a submarine cave in New South Wales, Australia. *Cahiers de Biologie Marine* **41**: 167-179.

Sørensen MV, Landers SC. 2014. Two new species of *Echinoderes* (Kinorhyncha: Cyclorhagida) from the Gulf of Mexico. *Frontiers in Marine Science* **1**: e8. https://doi.org/10.3389/fmars.2014.00008.

Sørensen MV, Landers SC. 2017a. Description of a new kinorhynch species, *Paracentrophyes sanchezae* n. sp. (Kinorhyncha: Allomalorhagida) from the Gulf of Mexico, with differential notes on one additional, yet undescribed species of the genus. *Zootaxa* **4242(1)**: 61-76. http://dx.doi.org/10.11646/zootaxa.4242.1.3.

Sørensen MV, Landers SC. 2017b. New species of Semnoderidae (Kinorhyncha: Cyclorhagida: Kentrorhagata) from the Gulf of Mexico. *Marine Biodiversity* **48(7)**: 1-29. https://doi.org/10.1007/s12526-017-0728-x.

Sørensen MV, Landers SC. 2018. New species of Semnoderidae (Kinorhyncha: Cyclorhagida: Kentrorhagata) from the Gulf of Mexico. *Marine Biodiversity* **48(1)**: 327-355. https://doi.org/10.1007/s12526-017-0728-x.

Sørensen MV, Pardos F. 2008. Kinorhynch systematics and biology – An introduction to the study of kinorhynchs, inclusive identification keys to the genera. *Meiofauna Marina* **16**: 21–73.

Sørensen MV, Pardos F. 2020. Kinorhyncha. In: Schmidt-Rhaesa A (ed.) *Guide to the Identification of Marine Meiofauna.* Verlag Dr. Friedrich Pfeil, Munich. pp. 391-414.

Sørensen MV, Pardos F, Herranz M, Rho HS. 2010a. New data on the genus *Paracentrophyes* (Homalorhagida, Kinorhyncha), with the description of a new species

from the west Pacific. *The Open Zoology Journal* **3**: 42-59. https://doi.org/ 10.2174/1874336601003010042.

Sørensen MV, Rho HS. 2009. *Triodontoderes anulap* gen. nov. et sp. nov. – a new cyclorhagid kinorhynch genus and species from Micronesia. *Journal of the Marine Biological Association of the United Kingdom* **89(6)**: 1269-1279. https://doi.org/10.1017/S0025315409000526.

Sørensen MV, Rho HS, Kim D. 2010b. A new species of *Condyloderes* (Cyclorhagida, Kinorhyncha) from Korea. *Zoological Science* **27**: 234-242. https://doi.org/ 10.2108/zsj.27.234.

Sørensen MV, Rho HS, Kim D. 2010c. A new species of the rare genus *Sphenoderes* (Cyclorhagida, Kinorhyncha), with differential notes on *S. indicus* Higgins, 1969. *Marine Biology Research* **6**: 472-484. https://doi.org/ 10.1080/17451000903334702.

Sørensen MV, Rho HS, Min WG, Kim D, Chang CY. 2012b. An exploration of *Echinoderes* (Kinorhyncha: Cyclorhagida) in Korean and neighbouring waters, with the description of four new species and a redescription of *E. tchenfouensis* Lou, 1934.*Zootaxa* **3368**: 161-196. http://dx.doi.org/10.11646/zootaxa.3368.1.8.

Sørensen MV, Rho HS, Min WG, Kim D, Chang SY. 2013. Occurrence of the newly described kinorhynch genus *Meristoderes* (Cyclorhagida: Echinoderidae) in Korea, with the description of four new species. *Helgoland Marine Research* **67(2)**: 291-319. https://doi.org/10.1007/s10152-012-0323-2.

Sørensen MV, Rohal M, Thistle D. 2018. Deep-sea Echinoderidae (Kinorhyncha: Cyclorhagida) from the Northwest Pacific. *European Journal of Taxonomy* **456**: 1-75. https://doi.org/10.5852/ejt.2018.456.

Sørensen MV, Thistle D, Landers SC. 2019. North American *Condyloderes* (Kinorhyncha: Cyclorhagida: Kentrorhagata): Female dimorphism suggests moulting among adult *Condyloderes*. *Zoologischer Anzeiger* **282**: 232-251. https:doi.org/10.1016/j.jcz.2019.05.015.

Southern R. 1914. Clare Island survey. Nemathelmia, Kinorhyncha, and Chaetognatha. *Proceedings of the Royal Irish Academy* **31(54/3)**: 1-80.

Spalding MD, Fox HE, Allen GR, Davidson N, Ferdaña ZA, Finlayson M, *et al.* 2007. Marine ecoregions of the world: bioregionalization of coastal and shelf areas. *BioScience* **57(7)**: 573-583. https://doi.org/10.1641/B570707.

Stillwell RC. 2010. Are latitudinal clines in body size adaptive? *Oikos* **119**: 1387-1390. https://doi.org/10.1111/j.1600-0706.2010.18670.x.

Sutherland TF, Levings CD, Petersen SA, Poon P, Piercey B. 2007. The use of meiofauna as an indicator of benthic organic enrichment associated with salmonid aquaculture. *Marine Pollution Bulletin* **54**: 1249-1261. https://doi.org/10.1016/j.marpolbul.2007.03.024.

Thistle D, Levin LA. 1998. The effect of experimentally increased near-bottom flow on metazoan meiofauna at a deep-sea site, with comparison data on macrofauna. *Deep-sea Research Part I: Oceanographic Research Papers* **45**: 625-638. https://doi.org/10.1016/S0967-0637(97)00101-5.

Thomsen I, Gust G. 2000. Sediment erosion thresholds and characteristics or re-suspended aggregates on the western European continental margin. *Deep-Sea Research Part I: Oceanographic Research Papers* **47**: 1881-1897. https://doi.org/10.1016/S0967-0637(00)00003-0.

Thorne-Miller B. 1999. *The living ocean: understanding and protecting marine biodiversity*. Island Press, Washington D.C. 1st ed., 240 pp.

Tidière M, Lemaître JF, Pélabon C, Gimenez O, Gaillard JM. 2017. Evolutionary allometry reveals a shift in selection pressure on male horn size. *Journal of Evolutionary Biology* **30:** 1826-1835. https://doi.org/10.1111/jeb.13142.

Tita G, Vincx M, Desrosiers G. 1999. Size spectra, body width and morphotypes of intertidal nematodes: an ecological interpretation. *Journal of the Marine Biological Association of the United Kingdom* **79**: 1007-1015. https://doi.org/10.1017/S0025315499001241.

Tomkins JL, Le Bas NR, Witton MP, Martill DM, Humphries S. 2010. Positive allometry and the prehistory of sexual selection. *The American Naturalist* **176**: 141-148. https://doi.org/10.1086/653001.

Traunspurger W, Majdi N. 2017. Meiofauna. In: Hauer F, Lamberti G (eds.) *Methods in Stream Ecology.* Elsevier, Amsterdam. pp. 273-295. https://doi.org/10.1016/B978-0-12-416558-8.00014-7.

Uozumi R, Yamasaki H, Euichi H. 2018. Mangrove forests may serve as stable environments for the meiobenthic *Echinoderes komatsui* (Kinorhyncha: Cyclorhagida): distribution patterns and population dynamics in a subtropical estuary. *Marine Biology Research* **14(3)**: 321-333. https://doi.org/10.1080/17451000.2017.1408916.

Vakati V, Eyun SI, Lee W. 2019. Unraveling the intricate biodiversity of the benthic harpacticoid genus *Nannopus* (Copepoda, Harpacticoida, Nannopodidae) in Korean waters. *Molecular Phylogenetics and Evolution* **130**: 366-379. https://doi.org/10.1016/j.ympev.2018.10.004.

Van Steenkiste NWL, Herbert ER, Leander BS. 2018. Species diversity in the marine microturbellarian *Astrotorhynchus bifidus* sensu lato (Platyhelminthes: Rhabdocoela) from the northeast Pacific Ocean. *Molecular Phylogenetics and Evolution* **120**: 259-273. https://doi.org/10.1016/j.ympev.2017.12.012.

Vanaberbeke J, Merckx B, Degraer S, Vincx M. 2011. Sediment-related distribution patterns of nematodes and macrofauna: two sides of the benthic coin? *Marine Environmental Research* **71**: 31-40. https://doi.org/10.1016/j.marenvres.2010.09.006.

Vanreusel A, De Groote A, Gollner S, Bright M. 2010. Ecology and biogeography of free-living nematodes associated with chemosynthetic environments in the deep-sea: a review. *PLoS ONE* **5**: e12449. https://doi.org/10.1371/journal.pone.0012449.

Vanreusel A, Fonseca G, Danovaro R, Da Silva MC, Esteves AM, Ferrero T, *et al.* 2009. The contribution of deep-sea macrohabitat heterogeneity to global nematode diversity. *Marine Ecology* **31(1)**: 6-20. https://doi.org/10.1111/j.1439-0485.2009.00352.x.

Varney RM, Funch P, Kocot KM, Sørensen MV. 2019. A new species of *Echinoderes* (Cyclorhagida: Echinoderidae) from the San Juan Islands, Washington State, USA, and insights into the kinorhynch transcriptome. *Zoologischer Anzeiger* **282**: 52-63. https://doi.org/10.1016/j.jcz.2019.06.003.

Walters RJ, Hassall M. 2006. The temperature-size rule in ectotherms: may a general explanation exist after all? *The American Naturalist* **167(4):** 510-523. https://doi.org/10.1086/501029.

Warwick RM, Platt HM, Clarke KR, Agard J, Gobin J. 1990. Analysis of macrobenthic and meiobenthic community structure to pollution and disturbance in Hamilton Harbour, Bermuda. *Journal of Experimental Marine Biology and Ecology* **138**: 119-142. https://doi.org/10.1016/0022-0981(90)90180-K.

Williams GC. 1966. *Adaptation and Natural Selection.* Princeton University Press, Princeton. 1st ed., 308 pp.

Wilson EO. 2004. Taxonomy as a fundamental discipline. *Philosophical Transactions of the Royal Society of London B* **359**: 739. https://doi.org/10.1098/rstb.2003.1440.

Yamasaki H. 2015. Two new species of *Dracoderes* (Kinorhyncha: Dracoderidae) from the Ryukyu Islands, Japan, with a molecular phylogeny of the genus. *Zootaxa* **3980(3)**: 359-378. https://doi.org/10.11646/zootaxa.3980.3.2

Yamasaki H. 2016. *Ryuguderes iejimaensis*, a new genus and species of Campyloderidae (Xenosomata: Cyclorhagida: Kinorhyncha) from a submarine cave in the Ryukyu Islands, Japan. *Zoologischer Anzeiger* **265**: 69-79. https://doi.org/10.1016/j.jcz.2016.02.003.

Yamasaki H. 2019. *Gracilideres mawatarii*, a new genus and species of Franciscideridae (Allomalorhagida: Kinorhyncha) - a kinorhynch with thin body cuticle, adapted to the interstitial environment. *Zoologischer Anzeiger* **282**: 176-188. https://doi.org/10.1016/j.jcz.2019.05.010.

Yamasaki H. 2021. Hiroshi Yamasaki Website. Study of Meiobenthos – Kinorhyncha, Loricifera, Priapulida, etc [Accessed at https://sites.google.com/a/meiobenthos.com/laboratory/home?authuser=0 on 2021-04-14].

Yamasaki H, Durucan F. 2018. *Echinoderes antalyaensis* sp. nov. (Cyclorhagida: Kinorhyncha) from Antalya, Turkey, Levantine Sea, Eastern Mediterranean Sea. *Species Diversity* **23(2):** 193-207. https:/doi.org/10.12782/specdiv.23.193.

Yamasaki H, Fujimoto S. 2014. Two new species in the *Echinoderes coulli* group (Echinoderidae, Cyclorhagida, Kinorhyncha) from the Ryukyu Islands, Japan. *ZooKeys* **382**: 27-52. https://doi.org/10.3897/zookeys.382.6761.

Yamasaki H, Fujimoto S, Tanaka H. 2020. Three new meiobenthic species from a submarine cave in Japan: *Echinoderes gama*, *E. kajiharai* and *E. uozumii* (Kinorhyncha:

Cyclorhagida). *Journal of the Marine Biological Association of the United Kingdom* **100(4)**: 537-558. https://doi.org/10.1017/s0025315420000429.

Yamasaki H, Grzelak K, Sørensen MV, Neuhaus B, George KH. 2018a. *Echinoderes pterus* sp. n. showing a geographically and bathymetrically wide distribution pattern on seamounts and on the deep-sea floor in the Arctic Ocean, Atlantic Ocean, and the Mediterranean Sea (Kinorhyncha, Cyclorhagida). *ZooKeys* **771**: 15-40. https://doi.org/10.3897/zookeys.771.25534.

Yamasaki H, Hiruta SF, Kajihara H. 2013. Molecular phylogeny of kinorhynchs. *Molecular Phylogenetics and Evolution* **67(2)**: 303-310. https://doi.org/10.1016/j.ympev.2013.02.016.

Yamasaki H, Kajihara H. 2012. A new brackish-water species of *Echinoderes* (Kinorhyncha: Cyclorhagida) from the Seto Inland Sea, Japan. *Species Diversity* **17(1)**: 109-118. https://doi.org/10.12782/sd.17.1.109.

Yamasaki H, Kajihara H, Mawatari SF. 2012. First report of kinorhynchs from Hokkaido, Japan, including a new species of *Pycnophyes* (Pycnophyidae: Homalorhagida). *Zootaxa* **3425**: 23-41. http://dx.doi.org/10.11646/zootaxa.3425.1.2.

Yamasaki H, Neuhaus B, George KH. 2018b. New species of *Echinoderes* (Kinorhyncha: Cyclorhagida) from Mediterranean seamounts and from the deep-sea floor in the North-eastern Atlantic Ocean, including notes of two undescribed species. *Zootaxa* **4387:** 541-556. https://doi.org/10.11646/zootaxa.4387.3.8.

Yamasaki H, Neuhaus B, George KH. 2018c. Three new species of Echinoderidae (Kinorhyncha: Cyclorhagida) from two seamounts and the adjacent deep-sea floor in the Northeast Atlantic Ocean. *Cahiers de Biologie Marine* **59**: 79-106. https://doi.org/ 10.21411/CBM.A.124081A9.

Yamasaki H, Neuhaus B, George KH. 2019. Echinoderid mud dragons (Cyclorhagida: Kinorhyncha) from Senghor Seamount (NE Atlantic Ocean) including general discussion of faunistic characters and distribution patterns of seamount kinorhynchs. *Zoologischer Anzeiger* **282**: 64-87. https://doi.org/10.1016/j.jcz.2019.05.018.

Yildiz NÖ, Sørensen MV, Karaytuğ S. 2016. A new species of *Cephalorhyncha* Adrianov, 1999 (Kinorhyncha: Cyclorhagida) from the Aegean Coast of Turkey. *Helgoland Marine Research* **70**: e24. https://doi.org/10.1186/s10152-016-0476-5.

Yushin VV, Adrianov AV, Malakhov VV. 1990. Intracellular procaryotes in gut epithelium of the kinorhynchan *Pycnophyes kielensis* (Kinorhyncha, Homalorhagida). *Proceedings of the Academy of Science of the USSR* **308**: 678-679.

Zelinka K. 1907. Zur Kenntnis der Echinoderen. *Zoologischer Anzeiger* **32**: 130-136.

Zelinka K. 1908. Zur Anatomie der Echinoderen. *Zoologischer Anzeiger* **33**: 629-647.

Zelinka K. 1912. Die Spermatozoen der Echinoderen und ihre Genese. In: Ritter von Stummer-Traunfels R. (ed.) *Verhandlungen des VIII. Internationalen Zoologen-Kongresses zu Graz vom 15.-20. August 1910*. Gustav Fischer, Jena, pp. 520-527.

Zelinka K. 1913. Die Echinoderen der Deutschen Südpolar Expedition 1901-1903. *Deutsche Südpolar Expedition, Zoologie* **14(6):** 419-437.

Zelinka K. 1928. *Monographie der Echinodera.* Verlag von Wilhelm Engelmann, Leipzig. 1st ed., 396 pp.

Zeppilli D, Canals M, Danovaro R. 2011. Pockmarks enhance deep-sea benthic biodiversity: a case study in the western Mediterranean Sea. *Diversity and Distributions* **18(8)**: 832-846. https://doi.org/10.1111/j.1472-4642.2011.00859.x.

Zeppilli D, Leduc D, Fontanier C, Fontaneto D, Fuchs S, Gooday AJ, *et al*. 2018. Characteristics of meiofauna in extreme marine ecosystems: a review. *Marine Biodiversity* **48**: 35-71. https://doi.org/10.1007/s12526-017-0815-z.

Zeppilli D, Pusceddu A, Trincardi F, Danovaro R. 2016. Seafloor heterogeneity influences the biodiversity-ecosystem functioning relationships in the deep-sea. *Scientific Reports* **6**: e26352. https://doi.org/10.1038/srep26352.